

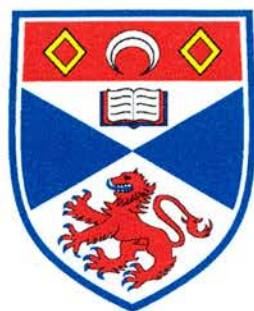
University of St Andrews



Full metadata for this thesis is available in
St Andrews Research Repository
at:

<http://research-repository.st-andrews.ac.uk/>

This thesis is protected by original copyright



University
of
St Andrews

Radical Nucleophilic Ring Closures:

Reactivity, Selectivity and Synthesis

A thesis presented by Mark D. Roydhouse to the
University of St Andrews in application for the degree of
Doctor of Philosophy.

Supervisor: Prof. J. C. Walton

September 2005



1950
1951
1952
1953
1954
1955
1956
1957
1958
1959
1960
1961
1962
1963
1964
1965
1966
1967
1968
1969
1970
1971
1972
1973
1974
1975
1976
1977
1978
1979
1980
1981
1982
1983
1984
1985
1986
1987
1988
1989
1990
1991
1992
1993
1994
1995
1996
1997
1998
1999
2000
2001
2002
2003
2004
2005
2006
2007
2008
2009
2010
2011
2012
2013
2014
2015
2016
2017
2018
2019
2020
2021
2022
2023
2024
2025

Radiochemical Nucleophilic Ring Closures

Activity, Selectivity and Synthesis

Dr. J. H. Goldstein, Department of Chemistry, University of California, San Diego, La Jolla, California 92037

1970

1971

DECLARATION

I, Mark David Roydhouse, hereby certify that this thesis, which is approximately 50,000 words in length, has been written by me, that it is the record of work carried out by me and that it has not been submitted in any previous application for a higher degree.

Date:

Signature of candidate:

26/09/05

I was admitted as a research student in October, 2001 and as a candidate for the degree of Doctor of Philosophy in July, 2002; the higher study for which this is a record was carried out in the University of St Andrews between 2001 and 2005.

Date:

Signature of candidate:

26/09/05

I hereby certify that the candidate has fulfilled the conditions of the Resolution and Regulations appropriate for the degree of Doctor of Philosophy in the University of St Andrews and that the candidate is qualified to submit the thesis in application for that degree.

Date:

Signature of supervisor:

26/9/05

(Prof. J. C. Walton)

COPYRIGHT DECLARATION

Unrestricted access

In submitting this thesis to the University of St Andrews I understand that I am giving permission for it to be made available for use in accordance with the regulations of the University Library for the time being in force, subject to any copyright vested in the work not being affected thereby. I also understand that the title and abstract will be published, and that a copy of the work may be made and supplied to any *bona fide* library or research worker.

Date:

Signature of candidate:

26/09/05

Abstract

Unimolecular radical nucleophilic substitution ($S_{RN}1$) is a chain process that was discovered in the early 1970's. The mechanism involves the formation by electron transfer of a radical centre which can then couple with a nucleophile to give a radical anion intermediate, which can transfer an electron to another molecule of starting material to give product and propagate the chain. Since then an exhaustive mechanistic and synthetic study has been carried out on the intermolecular version of the reaction. However, very little study has been made of the intramolecular $S_{RN}1$ reaction and even less study has been made of stereoselective $S_{RN}1$ processes.

This thesis reports the syntheses of substrates containing an aryl halide and a 2-oxazoline moiety joined by variable length carbon tethers. These precursor arylalkyl-2-oxazolines then undergo aryl radical-carbanion coupling to afford indanes, tetrahydronaphthalenes and benzosuberenes in good to excellent yield. Advantages of this synthetic protocol are that it enables sterically hindered quaternary centres to be made and a range of ring sizes can readily be attained. The process is facilitated by the use of lithium diisopropylamide as the base and tetrahydrofuran as the solvent. In the formation of benzosuberenes a rare *alpha-ortho* rearrangement was observed post ring closure.

It was demonstrated that when an oxazolidinone was used instead of a 2-oxazoline as a substrate, a novel fused tetracycle of the isoquinalone family was formed via a unique acyl migration followed by a nucleophilic ring closure cascade.

EPR observations of the intermediates from the oxazoline precursors enabled the ring closed radical anions to be detected and hence gave strong support to the $S_{RN}1$ character of the mechanism.

It was established that chiral arylpropyl-2-oxazolines undergo ring closure with modest selectivity to yield diastereoisomeric indanes that could be separated via conventional column chromatography.

An EPR study of cyclohexyl acyl radicals was undertaken showing for the first time that the axial and equatorial conformers could be distinguished and their concentrations measured. The acyl radicals show surprisingly large β & γ hyperfine splittings.

Acknowledgements

I would like to thank Prof. J. C. Walton for giving me the opportunity to carry out this PhD. Also would like to thank him for his unending support and encouragement though out the past 4 years. I would also like to thank Dr. R. A. Aitken for his help and useful discussions.

I would like to thank Melanja Smith and Dr. Tomas Lebl for the help and advice with NMR spectroscopy. I would also like to thank the DOH research group for the use of their GCMS and Prof A. M. Z. Slawin for carrying out X-ray analysis.

Thanks to all the Walton research group past and present, these are Fernando Portela, Eoin Scanlan, Patricia Minin, James Lymer and Franco Bella.

Many thanks to Caroline, Cristina, Sneh, Graham, Dean and Will for all their support and friendship over the years.

Finally, a big thank you to my family for the help and support over the years.

1	Abbreviations	i
1	Introduction	1
1.1	Stereoselectivity in Synthesis	2
1.1.1	Substrate-Controlled Methods	3
1.1.2	Auxiliary-Controlled Methods	6
1.1.3	Reagent-Controlled Methods	8
1.1.4	Catalyst-Controlled Methods	9
1.2	Radical Ring Closures	11
1.3	Unimolecular Radical Nucleophilic Substitution	18
1.3.1	The S _{RN} 1 Mechanism	20
1.3.1.1	Initiation	21
1.3.1.2	Propagation	23
1.3.1.2.1	Step 2: Radical Anion Fragmentation	23
1.3.1.2.2	Step 3: Radical Coupling With Nucleophiles	25
1.3.1.2.3	Step 4: Single Electron Transfer	27
1.3.2	Solvents and Bases	27
1.3.3	Nucleophiles	28
1.3.4	Substrates	31
1.3.5	Intramolecular S _{RN} 1 Reactions	38
1.3.6	Aryne Mechanism	41
1.3.7	Stereoselectivity in S _{RN} 1 Reactions	42
1.4	Project Aims and Objectives	45
1.4.1	Retrosynthetic Analysis of Procylic Species	48
1.5	Bibliography	52
2	Results and Discussion	64
2.1	2-(2-Halophenylalkyl)-2-oxazolines	65

2.1.1	2-Halophenylalkyl Halides from 2-Halophenylalkanoic Acids	65
2.1.1.1	2-Halophenethyl Halides.....	66
2.1.1.2	Chain Extension of 2-Halophenethyl Halides	68
2.1.2	Preparation of 2-Oxazolines from 1,2-Aminoalcohols	71
2.1.2.1	Non-chiral 2-Oxazolines	71
2.1.2.2	Chiral 2-Oxazolines.....	72
2.1.3	2-[3-(2-Halophenyl)propyl]-2-oxazolines	75
2.1.4	2-[3-(2-Halophenyl)-1-phenylpropyl]-2-oxazolines	78
2.2	3-Substituted 1-(2-Oxazolin-2-yl)-propen-2-ols	82
2.2.1	2-Bromophenylacetyl Chloride.....	82
2.2.2	Substituted Propen-2-ols	82
2.3	Hetero Atom Analogues of Arylalkyloxazolines.....	88
2.3.1	<i>N</i> -Substituted Anilines and <i>O</i> -Substituted Phenols.....	88
2.3.2	α -Cyano Esters and Amides	91
2.3.3	Potential Routes to Hetero Analogues of Arylalkyloxazolines	92
2.4	$S_{RN}1$ Reactions of Non Chiral 2-Oxazolines.....	94
2.4.1	$S_{RN}1$ Reactions Using DMSO/ ^t BuOK.....	96
2.4.2	$S_{RN}1$ Reactions Using MNH_2 /Ammonia.....	97
2.4.3	$S_{RN}1$ Reactions Using LDA/THF.....	98
2.4.3.1	2-[3-(2-Bromophenyl)-1-phenylpropyl]-4,4-dimethyl-2-oxazoline.....	99
2.4.3.2	2-[3-(2-Bromophenyl)propyl]-4,4-dimethyl-2-oxazoline	102
2.4.4	$S_{RN}1$ Reactions Using LDA/THF:Hexane	103
2.4.5	$S_{RN}1$ Reactions Using NaH/DMSO.....	104
2.4.6	Summary of Non-Chiral $S_{RN}1$ Reactions.....	106
2.5	Tetalins, Benzosuberenes and Benzocyclooctanes via $S_{RN}1$ Reactions	107
2.5.1	Formation of Substituted Tetalins using $S_{RN}1$ Protocols.....	107
2.5.2	Formation of Substituted Benzosuberenes Using $S_{RN}1$ protocols.....	108

2.5.2.1	NMR Structure Determination of Benzocycloheptane	150.. 110
2.5.2.2	Summary of $S_{RN}1$ Reactions of ϵ -Arylpentyl-2-oxazoline 121
2.5.2.3	Mechanism of Formation of Benzocycloheptane Derived Products.....	122
2.5.3	Formation of Benzocyclooctanes Using $S_{RN}1$ Protocols 127
2.5.4	Summary of $S_{RN}1$ Reactions to Afford Tetralins, Benzosuberenes and Benzocyclooctanes	129
2.6	EPR Study of $S_{RN}1$ Reactions of Arylalkyl-2-oxazolines.....	130
2.6.1	EPR Spectra and Computational Results.....	130
2.6.2	Mechanistic Considerations	139
2.7	Diastereoselective $S_{RN}1$ Reactions	143
2.7.1	Substituted (S)-4- <i>iso</i> -propyl-2-oxazoline.....	144
2.7.2	Substituted (S)-4- <i>tert</i> -Butyl-2-oxazoline	146
2.7.3	$S_{RN}1$ Reactions of Chiral Aryl and Benzyl-2-oxazolines	147
2.7.4	Substituted Chiral Cyclohexylmethyl-2-oxazolines	150
2.7.5	(-)-Spartiene: A Chiral Ligand for Lithium in $S_{RN}1$ Reactions	152
2.7.6	Summary of Stereoselective $S_{RN}1$ Reactions	153
2.8	Oxazolidinones in $S_{RN}1$ Reaction.....	155
2.8.1	$S_{RN}1$ Reactions of 2-Oxazolidinones.....	158
2.8.2	Cyclisation Mechanism	167
2.9	Conformational Study of Alicyclic Acyl Radicals.....	172
2.9.1	Preparation of Alicyclic Carbaldehydes	172
2.9.2	EPR and Computational Study of Cyclohexylacyl Radicals .	174
2.9.3	Summary of Study of Cyclohexylacyl Radicals.....	181
2.10	Conclusions.....	182
2.11	Bibliography	184
3	Experimental	189

3.1	Experimental Data Index.....	190
3.2	Instrumentation and General Techniques.....	194
3.2.1	NMR Spectroscopy	194
3.2.2	Infrared Spectroscopy.....	194
3.2.3	Mass Spectrometry	195
3.2.4	GC/MS.....	195
3.2.5	Elemental Analysis	195
3.2.6	Melting Points.....	195
3.2.7	Polarimetry.....	195
3.2.8	Chromatography	196
3.2.9	Reagents and Solvents.....	196
3.2.10	UV Photolysis	196
3.2.11	X-Ray Crystallography.....	196
3.2.12	EPR Spectroscopy	197
3.2.13	Computational Methods	197
3.3	2-Halophenylalkyl Iodides	198
3.3.1	2-Chlorophenethyl iodide.....	198
3.3.2	2-Bromophenalkyl Iodides	199
3.3.2.1	2-Bromophenylalkanoic Acids	199
3.3.2.2	2-Bromophenylalkanols	200
3.3.2.3	2-Bromophenylalkyl Iodides.....	201
3.4	Chiral Aminoalcohols	203
3.4.1	(S)-Valinol.....	203
3.4.2	(S)-Phenylglycinol.....	204
3.4.3	(S)-Serine Methyl Ester Hydrogen Chloride (S)-78.....	205
3.4.4	(S,S)-2-Amino-3-methoxy-1-phenylpropan-1-ol (S,S)-79	205
3.5	Acetimidate Esters	207
3.6	2-Oxazolines	208
3.6.1	Non Chiral Oxazolines	208
3.6.2	Chiral Oxazolines	208

3.7	2-(Arylalkyl)-2-Oxazolines	213
3.8	Substituted Propen-2-ols.....	222
3.9	γ-Substituted Propionic acids.....	224
3.10	Cyanoacetic acid Derivatives	226
3.11	S_{RN}1 Reactions	227
3.11.1	^tBuOK/DMSO	227
3.11.1.1	General Procedure.....	227
3.11.1.2	2-[3-(2-Chlorophenyl)propyl]-4,4-dimethyl-2-oxazoline 33a.....	227
3.11.1.3	2-[3-(2-Bromophenyl)-1-phenylpropyl]-4,4-dimethyl-2-oxazoline 34b.....	227
3.11.2	MNH₂/NH₃	228
3.11.2.1	General Procedure.....	228
3.11.2.2	2-[3-(2-Chlorophenyl)propyl]-4,4-dimethyl-2-oxazoline 33a.....	228
3.11.2.3	2-[3-(2-Bromophenyl)-1-phenylpropyl]-4,4-dimethyl-2-oxazoline 34b.....	228
3.11.3	LDA/THF & LDA THF/Hexane Without Iron(II) Salts	229
3.11.3.1	General Procedure.....	229
3.11.3.2	2-[3-(2-Bromophenyl)-propyl]-4,4-dimethyl-2-oxazoline 33b	229
3.11.3.3	2-[3-(2-Bromophenyl)-1-phenylpropyl]-4,4-dimethyl-2-oxazoline 34b.....	230
3.11.3.4	2-[3-(2-Bromophenyl)-1-phenylbutyl]-4,4-dimethyl-2-oxazoline 110	230
3.11.3.5	2-[3-(2-Bromophenyl)-1-phenylpentyl]-4,4-dimethyl-2-oxazoline 111.....	231
3.11.3.6	2-[3-(2-Bromophenyl)-1-phenylhexyl]-4,4-dimethyl-2-oxazoline 112.....	234
3.11.3.7	(4S)-2-[3-(2-Bromophenyl)-1-phenyl-propyl]-4-isopropyl-2-oxazoline (S)-103.....	234

3.11.3.8	2-[3-(2-Bromo-phenyl)-1-phenyl-propyl]-4- <i>tert</i> -butyl-2-oxazoline.....	236
3.11.3.8.1	With (-)-Spartiene	237
3.11.3.9	(4 <i>S</i>)-2-[3-(2-Bromo-phenyl)-1-phenyl-propyl]-4-phenyl-2-oxazoline (S)-105.....	238
3.11.3.10	(4 <i>S</i>)-2-[3-(2-Bromo-phenyl)-1-phenylpropyl]-4-cyclohexylmethyl-2-oxazoline (S)-107	238
3.11.4	LDA/THF & LDA THF/Hexane With Iron(II) Salts	238
3.11.5	NaH/DMSO	239
3.11.6	With Phenanthrene Radical Anion	240
3.11.7	Preparation of EPR Samples	240
3.12	Oxazolidinones	242
3.13	Cycloalkylcarbaldehydes	246
3.13.1	Synthesis	246
3.13.1.1	Carboxylic Acids	246
3.13.1.2	Cycloalkylmethanols	247
3.13.1.3	Cycloalkylmethanals	248
3.13.2	EPR Sample Preparation	249
3.13.3	Computations.....	249
3.14	Bibliography	250
Appendix A – X-Ray Crystal Data		253
Tetrahydronaphthalene 144.....		254
Benzosuberene 148.....		259
Flourene 149		264
(S,S)- β -Hydroxyamide (S,S)-175.....		269
Appendix B - NMR Data		274

Benzosuberene 150	275
Roytonone 191	278
Appendix C – EPR Spectra	281
Carbaldehyde <i>cis</i> -203	282
Carbaldehyde <i>trans</i> -203	283
Carbaldehyde <i>cis</i> -204	284
Carbaldehyde 206	285
Tetrahydronaphthalene Radical Anion 171	286
Benzosuberene Radical Anion 172	286
Appendix D - Kinetic Data	287
Cyclohexylacyl Radical 214	288
Appendix E - Publications	289

1 Abbreviations

AIBN	2,2-Azobisisobutyronitrile
Å	Angstrom
BDE	Bond Dissociation Energy
Bn	Benzyl Radical
°C	Degrees Centigrade, Temperature Unit
CI	Chemical Ionisation
COSY	Proton-Proton Correlation Spectroscopy
cm ³	Centimeters Cubed
DCC	1,3-Dicyclohexylcarbodiimide
DCM	Dichloromethane
D6-DMSO	Deuterated Dimethyl sulfoxide
d. e.	Diastereomeric Excess
δ	Chemical Shift in ppm
DMSO	Dimethyl sulfoxide
D8-THF	Deuterated tetrahydrofuran
DTBN	Di- <i>tert</i> -butylnitroxide
e. e.	Enantiomeric excess
EI	Electron impact, ionisation technique
equiv	Equivalents
EPR	Electron paramagnetic resonance
ES	Electrospray
Et	Ethyl Radical, CH ₃ CH ₂ -
ET	Electron Transfer
ether	diethyl ether
EWG	Electron Withdrawing Group
EtOAc	Ethyl Acetate
g	Grams
G	Gauss
h	Hours
hfs	Hyper Fine Splitting
HMBC	Heteronuclear Multiple Bond Connectivity

HMPA	Hexamethylphosphoramide
HOMO	Highest Occupied Molecular Orbital
HSQC	Heteronuclear Single Quantum Coherence
<i>hν</i>	Photons
ID	Internal Diameter
[•] Pr	2-Methylethyl Radical
IR	Infrared
<i>J</i>	Coupling constant
LDA	Lithium diisopropylamide
LiHMDS	Lithium bis(trimethylsilyl)amide
LUMO	Lowest Unoccupied Molecular Orbital
M	Concentration, mol.L ⁻¹
Me	Methyl radical, CH ₃ -
MHz	MegaHertz
min	Minutes
μL	Microlitres
mmol	Millimol
mp	Melting point
<i>m/z</i>	Mass over charge ratio
TEA	Triethylamine
THF	Tetrahydrofuran
nm	Nanometres
NMR	Nuclear Magnetic Resonance
Nu	Nucleophile
OD	Outer Diameter
ORD	Optical Rotatory Dispersion
Ph	Phenyl Radical, C ₆ H ₅ -
ppm	Parts Per Million
Py	Pyridine
R	Generic Group
R _f	Retention Factor, Chromatography
RT	Room Temperature
SET	Single Electron Transfer
S _H i	Intramolecular Homolytic Substitution

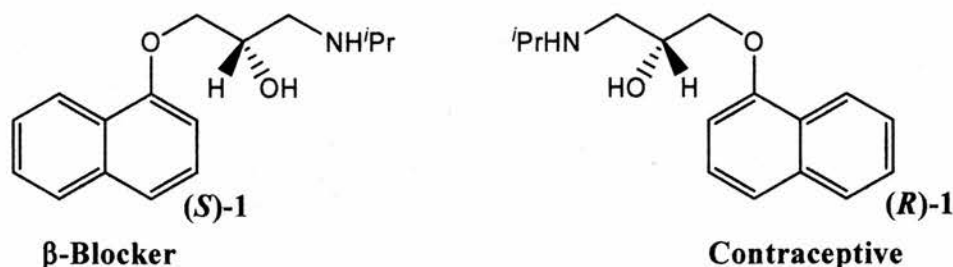
$S_{RN}1$	Unimolecular Radical Nucleophilic Substitution
S_N1	Unimolecular Nucleophilic Substitution
S_N2	Bimolecular Nucleophilic Substitution
S_{NAr}	Aromatic Nucleophilic Substitution
SOMO	Singly Occupied Molecular Orbital
tBu	2,2-Dimethylethyl Radical
THF	Tetrahydrofuran
TLC	Thin Layer Chromatography
TMS	Trimethylsilyl Radical
UV	Ultraviolet
ν	Wavenumber, cm^{-1}
X	Any Halogen

Section 1

Introduction

1.1 Stereoselectivity in Synthesis

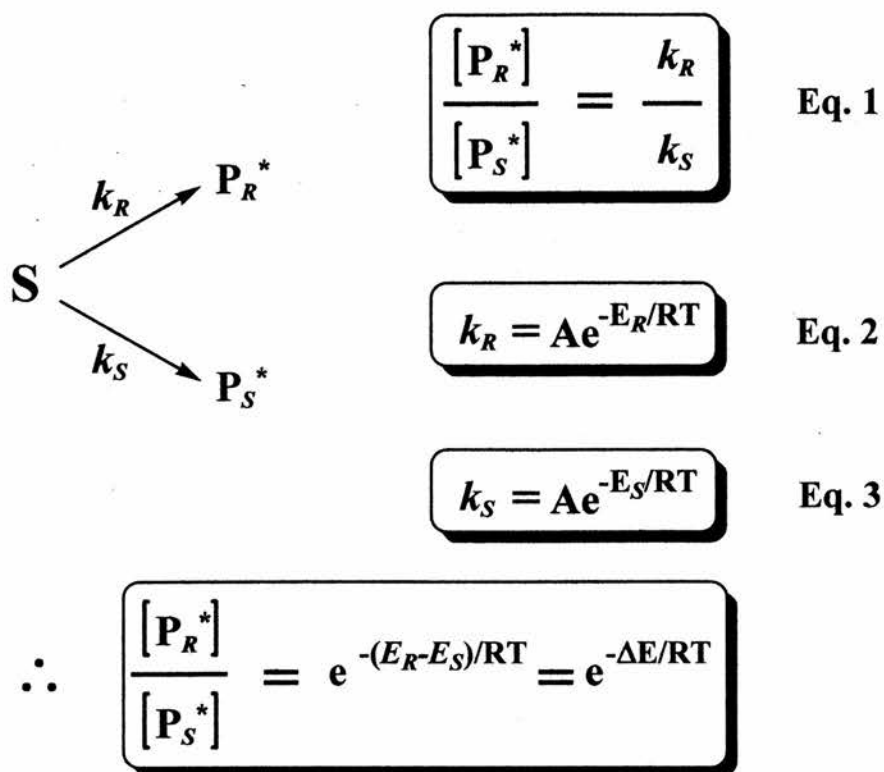
In the modern chemical arena, the ability to accurately control the regio- and stereo-chemistry of a given organic transformation is vitally important. This importance is due to economic, environmental and biological concerns. Traditionally many therapeutic compounds that contained a stereogenic aspect have been synthesised via racemic routes and have either been separated or used in the racemic form. Clearly, in today's present climate, such syntheses are becoming increasingly more uneconomical due to the costs associated with the disposal of the waste stereoisomer. Also different isomers can have different pharmacological properties. For instance, for the drug Propranolol **1** (Scheme 1), the two enantiomers have very different biological properties, one being a β -blocker while the other exhibits contraceptive properties.¹ Therefore it is clearly important that enantiomerically pure compounds can be prepared inexpensively with high purity with the minimum of waste.



Scheme 1

The concept of asymmetric synthesis is a relatively new area in organic synthesis only changing from a mechanistic interest in the 1960's to a important synthetic goal from the 1970's to the present day, culminating in the Nobel prize for chemistry being awarded to K. B. Sharpless, W. S. Knowles and R. Noyori for the work on catalytic asymmetric synthesis. An asymmetric synthesis may be defined as: "synthesis in which an achiral unit in an ensemble of substrate molecules is converted to a chiral unit such that the possible stereoisomers are formed in unequal amounts."²

Mechanistically, virtually all diastereomeric and enantiomeric excesses are kinetically controlled phenomena (Scheme 2). It can be seen from the derivation in Scheme 2 that as temperature decreases diastereomeric excess (d.e.) and enantiomeric excess (e.e.) increase although the overall rate decreases. $\Delta E = 8.4 \text{ kJ mol}^{-1}$ is enough to give 88 % d.e. (e.e.) at 298 K



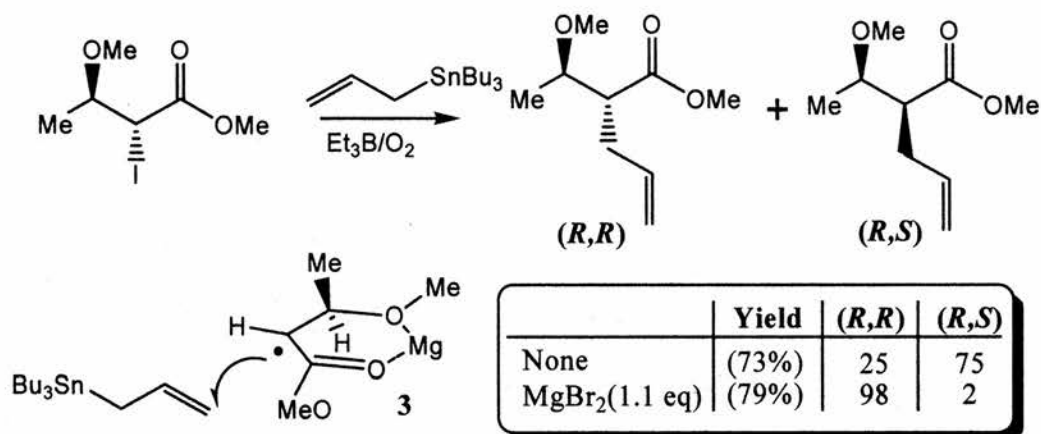
Scheme 2

The goal of asymmetric synthesis has been sought using a variety of methods. These can be categorised into roughly four distinct approaches,³ which are: 1) substrate-controlled methods; 2) auxiliary-controlled methods; 3) reagent controlled methods and 4) catalyst-controlled methods.

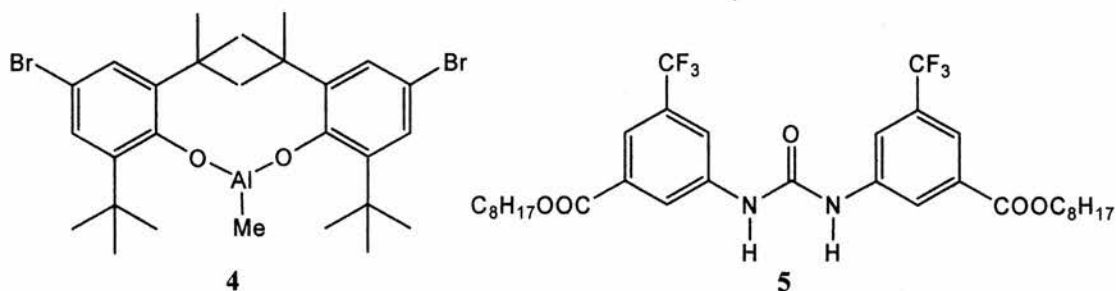
1.1.1 Substrate-Controlled Methods

This approach is the most simple of the four. The chiral unit is already present in the molecule and forms part of the intended final product. The already present stereogenic centre is used to intramolecularly induce selectivity at a prochiral centre within the molecule. Various strategies have been formulated to maximise the inductive capabilities of the pre-existing stereogenic group. These strategies include; 1) chelation of a metal by two or more groups in the molecule, in order to reduce the degrees of freedom; 2) complexation with a bulky group either through non-bonding interactions or dative bonding to a metal complex. In many cases the conformational restraints imposed by the pre-existing stereogenic centre are sufficient to induce respectable selectivity.

In order for metal chelation to occur a suitable nucleophilic centre needs to be present, also the spatial arrangement of such centres is important. Association with metals is usually best achieved using oxygen and nitrogen centres. Although a 1,3 arrangement is the optimum geometry, 1,2, 1,4 and 1,5 can be used. When two or more centres in a molecule are chelated to the same metal centre, temporary ring structures are formed. This reduces the geometric degrees of freedom, thus enabling a greater level selectivity to occur. Scheme 3 shows one such example with chelation involving Mg^{2+} and 1,3 oxygen functionality. As shown, this then forms the temporary cyclic structure **3**, thus enabling differentiation of the top and bottom faces, with the top face being more sterically hindered due to the methyl group, therefore radical attack takes place from the bottom face.

Scheme 3⁴

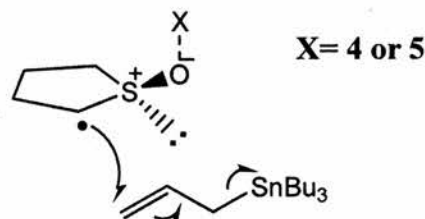
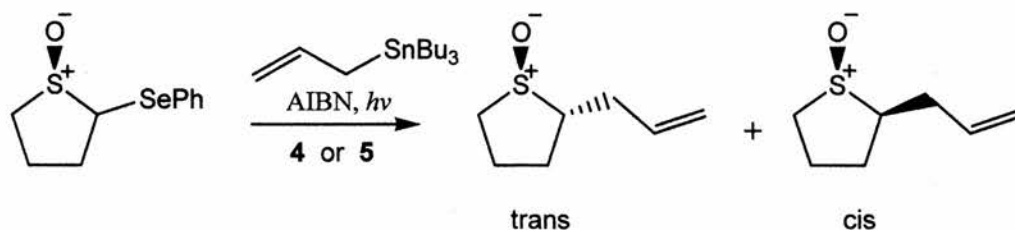
Introduction of a bulky group, be it a metal complex (e.g. **4**) or ligand (e.g. **5**), that can associate with one group around the stereogenic centre, can increase the overall steric effect of the group thus improving the asymmetry around the stereogenic centre.



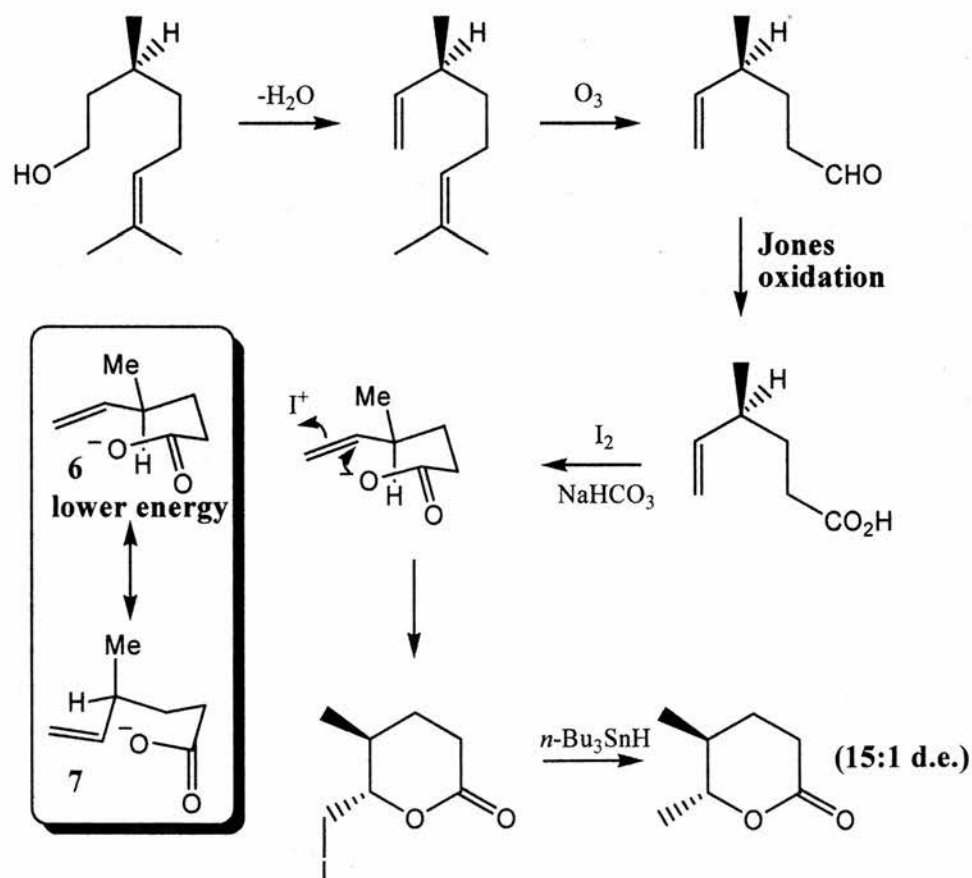
Scheme 4

The asymmetry at any pro-chiral centre elsewhere in the molecule is therefore increased, enabling a more selective attack of an incoming reactive group. An

example using a bulky metal complex **4** or ligand **5** associating with the oxygen of the chiral sulfinyl group is shown in Scheme 5.



	Yield	trans	cis
none	(78%)	70	30
4 (1.1eq)	(57%)	98.5	1.5
5 (1.1eq)	(81%)	88	12

Scheme 5⁵Scheme 6⁶

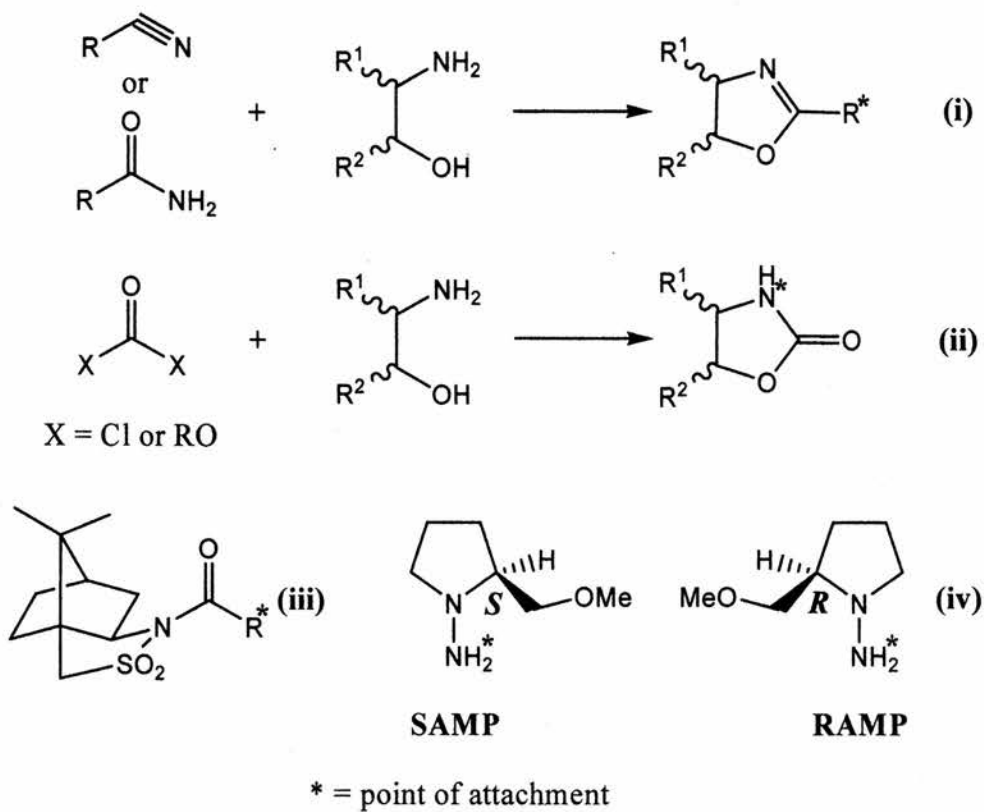
The inherent transition state geometric restraint of a chiral molecule can affect the outcome of a subsequent reaction at a pro-chiral centre elsewhere in the molecule. This is illustrated in Scheme 6. In the six membered chair type transition state the

methyl in a pseudo-equatorial position **6** is of lower energy than the methyl in a pseudo-axial position **7** which gives rise to the observed diastereomeric excess.

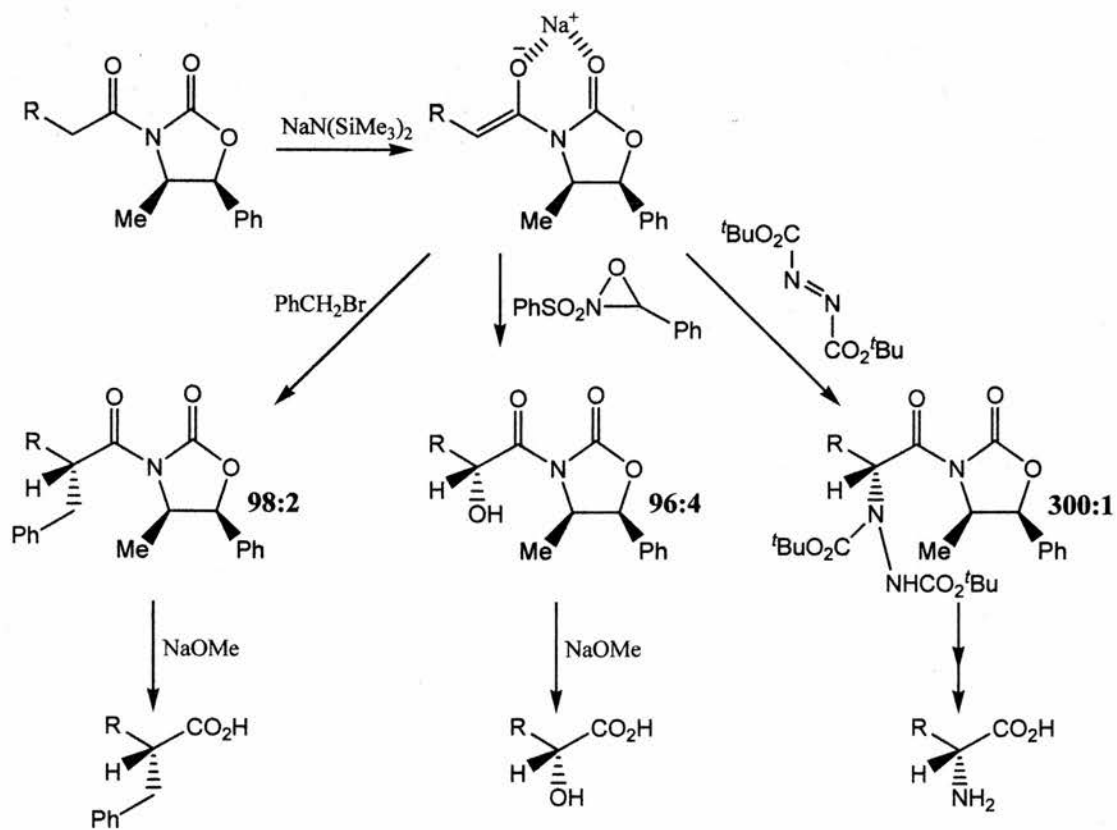
Overall substrate controlled methods offer simplicity, although the correct chiral motif has to be identified (usually from a natural source). Also, lots of scope exists to modify the selectivity by the use of chelating agents etc. This method could be considered as the poor person's asymmetric synthesis as the process only involves a selective modification of an existing chiral moiety. A new chiral molecule previously devoid of asymmetry has not been brought into being.

1.1.2 Auxiliary-Controlled Methods

Auxiliary controlled methods work on similar principal methods as substrate controlled methods, the difference being that the chiral inducing portion of the molecule is designed to be removed from the substrate after the introduction of the new chiral centre(s). The removable portion is termed the auxiliary. The auxiliary is designed to aid the reaction, induce chirality and be able to be easily removed and recycled. The ability to be recycled means that there is a net gain in chiral molecules created in the process as opposed to no net gain in the substrate-controlled method. The form of the auxiliary can vary greatly, but is always derived from the naturally occurring chiral pool. Some widely known chiral auxiliaries are 2-oxazolines,⁷ oxazolidinones,⁸ hydrazines⁹ and camphor sultams.¹⁰ 2-Oxazolines are derived from either nitriles or amides and a 1,2-aminoalcohol (Scheme 7i). Oxazolidinones are usually synthesised from either phosgene or dialkyl carbonates (Scheme 7ii) and a 1,2-aminoalcohol. The camphor sultams (Scheme 7iii) are obviously camphor derived. Enders' hydrazines, termed either RAMP or SAMP (Scheme 7iv), are synthesised from proline.

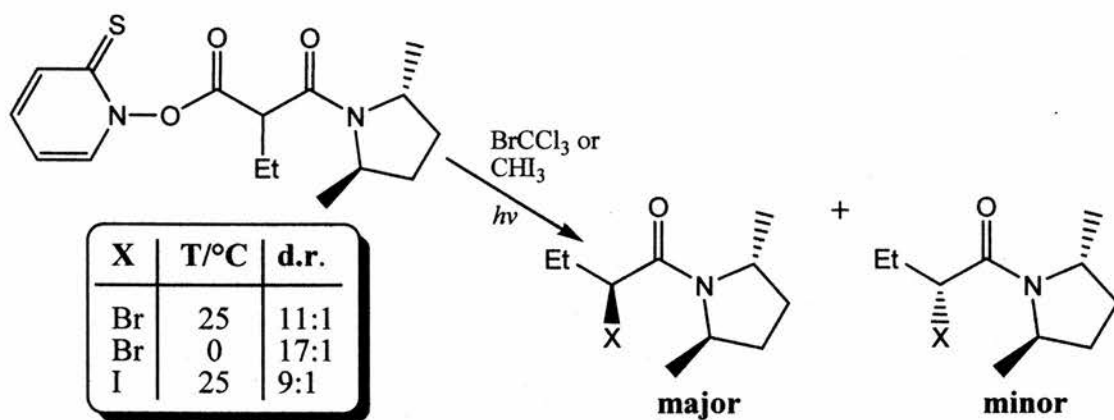


Scheme 7

Scheme 8^{8a-c}

An example of the use of oxazolidinones is shown in Scheme 8. The utility of the auxiliary-controlled method is shown, with the synthesis of amino acids, hydroxy-acids etc. all derived from the one intermediate oxazolidinone. The selectivities of these processes are extremely high, for example the production of enantiomerically pure unnatural α -amino acids.

The same utility is observed in many other auxiliary systems. As in substrate controlled methods, homolytic processes also benefit from auxiliary-controlled methods. One such example, involving the use of a tetrahydropyrrole, is displayed in Scheme 9, in which selectivity increases with a decrease in temperature as discussed previously.



Scheme 9 ¹¹

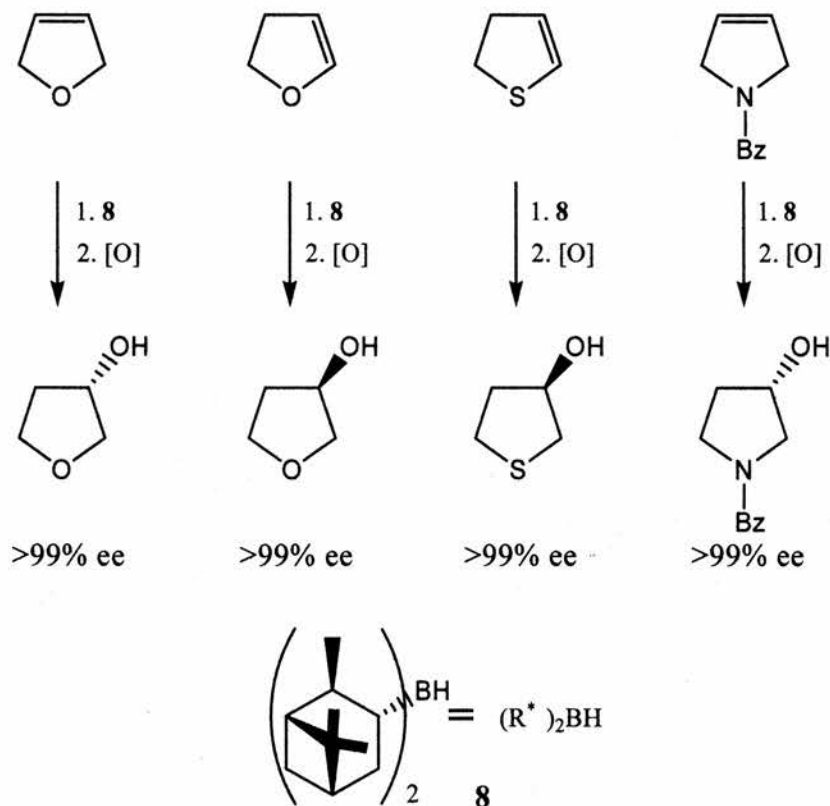
Overall auxiliary-controlled methods offer the same advantages as substrate-controlled methods, except that the ability to recycle the chiral inducing moiety is an added advantage. Although one major disadvantage of this methodology is the two extra steps needed to put on and remove the auxiliary, this can determine the feasibility of the synthetic use of a chiral auxiliary.

1.1.3 Reagent-Controlled Methods

One major disadvantage of the substrate and auxiliary controlled methods is the need to form the required chiral substrate prior to reaction. This is not always possible due to the limitations of the chiral pool; also auxiliary methods require two extra steps. In reagent-controlled methods these disadvantages are negated, as having a chiral reagent allows a wider range of possible substrates and no removal of an auxiliary is required post reaction. The chiral induction is now an intermolecular

process. Several different stereoselective reagents have been developed with great success; these include reducing reagents (borohydride,¹² and aluminium hydride¹³), acids¹⁴ and bases.¹⁵ The major disadvantage of this method is the lack of a variety of reagents.

Scheme 10, shows the stereoselective addition of a chiral borohydride reagent **8** to dihydro-furans, thiofurans and pyrroles. This yields, after oxidation of the organoborane intermediate, the 3-hydroxytetrahydro moieties in excellent enantiomeric excesses.



Scheme 10¹⁶

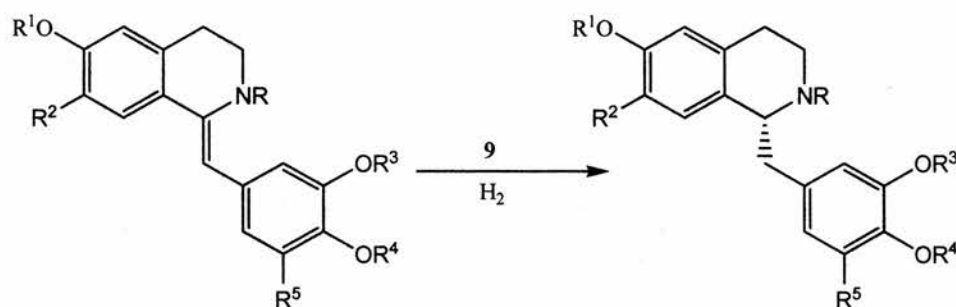
1.1.4 Catalyst-Controlled Methods

The most advanced method to date in the area of asymmetric synthesis is the use of a chiral catalyst. This method has distinct advantages over all other asymmetric synthetic methods in that the chiral agent does not need to be in stoichiometric amounts. Also, a catalytic substance should theoretically be unchanged by the reaction process, although in practise this is not always true. Amounts as small as 0.05 eq. have been used to bring about an asymmetric transformation of a pro-chiral molecule

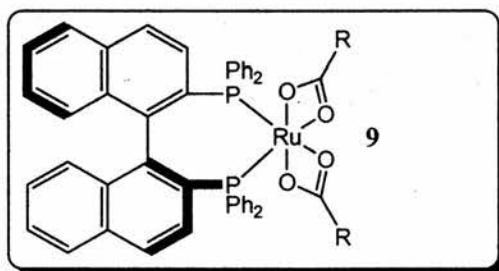
to a enantiomerically pure substance. This use of only small amounts of a chiral substance has an important impact especially on the industrial scale in terms of cost.

Many different reactions have had an asymmetric catalyst developed for them. These reactions include: Michael additions,¹⁷ 2+2 additions,¹⁸ Diels-Alder cycloadditions,¹⁸ epoxidations,¹⁹ oxidations of sulfides,²⁰ dihydroxylations²¹ and hydrogenations.²² Practically all the catalysts are transition metal chiral complexes, metals include Ti, Os, Ru, Rh, Fe and non-transition elements include Al, B & P.

Scheme 11 shows a ruthenium based binap complex **9** performing hydrogenation to yield in high enantiomeric excess intermediates in the synthesis of isoquinoline alkaloids.



- A** $R^1 = R^3 = R^4 = \text{CH}_3$; $R^2 = \text{OCH}_3$; 100% ee
 $R = R^5 = \text{H}$
- B** $R = R^1 = R^3 = R^4 = \text{CH}_3$; $R^2 = \text{OCH}_3$; 100% ee
 $R^5 = \text{H}$
- C** $R = R^2 = \text{H}$; $R^1 = R^4 = \text{CH}_3$; 97% ee
 $R^2 = \text{CH}_2\text{C}_6\text{H}_5$; $R^5 = \text{OCH}_2\text{C}_6\text{H}_5$
- D** $R = R^2 = R^3 = R^5 = \text{H}$; 95% ee
 $R^4 = \text{CH}_3$;



Scheme 11²³

Overall catalyst-controlled methods are the most efficient asymmetric process in terms of cost and net chiral molecules gained. The drawback of this method is the limited substrate scope of some of the catalysts, e.g. Sharpless asymmetric epoxidation is only successful for allylic alcohols.

1.2 Radical Ring Closures

Radical cyclisations form one of the most important branches of radical based organic synthesis. Synthetic routes to many important natural products and potential drugs²⁴ have utilised a radical cyclisation step to form the core ring system. Radical ring closures, like heterolytic ring closures, encompass a whole spectrum of mechanistic pathways, some of these are analogous to heterolytic processes and others unique to the special nature of radical reactions.

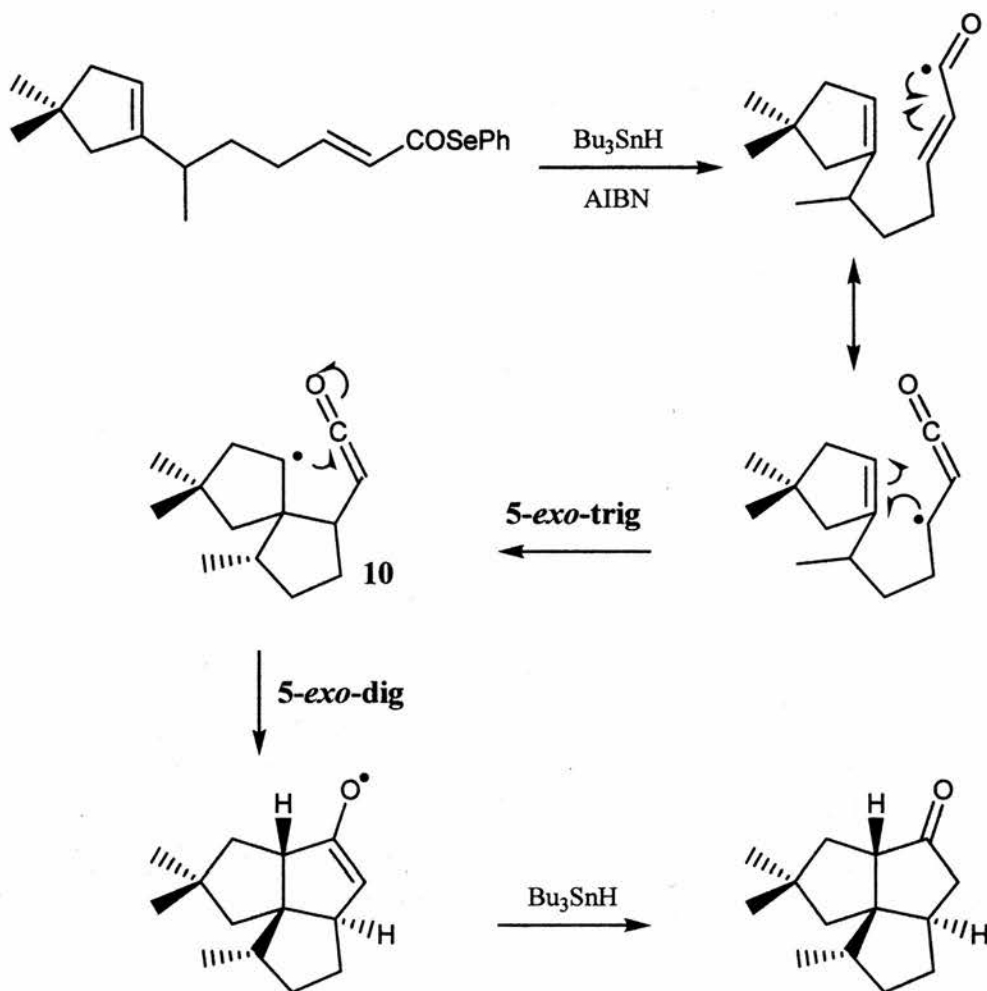
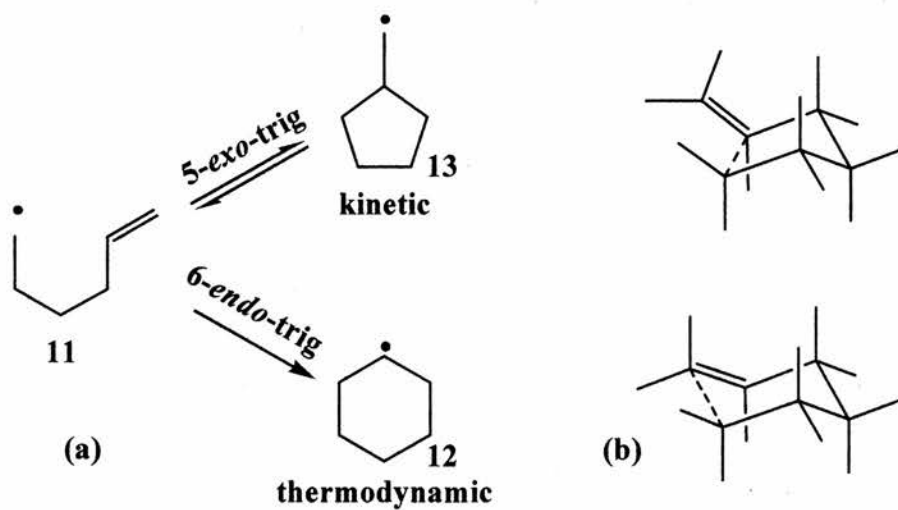
In 1976 Baldwin²⁵ identified and summarized a qualitative model describing general stereoelectronic constraints on cyclisation reactions, this model is known as Baldwin's rules or sometimes as the Beckwith-Baldwin rules.

In heterolytic ring closures Baldwin's rules define the mechanistic characteristics in relation to the ring size created, the resulting position of the electron pair and the hybridisation type of the electrophilic centre. Similarly, in homolytic ring closures, the ring size and acceptor centre are used, the only difference is that instead of the resulting electron pair position being definitive, the resulting position of the radical is. Baldwin's rules also predict the favourability of ring closure based upon geometric constraints on the interacting orbitals.

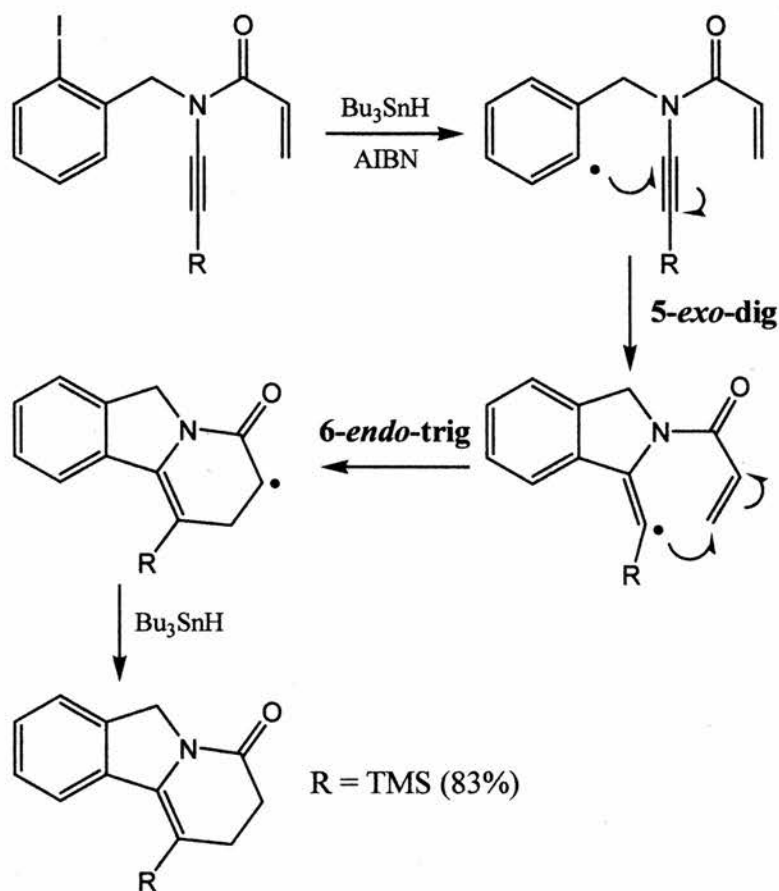
One of the most important and most frequently encountered ring closure types in radical cyclisations is 5-*exo*-trig. An example of this is shown in Scheme 12. The classic 5-*exo*-trig ring closure is onto a C=C bond,²⁶ although cyclisations onto C=O,²⁷ C=N,²⁸ N=N²⁸ etc. are known. Also in Scheme 12 is an example of 5-*exo*-dig process onto a ketene **10**,²⁶ other examples include alkynes,²⁹ nitriles,²⁸ isonitriles^{24e} and isocyanates.³⁰

It is worth noting that when two possible modes of cyclisation i.e. 5-*exo*-trig versus 6-*endo*-trig, are possible, kinetics and thermodynamics determine the product distribution. In Scheme 13a, a hex-5-enyl radical **11** is shown to cyclise and give two distinct products, which depend on the mode of cyclisation. The 6-*endo* product **12** is the thermodynamic product, due to the increased stability of the resultant secondary radical and it will predominate when reaction conditions allow equilibrium between open and closed ring structures (Scheme 13a). The 5-*exo* product **13**, which is the kinetic product is due to the better overlap of the SOMO and LUMO in the transition state that leads to the 5-membered product (Scheme 13b) and it will predominate if

termination/quenching of the resultant *exo* primary radical is fast compared to ring opening back to parent radical.

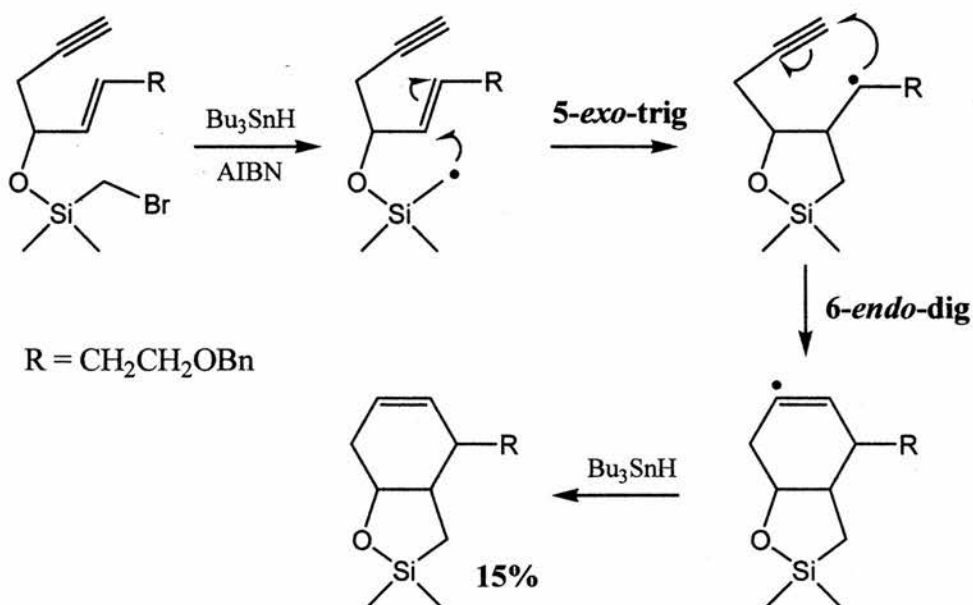
Scheme 12²⁶

Scheme 13

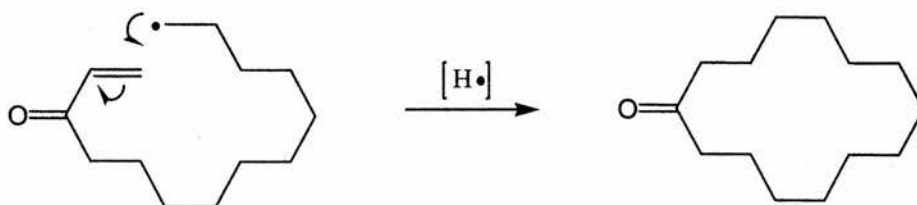
Scheme 14²⁹

In Scheme 14 an example of a 6-*endo*-trig cyclisation is shown. It can be seen clearly here that the predominance of the *endo* over *exo* is due to the high stability of the resultant radical alpha to the carbonyl group and the unfavourable sterics of the *exo* cyclisation.

The 6-*endo*-dig cyclisation mode has very few examples,³¹ due to the unfavourability of the bonding geometry and the faster and more favourable 5-*exo*-dig cyclisation mode. An example of 6-*endo*-dig is shown in Scheme 15.

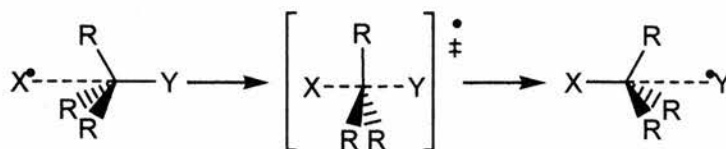
Scheme 15³²

As ring size increases, cyclisation becomes entropically unfavourable, but cyclisation can still be achieved, for example between a nucleophilic radical and an electron poor double bond (Scheme 16). A fuller explanation of factors influencing cyclisation products can be found in “Free Radicals in Organic Chemistry” by Fossey, Lefort and Sorba³³ and “Stereochemistry of Radical reactions” by Curran, Porter and Giese.³⁴



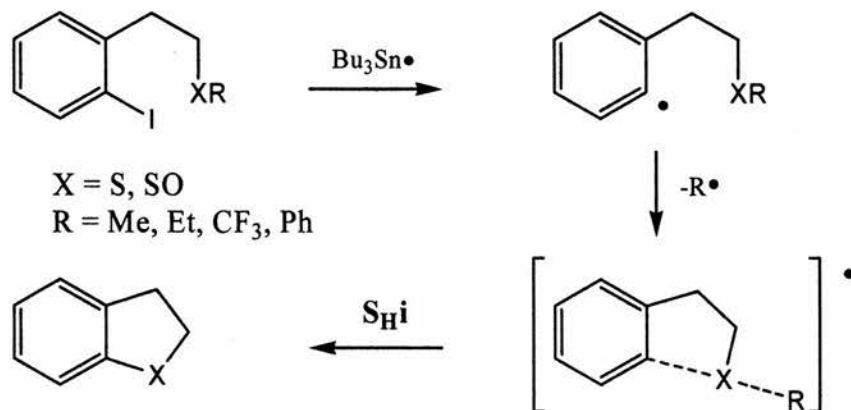
Scheme 16

So far only radical cyclisations onto unsaturated carbons have been reviewed,³⁵ another important class of reactions are the so called intramolecular radical substitutions ($S_{\text{H}}1$) or *exo-tet* ring closures. This class are analogous to the intramolecular $S_{\text{N}}2$ processes in ionic reactions. The transition state geometry is identical to the $S_{\text{N}}2$ transition state geometry in that the incoming radical approaches along the axis of the C-Y bond (Scheme 17).



Scheme 17

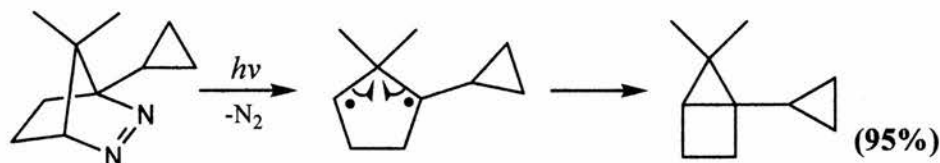
An example of S_{Hi} is shown in Scheme 18, showing a range of leaving groups and substitution centres. Another popular substitution centre is oxygen in the form of dialkylperoxides and peresters, which when undergoing S_{Hi} can form cyclic ethers and lactones³⁶ respectively. It should be noted that S_{Hi} reactions at sp^3 carbon atoms



Scheme 18³⁷

are very rare (they are restricted to strained centres e.g. cyclopropyl)³⁸ and this restriction limits the synthetic utility of this process.

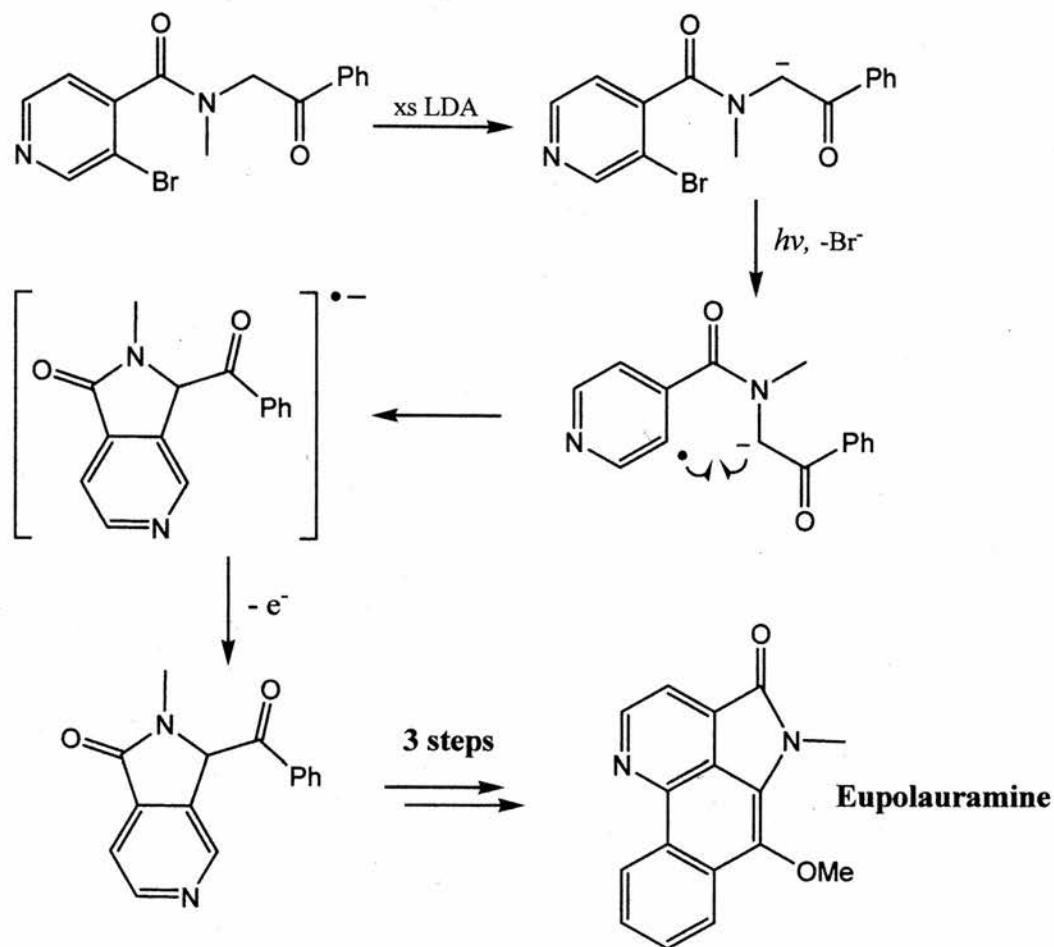
All radical species so far discussed in relation to cyclisations have contained only one unpaired electron. Species containing two unpaired electrons separated by one bond or more can be created in a synthetically useful setting and be employed to bring about ring closures³⁹ and other useful transformations.⁴⁰ These species with two unpaired electrons are known as biradicals. Many reactions of this class involve the loss of a neutral molecule e.g. N_2 to give the reactive biradical which then can combine to give a new bond. An example is shown in Scheme 19.



Scheme 19³⁹

So far, the examined mechanisms have featured radicals closing onto neutral centres of varying hybridisations and atom types, but another significant mechanism which is important in the formation of cycles involves the closure of a radical onto an anionic nucleophilic centre and/or group. This mechanism is known as unimolecular radical nucleophilic substitution ($S_{RN}1$). This mechanism involves the formation of a radical usually by electron transfer to an organic halide and the subsequent loss of X^- .

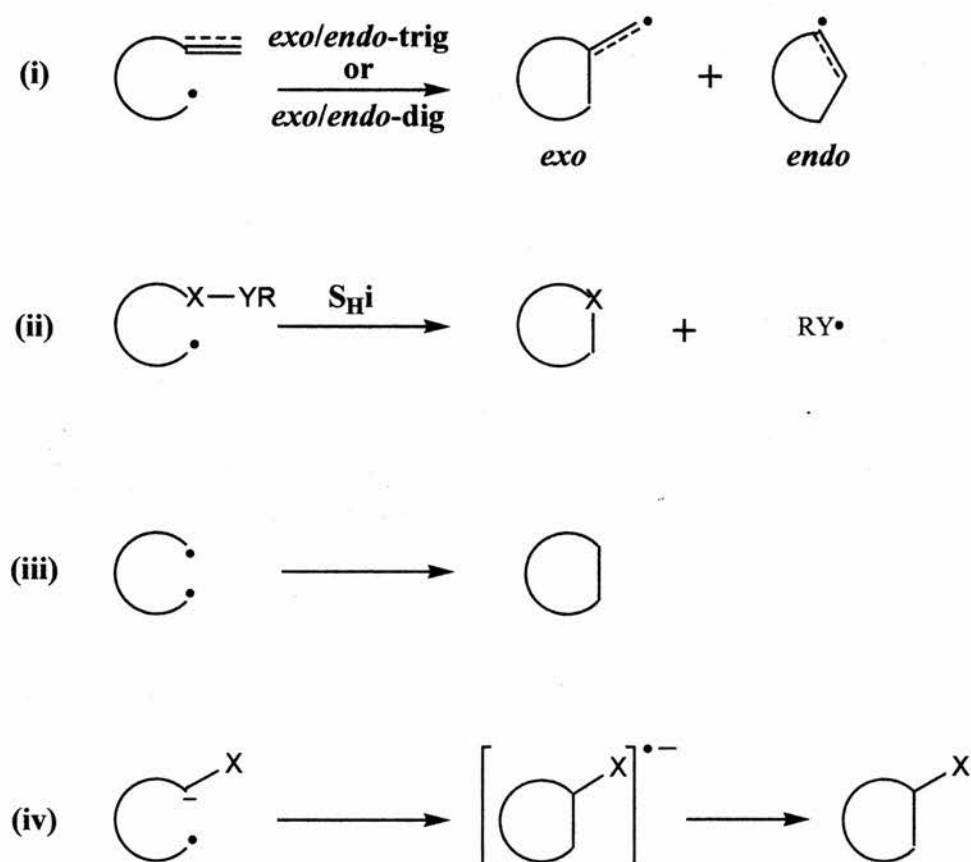
This radical then ring closes onto the nucleophile to give a radical anion followed by loss of an electron to give the cyclic product. This mechanism usually operates via a chain process. An example of a natural product formed by this process is shown in Scheme 20.



Scheme 20⁴¹

A summary of mechanistic pathways leading to ring formation via radical methods is shown in Scheme 21. Intramolecular addition to unsaturated centres (Scheme 21i), is by far the most synthetically used mode, with well understood reaction profiles due to intense research into the area. Intramolecular homolytic substitution at saturated centres ($\text{S}_{\text{H}}1$) (Scheme 21ii) is potentially synthetically useful. This usefulness however is limited by the need for a weak bond to the leaving group, and/or the potential for octet expansion, to incorporate a bond to the incoming radical. This in most cases excludes carbon due to its formation of strong bonds with almost all common elements and also its inability to expand its octet. Intramolecular radical-radical combination reactions (Scheme 21iii) in order to form rings, are in general not synthetically useful due to the need to incorporate a labile leaving group and the

inherent loss of control due to the high reactivity of biradicals. Unimolecular radical nucleophilic substitution ($S_{RN}1$) involves the coupling of a radical and an anion, and consequent bond formation induces ring closure (Scheme 21iv). From a mechanistic standpoint, $S_{RN}1$ reactions “sit on the fence” between homolytic and heterolytic chemistry. The literature details mechanistic aspects of $S_{RN}1$ reactions very thoroughly, although the synthetic utility has been under investigated. This may be due to the process fitting into neither the traditional areas of radical chemistry or ionic chemistry. The $S_{RN}1$ process is potentially a very useful transformation with much scope for innovation.



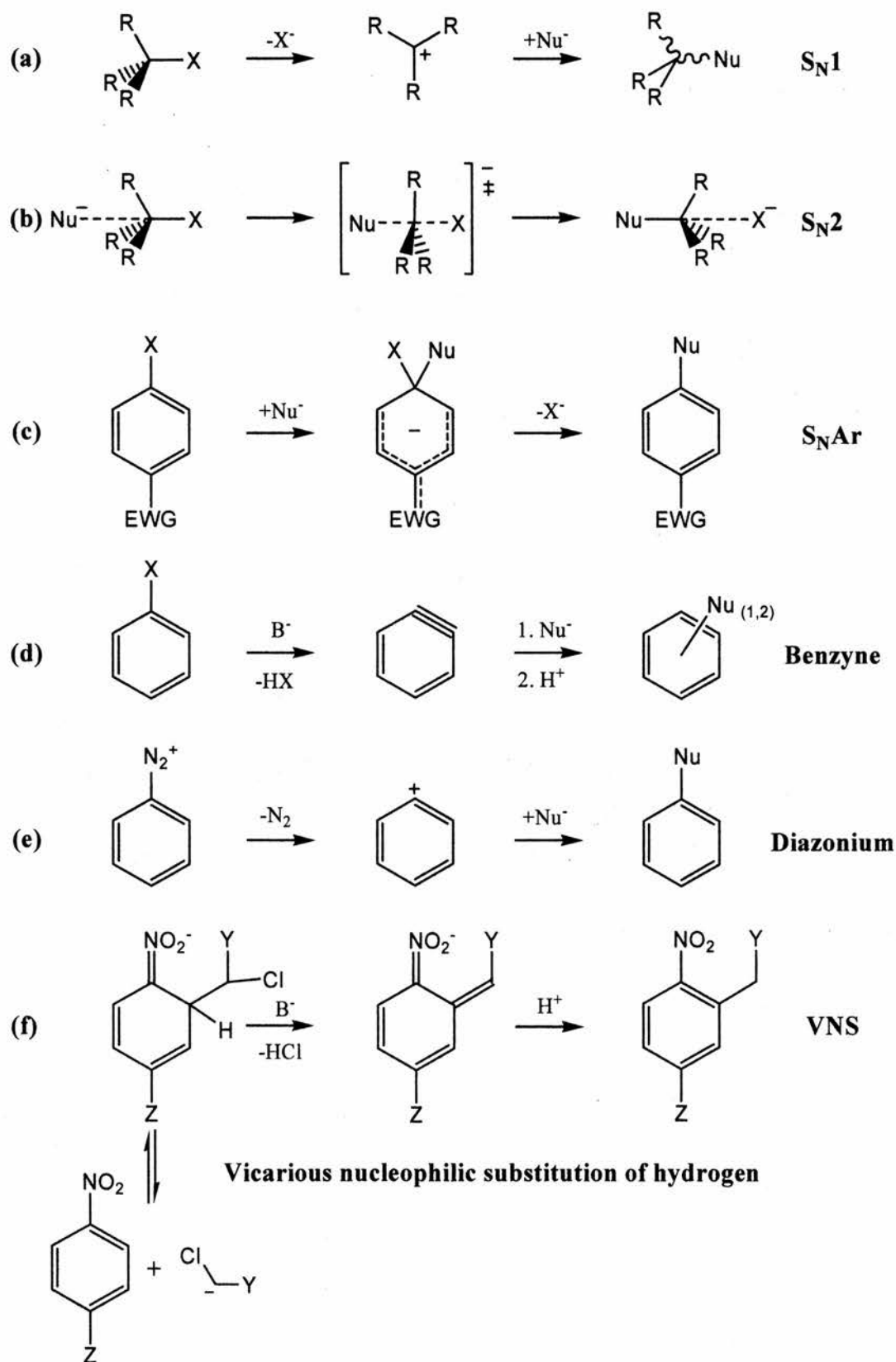
Scheme 21

1.3 Unimolecular Radical Nucleophilic Substitution

Nucleophilic substitution is one of the most frequently encountered mechanistic profiles in organic chemistry. S_N1 and S_N2 are the two nucleophilic substitution pathways that usually occur at sp^3 carbon atoms, S_N1 being the stepwise route and S_N2 the concerted (Scheme 22a & b). Nucleophilic substitution at aromatic centres was, up until the last 40-50 years, deemed relatively difficult as compared to electrophilic substitution. This is now known not to be the case. Common nucleophilic aromatic substitution mechanisms are detailed in Scheme 22c-f. The S_{NAr} process (Scheme 22c) requires the aromatic ring to be activated with an electron withdrawing group (EWG) or, if not activated, substitution can be facilitated by the use of chromium tricarbonyl.⁴² Reactions of aryl halides with strong bases can bring about substitution via the aryne mechanism (Scheme 22d). Nucleophilic substitution of diazonium ions (Scheme 22e) is an S_N1 process occurring at an aromatic centre due to N_2 being an extremely good leaving group. S_N2 processes at aromatic centres cannot occur due to the nucleophile attack vector being in the plane from the centre of the ring.⁴³ More recently vicarious nucleophilic substitutions of hydrogen (Scheme 22f) at an aromatic centre have been developed and championed by Makosza.⁴⁴

The nucleophilic substitution mechanisms so far discussed have been purely heterolytic in nature, one important mechanism left to be discussed, is the $S_{RN}1$ mechanism which will be looked at in detail. $S_{RN}1$ is nucleophilic substitution of a leaving group occurring by means of a single electron transfer chain process.

The first examples of aromatic $S_{RN}1$ mechanisms came to light as a result of an anomalous product distribution of a reaction involving 5- and 6-iodopseudocumenes with potassium amide in liquid ammonia reported by Kim and Bunnett,⁴⁵ supposedly occurring via the aryne mechanism. An excess of the respective *ipso* substitution was seen, more than could reasonably be explained by a common aryne intermediate. The *ipso* substitution was shown to be the result of a radical process, involving single electron transfer steps, which was inhibited by radical scavengers and promoted by one electron donors, e.g. solvated electrons from alkali metals in liquid ammonia.

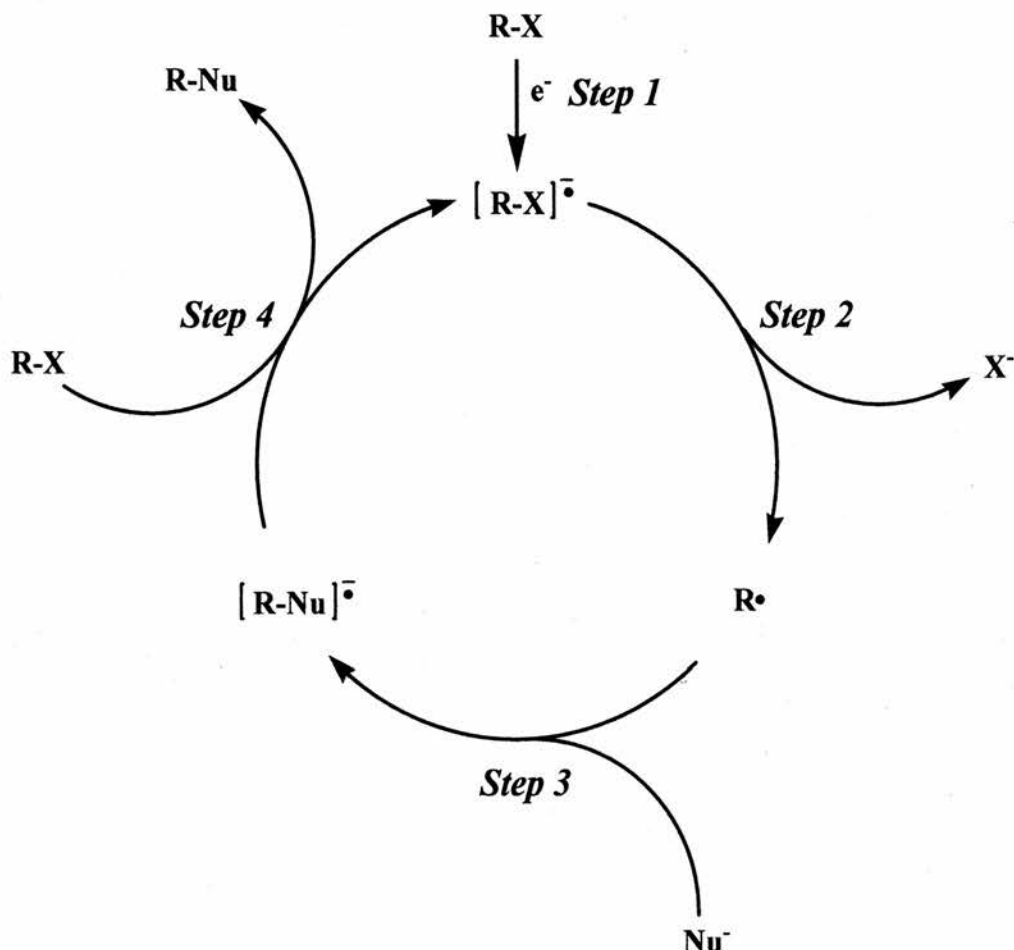


Scheme 22

This was shown to be the aromatic equivalent of an aliphatic process reported independently by Kornblum⁴⁶ and Russell⁴⁷ in 1966 featuring the reactions of *p*-

nitrobenzylic and α -nitroalkyl halides. The term $S_{RN}1$, standing for substitution, radical nucleophilic, unimolecular, was suggested by Bunnett^{45 & 48} and was widely adopted to describe reactions of this type.

1.3.1 The $S_{RN}1$ Mechanism



Scheme 23

The mechanism of the $S_{RN}1$ process is shown in Scheme 23. Initiation of the chain mechanism begins with a single electron transfer to RX (Step 1), followed by fragmentation with loss of X^- to give R^\bullet (Step 2). Coupling of R^\bullet and an incoming nucleophile results in the radical anion of RNu (Step 3), this then transfers an electron to another RX to complete the chain and give the substitution product RNu (Step 4). Several reviews of $S_{RN}1$ chemistry have been published over the years,⁴⁹ the most recent by Rossi *et al.*^{49a}

1.3.1.1 Initiation



Scheme 24

In step 1 of Scheme 23 the initiation of the $S_{\text{RN}}1$ mechanism is shown to occur by the addition of an electron to a molecule of RX , where X is a leaving group such as F , Cl , Br , I & SPh . This initial electron transfer (ET) has been widely studied and five main ET types have been identified, these are spontaneous or thermal, photostimulated, electrochemical, solvated electrons and reducing inorganic salts.

Spontaneous or thermal ET can occur from the nucleophile and/or base to the substrate RX , depending on the electron affinity of the substrate and the oxidation potential of the nucleophile and/or base. In most cases the $S_{\text{RN}}1$ substitution of aliphatic carbons with EWG can be initiated by thermal ET which can be stimulated by light.⁵⁰ Instances of spontaneous initiation with aromatic systems are relatively few. Cases can occur where the aromatic system is a good electron acceptor e.g. ArN_2SR ($\text{R} = \text{Ph}$ or $t\text{-Bu}$);⁵¹ or when the nucleophile is a good electron donor. This is seen in ketones and related compounds with high pK_a , as the higher the pK_a the better the conjugate base is as an electron donor;⁵² which increases the chance of a spontaneous initiation.

Photostimulation of $S_{\text{RN}}1$ reactions is the most popular method of initiation. The efficiency of reaction of a particular set of nucleophile and substrate can be altered by the choice of solvent and irradiation source. For example PhI does not react with $^-\text{CH}_2\text{COPh}$ under irradiation through a Pyrex flask in liquid ammonia,⁵³ but does in DMSO.⁵⁴ However, when a quartz immersion well is used the reaction proceeds in liquid ammonia.⁵⁵ Despite the popularity of photostimulation as a means of initiation very few studies have been done on the mechanism. A possible mechanism is photoexcitation of a charge transfer complex of Nu^- and substrate. The reaction of $^-\text{CH}_2\text{COMe}$ ions with PhI and PhBr in DMSO has been proposed to occur by this type of initiation.⁵⁶ Also, reactions of many other substrates and nucleophiles⁵⁷ have been suggested to undergo initiation via a photostimulated charge transfer complex mechanism. An electron transfer from an excited nucleophile is another possible mechanism. Due to the highly coloured nature of many nucleophiles e.g. $^-\text{PPh}_2$,⁵⁷ and thus high absorption in the UV-Vis region of the spectrum, it is deemed probable that

electron transfer from the excited nucleophile is occurring. Evidence has been put forward for this mechanism due to the fluorescence quenching of the diphenylindenyl anion by PhBr^{58} and of 2-naphthoxide by 1-iodoadamantane.⁵⁹ Evidence for many other photoinduced processes has been published. These include photohomolytic bond dissociation,⁶⁰ dye-photoinitiated⁶⁰ and visible light initiation, with a Ru complex as sensitizer and a Co complex as the intermediate electron carrier.⁶⁰

Work involving the investigation of electrochemical initiation of $\text{S}_{\text{RN}}1$ reactions⁶¹ has largely been carried out by Savéant and co-workers. Initiation by an electrochemical process allows for a quantitative analysis of fragmentation rate constants of radical anions. The absolute rate constants for coupling of a wide range of nucleophiles with radicals can also be determined. Many different scenarios can occur depending on the electrode potentials of $(\text{RX}/\text{RX}^{\cdot-})$ and $(\text{RNu}/\text{RNu}^{\cdot-})$ and the fragmentation rates of $\text{RX}^{\cdot-}$. If $E^0(\text{RX}/\text{RX}^{\cdot-}) \gg E^0(\text{RNu}/\text{RNu}^{\cdot-})$ and $\text{RX}^{\cdot-}$ fragments slowly, R^{\cdot} and $\text{RNu}^{\cdot-}$ are formed far away from the electrode and thus $\text{RNu}^{\cdot-}$ can be oxidised by either electrode or RX to form product or propagate the chain. This is then a process catalysed by few electrons which can lead to complete conversion of RX to RNu provided radical-nucleophile coupling is faster than potential side reactions. If $\text{RX}^{\cdot-}$ fragments fast then R^{\cdot} forms near the electrode and can be reduced to R^- before it couples with Nu^- . This can potentially be overcome by use of a mediator (M)⁶² which is reduced at a more positive potential than RX to form $\text{M}^{\cdot-}$. $\text{M}^{\cdot-}$ can then reduce RX away from the electrode enabling the reaction to proceed. Potential mediators are polyaromatics such as perylene. If $E^0(\text{RX}/\text{RX}^{\cdot-}) \ll E^0(\text{RNu}/\text{RNu}^{\cdot-})$ then $\text{RNu}^{\cdot-}$ formed cannot be oxidised by RX or at the electrode at the potential of the system. The process is an uphill process and is non-catalytic; one mole of product requires a stoichiometric quantity of electrons. An example of this is Ph^{\cdot} with CN^- .⁶³

The use of solvated electrons in liquid ammonia is an important initiation source, especially when products derived from an aryne mechanism are to be avoided. In the reaction of $p\text{-NCC}_6\text{H}_4\text{X}$ ($\text{X}=\text{Cl}, \text{Br}, \text{I}$) with $^-\text{CH}_2\text{CONMe}_2$ in liquid ammonia, using K metal as the source of solvated electrons, high yields of the substitution product are obtained with no aryne derived product seen.⁶⁴ If K metal is not present then aryne derived substituted anilines are obtained. A disadvantage of this initiation is the formation of reduced products.⁶⁵

Sodium amalgam has been used to initiate $S_{RN}1$ reactions where the substrate's redox potentials are close to, or more positive than, $Na(Hg)$.⁶⁶ If the radical anion of the substrate fragments quickly and therefore close to the surface of the $Na(Hg)$, as with $PhBr$ and $p\text{-MeOC}_6\text{H}_4Br$, substitution is inhibited by the consequent reduction of the intermediate radical; this can be alleviated by the use of a redox mediator⁶⁶ in a similar manner to the electroinduced case.

Inorganic salts have also been used to initiate $S_{RN}1$ reactions. Several have been tested⁶⁷ and ferrous ions are the most used, usually in the form of FeX_2 ($X=Cl$ or Br) in DMSO. Many possible mechanisms have been proposed, these are ET from Fe^{2+} to ArX , iron mediated ET from Nu^- to ArX , or direct capture of X from ArX with the formation of Ar^\bullet .⁶⁸ The Fe^{2+} salts are required in catalytic up to stoichiometric quantities, which is mechanistically very fascinating. Many substrates and nucleophiles have been used with yields as high as 86%.⁶⁹ Samarium iodide has also been used to initiate the $S_{RN}1$ process.⁷⁰

Many other approaches to initiation have been utilised with varying degrees of success, these are sonication,⁷¹ microwave irradiation,⁷² radiolysis with ^{60}Co ⁷³ and aromatic radical anions.⁷⁴

1.3.1.2 Propagation

1.3.1.2.1 Step 2: Radical Anion Fragmentation

Following the initiation of the chain by the addition of an electron to the substrate, the substrate can then undergo fragmentation to form a radical, R^\bullet , and a nucleofuge X^- (Scheme 25).



Scheme 25

When fragmentation is concerted, the RX bond is being broken as the electron is transferred. The barrier to the process depends on the bond dissociation energy for the neutral molecule as well as the solvent reorganisation energy associated with Marcus-Hush theory.⁷⁵ The fragmentation is stepwise if there is a π acceptor of sufficiently low energy to accommodate the incoming electron. An intramolecular electron transfer from π^* to σ^* of the RX bond can then occur, which leads to the

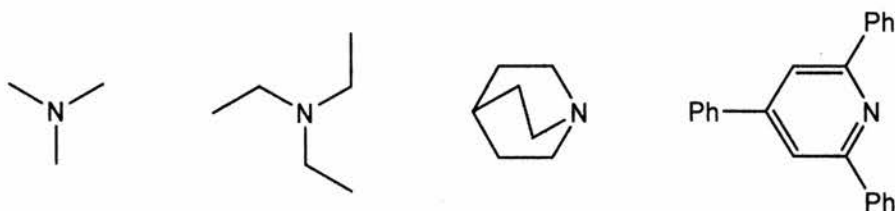
formation of a radical and nucleofuge. Thus, the main molecular factors affecting the transition between a stepwise and concerted sequence are the BDE (D), E^0 (RX/RX $^{\cdot-}$) and E^0 (X $^{\cdot-}$ /X $^-$).⁷⁶ For the fragmentation of [RX] $^{\cdot-}$ formed from initiation to take part in propagation of a chain it has to be fast, this rate is dependent on the ease of reduction of RX, E^0 (RX/RX $^{\cdot-}$) and the fragmentation rate of the resultant radical anion. This is highlighted by the relative reactivity of PhBr and ArBr towards $^-\text{CH}_2\text{CO}^t\text{Bu}$.⁷⁷ The reactivity increases from Ar = Ph to Ar = anthracenyl, regardless of the fact that the rate of fragmentation of the radical anion decreases from approximately 10^{10} s^{-1} (Ar=Ph) to $3 \times 10^5 \text{ s}^{-1}$ (Ar = anthracenyl). Conversely PhBr reacts faster than $\text{C}_6\text{H}_5\text{COC}_6\text{H}_4\text{Br-}p$. This was attributed to the fact that the $p\text{-C}_6\text{H}_5\text{COC}_6\text{H}_4\text{Br}$ radical anion fragments slowly ($6 \times 10^2 \text{ s}^{-1}$ in liquid ammonia) even though it is a better electron acceptor than PhBr.⁷⁷

Alkyl and benzyl halides unsubstituted by electron withdrawing groups fragment through a concerted pathway, due to the lack of a suitable low energy π LUMO. Aliphatic substrates with electron withdrawing groups such as NO_2 , dissociate through a stepwise mechanism. Although usually too unstable to be detected by ordinary EPR spectroscopy, some aliphatic radical anions have however been observed by EPR, these are 2-chloro- and 2-iodo-2-nitropropane,⁷⁸ p -nitrobenzyl,⁷⁹ p -nitrocumyl,^{79b} m -nitrobenzyl,⁸⁰ substituted-2-methyl-5-nitrofurans,⁸¹ 4-nitroimidazole derivatives⁸² and 5-X-2*H*,3*H*-benzo[*b*]thiophene-2,3-diones (X=F, Cl, Br or I).⁸³ Also, in some cases, fragmentation has been monitored by EPR. The structures of these radical anions revealed significant overlap between the π^* and σ^* molecular orbitals which is in agreement with results proposed by theoretical work.⁸⁴

Unsubstituted aromatic substrates generally undergo stepwise electron capture and fragmentation. In this family the π and σ are orthogonal to each other, unlike the benzyl system in which overlap exists. This helps to explain the low fragmentation rates of nitro-substituted aryl halides (10^{-3} - 10^2 s^{-1}).⁸⁵ Due to this, and the good electron acceptor ability of the nitrophenyl π system, nitro-substituted aryl halides are poor substrates for $\text{S}_{\text{RN}}1$ processes. Thus radical anions with low fragmentation rates, either through very low energy π systems, strong R-X bonds or orthogonal π - σ systems can cause this step to be rate determining in the overall chain.

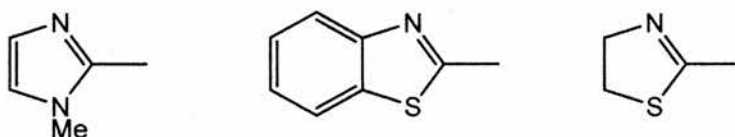
Many different leaving groups have been used in $\text{S}_{\text{RN}}1$ substrates, the most common groups used with all types of substrate are the halogens, Cl, Br, and I; with F being used less commonly. Other leaving groups include thiols, aromatic sulfines and

sulfones. The leaving group ability among halogens is $I > Br > Cl >> F$. Neutral tertiary amines can act as leaving groups from quaternary ammonium salt substrates (Scheme 26).^{86 & 121b}



Scheme 26

Thioazo and diazonium aromatic substrates have also been used in which on reduction N_2 is lost, as well as RS^- or the counter ion as the nucleofuge, e.g. $PhSN_2-Ar$, F_4BN_2-Ar and $tBuSN_2-Ar$. Diethyl phosphate has been used as a nucleofuge in aromatic substrates. N_3 , SCN , NO_2 , RCO_2 and polyaromatic alkoxides perform as leaving groups exclusively in aliphatic substrates. Bowman introduced some novel heterocyclic leaving groups in a variety of aliphatic substrates (Scheme 27).⁸⁷



Scheme 27

1.3.1.2.2 Step 3: Radical Coupling With Nucleophiles

After the formation of the radical, via fragmentation, coupling of the radical with the nucleophile can occur (Scheme 28).



Scheme 28

In the case of aromatic radicals, these rates have been determined by the use of electrochemical methods. In a large number of cases these rates were found to be close to the diffusion controlled limit. For example, the rates of the reactions of 2-, 3- and 4-cyanophenyl, 1-naphthyl and 3-pyridyl with PhS^- , $(EtO)_2PO^-$ and $^-CH_2COMe$ ions range from 10^9 to $10^{10} M^{-1} s^{-1}$ in liquid ammonia.⁸⁸ Overall it has been shown that phenyl radicals couple slower than other aryl radicals with rate between 10^7 and $10^8 M^{-1} s^{-1}$.⁸⁹ Radicals alpha to the nitrogen in a heteroaromatic system, such as 2-pyridyl radicals, also react at rates below the diffusion limit. This is thought to be due to the repulsion between the incoming nucleophile's electron pair and the nitrogen

lone pair.^{88a} Through competition reactions it has been shown that as Ar• radicals are soft electrophiles; they react faster with nucleophiles as they become softer, e.g., PhS⁻(1.00), PhSe⁻(5.8) and PhTe⁻(28).⁹⁰ On the basis of several studies the reactivity order of nucleophiles, with phenyl radicals in liquid ammonia has been obtained, this is: PhS⁻ (1.0), PhSe⁻ (5.8), NH₂⁻ (11.5), ⁻CH₂CO^tBu (13.0), (EtO)₂PO⁻ (18.0), PhTe⁻ (28.0), Ph₂PO⁻ (34), Ph₂P⁻, Ph₂As⁻, Me₃Sn⁻, and Ph₃Sn⁻ (74.0).^{49a, 90 & 91} Literature evidence is consistent with the view that nucleophiles and aryl radicals couple at or near the diffusion limit. Aromatic radical couplings with nucleophiles are insensitive to steric hindrance, even with ArX bearing *o*-methoxy or *o*-methyl groups, even an *o*-^tPr group does not inhibit the reaction, only when either two *o*-^tPr groups or an *o*-^tBu are present are the yields low.⁹²

In contrast with aryl radicals, very little is known about rates of coupling of aliphatic radicals with nucleophiles. Some absolute rates have been determined using the radical rearrangement approach.⁹³ The rate of reaction of nitronate ions with methyl radicals in DMSO decreases with increasing steric hindrance: ⁻CH₂NO₂ (1.35 x 10⁸ M⁻¹ s⁻¹), ⁻CHMeNO₂ (1.6 x 10⁷ M⁻¹ s⁻¹), ⁻CHEtNO₂ (1.35 x 10⁷ M⁻¹ s⁻¹) and ⁻CMe₂NO₂ (2.35 x 10⁶ M⁻¹ s⁻¹).⁹⁴ In general, the rate of coupling decreases as steric hindrance increases, but despite steric limitations, most of the C-alkylated products obtained in most reactions of alkyl halides with electron withdrawing groups are sterically crowded molecules. The counter ion of the nucleophile has a large effect on the relative rates of reactions; for example, the relative rates of ⁻CMe(CO₂Et)₂ vs. ⁻CMe₂NO₂ can be reversed from 10 with K⁺[2.2.2]-crypt to 0.24 in the presence of 2M Li⁺.⁹⁵ Solvent also has an appreciable effect, for example the relative rates of Li⁺ salts of ⁻CMe(CO₂Et)₂ versus ⁻CMe₂NO₂, were 0.22 in HMPA but 70 in THF.^{57f & 95}

In general the factors that affect the coupling rates are the reverse of those that affect cleavage of the initial substrate radical anion, [RX]⁻. These are a) the strength of bond formed in the coupled product; b) standard potential for reduction E^0 (RNu/RNu⁻); and c) standard potential for oxidation $-E^0$ (Nu[•]/Nu⁻). This explains the coupling rates of ⁻CH₂COMe (~10⁸), PhS⁻ (~10⁷) and CN⁻ (~10⁵). Despite there being thermodynamic evidence to the contrary for the latter, D_{Ph-SPh} = 326 kJ mol⁻¹, D_{Ph-CH₂COMe} = 403 kJ mol⁻¹ and D_{Ph-CN} = 548 kJ mol⁻¹. The low reactivity of the cyanide anion, which is a hard nucleophile, is attributed to the very positive standard

oxidation potential. Another contributing factor is the large reorganisation energy due to the strength of the bond being formed.⁷⁶

1.3.1.2.3 Step 4: Single Electron Transfer

Once the radical anion $[\text{RNu}]^{\cdot-}$ has formed, from coupling of the radical and nucleophile, there are several reaction pathways that could be followed. These are: a) transfer of an electron to another molecule of RX (Scheme 29), b) transfer of an electron to any other reducible species, or c) fragmentation.



Scheme 29

In order for the product radical anion to follow pathway (a), and transfer an electron to another RX and complete the chain to regenerate $[\text{RX}]^{\cdot-}$, $E^0(\text{RX}/\text{RX}^{\cdot-})$ has to be more positive than $E^0(\text{RNu}/\text{RNu}^{\cdot-})$. However if $E^0(\text{R}\cdot/\text{R}^-) > E^0(\text{RX}/\text{RX}^{\cdot-})$ then $\text{R}\cdot$ could be converted to R^- , which would result in termination of the chain. If any other species with a more positive reduction potential than RX is present then pathway (b) will be followed and propagation of the chain will not be achieved. If the product radical anion formed in step 3 has a leaving group with a cleavage rate faster than electron transfer, or the back reaction to $\text{R}\cdot$ and Nu^- is faster than single electron transfer (pathway (c)), then propagation will also not be accomplished. Clearly the overall product distribution from a given $\text{S}_{\text{RN}}1$ process will depend on the contribution of all these pathways which will also affect the overall rate.

1.3.2 Solvents and Bases

In choosing a solvent for an $\text{S}_{\text{RN}}1$ reaction a number of factors have to be taken into account, these are: a) The ability of solvent to dissolve all reactants. Generally an organic halide and alkali metal salts of various anions. b) In the case of photochemical initiation, the solvent should be transparent at the required frequencies. c) The solvent should be a poor hydrogen donor to reactive radicals present, as hydrogen donation can lead to termination of the chain mechanism. d) As the reactants include highly basic materials, then protic solvents with low pK_a are to be avoided. e) A solvent which accepts electrons either readily and/or irreversibly is

undesirable because the mechanism involves electron transfer steps. The traditional solvents used in $S_{RN}1$ processes are liquid ammonia and dimethyl sulfoxide, other solvents that have been used are dimethylformamide and hexamethylphosphoric triamide, all of which are polar aprotic solvents. The popularity of liquid ammonia as the solvent in nearly all aromatic $S_{RN}1$ reactions is in part due to the ease of formation of the strong bases, MNH_2 ($M = Li, Na \& K$) by reaction of alkali metals directly with the solvent. More recently solvents such as tetrahydrofuran, t -BuOH, acetonitrile and even water have been utilised with varying results. Results depend highly on individual reaction conditions and substrates, further information regarding the effectiveness of different solvents can be obtained from the many reviews⁴⁹ on $S_{RN}1$ reactions.

Bunnett *et al.*,⁹⁶ reported a study of the reaction of iodobenzene with diethyl phosphite anion using a range of solvents in order to ascertain the reactivity in each. It was discovered that as well as ammonia the reactions also proceeded in excellent yields in acetonitrile, dimethylformamide and to a lesser degree in *tert*-butyl alcohol. Poor solvents included hexamethylphosphoric triamide and other common polar aprotic solvents. While this result is indicative, it is by no means true in all cases, with the results in an individual solvent, as mentioned previously, depending greatly on the individual reaction parameters.

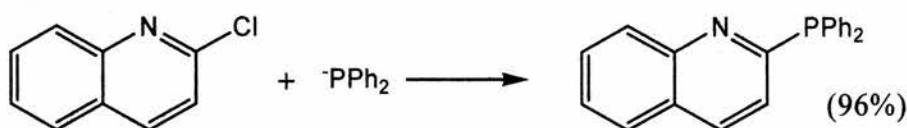
The most common bases used for $S_{RN}1$ reactions are alkali metal amides, and potassium *tert*-butoxide. More recently, lithium diisopropylamide has been used. The choice of base is heavily dependent on the pK_a of the conjugate acid of the nucleophile, and also the base's solubility in a given solvent.

1.3.3 Nucleophiles

Since the discovery and definition of the $S_{RN}1$ mechanism in the late nineteen sixties to early seventies, a whole plethora of nucleophiles have been evaluated. In this introductory review only enolate anions as nucleophiles will be evaluated in any detail although a quick survey of other types of nucleophiles will be made. In group 14 (IV) only carbon, germanium and tin nucleophiles are represented as far as the author is aware. Included in the nucleophiles epitomizing carbon are conjugate bases of ketones,⁵³ esters,⁵⁵ & ^{69a} amides,⁹⁷ thiazolines,⁹⁸ oxazolidinones,⁹⁹ oxazolines,⁹⁸ thioamides;¹⁰⁰ the cyanide anion,^{63b} nitriles,¹⁰¹ nitronates ($\text{C}(\text{NO}_2)\text{R}_2$),¹⁰² and

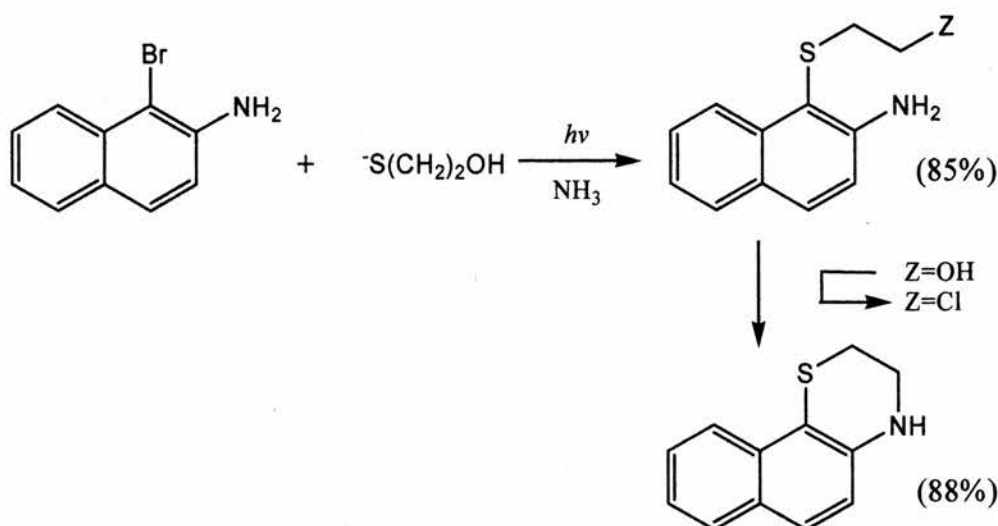
aryloxides (reactions occur *ortho* and *para* to oxygen).¹⁰³ In the cases of germanium and tin, only trialkyl and triaryl stannyl¹⁰⁴ and germanyl¹⁰⁵ anions have been used as nucleophiles. Group 15 (V) sees all members except bismuth taking part as nucleophiles. Nitrogen centred nucleophiles encompass the amide anion (NH_2^-),⁴⁵ alkyl and aryl amide anions,¹⁰⁶ NO_2^- ions,^{121c} N_3^- ions,^{121c} and heteroaromatic anions such as that derived from pyrrole.¹⁰⁷ Aromatic amide anions such as 2-naphthylamide, react both through the nitrogen and at the *ortho* position on the aromatic ring. The pyrrole derived anions reacts at both the 2 and 3 positions.

Phosphorus nucleophiles include $(\text{RO})_2\text{PO}^-$,¹⁰⁸ $(\text{RO})_2\text{PS}^-$,¹⁰⁹ PR_2^- ,^{66a & 71b} and P^{3-} .¹¹⁰ The reaction of diphenylphosphinide anions with aryl halides enables the synthesis of unsymmetrical triarylphosphines (Scheme 30).^{66a & 71b}



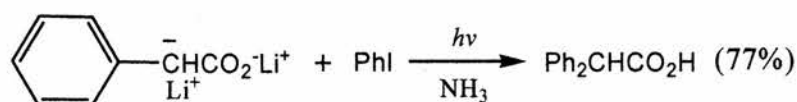
Scheme 30

Nucleophiles from the elements of periods 4 and 5, representatives of group 15, arsenic and antimony, both take part in $\text{S}_{\text{RN}}1$ reactions. They have the general formulas ($\text{M}=\text{As} \ \& \ \text{Sb}$) M^{3-} ,¹¹⁰ Ph_2M^- ,¹¹¹ and Ph_2MO^- .¹¹¹ Nucleophiles of group 16 (VI) elements include sulfur, selenium and tellurium-centred types. Enolate type nucleophiles react with aryl radicals almost exclusively through the carbon rather than oxygen centre (Section 1.3.5). The reason for this is proposed to be the greater bond strength of C-C (356 kJ mol^{-1}) versus C-O (336 kJ mol^{-1}) and also the hard nucleophilic nature of RO^- . Sulfur nucleophiles are wide and varied; they take the general formulas alkyl- S^- ,¹⁰⁸ ArS^- ,¹¹² ArSO_2^- ,¹¹³ RCOS^- ,¹¹⁴ and S_4^{2-} .¹¹⁵ An example of substitution on to an aminonaphthlene ring by an alkyl sulfide followed by an intramolecular cyclisation to form a tricyclic compound is shown in Scheme 31.¹⁰⁸ Selenium and tellurium nucleophiles have been less extensively studied, with only M_2Z ,¹¹⁶ M_2Z_2 ¹¹⁷ and RZ^- ¹¹⁸ ($\text{M} = \text{alkali metal}, \text{Z} = \text{Se} \ \& \ \text{Te}$) featuring.



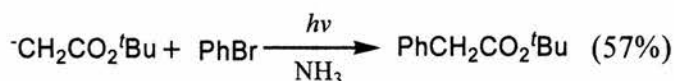
Scheme 31

$\text{S}_{\text{RN}}1$ reactions of carboxylic acid derivatives are widely known and when the substrate is an aryl halide, an alpha substituted carboxy compound can be formed. The dianions of carboxylic acids themselves can react with iodobenzene to form alpha aryl carboxylic acids (Scheme 32).¹¹⁹



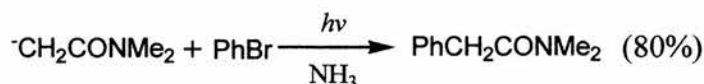
Scheme 32

A multitude of esters also fare well in radical nucleophilic substitutions and one example is shown in Scheme 33.^{55, 69a} It should be observed that a possibility for chiral induction is apparent here if chiral esters such as menthol ester are employed.



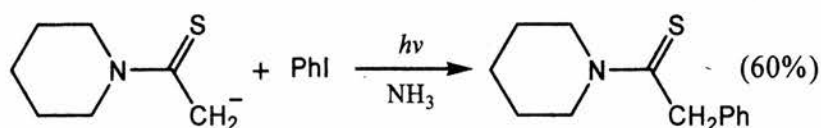
Scheme 33

Amides are also well represented in $\text{S}_{\text{RN}}1$ processes, with a wide variety of substrates reacting in moderate to excellent yields. An arylation of an N,N -dimethyl amide is shown in Scheme 34.⁹⁷



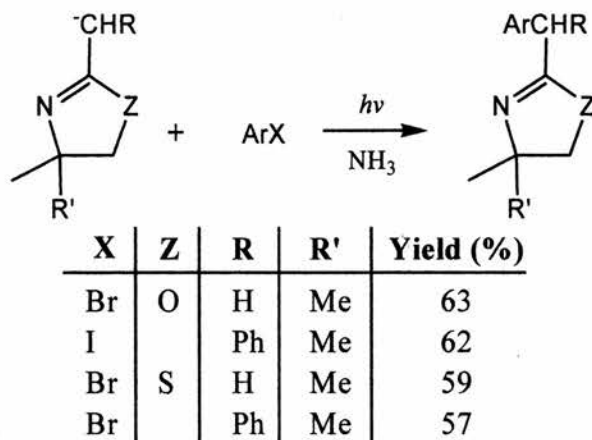
Scheme 34

Thioamides take part in $\text{S}_{\text{RN}}1$ reaction as well, although examples are limited,¹⁰⁰ they include the reaction of the piperidiny l thioamide with iodobenzene (Scheme 35).



Scheme 35

Even more elaborate derivatised carboxylic acids such as Meyers' heterocyclic 2-oxazolines⁷ and the closely related 2-thioxazolines, function as nucleophiles in $S_{RN}1$ reactions. The Wolfe research group has reacted substituted 2-oxazoline and 2-thioxazolines with aryl halides with good to moderate yields (Scheme 36).⁹⁸



Scheme 36

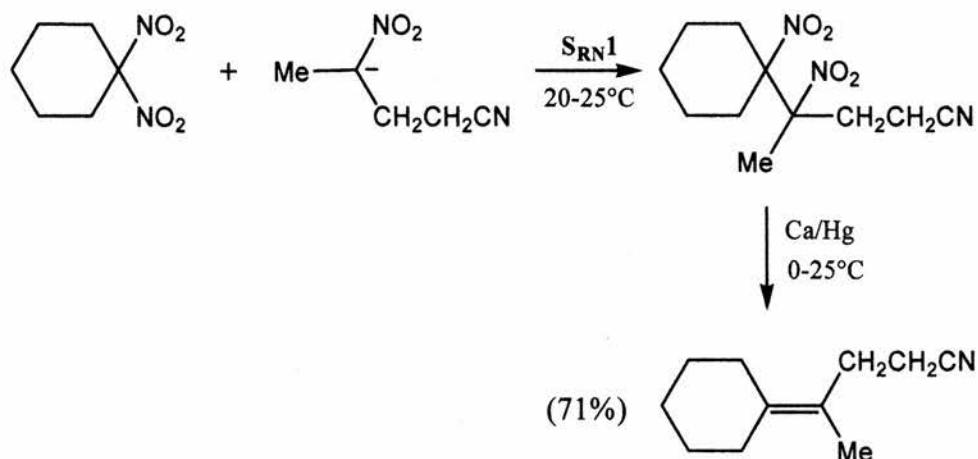
Also, the heteroaromatic, 2-bromopyridine reacted to afford heteroaryl substituted oxazolines and thioxazolines.⁹⁸ Historically chiral 2-oxazolines have been employed as chiral auxiliaries. Thus, development of a diastereoselective $S_{RN}1$ reaction protocol becomes a possibility. This would complement the already existing literature⁷ on 2-oxazolines due to the ability to produce 2-arylated 2-oxazolines and thus, after hydrolysis, alpha-arylated carboxylic acids.

1.3.4 Substrates

Many structurally diverse compounds have been used as substrates (RX) in $S_{RN}1$ reactions including aliphatics, allyl and aryl moieties. A full survey of the multitude of substrates that have been employed can be found in the many reviews on $S_{RN}1$ processes.⁴⁹

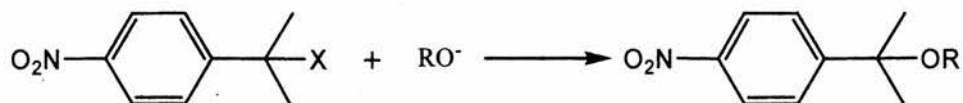
The most extensively studied aliphatic substrates since the first example, 2-bromonitropropane, are nitroalkanes. One interesting example of nitroalkanes is the reaction of *gem*-dinitroalkanes with a nitroalkane anion to form a 1,2-

dinitrosubstituted product, which can undergo reduction by Ca/Hg to form tetra substituted alkenes (Scheme 37).¹²⁰



Scheme 37

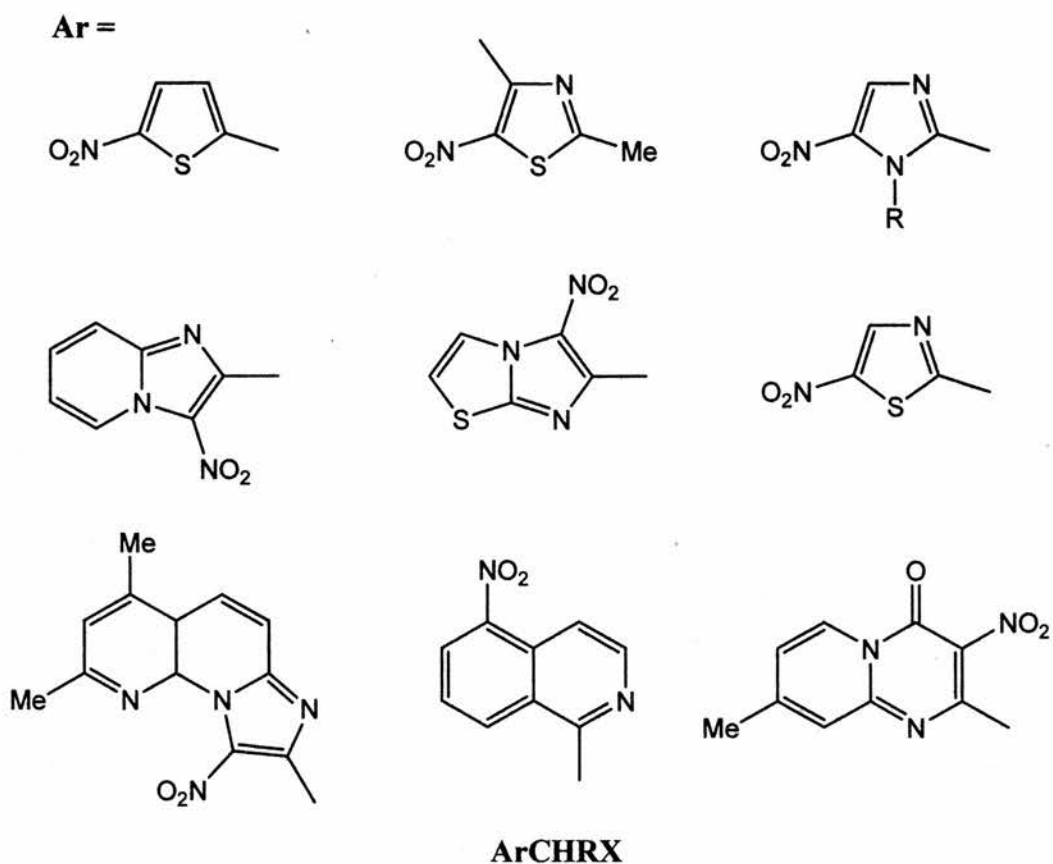
p-Nitrobenzyl and *p*-nitrocumyl substrates react with an extensive range of nucleophiles. An important example is the reaction of a range of *p*-nitrocumyl substrates with various alkoxides and phenoxides to form tertiary ethers in moderate yields (Scheme 38).¹²¹



R	X	Yield (%)
Me	NO_2	56
Ph	NO_2	66
Ph	quinuclidinium	57
1-methyl-2-naphthyl	Cl	62
1-methyl-2-naphthyl	NO_2	69

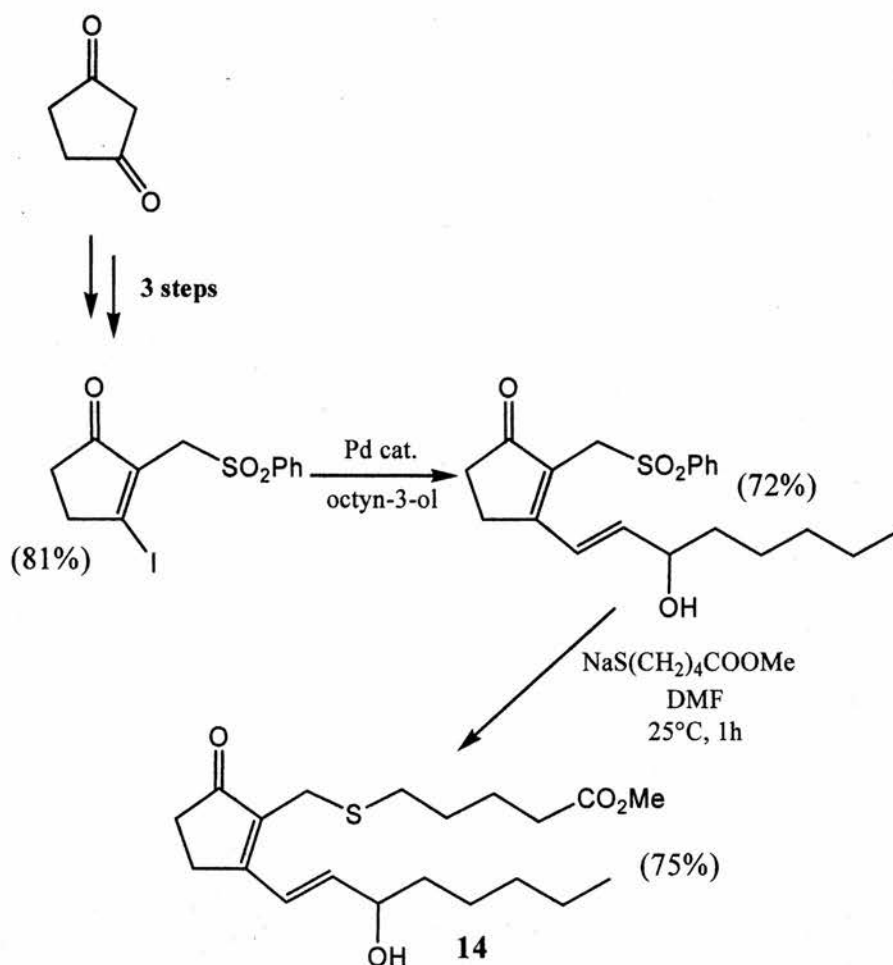
Scheme 38

A range of heteroaromatic analogues of *p*-nitrobenzyl and *p*-nitrocumyl substrates can also take part in $\text{S}_{\text{RN}}1$ couplings; Scheme 39 shows some of these analogues.¹²²



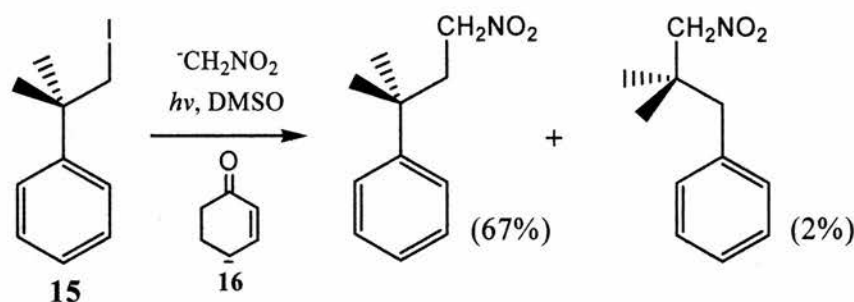
Scheme 39

Natural product analogues can be synthesised by utilising allyl substrates, such as allyl iodides. An example of a prostaglandin (PGB_1) **14** synthesised utilising an $\text{S}_{\text{RN}}1$ step is shown in Scheme 40.¹²³ It is interesting to note that, due to the wide variety of leaving groups tolerated, by judicious choice of leaving group other coupling steps such as palladium catalysed cross-coupling can occur sequentially with $\text{S}_{\text{RN}}1$ steps (Scheme 40).¹²³



Scheme 40

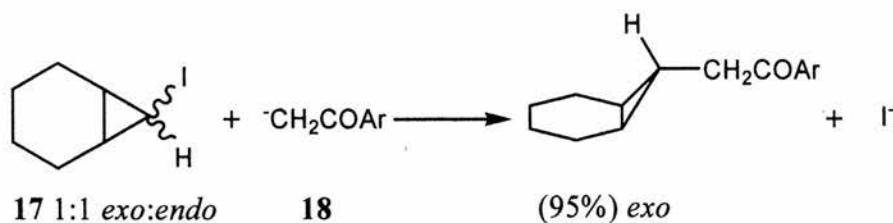
Unactivated alkyl halides also take part in $S_{RN}1$ substitutions. Substrates such as neopentyl and neophyl have been shown to be reactive. Neophyl iodide **15** reacts in a moderate yield of 67% with CH_2NO_2^- under entrainment with the anion of 3-cyclohexenone **16** (Scheme 41).^{57f} In the reactions of unactivated alkyl substrates other mechanistic pathways such as S_N1/S_N2 and halogen-metal exchange compete.¹²⁴



Scheme 41

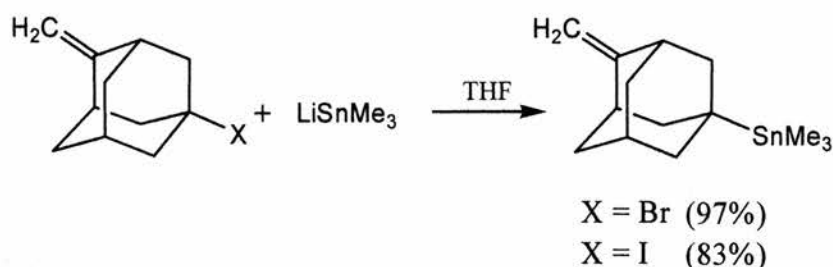
Substitution of 7-iodonorcarane **17** with acetophenone anion **18** occurs with a high degree of selectivity (Scheme 42).¹²⁵ Also, 7-bromonorcarane **17** reacts in liquid

ammonia under radiation with Ph_2P^- and Ph_2As^- with yields of 87% and 90% respectively.¹²⁶



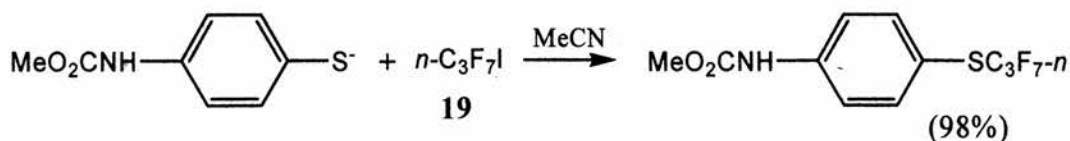
Scheme 42

Bridgehead substrates form an important group of reactants in $\text{S}_{\text{RN}}1$ reactions. These groups include adamantyl, bicyclo[2.2.2]octyl, norbornyl, and pentacyclo[6.4.0.0^{2,10}.0^{3,7}.0^{4,9}]dodecyl. All undergo substitution of a suitable leaving group by a nucleophile at the bridgehead carbon. Substitution at bridgehead carbons via the $\text{S}_{\text{N}}1$ and $\text{S}_{\text{N}}2$ mechanisms generally do not occur due to the instability of pyramidal cations in the $\text{S}_{\text{N}}1$ case and steric interactions precluding an attack from behind in the $\text{S}_{\text{N}}2$ case. The radical that is formed during an $\text{S}_{\text{RN}}1$ substitution at a bridgehead carbon results in a pyramidal radical which is generally not seriously energetically unfavoured plus the radical is a more stable tertiary radical. An example of an unsaturated adamantyl halide reacting with trimethylstannyl anions is shown in Scheme 43.¹²⁷ If the carbon double bond is replaced by a carbonyl functionality and the halide is iodide then the major product of the reaction is ring fission by a polar mechanistic pathway.¹²⁷



Scheme 43

The study of the functionality and reactivity of perfluoro organic compounds is of wide interest in organic chemistry at present. $\text{S}_{\text{RN}}1$ substitutions using perfluoroalkyl iodides offer a way to incorporate perfluoro groups into a molecule. Many different nucleophiles react with perfluoroalkyl iodides including carbonyls, heteroaromatics, phenols and thiophenols. An example of a substituted thiophenol reacting with *n*-perfluoropropyl iodide **19** is shown in Scheme 44.¹²⁸



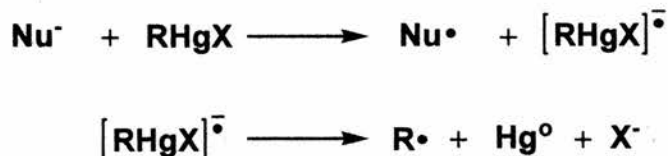
Scheme 44

The only substrates discussed so far have conformed to the motif R-X, but other substrate motifs are possible, one such motif is RMX in the form of RHgX. Alkylmercury halides have moderate activity in electrophilic substitutions and virtually no reactivity in nucleophilic substitutions at carbon due to the unfavourable polarity of the R-Hg bond, although alkylmercury halides are easily reduced to an alkyl radical, elemental mercury and a halide anion (Scheme 45).



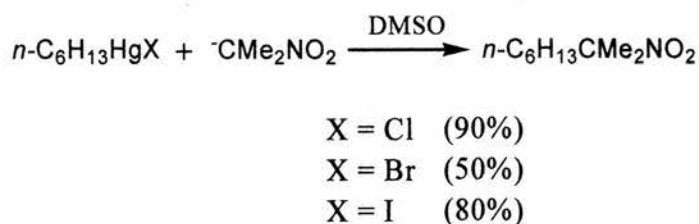
Scheme 45

This ease of reduction with the production of alkyl radicals makes it possible for RHgX, to undergo S_{RN}1 substitutions, with oxidation of a suitable nucleophile by RHgX enabling a chain reaction to be initiated (Scheme 46).



Scheme 46

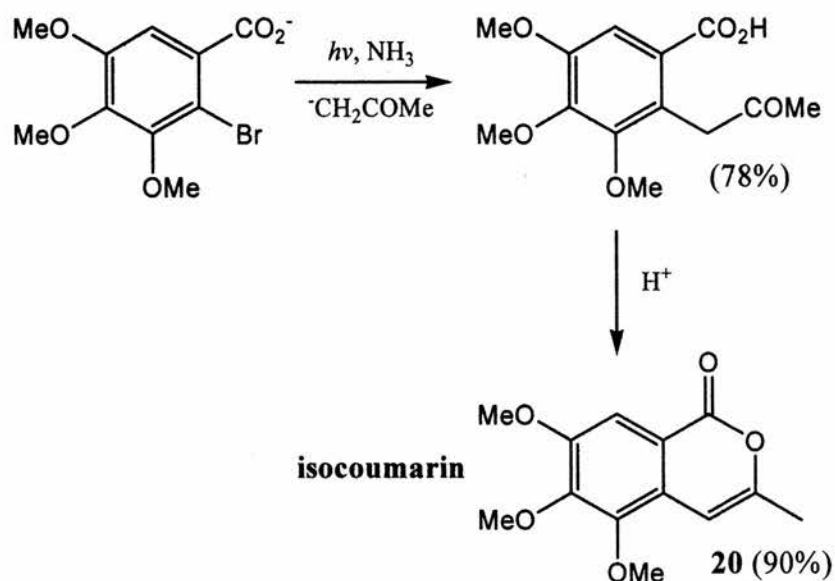
Scheme 47 shows an example of S_{RN}1 substitution using alkylmercury halides as substrates.¹²⁹



Scheme 47

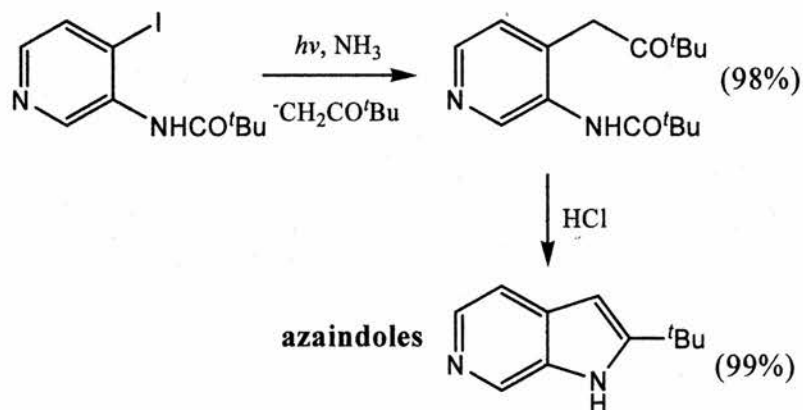
Aryl moieties form an important group of substrates in S_{RN}1 processes. They can be divided into three general groups; aromatic, heteroaromatic and polyaromatics. Members of all three groups can react efficiently in S_{RN}1 reactions.

A proficient synthesis of an isocoumarin **20** is demonstrated in Scheme 48 with substitution occurring on a structurally hindered aryl substrate in good yield of 78%.¹³⁰



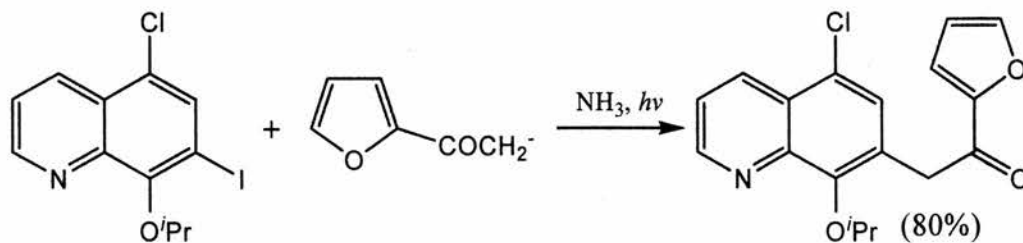
Scheme 48

When the substrate is heteroaromatic, the synthesis of azaindoles¹³¹ in 97% overall yield is possible, this is shown in Scheme 49.

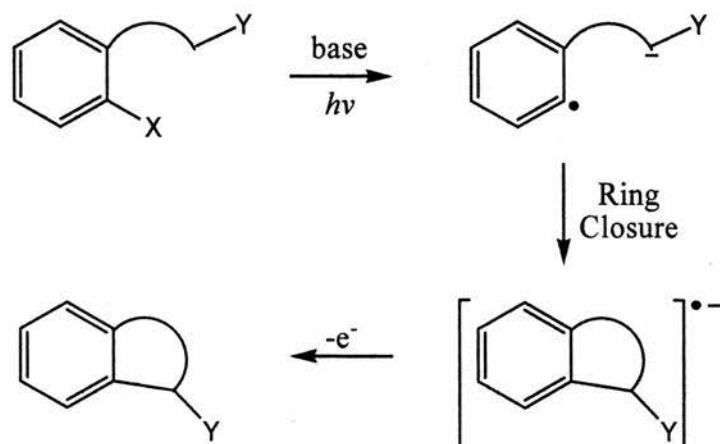


Scheme 49

A regioselective substitution of the heteroaromatic quinoline is exhibited in Scheme 50.¹³²

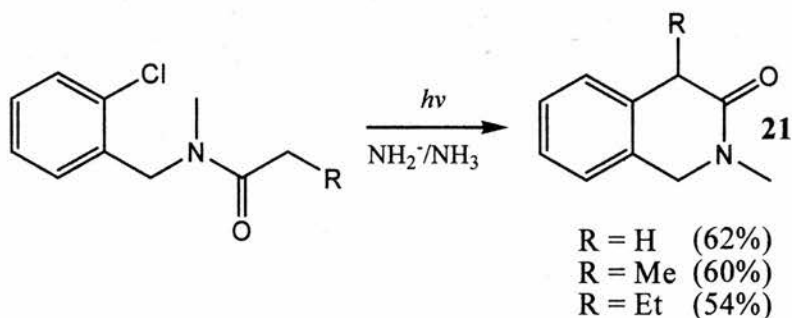


Scheme 50

1.3.5 Intramolecular $S_{RN}1$ Reactions

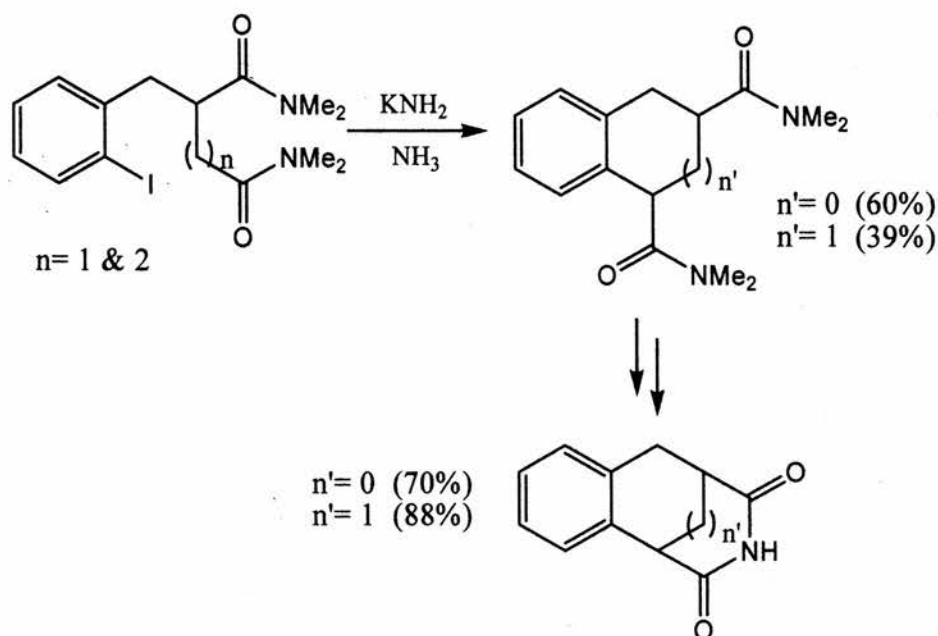
Scheme 51

Intramolecular $S_{RN}1$ reactions are less well known, with only a handful of examples in the literature, even though the unique nature of the $S_{RN}1$ mechanism has been fully exploited in other directions. In appropriately substituted precursors, intramolecular $S_{RN}1$ reactions could possibly lead to ring closure. A generalised reaction involving aryl radical formation and intramolecular coupling is shown in Scheme 51.

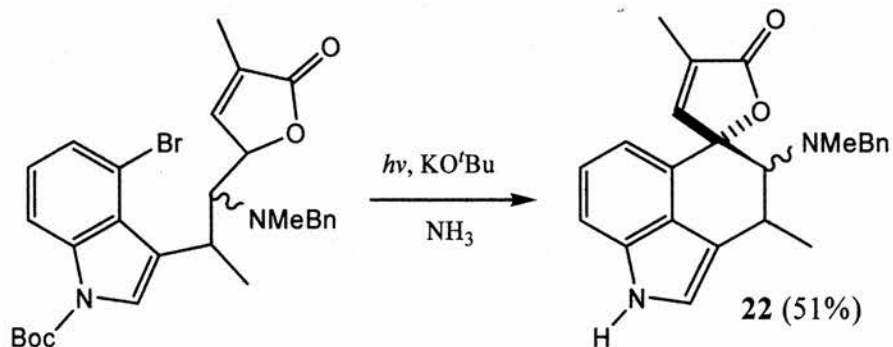
Scheme 52¹³⁴

The first class of intramolecular cyclisation reactions involve coupling of aromatic radicals on to conjugate base amides to form oxindoles¹³³ and isoquinolines.¹³⁴ The work has been mainly been carried out by Wolfe *et al.*¹³⁴ An example of isoquinoline **21** formation is shown in Scheme 52.

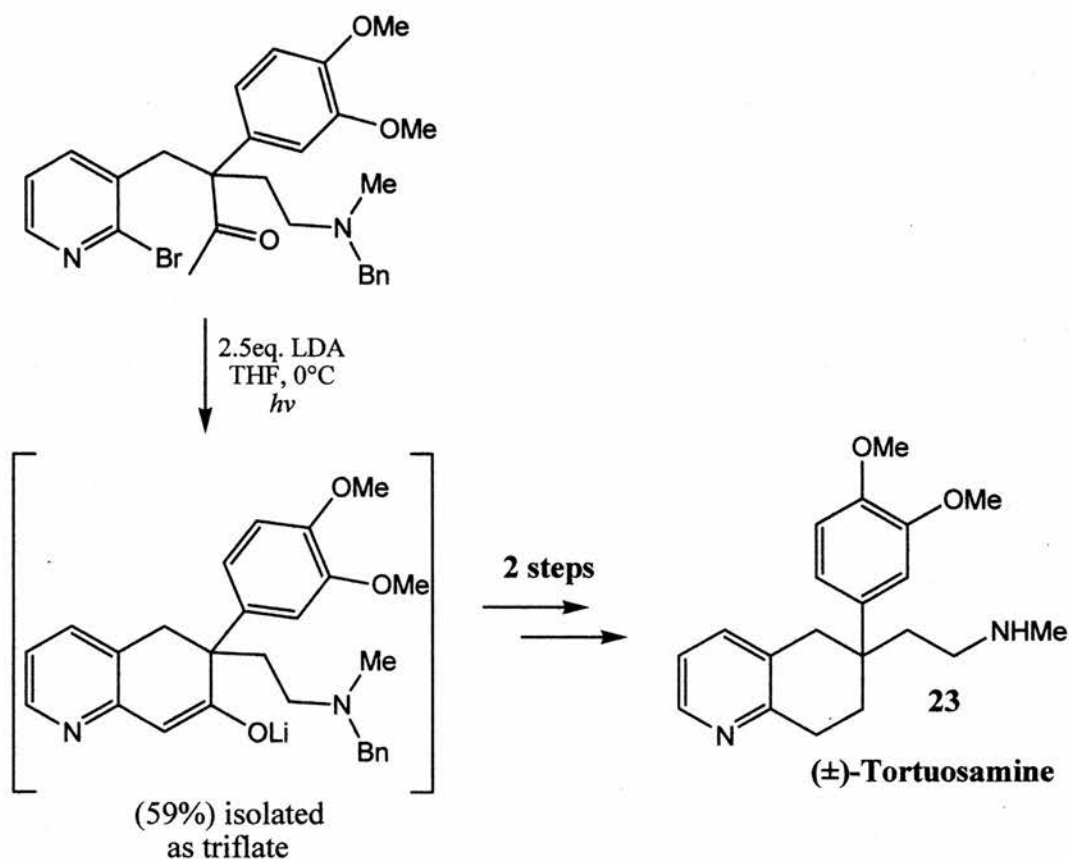
A more interesting example, also carried by Wolfe, is the cyclisation onto a diamide with subsequent condensation to form a tricyclic structure (Scheme 53).

Scheme 53¹³⁵

A few natural product structures have been assembled by intramolecular $S_{RN}1$ couplings. These include alkaloids and fused cyclic structures. The synthesis of an ergot type alkaloid **22** is shown in Scheme 54. This is a good example of the power of $S_{RN}1$ reactions in that the radical can couple with a sterically hindered centre to form, as in this case, a spiro centre.

Scheme 54¹³⁶

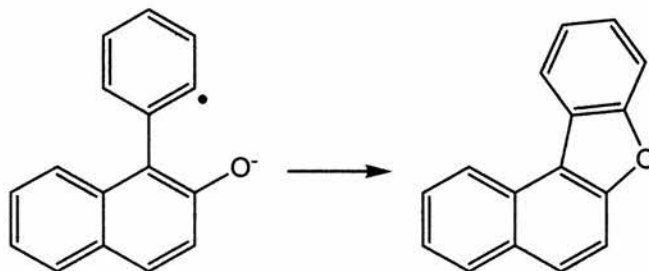
As well as the previously mentioned synthesis of europolaramine^{137a} (Section 1.2 : Radical Ring Closures) a key ring closure in the synthesis of (\pm)-tortuosamine **23**^{137b} has been carried out by the Goehring group (Scheme 55).



Scheme 55

Clearly, the examples shown, and others,¹³⁸ provide insight into the potential scope of intramolecular $S_{RN}1$ reactions.

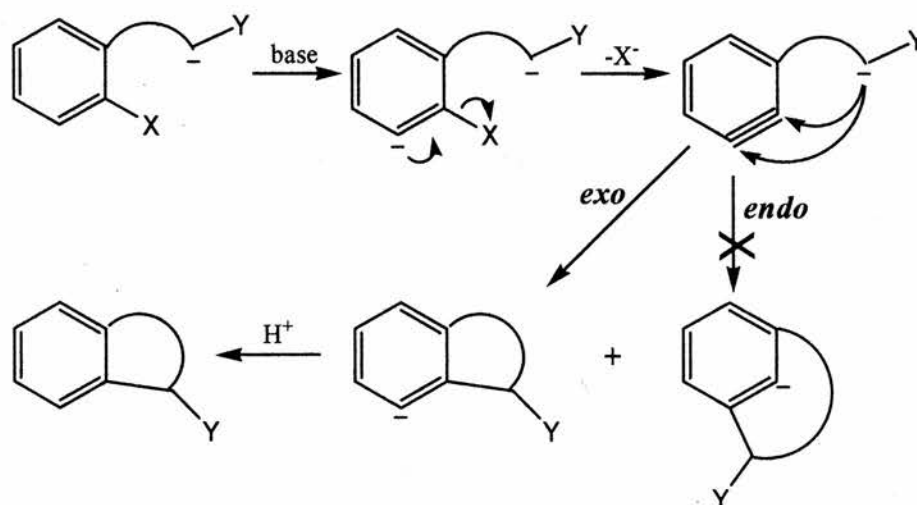
One other very interesting example of intramolecular cyclisation is direct O-arylation. Reactions of phenoxides normally occur intermolecularly through the alpha carbon and not the oxygen. However, in this intramolecular case, reaction was through the oxygen (Scheme 56).

Scheme 56¹³⁹

This is the only example known of a coupling of an aryl radical and an oxygen anion. It is thought to occur due to the proximity of the reacting sites.

1.3.6 Aryne Mechanism

A mechanism involving an aryne intermediate can often be written to explain the formation of the ring closed products (Scheme 57).



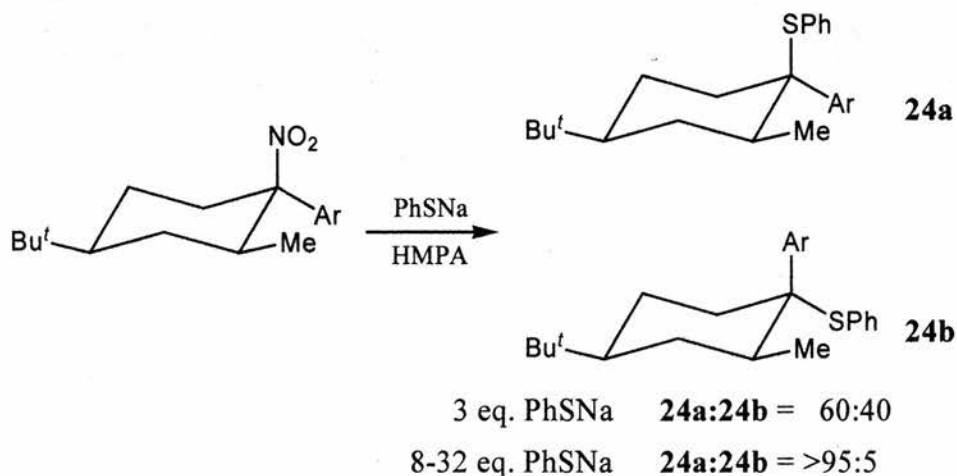
Scheme 57

In intermolecular $S_{RN}1$ reactions involving aryl radicals reacting with nucleophiles, confirmation of $S_{RN}1$ versus the aryne pathway can be obtained via product distribution. In intramolecular reactions, in small to medium size rings, only *ipso/exo* substitution is possible regardless of mechanism (Scheme 57). There are many different ways of determining if the reaction mechanism is $S_{RN}1$ in nature. The use of radical traps such as di-*tert*-butylnitroxide (DTBN), can determine the presence of radicals in the reaction pathway. This method can provide evidence in favour of the $S_{RN}1$ mechanism, but absence does not preclude the $S_{RN}1$ mechanism, as it is possible that either the coupling of nucleophile and radical (Step 3) and/or electron transfer from $[RNu]^-$ to RX (Step 4) is faster than reaction with the radical trap.¹⁴⁰ Clearly, in $S_{RN}1$ reactions involving aromatic substrates where the nucleophile's conjugate acid has low pK_A , then a relatively mild base is used to form the nucleophile; in this case the aryne mechanism can be ruled out because strong bases are required for aryne generation. The S_NAr pathway can also be dismissed if the aromatic moiety does not contain electron withdrawing groups. Only with detailed analysis of each reaction can the mechanism be established with certainty. More evidence for the $S_{RN}1$ mechanism in an intramolecular reaction can be obtained by comparison of the product

distribution of an analogous intermolecular system. If only the *ipso* product is observed then it is likely that the $S_{RN}1$ mechanism is the predominate one.

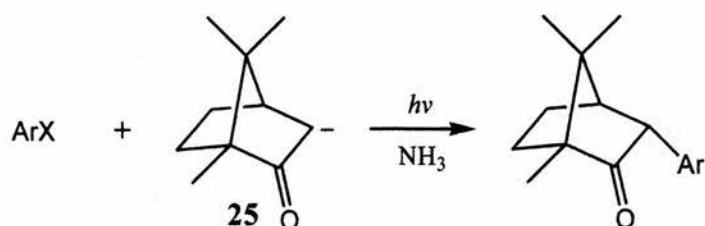
1.3.7 Stereoselectivity in $S_{RN}1$ Reactions

In reactions of alkyl halides with nucleophiles thought to be taking place via the $S_{RN}1$ chain mechanism, there can be contention as to nature of the mechanism. As well as other evidence for a radical route such as radical traps etc., another piece of evidence is the loss of stereochemical information at the centre of transformation. There are a number of examples in the literature of $S_{RN}1$ reactions of optically active alkyl halides and nitroalkanes undergoing substitution with a variety of nucleophiles with complete loss of optical activity. For example, optically active 2-(*p*-nitrophenyl)-2-nitrobutane with $^-CMe_2NO_2$, N_3^- , PhS^- and $PhSO_2^-$.¹⁴¹ Conversely $S_{RN}1$ reactions of cyclohexyl radicals bearing electron withdrawing groups have been shown to proceed with high retention of configuration (Scheme 58).¹⁴² Retention of configuration is highly dependent on the concentration of the incoming nucleophile with respect to the substrate.



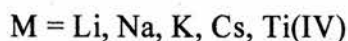
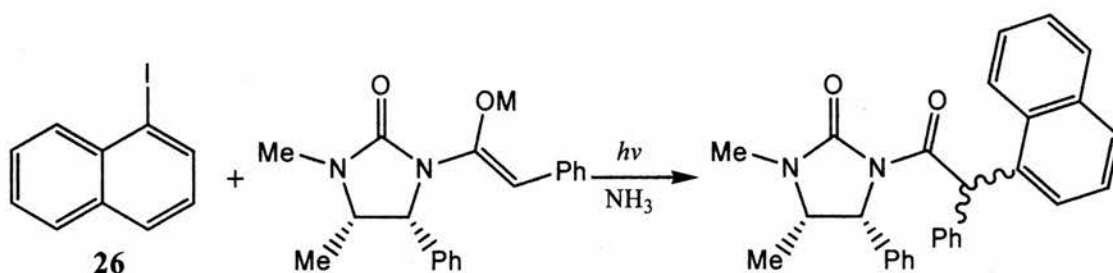
Scheme 58

This is thought to occur due to a fast formation and trapping of a pyramidal radical intermediate. In situations where pyramidal radical intermediates can be ruled out, but some inversion of configuration is observed, this is taken to be evidence of $S_{RN}1$ - S_N2 competition. This is occurring in the C-alkylation of the $^-CH(COMeCO_2Me)$ ion.¹⁴³



Scheme 59

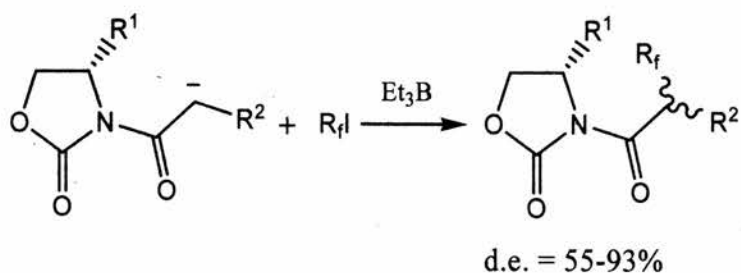
While aryl radicals themselves usually have no inherent chirality, they can react with chiral nucleophiles to form diastereoisomers. The enolate ion of (+)-camphor **25** can be arylated almost exclusively at C3 with high stereospecificity (Scheme 59).



Scheme 60

Chiral auxiliaries can also be used in $\text{S}_{\text{RN}}1$ reactions to form a mixture of diastereoisomers, an example is shown in Scheme 60. The result of this reaction with naphthyl iodide **26** was highly dependent on the choice of cation (Li^+ , Na^+ , K^+ , Cs^+ , and Ti(IV)). The highest diastereoselectivity was obtained with Li^+ and Ti(IV) cations.¹⁴⁴

A similar case of the use of chiral auxiliaries has been reported,⁹⁹ in which the auxiliary was an oxazolidinone (Scheme 61) instead of the imidazolidinone used in the previous example. The coupling of the perfluoroalkyl radical and enolate anion results in moderate to excellent diastereoselectivities (55-93%).



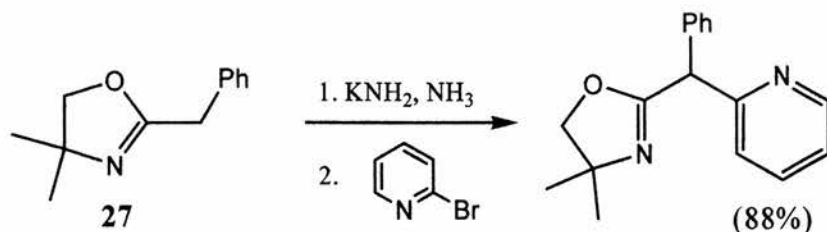
R_f	R^1	R^2	d.e
$n\text{-C}_6\text{F}_{13}$	$i\text{Pr}$	Me	71(<i>S</i>)
C_2H_5	$i\text{Pr}$	Me	74(<i>S</i>)
$(\text{CF}_3)_2\text{CF}(\text{CF}_2)_2$	$i\text{Pr}$	Me	79(<i>S</i>)
$n\text{-C}_6\text{F}_{13}$	Bn	Me	83(<i>S</i>)
$n\text{-C}_6\text{F}_{13}$	$i\text{Pr}$	$t\text{Bu}$	93

Scheme 61

These promising examples of chiral induction in intermolecular $S_{\text{RN}}1$ processes with the exception of the camphor arylation (Scheme 59) use removable chiral auxiliaries. This use of chiral auxiliaries as a means to effect chiral induction opens the possibility for use of many other substrates. At present no examples of stereocontrol in intramolecular $S_{\text{RN}}1$ reactions have been reported, therefore there is scope for a suitably designed substrate, incorporating an auxiliary, to undergo diastereoselective ring closure.

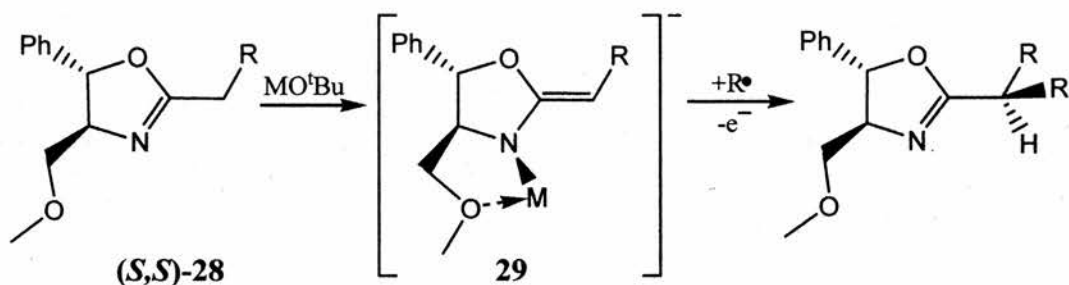
1.4 Project Aims and Objectives

Recently, in the literature, Wolfe *et al.*⁹⁸ reported that anions derived from oxazoline **27** could act as nucleophiles in $S_{RN}1$ reactions with aromatic and heterocyclic halides (Scheme 62). This was the first reported use of anions derived from 2-oxazolines in $S_{RN}1$ reactions.



Scheme 62

In view of this work it seemed probable that Meyers' chiral oxazolines (*S,S*)-**28** would take part in high yielding $S_{RN}1$ substitutions (Scheme 63), with a degree of stereoselection.

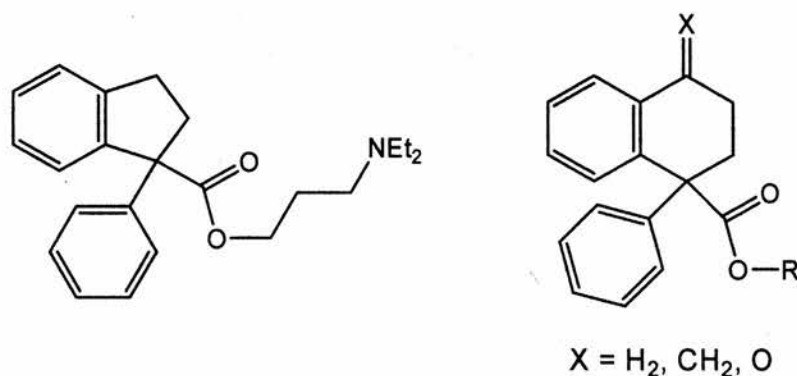


Scheme 63

Meyers' chiral oxazolines are synthesised easily from readily available chiral aminoalcohols and an appropriate carboxylic acid. R can also be introduced readily after oxazoline ring formation. Initial stereochemistry at the position alpha to the oxazoline ring in (*S,S*)-**28** is unimportant because carbanion formation takes place here. The product oxazolines are easily transformed into chiral alkylated acids, aldehydes, chloromethyl compounds, nitriles and epoxides.¹⁴⁵ Lithium is the metal most commonly used in heterolytic stereospecific reactions of Meyers' chiral oxazolines, whereas potassium in the form of KNH_2 or KO^tBu is generally used for $S_{RN}1$ reactions. Therefore the use of LiNH_2 and LiO^tBu will be investigated. If this proves to be disappointing, the use of Schlosser's base ($\text{BuLi}/\text{KO}^t\text{Bu}$) will be attempted. Successful use of lithium bases has been reported in $S_{RN}1$ reactions.^{123 & 146} Selectivity depends on the formation of Z-azaenolate **29** as well as complexation of

the metal. The measurement of ee's will be carried out by comparison with the well-documented $^1\text{H-NMR}$ spectra of oxazoline enantiomers.

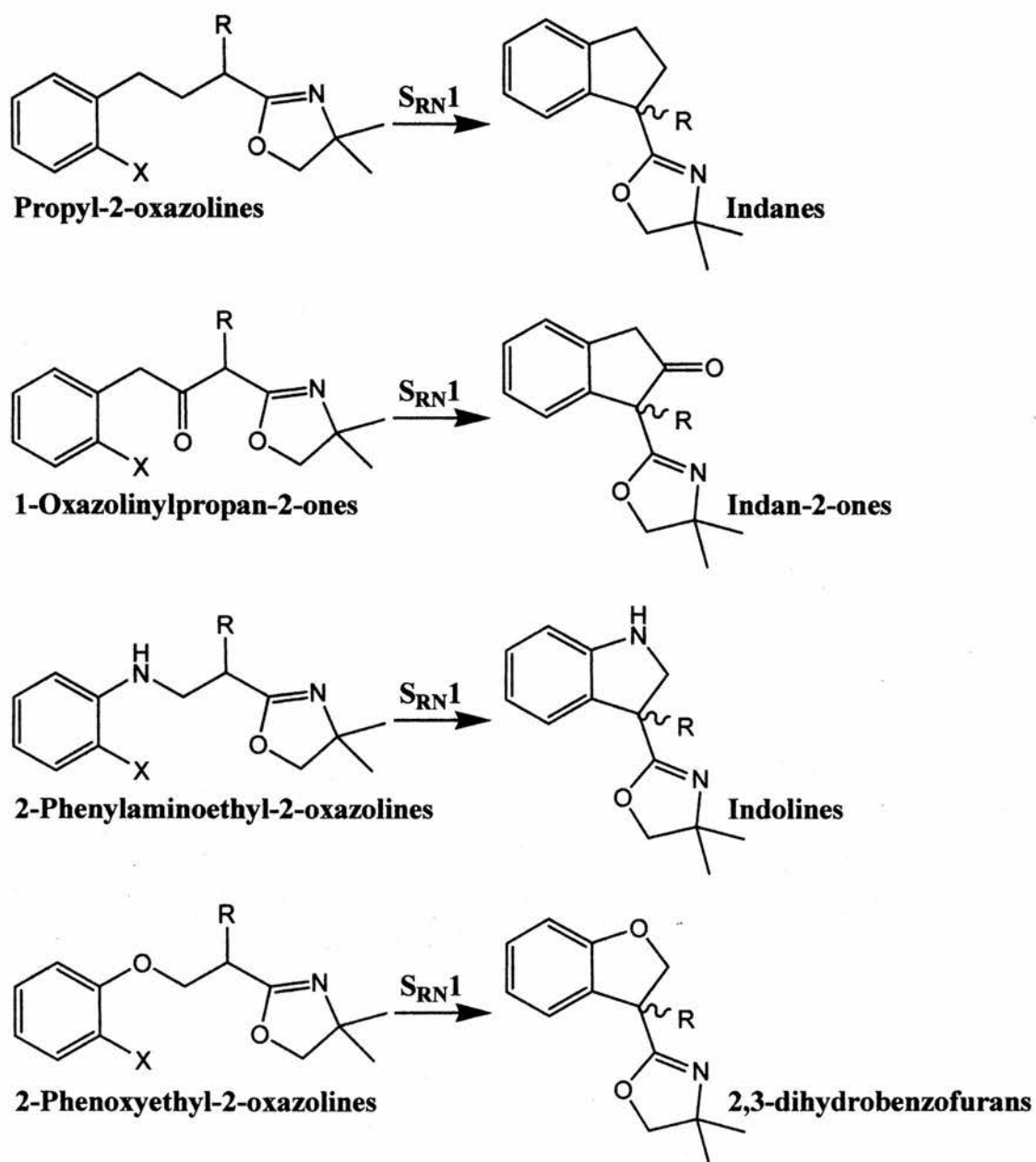
As expected, the costs of the enantiomerically pure chiral aminoalcohols needed to synthesise Meyers' oxazolines are high, therefore initial experimentation will be carried out using the non-chiral commercially available 2,4,4-trimethyl-2-oxazoline **30** and also 2-benzyl-4,4-dimethyl-2-oxazoline **27** which is easily prepared from the condensation of AMP **31** and phenylacetic acid **32** (Scheme 68).



Scheme 64

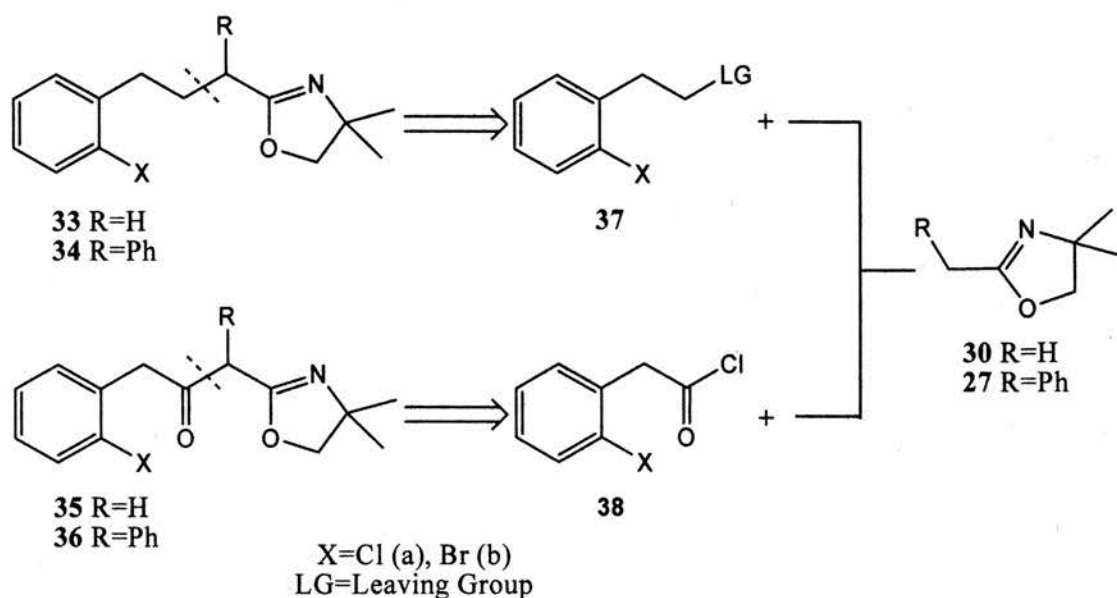
The initial focus will be on the intramolecular $\text{S}_{\text{RN}}1$ ring closure reactions to the five membered rings in the bicyclic systems shown in Scheme 65. These systems represent a variety of important basic ring systems some of which show biological activity (Scheme 64).¹⁴⁷ If the initial studies progress to success then the chiral equivalents will be investigated. It is envisaged that the $\text{S}_{\text{RN}}1$ conditions that will be employed, are: $\text{LiNH}_2/\text{NH}_3$, KNH_2/NH_3 , $\text{LiO}^t\text{Bu}/\text{DMSO}$, $\text{KO}^t\text{Bu}/\text{DMSO}$ and LDA/THF . All mentioned conditions will be attempted both in the dark and with photostimulation.

It is also intended that the intermediates of the $\text{S}_{\text{RN}}1$ cyclisations will be studied using EPR spectroscopic techniques. This will be one of only a few examples of *in-situ* study of radical anions during $\text{S}_{\text{RN}}1$ chain reactions. Also, *ab initio* DFT computations will be carried out using the Gaussian suite of programs to help in the analysis of any results gleaned from the EPR experiments.



Scheme 65

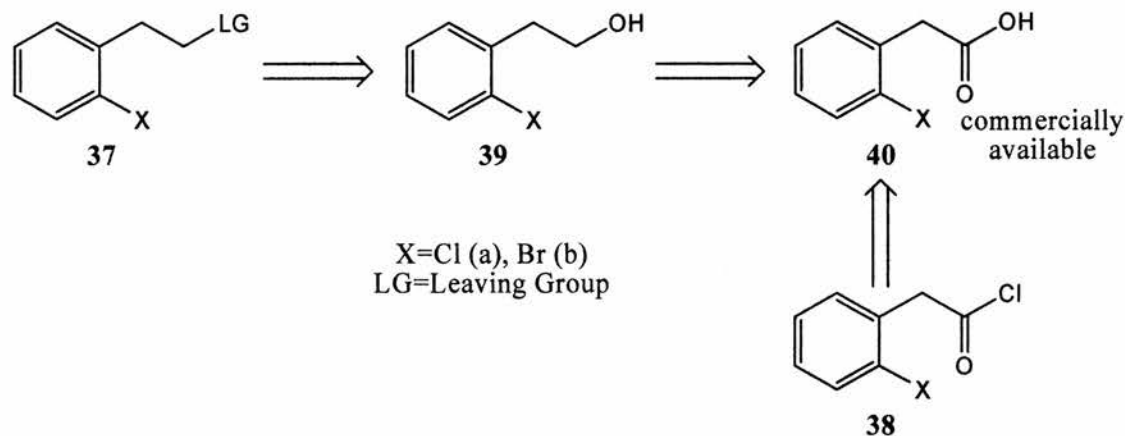
1.4.1 Retrosynthetic Analysis of Procyclic Species



Scheme 66

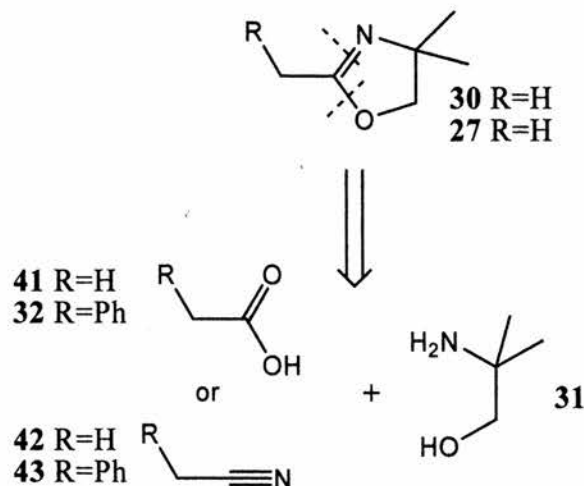
It is probable that functionalised oxazolines **33-36** could be derived from substituted 2-halophenylethanes **37** & **38** and oxazolines **27** & **30** (Scheme 66). The most likely reagents for this coupling are LDA or *n*-BuLi. The leaving group of **37** would likely be either a halogen (Br or I) or a tosyl group which are both easily made from an alcohol.

2-Halophenylethanes **37** & **38** could all be derived from a common acid **40** which is commercially available for X=Cl, Br (Scheme 67).



Scheme 67

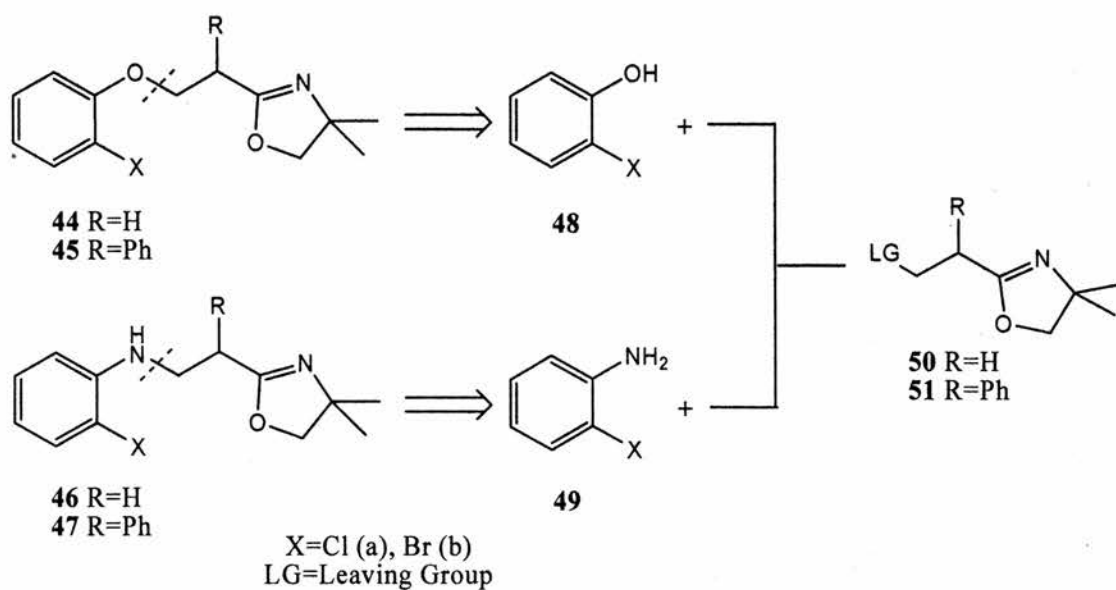
There are many methods recorded in the literature for the formation of 2-oxazolines.¹⁴⁸ These involve one and two step processes. One step processes involve the direct condensation of either a nitrile or a carboxylic acid with a 1,2-aminoalcohol. Two step processes either involve the preparation of acetimidate ethyl ester hydrochlorides from nitriles and condensing them with a 1,2-aminoalcohol, or the preparation of an acid chloride and condensation with a 1,2-aminoalcohol.



Scheme 68

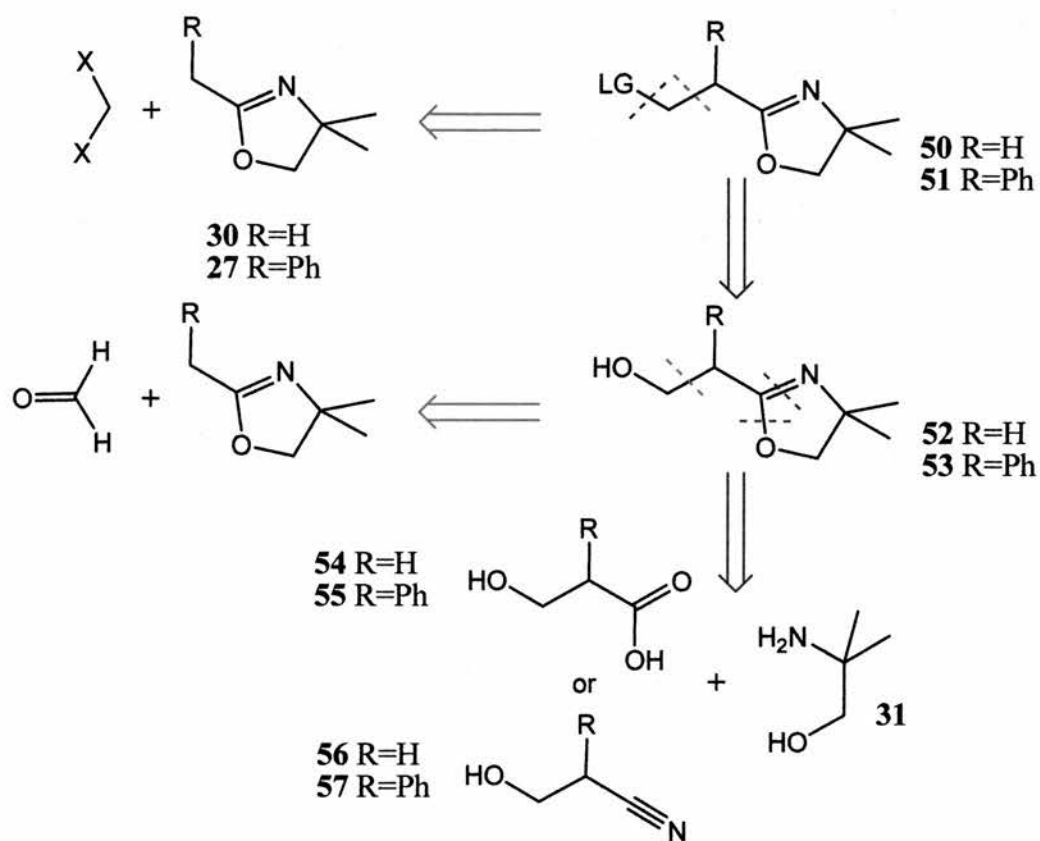
Oxazolines **27** & **30** could be derived in the common way for 2-oxazolines from the aminoalcohol **31** and acids **32** & **41** and nitriles **42** & **43**. The reaction condition would either be direct reaction in a high boiling point solvent with the removal of water in the case of the acids. Alternatively, the amide of the acid could be synthesised and then cyclised (Scheme 68).

Functionalised oxazolinyll ethers and amines **44-47** could be derived from the commercially available phenols **48** and anilines **49** coupled with 2-ethyloxazolines **50** & **51**. The coupling reactions to form **44-47** would probably involve the use of bases such as Et_3N , NaOH or K_2CO_3 . Possible leaving groups for **50** & **51** would be a halogen (Br & I) (Scheme 69).

**Scheme 69**

The substituted oxazolines **50** & **51** could be formed in several ways which are shown in Scheme 70. One route involves the use of the previously described oxazoline syntheses (Scheme 68). Another possible route starts with oxazoline **27** or **30** and adds a C1 unit to the 2-position of the oxazoline ring. Two ways of doing this are either coupling the oxazoline with formaldehyde to form an alcohol which could be converted to a good leaving group, or coupling the oxazoline with a dihalomethane such as CH_2Br_2 .

Initial synthetic effort will be given to the formation of the pure carbon chain oxazolines **33-36** and, if successful, investigations will progress towards the synthesis of hetero-atom containing oxazolines **44-47**.



Scheme 70

1.5 Bibliography

- 1 C. Y. Hong, *Br. J. Clin. Pharmacol.*, 1982, **13**, 285-293.
- 2 *Asymmetric Synthesis*, Eds. R. A. Aitken and S. N. Kilényi, Blackie, London, 1992.
- 3 Approaches categorised as in *Asymmetric Synthesis* (See ref. 2).
- 4 (a) D. J. Hart and H. C. Huang, *Tetrahedron Lett.*, 1985, **26**, 3749-3752; (b) D. J. Hart and H. C. Huang, *J. Am. Chem. Soc.*, 1989, **111**, 7509-7519; (c) Y. Guindon, J. F. Lavallée, M. Llinas-Brunnet, G. Horner and J. Rancourt, *ibid*, 1991, **113**, 9701-9702; (d) Y. Guindon, B. Guerin, C. Charbot, N. Mackintosh, and W. Ogilvie, *Synlett*, 1995, 12528-12535.
- 5 P. Renaud, N. Moufid, L. H. Kuo and D. P. Curran, *J. Org. Chem.*, 1994, **59**, 3547-3552.
- 6 D. R. William, B. A. Barner, K. Nishitani and J. G. Phillips, *J. Am. Chem. Soc.*, 1982, **104**, 4708-4710.
- 7 K. A. Lutomski and A. I. Meyers, in *Asymmetric Synthesis*, Vol. 3, Ed. J. D. Morrison, Academic Press, Orlando, 1984, Ch. 3.
- 8 (a) D. A. Evans, M. D. Ennis and D. J. Mathre, *J. Am. Chem. Soc.*, 1982, **104**, 1737-1730; (b) D. A. Evans, M. M. Morrissey and R. L. Dorow, *J. Am. Chem. Soc.*, 1985, **107**, 4346-4348; (c) D. A. Evans, T. C. Britton, R. L. Dorow and J. F. Dellaria, *J. Am. Chem. Soc.*, 1986, **108**, 6395-6397; (d) D. A. Evans, J. V. Nelson and T. R. Taber, *Top. Stereochem.*, 1982, **13**, 1-115; (e) D. A. Evans, *Aldrichimica Acta*, 1982, **15**, 23-32; (f) D. A. Evans and L. R. McGee, *J. Am. Chem. Soc.*, 1981, **103**, 2876-2878.
- 9 D. Enders, in *Asymmetric Synthesis*, Vol. 3, Ed. J. D. Morrison, Academic Press, Orlando, 1984, Ch. 4.
- 10 (a) W. Oppolzer, *Tetrahedron*, 1987, **43**, 1969-2004; (b) W. Oppolzer, *Pure Appl. Chem.*, 1990, **62**, 1241-1250.
- 11 N. A. Porter, R. Breyer, E. Swann, J. Nally, J. Pradhan, T. Allen and A. T. McPhail, *J. Am. Chem. Soc.*, 1991, **113**, 7002-7010.
- 12 (a) M. M. Midland, in *Asymmetric Synthesis*, Vol. 2, Ed. J. D. Morrison, Academic Press, Orlando, 1983, Ch. 2; (b) M. M. Midland, *Chem. Rev.*, 1989,

- 89, 1553-1561; (c) H. C. Brown and P. V. Ramachandran, *Acc. Chem. Res.*, 1992, **25**, 16-24.
- 13 E. R. Grandbois, S. I. Howard and J. D. Morrison, in *Asymmetric Synthesis*, Vol. 2, Ed. J. D. Morrison, Academic Press, Orlando, 1983, Ch. 3.
- 14 (a) L. Fuji, M. Node, S. Terada, M. Murata, H. Nagasuna, T. Taga and K. Machida, *J. Am. Chem. Soc.*, 1985, **107**, 6404-6406; (b) L. Duhamel, P. Duhamel, J. C. Launay and J. C. Plaquevent, *Bull. Soc. Chim. Fr. II*, 1984, 421-430.
- 15 P. J. Cox and N. S. Simpkins, *Tetrahedron Asymmetry*, 1991, **2**, 1-26.
- 16 H. C. Brown and J. V. N. Vara Prasad, *J. Am. Chem. Soc.*, 1986, **108**, 2049-2054.
- 17 (a) R. S. E. Conn, A. V. Lovell, S. Karady and L. M. Weinstock, *J. Org. Chem.*, 1986, **51**, 4710-4711; (b) K. Hermann and H. Wynberg, *ibid*, 1979, **44**, 2238-2244.
- 18 L. A. Paquette, in *Asymmetric Synthesis*, Vol. 3, Ed. J. D. Morrison, Academic Press, Orlando, 1984, Ch. 7.
- 19 (a) B. E. Rossiter, in *Asymmetric Synthesis*, Vol. 5, ed. J. D. Morrison, Academic Press, Orlando, 1985, Ch. 7; (b) A. Pfenninger, *Synthesis*, 1986, 89-116; (c) M. G. Finn and K. B. Sharpless, in *Asymmetric Synthesis*, Vol. 5, Ed. J. D. Morrison, Academic Press, Orlando, 1985, Ch. 8.
- 20 H. B. Kagan and F. Rebiere, *Synlett.*, 1990, 643-650.
- 21 S. G. Hentges and K. B. Sharpless, *J. Am. Chem. Soc.*, 1980, **103**, 4263-4265.
- 22 (a) J. Halpern, in *Asymmetric Synthesis*, Vol. 5, Ed. J. D. Morrison, Academic Press, Orlando, 1985, Ch. 2; (b) K. E. Koenig, in *Asymmetric Synthesis*, Vol. 5, Ed. J. D. Morrison, Academic Press, Orlando, 1985, Ch. 3.
- 23 M. Kitamura, Y. Hsiao, R. Noyori and H. Takaya, *Tetrahedron Lett.*, 1987, **28**, 4829-4832.
- 24 (a) P. Renaud, *Chimia*, 2001, **55**, 1045-1048; (b) C. P. Jasperse, D. P. Curran and T. L. Fevig, *Chem. Rev.*, 1991, **91**, 1237-1286; (c) U. Koert, *Angew. Chem. Int. Ed. Eng.*, 1996, **35**, 405-407; (d) F. Aldabbagh and W. R. Bowman, *Contemp. Org. Synth.*, 1997, 261-280; (e) *Radicals in Organic Synthesis*, Eds. P. Renaud and M. P. Sibi, Vol. 2, Wiley-VCH, Weinheim, 2001.

- 25 (a) J. E. Baldwin, *J. Chem. Soc., Chem. Commun.*, 1976, 734-736; (b) J. E. Baldwin, R. C. Thomas, L. I. Kruse and L. Silberman, *J. Org. Chem.*, 1977, **42**, 3846-3852.
- 26 N. M. Harrington-Frost and G. Pattenden, *Tetrahedron Lett.*, 2000, **41**, 403-405.
- 27 (a) R. A. Batey and D. B. Mackay, *Tetrahedron Lett.*, 1998, **39**, 7267-7270; (b) P. Devin, L. Fensterbank and M. Malacria, *ibid*, 1999, **40**, 5511-5514; (c) M. Chareyron, P. Devin, L. Fensterbank and M. Malacria, *Synlett*, 2000, 83-85.
- 28 A. G. Fallis and I. M. Brinza, *Tetrahedron*, 1997, **53**, 17543-17596.
- 29 F. Marion, C. Courillion and M. Malacria, *Org. Lett.*, 2003, **5**, 5095-5097.
- 30 P. L. Minin and J. C. Walton, *J. Org. Chem.*, 2003, **68**, 2960-2963.
- 31 (a) J. K. Choi, D. J. Hart and Y. M. Tsai, *Tetrahedron Lett.*, 1982, **23**, 4765-4768; (b) H. M. R. Hoffmann, U. Herden, M. Breithor and O. Rhode, *Tetrahedron*, 1997, **53**, 8383-8400; (c) J. Marco-Contelles, P. Ruiz, L. Martinez and A. Martinez-Grau, *ibid*, 1993, **49**, 6669-6694.
- 32 F. Beval, A. Fruchier, C. Chavis, J-L. Montero and M. Lucas, *J. Chem. Soc., Perkin Trans. 1*, 1999, 697-703.
- 33 J. Fossey, D. Lefort and J. Sorba, *Free Radicals in Organic Chemistry*, English Ed, Wiley, Paris, 1995, Ch. 13, p 151.
- 34 D. P. Curran, N. A. Porter and B. Giese, *Stereochemistry of Radical Reactions*, VCH, Weinheim, 1995, Ch 2, p 23.
- 35 (a) N. A. Porter, D. R. Magnin and B. T. Wright, *J. Am. Chem. Soc.*, 1986, **108**, 2787-2788; (b) N. A. Porter and V. H.-T. Chang, *ibid*, 1987, **109**, 4976-4981; (c) N. A. Porter, V. H.-T. Chang, D. R. Magnin and B. T. Wright, *ibid*, 1988, **110**, 3554-3560; (d) N. A. Porter, B. Lacher, V. H.-T. Chang and D. R. Magnin, *ibid*, 1989, **111**, 8309-8310; (e) P. Galatsis, S. D. Millan and T. Faber, *J. Org. Chem.*, 1993, **58**, 1215-1220.
- 36 (a) N. A. Porter and J. R. Nixon, *J. Am. Chem. Soc.*, 1978, **100**, 7116-7117; (b) B. Mailiard, E. Montaudon and F. Rakotomanana, *Tetrahedron*, 1985, **41**, 2727-2735; (c) B. Mailiard, A. Kharrat, F. Rakotomanana, E. Montaudon and C. Gardrat, *ibid*, 1985, **41**, 4047-4056; (d) B. Mailiard, E. Montaudon, F.

- Rakotomanana and M. J. Bourgeois, *ibid*, 1985, **41**, 5039-5043; (e) B. Mailiard, E. Montaudon and M. J. Bourgeois, *ibid*, 1986, **42**, 5309-5320; (f) B. Mailiard, D. Colombani, M. Degueil-Castaing and C. Navarro, *Synlett*, 1992, 587-588.
- 37 J. A. Kampmeier, R. B. Jordan, M. S. Liu, H. Yamanaka and D. J. Bishop, *ACS Symp Ser*, 1978, 275-289.
- 38 (a) R. J. Gritter and T. J. Wallace, *J. Org. Chem.*, 1961, **26**, 282-283; (b) R. E. Pincock and E. J. Torupka, *J. Am. Chem. Soc.*, 1969, **91**, 4593-4593; (c) B. B. Jarvis, *J. Org. Chem.*, 1970, **35**, 924-927; (d) J. C. Walton, *Acc. Chem. Res.*, 1998, **31**, 99-107.
- 39 P. S. Engel and K. L. Lowe, *Tetrahedron Lett.*, 1994, **35**, 2267-2270.
- 40 (a) J. A. Berson, *Acc. Chem. Res.*, 1978, **11**, 446; (b) K. K. Wang, *Chem. Rev.*, 1996, **96**, 207-222.
- 41 R. R. Goehring, *Tetrahedron Lett.*, 1992, **33**, 6045-6048.
- 42 F. Rose-Munch, V. Gagliardini, C. Renard and E. Rose, *Coordin. Chem. Rev.*, 1998, **178**, 249-268.
- 43 J. Clayden, N. Greeves, S. Warren and P. Wothers, *Organic Chemistry*, Oxford University Press, New York, 2001, p 589.
- 44 M. Makosa and J. Winiarski, *Acc. Chem. Res.*, 1987, **20**, 282-289.
- 45 J. F. Bunnett and J. K. Kim, *J. Am. Chem. Soc.*, 1970, **92**, 7463-7464; 7464-7466.
- 46 N. Kornblum, R. E. Michel and R. C. Kerber, *J. Am. Chem. Soc.*, 1966, **88**, 5662-5663.
- 47 G. A. Russell and W. C. Danen, *J. Am. Chem. Soc.*, 1966, **88**, 5663-5664.
- 48 J. F. Bunnett, *Acc. Chem. Res.*, 1978, **11**, 413-420.
- 49 (a) R. A. Rossi, A. B. Pierini and A. B. Peñéñory, *Chem. Rev.*, 2003, **103**, 71-167; (b) R. A. Rossi and R. H. de Rossi, *Aromatic Substitution by the $S_{RN}1$ Mechanism*, American Chemical Society, Washington, DC, 1983; (c) R. K. Norris, *Comprehensive Organic Synthesis*, Ed. B. M. Trost, Pergamon Press, London, UK, 1991, Vol. 4, p 451-482; (d) N. Kornblum, *The Chemistry of Functional groups*, Ed. S. Patai, Wiley, Chichester, UK, 1982, Suppl. F, Ch 10, p 361-393; (e) R. A. Rossi, A. B. Pierini and A. B. Peñéñory, *The*

- Chemistry of Functional groups*, Ed. S. Patai and Z. Rappoport, Wiley, Chichester, UK, 1995, Suppl. D2, Ch 24, p 1395-1485; (f) W. R. Bowman, *Chem. Soc. Rev.*, 1988, **17**, 283-316; (g) R. A. Rossi, A. B. Pierini and S. M. Palacios, *Adv. Free Radical Chem.*, 1990, **1**, 193-252.
- 50 (a) R. K. Norris, *The Chemistry of Functional Groups*, Ed. S. Patai and Z. Rappoport, Wiley, Chichester, UK, 1983, Suppl. D1, Ch. 16, p 681-701; (b) G. A. Russell and R. K. Norris, *J. Am Chem. Soc.*, 1971, **93**, 5839-5845.
- 51 (a) C. Dell'Erba, M. Novi, G. Petrillo, C. Tavani and P. Bellandi, *Tetrahedron*, 1991, **47**, 333-342; (b) C. Dell'Erba, M. Novi, G. Petrillo and C. Tavani, *ibid*, 1992, **48**, 325-334; (c) C. Dell'Erba, M. Novi, G. Petrillo and C. Tavani, *ibid*, 1993, **49**, 235-242; (d) C. Dell'Erba, M. Novi, G. Petrillo and C. Tavani, *Gazz. Chim. Ital.*, 1997, **127**, 361-366.
- 52 (a) F. G. Bordwell and X. Zhang, *Acc. Chem. Res.*, 1993, **26**, 510-517; (b) F. G. Bordwell, X. Zhang and R. Filler, *J. Org. Chem.*, 1993, **58**, 6067-6071.
- 53 J. F. Bunnett and J. E. Sundberg, *J. Org. Chem.*, 1976, **41**, 1702-1706.
- 54 G. L. Borosky, A. B. Pierini and R. A. Rossi, *J. Org. Chem.*, 1992, **57**, 247-252.
- 55 M. F. Semmelhack and T. M. Bargar, *J. Am. Chem. Soc.*, 1980, **102**, 7765-7774.
- 56 M. A. Fox, J. Younathan and G. E. Frynell, *J. Org. Chem.*, 1983, **48**, 3109-3112.
- 57 (a) B. Q. Wu, F. W. Zeng, M. Ge, X. Cheng and G. Wu, *Sci. China*, 1991, **34**, 777-786 [*Chem. Abstr.*, 1992, **116**, 58463]; (b) S. Hoz and J. F. Bunnett, *J. Am. Chem. Soc.*, 1977, **99**, 4690-4691; (c) C. Cheng and L. M. Stock, *J. Org. Chem.*, 1991, **56**, 2436-2443; (d) A. Boumekouez, E. About-Jaudet and N. J. Collignon, *Organomet. Chem.*, 1992, **440**, 297-301; (e) R. Beugelmans and M. Chbani, *New J. Chem.*, 1994, **18**, 949-952; (f) J. E. Argüello, A. B. Peñéñory and R. A. Rossi, *J. Org. Chem.*, 2000, **65**, 7175-7182.
- 58 L. M. Tolbert and S. Siddiqui, *J. Org. Chem.*, 1984, **49**, 1744-1751.
- 59 J. E. Argüello and A. B. Peñéñory, *J. Org. Chem.*, 2003, **68**, 2362-2368.
- 60 (a) V. L. Ivanov, J. Aurich, L. Eggert and M. G. Kuz'min, *J. Photochem. Photobiol. A. Chem.*, 1989, **50**, 275-281; (b) V. L. Ivanov, L. Eggert and M. G.

- Kuz'min, *High Energy Chem.*, 1987, 284-289; (c) V. L. Ivanov and A. Kherbst, *J. Org. Chem. USSR (Engl. Transl.)*, 1988, **24**, 1709-1713; (d) V. S. Savvina and V. L. Ivanov, *High Energy Chem.*, 1990, **24**, 205-210.
- 61 (a) C. P. Andrieux, P. Hapiot and J.-M. Savéant, *Chem. Rev.*, 1990, **90**, 723-738; (b) D. H. Evans, *Chem. Rev.*, 1990, **90**, 739-751; (c) J. Pinson and J.-M. Savéant, *Electroorg. Synth.*, 1991, **29**, 29-44; (d) J.-M. Savéant, *Acc. Chem. Res.*, 1980, **13**, 323-329; (e) J.-M. Savéant, *ibid*, 1993, **26**, 455-461; (f) J.-M. Savéant, *Adv. Phys. Org. Chem.*, 1990, **26**, 1-130; (g) J.-M. Savéant, *Bull. Soc. Chim. Fr.*, 1988, **125**, 225-237. (h) J.-M. Savéant, *New J. Chem.*, 1992, **16**, 131-150; (i) J.-M. Savéant, *Adv. Electron-Transfer Chem.*, 1994, **4**, 53-116.
- 62 (a) N. Alam, C. Amatore, C. Combellas, A. Thiébault and J. Verpeaux, *J. Org. Chem.*, 1990, **55**, 6347-6356; (b) C. Amatore, C. Combellas, N. E. Lebbar, A. Thiébault and J. N. Verpeaux, *J. Org. Chem.*, 1995, **60**, 18-26.
- 63 (a) C. Amatore, J.-M. Savéant, C. Combellas, S. Robveille and A. Thiébault, *J. Electroanal. Chem.*, 1985, **184**, 25-40; (b) C. Amatore, J.-M. Savéant, C. Combellas, S. Robveille and A. Thiébault, *J. Am. Chem. Soc.*, 1986, **108**, 4754-4760.
- 64 S. M. Palacios, S. E. Asis and R. A. Rossi, *Bull. Soc. Chim. Fr.*, 1993, **130**, 11-116.
- 65 (a) R. A. Rossi and J. F. Bunnett, *J. Am. Chem. Soc.*, 1972, **94**, 683-684; (b) R. A. Rossi, R. H. de Rossi and A. F. Lopez, *ibid*, 1976, **98**, 1252-1256; (c) R. R. Bard, J. F. Bunnett, X. Creary and M. J. Tremelling, *ibid*, 1980, **102**, 2852-2854; (d) M. J. Tremelling and J. F. Bunnett, *ibid*, 1980, **102**, 7375-7377.
- 66 (a) E. Austin, R. A. Alonso and R. A. Rossi, *J. Org. Chem.*, 1991, **56**, 4486-4489; (b) E. Austin, C. G. Ferrayoli, R. A. Alonso and R. A. Rossi, *Tetrahedron*, 1993, **49**, 4495-4502.
- 67 C. Calli and J. F. Bunnett, *J. Org. Chem.*, 1984, **49**, 3041-3042.
- 68 C. Calli and P. Gentili, *J. Chem. Soc., Perkin Trans. 2*, 1993, 1135-1140.
- 69 (a) M. Van Leeuwen and A. McKillop, *J. Chem. Soc., Perkin Trans. 1*, 1993, 2433-2440; (b) M. T. Baumgartner, M. H. Gallego and A. B. Pierini, *J. Org. Chem.*, 1998, **63**, 6394-6397; (c) M. T. Baumgartner, R. A. Rossi and A. B. Pierini, *ibid*, 1999, **64**, 6487-6489; (d) M. A. Nazareno and R. A. Rossi, *ibid*,

- 1996, **61**, 1645-1649; (e) M. C. Murguia and R. A. Rossi, *Tetrahedron Lett.*, 1997, **38**, 1355-1358.
- 70 M. A. Nazareno and R. A. Rossi, *Tetrahedron Lett.*, 1994, **35**, 5185-5188.
- 71 (a) P. G. Manzo, S. M. Palacios and R. A. Alonso, *Tetrahedron Lett.*, 1994, **35**, 677-680; (b) P. G. Manzo, S. M. Palacios R. A. Alonso and R. A Rossi, *Org. Prep. Procedure Int.*, 1995, **27**, 668-671; (c) M. J. Dickens and J. L. Luche, *Tetrahedron Lett.*, 1991, **32**, 4709-4712.
- 72 (a) P. Vanelle, A. Gellis, M. Kaafarani, J. Madonado and M. P. Crozet, *Tetrahedron Lett.*, 1999, **40**, 4343-4346; (b) P. Vanelle, T. Terme, A. Gellis and M. P. Crozet, *Res. Adv. Org. Chem.*, 2000, **1**, 27-41.
- 73 A. L. Scher and N. N. Lichtin, *J. Am. Chem. Soc.*, 1975, **97**, 7170-7171.
- 74 H. Lund, K. Daasbjerg, D. Ochiellini and S. U. Pedersen, *Russian J. Electrochem.*, 1995, **31**, 865-872.
- 75 (a) J.-M. Savéant, *J. Am. Chem. Soc.*, 1992, **114**, 10595-10602; (b) J.-M. Savéant, *Adv. Phys. Org. Chem.*, 2000, **35**, 117-192.
- 76 J.-M. Savéant, *J. Phys. Chem.*, 1994, **98**, 3716-3724.
- 77 C. Calli, *Gazz. Chim. Ital.*, 1988, **118**, 385-368.
- 78 (a) W. R. Bowman and M. C. R. Symons, *Tetrahedron Lett.*, 1981, **22**, 4549-4552; (b) W. R. Bowman and M. C. R. Symons, *J. Chem. Soc., Perkin Trans. 2*, 1983, 25-32; (c) W. R. Bowman and M. C. R. Symons, *J. Chem. Res. (S)*, 1984, 162-163.
- 79 (a) W. R. Bowman and M. C. R. Symons, *J. Chem. Soc., Chem. Commun.*, 1984, 1445-1446; (b) W. R. Bowman and M. C. R. Symons, *J. Chem. Soc., Perkin Trans. 2*, 1988, 583-589.
- 80 G. A. Russell and W. C. Danen, *J. Am. Chem. Soc.*, 1968, **90**, 347-353.
- 81 W. R. Bowman and M. C. R. Symons, *J. Chem. Soc., Perkin Trans. 2*, 1987, 1133-1138.
- 82 W. R. Bowman and M. C. R. Symons, *J. Chem. Soc., Perkin Trans. 2*, 1988, 1077-1082.
- 83 F. Ciminale, G. Bruno, L. Testaferri, M. Tiecco and G. Martelli, *J. Org. Chem.*, 1978, **43**, 4509-4513.

- 84 A. B. Pierini, J. S. Duca and M. T. Baumgartner, *THEOCHEM*, 1994, **311**, 343-352.
- 85 (a) R. G. Compton, R. A. W. Dryfe and A. C. Fisher, *J. Electroanal. Chem.*, 1993, **361**, 275-278; (b) R. G. Compton, R. A. W. Dryfe and A. C. Fisher, *J. Chem. Soc., Perkin Trans. 2*, 1994, 1581-1597; (c) R. G. Compton, R. A. W. Dryfe, J. C. Ekland, S. D. Page, J. Hirst, L. B. Nei, G. W. J. Fleet, K. Y. Hsia, D. Bethell and L. J. Martingale, *J. Chem. Soc., Perkin Trans. 2*, 1995, 1673-1677; (d) T. Teherani and A. J. Bard, *Acta Chem. Scand. B*, 1983, **37**, 413-422; (e) D. Behar and P. Neta, *J. Phys. Chem.*, 1981, **85**, 690-693; (f) H. B. Mereyala, P. Neta, R. K. Norris and K. Wilson, *ibid*, 1986, **90**, 168-173.
- 86 (a) J. Marquet, M. Moreno-Mañas, P. Pacheco, M. Prat, A. R. Katritzky and B. Brycki, *Tetrahedron*, 1990, **46**, 5333-5346; (b) C. D. Beadle and W. R. Bowman, *J. Chem. Res. S*, 1985, 150-151.
- 87 (a) W. R. Bowman and G. D. Richardson, *J. Chem. Soc., Perkin Trans. 1*, 1980, 1407-1413; W. R. Bowman, D. Rakshit and M. D. Valmas, *J. Chem. Soc., Perkin Trans. 1*, 1984, 2327-2336.
- 88 (a) C. Amatore, M. A. Oturan, J. Pinson, J.-M. Savéant and A. Thiébault, *J. Am. Chem. Soc.*, 1985, **107**, 3451-3459; (b) C. Amatore, J. Pinson, J.-M. Savéant and A. Thiébault, *ibid*, 1981, **103**, 6930-6937; (c) C. Amatore, M. A. Oturan, J. Pinson, J.-M. Savéant and A. Thiébault, *ibid*, 1984, **106**, 6318-6321.
- 89 C. Amatore, C. Combellas, J. Pinson, M. A. Oturan, S. Roveille J.-M. Savéant and A. Thiébault, *J. Am. Chem. Soc.*, 1985, **107**, 4846-4853.
- 90 A. B. Pierini, A. B. Peñéñory and R. A. Rossi, *J. Org. Chem.*, 1984, **49**, 486-490.
- 91 (a) C. Calli and J. F. Bunnett, *J. Am. Chem. Soc.*, 1981, **103**, 7140-7147; (b) C. Calli and J. F. Bunnett, *ibid*, 1979, **101**, 6137-6139; (c) R. A. Alonso, A. Bardon and R. A. Rossi, *J. Org. Chem.*, 1984, **48**, 3584-3587; (d) C. C. Yammel, J. C. Podesta and R. A. Rossi, *ibid*, 1992, **57**, 5720-5725.
- 92 (a) J. F. Bunnett, E. Mitchel, and C. Calli, *Tetrahedron*, 1985, **41**, 4119-4132; (b) J. F. Bunnett and J. E. Sundberg, *Chem. Pharm. Bull.*, 1975, **23**, 2620-2628.
- 93 A. L. J. Beckwith and S. M. Palacios, *J. Phys. Org. Chem.*, 1991, **4**, 404-412.

- 94 V. D. Veltwisch and K. D. Asmus, *J. Chem. Soc., Perkin Trans. 2*, 1982, 1143-1145.
- 95 G. A. Russell, F. Ros and B. Mudryk, *J. Am. Chem. Soc.*, 1980, **102**, 7601-7603.
- 96 J. F. Bunnett, R. G. Scamehorn and R. P. Traber, *J. Org. Chem.*, 1976, **41**, 3677-3682.
- 97 R. A. Rossi and R. A. Alonso, *J. Org. Chem.*, 1980, **45**, 1239-1241.
- 98 J.-W. Wong, K. J. Natalie Jr., G. C. Nwokogu, J. S. Pisipati, P. T. Flaherty, T. D. Greenwood and J. F. Wolfe, *J. Org. Chem.*, 1997, **62**, 6152-6159.
- 99 K. Isekia, M. Takahashi, D. Asada, T. Nagai and Y. Kobayashi, *J. Fluorine Chem.*, 1995, **74**, 269-271.
- 100 (a) M. C. Murguia and R. A. Rossi, *Tetrahedron Lett.*, 1997, **38**, 1355-1358; (b) M. C. Murguia, C. G. Ricci, M. I. Cabrera, J. A. Luna and R. J. Grau, *J. Mol. Catal. A. Chem.*, 2000, **165**, 113-120.
- 101 R. A. Rossi, R. H. de Rossi and A. F. Lopez, *J. Org. Chem.*, 1976, **41**, 3371-3373.
- 102 R. Beugelmans, T. Gharbaoui, A. Lechevallier and A. A. Madjdabadi, *J. Chem. Soc., Perkin Trans. 2*, 1995, 1-3.
- 103 R. Beugelmans and J. Chastanet, *Tetrahedron*, 1993, **49**, 7883-7890.
- 104 (a) A. B. Chopa, M. T. Lockhart and V. B. Dorn, *Organometallics*, 2002, **21**, 1425-1429; (b) M. T. Lockhart, A. B. Chopa and R. A. Rossi, *J. Organomet. Chem.*, 1999, **582**, 229-234.
- 105 W. Kitching, H. Olszuwy and J. Waugh, *J. Org. Chem.*, 1982, **47**, 1893-1904.
- 106 A. B. Pierini, M. T. Baumgartner and R. A. Rossi, *Tetrahedron Lett.*, 1987, **28**, 4653-4656.
- 107 M. Chahma, C. Combellas and A. Thiébault, *Synth. Stuttgart*, 1994, 366-386.
- 108 R. Beugelmans and M. Chbani, *Bull. Soc. Chim. Fr.*, 1995, **132**, 290-305; 306-313; 729-733.
- 109 J. E. Swartz and J. F. Bunnett, *J. Org. Chem.*, 1979, **44**, 4673-4677.
- 110 E. R. N. Bornancini, R. A. Alonso and R. A. Rossi, *J. Organomet. Chem.*, 1984, **270**, 177-183.

- 111 (a) R. A. Rossi, R. A. Alonso and S. M. Palacios, *J. Org. Chem.*, 1981, **46**, 2498-2502; (b) R. A. Rossi, R. A. Alonso and S. M. Palacios, *ibid*, 1982, **47**, 77-80; (c) E. R. N. Bornancini and R. A. Rossi, *ibid*, 1990, **55**, 2332-2336.
- 112 J. F. Bunnett and X. Creary, *J. Org. Chem.*, 1974, **39**, 3173-3174.
- 113 N. Kornblum, M. M. Kestner, S. D. Boyd and L. C. Cattran, *J. Am. Chem. Soc.*, 1973, **95**, 3356-3361.
- 114 G. Petrillo, M. Novi, G. Garbarino and M. Filiberti, *Tetrahedron Lett.*, 1988, **29**, 4185-4188.
- 115 M. Genesty and C. Degrand, *New. J. Chem.*, 1998, 349-354.
- 116 (a) R. A. Rossi and A. B. Peñeñory, *J. Org. Chem.*, 1981, **46**, 4580-4582; (b) L. A. Acampora, D. L. Dugger, T. Emma, J. Mohammed, M. F. Rubner, L. Samuelson, D. J. Sandman and S. K. Tripathy, *ACS Symp. Ser.*, 1995, No. **242**, 461-472.
- 117 D. J. Sandman, J. C. Stark, L. A. Acampora and P. Gagne, *Organometallics*, 1983, **2**, 549-551.
- 118 A. B. Pierini and R. A. Rossi, *J. Org. Chem.*, 1979, **44**, 4667-4673.
- 119 G. C. Nwokogu, J. W. Wong, T. D. Greenwood and J. F. Wolfe, *Org. Lett.*, 2000, **2**, 2643-2646.
- 120 (a) N. Kornblum, S. D. Boyd, H. W. Pinnick and R. G. Smith, *J. Am. Chem. Soc.*, 1971, **93**, 4316-4318; (b) N. Kornblum and L. Cheng, *J. Org. Chem.*, 1977, **42**, 2944-2945.
- 121 (a) N. Kornblum, M. T. Davies, G. W. Earl, G. S. Greene, N. L. Holy, R. C. Kerber, J. W. Manthey, M. T. Musser and D. H. Snow, *J. Am. Chem. Soc.*, 1967, **89**, 5714-5715; (b) N. Kornblum, P. Ackermann, J. W. Manthey, M. T. Musser, H. W. Pinnick, S. Singaram and P. A. Wade, *J. Org. Chem.*, 1988, **53**, 1475-1481; (c) N. Kornblum, L. Cheng, T. M. Davies, G. W. Earl, N. L. Holy, R. C. Kerber, M. M. Kestner, J. W. Manthey, M. T. Musser, H. W. Pinnick, D. H. Snow, F. W. Stuchal and R. T. Swiger, *J. Org. Chem.*, 1987, **52**, 196-204.
- 122 (a) P. Vanelle, S. Ghezali, J. Maldonado, M. P. Crozet, F. Delmas, M. Gasquet and P. Timon-David, *Eur. J. Med. Chem.*, 1993, **28**, 1-4; (b) F. I. Flower, P. J. Newcombe and R. K. Norris, *J. Org. Chem.*, 1983, **48**, 4202-4205; (c) M. P. Crozet and J. M. Surzur, *Tetrahedron Lett.*, 1985, **26**, 1023-1026; (d) P.

- Vanelle, N. Madadi, J. Maldonado, L. Giraud, J. Sabuco and M. P. Crozet, *Heterocycles*, 1991, **32**, 2083-2087; (e) P. Vanelle, S. Ghezali, J. Maldonado, O. Chavignon, A. Gueiffer, J. C. Teulade and M. P. Crozet, *ibid*, 1993, **36**, 1541-1551; (e) P. Vanelle, N. Madadi, C. Roubaud, J. Maldonado and M. P. Crozet, *Tetrahedron*, 1991, **47**, 5173-5184. (f) C. Roubaud, P. Vanelle, J. Maldonado and M. P. Crozet, *ibid*, 1995, **51**, 9643-9656.
- 123 R. Tamura, M. Kohno, S. Utsunomiya, K. Yamawaki, N. Azuma, A. Matsumoto and Y. Ishii, *J. Org. Chem.*, 1993, **58**, 3953-3959.
- 124 E. C. Ashby, W. Y. Su, and T. N. Pham, *Organometallics*, 1985, **4**, 1493-1501.
- 125 M. A. Nazareno and R. A. Rossi, *Tetrahedron*, 1994, **50**, 9267-9274.
- 126 R. A. Rossi, A. N. Santiago and S. M. Palacios, *J. Org. Chem.*, 1984, **49**, 3387-3388.
- 127 W. Adcock, C. I. Clark and N. A. Trout, *J. Org. Chem.*, 2001, **66**, 3362-3371.
- 128 V. N. Boiko and G. M. Shchupak, *J. Fluorine Chem.*, 1994, **69**, 207-212.
- 129 G. A. Russell, J. Hershberger and K. Owens, *J. Organomet. Chem.*, 1982, **225**, 43-58.
- 130 R. Beugelmans, H. Ginburg and M. Bois-Choussy, *J. Chem. Soc., Perkin Trans. 1*, 1982, 1149-1152.
- 131 L. Estel, F. Marsais and G. Queguiner, *J. Org. Chem.*, 1988, **53**, 2740-2744.
- 132 R. Beugelmans and M. Bois-Choussy, *Heterocycles*, 1987, **26**, 1863-1871.
- 133 J. F. Wolfe, M. C. Sleeve and R. R. Goehring, *J. Am. Chem. Soc.*, 1980, **102**, 3646-3647.
- 134 R. R. Goehring, Y. P. Sachdeva, J. S. Pisipati, M. C. Sleeve and J. F. Wolfe, *J. Am. Chem. Soc.*, 1985, **107**, 435-443.
- 135 S. A. Dandekar, S. N. Greenwood, T. D. Greenwood, S. Mabic, J. S. Merola, J. M. Tanko and J. F. Wolfe, *J. Org. Chem.*, 1999, **64**, 1543-1553.
- 136 (a) S. F. Martin and S. Liras, *J. Am. Chem. Soc.*, 1993, **113**, 10450-10451; (b) S. Liras, C. L. Lynch, A. M. Fryer, B. T. Vu and S. F. Martin, *ibid*, 2001, **123**, 5918-5924.
- 137 (a) R. G. Goehring, *Tetrahedron Lett.*, 1992, **33**, 6045-6048; (b) R. R. Goehring, *ibid*, 1994, **35**, 8145-8146.

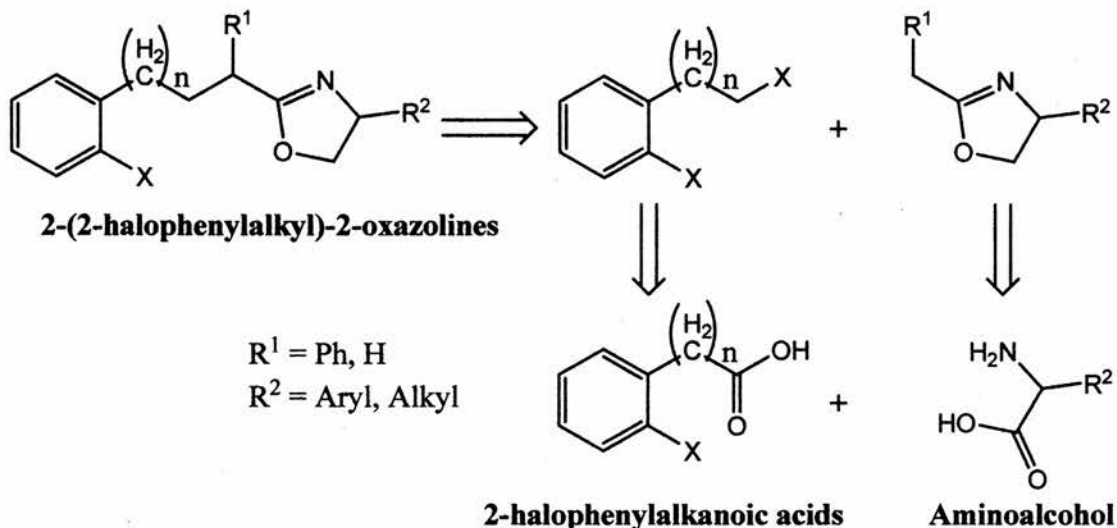
- 138 (a) W. R. Bowman, H. Heaney and P. H. G. Smith, *Tetrahedron Lett.*, 1982, **23**, 5093-5096; (b) M. F. Semmelhack, B. P. Chong, R. D. Stauffer, T. D. Rogerson, A. Chong and L. D. Jones, *J. Am. Chem. Soc.*, 1975, **97**, 2507-2511.
- 139 M. T. Baumgartner, A. B. Pierini and R. A. Rossi, *J. Org. Chem.*, 1993, **58**, 2593-2598.
- 140 M. Ahbala, P. K. Hapiot, A. Houmam, M. Jouini, J. Pinson and J.-M. Savéant, *J. Am. Chem. Soc.*, 1995, **117**, 11488-11498.
- 141 N. Kornblum and P. A. Wade, *J. Org. Chem.*, 1987, **52**, 5301-5305.
- 142 R. K. Norris and R. J. Smyth-King, *Tetrahedron*, 1982, **38**, 1051-1057.
- 143 D. Carbaret, N. Maigrot and Z. Welvart, *Tetrahedron*, 1985, **41**, 5357-5364.
- 144 G.A. Lotz, S. M. Palacios and R. A. Rossi, *Tetrahedron Lett.*, 1994, **35**, 7710-7714.
- 145 D. J. Ager, I. Prakash and D. R. Schaad, *Chem. Rev.*, 1996, **96**, 835-876.
- 146 R. Tamura, K. Yamawaki and N. Azuma, *J. Org. Chem.*, 1991, **56**, 5743-5745.
- 147 (a) D. L. Dehaven-Hudkins, J. T. Allen, R. L. Hudkins, J. F. Stubbins and F. C. Tortella, *Life Sciences*, 1995, **56**, 1571-1576; (b) M. B. Sommer, M. Begtrup and K. P. Bøgesø, *J. Org. Chem.*, 1990, **55**, 4822-4833.
- 148 a) H. Vorbrueggen and K. Krolkiewicz, *Tetrahedron Lett.*, 1981, **22**, 4471-4474; b) S. Serota, J. R. Simon, E. B. Murray and W. M. Linfield, *J. Org. Chem.*, 1981, **46**, 4147-4151; c) P. Zhou, J. E. Blubbaum, C. T. Burns and N. R. Natale, *Tetrahedron Lett.* 1997, **38**, 7019-7020; d) J. F. Hansen and S. Wang, *J. Org. Chem.*, 1976, **41**, 3635-3637.

Section 2

Results and Discussion

2.1 2-(2-Halophenylalkyl)-2-oxazolines

As outlined in section 1.4, a substituted oxazoline can be synthesised from a suitable aminoalcohol and a nitrile or carboxylic acid. Any further derivatisation of the 2-oxazoline can be achieved by deprotonation at the 2-position by a suitable base e.g. *n*-BuLi and subsequent nucleophilic attack by the anion on an alkyl halide or equivalent.



Scheme 71 Retrosynthetic analysis of 2-(2-halophenylalkyl)-2-oxazolines

As clearly shown in Scheme 71, the 2-halophenylalkyl portion of the 2-(2-halophenylalkyl)-2-oxazoline can ultimately be derived from an 2-halophenylalkanoic acid and, as mentioned earlier, the oxazoline portion comes from an aminoalcohol, usually derived from an amino acid.

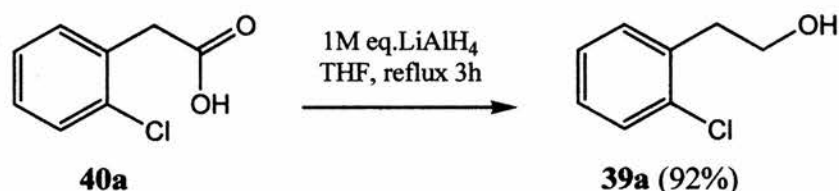
2.1.1 2-Halophenylalkyl Halides from 2-Halophenylalkanoic Acids

2-Halophenylalkyl halides are not commercially available, but the 2-halophenylacetic acids are (halogen equal to F, Cl, Br and I). Therefore, as previously mentioned, it was envisioned that 2-halophenylalkyl halides could be derived from 2-halophenylalkanoic acids via the intermediate alcohols. It was reasonably assumed that the 2-halophenylalkyl halides with propyl, butyl etc. chains could be obtained via chain elongation steps common in the literature.¹ Initially 2-halophenethyl halides will be synthesised to optimise reaction conditions.

2.1.1.1 2-Halophenethyl Halides

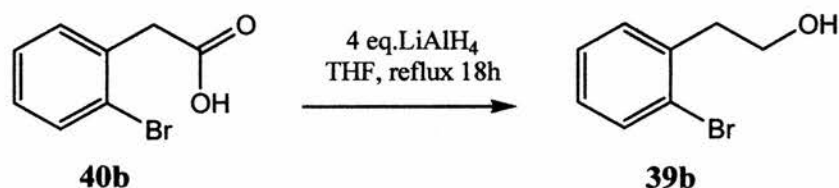
In order to synthesise the desired halides, first the commercially available acids had to be reduced to the corresponding alcohols. Only the 2-chloro, and 2-bromo acids will be utilised due to the lack of reactivity of the 2-fluorophenyl unit in $S_{RN}1$ reactions and the relative expense of 2-iodo compounds.

2-Chlorophenethyl alcohol **39a** was prepared by the reduction of 2-chlorophenylacetic acid **40a** using lithium aluminium hydride in tetrahydrofuran as detailed in the literature² (Scheme 72).



Scheme 72

When 2-bromophenylacetic acid **40b** was reduced (Scheme 73) using the literature method (4M excess LiAlH₄, reflux 18h, THF),³ the ¹H-NMR spectrum revealed an oddity in the aromatic region. In 2-bromophenylacetic acid the aromatic region showed three signals, they were 7.12-7.20 (1H, m, ArH), 7.28-7.31 (2H, m, ArH) and 7.57-7.60 (1H, m, ArH).



Scheme 73

On looking at the spectrum of the reduction product that was obtained, the three signals in the aromatic region were in the integral ratio of 1:43:1. Also there were two pairs of triplets, one pair was nearly on top of another at 3.75ppm and 3.74ppm with a total integration of 18.4 and the other pair at 2.94 ppm and 2.79ppm had a ratio of 2:16.8. This suggested that there were two products present. The evidence pointed to two aromatic ethyl alcohols, one being the desired product **39b** together with an unknown. If the integrations due to the desired product were subtracted in the aromatic region, and a comparison of the result made with the integration at 2.79ppm, a ratio of 5:2 was calculated, suggesting that the other product was phenylethanol. The literature ¹H-NMR was consulted and the major product was

indeed phenylethanol **58**.⁴ The ratio of desired product to phenylethanol was 1:8.5. In conclusion it appears that the reaction conditions had caused the reduction of the halogen on the phenyl ring.

A return to the literature revealed several other reaction conditions using only 1 equivalent of LiAlH₄ in diethyl ether at various temperatures and for various times, although slightly lower yields than the previous reference were reported.

1	4 eq LiAlH ₄ , 18h reflux, THF	11%	89%
2	1 eq LiAlH ₄ , 1.5h reflux, Et ₂ O	82%	18%
3	1 eq LiAlH ₄ , 30min r.t, Et ₂ O	89%	11%
4	1 eq LiAlH ₄ , 30min 0°C→r.t, Et ₂ O	95%	5%
5	1 eq LiAlH ₄ , 20min 0°C→r.t, Et ₂ O	98%	2%

Table 1 Optimisation of the reduction of 2-bromophenylacetic acid.

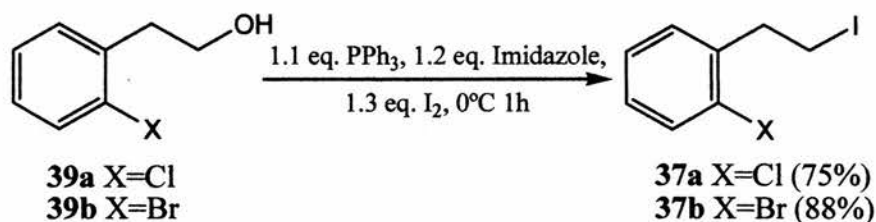
Therefore several reactions were carried out using different conditions, the results of which are detailed in Table 1. It can be seen that using very mild conditions virtually eliminates any phenylethanol **58** formation. The overall yield for entry 5 in the table was 84%. It can be concluded that the conditions originally described in the literature are either inaccurate or the quality of the lithium aluminium hydride used was poor.

Having now obtained the 2-halophenethyl alcohols in satisfactory yield conversion to the halide was now undertaken. A whole plethora of routes to alkyl bromides and iodides from the corresponding alcohols are described in the literature. Many of the methods involved corrosive or toxic reagents e.g chlorides – SOCl₂; bromides - HBr, CBr₄ and PBr₃; iodides – red phosphorus/I₂, and also long periods of heating. Only one method was found that used relatively mild conditions, i.e. I₂, PPh₃, imidazole, 0°C, 1-2 h. This method had been used previously⁵ to synthesise 2-

chlorophenethyl iodide **37a**, although no information was published on the individual yield of the reaction.

Thus 2-chlorophenethyl iodide **37a** was prepared using the literature method (Scheme 74) with a yield of 75%. This yield was comparable to those reported in the literature (even though much milder conditions were used) for the synthesis of 2-halophenethyl halides from the corresponding alcohols (58-78%).

Given the successful preparation of 2-chlorophenethyl iodide **37a** using the described procedure, 2-bromophenethyl iodide **37b** was prepared in similar good yield (88%) (Scheme 74).



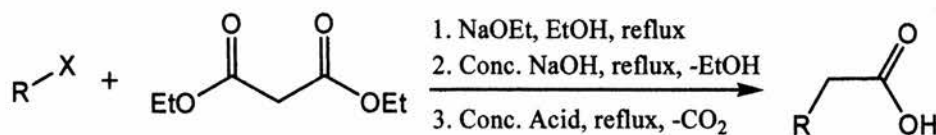
Scheme 74

2.1.1.2 Chain Extension of 2-Halophenethyl Halides

Having established a route from 2-halophenylethanoic acids to halophenethyl iodides using relatively mild conditions with good yield, access to the required iodides with longer chain length was now sought. In order to prepare arylalkyl iodides where alkyl equals propyl, butyl, pentyl, the corresponding acids were required. Unfortunately, the parent acids are not commercially available. Syntheses of 2-halophenylpropanoic acids have been achieved by reaction of 2-halobenzaldehydes with Meldrum's acid.⁶ Preparations of 2-halophenylbutanoic acids have previously been achieved via reactions of the appropriate 2-halophenethyl halides with diethyl malonate.⁷ The longer chain 2-halophenylpentanoic acids were unknown. It was envisaged that 2-halophenylpentanoic acids could be obtained from a C-2 addition to 2-halophenylpropyl halides.

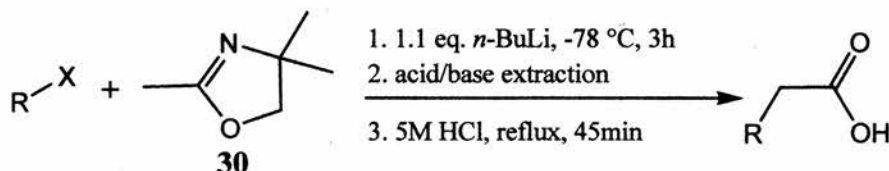
Therefore, as previously mentioned, the alkyl chain will have to be extended in order to afford the desired acids. Usually chain elongation methodology involves the addition of either a C-1 unit derived from the cyanide anion, or a C-2 unit derived from either diethyl malonate or ethylene oxide addition.⁸ Any reactions involving cyanide come with the inevitable safety concerns and restrictive protocols, therefore cyanide chemistry was avoided. Addition of a C-2 unit via malonate is technically

simple although widely variable in yield, mainly due to the de-esterification, decarboxylation step, which can be inefficient with certain substrates (Scheme 75).



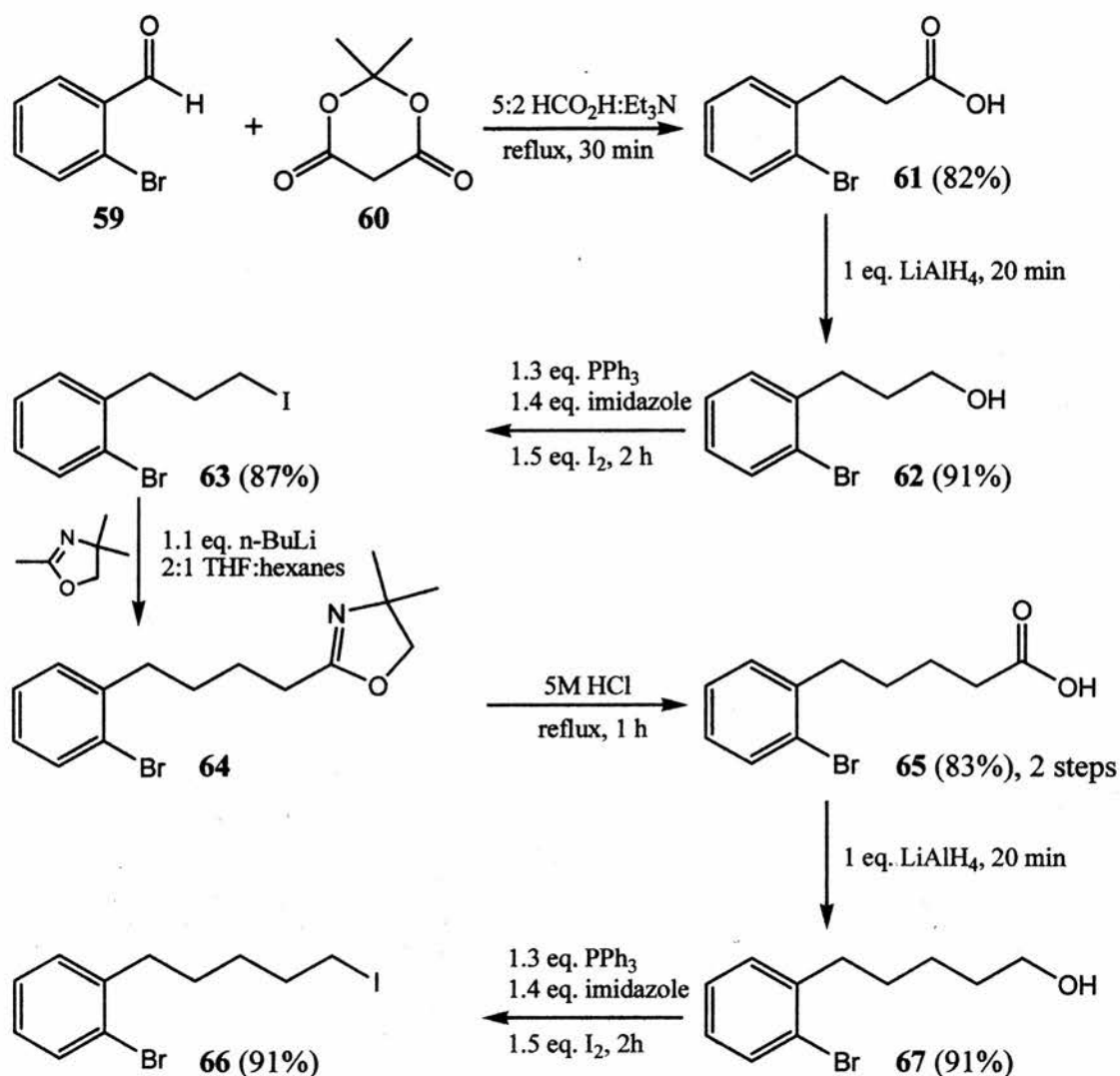
Scheme 75

The addition of alkyl halides to 2,4,4-trimethyl-2-oxazoline **30** is a well documented reaction with the product of said reaction being crudely purified (estimated >95 % by NMR) via an acid/base extraction (possibly due to the solubility of the oxazoline HCl salt in dilute acid).⁹ This reaction procedure, together with the knowledge that oxazolines are hydrolysed to the corresponding carboxylic acid in high yield using refluxing 5M HCl (usually within one hour), gives the possibility of a two step C-2 chain elongation protocol (Scheme 76). When this protocol is compared with the malonate method, it would seem it has distinct advantages such as the need for only one reflux and relatively mild reaction conditions. Also the experience of 2-halophenylalkyl iodides coupling with 2-oxazolines, acquired in this research, makes this the preferred, albeit non-conventional, method of C-2 chain elongation (see Section 2.1.2.1).



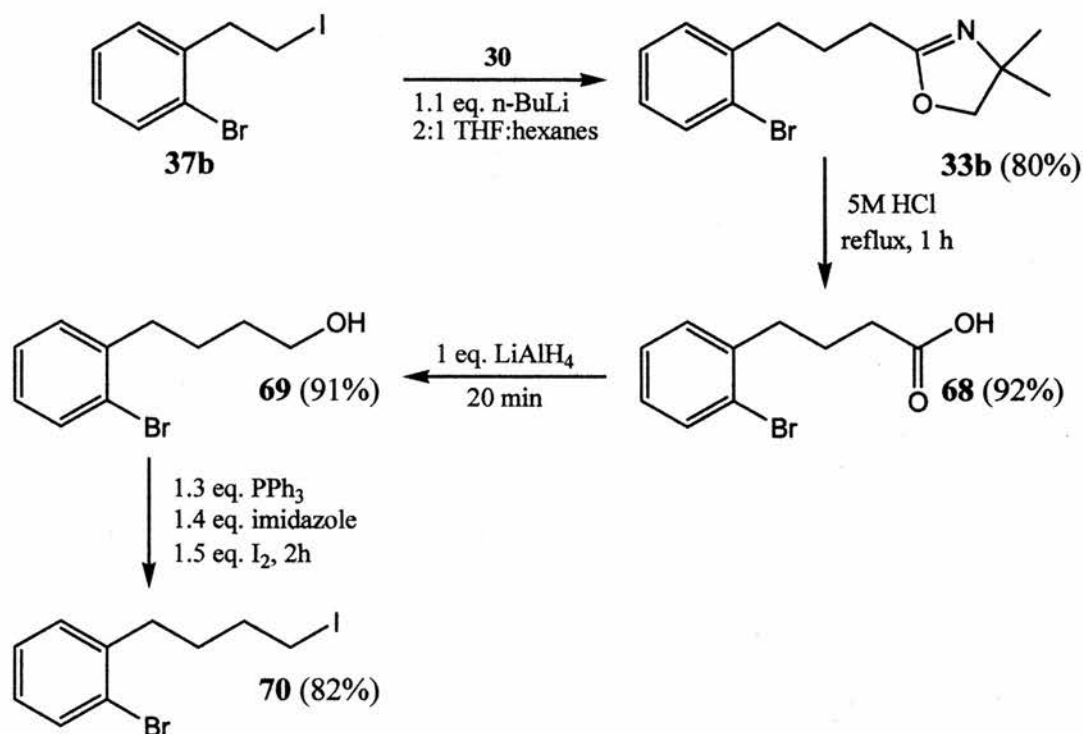
Scheme 76

Having designed a viable synthetic route to 2 halophenylpropanoic acids and 2-halophenylpentanoic acid and thus 2-halophenylpropyl iodides and 2-halophenylpentyl iodides, the syntheses were carried out with bromine as the aromatic halogen (Scheme 77). As shown in Scheme 77, 2-bromophenylpropyl iodide **63** was successfully prepared from 2-bromobenzaldehyde in an excellent overall yield of 65% following 3 synthetic steps. Similarly 2 bromophenylpentyl iodide **67** was prepared in an exceptional overall yield of 45% after 7 steps. It is worth noting that the only purifications employed were standard aqueous work-ups, except in the iodide formation steps, in which case a simple SiO₂ chromatographic column using pure hexane as the eluant was used. This was possible due to the purity of the reaction products after work up, typically >95 % as determined by NMR spectroscopy.



Scheme 77

Having firmly established the synthetic methodology, 2-bromophenylbutyl iodide **70** was obtained from the previously prepared 2-bromophenylethyl iodide **37b** in a good overall yield of 41% after 6 steps from the commercially available 2-bromophenylacetic acid **40b**.

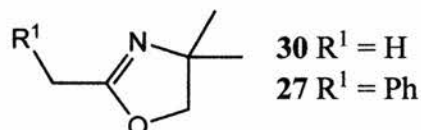


Scheme 78

2.1.2 Preparation of 2-Oxazolines from 1,2-Aminoalcohols

Having successfully completed the synthesis of the required 2-halophenylalkyl halides, the 2-oxazoline portion needs to be synthesised in order to obtain the desired 2-(2-halophenylalkyl)-2-oxazolines. Both achiral and chiral 2-oxazolines will be synthesised.

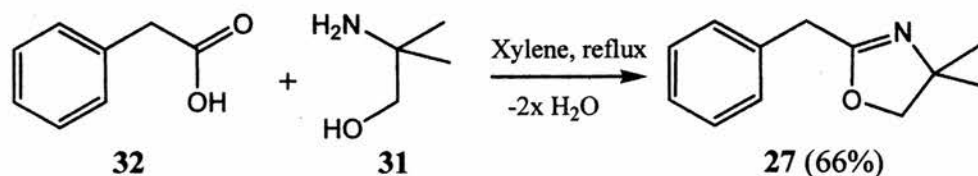
2.1.2.1 Non-chiral 2-Oxazolines



Scheme 79

Historically the most common non-chiral 2-oxazolines are the 4,4-dimethyl-2-oxazolines. These are generally obtained via condensation of 2-amino-2-methylpropan-1-ol **31** with the appropriate acid⁹ or nitrile,¹⁰ although many other synthetic routes have been used, including dehydration of β -hydroxyamides with thionyl chloride.¹¹ As 2,4,4-trimethyl-2-oxazoline **30** is available commercially, only

the structural analogue **27** needed to be synthesised (Scheme 79). Therefore 2-benzyl-4,4-dimethyl-2-oxazoline **27** was synthesised via condensation of 2-amino-2-methylpropan-1-ol **31** with phenylacetic acid **32** using a Dean-Stark trap to remove water generated *in situ*, as detailed in the literature (Scheme 80).^{11d}



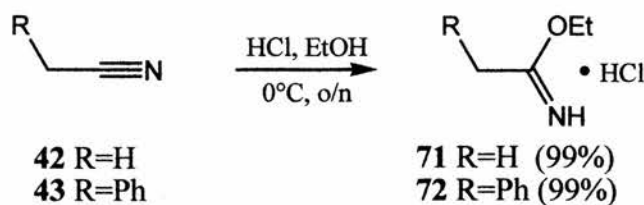
Scheme 80

The decision to use this method was based upon an evaluation of the variety of synthetic modes, carried out by S. Cobb in preliminary work.¹² Of all the procedures this condensation gave the highest observed yield (66%).

2.1.2.2 Chiral 2-Oxazolines

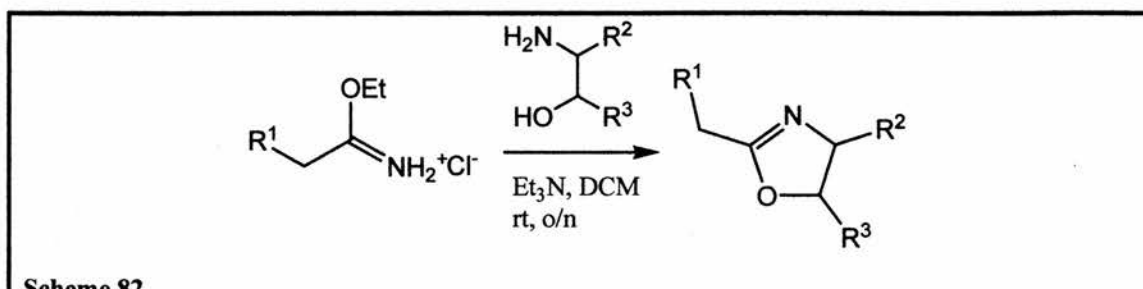
It was found that the one step process was useful for preparation of simple achiral 2-oxazolines, but the condensation conditions (refluxing in xylene for hours) were too harsh generally to afford pure chiral 2-oxazolines.

In the literature the preferred method for the synthesis of chiral 2-oxazolines, chosen by Meyers, was the condensation of an acetimidate ester, or its hydrochloride salt, with a 1,2-aminoalcohol.¹³ Acetimidate ester hydrochlorides are easily hydrolysed to the corresponding acetates, but when stored under anhydrous conditions in a dessicator they are still viable after 5 years. The synthesis of acetimidate ester hydrochlorides is very easy in large (molar) quantities from the corresponding nitrile and alcohol with excellent yields and 100% atom efficiency (Scheme 81). As only 2-benzyl and 2-methyl substituted 2-oxazolines were required, it was convenient to prepare one mole quantities of the two precursor acetimidate ethyl ester hydrochlorides **71** & **72**, from acetonitrile **42** and benzyl cyanide **43**, using the conditions shown in Scheme 81.



Scheme 81

Thus made, the two acetimidate salts **71** & **72** were combined with various chiral 1,2-aminoalcohols to afford chiral 2-oxazolines (Table 1). The acetimidate ethyl ester hydrochlorides were generally used as the free base by the *in situ* addition of 1 eq. triethylamine and similarly, where the aminoalcohol was obtained as the hydrochloride, *in situ* addition of triethylamine afforded the free amine also.



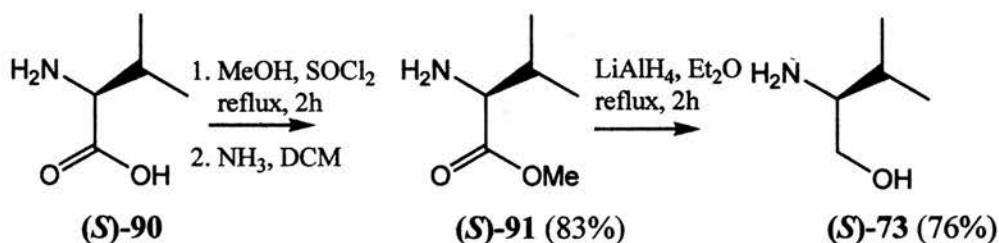
Scheme 82

Entry	A. Alcohol	R ¹	R ²	R ³	2-oxazoline	Yield/%
1	(<i>S</i>)- 73	H	<i>iso</i> -propyl	H	(<i>S</i>)- 81	60
2	(<i>S</i>)- 73	Ph	<i>iso</i> -propyl	H	(<i>S</i>)- 82	59
3	(<i>R</i>)- 73	Ph	<i>iso</i> -propyl	H	(<i>R</i>)- 82	33
4	(<i>S</i>)- 74	Ph	<i>tert</i> -butyl	H	(<i>S</i>)- 83	33
5	(<i>R</i>)- 74	Ph	<i>tert</i> -butyl	H	(<i>R</i>)- 83	34
6	(<i>S</i>)- 75	Ph	Ph	H	(<i>S</i>)- 84	75
7	(<i>S</i>)- 76	Ph	Bn	H	(<i>S</i>)- 85	55
8	(<i>S</i>)- 77	Ph	<i>c</i> -C ₆ H ₁₁ CH ₂	H	(<i>S</i>)- 86	56
9	(<i>S</i>)- 78	Ph	CO ₂ Me	H	(<i>S</i>)- 87	30
10	(<i>S,S</i>)- 79	Ph	CH ₂ OMe	Ph	(<i>S,S</i>)- 88	85
11	(<i>S</i>)- 80 *	Ph	CPh ₂ OH	H	(<i>S</i>)- 89	50

Table 2

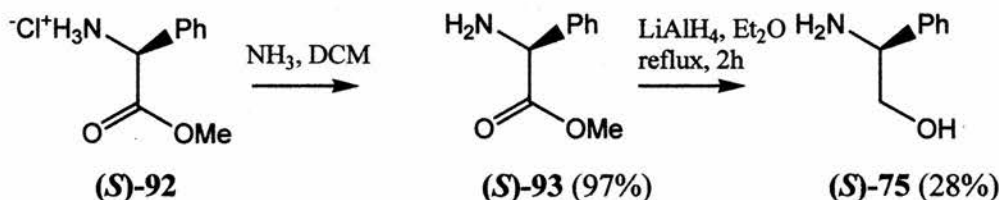
Synthesis of chiral 2-oxazolines from condensation of 1,2-aminoalcohols and acetimidate esters. * Oxazoline was formed from pre-existing 2-oxazoline (*S*)-**87** via reaction with PhMgBr.

Aminoalcohols (*S*)-**74**, (*S*)-**76**, (*S*)-**77**, (*S*)-**78**, (*R*)-**73** and (*R*)-**74** were all commercially available either as hydrochloride salts or as the free base, and they were used as obtained. (*S*)-Valinol (*S*)-**73**, was prepared in three steps from (*S*)-valine (*S*)-**90** in an overall yield of 63% (Scheme 83). Direct reduction of (*S*)-**90** to the alcohol was attempted but proved to be troublesome and required extremely harsh conditions (1.5 eq. LiAlH₄, THF reflux 4 days) chiefly because of the zwitterionic nature of the amino acid. However, conversion to the methyl ester (*S*)-**91** enabled a cleaner and milder reduction (1 eq. LiAlH₄, Et₂O, 2 h, reflux).



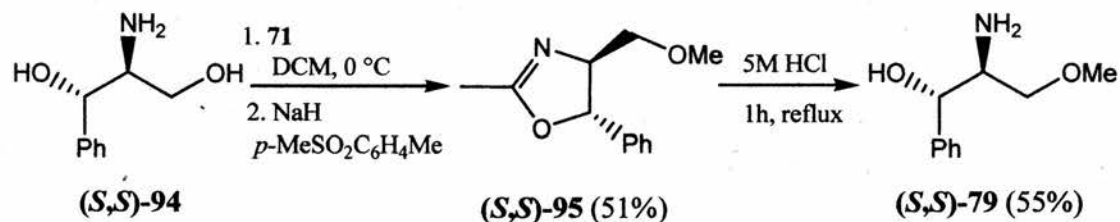
Scheme 83

Similarly phenylglycinol (**S**)-75 was synthesised by the reduction of phenylglycine methyl ester (**S**)-93 (Scheme 84).



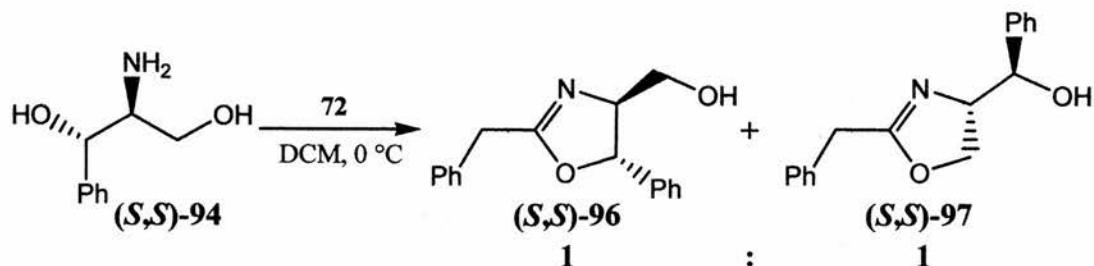
Scheme 84

Formation of aminoalcohol (**S,S**)-79 was via the 2-methyl-2-oxazoline (**S,S**)-95, which in turn was derived from commercially available (**S,S**)-2-amino-1-phenylpropane-1,3-diol (**S,S**)-94 (Scheme 85).



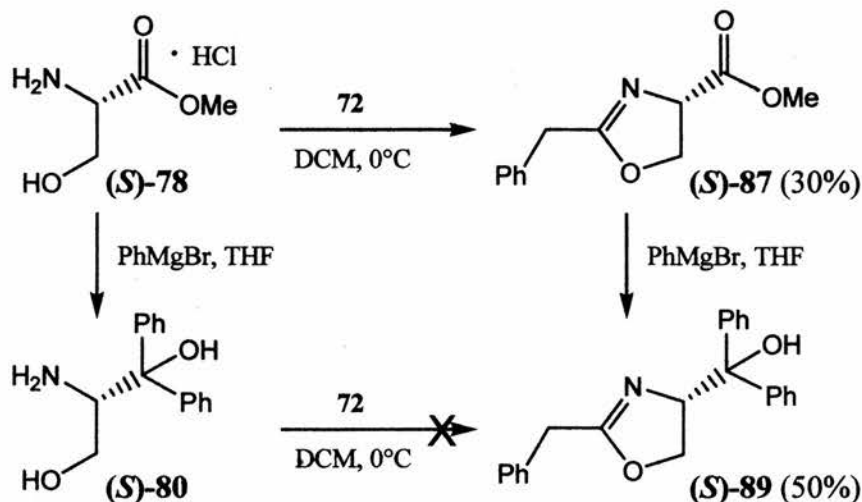
Scheme 85

This route was devised by Meyers *et al.* and oxazolines of this type are known as Meyers' oxazolines.¹⁴ The direct two step formation of Meyers' oxazoline (**S,S**)-88 (Scheme 86) is precluded due to the formation of an almost equal mixture of regioisomers when (**S,S**)-94 is reacted with 72, whereas the reaction of acetimidate ester 71 with propanediol (**S,S**)-94 proceeded with almost exclusive formation of the desired regioisomer. The small amount of the undesired isomer (< ca. 10 %) was easily removed by crystallisation.



Scheme 86

Diphenylmethanol substituted 2-oxazoline (**S**)-**89** was prepared from serine derived oxazoline (**S**)-**87**, the direct reaction of the corresponding aminoalcohol (**S**)-**80** with the phenylacetimidate ester **72** being inefficient (Scheme 87).

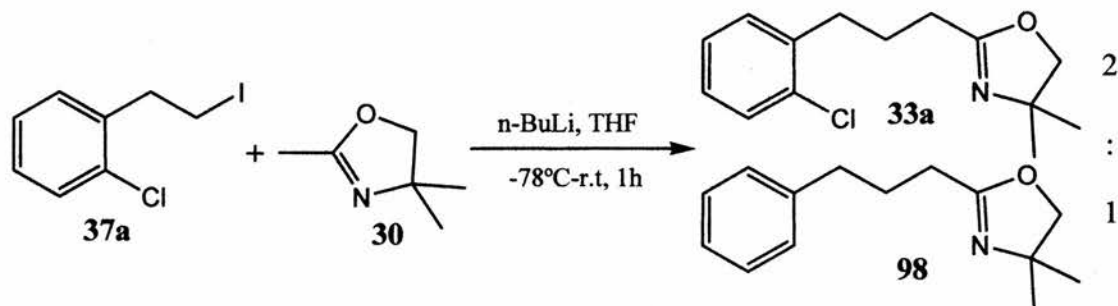


Scheme 87

2.1.3 2-[3-(2-Halophenyl)propyl]-2-oxazolines

Following completion of the 2-haloaromatic and 2-oxazoline portions of the desired 2-(2-halophenylalkyl)-2-oxazolines, coupling of the two sections was next accomplished.

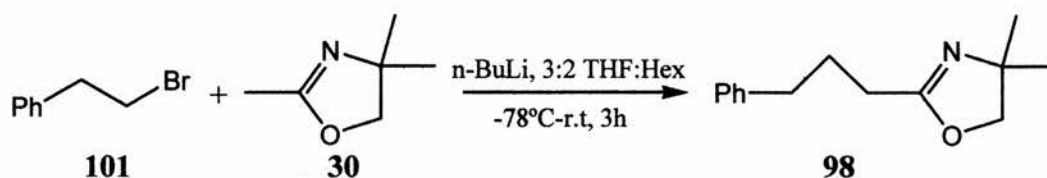
Preparation of 2-[3-(2-chlorophenyl)propyl]-4,4-dimethyl-2-oxazoline **33a** was attempted by coupling iodide **37a** with 2,4,4-trimethyloxazoline **30** using 1 eq. of *n*-BuLi at -78 °C. The initial attempt revealed a 2:1 mixture of products. Analysis showed the major product to be the anticipated oxazoline **33a** and the minor product as 2-(3-phenylpropyl)-4,4-dimethyl-2-oxazoline **98**, presumably deriving from lithium halogen exchange followed by protonation (Scheme 88). Attempted separation of the mixture via column chromatography unfortunately failed.



Scheme 88

dimerisation, the reaction has to be carried out at $-78\text{ }^{\circ}\text{C}$. Because it was difficult to transfer via canula while maintaining a stable low temperature, another possible solution was investigated i.e. the solvent system.

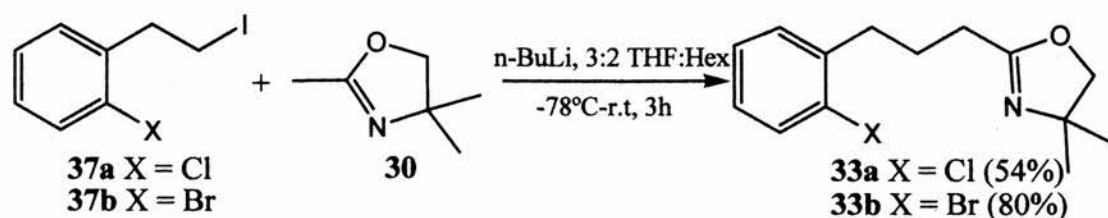
An examination of the solvent system employed by Meyers *et al*¹⁶ revealed the reactions with *n*-BuLi were carried out in a less polar solvent system. We used a 2.5 M *n*-BuLi solution in hexanes whereas Meyers used 1.6 M *n*-BuLi solution in hexanes. This difference results in hexane accounting for a higher portion of the overall solvent volume in Meyers' reactions, and therefore results in a less polar solvent system. Analysis revealed Meyers' overall solvent mixture was 3:2 THF:hexanes, whereas we used a 4:1 THF:hexanes combination. After adjustments were calculated to harmonize our solvent system with that of Meyers', a test reaction was carried out with phenethyl bromide **101** instead of iodide **37a** (Scheme 90).



Scheme 90

Dried and distilled hexane was added to the initial THF solution of oxazoline **30** in order to reduce the solvent polarity to match Meyers and thus on the addition of 2.5M *n*-BuLi solution in hexanes the resulting solvent mixture would result in a 3:2 ratio of THF to hexanes. The $^1\text{H-NMR}$ spectrum of the crude mixture was examined and found to be exceptionally clean, containing mainly the correct product and a small amount of starting material, thus proving that the reaction proceeded smoothly in the reduced polarity solvent to give predominantly the expected product.

Given this encouraging result, the reaction was repeated using the original iodide **37a**. The $^1\text{H-NMR}$ spectrum revealed the crude reaction mixture to contain almost exclusively the desired oxazoline **33a**. The minor impurities were 2-chlorostyrene (~2%) and 2-chlorophenethyl iodide **37a**. Most importantly, the crude reaction mixture did not contain the dehalogenated product **98**. Column chromatography afforded the pure substituted 2-propyl-4,4-dimethyl-2-oxazoline **33a** in a moderate yield of 54% (Scheme 91).



Scheme 91

Using the developed reaction conditions, 2-bromophenethyl iodide **37b** was added to azaenolate **99** to afford oxazoline **33b** in a good yield of 80% (Scheme 91).

2.1.4 2-[3-(2-Halophenyl)-1-phenylpropyl]-2-oxazolines

Iodide **37a** was reacted with the azaenolate of 2-benzyl-4,4-dimethyl-2-oxazoline **27**, using previously derived reaction conditions (Section 2.1.3, Scheme 91). After column chromatography of the crude mixture, the $^1\text{H-NMR}$ spectrum of the major product contained 9 signals, these were 1.27 (3H, s), 1.28 (3H, s), 2.07-2.19 (1H, m), 2.32-2.44 (1H, m), 2.63-2.80 (2H, m), 3.60 (1H, t, $J=7.8$), 3.87 (2H, s), 7.07-7.20 (3H, m) and 7.22-7.37 (6H, m). The product oxazoline **34a** was expected to contain 8 signals in its $^1\text{H-NMR}$ spectrum. The mass spectrum revealed a MH^+ peak of 328, with MH^+ and MH^+2 in a 3:1 ratio which is consistent with a molecule containing a single chlorine atom. The accurate mass of the MH^+ peak was consistent to 3 ppm with the molecular formula $\text{C}_{20}\text{H}_{23}\text{NO}^{35}\text{Cl}$, expected of oxazoline **34a**. The aromatic resonances at 7.07-7.20 & 7.22-7.37 ppm with a total integration of 9 are consistent with one phenyl ring plus a di-substituted aromatic ring. Characteristic peaks of the 2-oxazoline moiety were present at 1.27, 1.28, and 3.87 ppm corresponding to the bis methyls and methylene alpha to the oxygen. The remaining signals at 2.07-2.19, 2.32-2.44, 2.63-2.80 & 3.60 have a total integration of five which accords with the C3 aliphatic chain present in **34a**. In order to clarify the aliphatic signals more clearly a $^1\text{H-}^1\text{H}$ COSY experiment was carried out; a portion of the resultant spectrum is detailed in Figure 1.

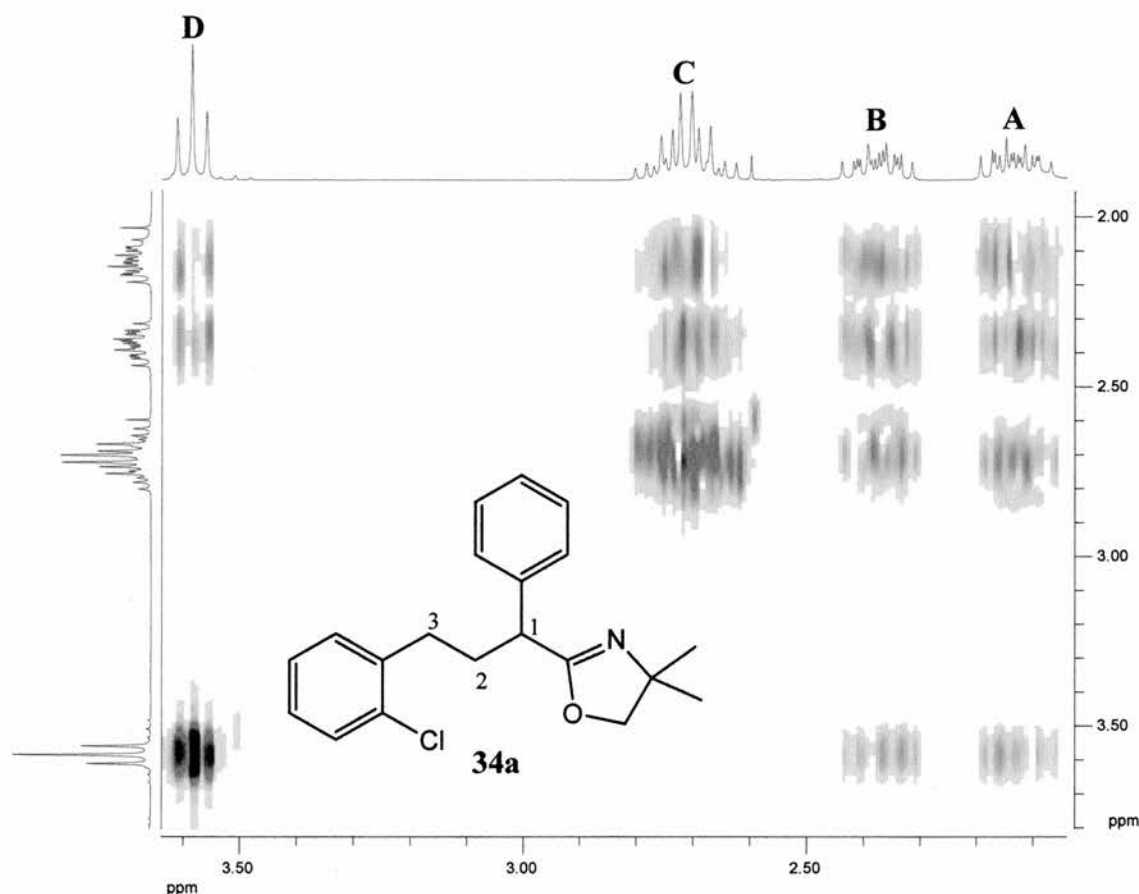


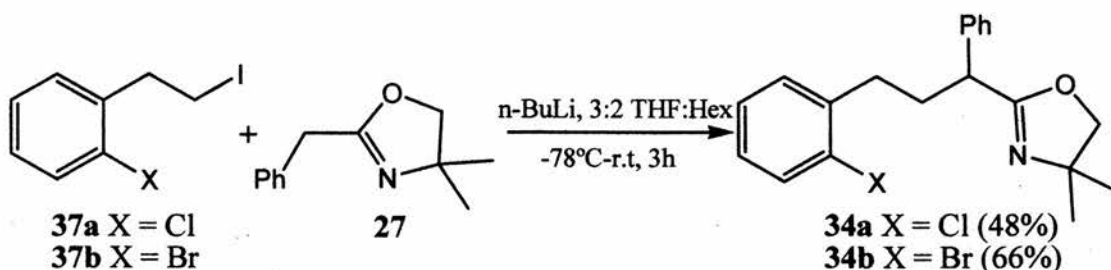
Figure 1 Aliphatic region of COSY spectrum of substituted 2-oxazoline **34a**.

ID	Integration	Correlation	Carbon
A	1	B, C & D	2
B	1	A, C & D	2
C	2	A & B	3
D	1	A & B	1

Table 3 Summary of aliphatic correlations in the COSY spectrum of **34a**.

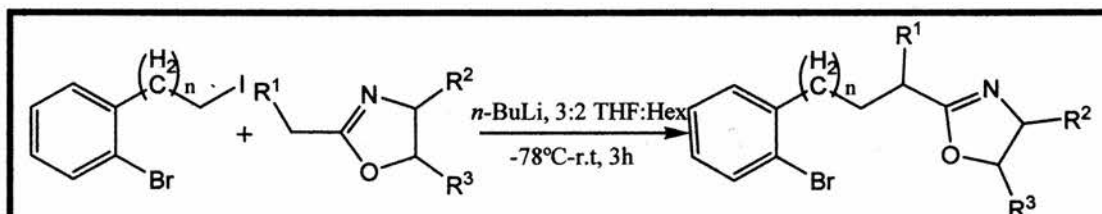
Assignment of ^1H resonance D with C-1 hydrogen is evident due to the triplet nature of the signal and the integration value of 1 and also the down field nature of the chemical shift. Signal D is correlated to signals A & B which is consistent with signals A & B being due to the hydrogens of C-2, as the hydrogens can reasonably be expected to be non-equivalent due to the presence of the stereotopic carbon C-1. Signal C only correlates with A & B which is concordant with it being due to carbon 3. Confirmation of this assignment was obtained via ^{13}C NMR and IR (This is detailed in the experimental section). A summary of the assignments of the aliphatic

signals is set out in Table 3. Clearly, this evidence shows that the required product had been formed in a moderate yield of 48% (Scheme 92).



Scheme 92

2-Bromophenethyl iodide **37b** was reacted in the same way with oxazoline **27** to give substituted 2-propyl-4,4-dimethyl-2-oxazoline **34b** in a good yield of 66%. The $^1\text{H-NMR}$ spectrum was very similar to that of oxazoline **34a**, the major difference being in the aromatic region, in which were observed three signals with integrals of 1:7:1 which is typical, in this class of compounds, of an *o*-bromo substituted aromatic ring plus a phenyl ring.



Scheme 93

ID	R ¹	R ²	R ³	n	Yield/%
(S)-102	H	<i>iso</i> -propyl	H	1	50
(S)-103	Ph	<i>iso</i> -propyl	H	1	71
(R)-103	Ph	<i>iso</i> -propyl	H	1	68
(S)-104	Ph	<i>tert</i> -butyl	H	1	72
(R)-104	Ph	<i>tert</i> -butyl	H	1	80
(S)-105	Ph	Ph	H	1	40
(S)-106	Ph	Bn	H	1	88
(S)-107	Ph	<i>c</i> -C ₆ H ₁₁ CH ₂	H	1	49
(S,S)-108	Ph	CH ₂ OMe	Ph	1	55
(S)-109	Ph	CPh ₂ OH	H	1	41
110	Ph	2xCH ₃	H	2	69
111	Ph	2xCH ₃	H	3	60
112	Ph	2xCH ₃	H	4	61

Table 4

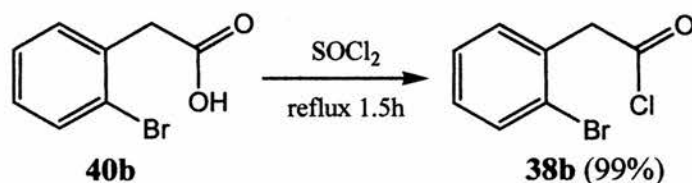
Having now established a viable protocol for substitution at the 2-position of the 2-oxazoline ring, a wide variety of different substituted oxazolines were prepared via the coupling of combinations of the previously prepared 2-oxazolines and 2-halophenylalkyl halides. The results of these combinations are detailed in Table 4.

With only a few exceptions, yields were above 60 % and, as expected, were essentially independent of the length of the alkyl chain. In cases where a new stereogenic centre was generated during coupling ($R^1 = Ph$) the product was formed as a mixture of inseparable diastereoisomers. The diastereoselectivities obtained were in the range 0 to 34 %.

2.2 3-Substituted 1-(2-Oxazolin-2-yl)-propen-2-ols

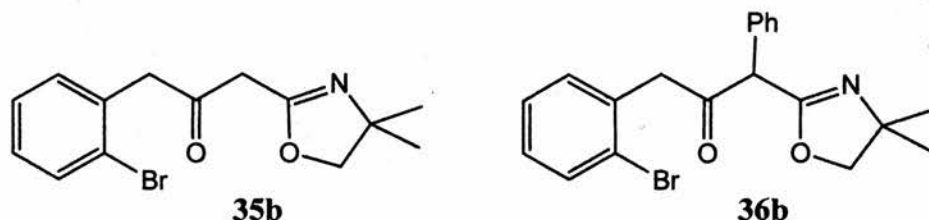
2.2.1 2-Bromophenylacetyl Chloride

2-Bromophenylacetyl chloride **38b** was synthesised in the usual way for acid chlorides from 2-bromophenylacetic acid **40b** in quantitative yield. After the excess thionyl chloride was removed the crude product was used without further purification (Scheme 94).



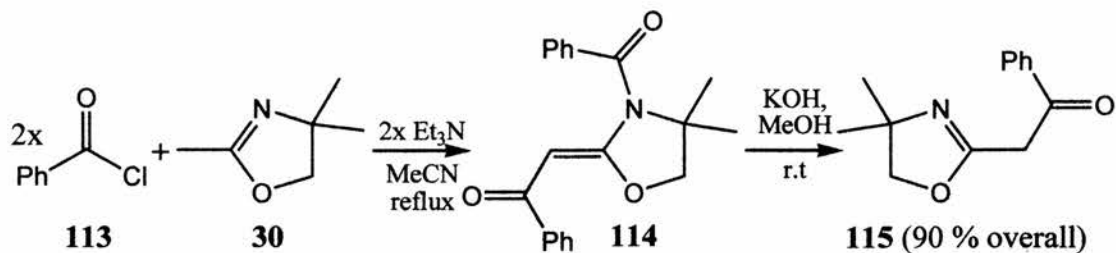
Scheme 94

2.2.2 Substituted Propen-2-ols



Scheme 95

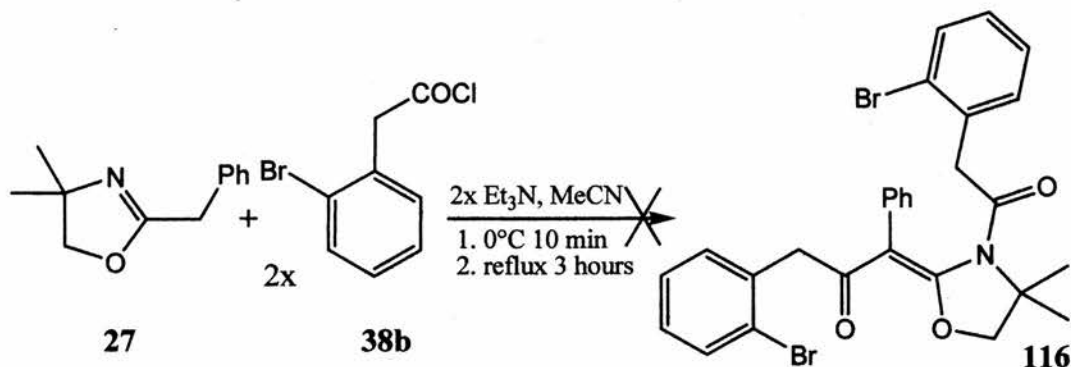
Two approaches to the synthesis of substituted oxazolines **35b** & **36b** from 2-bromophenylacetyl chloride **38b** were evaluated. The first approach had been previously employed by Tohda *et al.*¹⁷ to synthesise oxazolinyl ketone **115** (Scheme 96). The second approach involves the reaction of 2-bromophenylacetyl chloride **38b** with the aza-enolate of the appropriate oxazoline.



Scheme 96

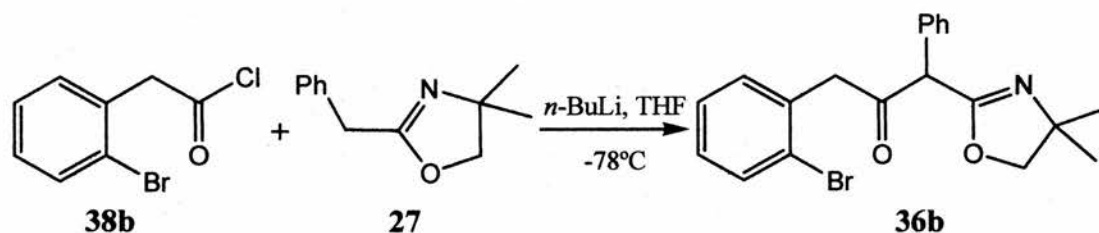
The di-acylation reaction of 2,4,4-trimethyl-2-oxazoline **30** with acid chloride **38b** using triethylamine gave mainly unreacted 2-oxazoline **27** plus multiple

unidentified products containing an aromatic moiety (Scheme 97). Tohda *et al.* reported success of this reaction with the following groups: C₆H₅, *p*-O₂NC₆H₄, 2-furyl, *t*-C₄H₉.



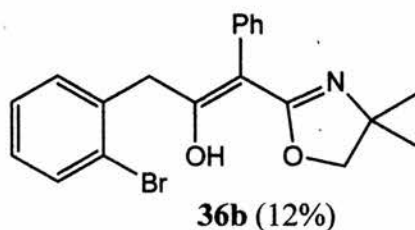
Scheme 97

Further discussion by Tohda *et al.* revealed that acid chlorides with alpha protons decompose under the reaction conditions, which could explain the plethora of aromatic by-products observed. Therefore further attempts to synthesis oxazolines **35b** and **36b** were not made using this procedure.



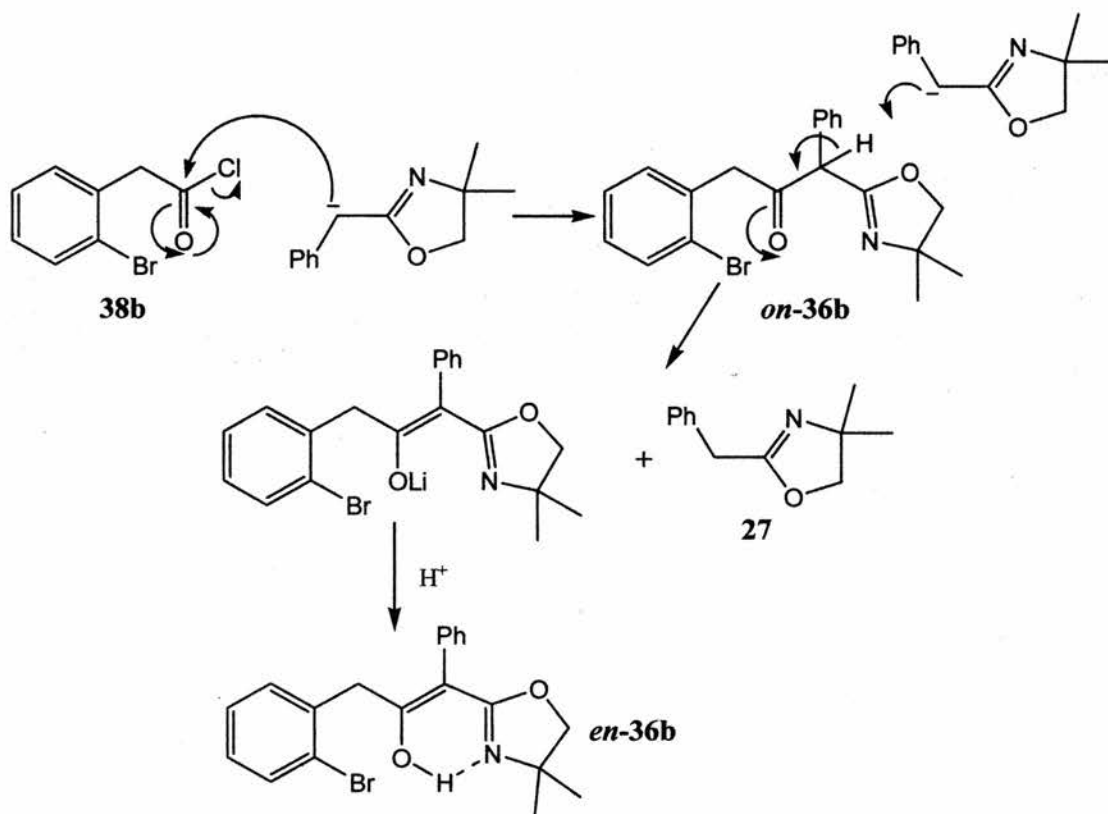
Scheme 98

The reaction of benzyl-2-oxazoline **27** and acid chloride **38b** facilitated by *n*-BuLi (Scheme 98) gave a product which contained four singlet signals 1.38ppm (6H), 3.70 ppm (2H), 4.05 (2H) & 10.22 (1H), also aromatic signals equating to nine hydrogens in the ¹H-NMR spectrum. The signal at 10.22 ppm was broad which could be indicative of a carboxylic acid, enol or aldehyde. Accurate mass measurements were consistent to 2.5 ppm with the formula C₂₀H₂₀NO₂Br which is in accord with the proposed product. The ¹³C-NMR spectrum showed the expected peaks for the anticipated structure. Therefore it was tentatively concluded that the substituted oxazoline **36b** exists exclusively in the enol form which is supported by the spectroscopic evidence (Scheme 99). Also research in the literature revealed that some β-keto-2-oxazolines do in fact exist as the enol tautomers.¹⁷



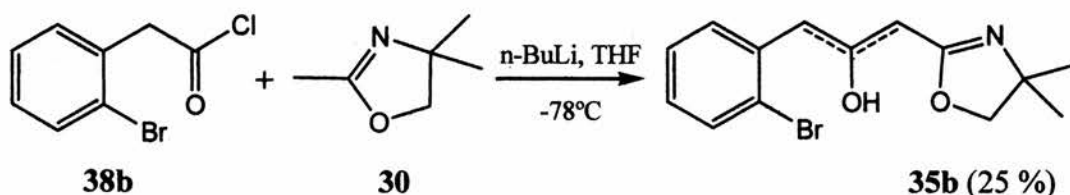
Scheme 99

The poor yield of the reaction can be explained as a combination of two factors, one being problems relating to isolation. The second factor is proposed to be that the acidity of the product formed is greater than the lithio azaenolate of 2-oxazoline **27**, which would result in the product being deprotonated as soon as it is formed. This would lead to loss of the active azaenolate reactant and therefore lower the overall yield of the reaction (Scheme 100).



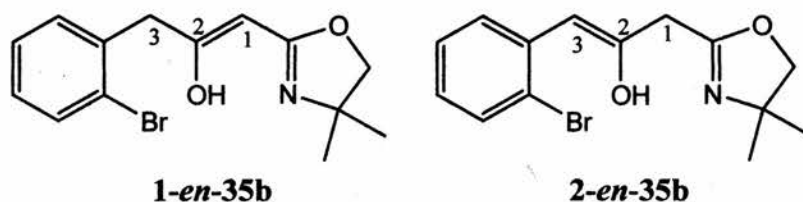
Scheme 100

The E/Z configuration of the double bond was unknown but it was proposed that it is Z due to the possible hydrogen bonding interaction between the enolic hydrogen and the nitrogen lone pair.



Scheme 101

In the same way oxazoline **30** was reacted with acid chloride **38b** to give enol **35b** (Scheme 101). Unfortunately due to the absence of a phenyl ring at the 2-position of the oxazoline, the location of the double bond could not be determined by one dimensional NMR spectroscopy (Scheme 102).



Scheme 102

In order to address this problem a two dimensional HMBC experiment was carried out. If C-3 is a methylene group, and thus the double bond is in the one position (**1-en-35b**, Scheme 102), then the two hydrogen singlet at 3.75 ppm (A) should show 3J couplings to the aromatic carbon signals (*ar*). Also the methine 1H -NMR signal at 4.82 ppm (B) should have couplings to carbon signals of the oxazoline (*ox*). Clearly the opposite holds true for the previous statements if the double bond is in the two position (**2-en-35b**, Scheme 102). Analysis of the HMBC spectrum showed that the 1H -NMR signal A does indeed show correlations to the aromatic carbon peaks (cross peaks i, Figure 2) but signal B doesn't show any correlations to any oxazoline or aromatic carbons. Only a weak correlation is observed to the enolic carbon C-2 (*en*) (cross peak ii, Figure 2) which is a weak 2J correlation between the methine 1H -NMR signal and the C-2 resonance. This lack of correlations could be due to the unavailability of any possible 3J couplings with the oxazoline ring. The only couplings possible are 2J and 4J , which are both weak in the HMBC spectrum. Based on this evidence it is probable that the product of reaction was **1-en-35b**.

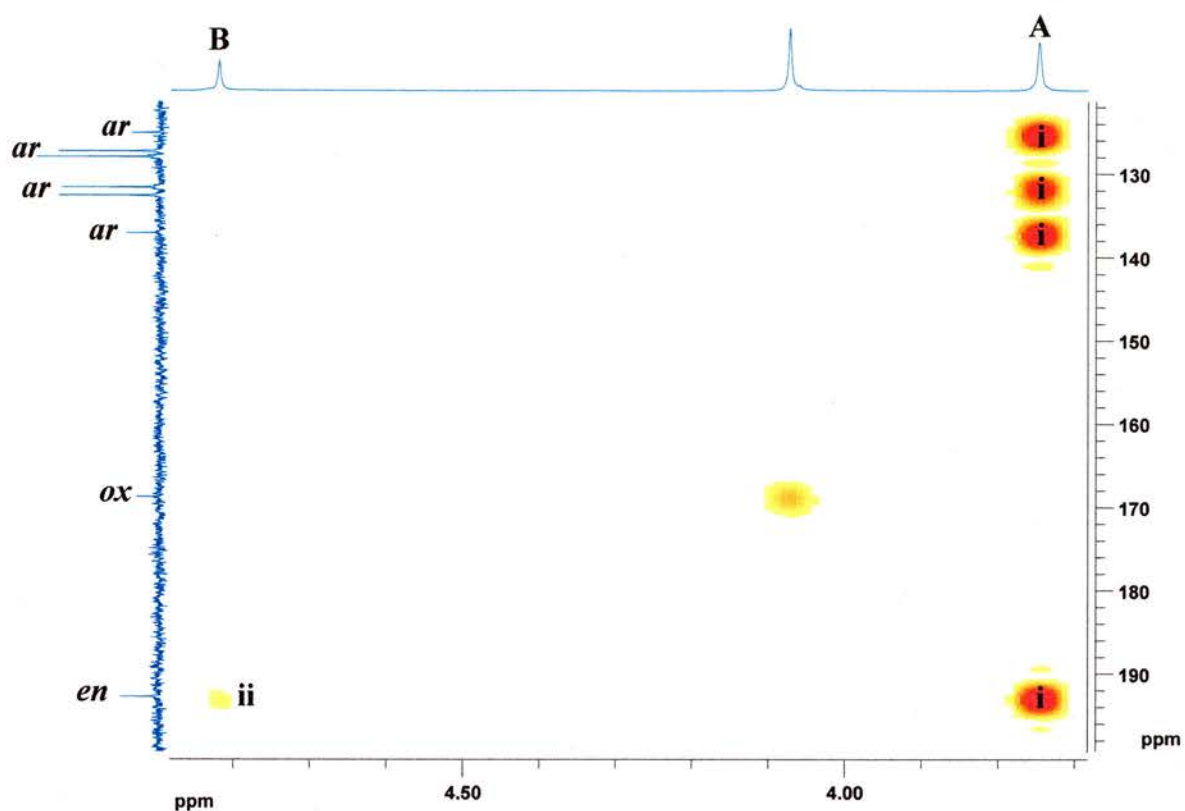
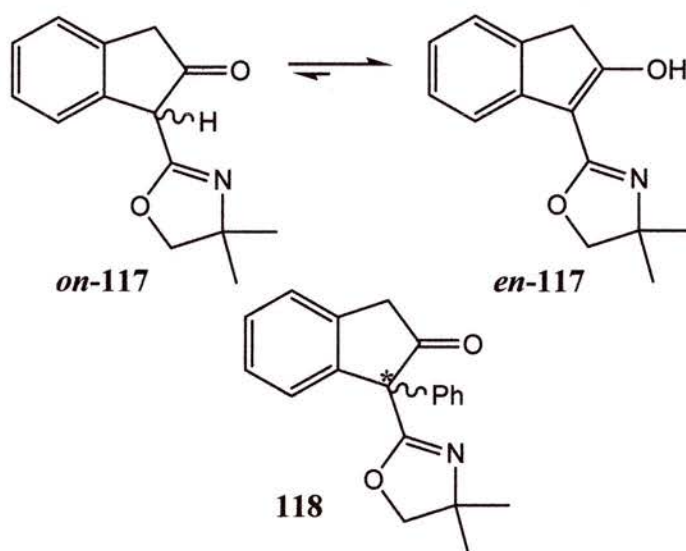


Figure 2 Region edited HMBC spectrum of propenol **35b**

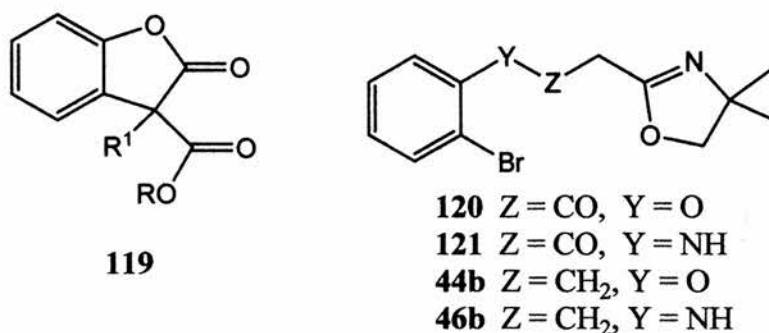
It was decided that no further interest would be taken in this class of compounds due to 2-oxazolines **35b** & **36b** existing in purely the enol form and thus not being suitable precursors for stereocontrol of $S_{RN}1$ chemistry.



Scheme 103

This is because the goal of a successful $S_{RN}1$ is to form a new chiral centre and cyclised indan-2-one **117** is expected to exist at least partly in enolic form after cyclisation which would result in loss of any stereochemical information gained (Scheme 103). Although indan-2-one **118** can only exist in the keto form (Scheme 103) due to the presence of the quaternary centre, it was felt that the low yield and difficulty of isolation precluded it also.

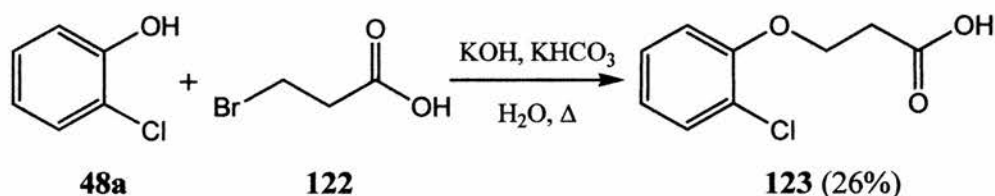
2.3 Hetero Atom Analogues of Arylalkyloxazolines



Scheme 104

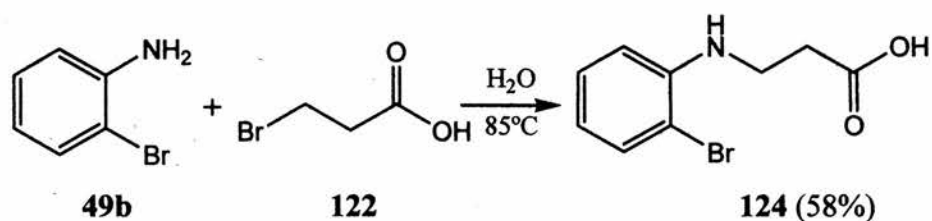
It is well known that many biological molecules include heteroatom containing rings with diverse functionality. A new method for forming cycles of this type would enhance the value of this field of synthetic methodology. For example, the simple lactone **119** has been shown to exhibit anticancer activity (Scheme 104). It is envisaged that this core structure could be synthesised by the S_{RN}1 ring closure of ester **120**. Attempts were made to synthesise ester **120** and the close analogues **121**, **44b** & **46b** (Scheme 104). The retrosynthetic analysis of this class of compounds is shown in Section 1.4.1.

2.3.1 N-Substituted Anilines and O-Substituted Phenols



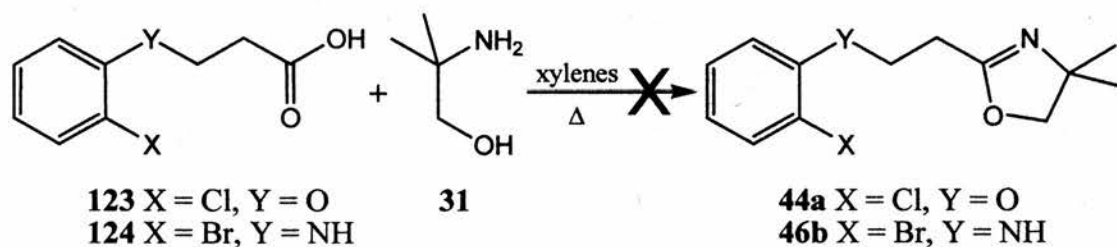
Scheme 105

Initially an attempt at synthesising the chloro analogue of **44** was made due to our having 2-chlorophenol **48a** at hand. The synthesis of aryloxyl acid **123** was achieved by refluxing 3-bromopropionic acid **122** in a basic aqueous solution with 2-chlorophenol **48a** for 2 hours (Scheme 105).¹⁸ Unfortunately some difficulty was encountered in the isolation of the acid from the aqueous reaction mixture and this was the cause of the poor yield (26 %).



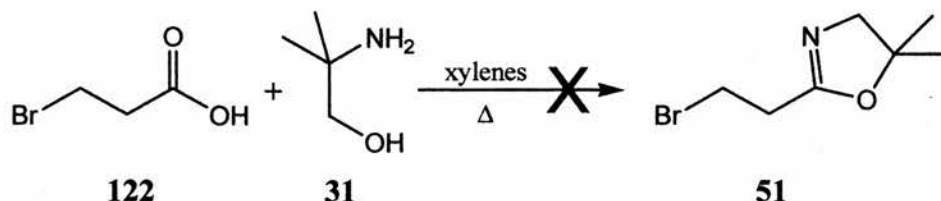
Scheme 106

β -Amino acid **124** was prepared from 2-bromoaniline **49b** by heating in water with bromoacetic acid **122** (Scheme 106). Difficulty was again encountered with the isolation of the product. The pH of the reaction mixture was found to be critical, with the product precipitating from aqueous media as the free base at pH 4. Neither the anilino nor the carboxy protons were evident in the $^1\text{H-NMR}$ spectrum (d^6 -acetone) over the normal spectral range (-0.5 – 12 ppm). This could be because of one of two reasons: firstly the anilino moiety could be protonated, in which case the resonance may occur at greater than 12 ppm; or secondly the protons of the aniline and carboxyl groups could be exchanging, in which case they may go unobserved. The $^{13}\text{C-NMR}$ spectrum showed the requisite number of resonances and the accurate mass was found to be correct.



Scheme 107

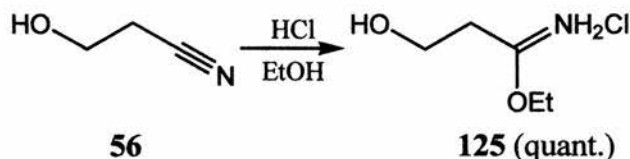
In order to form the desired oxazolines **44a** and **46b**, the acids **123** and **124** need to be condensed with aminoalcohol **31**. The traditional condensation route to 2-oxazolines via azeotropic removal of water resulted in intractable tarry mixtures being obtained in both cases (Scheme 107).



Scheme 108

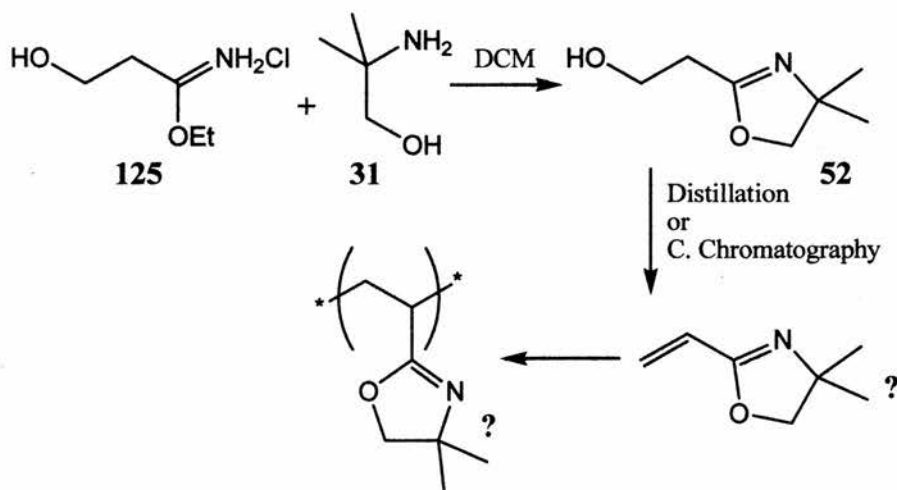
Due to the unsuccessful attempts to form the oxazoline functionality, post formation of the ether & amine linkages en route to **44a** and **46b**, it was decided to try

to pre-form the oxazoline first. 3-Bromopropionic acid **122** was heated under Dean-Stark conditions with aminoalcohol **31** but unfortunately no isolatable product was obtained (Scheme 108). The $^1\text{H-NMR}$ spectrum of the crude mixture suggested polymeric products had been formed. This was possibly due the elimination of HBr followed by polymerisation. Given the elimination problem it was decided to use the mild method of oxazoline formation, i.e. via the acetimidate ester. The corresponding alcohol was also used in the hope of curtailing any elimination reactions of the products.



Scheme 109

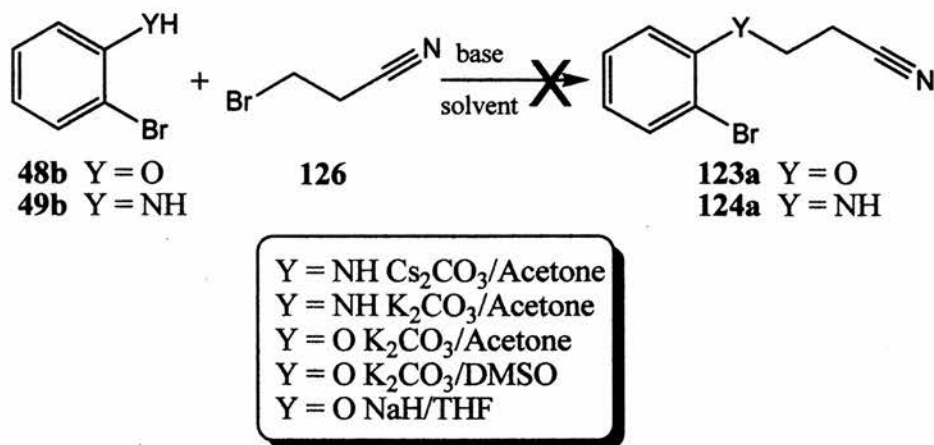
Therefore, 3-hydroxypropionitrile **56** was treated with ethanol and hydrogen chloride gas at $0\text{ }^\circ\text{C}$ as detailed in the literature¹⁹ to afford the imidate **125** in a quantitative yield (Scheme 109). The imidate **125** was then stirred in dichloromethane with aminoalcohol **31**. The crude $^1\text{H-NMR}$ spectrum clearly showed the presence of the product but all attempts to purify the oxazoline **52** led to a tarry product which gave a $^1\text{H-NMR}$ spectrum with broad peaks. This was assumed to be a polymer derived from elimination of water and subsequent polymerisation (Scheme 110).



Scheme 110

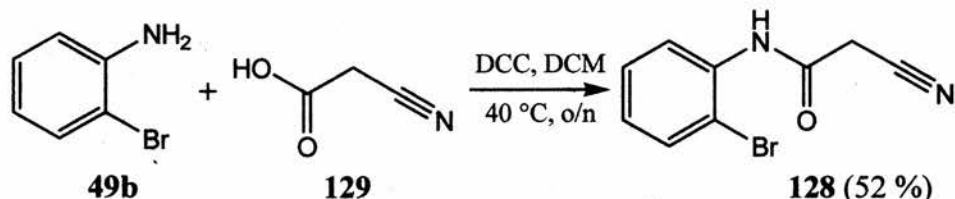
Given this failure an alternate tack was taken. It was envisaged that the nitriles **123a** & **124a** could be synthesised, followed by imidate formation to lead ultimately to the desired structures **44b** & **46b**. Various base-solvent combinations were employed to effect the coupling of phenol **48b** and aniline **49b** with 3-

bromopropionitrile **126**; unfortunately to no avail (Scheme 111). Possible alternate routes to **44b** and **46b** are discussed in section 2.3.3.



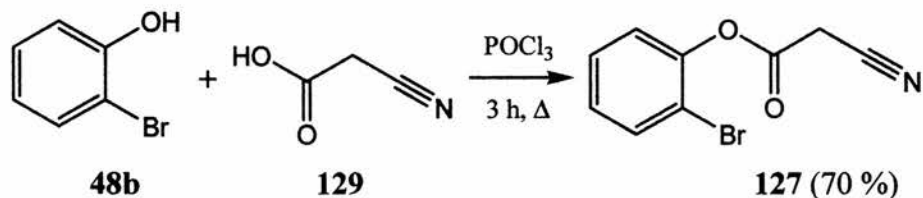
Scheme 111

2.3.2 α -Cyano Esters and Amides



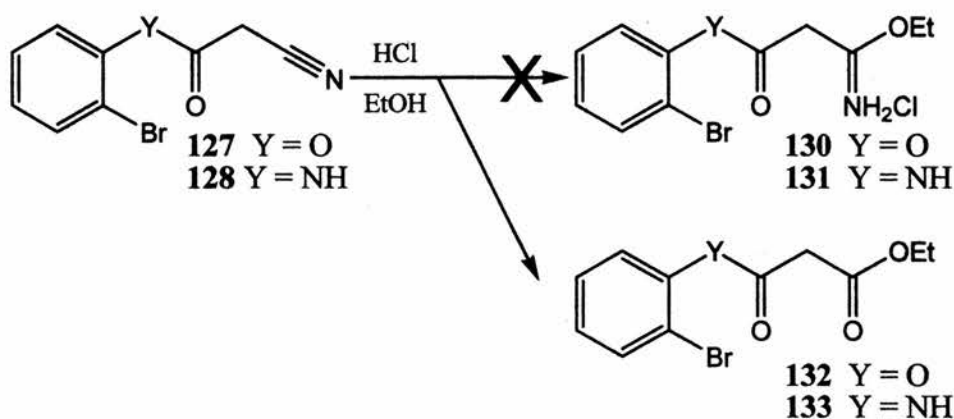
Scheme 112

Amide **128** was prepared via the DCC coupling of aniline **49b** and cyanoacetic acid **129** in moderate yield of 52 % (Scheme 112).²⁰ Similarly ester **127** was prepared from the phosphorus oxychloride promoted coupling of phenol **48b** and cyanoacetic acid **129** (Scheme 113).²¹



Scheme 113

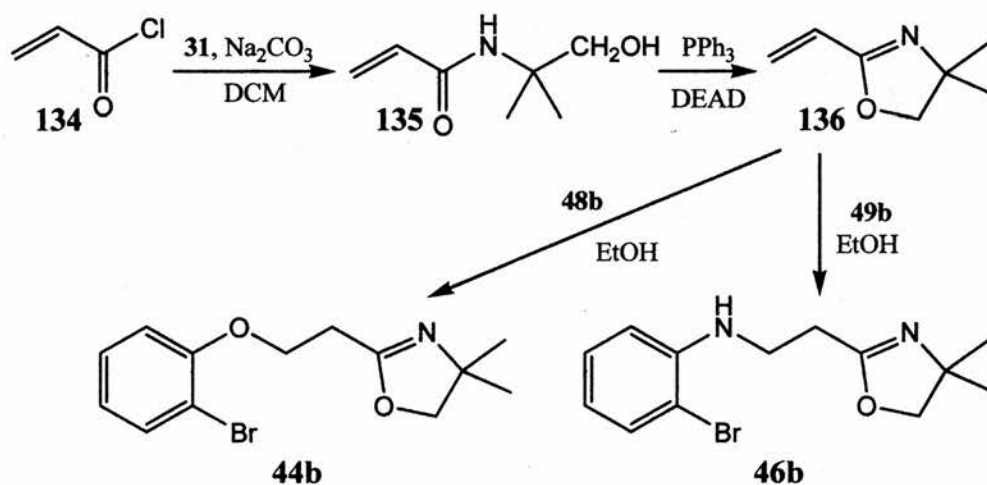
The cyanoacetamide **128** and cyanoester **127** were then treated with dry hydrogen chloride and “super dry”²² ethanol to yield disappointingly the corresponding ethylesters **132** and **133** (Scheme 114). It is thought that this failure is due to the immediate hydrolysis on any attempt to isolate the imidates **130** & **131** from the reaction solvent (ethanol).



Scheme 114

Several other methods of formation of the imidates of 130 and 131 were attempted. These included in situ generation of $\text{HCl}_{(g)}$ with incidental drying of the ethanol, facilitated by acetyl chloride in ethanol. However, little success was obtained. Viable alternate routes to the wanted 120 and 121 are discussed below.

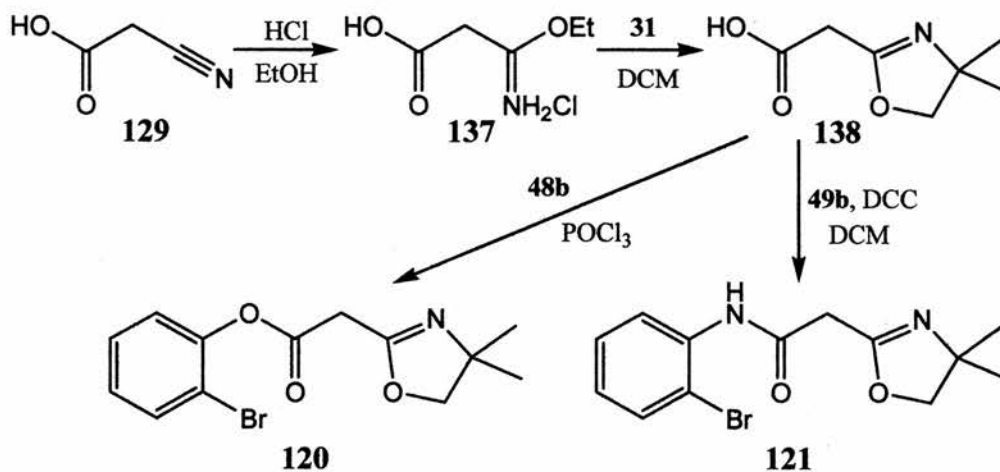
2.3.3 Potential Routes to Hetero Analogues of Arylalkyloxazolines

Scheme 115^{23, 24}

Given time and resources the following possible alternate routes, which are based on experience already gained, could be explored.

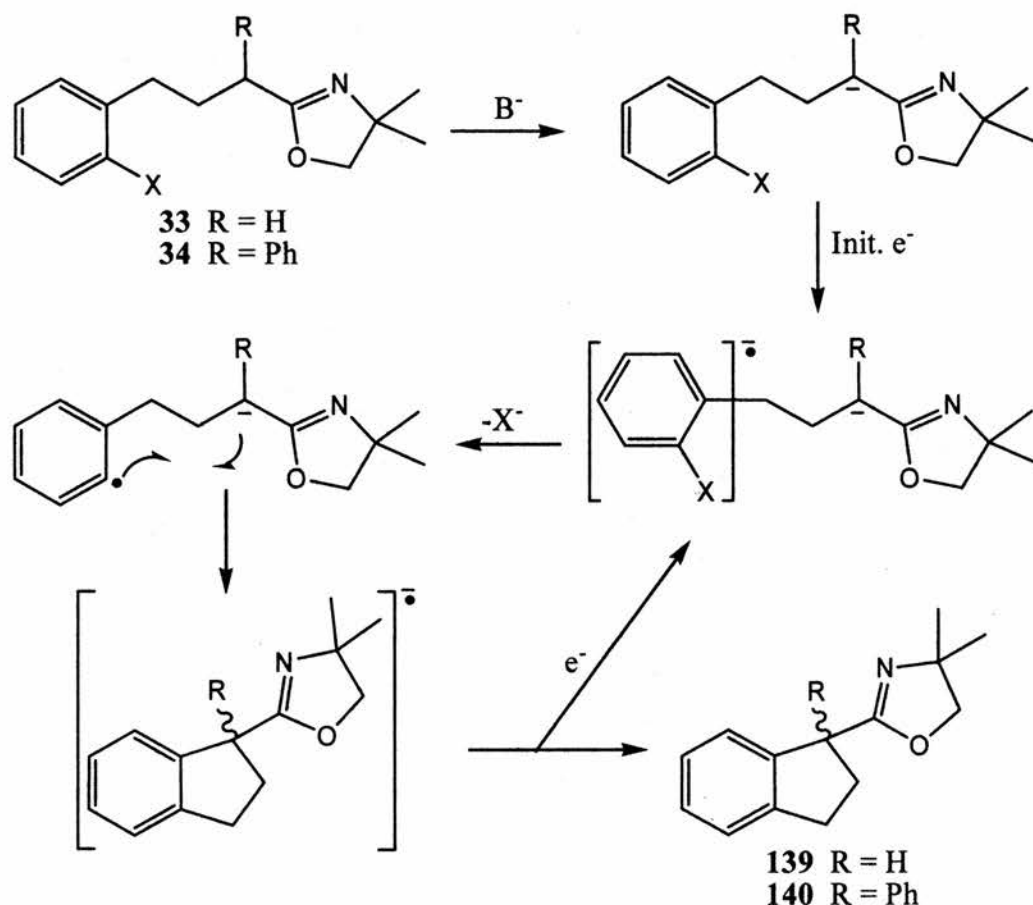
Scheme 115 shows a possible route to 44b and 46b via the intermediate vinyl oxazoline 136. It is envisaged that aminoalcohol 31 could be reacted with acryloyl chloride 134, followed by ring closure with DEAD & triphenylphosphine, to afford 136.²³ 136 could then undergo Michael addition using either nucleophile 48b or 49b to give the desired ether 44b or amine 46b respectively.²⁴

An alternative route to amide **121** and ester **120** is shown in Scheme 116. The imidate ester **137** of cyanoacetic acid **129** could be formed²⁵ followed by condensation with aminoalcohol **31** to yield carboxyoxazoline **138**. **138** could then be coupled with either aniline **49b** or phenol **48b** to furnish amide **121** or ester **120** respectively.

Scheme 116²⁵

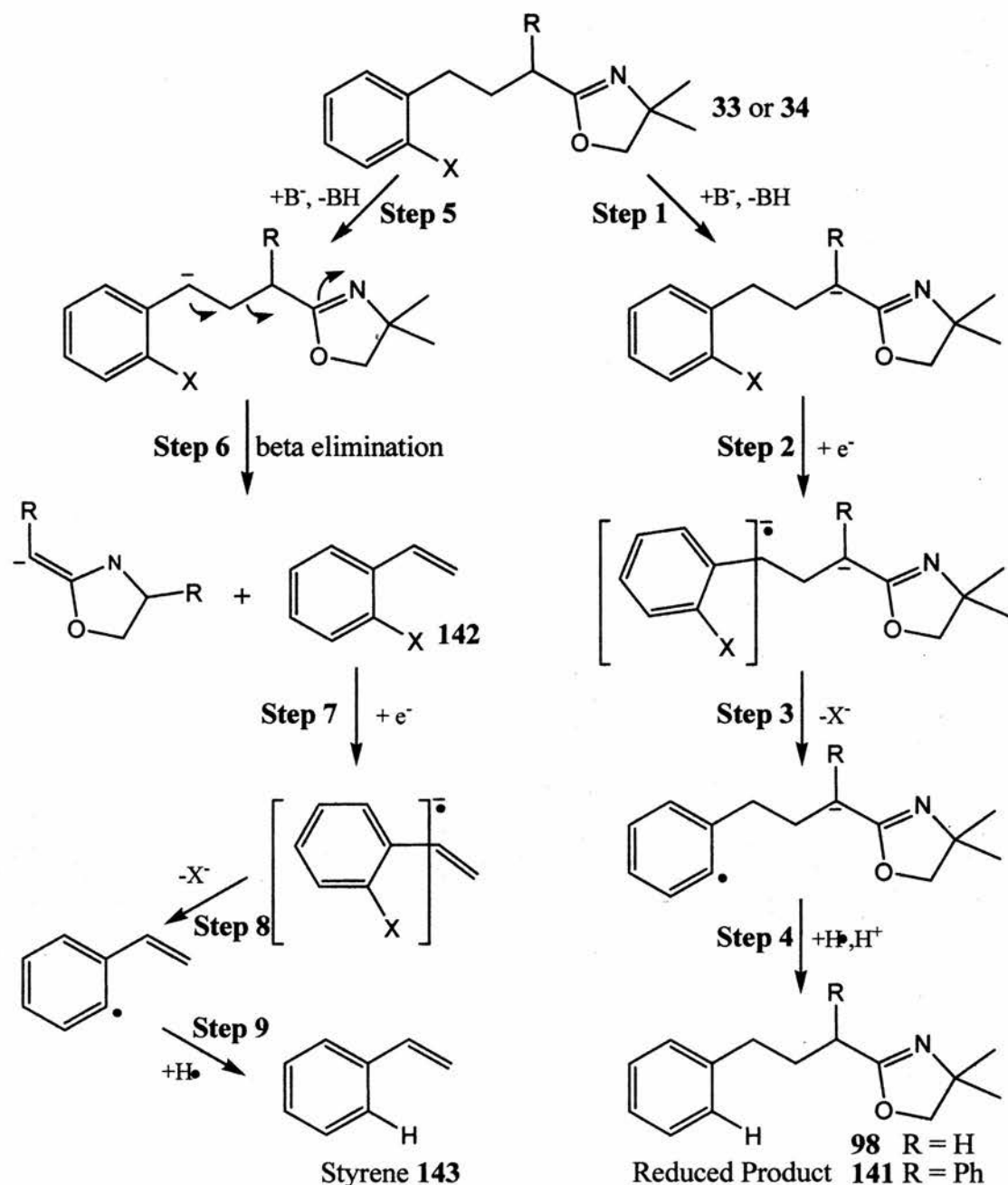
2.4 S_{RN}1 Reactions of Non Chiral 2-Oxazolines

Following the successful preparation of substituted 2-oxazolines, their evaluation under S_{RN}1 conditions was carried out.²⁶ This was achieved using a variety of common protocols previously discussed in section 1.3. Initially only S_{RN}1 reactions of γ -arylpropyl-2-oxazolines **33a**, **33b**, **34a** & **34b**, which on successful cyclisation will yield substituted indanes **139** & **140**, were studied. A wide variety of conditions were evaluated in order to optimise ring closure conditions. The expected mechanistic pathway is shown in Scheme 117.



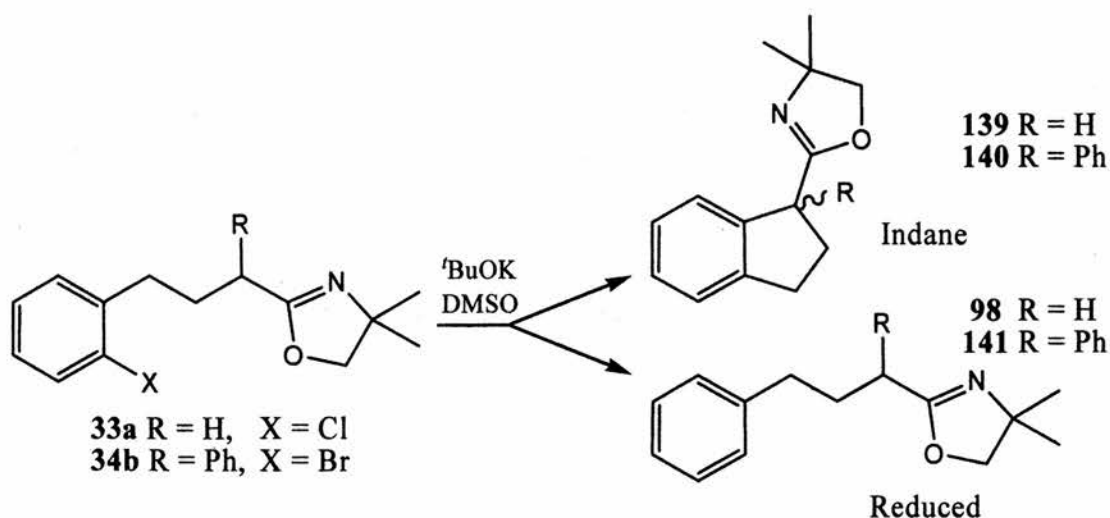
Scheme 117

During the course of the study, three additional products were observed in the S_{RN}1 cyclisations. These were the direct reduction product **98** or **141**, o-halostyrene **142** and styrene **143**. The proposed mechanisms that would account for these products are shown in Scheme 118.



Scheme 118

The reduced product is proposed to come from the initially generated phenyl radical (steps 1-3, Scheme 118) abstracting a hydrogen atom from either solvent or base (step 4, Scheme 118). In reactions where UV irradiation is used, another possible source of the initial aryl radical is photolytic cleavage. The styrene probably originates from a deprotonation of the substrate at the aryl benzyl position followed by β -elimination of the oxazolinyl moiety (steps 5 & 6, Scheme 118). The 2-halostyrene formed can undergo reduction to form radical anion; subsequent halide loss could then occur to give a styryl radical (steps 7 & 8, Scheme 118). Hydrogen capture would then result in styrene formation (step 9, Scheme 118).

2.4.1 SRN1 Reactions Using DMSO/^tBuOK

Scheme 119

Entry	ID	Conditions	Unreacted Substrate (%)	Indane (%)	Reduced (%)
1	33a	3h, UV, rt, Et ₃ N*	100	-	-
2	34b	4h, UV, rt, Et ₃ N [†]	1	-	2

Table 5 Summary of SRN1 Reactions using ^tBuOK/DMSO. * NMR yields [†] ratio

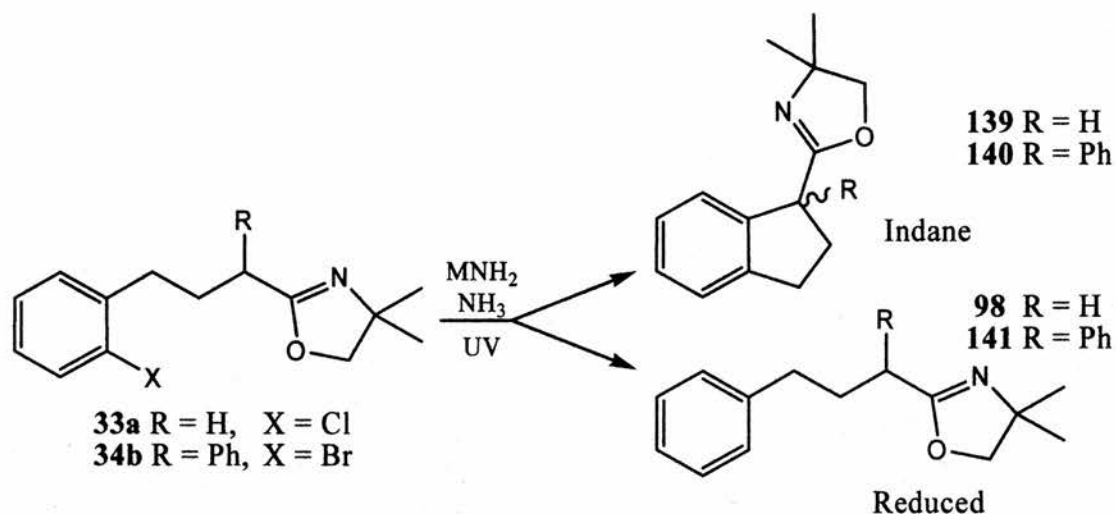
One of the two traditional conditions for SRN1 processes utilises ^tBuOK as base and DMSO as solvent. Reactions are usually carried out with UV irradiation. The other traditional process involves an alkali metal amide in liquid ammonia with or without irradiation (results are shown in Section 2.4.2).

Table 5, shows the result of SRN1 reactions of 2-oxazolines **33a** & **34b** in DMSO using potassium *tert*-butoxide as a base. Freshly sublimed butoxide was dissolved in DMSO, the oxazoline was then added. Irradiation was carried for between three and four hours (Scheme 119). One equivalent of triethylamine, which is well known as an electron transfer catalyst, was also added prior to irradiation,.

The results (Table 5) clearly show that no cyclised product was formed under the described conditions. The fact that no reaction occurred with 2-oxazoline **33a** (R = H, X = Cl) was unsurprising because aromatic chlorides are known to be poor substrates for aromatic SRN1 processes. This was especially highlighted by the fact that no reduced product was formed. This indicated that either radical anion formation did not occur or that intramolecular SET from the π^* orbital to the σ^* orbital did not

occur due to the high energy nature of the C-Cl σ^* orbital. In the case of bromide **34b**, formation of reduced product **141** was observed, signifying that radical anion formation followed by intramolecular SET and expulsion of bromide was taking place. That no indane product **140** formed was thought to be because the pK_a of potassium *tert* butoxide ($pK_a = 19$) was insufficient to efficiently deprotonate the 2-oxazoline moiety to give the azaenolate ($pK_a = 20-25$),

2.4.2 $S_{RN}1$ Reactions Using MNH_2 /Ammonia



Scheme 120

Entry	ID	Conditions	Unreacted Substrate (%)	Indane (%)	Reduced (%)
1	33a	2h, UV, -33°C (M = Li) [†]	5	-	1
2	34b	1h UV, -33°C (M = K) [*]	54	16	31
3	34b	1h, UV, -33°C 1/10 dil (M = K) [†]	1	-	1

Table 6 Summary of $S_{RN}1$ reaction using MNH_2/NH_3 . * NMR yields [†] ratio

As previously mentioned, alkali metal amides in liquid ammonia are one of the traditional set of conditions in which to carry out $S_{RN}1$ reactions. The same 2-oxazolines **33a** & **34b**, which were evaluated using ^tBuOK/DMSO conditions (Section 2.4.1), were appraised using these conditions. Both lithium and potassium amide in liquid ammonia were used.

The solution of alkali metal amide in ammonia was generated by the addition of three equivalents of alkali metal to refluxing ammonia along with 0.1 % iron(III) nitrate. Initially, solvated electrons were observed (blue colour), but, after stirring for thirty minutes, a grey suspension of the alkali metal amide was formed. The oxazoline dissolved in tetrahydrofuran was then added and the resultant mixture irradiated for one to two hours in the quartz vessel.

The reaction of chloride **33a** again gave a very poor yield mostly of starting material plus a small amount of the dehalogenated product **98** (entry 1, Table 6). When bromide **34b** was reacted under the same conditions, the expected indane **140** was obtained albeit in a poor yield of 16% (entry 2, Table 6). Disappointingly though, nearly twice as much of the reduced product **141** was formed. This may be due to a one electron reduction of the intermediate phenyl radical to the anion by free electrons in solution. In order to determine if the concentrations of the reactants played an important role in the process, the reaction was repeated with a 1/10 dilution of all reactants. Unfortunately no indane product **140** was obtained. Only a 1:1 mixture of the starting material **34b** and the dehalogenated product **141** was observed.

In the intermolecular reactions carried out by Wolfe *et al.*,²⁷ a three fold excess of the aryl bromide was used, which could explain the relatively high yields obtained by Wolfe (57 %, 2-benzyl-4,4-dimethyl-2-oxazoline **27**, bromobenzene).²⁷ It was postulated that possibly liquid ammonia was a poor solvent for intramolecular $S_{RN}1$ reactions of 2-oxazolines.

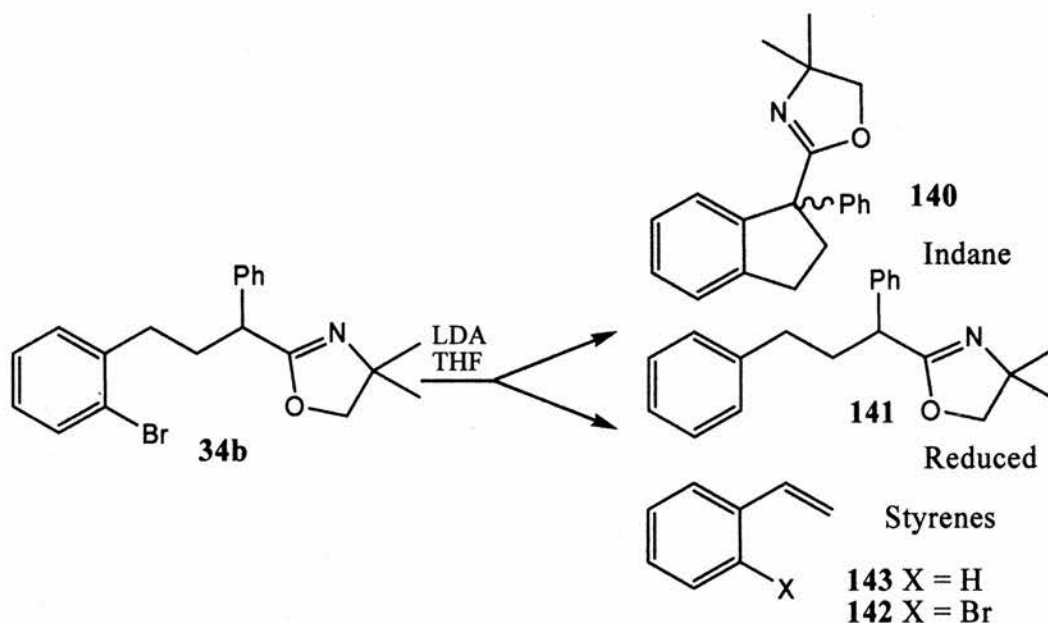
The $S_{RN}1$ reaction of **34b** was repeated in THF as the solvent and commercially available sodamide was used as a base. A 1:1 ratio of the starting material **34b** and reduced **141** was obtained after work up. This was thought to be because of lack of deprotonation of the oxazoline due to the poor solubility of sodamide in THF.

2.4.3 $S_{RN}1$ Reactions Using LDA/THF

A less common but widely used base and solvent combination for $S_{RN}1$ reactions is lithium diisopropylamide and tetrahydrofuran. The general procedure for the reactions involved a solution of the substrate being added to a stirred solution of one to three equivalents of lithium diisopropylamide in tetrahydrofuran at -78 °C. The

mixture was then allowed to warm up to room temperature for thirty to forty minutes, after which a variety of different conditions were employed.

2.4.3.1 2-[3-(2-Bromophenyl)-1-phenylpropyl]-4,4-dimethyl-2-oxazoline



Scheme 121

Table 7 shows a summary of yields of $S_{RN}1$ reaction products from bromide **34b** using variety of conditions. All reactions involved the bromide **34b** in THF with 3 eq. of lithium diisopropylamide, unless otherwise indicated.

The results show that the $S_{RN}1$ process proceeds at an appropriate rate at room temperature without additional stimulus (entries 1-3, Table 7). Full consumption of the starting materials required forty eight hours, which furnished, after work up, the expected indane **140** in a good yield of 75 %. A small amount, ca. 2 %, of styrenes **142** & **143** was formed. When the reaction mixture, after being allowed to warm to room temperature, was irradiated with a 400 W medium pressure mercury vapour UV lamp, all of the starting material was consumed, 57 % of the cyclised product **140** was obtained after isolation via column chromatography (entry 4, Table 7). Also, 15 % of the reduced homologue **141** and 7 % of styrenes **142** & **143** was produced as well. It is clear from these results that a cleaner reaction results without irradiation at the expense of rate. Rate acceleration by UV photolysis is a hallmark of $S_{RN}1$ processes.

Absence of oxygen was very important, with trace oxygen resulting in poor to no product yield; this is another indicator of a radical process.

Entry	Conditions	Unreacted S. M. (%)	Indane (%)	Reduced (%)	Styrene (%)
1	0h, rt	50	34	-	2
2	20h, dark, rt	20	50	-	8
3	48h, dark, rt	<1	75	-	2
4	6h, UV, rt	<1	57 [†]	15 [†]	7 [†]
5	3h, dark, reflux	40	45	-	5
6	2h, dark, rt*	32	11	13	2
7	1h, 0.1 eq. FeCl ₂ , rt	38	25	-	6
8	1h, 1 eq. FeCl ₂ , rt	38	23	16	8
9	1 eq. LiCl, 0.1eq. _‡ [P] ^{•-} , -78°C, 4 h	99	-	-	-
10	1 eq. LiCl, 0.2eq. _‡ [P] ^{•-} , -78°C, 4 h	99	-	-	-
11	1 eq. LiCl, 0.3eq. _‡ [P] ^{•-} , -78°C, 4 h	99	-	-	-
12	1 eq. LiCl, 0.4eq. _‡ [P] ^{•-} , -78°C, 4 h	99	-	-	-
13	1 eq. LiCl, 0.5eq. _‡ [P] ^{•-} , -78°C, 4 h	99	-	-	-
14	1 eq. BuLi, 1 eq. [P] ^{•-} , -78°C, 4 h [‡]	35	-	28	4

Table 7 Summary of S_{RN1} reactions of bromide **34b**. * 1 eq. LDA, [†] isolated yields, [‡] No LDA.

When the reaction mixture was heated to reflux in place of UV irradiation a moderate increase in product yield was detected (entry 5, Table 7). Although this was advantageous in terms of ease of reaction, for a chiral homologue, any diastereoselectivity would be diminished under such conditions.

The necessity of 3 eq. LDA was shown by the poorer yield observed when only one eq. of LDA was employed (entry 6, Table 7). This may be because the LDA was acting as an electron transfer reagent and/or a electron donor as well as a base (Scheme 122).



Scheme 122

It was reported in the literature that in some systems where S_{RN1} processes occur, iron(II) salts were found to act as one electron donors and increase initiation events, therefore enhancing overall reaction efficiency. When Fe(II)Cl₂ was used in

our system (entries 7 & 8, Table 7) the results were disappointing. At the very least the yields were unaffected and at the worst, yields were actually depressed. Only 50-60% overall material was recovered. It is known from the literature that 2-oxazolines form stable complexes with iron.²⁸ This may explain the particular messy work up for these reactions and the low recovery of material at the end of reaction. When going from 10 mol% to 1 eq. Fe(II)Cl₂ the yields of product did not change but significant amounts of the reduction product were produced. Based on this observation it is evident that the iron salt is indeed acting as a reductant, but the phenyl radicals produced are then being further reduced to the phenyl anion.

Polyaromatics such as anthracene and phenanthrene have been used in electrochemistry as redox mediators in order to transport electrons from the anode. This is needed in order to avoid over reduction of the organo-halide at the anode.²⁹ It is therefore evident that the polyaromatic radical anions are capable of initiating a chain process via electron transfer to a suitable organic halide.

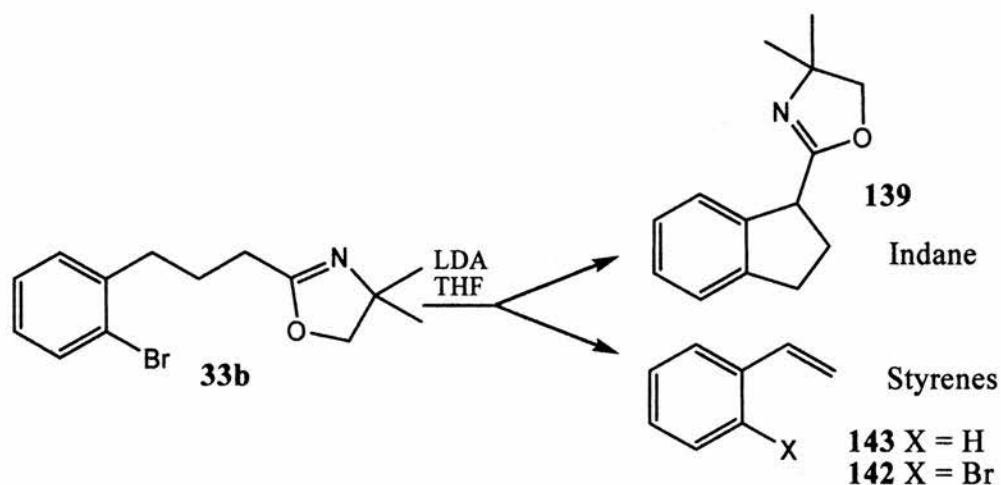
Phenanthrene radical anion [P]^{•-} was synthesised via addition of one equivalent of sodium metal to a dry, deoxygenated solution of phenanthrene under nitrogen with stirring over night to give a deep green solution. The S_{RN1} reaction of halide **34b** was repeated using 1 eq. LDA, 1 eq. LiCl at -78 °C. 0.1–0.5 equivalents of the prepared 0.02 M solution of phenanthrene radical anion [P]^{•-} were then added and the solution stirred at -78 °C for 4 hours (entries 9-13, Table 7). At which time the reaction was quenched by the addition of a saturated solution of ammonium chloride. Lithium chloride was used because it is known to help form aggregates at low temperature in THF, which would be helpful in S_{RN1} reactions of chiral homologues of **34b** in order to ensure a high diastereoselectivity.

Unfortunately, no reaction was observed. The reaction was repeated without LDA or LiCl, and only 1 eq. BuLi was added to obtain the anion. Also 1 eq. of the phenanthrene radical anion was added (entry 14, Table 7). This time a reaction occurred but it only led to 28 % of the reduced product **141** and 4 % of styrenes **142** & **143**. Clearly addition of phenanthrene did not bring about any formation of the desired indane **140**. This may be due to a problem of over reduction (as in the case of entry 14, Table 7) or the reaction temperature being too low.

The yield of the minor product of this system, styrenes **142** & **143**, doesn't appear to follow any pattern with regard to reaction conditions. The yield of styrene

may be due to minor fluctuations in the initial starting conditions or minor impurities, although styrene production never reaches more than 8 % (Table 7).

2.4.3.2 2-[3-(2-Bromophenyl)propyl]-4,4-dimethyl-2-oxazoline

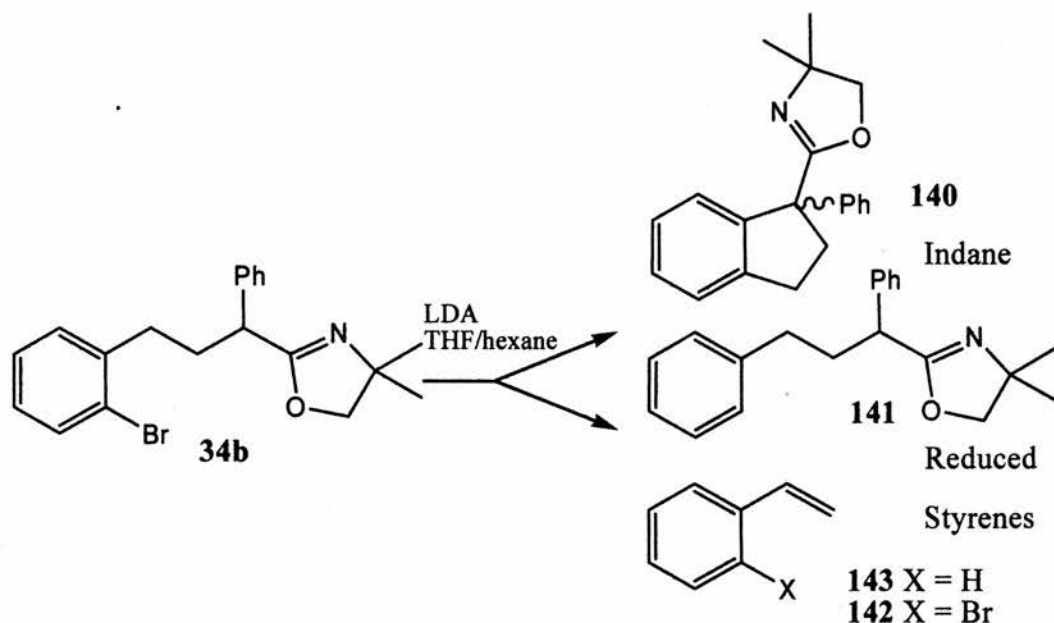


Scheme 123

Entry	Conditions	Unreacted S.M (%)	Indane (%)	Reduced (%)	Styrene (%)
1	Pyrex, 4h, UV, rt	22	9	-	0
2	Quartz, 4h, UV, rt	29	58	-	10

Table 8 Summary of SRN1 Reaction of **33b** using LDA/THF. All yields are isolated.

SRN1 reactions of bromide **33b** were carried out as described previously for reactions in section 2.4.3.1 (Scheme 123) and the results are summarised in Table 8. Reactions in Pyrex were poor with only a small amount of indane **139** formed (9 %) (entry 1, Table 8). After 4 hours of irradiation in quartz glassware a good yield of **139** was obtained (58 %), although 29 % of starting material **33b** was recovered (entry 2, Table 8). Pyrex glassware is opaque to most UV radiation whereas quartz is not, therefore these results were not unexpected. Isolation of the product via column chromatography was more difficult than with the previously reacted bromide **34b**. This may be due to the presence of a phenyl ring in **34b**. Interestingly, no reduced product could be detected which suggested that the phenyl group of **34b** may play a role in the formation of the reduced product **141**.

2.4.4 S_{RN}1 Reactions Using LDA/THF:Hexane

Scheme 124

In order to obtain a fuller picture of the use of LDA as a base in S_{RN}1 reactions, a more non polar solvent system was investigated (Scheme 124, Table 9). A 2:1 mixture of THF:hexane was used instead of purely THF. All other conditions remained unchanged.

As previously observed, the yield upon irradiation in Pyrex glassware (entry 1, Table 9) is lower than the corresponding reaction in quartz (entry 2, Table 9). The yield (41 %, after 3 hours) in quartz glassware is comparable to that which was obtained previously in purely THF (57 % after 6 hours, entry 4, Table 7). The yield of indane **140** when 0.1 equivalent of iron(II) chloride was employed (entry 3, Table 9) was comparable to previous results (entry 7, Table 7). Although the reduced product **141** was observed in this case. When one equivalent of iron(II) chloride was added, yields of the indane **140** (entry 4, Table 9) were slightly decreased in comparison with the more polar solvent case (entry 8, Table 7). This was probably due to the lower solubility of any aggregates formed during the reaction, appropriated to the high concentration of the iron salts.

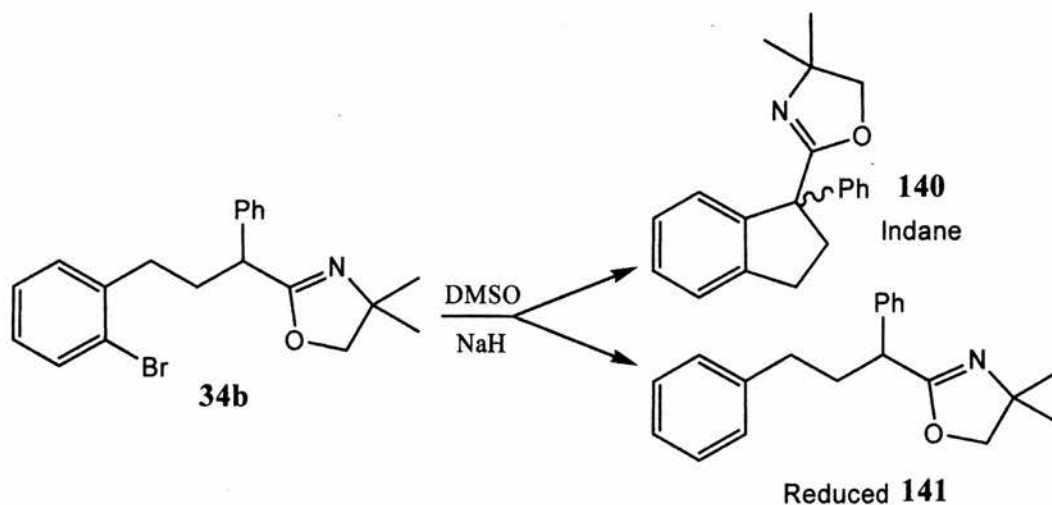
Entry	Conditions	Unreacted Substrate (%)	Indane (%)	Reduced (%)	Styrene (%)
1	Pyrex, 3h, UV, rt*	27	18	5	4
2	Quartz, 3h, UV, rt*	31	41	12	6
3	1h, 0.1.eq FeCl ₂ , rt [†]	24	25	17	8
4	1h, 1 eq, FeCl ₂ , rt [†]	50	17	8	3

Table 9 Summary of *S_{RN1}* reactions of **34b** using LDA/THF:hexane. * isolated Yields [†] NMR yields

Overall it appears that a less polar solvent system does not appreciably affect the yields of reactions carried out without ferric salts.

2.4.5 *S_{RN1}* Reactions Using NaH/DMSO

As previously mentioned, one of the most common base/solvent combinations for *S_{RN1}* reactions is *t*BuOK/DMSO. As discussed in Section 2.4.1, *t*BuOK was unable to deprotonate 2-oxazoline substrates. Dimethyl sulfoxide is deemed a good polar aprotic solvent for *S_{RN1}* reactions, so maybe a strong base would suffice to give a viable *S_{RN1}* reaction. 2-Oxazolines have *pK_a*'s in the range of 20-25, which is why LDA (*pK_a* 36) is able to deprotonate them easily. Dimethyl sulfoxide has a *pK_a* of 35 therefore, if LDA was used in DMSO, the dimethyl sulfoxide would be deprotonated to give the lithium salt. This would be acceptable as the sulfoxide base should still be able to deprotonate 2-oxazolines. The only problem is the presence of undesirable diisopropylamine. If NaH (*pK_a* = 36) were used in place of LDA then a pure solution of dimethyl sulfoxide sodium salt (dimethyl sodium) in DMSO should result.



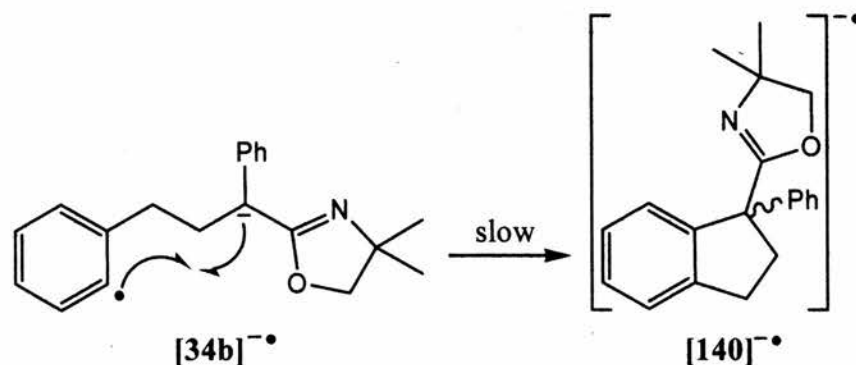
Scheme 125

Entry	Conditions	Unreacted Substrate (%)	Indane (%)	Reduced (%)
1	4h, dark, rt	99	-	-
2	4h, UV, rt	4	-	96
3	4h, dark, 60°C	99	-	-
4	10min, UV, 100°C	16	34	39
5	4h, UV, 100°C	-	66	-
6	4h, 1 eq. FeCl ₂ , rt	99	-	-

Table 10 Summary of S_{RN1} reactions of **34b** using NaH/DMSO. All yields are NMR yields.

Reactions were carried out by the addition of a DMSO solution of the substrate **34b** to a freshly prepared solution of dimethyl sodium in dry DMSO at room temperature under nitrogen. The reaction was quenched by the addition of finely ground ammonium chloride (Scheme 125, Table 10).

It was evident that the reaction was not spontaneous at room temperature contrasting with the examples for LDA/THF system (entry 1, Table 10). Irradiation at room temperature for 4 hours led to a 96 % yield of the reduced diphenyl **141** (entry 2, Table 10), suggesting photolytic cleavage of the C-Br bond as the main process. On heating the mixture a colour change from pale yellow to bright orange was observed. This possibly indicated an improved generation of the anion. However, after 4 hours heating at 60 °C no reaction was detected (entry 3, Table 10). When both heating at 100 °C and irradiation were employed the desired indane was obtained in moderate yield of 34 % after only 10 minutes. More disappointingly though, 39 % of the reduced product **141** was formed with 16 % unreacted starting material recovered (entry 4, Table 10). This contrasted with a 66 % yield of the indane **140** after 4 hours irradiation at 100 °C with no detectable reduced **141** or starting material **34b** (entry 5, Table 10). This observation can be explained if the coupling of the phenyl radical and the anion is slow and therefore rate determining (Scheme 126), which would explain the large amount of reduced product observed after only ten minutes irradiation (entry 4, Table 10).



Scheme 126

One equivalent of iron salts seems to have no effect, with starting material being fully recovered after 4 hours at room temperature, although this may indicate that the anion was not generated sufficiently. No styrene was formed under these conditions, which contrasts with the use of LDA and THF/hexane solvent mixtures. This can be explained by the lack of excess base.

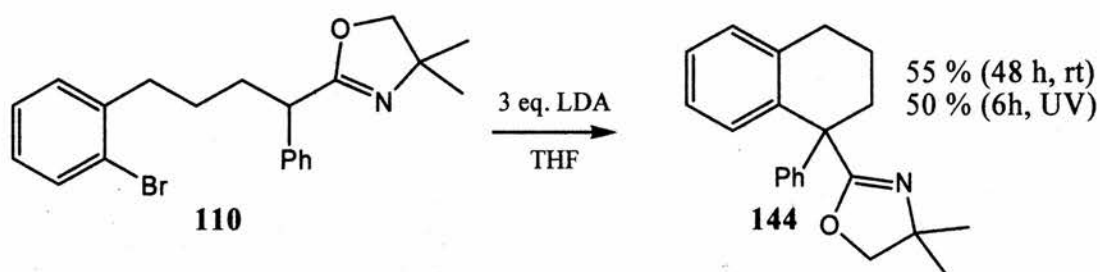
2.4.6 Summary of Non-Chiral $S_{RN}1$ Reactions

t BuOK/DMSO, of all the various base/solvent combinations, was the only combination not to afford the desired substituted indanes **139** & **140**. The MNH_2/NH_3 combination gave an excess of reduced product. LDA/THF gave the highest yields of cyclised product, of which the reaction without UV irradiation gave the cleanest reaction. Reactions involving iron(II) salts showed no enhancement of yields, and also crude reaction mixtures were intractable. A phenyl ring alpha to the oxazoline ring aided separation of the product. It was decided that for further reactions on chiral and chain extended analogues only the optimum conditions i.e. LDA/THF with either 48 h at room temperature or 6 hours irradiation would be employed. An EPR study was also carried out also using these optimised conditions to identify any radical intermediates (Section 2.6).

2.5 Tetralins, Benzosuberenes and Benzocyclooctanes via S_{RN}1 Reactions

The feasibility of forming tetralins, benzosuberenes and benzocyclooctanes was evaluated following the successful preparation of indanes involving the creation of sterically hindered centres. Reactions were carried out using the optimum conditions identified in the formation of indanes i.e. three equivalents of LDA in THF, with either 6 hours UV irradiation or 48 hours stirring in the dark at room temperature (Section 2.4.3). The preparation of the analogous precursors is detailed in Section 2.1.4.

2.5.1 Formation of Substituted Tetralins using S_{RN}1 Protocols



Scheme 127

δ -Arylbutyl-2-oxazoline **110** was added to a stirred solution of LDA at $-78\text{ }^{\circ}\text{C}$ under nitrogen and then the mixture was allowed to warm to room temperature. Irradiation for 6 hours, or stirring for 48 hours in the dark, was then carried out. After work up, one product was observed in both cases via $^1\text{H-NMR}$ spectroscopy, which formed white crystals after crystallisation via diffusion of hexane into a solution of the product in ethyl acetate. These crystals were submitted for X-ray structural analysis to reveal that the expected product **144** had been formed in moderate yields of 55% (48 hours, r.t.) and 50% (6 hours, UV) (Scheme 127, Figure 3, Appendix A).

The slightly lower yield of formation of tetralin **144** versus formation the analogous indane **140** (Section 2.4) is possibly due to a slightly slower rate of six membered ring closure.

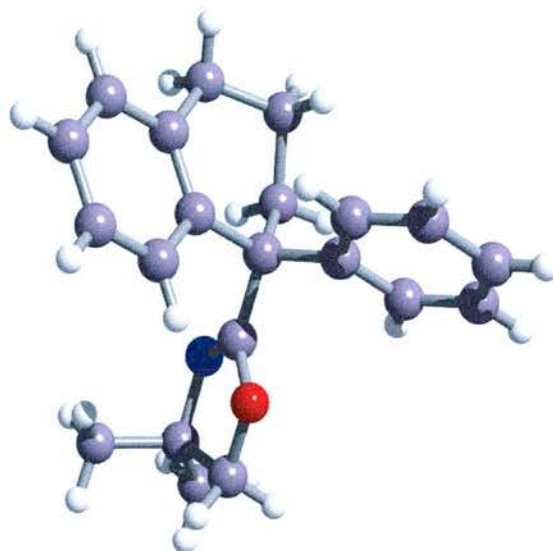
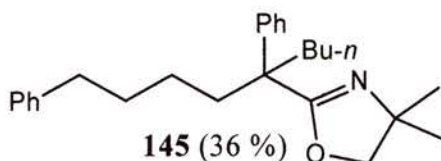


Figure 3 X-ray structure of tetralin **144**

The X-ray analysis of tetralin **144** showed a single conformer of the expected half-chair 6-membered ring with the oxazoline in the pseudo-equatorial orientation and the phenyl ring in the pseudo-axial orientation (Figure 3). The C-C bonds to the quaternary C-atom in the 6-membered ring were 1.542 Å (to benzo sp^2 C-atom), 1.547 Å (to ring CH_2), 1.547 Å (to Ph) and 1.532 Å (to oxazoline). As expected from the crowded nature of this centre, these bonds were significantly longer than unencumbered C-C bonds. For comparison, the sp^3 CH_2-CH_2 bonds in the new 6-membered ring were 1.524 Å, and 1.516 Å in length.

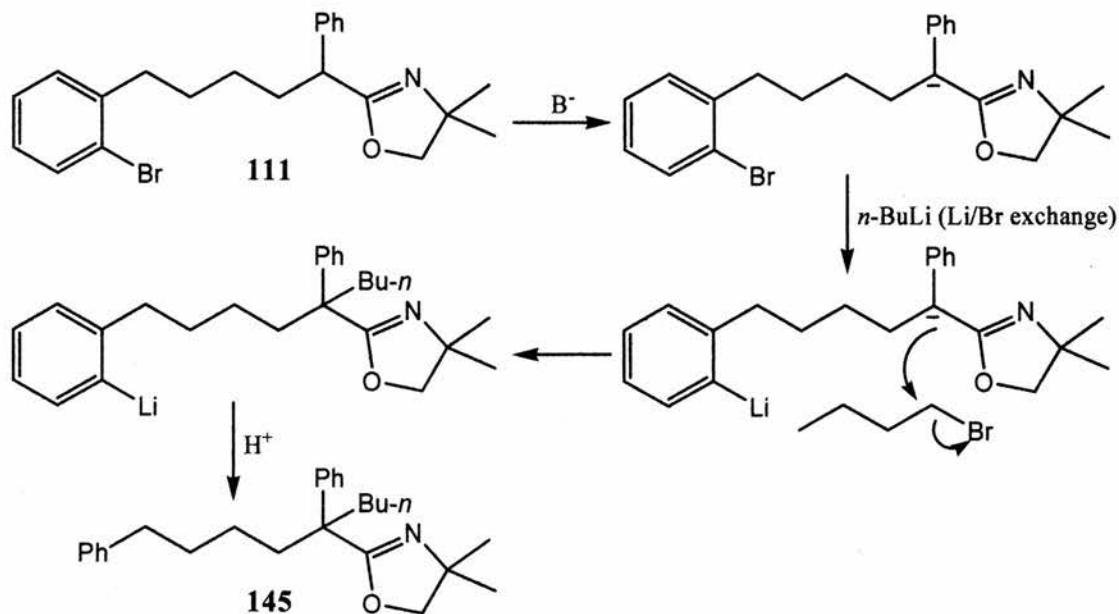
2.5.2 Formation of Substituted Benzosuberenes Using $S_{RN}1$ protocols

On reaction of ϵ -arylpentyl-2-oxazoline **111** with three equivalents of LDA at r.t. for 48 hours the expected product was not observed. After analysis of the NMR spectra it was determined that butyl derivative **145** was the only identifiable product, formed in 36 % yield (Scheme 128); 15 % of the starting material was recovered.



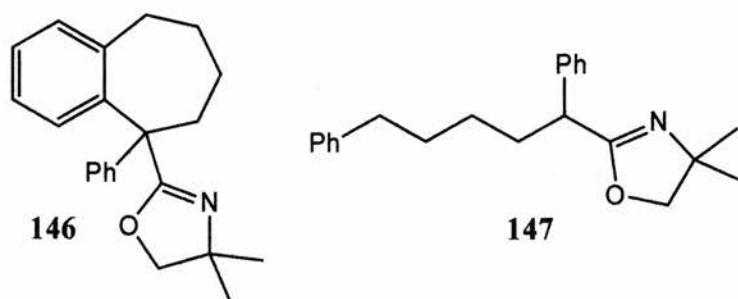
Scheme 128

The formation of the butyl product is thought to have occurred due to an inaccurate amount of either *n*-BuLi and/or diisopropylamine being used. A plausible mechanism to account for its formation is shown in Scheme 129.



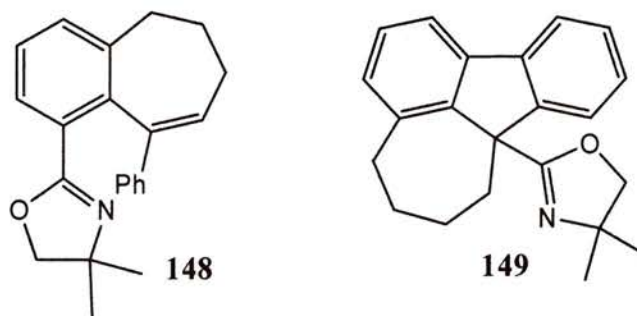
Scheme 129

The reaction was repeated with fresh LDA and several different products were revealed after column chromatography. However, the expected benzosuberene **146** (Scheme 130) was not among them.



Scheme 130

One of the products which was identified, was the simple dehalogenated product **147** (Scheme 130). Crystals of two of the remaining products were obtained and submitted for X-ray analysis, to reveal alkene **148** (Scheme 131, Figure 4) and fluorene derivative **149** (Scheme 131, Figure 4).



Scheme 131

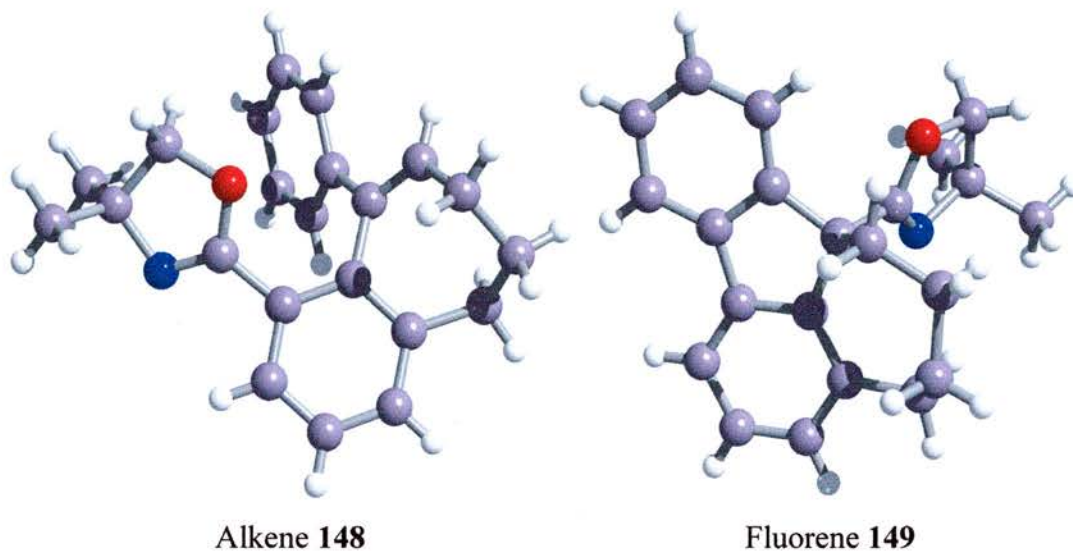
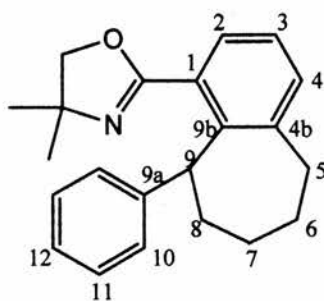


Figure 4 X-ray structures of alkene **148** and fluorene **149**

2.5.2.1 NMR Structure Determination of Benzocycloheptane **150**

Unfortunately the fourth and final product **150** could not be crystallised. It gave an accurate mass result consistent with $C_{22}H_{25}ON$, which was two mass units higher than the alkene **148** obtained (Scheme 131). The presence of signals with an integration value of eight in the aromatic region suggested that the structure was related to the unsaturated product **148**, therefore the analogous saturated rearranged structure was proposed (Scheme 132). Structural determination was carried out using a combination of one dimensional NMR (1H & ^{13}C) and two dimensional NMR (COSY, HSQC & HMBC). It should be noted that the NMR spectra contain extraneous signals due to small amounts of impurities. The COSY spectrum confirmed that these peaks were not related to the main structure and they are ignored in the analysis.



Scheme 132

¹ H Signal	PPM (Integration, Multiplicity)	¹³ C Signal	PPM (Type)
α	1.24 (3H, s)	A	25.1 (CH ₂)
β	1.28 (3H, s)	B	27.4 (CH ₂)
γ	1.30-1.40 (1H, m)	C	28.0 (CH ₃)
δ	1.68-1.89 (3H, m)	D	28.1 (CH ₃)
ε	1.95-2.06 (1H, m)	E	30.7 (CH ₂)
ζ	2.47-2.66 (3H, m)	F	35.9 (CH ₂)
η	3.89 (1H, d)	G	44.4 (CH)
θ	3.94 (1H, d)	H	67.5 (C _q)
ι	5.01 (1H, dd)/	I	78.9 (CH ₂)
κ	7.05 (2H, d)	J	125.1 (CH _{Ar})
λ(1)	7.10-7.30* (~1H, br. t)	K	126.3 (CH _{Ar})
λ(2)	(~2H, m)	L	127.4 (CH _{Ar})
λ(3)	(~2H, m)	M	127.8 (CH _{Ar})
μ	7.44 (1H, dd)	N	128.0 (CH _{Ar})
/		O	130.2 (C _q)
		P	132.2 (CH _{Ar})
		Q	142.2 (C _q)
		R	142.3 (C _q)
		S	144.2 (C _q)
		T	163.9 (C _q)

Table 11 Summary of 1D ¹H and ¹³C NMR experiments of unknown 150

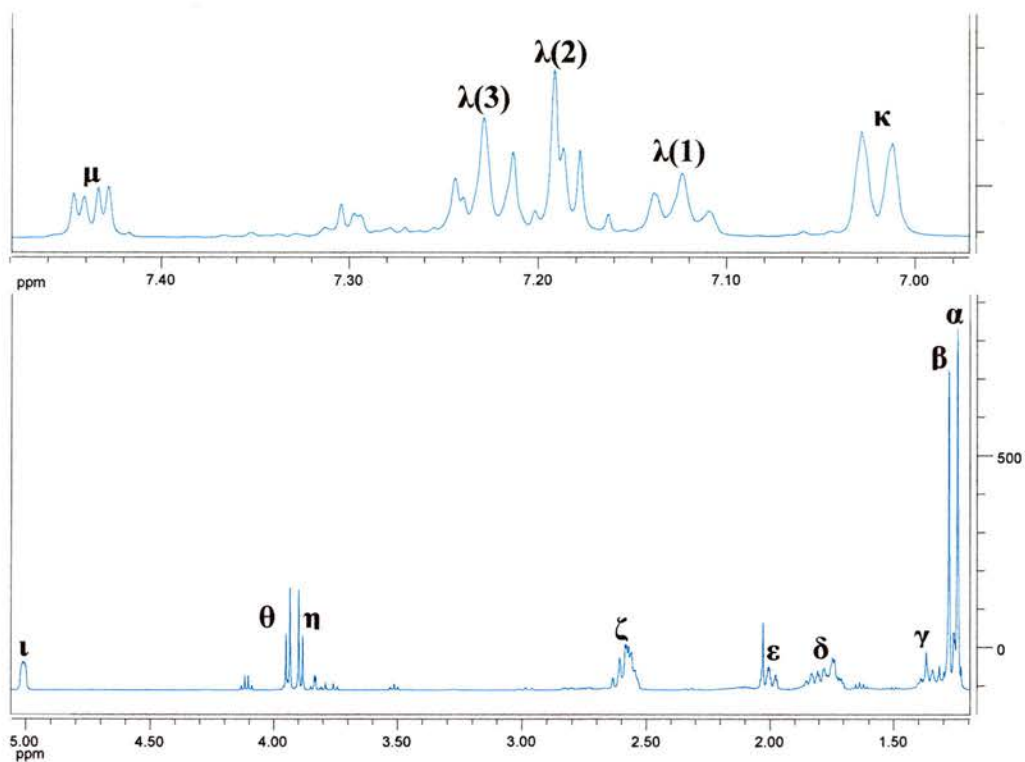


Figure 5 ¹H-NMR (500MHz, CDCl₃) of unknown product **150**

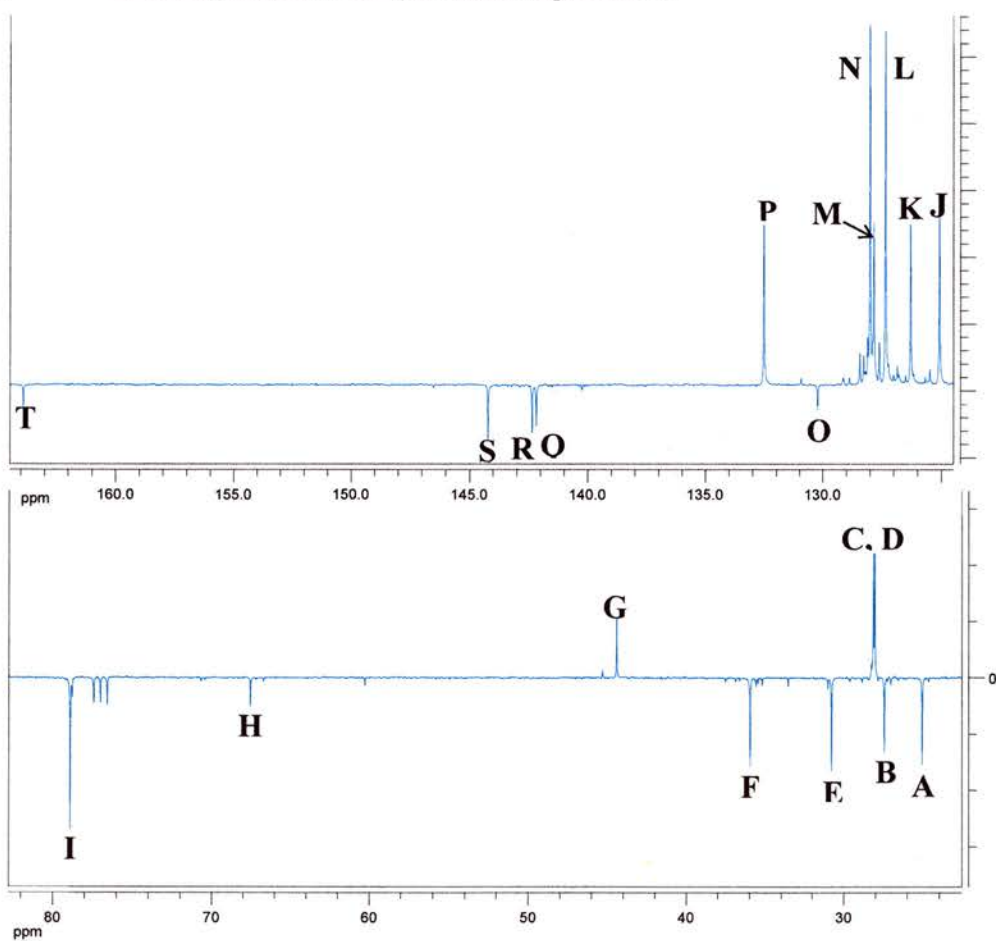


Figure 6 ¹³C-NMR (300MHz, CDCl₃, pendant) of unknown product **150**

Figure 5 and Figure 6 show the graphical representation of the one dimensional spectra. Table 11 shows a summary of the ^1H and ^{13}C NMR spectra with ^1H signals labelled with Greek letters and ^{13}C signals labelled with Latin letters. The limited assignment in ^{13}C NMR was achieved in terms of multiplicity and relative peak height. Generally, peaks corresponding to quaternary peaks are less intense, and similarly peaks accounting for two or more carbon nuclei are usually larger in size.

The ^1H -NMR shows characteristic 3H singlet signals α & β (Table 11 & Figure 5) and two AB doublet signals η & θ of the dimethyl-2-oxazoline moiety. This was confirmed by the presence of two methyl signals C & D (Table 11, Figure 6) and quaternary signals H & T (C=N), and also methylene signal I in the ^{13}C NMR. The HSQC spectrum showed the required cross peaks supporting this analysis (i & ii (circled), Figure 7).

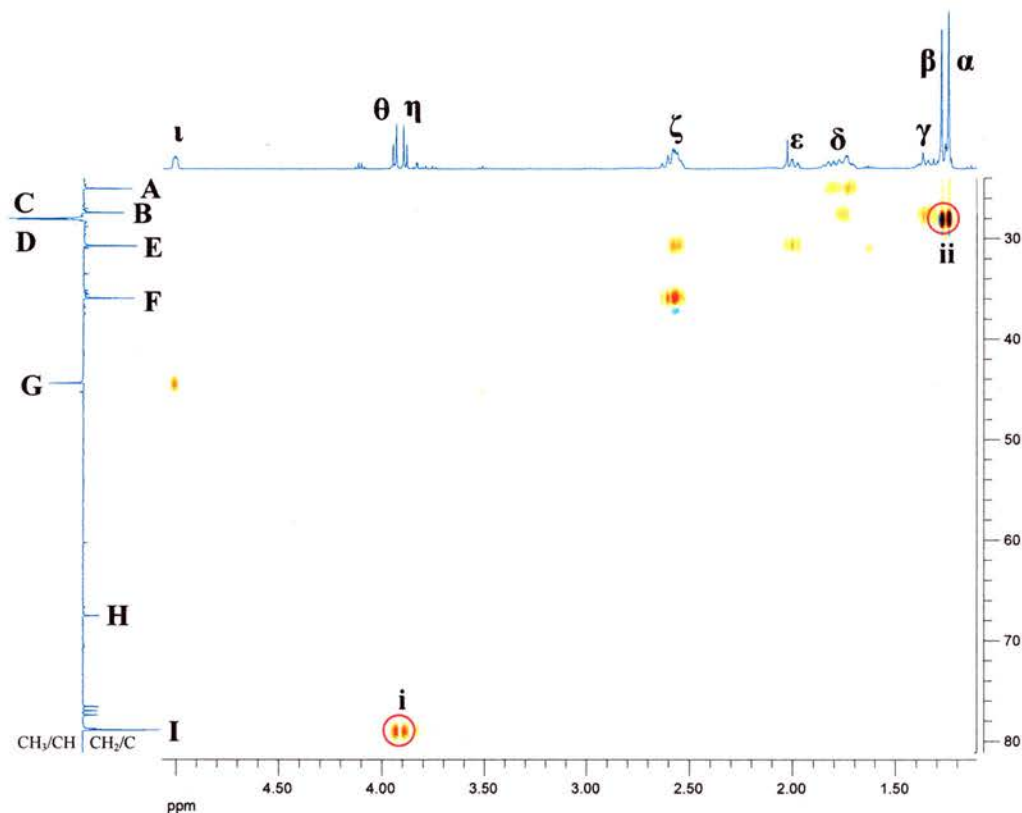


Figure 7 Aliphatic region of HSQC spectrum of unknown **150**

Assignment of signals γ - ζ and ι in the ^1H NMR was achieved using initially the HSQC spectrum to determine the multiplicity of the carbon atom to which they are attached (Figure 7). In the ^{13}C NMR spectrum, methylene signal B correlates with two ^1H resonances (γ & δ) indicating the presence of a CH_AH_B fragment. Similarly methylene signal E corresponds with two ^1H signals (ϵ & ζ) as well. ^{13}C signals A & F

only show a relationship with one ^1H resonance each (δ & ζ respectively). This evidence taken in conjunction with the integral values of the ^1H signals, confirms their initial assignment as methylenes. The ^{13}C methine signal G at 44.4 ppm only correlates with the ^1H signal at 5.01 ppm (ι) (integral of 1), and therefore can be assigned to C-9. The establishment of four methylene and one methine group in the NMR spectra equates with the proposed structure. Connectivity was established through analysis of the COSY spectrum (Figure 8).

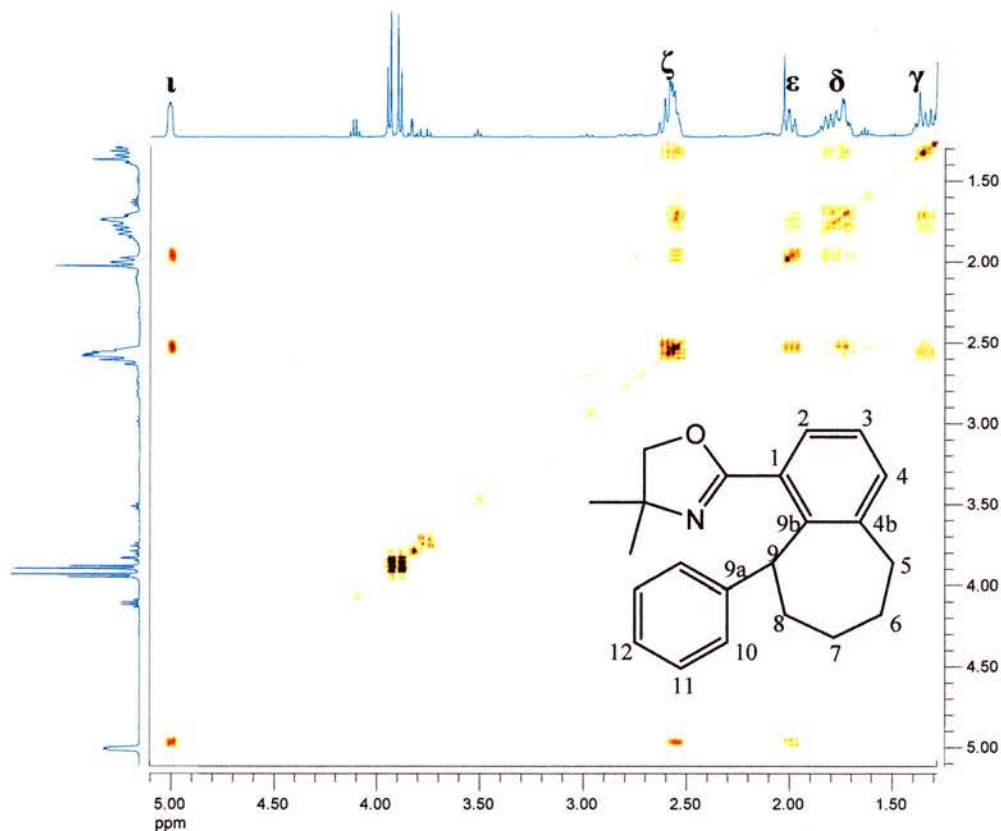


Figure 8 Aliphatic region of COSY spectrum of unknown **150**

Having determined the ^1H signal ι is due to C^9H , using the HSQC spectrum, elucidation of the connectivity of the four methylene groups can be achieved by the use of the ^1H - ^1H COSY spectrum. Signal ι correlates with signals ζ & ϵ , which are known to be associated with carbon resonance E, therefore C-8 is assigned. ζ correlates to signals ϵ , δ & γ , but ϵ only correlates to δ , therefore two hydrogens of signal δ which are associated with the ^{13}C methylene signal A are assigned to C-7. Given that resonances γ & δ both correlate with signal ζ and δ but not ϵ must mean they can be assigned to C-6 along with the ^{13}C signal B. The remaining 2 protons of signal ζ can therefore be assigned to C-5 together with ^{13}C methylene signal F.

Information relating to the elucidation of the five carbon aliphatic sequence is summarised in Table 12.

Entry	¹ H Signal	¹³ C signal	Type/Multiplicity	Assignment
1	γ & δ	B	CH _A H _B	C-6
2	δ	A	CH ₂	C-7
3	ε & ζ	E	CH _A H _B	C-8
4	ζ	F	CH ₂	C-5
5	ι	G	CH	C-9

Table 12 Summary of HSQC and COSY analysis of the aliphatic portion of unknown 150

Having now determined the presence of a five carbon sequence, which is concordant with our proposed structure, attention was turned to assignment and connectivity of the aromatic portion.

The ¹H-¹H COSY spectrum of the aromatic region shows clearly two sets of coupled signals (Figure 9, red and blue circled).

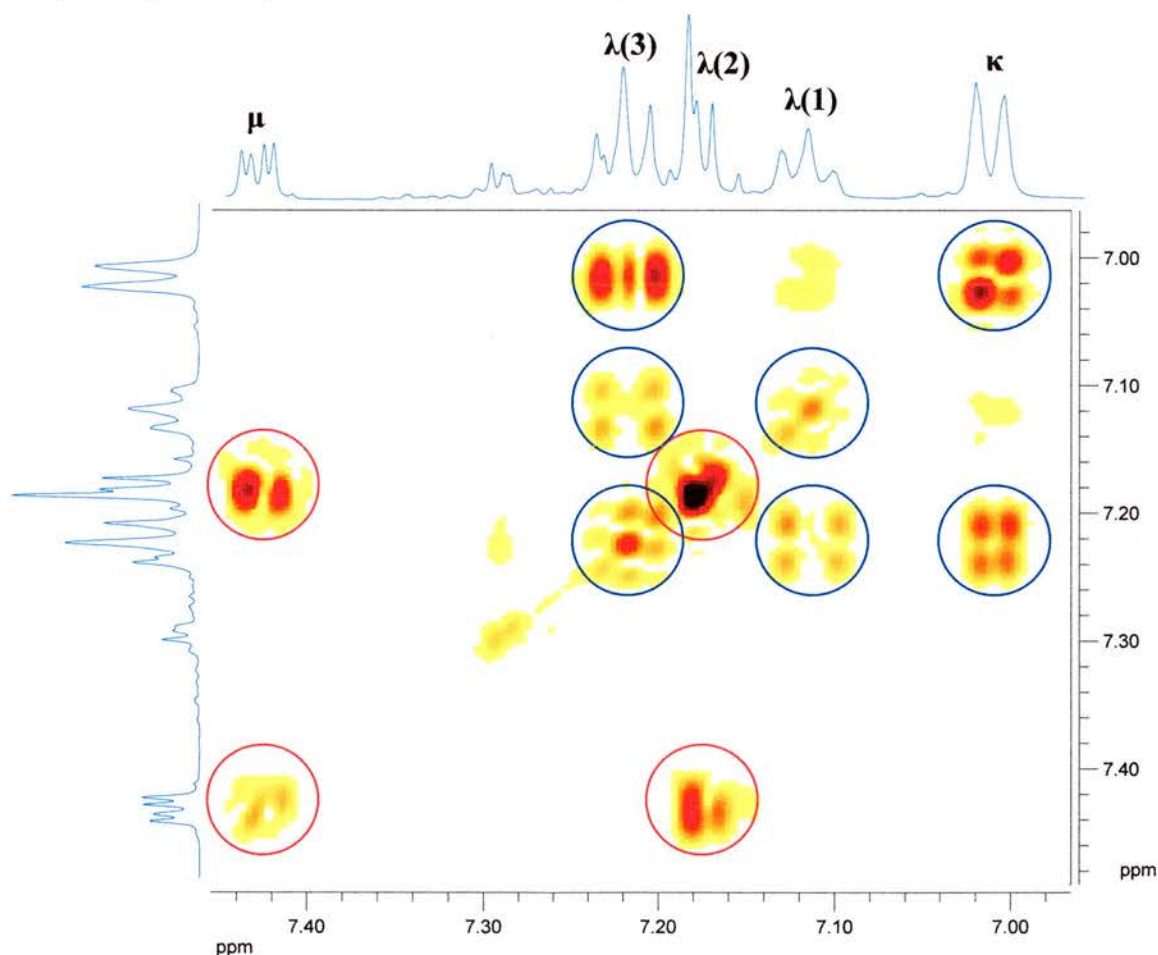


Figure 9 Aromatic region of COSY spectrum of unknown 150

From the integration of the ^1H signals the blue coupled set of signals (Figure 9, κ , $\lambda(1)$ & $\lambda(3)$) is equivalent to five hydrogens and the red set (Figure 9, $\lambda(2)$ & μ) is equal to three hydrogens. The blue set of coupled signal integrals is in the ratio of $2(\kappa):1(\lambda(1)):2(\lambda(3))$, as well as signal κ being a doublet and $\lambda(1)$ and $\lambda(3)$ being a triplet and multiplet respectively which is typical of a phenyl ring. Corroborative evidence was obtained from the aromatic region of the HSQC spectrum (cross peaks i, Figure 10). Signals κ and $\lambda(3)$ both correlate with the double intensity ^{13}C peaks L and M. As κ is a two hydrogen doublet it can be assigned to C-10 along with ^{13}C signal L and by deduction the two hydrogen multiplet $\lambda(3)$ can be assigned to C-11. This logically leaves the one hydrogen triplet $\lambda(1)$ and ^{13}C peak J belonging to C-12. The red set of signals has a combined integral value of three. Signal μ is a double doublet with a chemical shift of 7.44 and coupling constants of 5.8 and 3.4 Hz, and signal $\lambda(2)$ is a two hydrogen multiplet. This evidence is consistent with signal μ being assigned to C-2 and signal $\lambda(2)$ being a combination of C-3 and C-4 methine Hs. An inspection of the HSQC spectrum (cross peaks ii, Figure 10) reveals ^{13}C signal M as belonging to C-2 and signals K and P either C-3 or C-4.

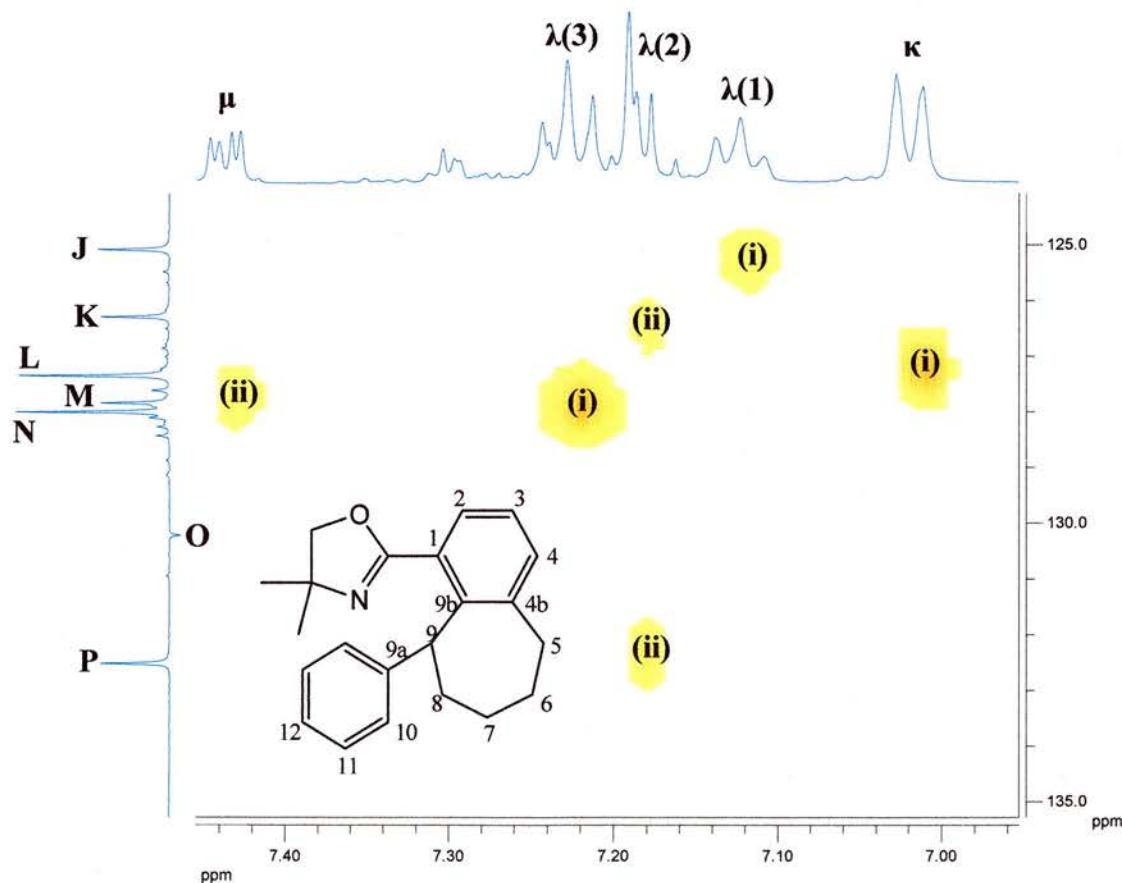


Figure 10 Aromatic region of HSQC spectrum of unknown **150**

In order to prove the NMR data are consistent with the proposed structure, the assignment and connectivity of the quaternary carbon signals O, Q, R & S needs to be carried out. In order for the proposed structure to be correct, C-5 hydrogens should have a 3J coupling with carbons 4, 9b & 7, and maybe a weak 4J coupling to C-3 & C-8 and also possibly weak 2J couplings to C-6 & C-4b. Analysis of the HMBC spectrum reveals that the C-5 hydrogen signal ζ has correlations with ^{13}C signals A(C-7), B(C-6), P, Q, R & S (circled cross peaks, Figure 11). As signal ζ also has one hydrogen of C-8 (ϵ & ζ), then the strong cross peak with ^{13}C signal B(C-6) can be assumed to derive from a combination of the C-5 – C-6 2J coupling and the 3J coupling C-8 – C-6 (cross peak i, Figure 11). This disregards signal B, but not signals Q & R, as they are quaternary and as yet to be defined. This is because C-5 hydrogens should have a 3J coupling to 9b (cross peak ii, Figure 11), and C-8 hydrogens would have 3J couplings to C-9a and C-9b (cross peaks i & ii, Figure 11) but Q & R are very close together quaternary signals that could belong to either 9a or 9b.

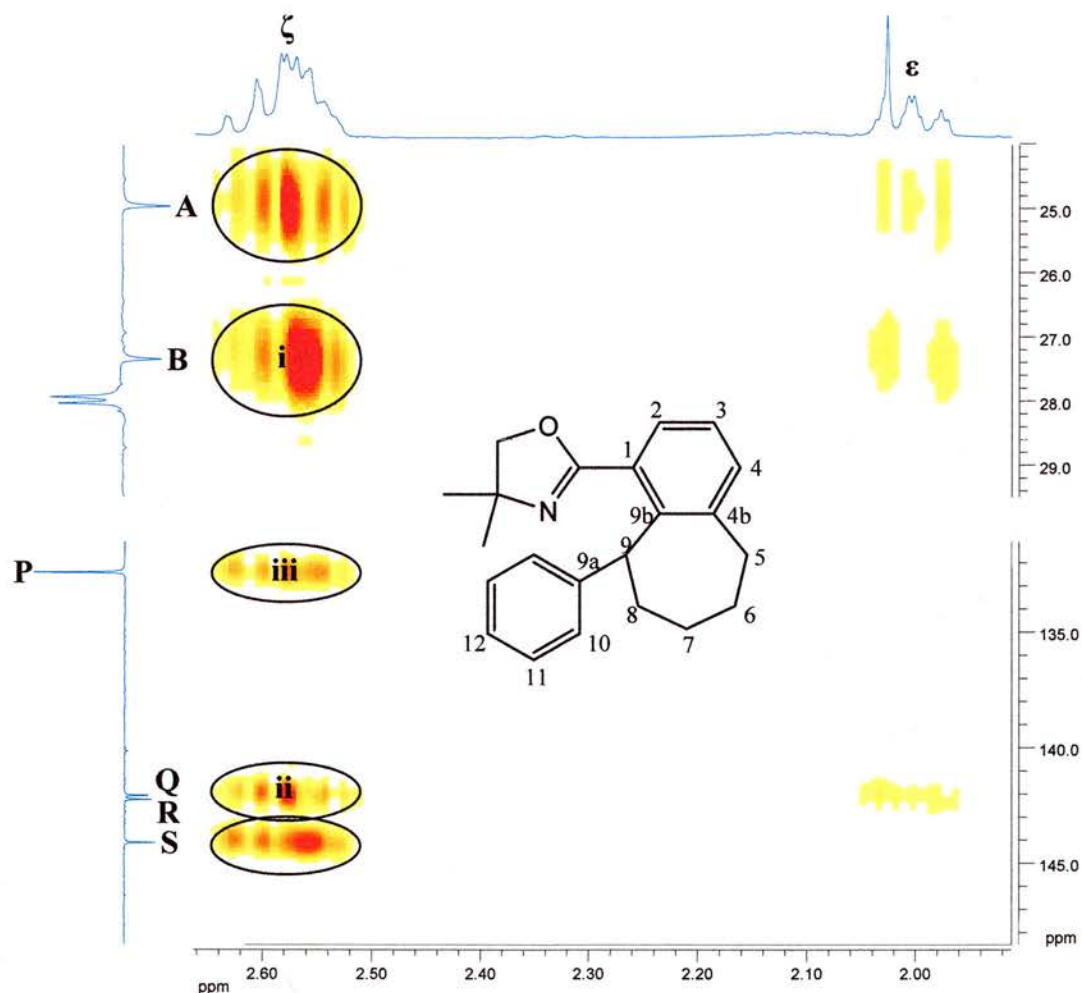


Figure 11 Region edited HMBC spectrum of unknown **150**

As the C-5 ^1H (ζ) signal is the only one to correlate with methine carbon signal P then it can be assigned to C-4 (cross peak iii, Figure 11). Further evidence for this assignment can be gleaned from the fact that C-2 hydrogens (μ) have a cross peak with ^{13}C signal P and vice versa ($\lambda(2)$ vs. M) (circled cross peaks, Figure 12).

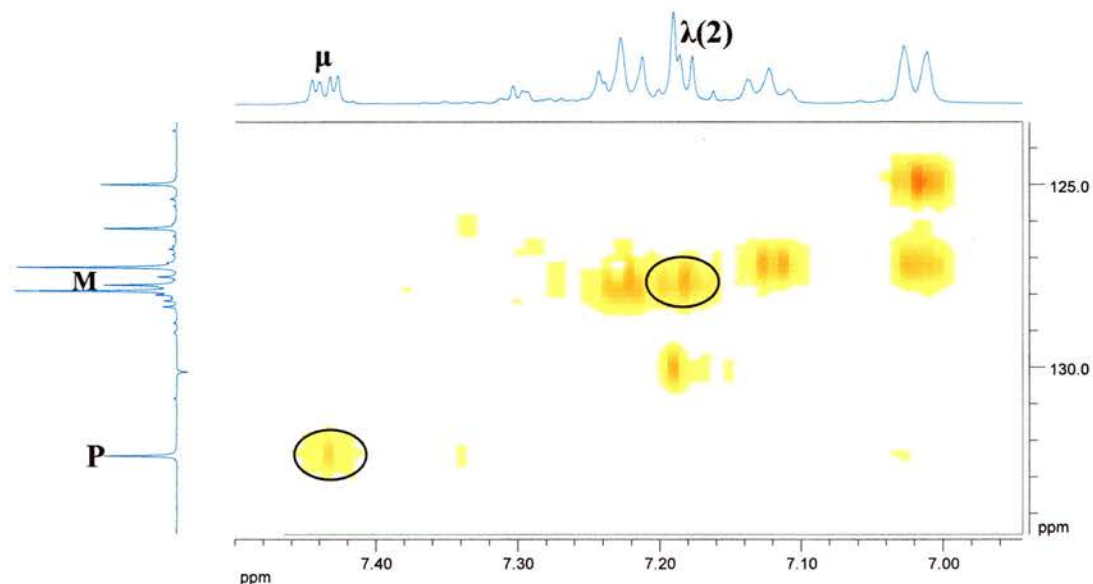


Figure 12 Region edited HMBC spectrum of unknown **150**

Therefore, by elimination, C-3 must be assigned to peak K. Signal ζ (C-5) also has a correlation with signal S, this could be a ^2J coupling. Assignment of quaternary carbon 4b to ^{13}C peak S, can be corroborated by the fact that only ^1H signals γ & δ (C-6), ζ (C-5), ι (C-9) and $\lambda(2)$ (C-3/4) show a strong correlation (circled cross peaks, Figure 13).

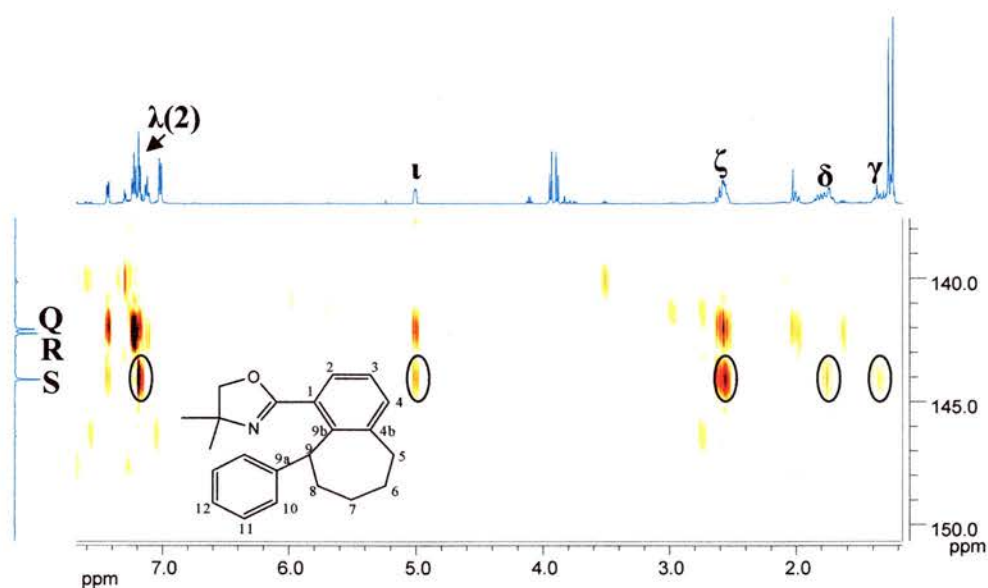


Figure 13 Region edited HMBC spectrum of unknown **150**

The only unassigned ^{13}C peaks are O, Q & R which should correspond to undesigned carbons 1, 9a and 9b. C-1 should have ^3J couplings with hydrogens of C-9(i) & C-3($\lambda(2)$). ^{13}C peak O is the only peak to show these correlations and is therefore assigned to C-1 (blue circles, Figure 14).

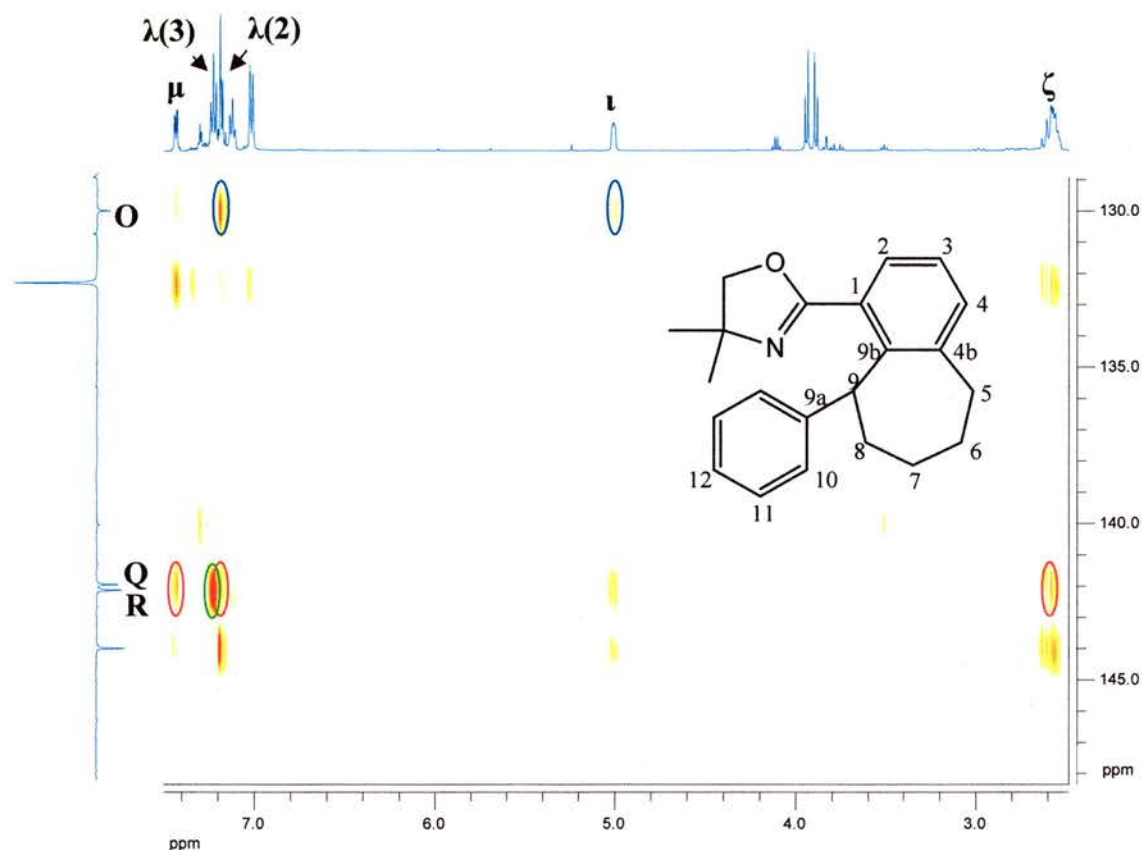


Figure 14 Region edited HMBC spectrum of unknown **150**

The close proximity of peaks Q and R to each other makes unambiguous assignment of them to either carbon 9a or 9b troublesome. C-2, C-4 & C-5 hydrogen signals (μ , $\lambda(2)$ & ζ) should show exclusive cross peaks to the ^{13}C signal attributed to carbon 9b (red circle, Figure 14) and C-11($\lambda(3)$) should show exclusive cross peaks to 9a (green circles, Figure 14). The difficulty lies in the fact that because the chemical shifts of ^{13}C peaks Q & R are so close, there is insufficient resolution to differentiate which cross peak correlates with which ^{13}C signal. A tentative assignment of peak Q to C-9b and thus peak R to C-9a has been made and is supported by the following evidence. A 3D projection of the 2D spectrum is analysed, where the ^1H signals for C-2(μ) and C-11($\lambda(3)$) correlate with peaks Q and R (Figure 15). It can be seen that the maxima for the cross peak relating to C-3(μ) and Q & R is slightly upfield (with

reference to the ^{13}C dimension) than the cross peak for the C-11($\lambda(3)$) and Q & R, therefore justifying the tentative assignment of resonance Q to C-9b (stated thus in the experimental description Section 3.10.7).

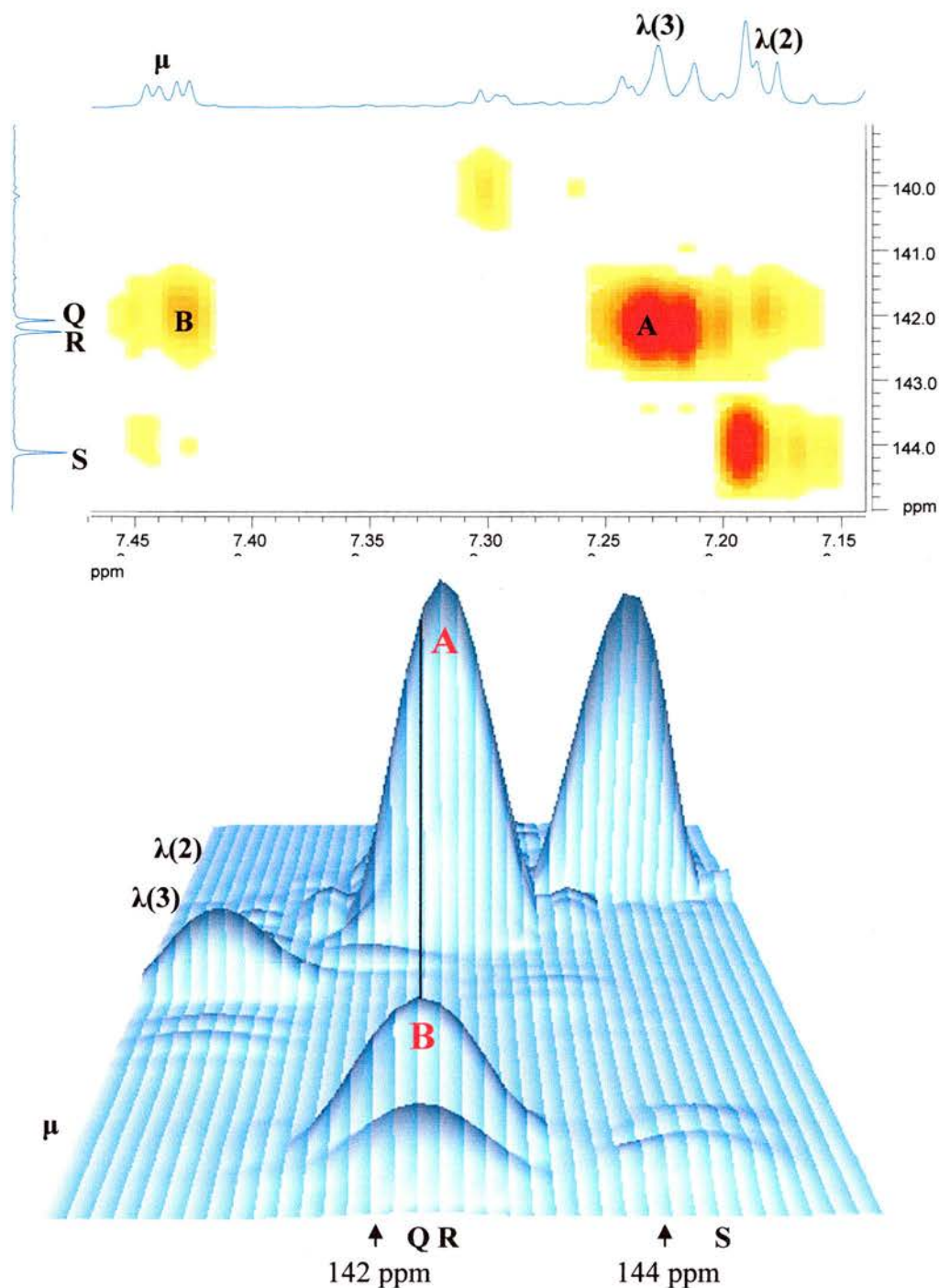


Figure 15 3D Projection and region edited HMBC spectrum of unknown **150**

Having now satisfactorily assigned resonances both in the ^{13}C and ^1H spectra to their respective carbons and hydrogens, confirmation of the phenyl ring at C-9 and

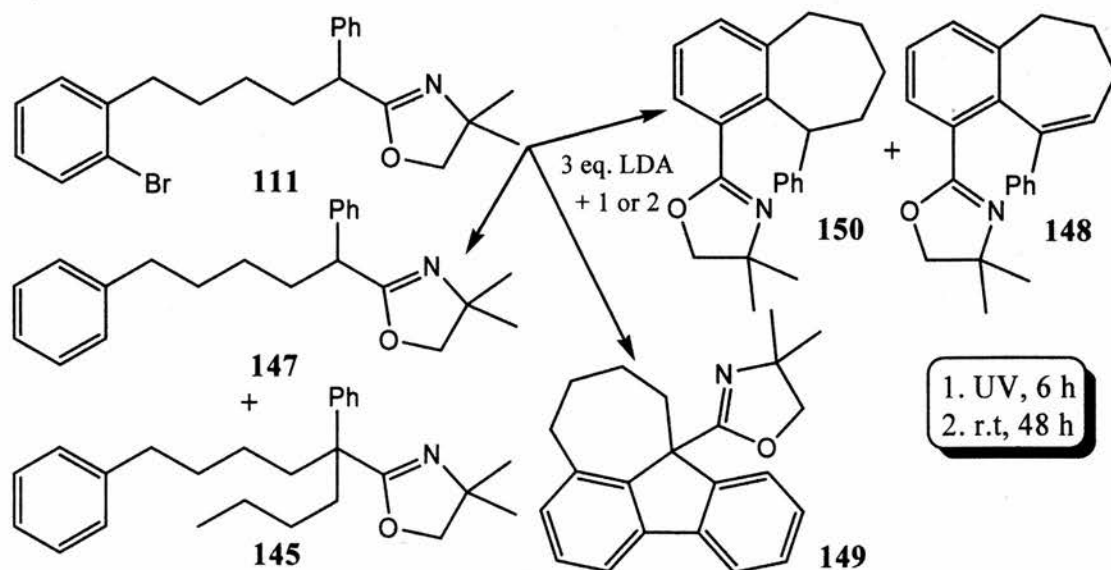
thus the oxazoline fragment at C-1 needed to be obtained. If C-10 hydrogens show a ^3J coupling to C-9 and vice versa, then confirmation would indeed be obtained. Examination of the relevant area of the HMBC spectrum shows this to be true. Therefore it can be concluded that the proposed structure **150** is concordant with experimental evidence.

2.5.2.2 Summary of $\text{S}_{\text{RN}}1$ Reactions of ϵ -Arylpentyl-2-oxazoline

The $\text{S}_{\text{RN}}1$ reaction of pentyl 2-oxazoline **111** was carried out again using the alternative reaction conditions involving irradiation for six hours. The product analysis results for this reaction and the previous two involving pentyl-2-oxazoline **111** are summarised in Table 13 & Scheme 133.

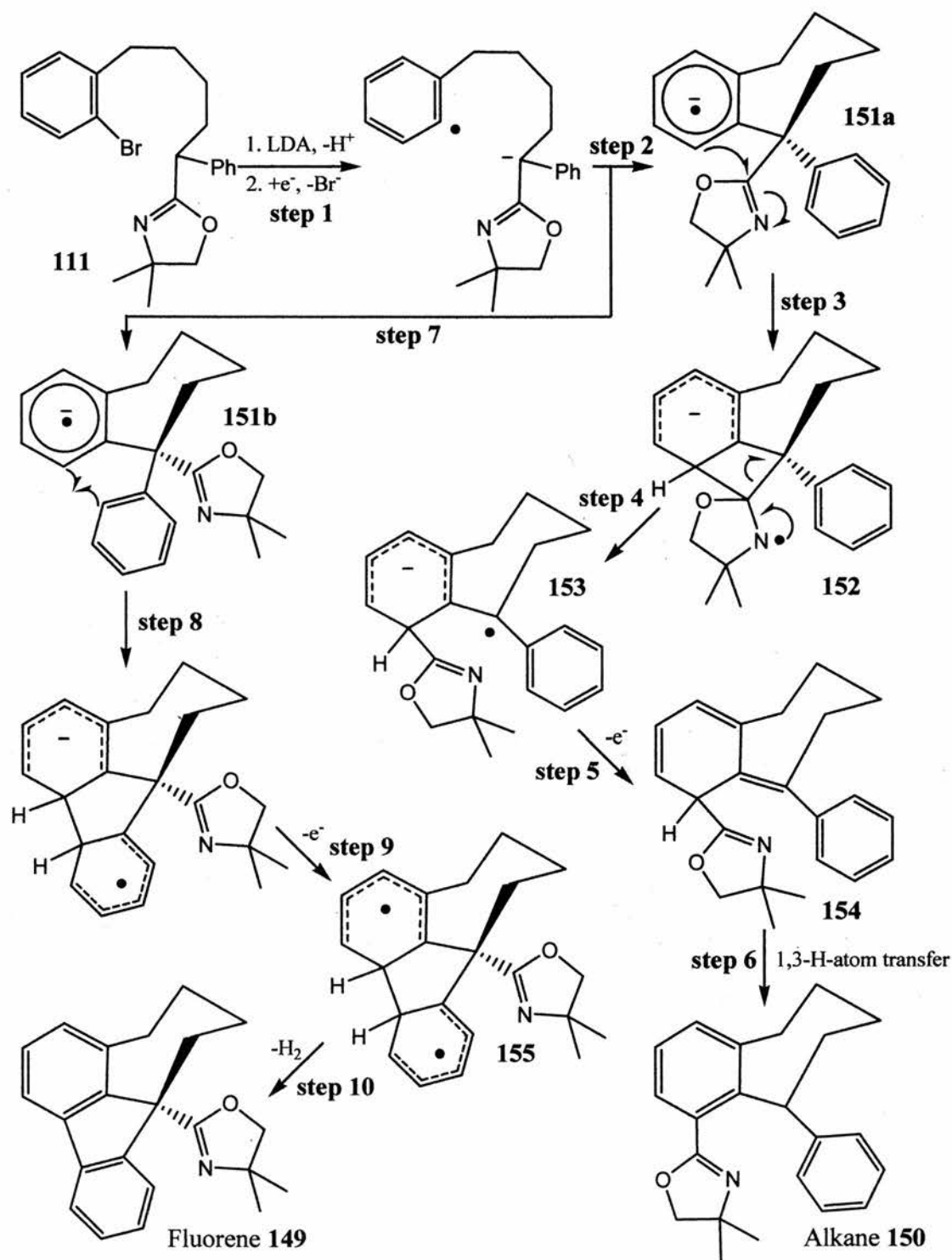
Entry	Conditions	S.M 111 (%)	Reduced 147 (%)	Alkane 150 (%)	Alkene 148 (%)	Fluorene 149 (%)	<i>n</i> -Butyl 145 (%)
1	(1) r.t, 48 h	15	-	-	-	-	36
2	(2) r.t, 48 h	-	7	19	25	6	13
3	UV, 6 h	-	10	30	6	3	-

Table 13 Summary of $\text{S}_{\text{RN}}1$ reactions of 2-oxazoline **111**



Scheme 133

2.5.2.3 Mechanism of Formation of Benzocycloheptane Derived Products



Scheme 134

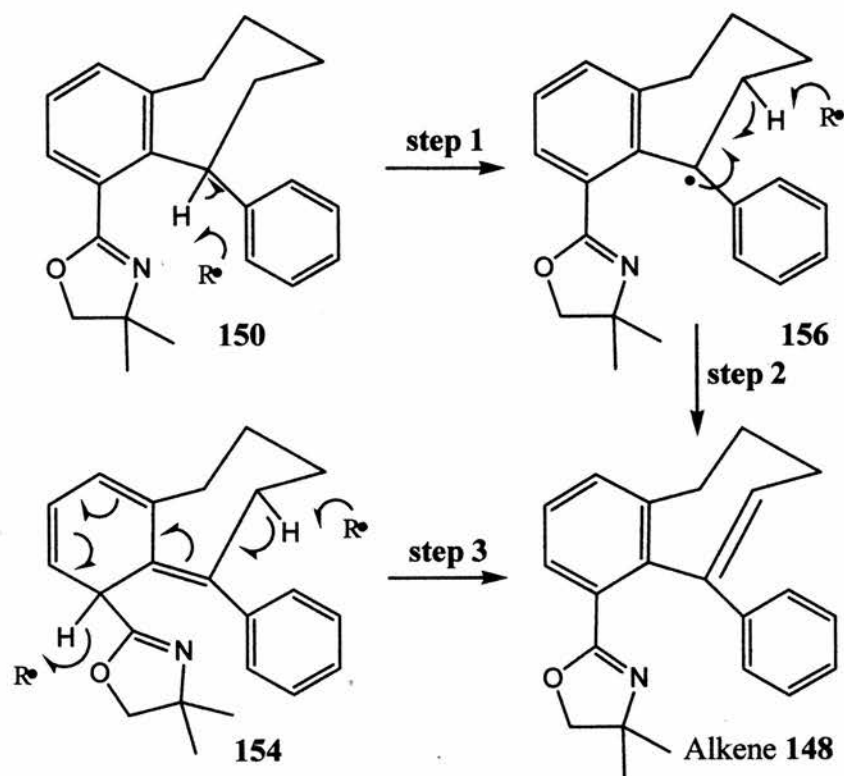
Two conceivable mechanistic paths can be considered to account for the formation of the diverse products from the $S_{RN}1$ reaction of pentyl-2-oxazoline 111

(Scheme 133). The first being a radical/radical anion pathway and the second being a benzyne/anionic pathway.

Shown in Scheme 134 is a summary of a proposed radical/radical anion pathway to explain the formation of cycloheptanes **149** & **150**.

The $S_{RN}1$ reaction is proposed to form the expected ring closure intermediate radical anion **151** via the normal pathway (steps 1 & 2, Scheme 134), after which the two different conformers **151a** and **151b** can react further to give **150** and **149** respectively. In radical anions **151a** and **151b** the unpaired electron will actually be distributed over both aromatic rings and part of the oxazoline moiety. However, for simplicity, a single resonance structure of each is shown. Conformer **151a** can undergo a 4-*exo*-trig attack by the benzene radical anion onto the oxazolanyl C=N to afford a cyclobutene-containing species **152** (step 3, Scheme 134), which then ring opens to give intermediate radical anion **153** (step 4, Scheme 134). The cyclobutene-containing species **152** might be a transition state rather than an intermediate. **153** can lose an electron to give cyclohexadiene **154** (step 5, Scheme 134), which then undergoes a rearomatisation via an allyl rearrangement to give alkane **150** (step 6, Scheme 134). Conformer **151b** performs a 5-*endo*-trig cyclisation involving the benzene radical anion and phenyl ring (step 8, Scheme 134). This is then followed by oxidation via a single electron transfer to give diradical **155** (step 9, Scheme 134) which readily eliminates dihydrogen to afford fluorene **149** (step 10, Scheme 134).

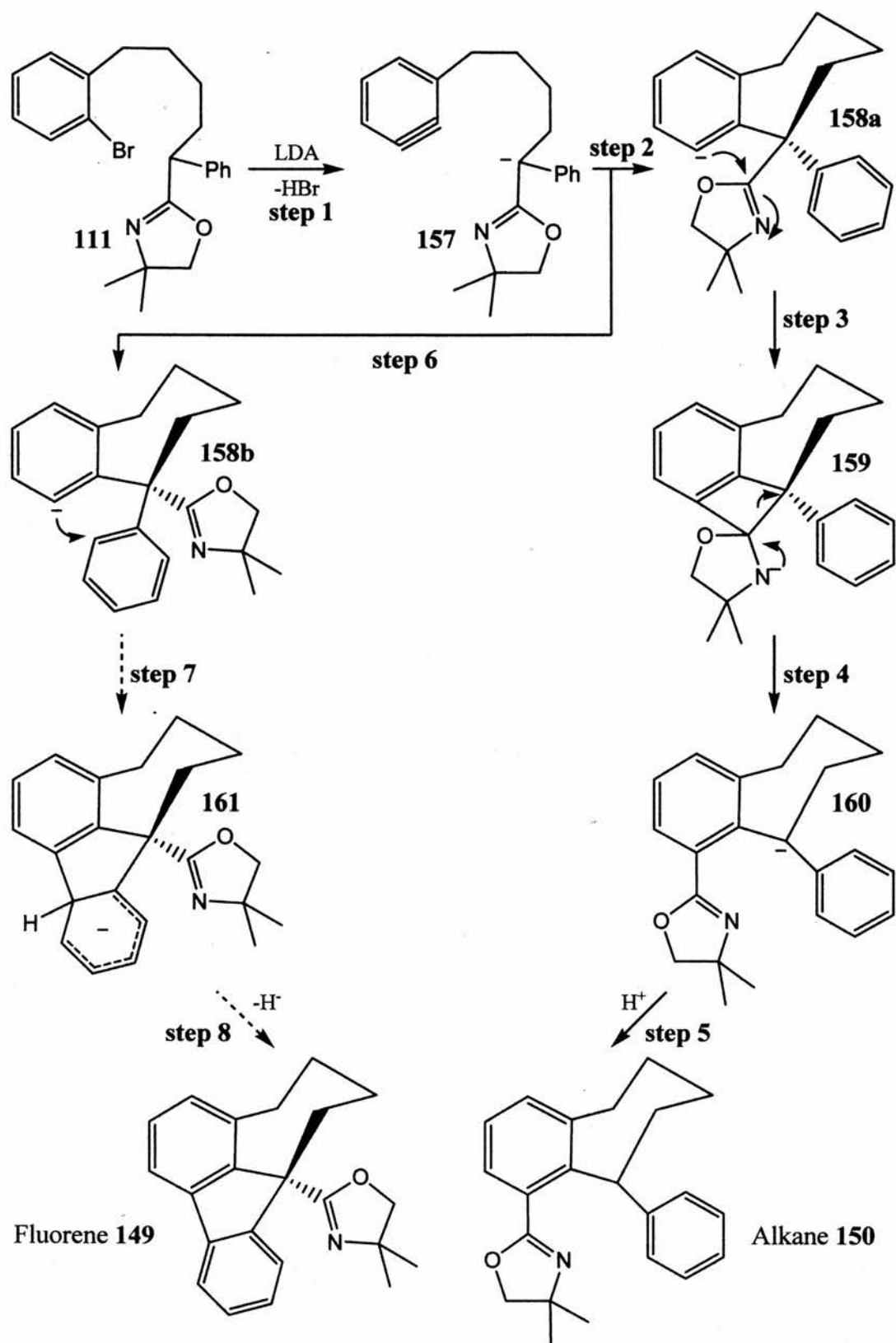
Alkene **148** could be formed via an adjunct to the pathway involving the formation of alkane **150** (steps 1-6, Scheme 134). This would occur via concerted H-atom abstractions from cyclohexadiene **154** (step 3, Scheme 135). An alternate route to alkene **148** is via a two step H-atom abstraction process from alkane **150**. The first step involves the formation of the resonance stabilised diphenylmethyl radical **156** (step 1, Scheme 135) followed, secondly, by β -hydrogen abstraction i.e. disproportionation (step 2, Scheme 135).



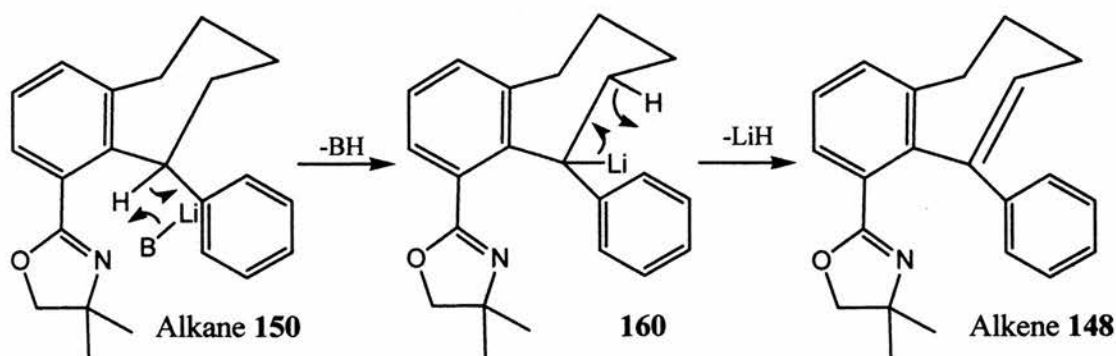
Scheme 135

The second mechanistic type, the benzyne route, to alkane **150** and fluorene **149** is summarised in Scheme 136.

As in the radical route the initial steps were envisaged to be the formation of an anionic intermediate **158**, only in this instance it is formed via an aryne intermediate **157**, which was created by the base induced loss of HBr from the aromatic ring (steps 1 & 2, Scheme 136). Conformer **158a** can proceed in a similar way to the radical case, by performing a 4-*exo*-trig cyclisation, by the aryl anion onto the C=N bond (step 3, Scheme 136). As before, this intermediate cyclobutene **159** should quickly ring open to afford diphenylmethyl anion **160** (step 4, Scheme 136). **160** can then pick up a proton to form alkane **150** (step 5, Scheme 136). Conformer **158b** is theoretically of the right orientation for a nucleophile attack on the phenyl ring by the aryl anion and thus via hydride abstraction afford fluorene **149** (steps 7 & 8, Scheme 136). However, this is deemed unlikely due to the unactivated status of the phenyl ring.



Scheme 136



Scheme 137

Production of alkene **148** via an anionic mechanism, is thought to possibly occur via LiH loss from the lithiated alkane **160** (Scheme 137). This process of LiH loss is a known process occurring under similar conditions.³⁰

The unusual benzyl-*ortho* rearrangement of the oxazolinyl moiety which ultimately results in alkane **150** and alkene **148** is supported by literature precedent in both mechanistic cases. Arynes have been shown to react with diethyl malonate with a 1,3-shift of one of the carboxy ethyl ester moieties to form 2-ethoxycarbonylmethylbenzoates.³¹ Also, polyaromatic radical anions have been revealed to react in a S_N2 fashion with cyclopropylmethyl bromides to afford the substitution product with loss of bromide.³²

The formation of the fluorene **149** is more likely to have occurred via the radical mechanism due the fact that phenyl radical attack on to another aromatic ring is a facile process whereas attack of a phenyl anion is not.

Analysis of the yields of alkenic product **148** with or without UV irradiation for 6 hours reveals that under UV irradiation much less is formed (6 % with, 25 % without) (Table 13). One possible explanation for this is that the mechanism of formation of the alkene is different under the two sets of conditions. Another more likely explanation based on the facts is that formation of the alkene is a result of a thermally induced dehydrogenation process based upon β-hydrogen loss from either the diphenylmethyl radical **156** or anion **160**.

Clearly contributions from both mechanistic types could be taking part in the formation of the observed products and only a detailed study would enable the full picture to emerge. However, it can be concluded that a major contribution by the radical anion mechanism is very likely based upon the following facts: a) in the formation of the indanes (Section 2.4) UV irradiation increased the rate of product

formation which is indicative of a $S_{RN}1$ type process; b) EPR spectra of radical anion intermediates were detected (Section 2.6).

2.5.3 Formation of Benzocyclooctanes Using $S_{RN}1$ Protocols

$S_{RN}1$ reactions of ζ -arylhexyl-2-oxazoline **112** were carried out using the usual conditions. Unfortunately, due to the lengthy synthesis and limited time and resources, only a small amount ca. 100 mg, was available. When the $S_{RN}1$ reactions were carried out (one at room temperature for 48 h and one under UV irradiation for 6 h) a multitude of products was observed in the $^1\text{H-NMR}$ spectrum. Due to the large number of products and the paucity of material, crude mixtures from both reactions were combined in the hope that after column chromatography enough of each product would be obtained to enable identification. Disappointingly, the NMR data obtained from each fraction from the column were not of high enough quality to enable complete identification; mainly due to mixtures of products. GCMS analysis of each fraction was carried out in the hope that evidence for products analogous to the benzosuberenes (section 2.5.2) could be obtained. Table 14 shows the results of the GCMS analysis together with tentative assignment, also included is a comparison of characteristic $^1\text{H-NMR}$ peaks of the benzosuberenes with the $^1\text{H-NMR}$ data found for the benzocyclooctanes.

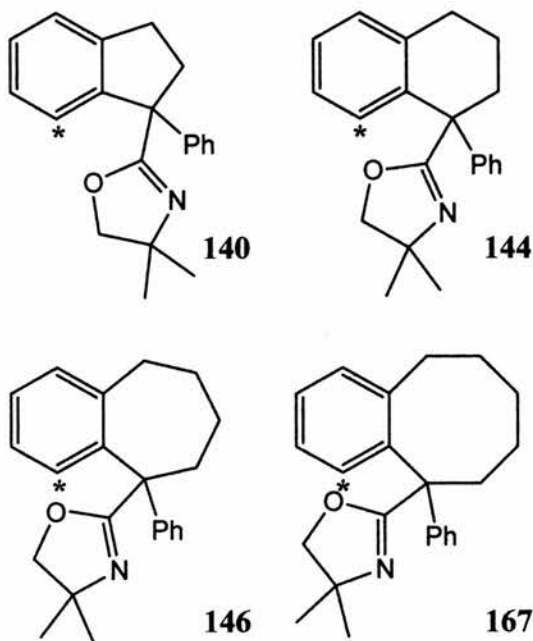
Evidence for the formation of the alkane **162** is based upon the obtained molecular ion mass and the presence of an unusually high aliphatic proton resonance, thought to account for the PhCH proton; this was also comparable to the 7-membered ring analogue **150** (entry 1, Table 14). Similarly alkene **163** was identified. Using the mass spectrum information alone, the alkene **163** can be distinguished from the fluorene **164** (both have $M^+ = 331$) by the presence in the alkene spectrum of 1:1 M^+ and M^+-1 peaks signifying the loss of the alkenic proton indicated, which is not the case in the fluorene **164** mass spectrum (entries 2 & 3, Table 14). Absolute differentiation can be made through the $^1\text{H-NMR}$ evidence (entry 2 & 3, Table 14). The reduced product **165**, *n*-butyl **166** and 1,1-octane **167** were all obtained as minor products, and therefore no clear NMR evidence could be obtained. They were tentatively identified purely on the basis of the mass spectral data (entries 4-6, Table 14).

Entry	I.D	Structure	MS (EI)	¹ H-NMR Data	Suberane NMR Data
1	Alkane 162		M ⁺ = 333 318, 304, 290	4.75 (br. dd, PhCH)	5.01 (dd, PhCH)
2	Alkene 163		M ⁺ = 331 330, 302, 276	3.48 (d, J = 7.9, CH _A H _B O) 3.79 (d, J = 7.9, CH _A H _B O) 6.32 (dd, J = 9.7 & 7.1, CH)	3.22 (d, J = 7.8, CH _A H _B O) 3.71 (d, J = 7.8, CH _A H _B O) 6.54 (t, J = 7.4, CH)
3	Fluorene 164		M ⁺ = 331 302, 278, 232	Broad Peaks at 7.5 – 7.8	Broad Peaks at 7.53 – 7.71
4	Reduced 165		M ⁺ = 335 244, 203, 189		
5	n-Butyl 166		M ⁺ = 391 260, 231, 189		
6	1,1- octane 167		M ⁺ = 333 276, 178, 126		

Table 14 Summary of GCMS and ¹H-NMR results of S_{RN1} reaction of 112

Clearly, additional work needs to be done in order to satisfactorily identify and characterise these products.

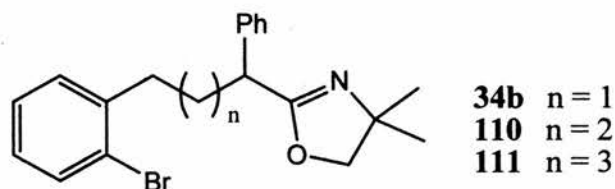
2.5.4 Summary of $S_{RN}1$ Reactions to Afford Tetralins, Benzosuberenes and Benzocyclooctanes



Scheme 138

The tetralin **144** was formed in moderate yields in an analogous manner to the indanes **139** & **140** reported in Section 2.4. When ϵ & ζ -arylalkyl-2-oxazolines **111** & **112** were reacted under the same conditions mostly rearrangement products were observed. These were derived from attack by a reactive centre at the *ortho* position of the fused benzo moiety. One rationale for these observations is that on moving from 6-5 fused ring system to a 6-8 system the conformational flexibility of the alkane ring is increased. This would bring the alkane ring portion into the sphere of reactivity around the *ortho*-benzo position and increase the likelihood of a reaction taking place between the *ortho*-aromatic position and either the nearby phenyl ring or oxazolinyli moiety (Scheme 138).

2.6 EPR Study of S_{RN}1 Reactions of Arylalkyl-2-oxazolines



Scheme 139

The reactions of the three homologous arylalkyl-2-oxazolines **34b**, **110** & **111** (Scheme 139), were studied using 9 GHz EPR spectroscopy. A solution of LDA in dry THF (7.5 or 1.5 mmol) was prepared under nitrogen and to this was added a THF solution of the precursor (2.5 mmol for **34b** and 0.5 mmol for **110** or **111**, 0.33 eq.).

The mixture was allowed to warm to room temperature and a 0.02 cm³ aliquot was transferred to a quartz capillary tube (1 mm i.d.) and photolysed in the resonant cavity of the EPR spectrometer with irradiation via unfiltered light from a 500 Watt super pressure Hg lamp.

2.6.1 EPR Spectra and Computational Results

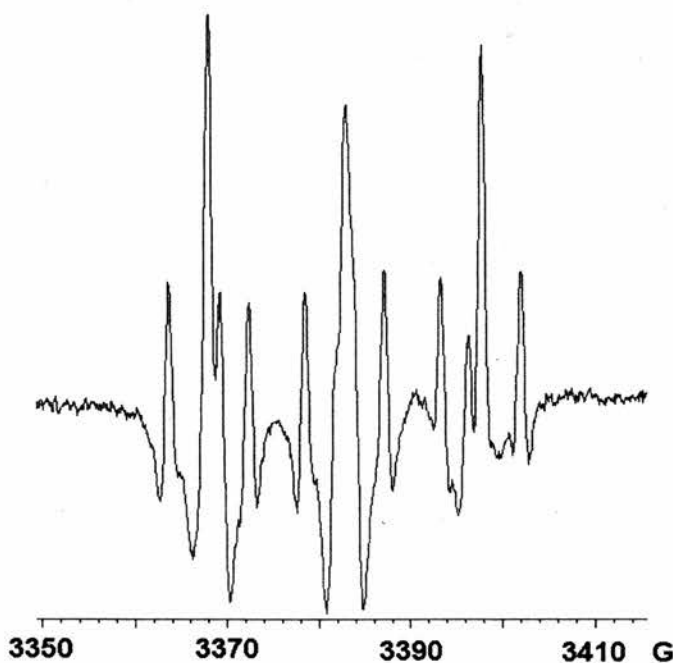


Figure 16 2nd Derivative EPR spectrum obtained from **34b** and LDA in THF at 290 K in the presence of traces of oxygen

When traces of oxygen were present, spectra similar to that shown in Figure 16 were obtained. The EPR parameters of the main spectrum ($g = 2.006$, $a(\text{N}) = 14.6$,

$a(2H) = 4.2$ G at 290 K) showed that this was due to the di-isopropyl nitroxide [aminoxyl radical, $(Me_2CH)_2NO\cdot$].^{33, 34}

The radical in this spectrum was comparatively short lived and the spectrum weakened over a period of about 1 h so that only weak broad signals from the second minor unidentified nitroxide remained.

The sample that gave rise to the observed nitroxide signals was prepared using standard preparative inert atmosphere conditions which illustrates the sensitivity of the reaction mixture to oxygen. Only when oxygen was rigorously removed via degassing the sample after addition into the tube, with a stream of nitrogen bubbled through a capillary was the nitroxide not observed. In the absence of the nitroxide, with precursor **34b** a longer lived species was observed having g -factor of 2.0030. The isotropic EPR signal was broad at 300 K and its intensity increased with UV photolysis. On lowering the temperature the intensity increased again and better resolution was obtained at temperatures of about 205 K (Figure 17).

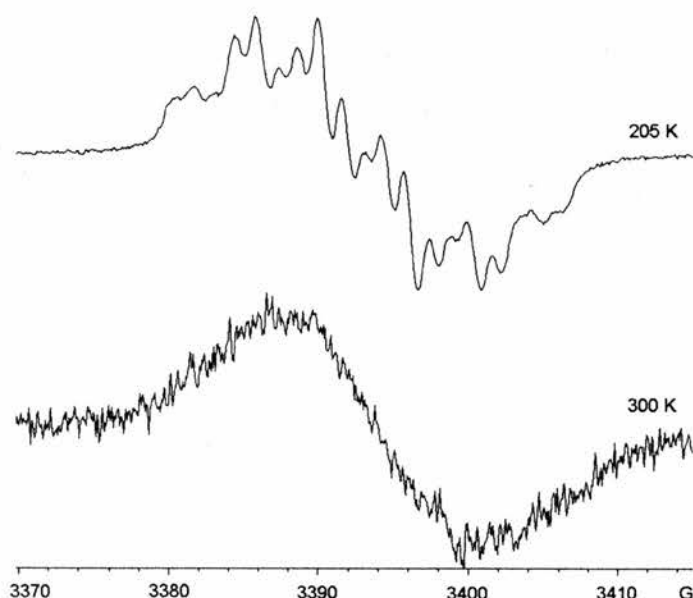


Figure 17 1st Derivative EPR spectra obtained from **34b** and LDA (3 equiv.) in THF with UV photolysis and complete exclusion of oxygen.

This spectrum was observable for many hours although its intensity gradually weakened. Broadly similar long-lived EPR spectra, with essentially identical g -factors, were obtained on treatment of precursors **110** and **111** with LDA in THF and illumination with UV light (Figure 18). A good computer simulation ($R = 0.991$)³⁵

was obtained for the 2nd derivative spectrum of **34b** (A, Figure 18) with the hyperfine splittings (hfs) listed in Table 15. The spectrum obtained from precursor **110** was considerably broader than the others (B, Figure 18). The asymmetry was caused by the presence of an additional signal originating from the quartz tube (probably an F-centre). Although satisfactory simulations could be obtained, these were very “soft” due to the poor resolution, so that reliable hfs could not be derived. However, the *g*-factor (2.0031), spectral width, and lifetime, all suggested the species responsible for this spectrum was analogous to that derived from the other precursors.

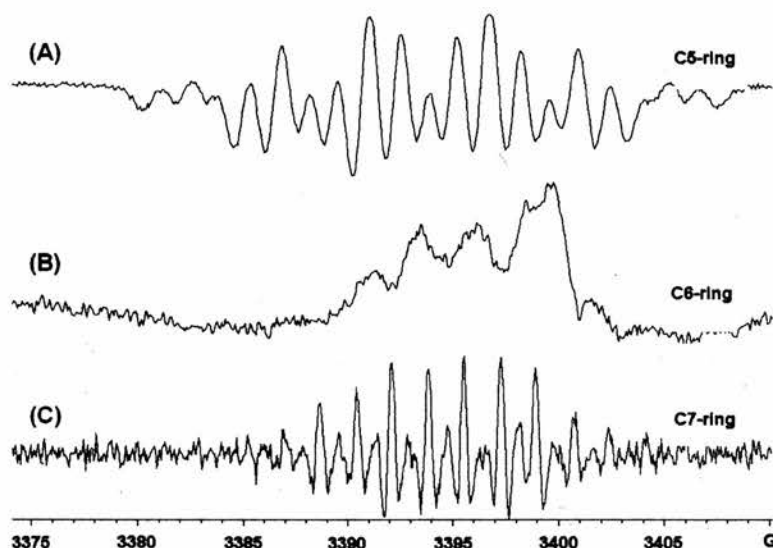


Figure 18 2nd Derivative EPR spectra obtained from (2-bromophenyl)alkyl-1-phenyl-dimethyl-2-oxazolines and LDA on UV illumination in THF solution. Top: from propyl-precursor **34b** at 205K. Middle: from butyl-precursor **110** at 194 K. Bottom: from pentyl-precursor **111** at 195 K.

The spectrum obtained from pentyl-precursor **111** was well resolved and the 2nd derivative presentation (C, Figure 18) suggested that two similar paramagnetic species were present. A satisfactory simulation including both species (*R* = 0.922) was obtained with the parameters shown in Table 17, and this is displayed in Figure 19.

The *g*-factors and the magnitudes of the hfs of these species suggested they were aromatic radical anions. Cyclo-coupling of the aromatic radical-carbanion derived from **34b** will give a radical-anion that contains an indane unit substituted by phenyl and oxazoline rings i.e. **168**. The experimental hfs were tentatively assigned to specific H-atoms of **168** with the aid of DFT computations (Table 15) and are compared with experimental data from the literature (Figure 20) for the model radical

anions of diphenylmethane **169**³⁴ and indane **170**³⁶ which had been prepared by treatment of the corresponding hydrocarbons with K metal. The data for **168** is sufficiently similar to that of **169** and **170** to support the attribution of our spectrum to radical anion **168**. A noteworthy feature is that the spin density is equally distributed to both phenyl rings in **169**. In radical anion **168** spin density is also distributed to both rings but the two rings are not chemically or magnetically equivalent so the spin is not equally partitioned.

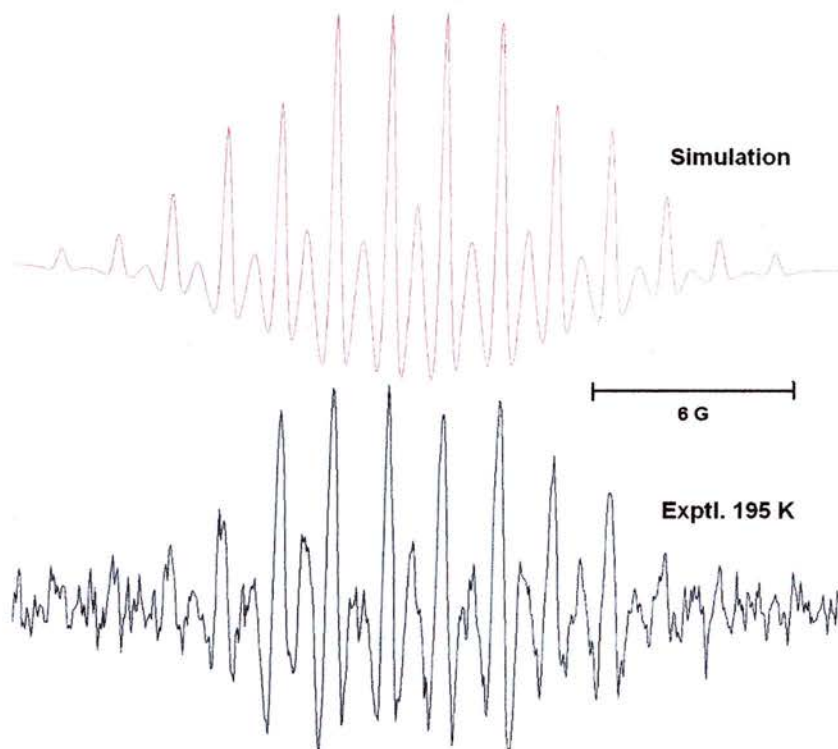


Figure 19 Comparison of experimental and computed spectra for species **172Ax** and **172Eq** derived from precursor **111**.

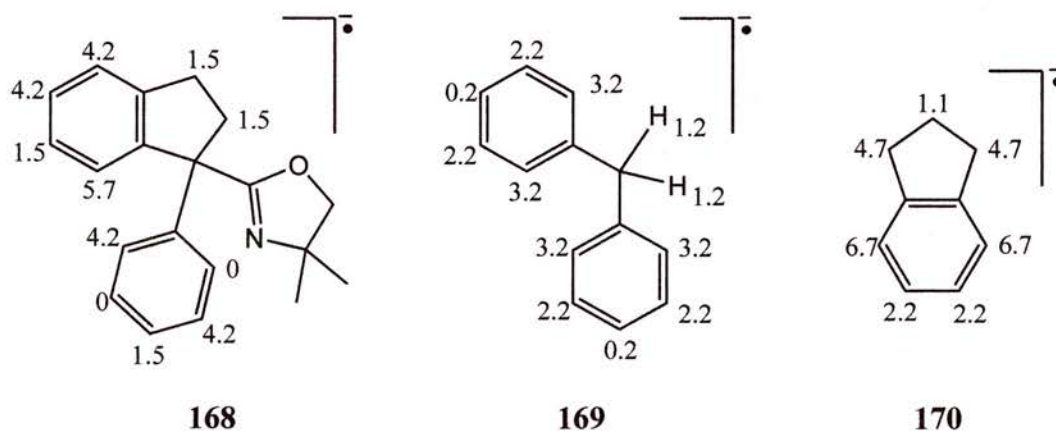


Figure 20 Isotropic EPR H-atom hfs of aromatic radical-anions. Counter ions for **168**: Li^+ , and for **169** and **170**: K^+ .

The structures and energies of the parent indane **140** and radical anion **168** were computed using DFT methods.³⁷ Two views of the structure of **168** computed using the UB3LYP functional with a 6-31G(d,p) basis set are shown in Figure 21.

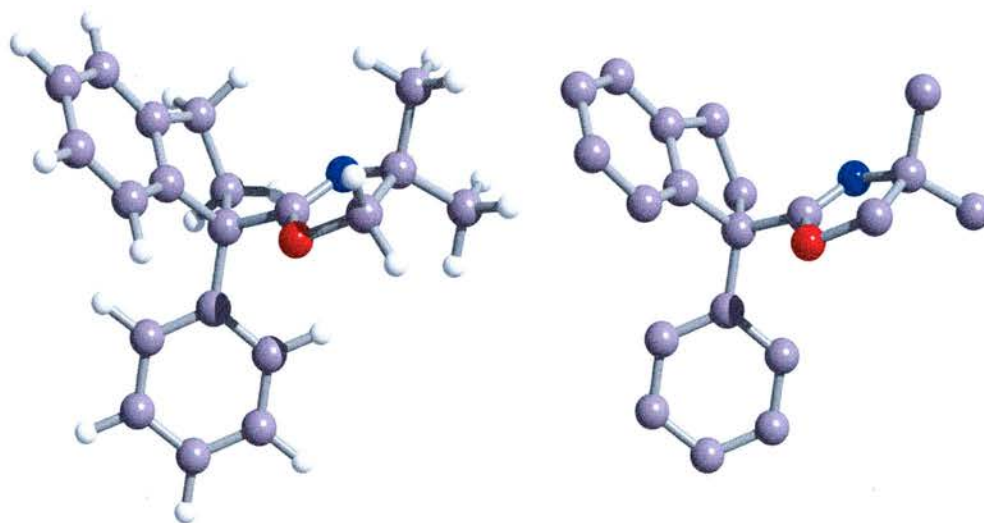
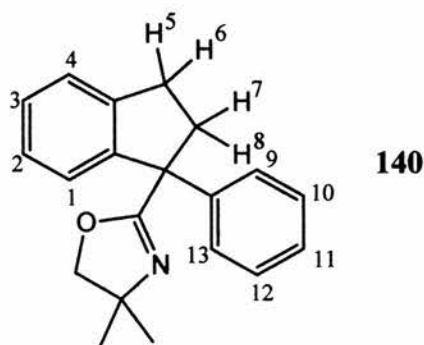


Figure 21 DFT computed structure of radical anion **168**. Left: including H-atoms. Right: no Hs

The 5-membered ring of the indane unit showed a definite pucker in the computed structure, but the pseudo-rotation barrier would be very low and hence only a single conformer of the molecule will be detectable on the EPR timescale. Of course, two enantiomers (1:1) are formed in the cyclisation step, but their EPR spectra would be identical. The EPR hfs computed for **168** using various basis sets, including the triple-zeta quality EPR-III basis set specially developed for hfs by Barone,³⁸ are shown in Table 15.

Basis Set	Hydrogen Atom												
	1	2	3	4	5	6	7	8	9	10	11	12	13
6-31G (d)	-5.6	1.0	-4.4	-3.8	-1.0	-0.7	1.0	0.1	0.2	-3.6	-1.4	0.1	-4.0
6-31G (d, p)	-4.3	0.4	-2.6	3.6	-1.0	-0.5	1.1	0.4	-0.5	-2.9	-0.3	-0.6	2.7
EPR-III	-3.2	0.4	-2.0	-2.6	-0.7	-0.4	0.8	0.2	-0.1	-2.2	-0.3	-0.3	2.0
Exptl. (205 K)	5.7	1.5	4.2	4.2	1.5	-	1.5	-	-	4.2	1.5	-	4.2

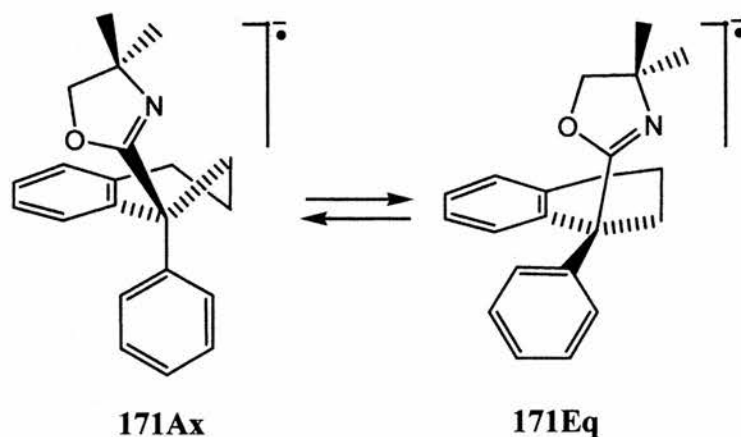
Table 15 EPR hfs/G computed for radical-anion **168** using the UB3LYP functional and the molecular geometry optimised with the 6-31G+(d,p) basis set. Shown in Scheme 140 is indane **140** with hydrogens numbered.



Scheme 140

The computations clearly show that spin density is distributed to both phenyl rings. This distribution will depend critically on the torsion angle about the C-C bond connecting the Ph ring to the indane unit. The barrier about this single bond will be very low because the Ph and oxazoline rings can easily rotate together in a propeller type motion. In view of this, great precision in the computed hfs cannot be expected. The experimental hfs were assigned to specific H-atoms simply on the basis of the computed data and hence the assignments are only tentative. However, the data gives good support for the assignment of the spectrum to radical-anion **168**.

The EPR spectrum from precursor **110** was comparatively broad. The computed structure for the tetralin ring of the cyclised radical anion **171** showed that the cyclohexene-type ring adopts a half-chair structure (Figure 22). In this conformation the pseudo-axial and pseudo-equatorial orientations are not equivalent and hence two conformers of the radical anion are expected to result from the cyclisation step i.e. **171Ax** and **171Eq** (Scheme 141). Each of these will be present as a 1:1 mixture of enantiomers. The barrier to inversion for the unsubstituted cyclohexene ring is about 5 kcal mol⁻¹.³⁹ The barrier to interchange of structures **171Ax** and **171Eq** will probably also be of this order, i.e. comparatively low.



Scheme 141

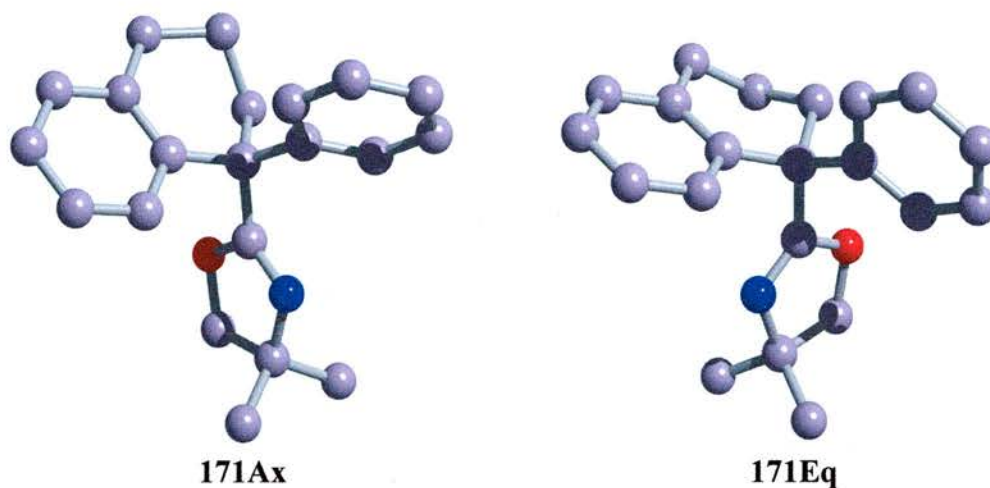


Figure 22 Structures of **171Ax** and **171Eq** computed with the UB3LYP functional and a 6-31G(d) basis set.

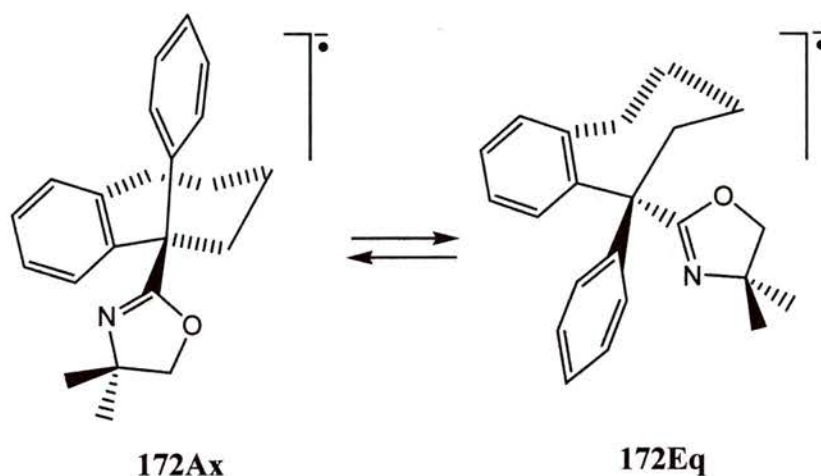
The energy differences of the conformers of the tetralin and benzocycloheptane radical anions and of the corresponding neutral products, computed with the UB3LYP functional and the 6-31G(d) basis set, are shown in Table 16.

	ΔH_o Radical-anions E(Eq-Ax) kcal/mol	ΔH_o Neutral products E(Eq-Ax) kcal/mol
Tetralin 144	-1.6	-0.7
Benzocycloheptane 146	4.6	0.5

Table 16 DFT computed energy differences between conformers of **144** & **146** and the corresponding radical anions **171** & **172**.

For the 6-member ring radical-anions (tetralins) the conformer with the Ph group axial was calculated to be lower in energy whereas for the 7-member ring analogues the conformer with the Ph group equatorial was lower in energy. The small computed energy difference between the tetralin conformers suggests the barrier to inversion will be low. It follows that this inversion may be taking place at ‘intermediate’ rate during the EPR experiments, i.e. the observed spectral broadening may be due to this internal motion.

The benzocycloheptane structure **172**, that results from cyclisation of precursor **111**, contains a cycloheptene type ring and hence two conformations were also expected, i.e. **172Ax** and **172Eq** (Scheme 142).



Scheme 142

DFT computed structures for these radical anions are shown in Figure 23. The 7-membered ring in the parent, unsubstituted cycloheptene also has an experimental barrier to inversion of ca. 5 kcal mol⁻¹.^{39 & 40} However, the two conformers of **172** are much more crowded than the conformers of **171** and interchange of the pseudoaxial and pseudoequatorial substituents is seriously impeded by the proximity of atoms from the benzocycloheptane unit. Therefore the barrier in **172** is likely to be significantly higher.

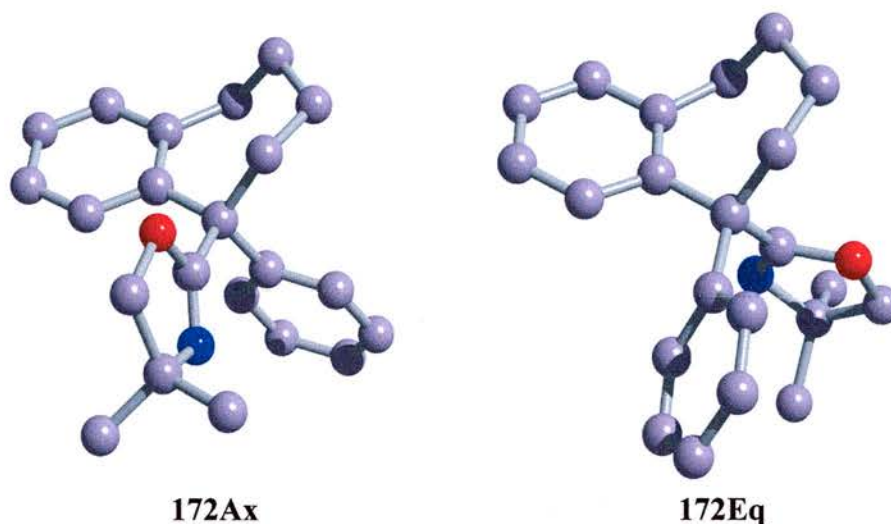


Figure 23 Structures of **172Ax** and **172Eq** computed with the UB3LYP functional and a 6-31G(d) basis set.

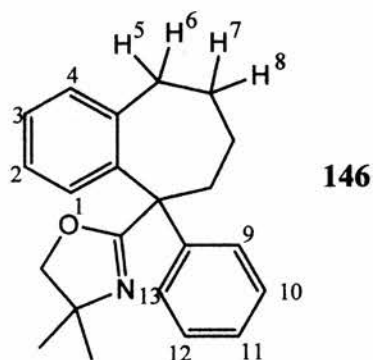
The computed energy difference between **172Ax** and **172Eq** was significantly greater than in the case of the tetralin conformers (Table 16). The energy of the **172Eq** structure, with the Ph ring equatorial, was found to be 4.6 kcal mol⁻¹ lower than the **172Ax** structure with the 6-31G(d) basis set and 3.8 kcal mol⁻¹ lower with the much larger EPR-III basis set. The crowded nature of **172** implies that the ring

inversion barrier will be significantly greater than 5 kcal mol^{-1} , as does the computed energy difference between **172Eq** and **172Ax**. This probably explains why the spectrum was not broadened, i.e. because interchange of structures **172Eq** and **172Ax** was slow on the EPR timescale. In view of this, the two species in the experimental EPR spectrum (Figure 19) were assigned as the equatorial and axial conformers **172Eq** and **172Ax**. Table 17 shows the experimental hfs compared with *ab initio* calculations with two basis sets. Experimental hfs were assigned to specific H-atoms simply by comparison with the magnitudes of the computed hfs and are obviously quite tentative.

Basis Set	172Ax Hydrogen Atom												
	1	2	3	4	5	6	7	8	9	10	11	12	13
6-31G (d)	-0.2	-1.4	-6.4	-4.0	3.3	0.5	-0.2	0.2	-0.5	-3.1	-0.2	-0.5	3.1
EPR-III	0.2	-0.9	-3.8	1.0	1.1	-0.4	-0.1	-0.2	-0.2	-1.7	-0.1	-0.4	1.7
Exptl. (205 K)	-	1.5	3.4	1.5	1.5	-	-	-	1.5	3.4	1.5	1.5	3.4

Basis Set	172Eq Hydrogen Atom												
	1	2	3	4	5	6	7	8	9	10	11	12	13
6-31G (d)	-1.4	-0.3	0.0	-1.2	0.3	0.7	0.0	0.0	-1.4	-0.4	-7.1	0.7	-3.7
EPR-III	-1.2	-0.1	0.0	-1.2	0.3	0.1	0.0	0.0	-0.8	-0.5	-6.2	0.6	-3.0
Exptl. (205 K)	3.4	-	-	3.4	-	-	-	-	3.4	1.8	5.1	1.8	3.4

Table 17 EPR hfs/G computed for radical-anions **172Ax** (upper) and **172Eq** (lower) using the UB3LYP functional and the molecular geometry optimised with the 6-31G(d) and EPR-III basis sets. Scheme 143 shows cycloheptane **146** with hydrogens numbered.



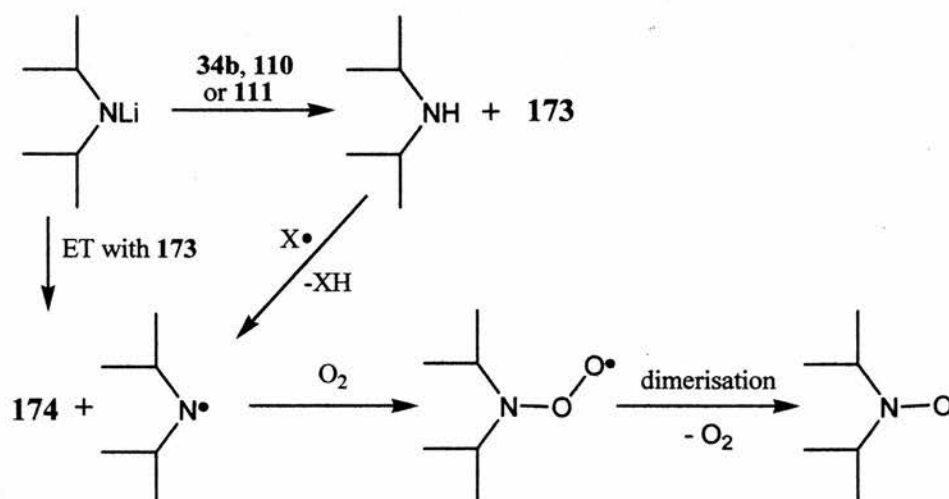
Scheme 143

Table 17 shows that there is a reasonable correlation between the experimental and the computed hfs. In particular, the experimental spectrum of the major species

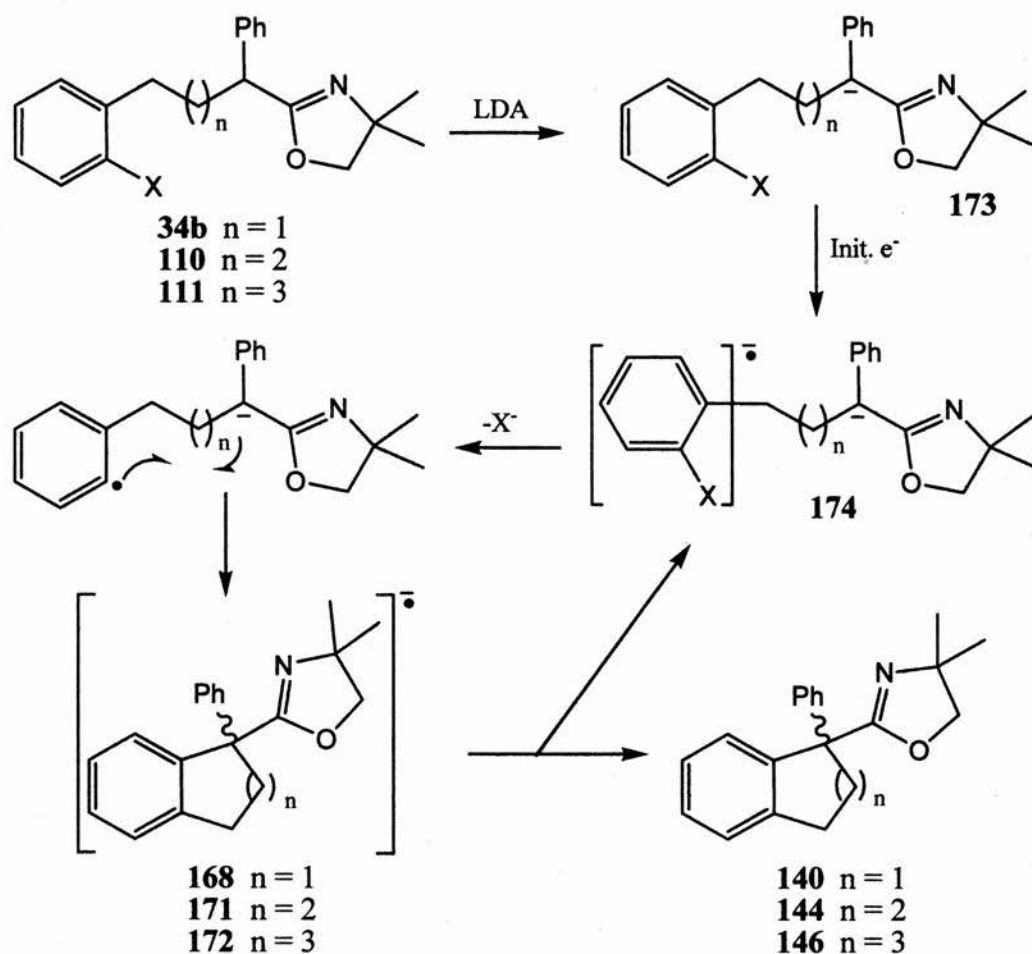
had one large hfs (5.1 G), not present in the spectrum of the minor species, and this correlates well with the computed data for **172Eq** which also has one large hfs (H-11).

2.6.2 Mechanistic Considerations

Wolfe,²⁷ Goehring,⁴¹ and others⁴² have argued that the mechanism for photo-stimulated inter- and intra-molecular reactions of haloaromatics with carbanions, promoted by LDA/THF or MNH₂/liq. NH₃ (M = Li, Na, K), is the S_{RN1} chain process (Scheme 145), rather than a mechanism involving aryne formation followed by inter- or intra-molecular nucleophilic attack by the carbanion (Section 2.5.2.3, Scheme 136). The main evidence for this was: (i) the fact that the reactions were inhibited by radical traps including di-*t*-butyl nitroxide and *p*-dinitrobenzene, (ii) the fact that UV photolysis accelerated the reactions, (iii) the sensitivity of the reactions to oxygen (Scheme 144), (iv) the fact that haloaromatics incapable of producing arynes, because they lacked H-atoms adjacent to the halogen, gave the expected coupled or cyclo-coupled products and (v) that minor amounts of dimers (e.g. biphenyl from bromobenzene) were produced.



Scheme 144 Mechanism of nitroxide formation observed in EPR experiments with trace oxygen present.



Scheme 145 Mechanism of photo-stimulated, base-promoted reactions of (2-bromophenyl)alkyl-2-oxazolines.

The EPR spectroscopic data obtained from the reactions of **34b**, **110** & **111** with 3 eq. LDA in THF fully support the $S_{RN}1$ mechanism. The EPR spectra that were obtained from precursors **34b**, **110** & **111** can reliably be attributed to the radical anions **168**, **171** & **172** that are expected as intermediates in an $S_{RN}1$ type cyclo-coupling step. The concentrations of **168**, **171**, and **172** were determined by double integration of their EPR spectra and comparison with the signal from a solution of DPPH of known concentration (1 mM) in the same capillary tube as used for the LDA experiments. The signal intensities increased significantly during UV photolysis, as expected for the $S_{RN}1$ process with photo-stimulation of the initiation step. Signal intensities decreased slowly over time; therefore values from shortly after the start of photolysis are displayed in Figure 8.

The measured radical anion concentrations ranged from 4×10^{-6} M for **172** to 3×10^{-4} M for **168**. At the temperature of the preparative experiments (ca. 290 K) somewhat lower concentrations will prevail. The measured concentrations expressed

as a percentage of the initial concentrations of the individual precursors were extrapolated to 290 K (Table 18).

Ratio	[168/34b]	[171/110]	[172/111]
% at 290 K	1.5	0.8	0.6

Table 18 Radical anion concentration at 290 K.

These values represent a significant proportion of the concentration of the precursor molecules and hence the EPR spectra are not minor, stray species, but important intermediates that help propagate the chains.

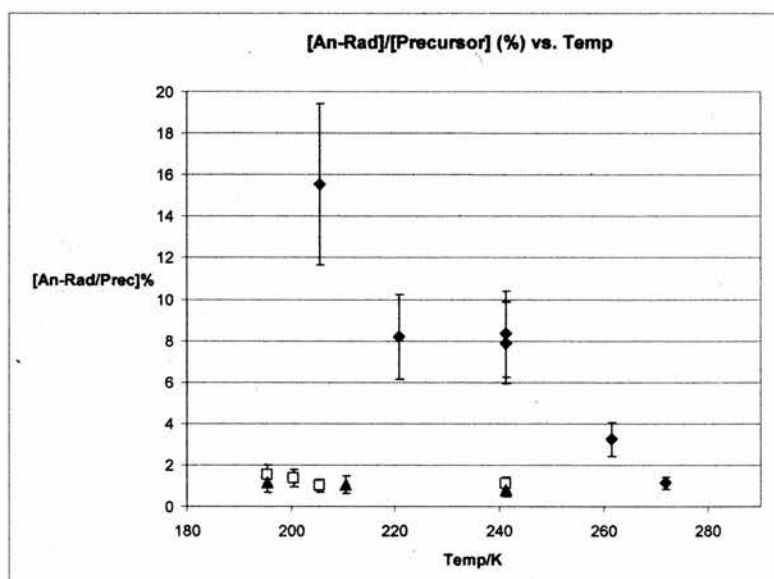


Figure 24 Plots of the concentrations of radical anions, relative to the concentrations of the precursors vs. temperature. ◆: [168/34b]%, □: [171/110]%, & ▲: [172(Eq+Ax)/111]%

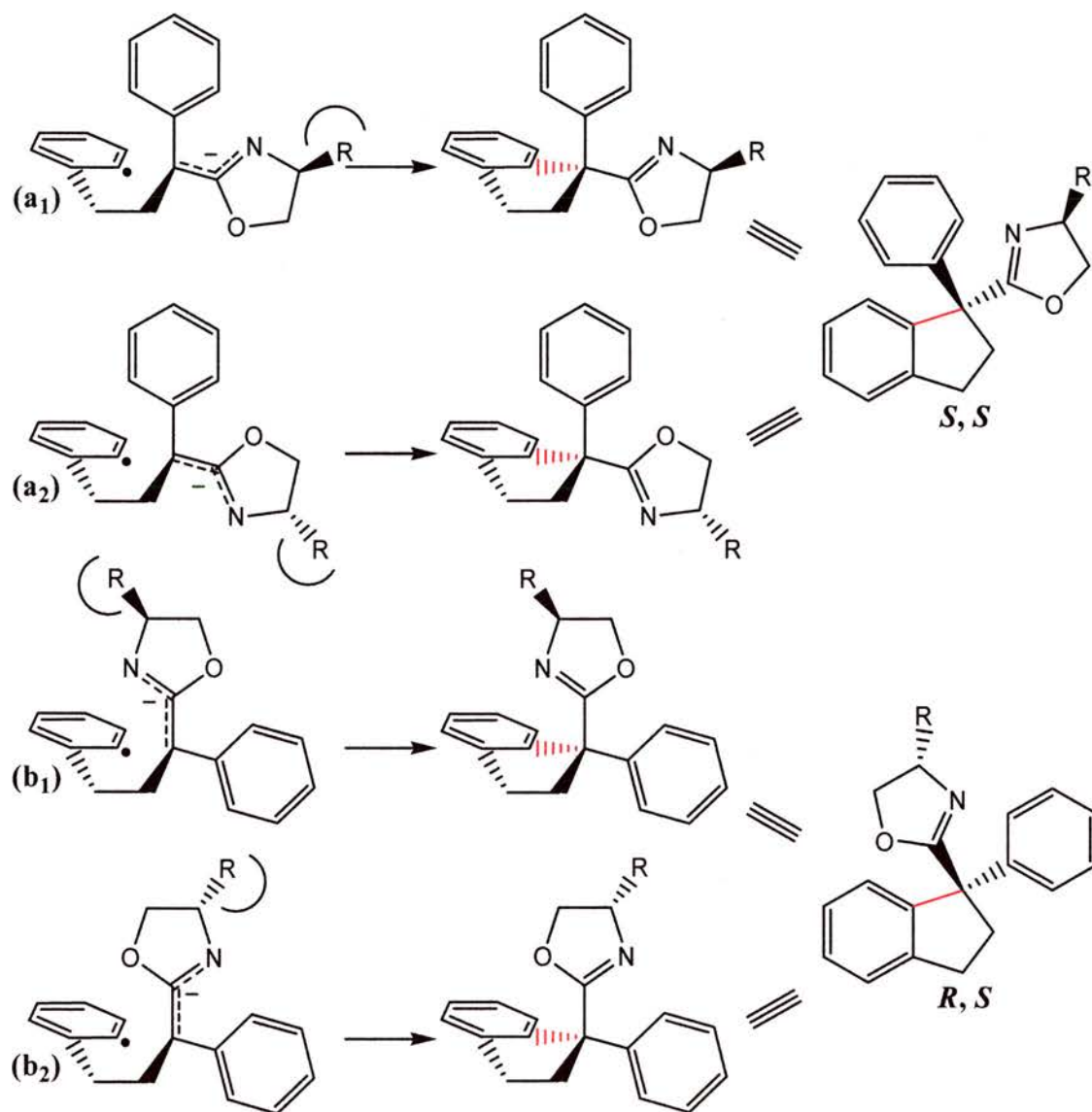
The data are consistent with a chain process of moderate length. Figure 24 shows that the concentration of each radical anion was increased at lower temperatures. This is as would be expected if chain propagation was slower at lower temperatures. In particular, Scheme 145 proposes that the radical anions decay by bimolecular electron transfer (ET) to more precursor. This step would slow down as temperature was lowered and hence, if this is the slow rate limiting step, the concentration of the radical anions would be expected to build up; exactly as observed.

The detection of di-isopropyl nitroxide in the presence of oxygen is further evidence in favour of a radical-mediated chain. The nitroxide is probably derived from di-isopropylaminy radicals generated from LDA (Scheme 144). Two routes to this radical can be envisaged. The $i\text{-Pr}_2\text{N}^-$ anion could transfer an electron to a precursor molecule **173** thus initiating a new chain and generating the $i\text{-Pr}_2\text{N}^\bullet$ radical together with species **174**. This amounts to an initiation step and would account for the fact that excess LDA was always found to be advantageous. Alternatively, $i\text{-Pr}_2\text{N}^\bullet$ could be formed by some other radical (or radicals) in the system (X^\bullet) abstracting an H-atom from $i\text{-Pr}_2\text{NH}$. The $i\text{-Pr}_2\text{N}^\bullet$ radical will capture dioxygen to give the corresponding peroxy radical $i\text{-Pr}_2\text{NOO}^\bullet$ and coupling of two peroxy radicals will produce the observed di-isopropyl nitroxide together with oxygen. This is a secondary nitroxide and will decay by disproportionation to the corresponding oxime and nitrene. However, it will also inhibit the $S_{\text{RN}}1$ chain, and this is consistent with the observed sensitivity of the reactions to oxygen. In summary, the EPR data fully support the $S_{\text{RN}}1$ chain mechanism and suggest that the aryne route is unimportant in these photo-stimulated reactions.

2.7 Diastereoselective $S_{RN}1$ Reactions

Having shown that azaenolates of achiral 2-oxazolines can take part in intramolecular $S_{RN}1$ reactions, it was envisaged that diastereoselectivity could be achieved in the reactions of analogous precursors containing chiral 2-oxazolines.

It was hoped that by attaching bulky groups to the 2-oxazoline moiety the facial selectivity of the coupling of the aryl radical to the azaenolate could be influenced (Scheme 146). It was expected that the reaction would proceed along the normal reaction pathway (Section 2.4) to give four intermediate conformers (a_1 , a_2 , b_1 & b_2 , Scheme 146).

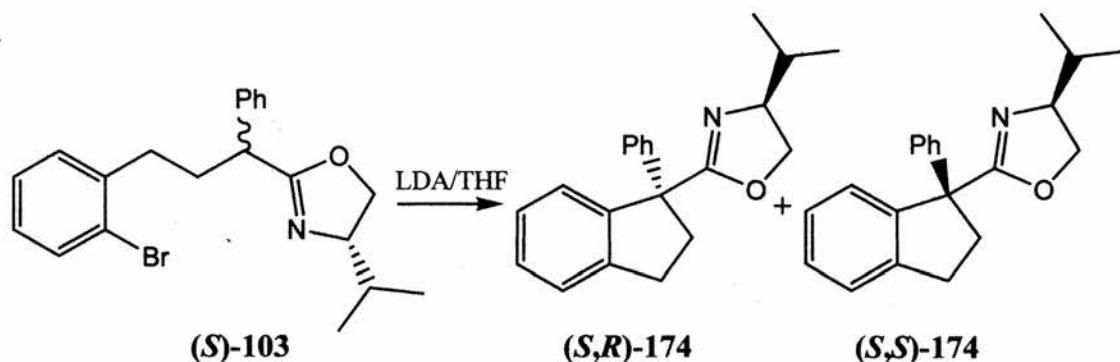


Scheme 146

Conformers a_1 and b_1 are expected to be favoured over a_2 & b_2 due to the smaller steric interactions of the R-group with the approaching radical. It was expected that the two pathways that lead to product formation would be derived from a_1 & b_2 , but unfortunately they lead to opposite diastereomers. Therefore, the selectivity of the $S_{RN}1$ ring closure will depend on the concentrations of the two conformer's a_1 & b_1 and to a lesser extent a_2 & b_2 .

The $S_{RN}1$ reactions of the chiral analogs were carried out using the previously optimised conditions i.e. 3 eq. LDA with either 48 h at r.t or 6 h with UV irradiation. Determination of the d.e.'s was carried out using the most convenient method, either GCMS or 1H NMR spectroscopy.

2.7.1 Substituted (S)-4-iso-propyl-2-oxazoline



Scheme 147

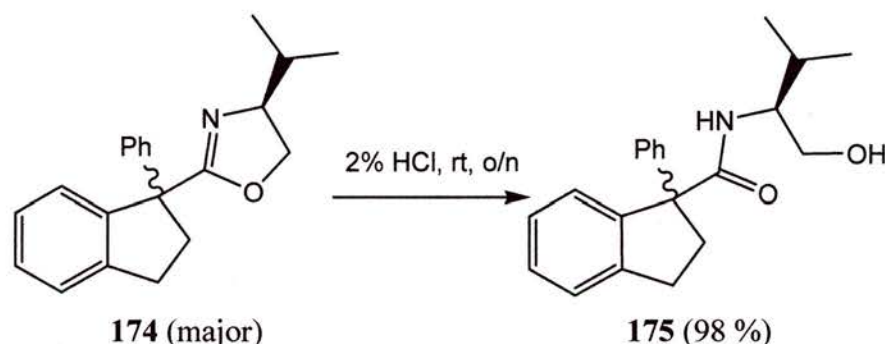
The results for the $S_{RN}1$ reactions of chiral oxazoline (S)-103 (Scheme 147) are shown in Table 19. The composition of precursor oxazoline (S)-103 was a 2:1 mixture of diastereoisomers, but this should not affect the outcome of the reaction because the stereo centre responsible is destroyed, via deprotonation, during the course of the reaction.

Entry	Conditions	Product (%)	d.e.(%)
1	6h, UV, rt	55	18 [†]
2	48h, dark, rt	72	42 [‡]
3	48h, dark, 0 °C	50	48 [†]

Table 19 Results of the $S_{RN}1$ reactions of *iso*-propyloxazoline (S)-103. [†] Obtained by GCMS. [‡] Ratio of isolated products.

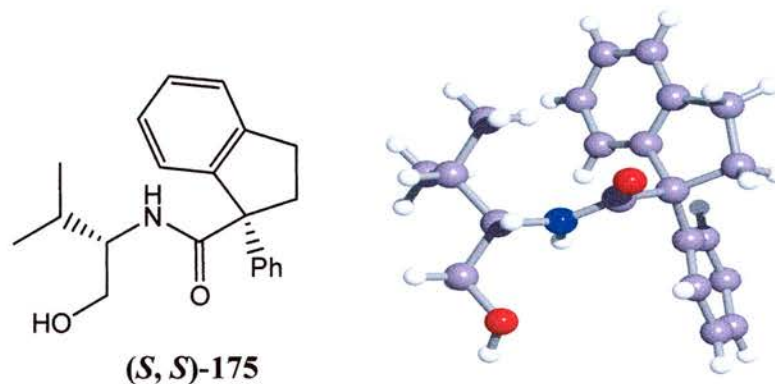
The yield (72 %), obtained under the standard non-irradiated conditions was comparable to that which was obtained for the dimethyl analogue **34b** (entry 2, Table 19). A moderate selectivity (42 % d.e.) was obtained under these conditions. The highest d.e. (48 %) was attained when the reaction was carried out at 0 °C for 48 h albeit with a reduction in yield (entry 3, Table 19). When the reaction mixture was irradiated for 6 h a diastereoselectivity of only 18 % was observed (entry 1, Table 19), this reduced value is thought to be due to the incidental heating of the reaction from the UV lamp. An attempt to carry out the reaction at the lower temperature of -33 °C so as to increase the selectivity resulted in an intractable mixture in which no product was evident.

It was found that the two diastereoisomers were easily separable via column chromatography. Unfortunately crystals of either isomer were unobtainable. Therefore the major isomer was mildly hydrolysed to form the β -hydroxyamide **175** (Scheme 148).



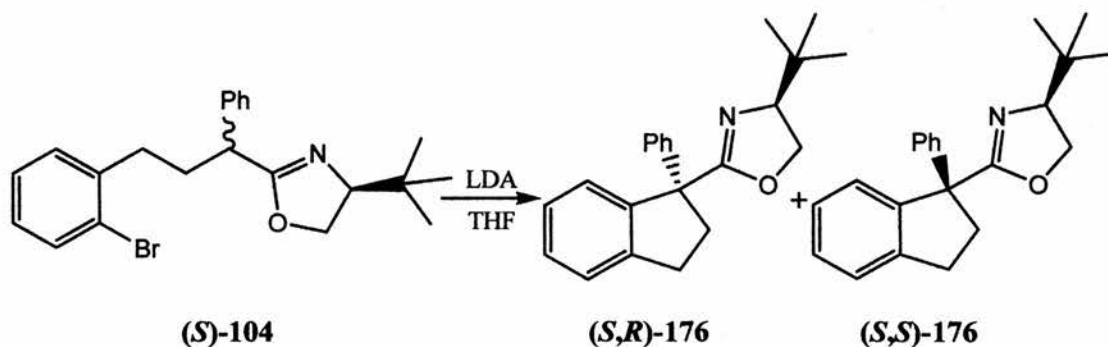
Scheme 148

X-ray quality crystals of β -hydroxyamide **175** were obtained and the subsequent crystal structure determination revealed the configuration to be *S,S* (Figure 25) and thus the absolute configuration of the major isomeric indane **174** was also *S,S*.

Figure 25 X-ray structure of β -hydroxyamide (*S,S*)-**175**.

It appeared that conformer a_1 was the major intermediate in the reaction based upon assumptions made previously (Scheme 146 & Section 2.7).

2.7.2 Substituted (*S*)-4-*tert*-Butyl-2-oxazoline



Scheme 149

Chiral 2-oxazoline (*S*)-104 was reacted using similar conditions to those employed previously (Scheme 149). As before, the mixture of stereoisomers of (*S*)-104 was used as prepared. The results for the $S_{RN}1$ reactions of (*S*)-104 are shown in Table 20.

Entry	Conditions	Product (%)	d.e.(%)
1	6h, UV,rt	60	33 [†]
2	48h, dark, rt	85	16 [‡]

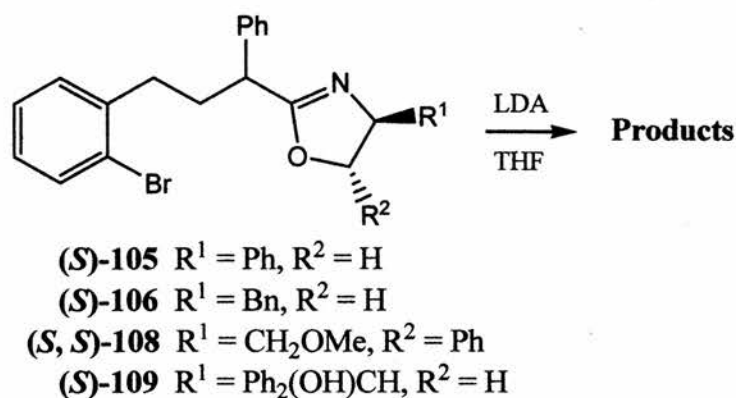
Table 20 Results of the $S_{RN}1$ reactions of *tert*-butyloxazoline (*S*)-104. [†] Obtained by GCMS. [‡] Obtained from NMR spectra.

The yield of 85 %, obtained when oxazoline (*S*)-104 was stirred with 3 equivalents of LDA at room temperature for forty-eight hours, was the highest overall we have achieved for an intramolecular $S_{RN}1$ cyclisation involving LDA/THF (entry 2, Table 20). The d.e. for this reaction was only 16 % which was disappointing. The reaction was also repeated with six hours of irradiation in the place of stirring in the dark. This afforded a moderate yield (60 %) and a d.e. of 33 % (entry 1, Table 20) which was surprisingly low in the light of the earlier results with the *iso*-propyl analogue (*S*)-103 (Section 2.7.1). An attempt was made to carry out the reaction below 0 °C (-30 °C) in order to increase selectivity but, as before, this resulted in an intractable mixture of products. The products were isolated after column

chromatography as the β -hydroxyamide derivatives. Unfortunately due to the expense of the starting material, not enough of the product was formed to grow X-ray quality crystals. It was assumed though, that the sense of selectivity was similar to the *iso*-propyl case as they are similar in topology (Section 2.7.1).

2.7.3 S_{RN}1 Reactions of Chiral Aryl and Benzyl-2-oxazolines

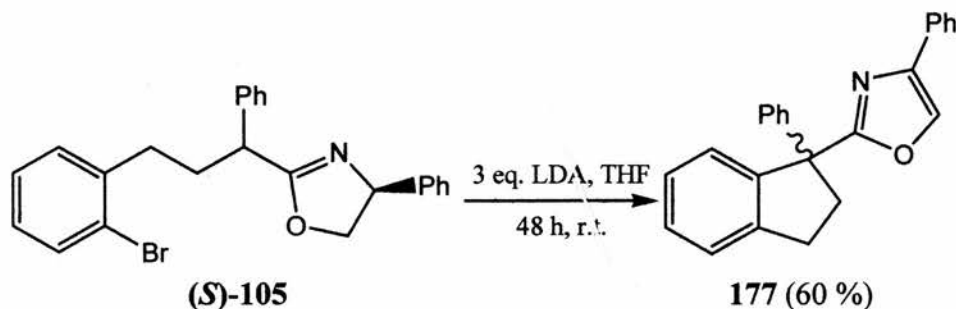
In order to attempt to increase the diastereoselectivity of the reaction 2-oxazolines with larger groups attached were evaluated.



Scheme 150

Chiral oxazolines containing either aryl or benzyl moieties on the oxazoline ring were reacted under the standard LDA/THF S_{RN}1 conditions (Scheme 150).

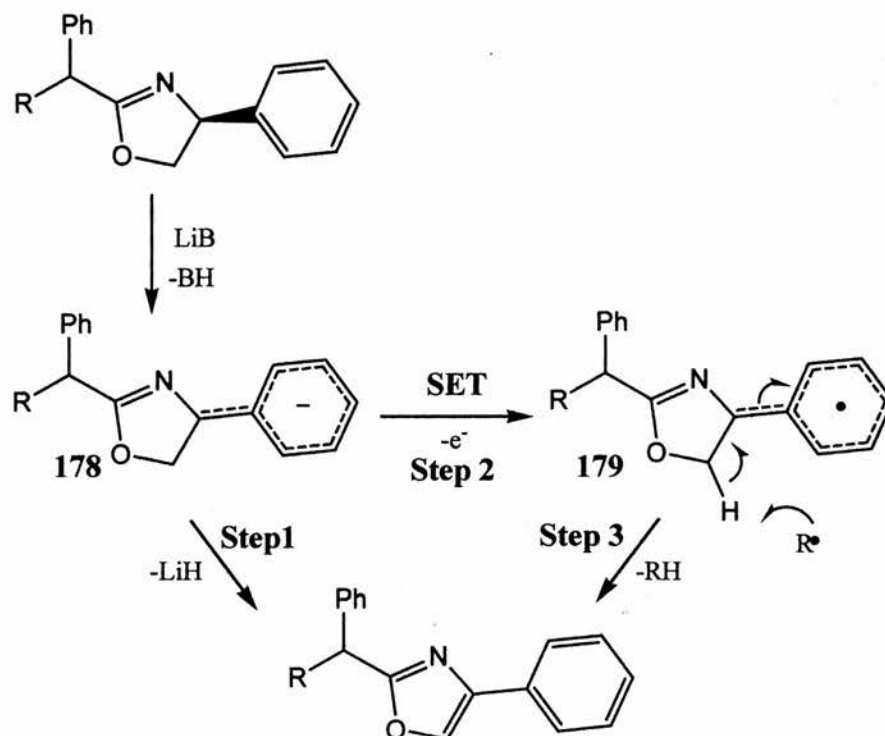
When the phenyl substituted oxazoline **(S)**-105 was reacted over 48 hours at room temperature only one product other than starting material was recovered. Identification of the product was carried out using NMR analysis and it was revealed to be the oxazole **177** (Scheme 151).



Scheme 151

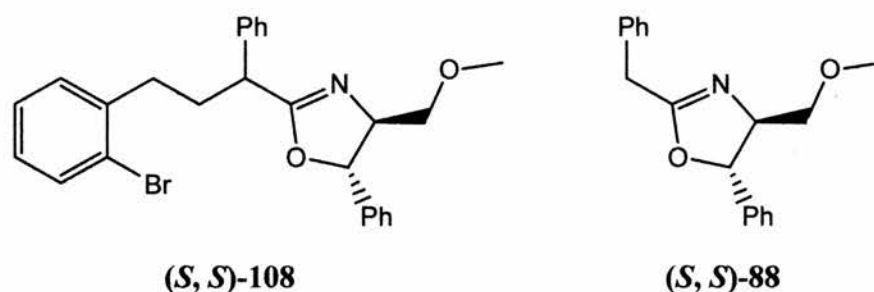
Formation of this product is thought to arise from the acidity of the proton at the 4-position of the oxazolinyl ring of the starting material **(S)**-105. A possible mechanism to account for the formation of the oxazole can be postulated. The first

step involves the elimination of LiH after lithiation of the oxazoline ring, the driving force for which would be the aromatisation of the ring (Step 1, Scheme 152). The second alternative mechanism would involve the oxidative SET from the formed oxazolinyl anion **178** to a more electropositive moiety to give the stabilised benzyl radical **179** (Step 2, Scheme 152). Hydrogen atom extraction by another radical would then form the observed oxazole (Step 3, Scheme 152). In both cases loss of H₂ could have arisen either before or after S_{RN1} ring closure took place.



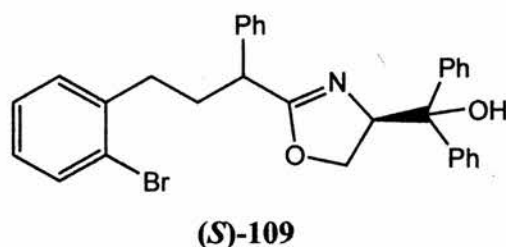
Scheme 152

Due to the loss of the predefined chiral centre in the molecule, the determination of any selectivity could not be carried out by normal means. Therefore chiral GCMS was employed in order to determine if any selectivity had arisen during the ring closure step. Unfortunately these results were inconclusive due to only one peak of the required mass being identifiable.



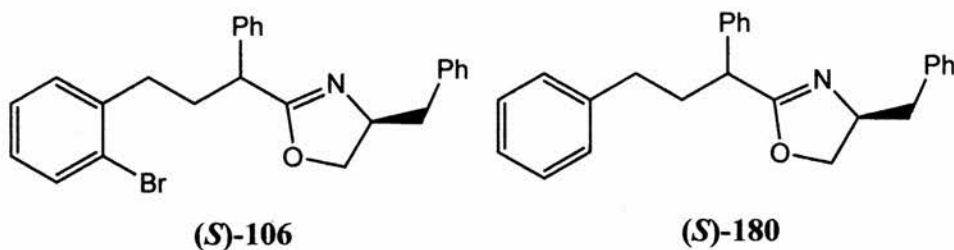
Scheme 153

The γ -arylpropyl-2-oxazoline (*S,S*)-108, which is derived from the "classic" Meyers' 2-oxazoline (*S,S*)-88 (Scheme 153), was reacted using the $S_{RN}1$ conditions described previously, to form an intractable mixture of products. The $^1\text{H-NMR}$ of the crude mixture indicated many aromatic environments with complete loss of the signals due to the 2-oxazolinyll moiety. This was indicative once again that, probably, the 2-oxazoline ring protons had been lost, and thus the unsaturated aromatic analogue formed (either cyclised or not). Clearly either the intermediate anion or radical proposed previously could also take part in mechanistic pathways other than that which leads to aromatisation; this would explain the multitude of products observed. Although GCMS evidence did indicate the presence of indanyl fragments no positive identification could be made.



Scheme 154

The same behaviour under the LDA/THF $S_{RN}1$ reaction conditions was observed for diphenylmethanol derivative (*S*)-109 (Scheme 154). A large amount of diverse products were detected. This was unexpected due to the phenyl groups being attached to a quaternary centre and not directly attached to the ring and, also an extra equivalent of LDA was present to ensure deprotonation of the alcohol functionality. On further contemplation it was postulated that water could have been lost and the resultant double bond isomerised to give the aromatic oxazole, although no mechanistic pathway at present can be suggested. The GCMS of the reaction mixture identified the presence of the indane ring system in the structures of some of the products, indicating that ring closure again was occurring.



Scheme 155

It was thought that the benzyl substituted oxazoline (**S**)-106 (Scheme 155) should not undergo any side reaction due to the absence of a possible dehydration route or aromatisation. Disappointingly, this was not the case, and a multitude of products was again observed when either 6 h, UV or 48 h, r.t were used in conjunction with 3 equivalents of LDA in THF. In order to circumvent these undesired products the reaction was repeated with only 1 equivalent of LDA and photolysed for 6 hours. This revealed a 2:1 mixture of starting material (**S**)-106 to reduced (**S**)-180 (Scheme 155). An excess of the weaker base, ^tBuOK in THF was also assessed in the hope that product formation would occur. This turned out not to be the case and only starting material was recovered when the mixture was stirred at room temperature for 48 hours. Upon irradiation for 6 hours only the reduced product (**S**)-180 was observed. The base, LiHMDS which is comparable to LDA was also used in THF with a short irradiation period (1 h) but to no avail with only an intractable mixture of products being formed.

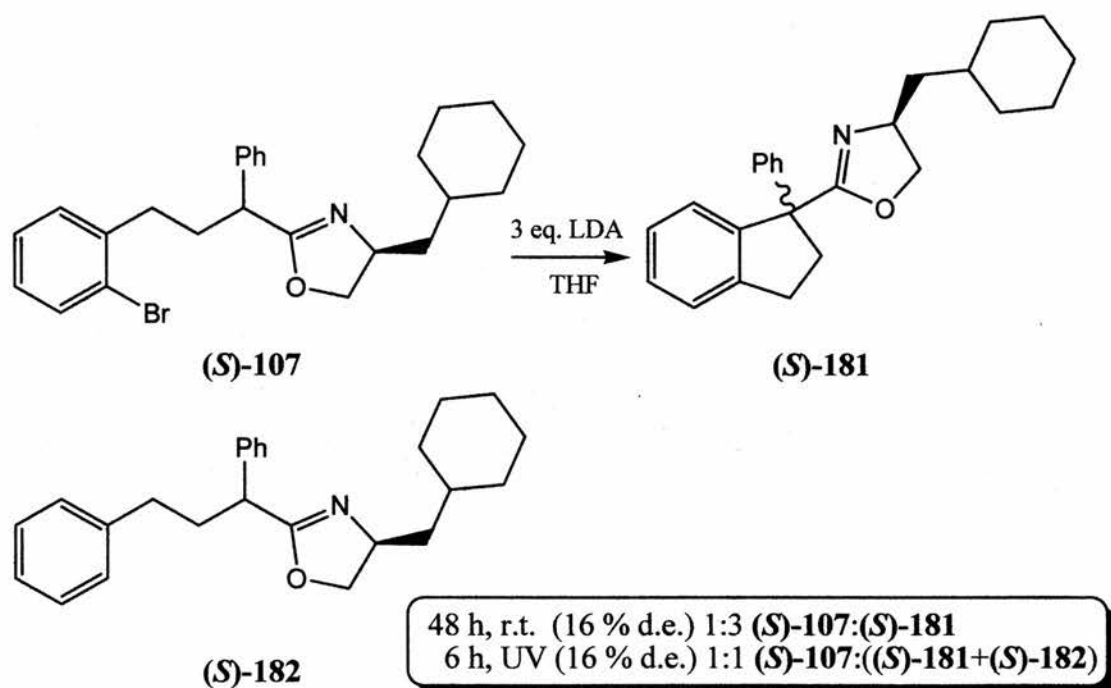
It is evident that when the optimised conditions, which brought success in the case of S_{RN1} ring closures with alkyl substituted oxazolines, were applied to aromatically substituted oxazolines they failed. Although evidence for indane formation was present, the loss of the stereo centre which was to impart selectivity at the newly formed chiral centre resulted in the ultimate failure of these substrates.

2.7.4 Substituted Chiral Cyclohexylmethyl-2-oxazolines

It became clear in the previous section (Section 2.7.3) that oxazolines with groups attached that increase the acidity of the ring protons degrade during the S_{RN1} reaction conditions resulting in loss of stereo induction. In order to solve this problem and hopefully see an increase in selectivity, the saturated analogue of (**S**)-106, cyclohexylmethyloxazoline (**S**)-107 was evaluated.

When oxazoline (**S**)-107 was reacted under the standard conditions with stirring for 48 hours at room temperature the indane product (**S**)-181 was indeed formed (as determined by ¹H-NMR and GCMS analysis) in a ratio of 1:3 with the starting material. The diastereomeric excess obtained was poor (16 %) (Scheme 156). The low ratio of product formed indicating that the reaction rate was slow under these conditions.

The slow rate of reaction could be explained in two ways: a) the large cyclohexylmethyl moiety was sterically hindering the coupling step and therefore inhibiting the reaction; b) the solubility of the initial azaenolate was low due to the presence of the cyclohexane ring and therefore electron transfer to the aryl bromide moiety was inhibited. If statement A was to hold true then an amount of reduced product would be expected to be formed due to the intermediate phenyl radical being more likely to react with a hydrogen atom source and also the selectivity would be expected to be considerably higher for the portion of product obtained. It is clear that as this was not observed so therefore statement B, or an alternate explanation, must hold true.

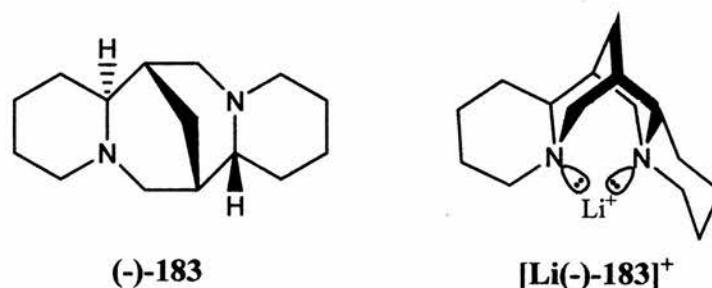


Scheme 156

When the reaction was carried out with 6 hours of UV photolysis the selectivity obtained was identical (16 % d.e.). Reduced product (S)-182 was formed as well as the indane product (S)-181. The presence of reduced product and a higher yield of indane, yet a similar d.e. as compared to reaction in the dark, adds weight to the theory that electron transfer is slow due to the low solubility of the initial azaenolate. The increased yield was probably due to the presence of more initiation events which should more efficiently form the intermediate phenyl radical despite the low solubility of the azaenolate.

2.7.5 (-)-Spartiene: A Chiral Ligand for Lithium in $S_{RN}1$ Reactions

(-)-Spartiene (-)-**183** has been used as a bidentate ligand for lithium cations (Scheme 157) in stereoselective synthesis with varying degrees of success.⁴³ When lithium chiral ligating agents are used in conjunction with the presence of chiral auxiliaries there is a possibility of either an enhancement (matched pair) or decrease/reversal in selectivity (mismatched pair).



Scheme 157

Thus in order to try and improve the diastereoselectivity of the $S_{RN}1$ ring closures several experiments were carried out using varying amounts of (-)-sparteine (-)-**183** with differing substrate concentrations. The (*S*)-*tert*-butyl substrate (**S**)-**104** was initially used, chosen due to it delivering the cleanest $S_{RN}1$ ring closure. The reaction were carried using the usual conditions i.e. 3 eq. LDA, THF, 48 h, r.t. When 3.5 equivalents of (-)-**183** were used with a substrate concentration of 0.036 M a reduced selectivity of 2 % d.e. compared with blank (16 % d.e.) was observed (entry 2, Table 21). The substrate concentration was increased (0.1 M) to yield a reversal of selectivity (-4 % d.e.) (entry 3, Table 21). If the (-)-sparteine (-)-**183** concentration was increased to 10 equivalents an increased reversal of selectivity was observed (-14 % d.e.) (entry 4, Table 21). Clearly the data indicates that this is a case of a mismatched pair between the (-)-sparteine (-)-**183** and the oxazoline auxiliary.

Therefore the opposite enantiomer of **104** was prepared from (*R*)-*tert*-leucinol (**R**)-**74** (Section 2.1.2.2). The $S_{RN}1$ reaction was then repeated as before using either 3.5 or 10 equivalents of (-)-**183** and a substrate concentration of 0.1 M. A slightly increased selectivity was observed (21 % d.e.) when 3.5 equivalents of (-)-**183** were present (entry 5, Table 21) but a poorer selectivity was observed in the case of 10 equivalents (entry 6, Table 21). These disappointing results are probably due to the fact that as the starting material is expensive only a small amount of the substrate (**R**)-**104** was obtained. As a result these reactions could only be carried out on a small

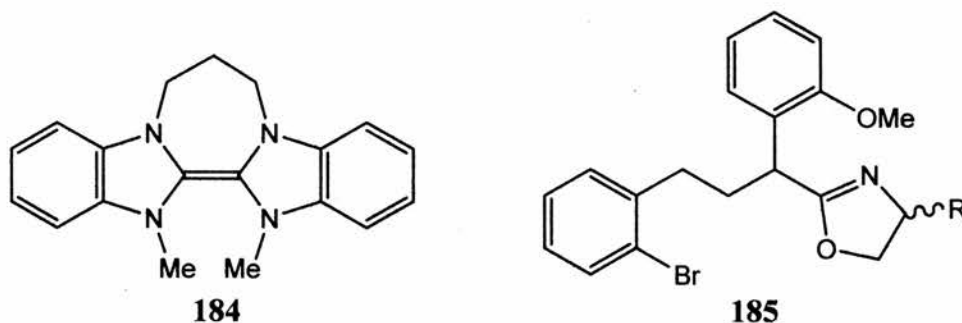
scale. This lead to problems in reaction solvent retention under a nitrogen flow and thus it is thought the results obtained are not representative (entries 5 & 6, Table 21). Unfortunately time and resource pressure prohibited a repetition of these reactions.

Entry	104	[104]/M	[(-)-183]/eq.	d.e./%
1	<i>S</i>	0.036	0	16
2	<i>S</i>	0.036	3.5	2
3	<i>S</i>	0.1	3.5	-4
4	<i>S</i>	0.1	10	-14
5	<i>R</i>	0.1	3.5	21
6	<i>R</i>	0.1	10	14

Table 21 $S_{RN}1$ Reactions of (*S/R*)-104 using (-)-sparteine (-)-183.

2.7.6 Summary of Stereoselective $S_{RN}1$ Reactions

In summary, a diastereoselective $S_{RN}1$ reaction of γ -arylpropyl-2-oxazolines to from stereoisomeric indanes was achieved albeit in moderate selectivity (48 % d.e.). A redeeming feature is the separability of the two diastereoisomers by conventional chromatography. It is also evident that groups that enhance the acidity of the protons on the oxazolinyl moiety are not tolerated. The use of chiral cationic ligating agents was shown to effect the selectivity, as was temperature. Unfortunately in the case of ligating agents, this effect was unable to be fully evaluated. In order to carry out the $S_{RN}1$ reaction at lower temperature it is postulated that an efficient single electron transfer reagent would be needed. This is because the thermally spontaneous process ceases at lower temperatures and UV irradiation is problematic. One such reagent **184** has recently been reported by Murphy *et al.*⁴⁴ to reduce aryl iodides to the corresponding radical (Scheme 158).

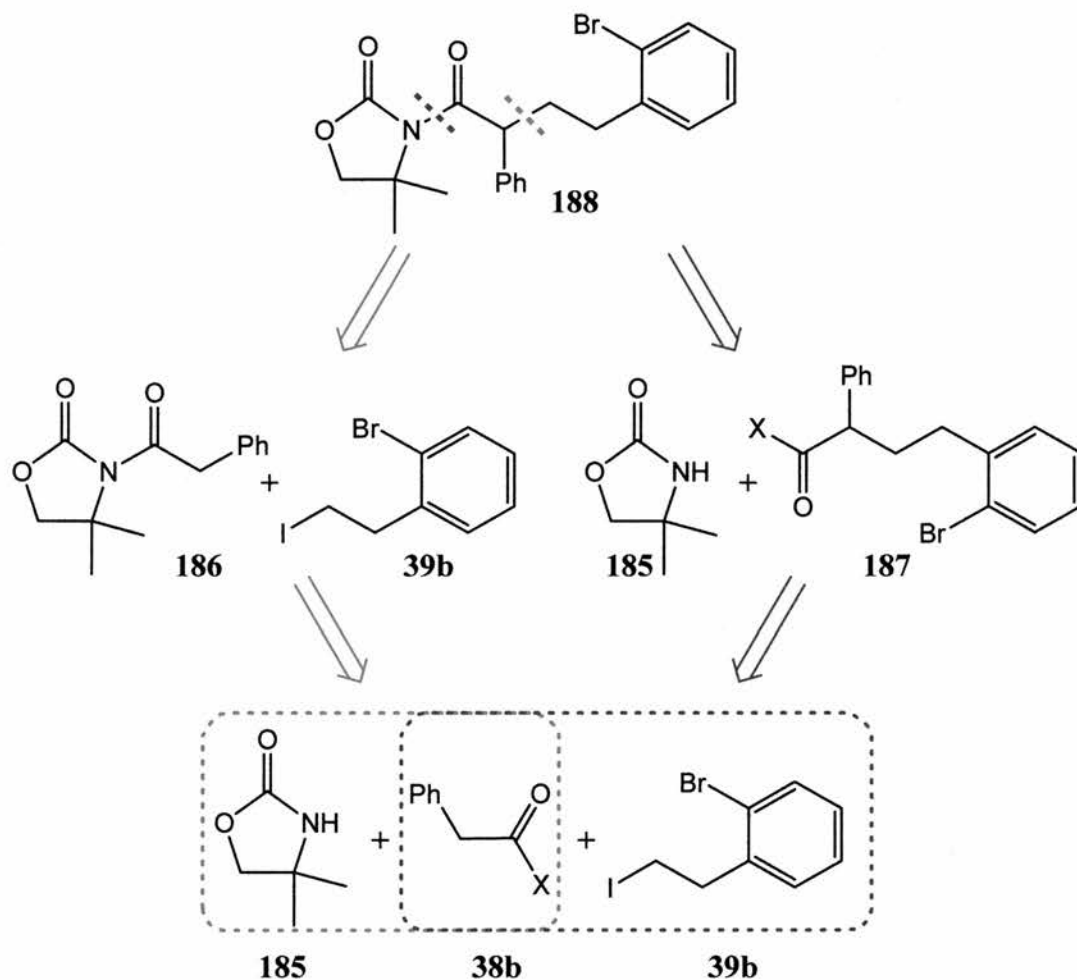


Scheme 158

One other possibility for increasing the selectivity would involve the placement of additional coordinating groups in the molecule which would restrict conformational flexibility. An example **185**, is shown in Scheme 158, with an *o*-methoxyphenyl substituent. It is postulated that on deprotonation by a lithium base, the lithium would coordinate to the O and the N centres thus limiting the conformational flexibility of the anion.

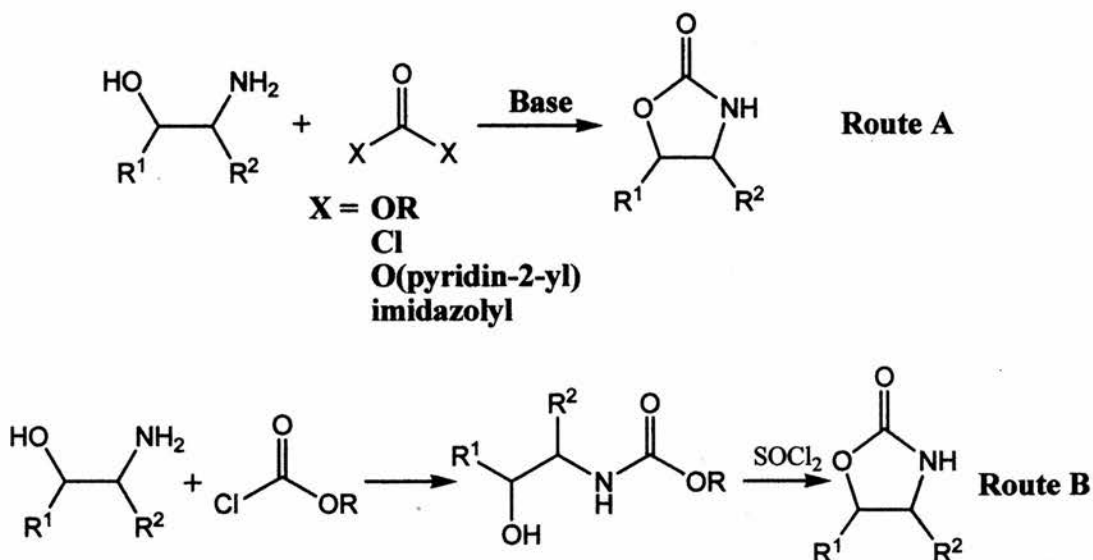
2.8 Oxazolidinones in $S_{RN}1$ Reaction

It was decided, following the success of azaenolates of 2-oxazolines as nucleophiles in achiral intramolecular $S_{RN}1$ cyclisations, to investigate the use of another common auxiliary, oxazolidinones. To this end, a retrosynthetic analysis of analogous oxazolidinone **188** was carried out (Scheme 159).



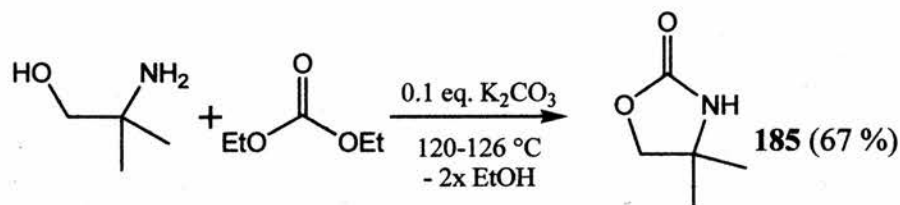
Scheme 159

The red synthetic route was deemed the most feasible and is analogous to the preparation of the 2-oxazoline counterpart (Section 2.1.4). Several methods are available to prepare dimethyloxazolidinone **185** and these include: a) base catalysed condensation of a 1,2-aminoalcohol with a dialkylcarbonate or equivalent (Route A, Scheme 160),⁴⁵ b) formation of an intermediate carbamic acid ester from a 1,2-aminoalcohol and an alkyl chloroformate followed by dehydration by thionyl chloride to form the oxazolidinone ring (Route B, Scheme 160).⁴⁶



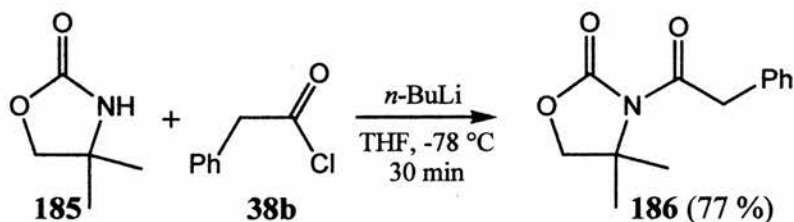
Scheme 160

As route A was only a single step, a literature procedure involving this route was chosen,⁴⁵ and the desired oxazolidinone **185** was obtained in a good yield of 67 % (Scheme 161).



Scheme 161

The next synthetic step was the coupling of phenylacetyl chloride **38b** to the prepared oxazolidinone **185**. This was carried out via deprotonation of the oxazolidinone at low temperature, followed by slow addition of the acid chloride in THF solution to give the *N*-substituted oxazolidinone **186** in good yield (77 %) (Scheme 162).



Scheme 162

Following this success, phenylacetyloxazolidinone **186**, was reacted with iodide **39b** using standard conditions developed for 2-substitution of 2-oxazolines (Section 2.1.4). Unfortunately no reaction occurred although the yellow colouration due to anion formation was observed. Further scrutiny revealed that the yellow

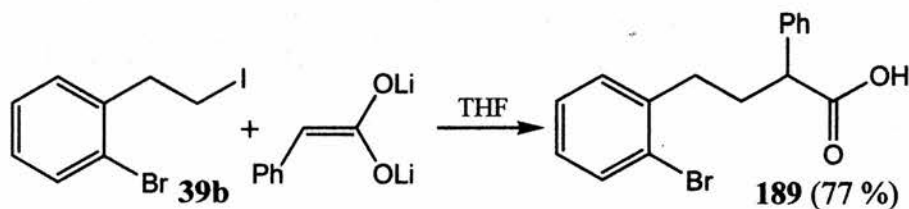
colouration was due to a precipitate in the reaction vessel. It was concluded from this that the formed anion was insoluble in the reaction solvent system at $-78\text{ }^{\circ}\text{C}$. In order to address this lack of reactivity, a series of reactions was carried out. These involved different enolate concentrations and solvent polarities as shown in Table 22.

Entry	Anion Concentration (M)	THF/Hexane	Result
1	0.95	0.70	No Reaction
2	0.21	1.55	No Reaction
3	0.21	3.40	No Reaction
4	0.31	6.90	No Reaction

Table 22 Table of different condition used in deprotonation of oxazolidinone **186**.

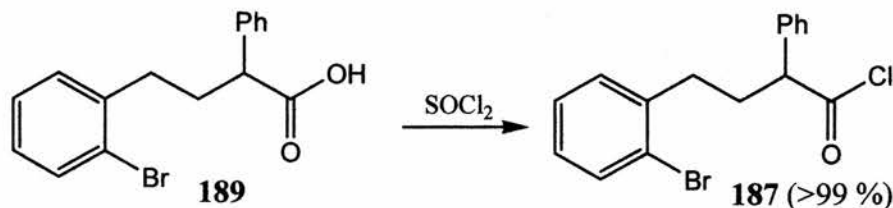
However, no reaction was observed to occur under any of these conditions and it was therefore decided to try and form the desired 2-oxazolidinone via the alternative route detailed previously (blue route, Scheme 159).

Substituted phenylacetic acid **189** was prepared very easily from addition of iodide **39b** to phenylacetic acid dilithium salt (prepared from phenylacetic acid and 2 eq. of *n*-BuLi in THF at $-78\text{ }^{\circ}\text{C}$) at $-78\text{ }^{\circ}\text{C}$ in a good yield of 77 % (Scheme 163).



Scheme 163

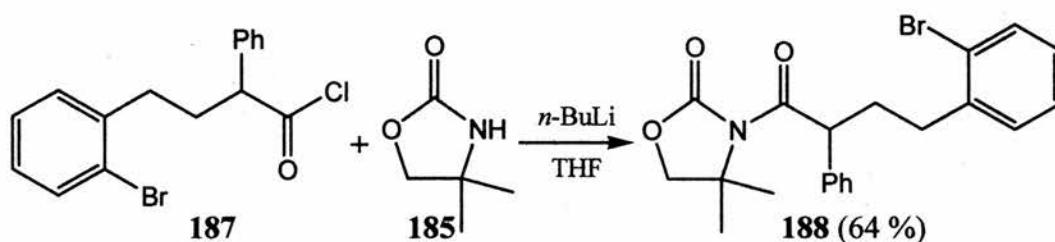
Using standard protocols (SOCl_2 , reflux, 30 min) acid **189** was smoothly converted to the required acid chloride **187**, effectively quantitatively (Scheme 164).



Scheme 164

It was now hoped that, given the reactivity of acid chlorides towards nucleophiles, the anion of simple oxazolidinone **185**, would react smoothly to give the required amide **188**. Hence, a THF solution of **187** was added dropwise to a stirred solution of the deprotonated oxazolidinone **185**. Examination of the $^1\text{H-NMR}$

spectrum of the crude reaction mixture indeed revealed the desired oxazolidinone had been made in a modest yield of 64 % after column chromatography (Scheme 165).

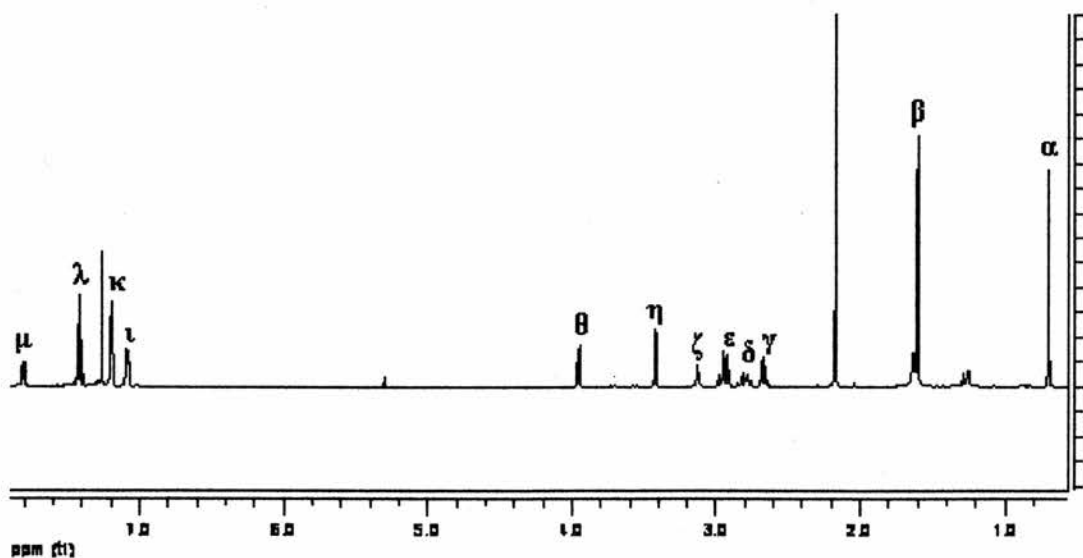


Scheme 165

2.8.1 $S_{RN}1$ Reactions of 2-Oxazolidinones

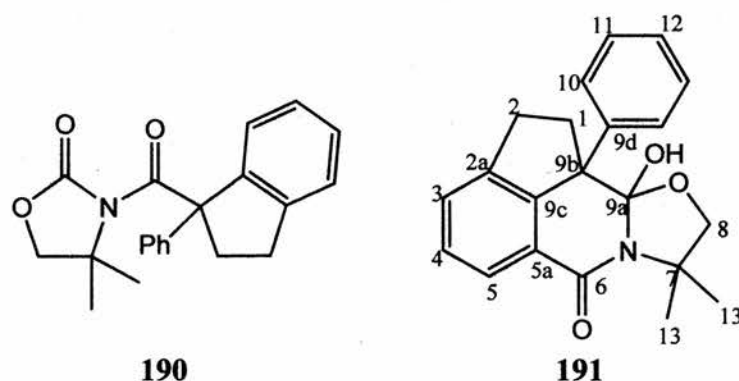
2-Oxazolidinone **188** was reacted using standard $S_{RN}1$ conditions developed for 2-oxazolines, i.e. 3eq. LDA at r.t. for 48 h. A white waxy solid was obtained in a 75% yield (based on MW of expected indane product **190** (Scheme 166)). However, examination of the ^1H NMR spectrum showed the structure could not be that of the indane product **190**. Unfortunately, all attempts to gain X-ray quality crystals failed.

The mass spectrum (CI) of the unknown gave an accurate mass of 336.1604 indicating an elemental composition $\text{C}_{21}\text{H}_{22}\text{NO}_3$, identical with that of the molecular ion of indane **190**. However, in view of the NMR evidence we concluded that a rearrangement to an isomeric structure may have occurred, possibly similar to that which was reported in Section 2.5.2. Preliminary evidence for this postulate was obtained from the ^1H -NMR spectrum (Figure 26).

Figure 26 ^1H -NMR spectrum of unknown **191**

The ^1H -NMR spectrum showed the presence of characteristic peaks for the oxazolidinone moiety (peaks α , β , η & θ , Figure 26) but also an OH signal (peak ζ , Figure 26) and multiplets equating to only eight hydrogens in the aryl region (peaks ι , κ , λ & μ , Figure 26). This was indicative of either a phenyl ring and a trisubstituted aromatic ring or two disubstituted aromatic rings. Also, the presence of a one hydrogen doublet (simplification) at 7.81 ppm (peak μ , Figure 26) was taken as evidence for a carbonyl moiety attached directly to an aromatic ring. The oxazolidinone moiety was assumed to be held rigid or to be sterically crowded, due to the large difference in the resonances of the geminal methyls (~ 0.9 ppm) and also the two hydrogens attached to the carbon adjacent to the oxygen in the ring (~ 0.6 ppm). Using the above evidence, the structure **191** shown in Scheme 166, was proposed with unknown stereochemistry at carbons 9a and 9b.

One dimensional ^1H and ^{13}C and two dimensional COSY, HSQC & HMBC 500 MHz NMR spectra were obtained for the unknown substance in order to confirm or refute the proposed structure **191**.



Scheme 166

Summaries of the ^1H and ^{13}C -NMR spectra are shown in Table 23. A pictorial representation of the ^1H -NMR spectrum is shown in Figure 26 and the ^{13}C spectrum is in Figure 27. The HSQC spectrum shows that both ^1H signals η & θ correlate with ^{13}C signal G thus confirming the previous proposition that the signals are due to the oxazolidinyl methylene protons (Figure 28). Thus, with respect to the proposed structure, ^1H signals η & θ and ^{13}C signal G can be assigned to C-8. ^1H -NMR resonances α & β , earlier attributed to the oxazolidinyl geminal methyls have, in the HSQC spectrum, respective couplings with ^{13}C -NMR signals A & B. ^{13}C -NMR signals A & B are identifiable as belonging to methyl type carbons, which confirms

the presence of two methyl groups. Consequently, ^1H -NMR signals α & β and ^{13}C -NMR resonances will be assigned to C-13s.

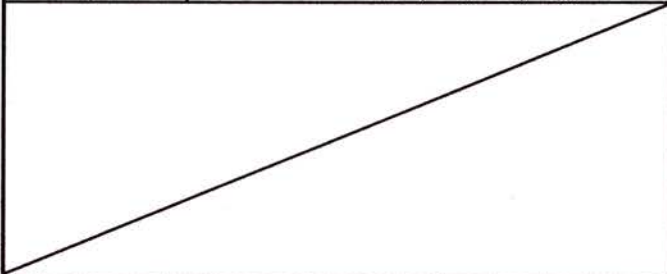
^1H Signal	PPM (Integration, Multiplicity)	^{13}C Signal	PPM (Type)
α	0.70 (3H, s)	A	22.4 (CH ₃)
β	1.60 (3H, s)	B	25.0 (CH ₃)
γ	2.64-2.69 (1H, m)	C	31.3 (CH ₂)
δ	2.76-2.85 (1H, m)	D	36.3 (CH ₂)
ϵ	2.91-2.99 (2H, m)	E	58.9 (C _q)
ζ	3.13 (1H, br. s)	F	59.5 (C _q)
η	3.42 (1H, d, $J = 8.2$)	G	78.1 (CH ₂)
θ	3.94 (1H, d, $J = 8.2$)	H	112.4 (C _q)
ι	7.07-7.10 (2H, m)	I	123.8 (CH _{Ar})
κ	7.17-7.21 (3H, m)	J	127.1 (CH _{Ar})
λ	7.40-7.45 (2H, m)	K	127.4 (CH _{Ar})
μ	7.80-7.82 (1H, m (~d))	L	128.0 (C _q)
		M	128.5 (CH _{Ar})
		N	128.8 (CH _{Ar})
		O	129.6 (CH _{Ar})
		P	139.1 (C _q)
		Q	142.5 (C _q)
		R	145.8 (C _q)
		S	162.6 (C _q)

Table 23 Summary of ^1H and ^{13}C NMR Spectra of unknown **191**

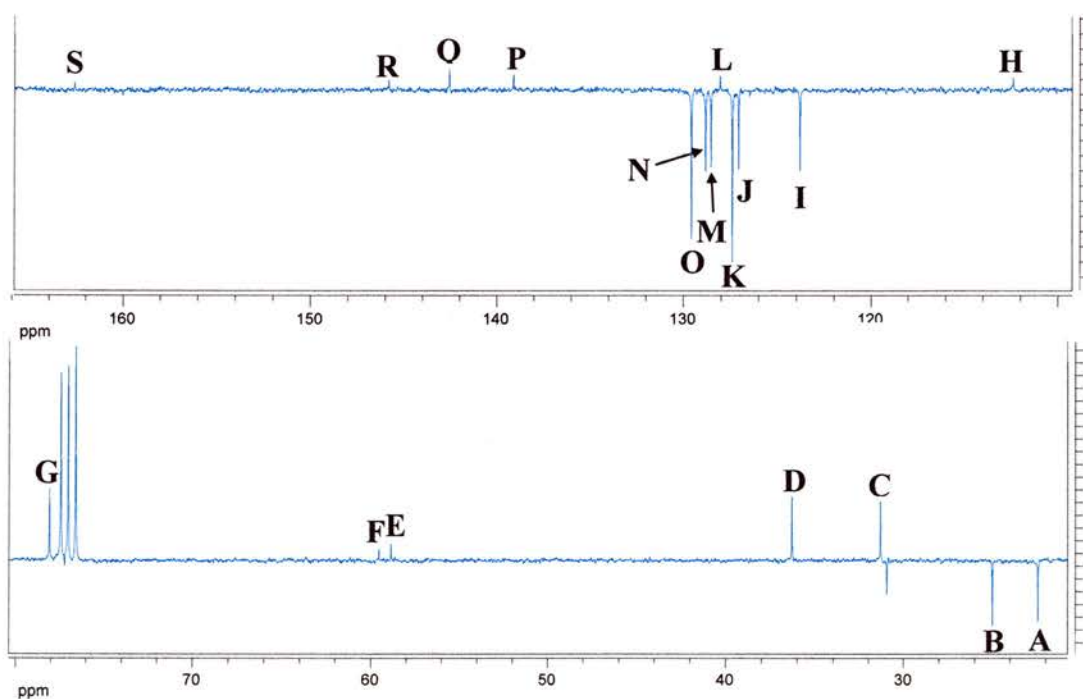


Figure 27 ^{13}C -NMR spectrum of unknown **191**

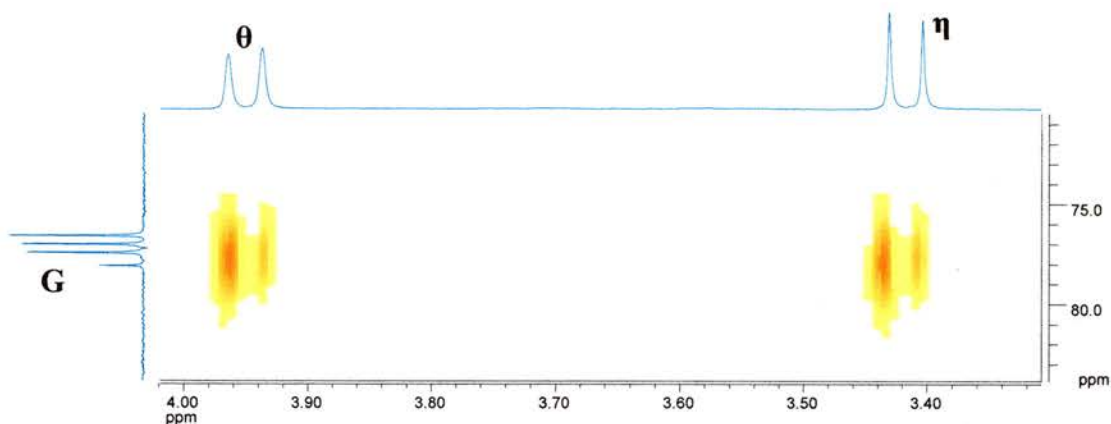


Figure 28 Region edited HSQC spectrum of unknown **191**

In the HMBC spectrum ^1H -NMR resonances α & β (C-13s) correlate with ^{13}C -NMR signals E & G (C-8) (cross peaks i, Figure 29) and ^1H -NMR signals η (C-8) & θ (C-8) have cross peaks with ^{13}C -NMR resonances A (C-13), B (C-13) & E (cross peaks ii, Figure 29). ^{13}C -NMR signal E belongs to a quaternary carbon. Thus, based on the HMBC evidence it can be assigned to C-7.

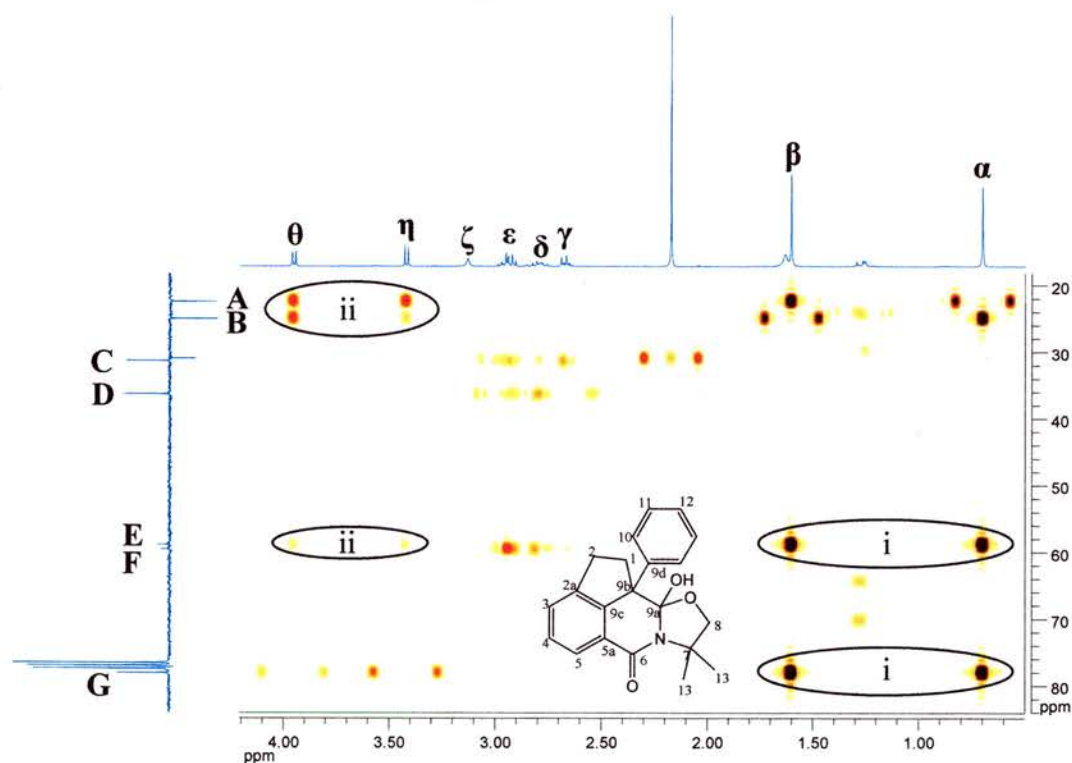


Figure 29 Region edited HMBC spectrum of unknown **191**

δ & ϵ ^1H -NMR signals both correlate with ^{13}C -NMR methylene signal C (cross peaks i, Figure 30) and γ & ϵ signals correlate with D (cross peaks ii, Figure 30) in the HSQC spectrum. This information, along with fact that the ^1H -NMR signals have correlations with each other in the COSY spectrum, indicates that these signals

are due to C-1 and C-2, although no differentiation as to which carbon belongs to which set of signals is made yet.

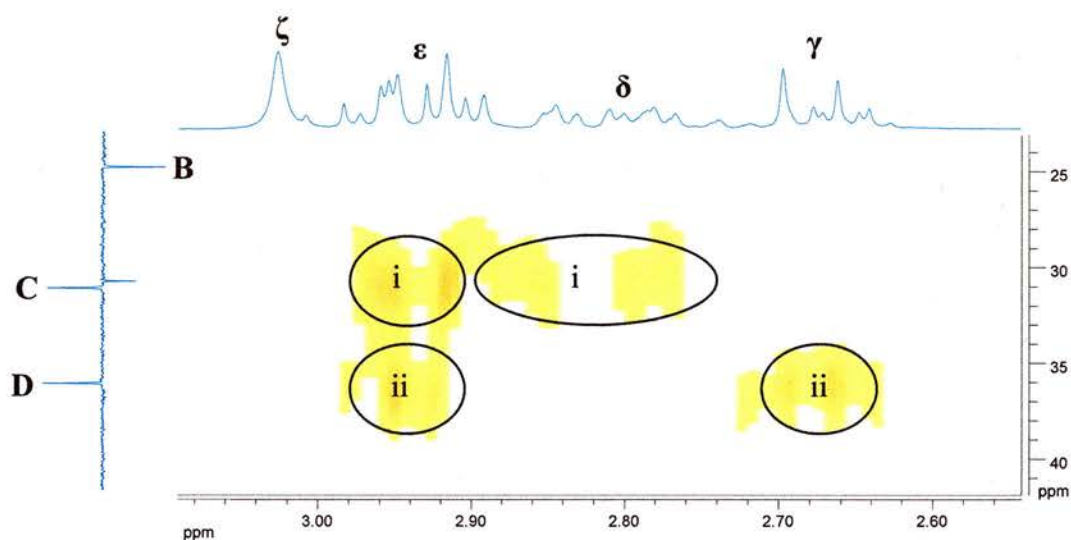


Figure 30 Aliphatic region of HSQC spectrum of unknown **191**

As previously mentioned, the $^1\text{H-NMR}$ aromatic region contain 4 signals (ι , κ , λ & μ). The $^1\text{H-}^1\text{H}$ COSY spectrum clearly shows two distinct correlation patterns (Figure 31).

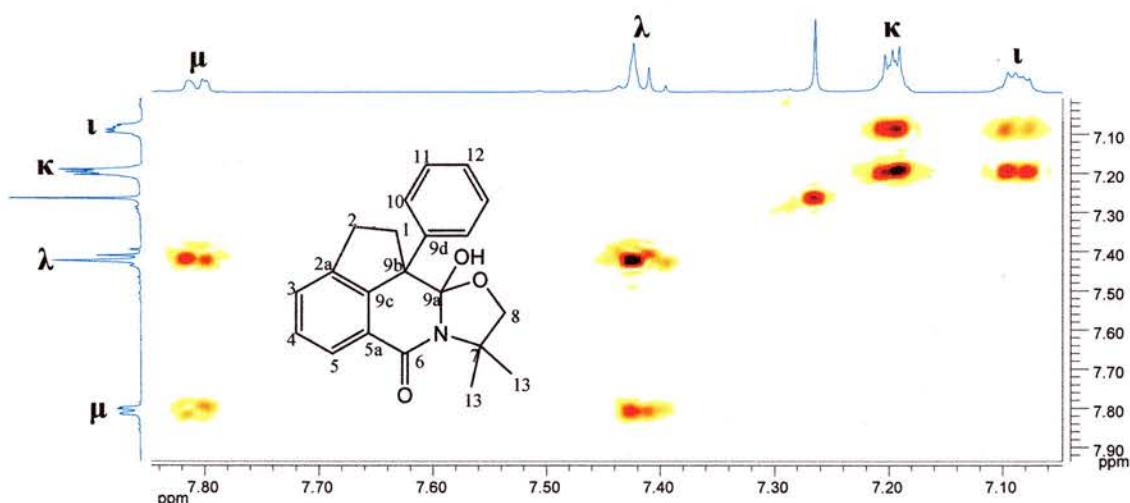


Figure 31 Aromatic Region of COSY Spectrum of unknown **191**

$^1\text{H-NMR}$ signals ι & κ belong to one aromatic ring which, based upon the value of the integrations (5) of the two signals, indicates the presence of a phenyl ring. The other two signals λ & μ with a combined integration value of three, indicate the existence of a trisubstituted aromatic ring which is consistent with the proposed

structure **191**. The chemical shift of $^1\text{H-NMR}$ signal μ (7.81) indicates it is probably *ortho* to a C=O , therefore it is assigned to C-5. It can then be deduced that $^1\text{H-NMR}$ multiplet λ must be assigned to C-3 and C-4. The HSQC spectrum shows that $^{13}\text{C-NMR}$ signal I correlates with $^1\text{H-NMR}$ signal μ and hence is assigned to C-5 (Figure 32). $^{13}\text{C-NMR}$ resonances M & N both show a cross peak with $^1\text{H-NMR}$ signal λ and are consequently attributed to C-3 and C-4 (Figure 32).

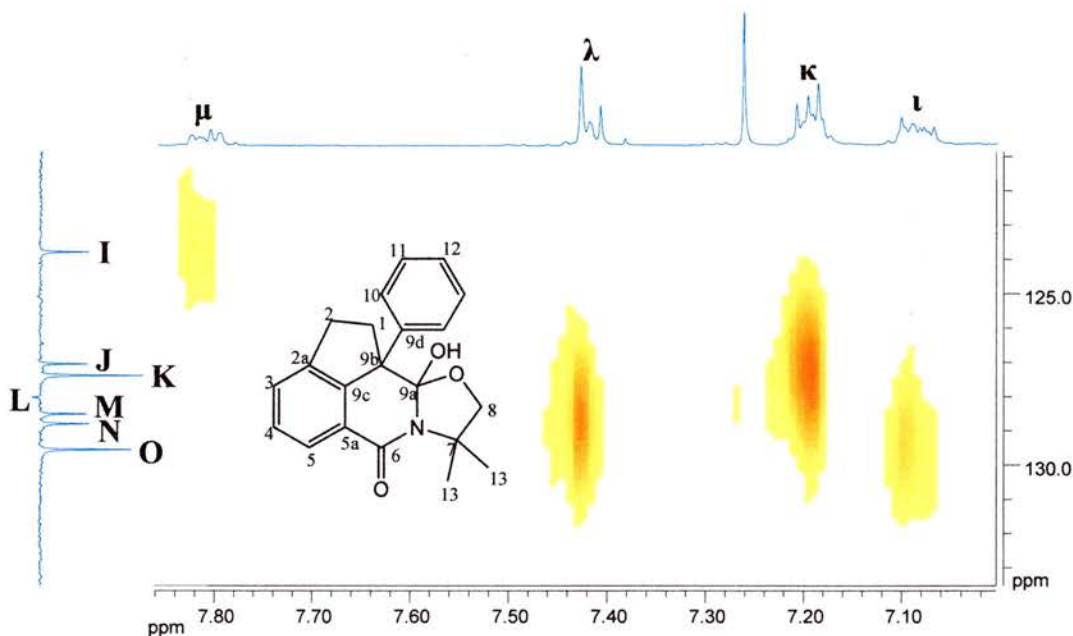


Figure 32 Aromatic region of HSQC spectrum of unknown **191**

The phenyl ring $^{13}\text{C-NMR}$ resonances, by a process of elimination, can be associated with signals J, K & O. Signal J can be specifically assigned to C-12 (κ) due to its relative size (Figure 32).

Analysis of the aromatic region of the HMBC spectrum discloses a strong ^3J correlation of $^{13}\text{C-NMR}$ signal J (κ , C-12) with $^1\text{H-NMR}$ signal ι (cross peak i, Figure 33), thus C-10 can be assigned to resonances ι & O. This can be corroborated by the presence of a correlation between $^1\text{H-NMR}$ signal κ and $^{13}\text{C-NMR}$ signal O (cross peak ii, Figure 33). Therefore it can be concluded that $^{13}\text{C-NMR}$ signal K can be assigned to C-11 along with two hydrogen equivalents of $^1\text{H-NMR}$ signal κ . The weak correlations between signals ι & O (both C-10) and κ and K (both C-11) (cross peaks iii, Figure 33) are due to the fact that although both *ortho* protons are chemically equivalent they are not magnetically equivalent. This is also the case with the *meta* protons. $^1\text{H-NMR}$ signal κ also has a correlation to quaternary $^{13}\text{C-NMR}$ signal P and is thus assigned to C-9d (cross peak iv, Figure 33).

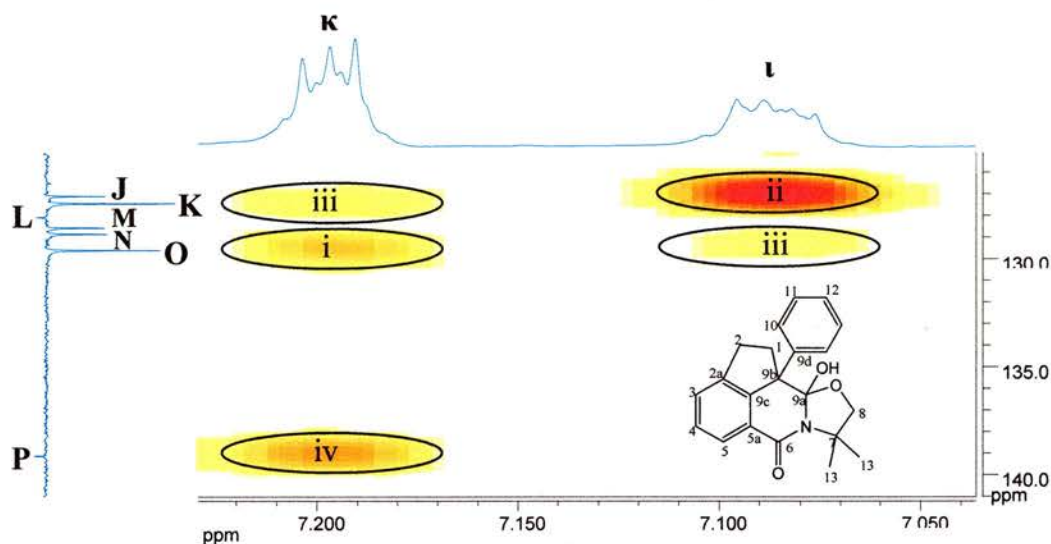
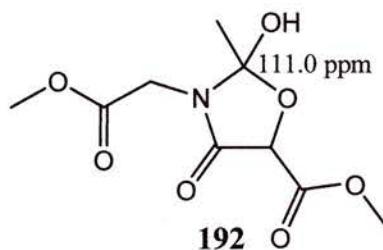


Figure 33 Phenyl Region of HMBC spectrum of unknown **191**

The $^1\text{H-NMR}$ signals responsible for C-1 should also correlate strongly with $^{13}\text{C-NMR}$ signal P (C-9d). Signals δ & ϵ indeed show this relationship and therefore one hydrogen from composite signal ϵ and signal δ are assigned along with $^{13}\text{C-NMR}$ signal C to C-1 (cross peaks i, Figure 34). Accordingly, one hydrogen equivalent from $^1\text{H-NMR}$ ϵ and signal γ , together with $^{13}\text{C-NMR}$ resonance D, are attributed to C-2.

$^{13}\text{C-NMR}$ resonance H has cross peaks with $^1\text{H-NMR}$ signals γ (C-1), ϵ (C-1/2), η (C-8) & θ (C-8) which is indicative of it being due to hydroxyl quaternary C-9a (cross peaks ii, Figure 34). Comparison with the literature was made due to the unusual nature of quaternary C-9a and the unusual chemical shift of signal H (112.4 ppm). The model hydroxy-amide **192** shown in Scheme 167 exhibits a similar chemical shift (111.0 ppm)⁴⁷ due to its hydroxyl quaternary centre, therefore confirming the assignment of resonance H to C-9a.



Scheme 167

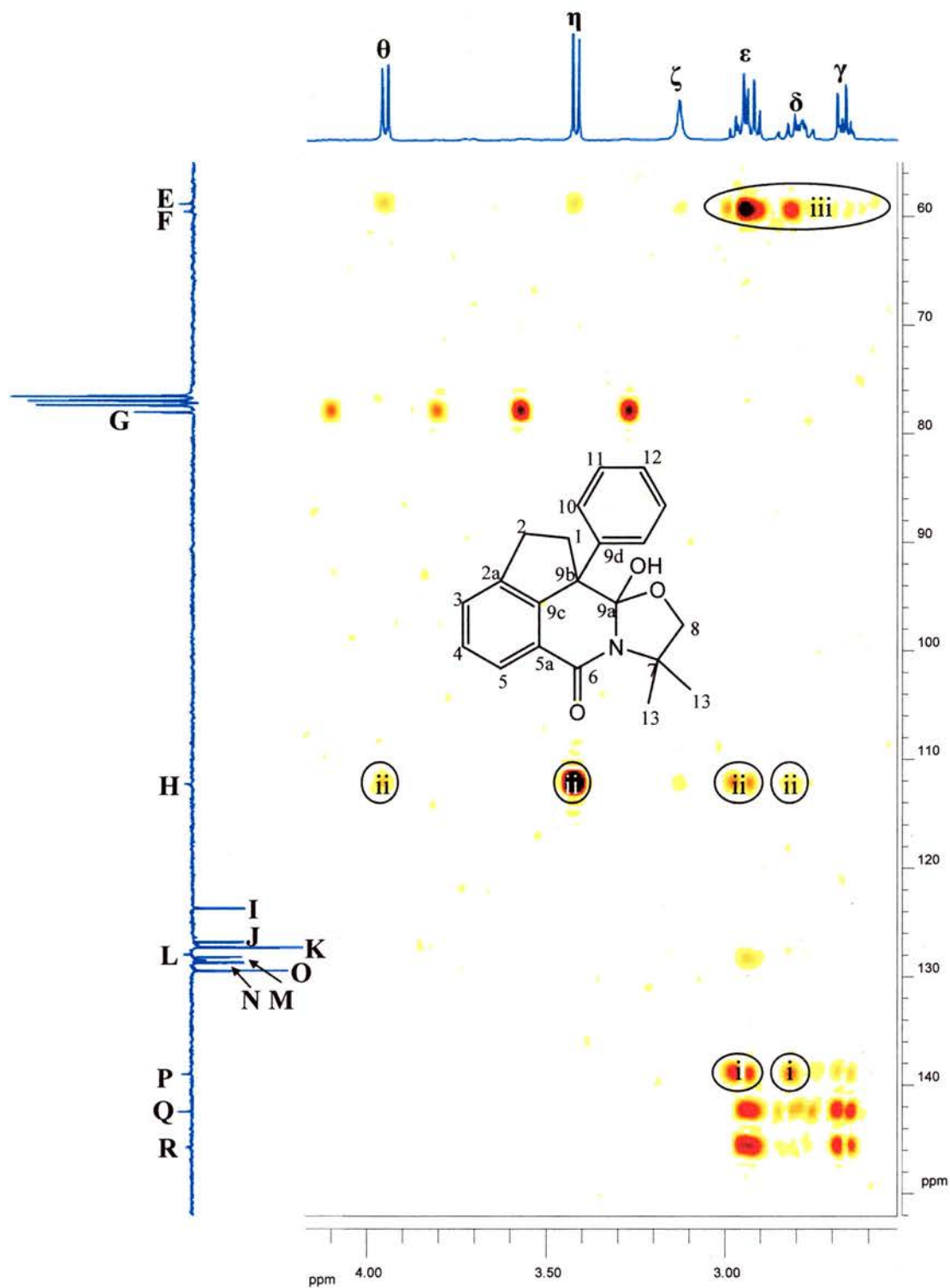


Figure 34 Region edited HMBC spectrum of unknown **191**

^1H -NMR resonances due to C-1 and C-2 all show coupling with ^{13}C -NMR signal F which is concordant with F being assigned to C-9b (cross peaks iii, Figure 34).

Carbon resonance M shows a correlation with hydrogen peak ϵ (C-1/2) indicating it is due to C-3 rather than C-4 (cross peak iv, Figure 34). Further evidence for this assignment is provided by the existence of a correlation between $^1\text{H-NMR}$ signal μ (C-5) and $^{13}\text{C-NMR}$ signal M (C-3) (cross peak i, Figure 35). Thus C-4 can be accounted for by $^{13}\text{C-NMR}$ peak N.

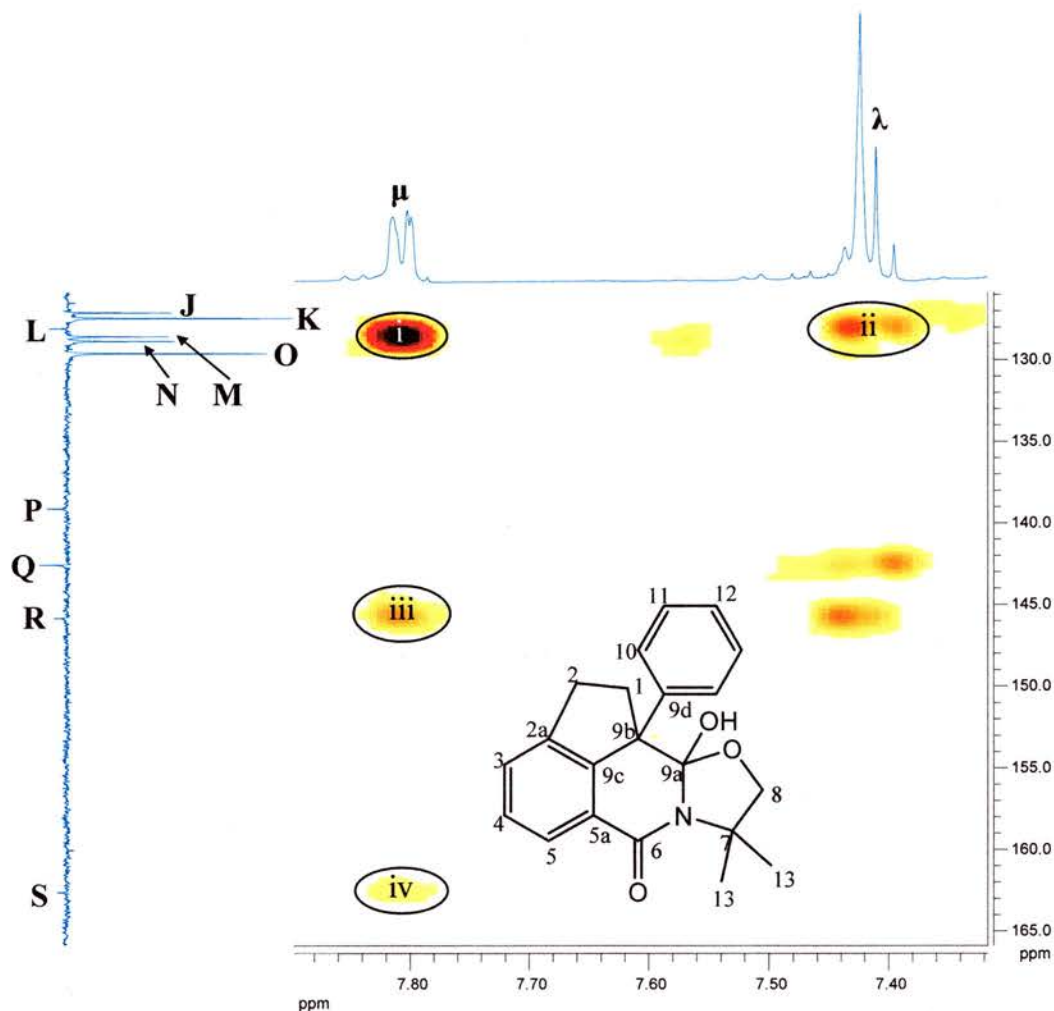


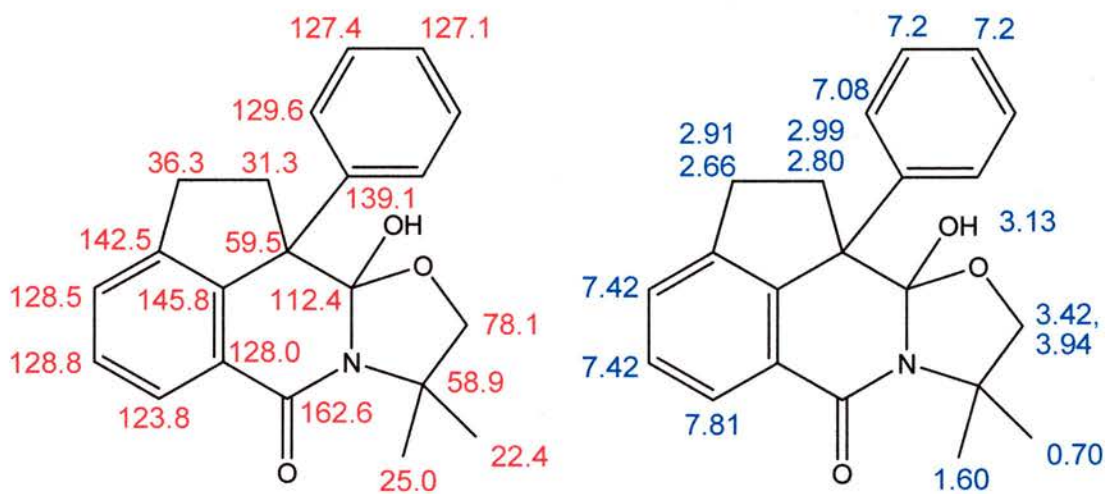
Figure 35 Region edited HMBC spectrum of unknown **191**

$^1\text{H-NMR}$ signals due to C-3 & C-4 (λ) have a cross peak with quaternary carbon signal L (cross peaks ii, Figure 35) but C-1 & C-2 (γ , δ & ϵ) do not, therefore L is allocated to C-5a. Carbon-9c can be assigned to $^{13}\text{C-NMR}$ signal R because C-5's hydrogen resonance (μ) only correlates with that aryl quaternary signal (cross peak iii, Figure 35). It may therefore be deduced that carbon signal Q must be assigned to C-2a.

The allocation of $^{13}\text{C-NMR}$ signal S to carbonyl carbon 6 owing to its chemical shift is further corroborated by the presence of a correlation between signals

μ (C-5) and S (C-6) (cross peak iv, Figure 35). This is crucial evidence of the bond between C-6 and C-5a.

In instances where the two hydrogens of a methylene group show unequal 2J and 3J coupling strengths, it is thought that this is due to the rigid nature of the structure which therefore allows unusual dihedral angles. The latter is what determines the strength of the coupling between particular nuclei. The final assignments of ^{13}C and ^1H NMR resonances to specific atoms are shown below:

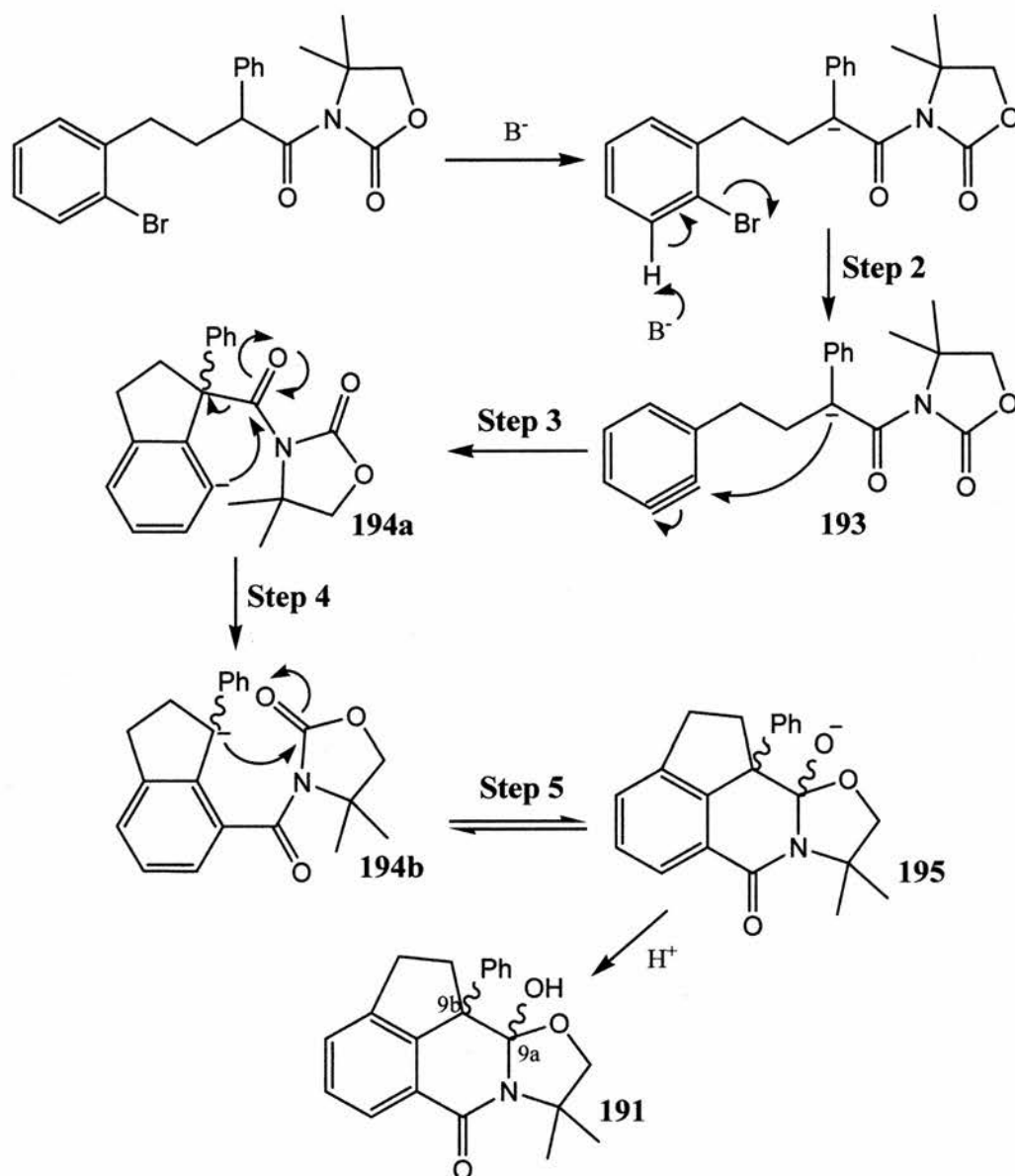


2.8.2 Cyclisation Mechanism

The confirmation of the structure of fused tetracycle **191** posed mechanistic questions. It is proposed that an aryne type or a radical anion type process could account for the formation of tetracycle **191**. Scheme 168 shows a plausible aryne-based mechanism.

After initial deprotonation adjacent to the carbonyl group, a second deprotonation occurs to form the intermediate aryne **193** (step 2, Scheme 168). Aryne **193** can then undergo ring closure involving intramolecular nucleophilic attack by the azaenolate to form indanyl anion **194a** (step 3, Scheme 168). Attack on the oxazolidinyl carbonyl by the resultant aryl anion to give a 1,3 shift of the oxazolidinone moiety could then occur (step 4, Scheme 168). There are several precedents in the literature for this type of carbonyl migration process involving anions derived from arynes.³¹ This would immediately be followed by a 6-*exo*-trig ring closure to form alkoxide anion **195** (step 5, Scheme 168). Proton addition would

then result in the formation of the novel tetracycle **191**. It is thought that, in the absence of a proton donor, that ring closure to **195** may be reversible. This would inevitably lead to the most thermodynamically stable product.



Scheme 168

Two stereoisomers with the OH and Ph groups *cis* or *trans* about the C9a-C9b bond are possible. Distinction between these two could not be made with certainty on the basis of the NMR spectra. Bond C9a-C9b forms during closure of the second ring in which the anionic centre (or radical centre, Scheme 169) approaches from above or below the oxazolidinone carbonyl group. Models suggested there was less steric hindrance in the mode leading to formation of the *trans* product. To shed further light on the situation the geometries and energies of the *cis*- and *trans*-isomers were

computed using the empirical MM2 method, the semi-empirical AM1 method and the ab initio DFT method with the B3LYP functional. The optimised geometries obtained with the AM1 method are shown in Figure 11 and the energies computed with all three methods are in Table 3.

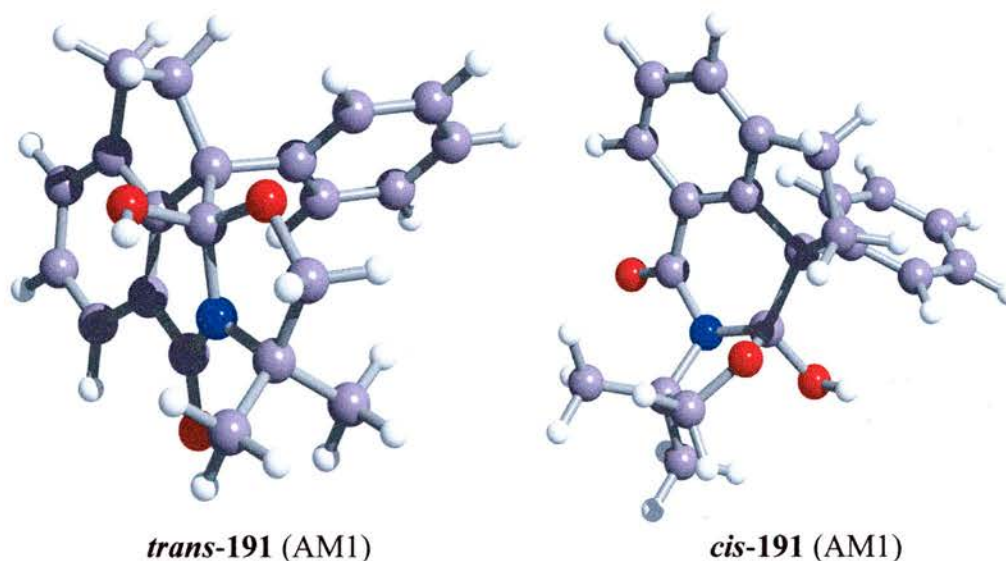


Figure 36 Graphical representation of the energy minimised structures for *cis/trans* 191

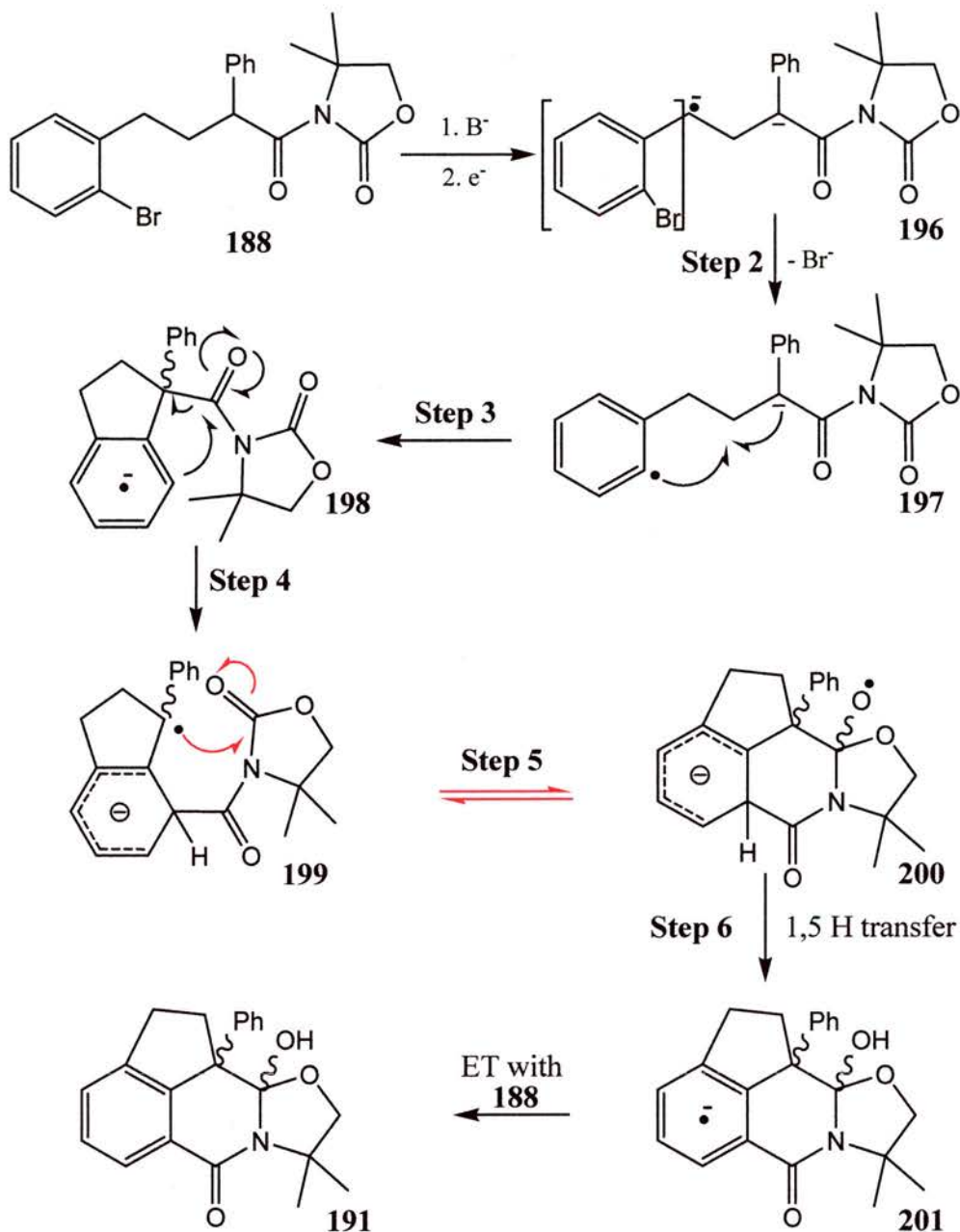
	MM2 steric energies (kcal mol ⁻¹)	AM1 heats of formation (kcal mol ⁻¹)	B3LYP/6-31G(d) total energies (Hartrees)
<i>trans</i>	20.4	-51.8	-1093.326960
<i>cis</i>	30.8	-41.1	-1093.309441
$\Delta E(\text{trans-cis})^*$	-10.4	-10.7	-11.0

Table 24 Computed energies of *cis* and *trans* 191. * In kcal mol⁻¹

The three computational methods all predict that the *trans*-isomer is 10 to 11 kcal mol⁻¹ lower in energy than the *cis*-isomer. On thermodynamic grounds therefore the *trans*-structure is more likely to form, particularly if the ring closure is reversible. The stereochemistry of 191 is therefore tentatively assigned as *trans* about the C9a-C9b bond.

Scheme 169 shows an alternative radical-anion mechanism analogous to that proposed for the 2-oxazoline precursors (Section 2.5.2.3). Following the initial deprotonation and electron transfer to the precursor, intermediate 196 would be formed which would lose bromide to give radical anion 197 (step 2, Scheme 169).

This radical-anion could then undergo classical $S_{RN}1$ intramolecular coupling to form indanyl radical anion **198** (step 3, Scheme 169).

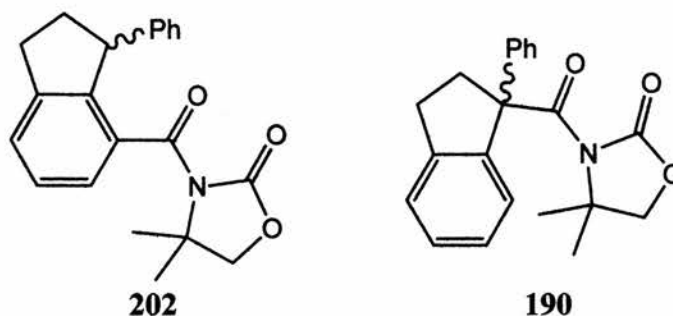


Scheme 169

Then, in a similar way to that illustrated in Section 2.5.2.3, the aryl radical anion could attack the carbonyl group to form 1,3 rearranged product **199** (step 4, Scheme 169). Intermediate **199** first undergoes a 6-*exo-trig* cyclisation (step 5, Scheme 169) and subsequently a 1,5-H-atom transfer to give tetracyclic radical anion **201** (step 6, Scheme 169). In the structure of intermediate **200**, with the HO and Ph groups *trans*, the *tertiary* H-atom is particularly well placed to migrate to the oxygen. Electron transfer to more of the precursor will give the observed product **191** (step 7,

Scheme 169) and continue the $S_{RN}1$ chain process. It is assumed that the one stereoisomer formed is the *trans* isomer for reasons detailed above (Table 24, Figure 36).

In either the aryne or the radical-anion pathway the quenching of either **194b** or **199** by a proton or hydrogen atom is not a significant event because no indane **202** was observed (Scheme 170). The 1,3 rearrangement of the oxazolidinone must be a facile process because none of indane **190** was detected (Scheme 170).



Scheme 170

Labelling experiments could be carried out to ascertain which mechanistic pathway was occurring. Also, EPR experiments could help to determine if any radical intermediates are present in the reaction mixture. Confirmation of the relative stereochemistry could be obtained by selective derivatisation in order to obtain a single crystal suitable for X-ray analysis.

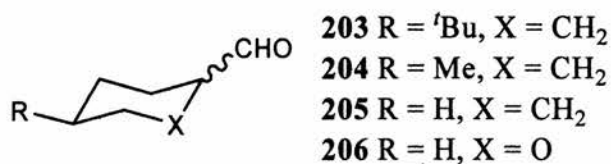
A substructure search in the literature revealed that tetracycle **191** was a completely novel fused ring structure; derivatives thereof may show interesting biological activity. The amide linkage in **191** would probably be difficult to selectively hydrolyse and acid treatment would probably lead to molecular rearrangement(s).

The results obtained with the oxazolidinone precursor suggest that the initial course of the reaction with LDA is analogous to that of the 2-oxazoline precursors, i.e. cyclo-coupling to give an indane-type structure. However, in the case of the oxazolidinone, the presence of two electronegative carbonyl groups promotes additional intramolecular processes leading to a cascade rearrangement.

In view of the good yield of product **191** obtained under $S_{RN}1$ conditions with achiral precursor **188**, it is probable that similar reactions could be accomplished with a range of other oxazolidinones. In particular, a promising future project would be to examine the control of the stereochemistry of the first ring closure by using a chiral oxazolidinone.

2.9 Conformational Study of Alicyclic Acyl Radicals

The structural, mechanistic and synthetic properties of acyl radicals have received much interest in recent times.⁴⁸ Acyl radicals including alicyclic acyl radicals have been used successfully in the preparation of acyl halides,⁴⁹ esters⁵⁰ and in a wide range of routes to carbonyl compounds.^{48, 51, 52} Furthermore acyl generation by carbonylation of C-centred radicals, which is synthetically important,^{52d} has been investigated for cyclohexyl radicals.⁵³ Due to the conformationally labile nature of cyclohexane rings, the acyl radical moiety can exist either axially or equatorially. Thus far no study of this phenomenon has been carried out, although cyclopropylacyl and cyclobutylacyl radicals have been shown by EPR to exist in both *s-cis* and *s-trans* conformations in which the plane of the acyl group bisects the ring.⁵⁴ An EPR spectroscopic method for distinguishing axial and equatorial cyclohexylcarbinyl radicals, which depends on their differing H_{β} hfs, had been established previously by Walton and Ingold.⁵⁵ Acyl radicals are σ -radicals with small H_{β} hfs and low g -factors,⁵⁶ unlike the π -type cycloalkylcarbinyl radicals. In order to ascertain if axial and equatorial cyclohexylacyl radical conformations could be differentiated via EPR spectroscopy, a series of EPR experimental observations were proposed, for solutions of the radicals prepared by hydrogen abstraction from alicyclic carbaldehydes of the type shown in Scheme 171. This work has been recently published in the literature.⁵⁷

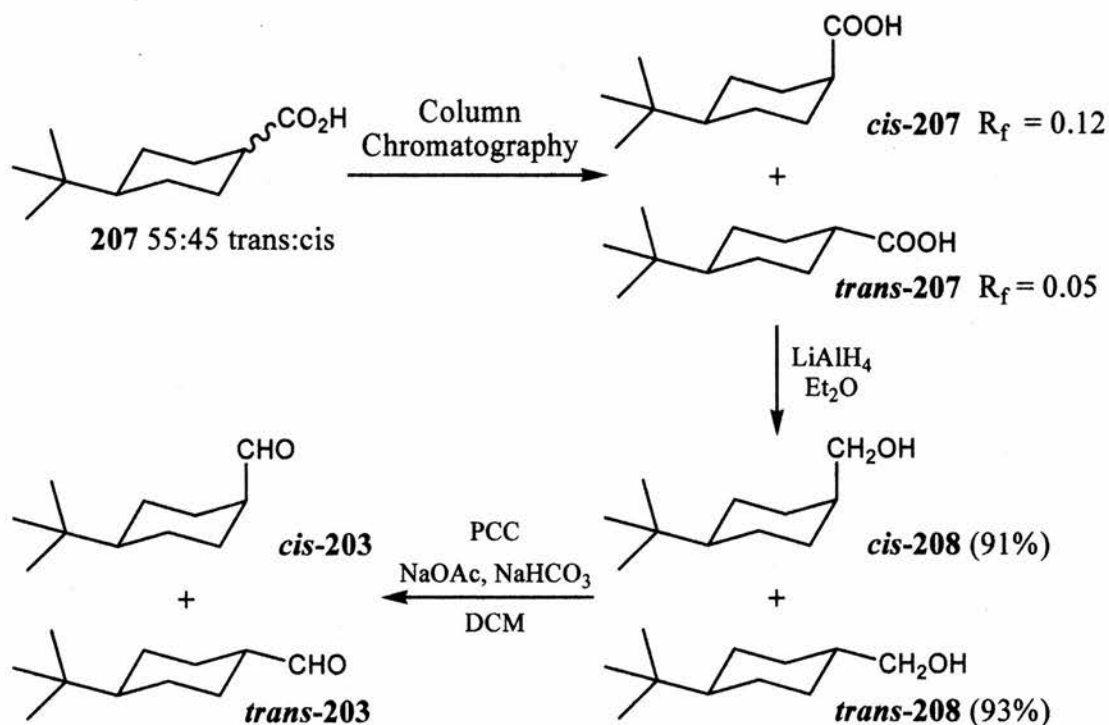


Scheme 171

2.9.1 Preparation of Alicyclic Carbaldehydes

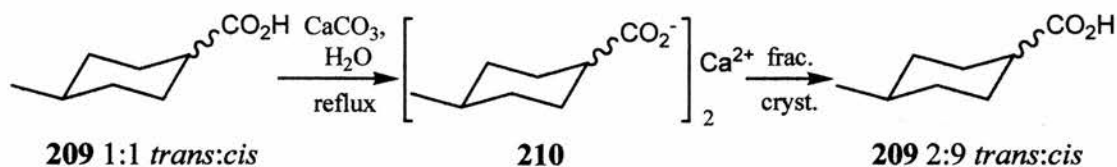
Cyclohexanecarbaldehyde **205** was commercially available and was distilled prior to use. *Cis* & *trans*-4-*tert*-butylcyclohexanecarbaldehydes *cis*-**203** & *trans*-**203** were not commercially available, but their parent acids *cis*-**207** & *trans*-**207** were commercially available as a 45:55 mixture. Separation of the two isomers of **207** was facilitated simply by passage through a silica column (3.5 x 20 cm) using

dichloromethane as eluant (Scheme 172). Reduction using lithium aluminium hydride followed by mild oxidation by pyridinium chlorochromate yielded the desired isomeric carbaldehydes *cis*-207 and *trans*-207 (Scheme 172).⁵⁸



Scheme 172⁵⁸

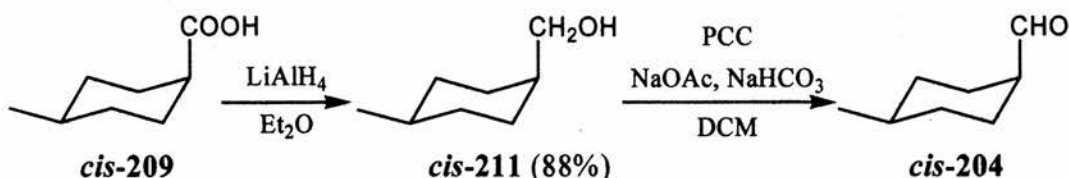
The conformationally labile *cis*-4-methylcyclohexancarbaldehyde *cis*-204 was also not available commercially. As before, the parent acid *cis*-209 was available, although as a 1:1 mixture with the *trans* isomer *trans*-209. Unfortunately separation could not be achieved via column chromatography. A survey of the literature revealed a separation of the calcium salts via fractional crystallisation reported by Perkin Jr. *et al.*⁵⁹ in 1911. The calcium salt was formed by refluxing the isomeric acids in an aqueous suspension of calcium carbonate. Thus formed, the calcium salts **210** were repeatedly recrystallised from water to obtain a 9:2 mixture (from the 4th crop) of the *cis:trans* calcium carboxylates **210** which was deemed an acceptable ratio (Scheme 173).



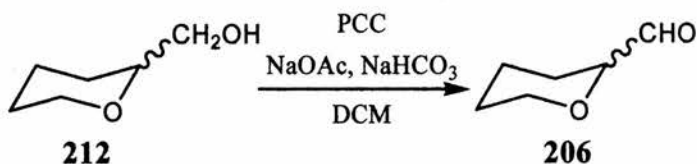
Scheme 173

Acidification of the calcium salt with 1M hydrochloric acid furnished the free acid *cis*-209. The acid was reduced as before with lithium aluminium hydride

followed by mild oxidation to afford the carbaldehyde *cis*-**204** (Scheme 174).⁵⁸ The carbaldehyde was distilled prior to use.

Scheme 174⁵⁸

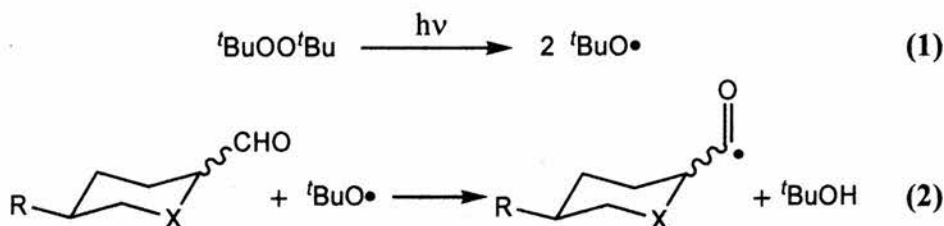
Tetrahydropyran-2-carbaldehyde **206** was obtained by oxidation of the commercially available racemic tetrahydropyran-2-ylmethanol **212** and distilled prior to use as before (Scheme 175).⁵⁸

Scheme 175⁵⁸

2.9.2 EPR and Computational Study of Cyclohexylacyl Radicals

The EPR samples were prepared by the addition of either cyclopropane or *n*-propane to a mixture of di-*tert*-butylperoxide (20 μ l) and the carbaldehyde (0.14 M), followed by several freeze-pump-thaw cycles in order to degas the sample, after which the tube was sealed.

The mechanism of formation of acyl radicals upon UV irradiation in the EPR resonant cavity is shown in Scheme 176. Upon irradiation homolytic fission of the di-*tert*-butylperoxide O-O bond will occur to form *tert*-butoxy radicals (Eq. 1, Scheme 176) which then abstract a hydrogen atom from the carbaldehyde to form the corresponding acyl radical and *tert*-butyl alcohol (Eq. 2, Scheme 176).



Scheme 176

In cycloalkanes the bulky *tert*-butyl always maintains an equatorial or pseudoequatorial position, thus *cis*-**203** should always retain the formyl group axial

and *trans*-203 equatorial. EPR experiments of carbaldehydes *cis*-203 and *trans*-203 were run under similar conditions to furnish spectra of the corresponding acyl radicals *cis*-213 and *trans*-213 as illustrated in Figure 37.⁶⁰

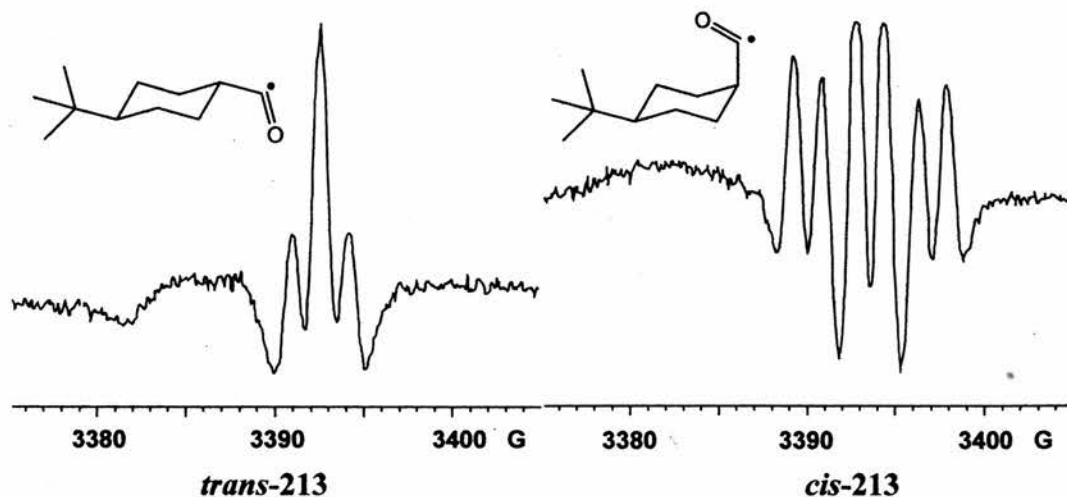
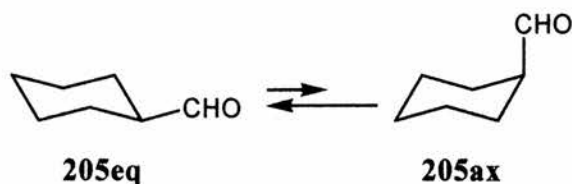


Figure 37 2nd Derivative EPR spectra of *cis* and *trans* acyl radicals **213** in cyclopropane at 140 K.

Surprisingly the spectrum of *trans*-213 showed a triplet multiplicity which was not expected of an acyl radical with a single beta hydrogen (Figure 37).⁶¹ The spectrum had a low *g*-factor (2.0007) appropriate for a σ -acyl radical with an $a(2H)$ of 1.6 G (Table 25). It can be assumed that, due to the absence of a doublet in the spectrum, the $a(H_\beta)$ is less than the line width (<1 G) and the observed $a(2H)$ is due to long range interactions. The axial acyl radical *cis*-213 showed a significantly larger $a(H_\beta)$ (1.6 G at 140 K) leading to a distinct *dt* pattern (Figure 37, Table 25). EPR spectra of *cis* & *trans* **213** showed significant broadening above 160 K (Appendix C).

Cyclohexanecarbaldehyde **205** is expected to exist in both the axial and equatorial conformers at equilibrium and as will the analogous acyl radical **214** (Scheme 177). It is expected that the **205eq** will be the predominate conformer.



Scheme 177

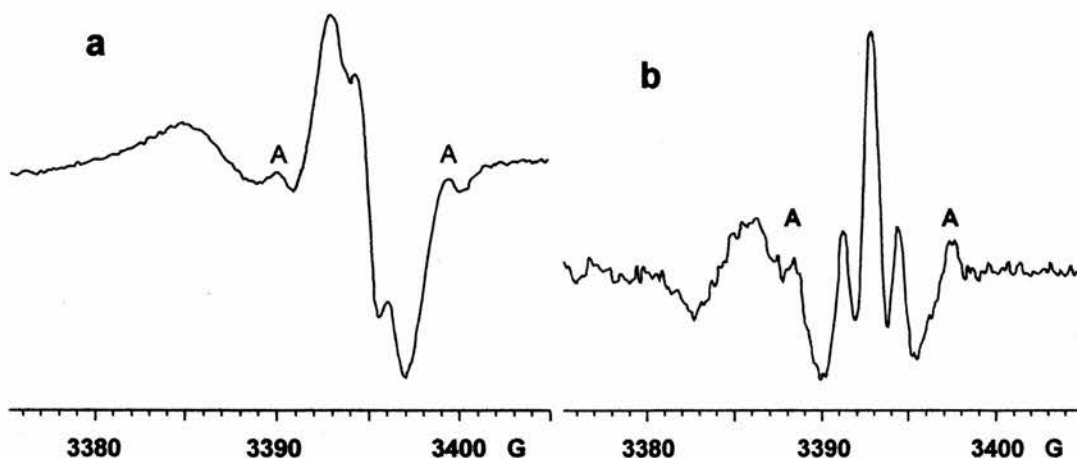
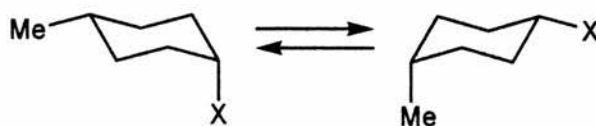


Figure 38 (a) 1st Derivative EPR spectrum of **214** in *n*-propane at 120 K; (b) 2nd Derivative EPR spectrum of **214** in cyclopropane at 140K.

The EPR spectra of acyl radical **214** in either cyclopropane or *n*-propane⁶⁰ showed a prominent triplet (Figure 38) with small additional features (marked A, Figure 38). The triplet had a low *g*-factor (2.0001) similar to that observed in the case of *cis*-**213** and *trans*-**213**. The dominant triplet has $a(2H) = 1.6$ which is essentially identical to that observed for *trans*-**213**, thus the signal can be attributed to the equatorial conformer **214eq** (Table 25). Again the $a(H_\beta)$ was assumed to be less than the line width. The small features (marked A, Figure 38) have a separation (w) of 8.9 G, which is very close to the separation (8.7 G at 140 K) of the outer peaks of the spectrum of *cis*-**213** (axial formyl) (Figure 37). This leads to the conclusion that these features are due to the presence of the minor conformer **214ax**, the central portion of the multiplet being obscured by the stronger **214eq** signal. This data shows for the first time, that axial and equatorial acyl radicals can be distinguished by EPR spectroscopy. A broad line at lower field ($g = 2.0046$) was also observed in these spectra and that of *cis* & *trans* **213**. Redistilled aldehyde showed the same broad feature, as did spectra from all the other aldehydes of this study; therefore, these features were deemed not due to impurities. Most likely they are due to the 1-formylcyclohexyl radicals generated by abstraction of the tertiary H-atoms adjacent to the formyl groups. The *g*-factor of the analogous $Me_2C(\cdot)CHO$ radical is 2.0045, in close agreement.⁶²

Unlike the *tert*-butyl group, a methyl group on a cyclohexane ring can exist in either the axial or equatorial orientation depending on the steric demands of other groups attached to the ring (Scheme 178).



Scheme 178

The EPR spectrum (Figure 39) of acyl radical *cis*-**215**, obtained in the usual way, from *cis*-4-methylcyclohexancarbaldehyde *cis*-**204** after H-atom abstraction revealed the main signal to be a *dt* with parameters very similar to those obtained for *cis*-**213** (Table 25). Therefore the formyl group is deemed to be axial.

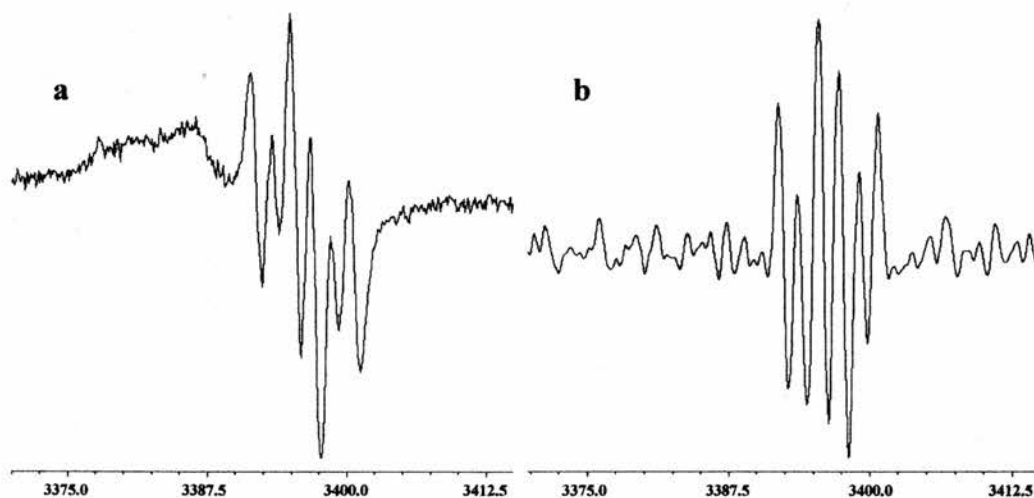


Figure 39 EPR spectra (1st derivative = a, 2nd derivative = b) of *cis*-**215** in cyclopropane at 140 K.

The radical **216** derived from H-atom abstraction from pyranaldehyde **206** was also studied. The spectrum revealed a main signal with a *dd* multiplicity (Table 25) having a *g*-factor (2.0001) indicative of a acyl radical and many small features which can be divided into two groups (A and B, Figure 40). The first set of small features (A, Figure 40) show a small doublet splitting of approximately 0.7 G with a separation of 7.7 which is of the same order as seen in previous axial acyl radicals (Table 25) and is therefore tentatively assigned to **216aq**, with main *dd* signal assigned to **216eq** (Scheme 179). The other set of minor signals had a *g*-factor of 2.0042 and was probably due to the tertiary 2-formyltetrahydropyran-2-yl radical **217** (Scheme 179).

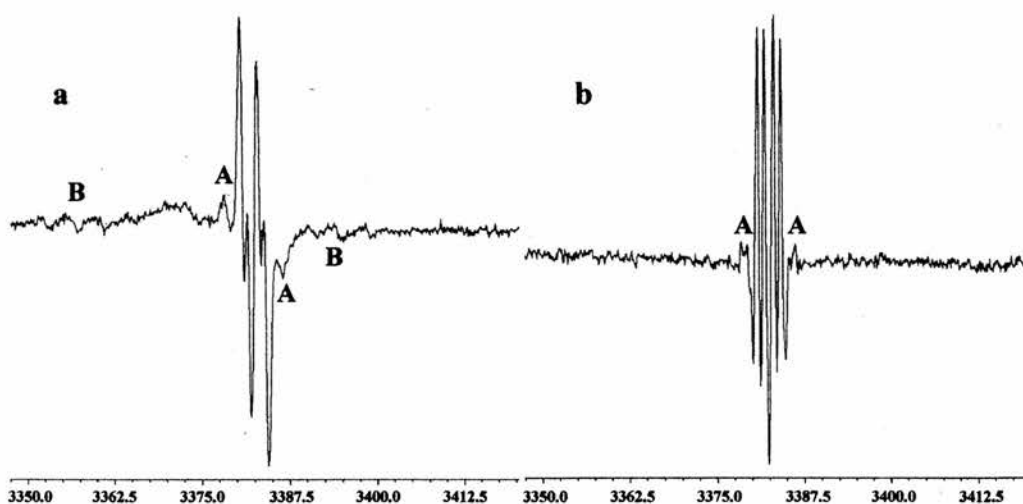
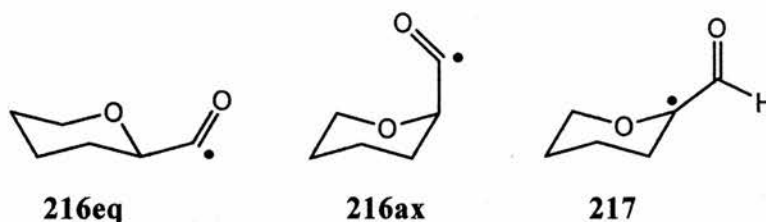
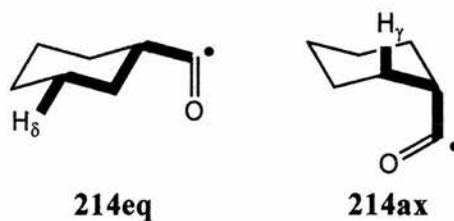


Figure 40 EPR spectra (1st derivative = a, 2nd derivative = b) of **216** in cyclopropane at 140 K.



Scheme 179

Theoretical hyperfine splittings were calculated by co-workers⁶³ for the axial and equatorial conformers of acyl radical **214** using the UB3LYP method with the EPR-III basis set (structures at B3LYP/6-31G*)³⁸ implemented in the Gaussian 03 suite of programs.³⁷ $a(H_\beta)$ Values of -1.6 and -2.2 G were obtained for **214eq** and **214ax** respectively (Table 25). The computations suggested the triplet long range hfs of **214eq** were due to equatorial H_δ s whereas the long range hfs of **214ax** were associated with axial H_γ s. In both cases these are the H-atoms with all-*trans* (W-Plan) arrangement of bonds with respect to the radical centre (Scheme 180).⁶⁴



Scheme 180

Radical	T/K or Comp. method	g-factor	$a(H_\beta)/G$	$a(2H)/G$	w/G
214eq [†]	120	2.0001	<1.0	1.6	-
214eq	UB3LYP/EPR-III	-	-1.6	1.6(H _δ)	-
214ax [†]	120	2.0001	-	-	8.9
214ax	UB3LYP/EPR-III	-	-2.2	3.7(H _γ)	9.6
<i>cis</i> -213	140	2.0001	1.8	3.6	9.0
<i>trans</i> -213	145	2.0007	<1.0	1.6	-
<i>cis</i> -215	140	2.0007	1.5	3.6	8.7
216eq	140	2.0000	2.4	1.1 [‡]	-
216ax	140	2.0000	[7.0]	[0.7] [‡]	7.7

Table 25 EPR parameters for cyclohexylacyl and related radicals in cyclopropane. [†] Solvent *n*-propane. [‡] $a(1H)$.

The concentrations of **214eq** and **214ax** were determined from the double integration of the EPR signals.⁶⁵ The error limits were large due to the limited resolution of the two species (Figure 41, Appendix D). At these temperatures (120-150 K) 6-membered ring inversion is expected to be slow compared to the loss of the radicals in bimolecular termination processes. Therefore the concentration ratios measured by EPR spectroscopy probably do not reflect their equilibrium ratio at the temperature of the measurements.

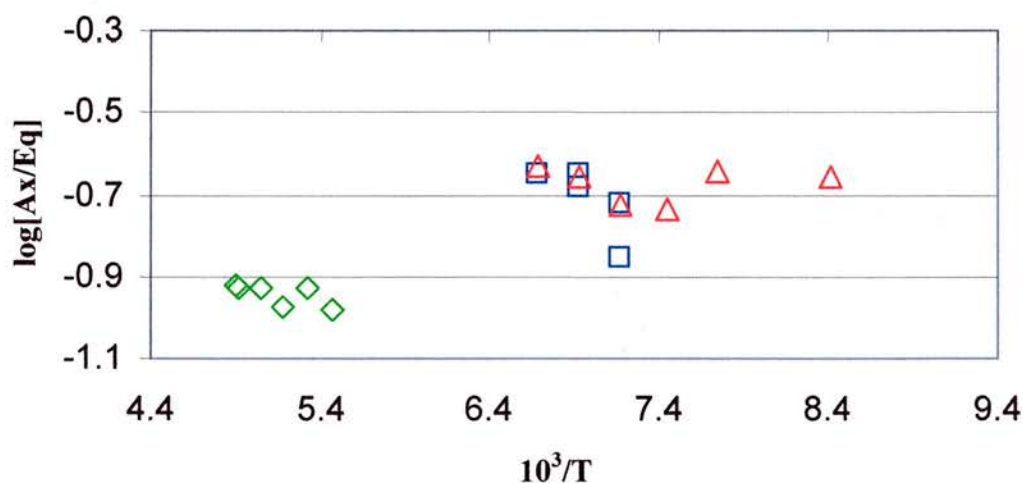


Figure 41 Plot of $\log[Axial]/[Equatorial]$ ratios vs. $10^3/T$. Δ : EPR data for **[214ax]/[214eq]** in *n*-propane (Appendix D). \square : EPR data for **[214ax]/[214eq]** in cyclopropane (Appendix D). \diamond : NMR data for **[205ax]/[205eq]** in dichloromethane (Section 3.11.1.3).

The ratio $[205_{ax}]/[205_{eq}]$ was also measured via integration of the formyl signals of the axial and equatorial aldehydes in their low temperature $^1\text{H-NMR}$ spectra in CD_2Cl_2 (Figure 41). Coalescence of the formyl signals was observed at 213 K and therefore ring inversion will be very slow at lower temperatures. The EPR experiments were conducted at 120 – 165 K so the measured $[214_{aq}]/[214_{eq}]$ ratios probably reflect the ratio of the concentrations of the two aldehydes that was “frozen” in as the sample was cooled. Examination of Figure 41 supports this conclusion. The $\log \{[214_{ax}]/[214_{eq}]\}$ ratio is practically independent of the temperature, as is the ratio obtained for the aldehyde **205** in CD_2Cl_2 at higher temperature. The latter, measured in the more polar solvent appears lower than the ratios obtained for the analogous acyl radical in the non-polar *n*-propane and cyclopropane (Figure 41). This could possibly be due to a small solvent dependence of the axial/equatorial ratios.

A simulation of the 2nd derivative EPR spectrum of **214** (Figure 38a) was carried out using the Winsim 2002 beta simulation package.⁶⁶ As an approximation the hfs determined for *cis*-**213** were used for the mostly obscured signal of **214_{ax}** (Figure 38a). The relative areas of the two species were optimised using a quadratic optimisation protocol, to give the $[214_{ax}]/[214_{eq}]$ ratio as 0.33 with $R = 0.96$ (Figure 42). This ratio is of the same order as obtained via double integration of the actual EPR spectra.

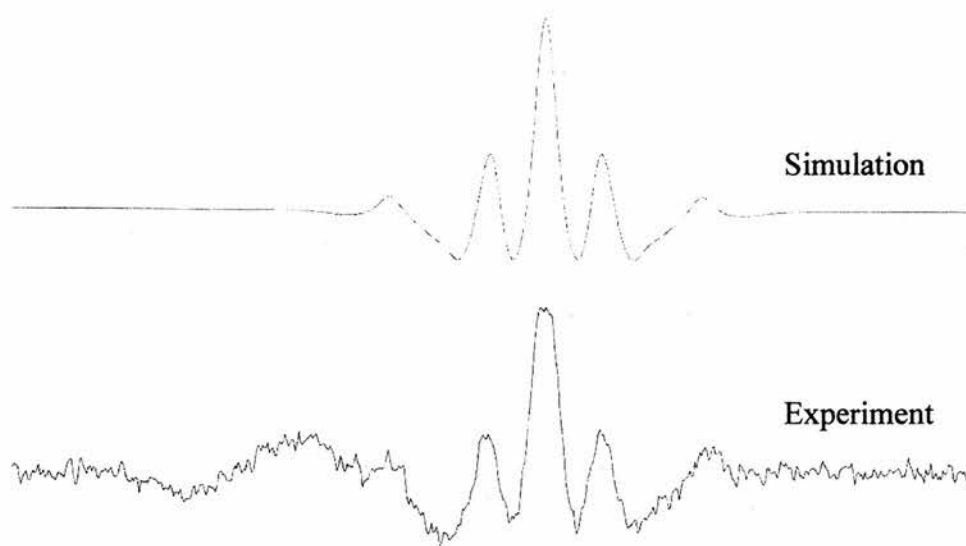
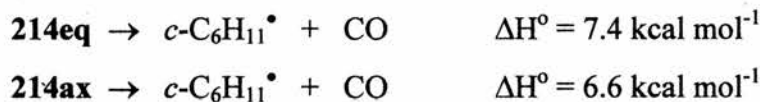


Figure 42 Simulation of the EPR spectrum of **214** in cyclopropane at 140 K.

2.9.3 Summary of Study of Cyclohexylacyl Radicals

In summary, it has been shown that cyclohexylacyl radicals exist in two conformations and that they can be characterized and their concentrations tracked by an EPR spectroscopic method. As with cycloalkylcarbinyl radicals, the key difference between axial and equatorial species lies in the larger H_β hfs of the former. Computational results⁶³ indicated that this derives from the higher rotational barrier about the $C_\beta-C_\alpha(O)$ bond which results from 1,3-interactions of the CO group with the axial H_β -atoms of the ring. The method also works for tetrahydropyranylacyl radicals and, judging by cycloalkylmethyl analogs,^{39b, 40 & 67} it is probable that it can also be successfully applied for a variety of alicyclic rings including cyclohex-2-enyl-1-acyl, and cyclohept-4-enyl-1-acyl.

The conformational equilibria will lead to subtle chemical consequences. For example, it is likely that the rates of decarbonylations of the axial and equatorial radicals will differ since computations (B3LYP/EPR-III//B3LYP/6-31G*)⁶³ give different enthalpies for these reactions:



Thermodynamically, loss of CO is predicted to be somewhat easier from the axial conformation and this is in accord with expectation.

2.10 Conclusions

A viable synthetic route to arylalkyl-2-oxazolines has been developed from readily available starting materials. Although in the case of chiral 2-oxazolines, several more synthetic steps are needed, this is mainly due to the need to obtain the chiral moiety in the correct oxidation state from the existing chiral pool (Section 2.1).

Although attempts to form heteroatom analogues of arylalkyl-2-oxazolines failed, viable alternative routes have been identified (Section 2.3).

It has been shown that arylalkyl-2-oxazolines undergo radical nucleophilic ring closure, which is stimulated by UV light, to give indanes, tetrahydronaphthalenes and benzosuberenes with strained quaternary centres in good to high yield. Thus, it is demonstrated for the first time that 2-oxazoline nucleophiles take part in intramolecular $S_{RN}1$ reactions. The optimum conditions for ring closure were found to be 3 eq. LDA in THF with either stirring at room temperature for 48 h or UV irradiation for 6 h (Section 2.4).

Arylpropyl-2-oxazolines and arylbutyl-2-oxazolines proceed to form the direct ring closed indanes and tetrahydronaphthalenes whereas arylpentyl-2-oxazolines and arylhexyl-2-oxazoline undergo rearrangement reactions post ring closure (Section 2.5). This rearrangement involves a rare *alpha-ortho* shift of the oxazolinylium moiety which has only previously been reported in the case of the alkyne mechanism.³¹ This rearrangement is thought to proceed via a cyclic four membered transition state.

The intermediate radical anions have been observed by EPR spectroscopy during the course of ring closure reactions. This strongly indicates the $S_{RN}1$ mechanism is the dominant process (Section 2.6). This is believed to be only the second time radical anion intermediates in $S_{RN}1$ reactions have been observed *in situ*.⁶⁸

Modest diastereoselectivities have been observed when chiral arylpropyl-2-oxazolines undergo radical nucleophilic ring closures. When an isopropyl substituted 2-oxazoline was utilised the product indanes were easily separated via column chromatography to afford, after removal of the oxazoline group, the pure enantiomeric indane carboxylic acids containing a sterically hindered stereogenic quaternary centre (Section 2.7).

When an oxazolidinone moiety was employed instead of the 2-oxazoline functionality, the base induced ring closure occurred, to form the indane which was then observed to undergo an *alpha-ortho* shift of the oxazolidinone group which was followed by a second ring closure onto the carbonyl group of the oxazolidinone to form a novel fused tetracyclic ring structure in good yield (75 %) (Section 2.8). This novel ring structure, and analogues thereof, may exhibit interesting biological activity as it contains the biologically active isoquinolinone motif.

It has been shown that concentrations of axial and equatorial cyclohexylacetylradicals, for the first time, can be distinguished by EPR spectroscopy and their concentrations measured (Section 2.9).

2.11 Bibliography

- 1 R. J. Fessenden and J. S. Fessenden, *Organic Chemistry*, Wadsworth, Belmont CA, 1990, p 705.
- 2 R. A. Glennon, J. J. Salley, O. S. Steinstand and S. Nelson, *J. Med. Chem.*, 1981, **24**, 678-683.
- 3 R. Faust, P. J. Garrett, R. Jones, Li-Kuan Yeh, A. Tsotinis, M. Panoussopoulou, T. Calogeropoulou, Muy-Teck Teh and D. Sugden, *J. Med. Chem.*, 2000, **43**, 1050-1061.
- 4 S. Tanaka, H. Saburi, Y. Ishibashi and M. Kitamura, *Org. Lett.*, 2004, **11**, 1873-1876.
- 5 P. L. Ornstein, T. J. Bleisch, B. M. Arnold, J. H. Kennedy and R. A. Wright, *J. Med. Chem.*, 1998, **41**, 358-378.
- 6 G. Toth and K. E. Kover, *Synth. Commun.*, 1995, **25**, 3067-3074.
- 7 M. Adamczyk, D. S. Watt and D. A. Netzel, *J. Org. Chem.*, 1984, **49**, 4226-4237.
- 8 R. J. Fessenden and J. S. Fessenden, *Organic Chemistry*, Wadsworth, Belmont CA, 1990, p 321.
- 9 A. I. Meyers, D L. Temple, R L. Nolen and E D. Mihelich, *J. Org. Chem.*, 1974, **39**, 2778-2783.
- 10 M. D. Fryzuk, L. Jafarpour and S. J. Rettig, *Tetrahedron: Asymmetry*, 1998, **9**, 3191-3202.
- 11 (a) H. Vorbrueggen and K. Krolkiewicz, *Tetrahedron Lett.*, 1981, **22**, 4471-4474; (b) S. Serota, J. R. Simon, E. B. Murray, and W. M. Leinfield, *J. Org. Chem.*, 1981, **46**, 4147-4151; (c), P. Zhou, J. E. Blubaum, C. T. Burns and N. R. Natale, *Tetrahedron Lett.*, 1997, **38**, 7019-7020; (d) J. F. Hansen, and S. Wang, *J. Org. Chem.*, 1976, **41**, 3635-3637.
- 12 S. Cobb, MChem project report, University of St Andrews, 2001.
- 13 T. G. Gant and A. I. Meyers, *Tetrahedron*, 1994, **50**, 2297-2360.
- 14 A. I. Meyers, G. Knaus, K. Kamata, and M. E. Ford, *J. Am. Chem. Soc.*, 1976, **98**, 567-576.
- 15 P. Beak, D. J. Allen, and W. K. Lee, *J. Am. Chem. Soc.*, 1990, **112**, 1629-1630.

- 16 A. I. Meyers, D. L. Temple, R. L. Nolen and E. D. Mihelich, *J. Org. Chem.*, 1974, **39**, 2778-2783.
- 17 Y. Tohda, T. Kawashima, M. Ariga, R. Akiyama, K. Shuhoh and Y. Mori, *Bull. Chem. Soc. Jpn.*, 1984, **57**, 2329-2330.
- 18 D. Chakravarti, *J. Indian Chem. Soc.*, 1939, **16**, 639-644.
- 19 H. Emtenäs, L. Alderin and F. Almqvist, *J. Org. Chem.*, 2001, **66**, 6756-6761.
- 20 E. A. Kuo, P. T. Hambleton, D. P. Kay, P. L. Evans, S. S. Matharu, E. Little, N. McDowall, C. B. Jones, C. J. R. Hedgecock, C. M. Yea, A. W. E. Chan, P. W. Hairsine, I. R. Ager, W. R. Tully, R. A. Williamson, and R. Westwood, *J. Med. Chem.*, 1996, **39**, 4608-4621.
- 21 E. Ziegler, *Justus Liebigs Ann. Chem.*, 1976, 250-256.
- 22 Prepared by distilling from an ethanolic solution of magnesium ethoxide.
- 23 F. Michelon, A. Pouilhès, N. Van Bac and N. Langlois, *Tetrahedron Lett.*, 1992, **33**, 1743-1746.
- 24 H. Bartsch and T. Erker, *Arch. Pharm.*, 1991, **324**, 79-82.
- 25 E. Ziegler, *Monatsh. Chem.*, 1957, **88**, 164-166.
- 26 Aspects of which are published: M. D. Roydhouse and J. C. Walton, *Chem. Commun.*, 2005, 4453-4455.
- 27 J.-W. Wong, K. J. Natalie Jr., G. C. Nwokogu, J. S. Pisipati, P. T. Flaherty, T. D. Greenwood and J. F. Wolfe, *J. Org. Chem.*, 1997, **62**, 6152-6159.
- 28 S. C. Bart, E. J. Hawrelak, A. K. Schmisser, E. Lobkovsky and P. J. Chirik, *Organometallics*, 2004, **23**, 237-246.
- 29 (a) M. Ahbala, P. K. Hapiot, A. Houmam, M. Jouini, J. Pinson and J.-M. Saveánt, *J. Am. Chem. Soc.*, 1995, **117**, 11488-11498; (b) N. Alam, C. Amatore, C. Combellas, A. Thiébault and J. N. Verpeaux, *J. Org. Chem.*, 1990, **55**, 6347-6356; (c) C. Amatore, C. Combellas, N. E. Lebbar, A. Thiébault and J. N. Verpeaux, *J. Org. Chem.*, 1995, **60**, 18-26.
- 30 R. Withnall, I. R. Dunkin and R. Snaith, *J. Chem. Soc., Perkin Trans. 2*, 1994, 1973-1977.
- 31 (a) H. Yoshida, M. Watanabe, J. Ohshita and A. Kunai, *Chem. Commun.*, 2005, 3292-3294, 3454-3456.
- 32 H. Jensen, H. S. Sørensen, S. U. Pedersen and K. Daabjerg, *J. Chem. Soc., Perkin Trans. 2*, 2002, 1423-1428.

- 33 (a) A. Hudson and H. A. Hussain, *J. Chem. Soc. (B)* 1967, 1299-1300; (b) E. Flesia and J.-M. Surzur, *Tetrahedron Lett.* 1974, **15**, 123-126.
- 34 (a) F. Gerson and W. B. Martin Jr. *J. Am. Chem. Soc.* 1969, **91**, 1883-1891; (b) F. Correadu-Duran, A. L. Allred and R. J. Loyd, *J. Organometal. Chem.* 1973, **49**, 373-379.
- 35 D. R. Duling, *J. Magn. Reson, Ser B*, 1994, **104**, 105-110.
- 36 N. L. Bauld and F. R. Farr, *J. Am. Chem. Soc.* 1974, **96**, 5633-5634.
- 37 Gaussian 03, Revision A.1, M. J. Frisch, G. W. Trucks, H. B. Schlegel, G. E. Scuseria, M. A. Robb, J. R. Cheeseman, J. A. Montgomery, Jr., T. Vreven, K. N. Kudin, J. C. Burant, J. M. Millam, S. S. Iyengar, J. Tomasi, V. Barone, B. Mennucci, M. Cossi, G. Scalmani, N. Rega, G. A. Petersson, H. Nakatsuji, M. Hada, M. Ehara, K. Toyota, R. Fukuda, J. Hasegawa, M. Ishida, T. Nakajima, Y. Honda, O. Kitao, H. Nakai, M. Klene, X. Li, J. E. Knox, H. P. Hratchian, J. B. Cross, C. Adamo, J. Jaramillo, R. Gomperts, R. E. Stratmann, O. Yazyev, A. J. Austin, R. Cammi, C. Pomelli, J. W. Ochterski, P. Y. Ayala, K. Morokuma, G. A. Voth, P. Salvador, J. J. Dannenberg, V. G. Zakrzewski, S. Dapprich, A. D. Daniels, M. C. Strain, O. Farkas, D. K. Malick, A. D. Rabuck, K. Raghavachari, J. B. Foresman, J. V. Ortiz, Q. Cui, A. G. Baboul, S. Clifford, J. Cioslowski, B. B. Stefanov, G. Liu, A. Liashenko, P. Piskorz, I. Komaromi, R. L. Martin, D. J. Fox, T. Keith, M. A. Al-Laham, C. Y. Peng, A. Nanayakkara, M. Challacombe, P. M. W. Gill, B. Johnson, W. Chen, M. W. Wong, C. Gonzalez, and J. A. Pople, Gaussian, Inc., Pittsburgh PA, 2003.
- 38 V. Barone, *Recent Advances in Density Functional Theory*, Ed. D. P. Chong; World Scientific Publishing Co. Singapore, 1996.
- 39 (a) F. A. L. Anet and R. Anet, *Dynamic Nuclear Magnetic Resonance Spectroscopy*, eds. L. M. Jackman and F. A. Cotton, Academic, New York, 1975, ch. 14, p. 543; (b) J. C. Walton, *J. Chem. Soc., Perkin Trans. 2*, 1986, 1641-1646.
- 40 A. C. Hindson and J. C. Walton, *J. Chem. Soc. Faraday Trans.*, 1990, **86**, 3237-3241.
- 41 (a) R. R. Goehring, *Tetrahedron Lett.*, 1992, **33**, 6045-6048; (b) R. R. Goehring, *Tetrahedron Lett.*, 1994, **35**, 8145-8146.
- 42 R. A. Rossi, A. B. Pierini and A. B. Peñeñory, *Chem. Rev.* 2003, **103**, 71-168.

- 43 D. Hoppe and T. Hense, *Angew. Chem. Int. Ed.*, 1997, **36**, 2282-2316.
- 44 J. A. Murphy, T. A. Khan, S.-Z. Zhou, D. W. Thomson and M. Mahesh, *Angew. Chem. Int. Ed.*, 2005, **44**, 1356-1360.
- 45 S. Jones and C. Smannoo, *Tetrahedron Lett.*, 2004, **45**, 1585-1588.
- 46 C. Gaul, P. I. Arvidsson, W. Bauer, R. E. Gawley and D. Seebach, *Chem. Eur. J.*, 2001, **7**, 4117-4125.
- 47 M. Prein, P. J. Manley and A. Padwa, *Tetrahedron*, 1997, **53**, 7777-7794.
- 48 C. Chatgililoglu, D. Crich, M. Komatsu, and I. Ryu, *Chem. Rev.*, 1999, **99**, 1991-2069.
- 49 (a) W. A. Thaler, *J. Am. Chem. Soc.*, 1966, **88**, 4278; (b) *ibid*, *J. Am. Chem. Soc.*, 1967, **89**, 1902-1908.
- 50 (a) I. E. Marko and A. Mekhalifa, *Tetrahedron Lett.*, 1990, **31**, 7237-7240; (b) I. E. Marko, A. Mekhalifa and W. D. Ollis, *Synlett*, 1990, 347-348.
- 51 D. L. Boger and R. J. Mathvink, *J. Org. Chem.*, 1992, **57**, 1429-1443.
- 52 (a) G. Keck, E. J. Enholm, J. B. Yates and M. R. Wiley, *Tetrahedron*, 1985, **41**, 4079-4094; (b) D. P. Curran, P. A. van Elburg, B. Giese and S. Gilges, *Tetrahedron Lett.*, 1990, **31**, 2861-2864; (c) I. Ryu, H. Yamazaki, A. Ogawa and N. Sonoda, *J. Am. Chem. Soc.*, 1991, **113**, 8558-8560; (d) I. Ryu, T. Niguma, S. Minakata, M. Komatsu, Z. Luo and D. P. Curran, *Tetrahedron Lett.*, 1999, **40**, 2367-2370.
- 53 W. T. Boese and A. S. Goldman, *Tetrahedron Lett.*, 1992, **33**, 2119-2122.
- 54 (a) A. G. Davies and R. Sutcliffe, *J. Chem. Soc., Perkin Trans. 2*, 1982, 1483-1488; (b) P. Blum, A. G. Davies and R. Sutcliffe, *J. Chem. Soc., Chem. Commun.*, 1979, 217-218; (c) H. G. Korth, J. Lusztyk and K. U. Ingold, *J. Chem. Soc., Perkin Trans. 2*, 1990, 1997-2007; (d) D. M. Pawar and E. A. Noe, *J. Org. Chem.*, 1998, **63**, 2850-2853.
- 55 (a) K. U. Ingold and J. C. Walton, *J. Am. Chem. Soc.*, 1985, **107**, 6315-6317; (b) K. U. Ingold and J. C. Walton, *J. Chem. Soc., Perkin Trans. 2*, 1986, 1337-1344.
- 56 (a) J. E. Bennett and B. Mile, *Trans. Faraday Soc.*, 1971, **67**, 1587-1597; (b) A. G. Davies and R. Sutcliffe, *J. Chem. Soc., Perkin Trans. 2*, 1980, 819-824; (c) M. Guerra, *J. Chem. Soc., Perkin Trans. 2*, 1996, 779-782.

- 57 G. A. DiLabio, K. U. Ingold, M. D. Roydhouse and J. C. Walton, *Org. Lett.*, 2004, **6**, 4319-4322
- 58 Aldehydes were purified via filtration of the crude reaction mixture through a pad of silica followed by distillation under reduced atmosphere. At which time a portion was taken and place directly into the quartz EPR tube, therefore no yields were obtained for the oxidation step.
- 59 T. Q. Chou and W. H. Perkin Jr., *J. Chem. Soc., Trans.*, 1911, 526-538.
- 60 Full sets of EPR spectra obtained for all carbaldehydes are shown in Appendix C.
- 61 The analogous acyclic acyl, i.e. $\text{Me}_2\text{CHC}(\cdot)\text{O}$, had $a(\text{H}_\beta) < 1.5 \text{ G}^{56c}$, i.e. within the linewidth, so that a singlet or doublet was anticipated.
- 62 T. Foster, D. Klapstein and P. R. West, *Can. J. Chem.*, 1974, **52**, 524-526.
- 63 G. A. DiLabio, NINT, Edmonton, Canada, personal communication, 2004.
- 64 (a) Y. Ellinger, A. Rassat, R. Subra and G. Berthier, *J. Am. Chem. Soc.*, 1973, **95**, 2372-2373; (b) Y. Ellinger, R. Subra, B. Levy, P. Millie and G. Berthier, *J. Chem. Phys.*, 1975, **62**, 10-29; (c) K. U. Ingold, D. C. Nonhebel and J. C. Walton, *J. Phys. Chem.*, 1986, **90**, 2859-2869.
- 65 (a) D. Griller and K. U. Ingold, *Acc. Chem. Res.*, 1980, **13**, 193-200; (b) D. Griller and K. U. Ingold, *Acc. Chem. Res.*, 1980, **13**, 317-323.
- 66 D. R. Duling, "Simulation of Multiple Isotropic Spin Trap EPR Spectra", *J. Mag. Res., Series B*, 1994, **104**, 105-110.
- 67 F. MacCorquodale, J. C. Walton, L. Hughes and K. U. Ingold, *J. Chem. Soc., Perkin Trans. 2*, 1991, 1893-1899.
- 68 R. G. Scamehorn, L. A. Mahnke, R. D. Krause, B. L. Frey, D. L. Hendriksen, K. S. Jahn, S. G. Kultgen and J. C. Walton, *Org. Lett.*, 2000, **2**, 827-829.

Section 3

Experimental

3.1 Experimental Data Index

2-Benzyl-4,4-dimethyl-2-oxazoline 27	208
2-[3-(2-Chlorophenyl)propyl]-4,4-dimethyl-2-oxazoline 33a	213
2-[3-(2-Bromophenyl)-propyl]-4,4-dimethyl-2-oxazoline 33b	213
2-[3-(2-Chlorophenyl)-1-phenylpropyl]-4,4-dimethyl-2-oxazoline 34a	214
2-[3-(2-Bromophenyl)-1-phenylpropyl]-4,4-dimethyl-2-oxazoline 34b	214
3-(2-Bromophenyl)-1-(4,4-dimethyl-2-oxazolin-2-yl)propen-2-ol 35b	222
3-(2-Bromophenyl)-1-(4,4-dimethyl-2-oxazolin-2-yl)-1-phenylpropen-2-ol 36b	223
2-Chlorophenethyl iodide 37a	198
2-Bromophenethyl Iodide 37b	202
2-Bromophenylacetyl chloride 38b	222
2-Chlorophenethyl alcohol 39a	198
2-Bromophenylethanol 39b	200
2-Bromophenylpropanoic acid 61	199
2-Bromophenylpropanol 62	201
2-Bromophenylpropyl Iodide 63	202
2-[3-(2-Bromophenyl)butyl]-4,4-dimethyl-2-oxazoline 64	219
2-Bromophenylpentanoic acid 65	200
2-Bromophenylpentanol 66	201
2-Bromophenylpentyl Iodide 67	202
2-Bromophenylbutanoic acid 68	199
2-Bromophenylbutanol 69	201
2-Bromophenylbutyl Iodide 70	202
Acetimidic acid ethyl ester hydrochloride 71	207
2-Phenylacetimidic acid ethyl ester hydrochloride 72	207
(<i>S</i>)-Valinol (<i>S</i>)- 73	203
(<i>S</i>)-Phenylglycinol (<i>S</i>)- 75	204
(<i>S</i>)-Serine Methyl Ester Hydrogen Chloride (<i>S</i>)- 78	205
(<i>S,S</i>)-2-Amino-3-methoxy-1-phenylpropan-1-ol (<i>S,S</i>)- 79	205
(<i>S</i>)-4-Isopropyl-2-methyl-2-oxazoline (<i>S</i>)- 81	209
(<i>S</i>)-2-Benzyl-4- <i>iso</i> -propyl-2-oxazoline (<i>S</i>)- 82	209
(<i>R</i>)-2-Benzyl-4- <i>iso</i> -propyl-2-oxazoline (<i>R</i>)- 82	209

(<i>S</i>)-2-Benzyl-4- <i>tert</i> -butyl-2-oxazoline (<i>S</i>)-83.....	209
(<i>R</i>)-2-Benzyl-4- <i>tert</i> -butyl-2-oxazoline (<i>R</i>)-83.....	210
(<i>S</i>)-2-Benzyl-4-phenyl-2-oxazoline (<i>S</i>)-84.....	210
(<i>S</i>)-2,4-Dibenzyl-2-oxazoline (<i>S</i>)-85.....	210
(<i>S</i>)-2-Benzyl-4-cyclohexylmethyl-2-oxazoline (<i>S</i>)-86.....	210
(<i>S</i>)-2-Benzyl-2-oxazoline-4-carboxylic acid methyl ester (<i>S</i>)-87.....	211
(<i>S,S</i>)-2-Benzyl-4-methoxymethyl-5-phenyl-2-oxazoline (<i>S,S</i>)-88.....	211
(<i>S</i>)-1-(2-Benzyl-2-oxazolinyldiphenylmethanol (<i>S</i>)-89.....	211
(<i>S</i>)-Valine methyl ester (<i>S</i>)-91.....	203
(<i>S</i>)-Phenylglycine methyl ester (<i>S</i>)-93.....	204
4,4-Dimethyl-2-(3-phenylpropyl)-2-oxazoline 98.....	221
(4 <i>S</i>)-2-[3-(2-Bromophenyl)propyl]-4-isopropyl-2-oxazoline (<i>S</i>)-102.....	214
(4 <i>S</i>)-2-[3-(2-Bromophenyl)-1-phenyl-propyl]-4-isopropyl-2-oxazoline (<i>S</i>)-103.....	215
(4 <i>R</i>)-2-[3-(2-Bromophenyl)-1-phenyl-propyl]-4-isopropyl-2-oxazoline (<i>R</i>)-103.....	215
(4 <i>S</i>)-2-[3-(2-Bromo-phenyl)-1-phenyl-propyl]-4- <i>tert</i> -butyl-2-oxazoline (<i>S</i>)-104.....	216
(4 <i>R</i>)-2-[3-(2-Bromo-phenyl)-1-phenyl-propyl]-4- <i>tert</i> -butyl-2-oxazoline (<i>R</i>)-104.....	216
(4 <i>S</i>)-2-[3-(2-Bromo-phenyl)-1-phenyl-propyl]-4-phenyl-2-oxazoline (<i>S</i>)-105.....	216
(4 <i>S</i>)-2-[3-(2-Bromophenyl)-1-phenylpropyl]-4-benzyl-2-oxazoline (<i>S</i>)-106.....	217
(4 <i>S</i>)-2-[3-(2-Bromo-phenyl)-1-phenylpropyl]-4-cyclohexylmethyl- 2-oxazoline (<i>S</i>)-107.....	217
(4 <i>S,5S</i>)-2-[3-(2-Bromophenyl)-1-phenylpropyl]-4-methoxy-5- phenyl-2-oxazoline (<i>S,S</i>)-108.....	218
(4 <i>S</i>)-{2-[3-(2-Bromophenyl)-1-phenylpropyl]-2-oxazolin-4-yl}- diphenylmethanol (<i>S</i>)-109.....	218
2-[3-(2-Bromophenyl)-1-phenylbutyl]-4,4-dimethyl-2-oxazoline 110.....	219
2-[3-(2-Bromophenyl)-1-phenylpentyl]-4,4-dimethyl-2-oxazoline 111.....	220
2-[3-(2-Bromophenyl)-1-phenylhexyl]-4,4-dimethyl-2-oxazoline 112.....	220
3-(2-Chlorophenoxy)propionic acid 123.....	224
3-(2-Bromophenylamino)propionic acid 124.....	224
2-Bromophenyl cyanoacetate 127.....	226
<i>N</i> -(2-Bromophenyl)-2-cyanoacetamide 128.....	226
4,4-Dimethyl-2-indan-1'-yl-2-oxazoline 139.....	229
4,4-Dimethyl-2-(1'-phenyl-indan-1'-yl)-2-oxazoline 140.....	228
2-[1,3-Diphenylpropyl]-4,4-dimethyl-2-oxazoline 141.....	227

2-Bromostyrene 142	230
Styrene 143	230
4,4-Dimethyl-2-(1-phenyl-1,2,3,4-tetrahydronaphthalen-1-yl)-2-oxazoline 144	230
2-(1-Butyl-1,5-diphenylpentyl)-4,4-dimethyl-2-oxazoline 145	231
2-[1,5-Diphenylpentyl]-4,4-dimethyl-2-oxazoline 147	233
4,4-Dimethyl-2-(9-phenyl-6,7-dihydro-5H-benzocyclohepten-1-yl)- 2-oxazoline 148	232
4,4-Dimethyl-2-(4,5,6,7-tetrahydro-cyclohepta[jk]fluoren-7a-yl)-2-oxazoline 149 .	232
4,4-Dimethyl-2-(9-phenyl-6,7,8,9-tetrahydro-5H-benzocyclohepten-1-yl)- 2-oxazoline 150	233
(4 <i>S</i> ,1' <i>R</i>)-4-Isopropyl-2-(1'-phenyl-indan-1'-yl)-2-oxazoline (<i>S,R</i>)- 174	234
(4 <i>S</i> ,1' <i>S</i>)-4-Isopropyl-2-(1'-phenyl-indan-1'-yl)-2-oxazoline (<i>S,S</i>)- 174	235
(1 <i>S</i> ,1' <i>S</i>)-1'-Phenyl-indan-1'-carboxylic acid (2-hydroxy-1-isopropylethyl)- amide (<i>S,S</i>)- 175	235
(4 <i>S</i>)-4- <i>tert</i> -Butyl-2-(1'-phenyl-indan-1'-yl)-2-oxazoline (<i>S</i>)- 176	236
4-Phenyl-2-(1'-phenyl-indan-1'-yl)-oxazole 177	238
4-Cyclohexylmethyl-2-(1'-phenylindan-1'-yl)-2-oxazoline 181	238
4,4-Dimethyloxazolidin-2-one 185	243
4,4-Dimethyl-3-phenylacetyloxazolidin-2-one 186	243
4-(2-Bromophenyl)-2-phenylbutyryl chloride 187	242
3-[4-(2-Bromophenyl)-2-phenylbutyryl]-4,4-dimethyloxazolidin-2-one 188	244
4-(2-Bromophenyl)-2-phenylbutyric acid 189	242
7,7-Dimethyl-9a-hydroxy-9b-phenylroytonone 191	244
<i>trans</i> -4- <i>tert</i> -Butylcyclohexane carbaldehyde <i>trans</i> - 203	248
<i>cis</i> -4- <i>tert</i> -Butylcyclohexane carbaldehyde <i>cis</i> - 203	248
<i>cis</i> -4-Methylcyclohexane carbaldehyde <i>cis</i> - 204	249
Cyclohexane carbaldehyde (<i>axial/equatorial</i> mixture) 205	248
Tetrahydropyran-2-carbaldehyde (<i>axial/equatorial</i> mixture) 206	249
<i>cis</i> -4- <i>t</i> -Butylcyclohexane carboxylic acid <i>cis</i> - 207	247
<i>trans</i> -4- <i>tert</i> -Butylcyclohexane methanol <i>trans</i> - 208	247
<i>cis</i> -4- <i>tert</i> -Butylcyclohexane methanol <i>cis</i> - 208	247
<i>cis</i> -4-Methylcyclohexane carboxylic acid calcium salt <i>cis</i> - 210	246
(<i>S</i>)-Valine methyl ester hydrochloride (<i>S</i>)- 218	203
(<i>S,S</i>)-4-Hydroxymethyl-2-methyl-5-phenyl-2-oxazoline (<i>S,S</i>)- 219	211

(1'*S*)-1-Phenyl-indan-1-carboxylic acid (1'-hydroxymethyl-2',2'-
dimethyl-propyl)-amide (*S*)-220237

3.2 Instrumentation and General Techniques

3.2.1 NMR Spectroscopy

^1H Nuclear magnetic resonance (NMR) spectra were recorded on a Bruker Avance 300 (300.1 MHz), Bruker Avance 500 (499.9 MHz) or a Varian Gemini 2000 (300.0 MHz) spectrometer, using deuteriochloroform (or other indicated solvent) as reference or internal deuterium lock.

^{13}C NMR spectra were recorded using the PENDANT sequence and internal deuterium lock were recorded on a Bruker Avance 300 (75.5 MHz) or a Bruker Avance 500 (125.7 MHz) spectrometer. All other ^{13}C spectra were recorded on a Varian Gemini 2000 (75.5 MHz) spectrometer using composite pulse ^1H decoupling.

Two-dimensional NMR spectroscopy such as ^1H - ^1H COSY spectra (Correlated Spectroscopy), ^1H - ^{13}C COSY spectra (HSQC: Heteronuclear Single Quantum Coherence) and long-range ^1H - ^{13}C COSY spectra (HMBC: Heteronuclear Multiple Bond Connectivity), were carried out to determine the correlation between ^1H and ^{13}C .

Both the ^1H -NMR and ^{13}C -NMR spectra were obtained from solutions in CDCl_3 unless otherwise stated. All spectra were referenced to internal tetramethylsilane and the chemical shifts for all NMR spectra are expressed in parts per million to high frequency of the reference. $5\mu\text{l}$ Dibromomethane was used as the internal standard as reference for NMR yields. Coupling constants (J) are quoted in Hz and are recorded to the nearest 0.1 Hz. The multiplicity of each signal is indicated by the following abbreviations: s, singlet; d, doublet; dd, doublet of doublets; ddd, doublet of doublet of doublets; dt, doublet of triplets; t, triplet; q, quartet; ddq, doublet of doublet of quartets; m, multiplet and br, broad.

3.2.2 Infrared Spectroscopy

The IR spectra were obtained on a Perkin Elmer FT-IR Paragon 1000 spectrometer. Solids were run as nujol mulls and liquids were run as thin films on NaCl plates.

3.2.3 Mass Spectrometry

Low resolution and high-resolution (HR) mass spectral analysis (EI and CI) were recorded using a VG AUTOSPEC mass spectrometer or a Micromass GCT (Time-of-Flight), high performance, orthogonal acceleration spectrometer coupled to an Agilent Technologies 6890N GC system. Electrospray mass spectrometry (ESMS) was recorded on a high performance orthogonal acceleration reflecting TOF mass spectrometer, coupled to a Waters 2975 HPLC. Only major peaks are reported and intensities are quoted as percentages of the base peak.

3.2.4 GC/MS

GC/MS analyses were run on a Finnigan Incos 50 quadrupole instrument coupled to a Hewlett Packard HP 5890 chromatograph fitted with a 25 m HP 17 capillary column (50 % phenyl methyl silicone).

3.2.5 Elemental Analysis

Microanalysis was carried out for C, H and N using an EA 1110 CHNS CE instruments elemental analyser.

3.2.6 Melting Points

Routine melting points were carried out on a Gallenkamp melting point apparatus. All melting points are uncorrected. Values are quoted to the nearest 0.5 °C.

3.2.7 Polarimetry

Specific Optical Rotation measurements were performed using an Optical Activity AA-1000 automatic polarimeter (Optical Activity Ltd. Polarimeter millidegree-autoranging), operating at 589 nm using a 2 mL solution cell with a 20 cm path length. The concentration (*c*) is expressed in g/100 mL (equivalent to g/0.1 dm³). Specific rotations are denoted $[\alpha]_D^T$ and are given in units of 10⁻¹ deg cm² g⁻¹ (T= ambient temperature in °C).

3.2.8 Chromatography

TLC was carried out using either Polygram silica plates (0.2mm with 254nm fluorescent dye) or Fluka alumina plates (0.2mm with 254nm fluorescent dye). The components were observed under ultraviolet light (254 nm/365 nm) and stained with ninhydrin (1-2 % in EtOH) or KMnO₄ aqueous solution. Column chromatography was performed using silica gel (40-63 μm, Fluorochem).

3.2.9 Reagents and Solvents

Ether and THF were freshly distilled from sodium benzophenone ketyl. Dry hexane was obtained by distillation from sodium. Where dry DCM was used, it was distilled over CaH₂. DMSO was dried, distilled from CaH₂ and stored over 4 Å molecular sieve. Liquid Ammonia was distilled direct from a cylinder. All amines were distilled from potassium hydroxide under a nitrogen atmosphere prior to use. Other organic compounds were used as received, without further drying. Organic solutions were dried by standing over anhydrous magnesium sulfate or sodium sulfate. Solvents were evaporated under reduced pressure on a rotary evaporator. Nitrogen gas was dried (NaOH, CaCl₂, 4 Å molecular sieve) prior to use. Glassware was oven dried for at least 2 h for all oxygen/water free reactions.

3.2.10 UV Photolysis

Ultra Violet irradiation was carried out in quartz apparatus using a 400 W medium pressure Hg lamp.

3.2.11 X-Ray Crystallography

X-Ray Crystallography data were recorded on: a) Bruker SMART diffractometer with graphite-monochromated Mo-K α radiation ($\lambda = 0.71073 \text{ \AA}$), sealed tube and CCD detector, b) Mer-Rigaku, mercury detector 007 with Mo-K α radiation ($\lambda = 0.71073 \text{ \AA}$) generator (rotating anode), c) Cop-Saturn 92 detector 007, Cu-K α radiation with rotating anode.

3.2.12 EPR Spectroscopy

EPR spectra were obtained with a Bruker EMX 10/12 spectrometer operating at 9.5 GHz with 100 KHz modulation. Irradiation of samples was carried out in the resonant cavity by unfiltered light from a 500 W super pressure Hg arc. Samples were contained in 4mm od quartz tubes. In all cases where spectra were obtained, hfs were assigned with the aid of computer simulations using the Bruker Simfonia software package or Winsim 2002 beta suite. For concentration measurements, signals were double integrated using the Bruker WinEPR software and radical concentrations were calculated by reference to a known concentration of DPPH,

3.2.13 Computational Methods

Quantum chemical calculations were carried out with the Gaussian 98W and 03W packages. Density functional theory with the UB3LYP functional was employed. The equilibrium geometries were fully optimised with respect to all geometric variables, no symmetry being assumed, with various basis sets as indicated in the text. Computed $\langle S^2 \rangle$ values for all types of radicals were 0.7500 after annihilation of higher multiplicity spin states. Isotropic EPR hfs were derived from computed Fermi contact integrals evaluated at the H-nuclei. The hfs were taken directly from the Gaussian output files.

The computations for the cycloalkyl radicals were carried by Dr G. DiLabio at the National Institute of Nanotechnology, NRCC, Edmonton, Canada.

3.3 2-Halophenylalkyl Iodides

3.3.1 2-Chlorophenethyl iodide

2-Chlorophenethyl alcohol **39a**¹

To a stirring solution of 2-chlorophenylacetic acid **40a** (5 g, 29.3 mmol) in freshly distilled dry THF (400 cm³) at 0 °C, was added LiAlH₄ (4.5 g, 118 mmol) in several portions carefully. The mixture was then allowed to warm to room temperature and heated under reflux for 3 h. After cooling to 0 °C, water (50 cm³) was added carefully dropwise with stirring. The resulting white suspension was allowed to reach room temperature and stirred for 15 min, after which the solids were removed by centrifugation. The liquid portion was taken up in ethyl acetate (400 cm³), the organic layer was washed with water (2x50 cm³) and brine (50 cm³), dried (Na₂SO₄) and concentrated in vacuo to give the known crude alcohol **39a** (4.22 g, 92 %) as a viscous clear liquid. The crude alcohol was deemed pure enough by ¹H-NMR spectroscopy to use in the next synthetic step; δ_{H} 2.19 (1H, br s, OH), 2.99 (2H, t, $J=6.8$, CH₂), 3.83 (2H, t, $J=6.8$, CH₂O) and 7.12-7.36 (4H, m, ArH).

2-Chlorophenethyl iodide **37a**²

At 0 °C 2-chlorophenethyl alcohol **39a** (2.0 g, 13.0 mmol) in dichloromethane (3 cm³) was added dropwise to a stirring solution of triphenylphosphine (4.4 g, 17.0 mmol) and imidazole (1.2 g, 18.0 mmol) in dichloromethane (45 cm³). After 10 min iodine (4.9 g, 20.0 mmol) was added and the resulting dark brown mixture allowed to stir for 1 h at 0 °C. A saturated solution of sodium thiosulphate (50 cm³) was added and the mixture allowed to warm to room temperature over 10 min with stirring. The organic layer was then washed with further portions of saturated sodium thiosulfate solution until the organic layer was pale yellow in colour. The aqueous layers were extracted with dichloromethane (2x30 cm³) and the combined organic layers were then dried (MgSO₄) and concentrated in vacuo. The crude product was purified by column chromatography (SiO₂, hexane) to give the known pure iodide **37a** (2.6 g, 75

%) as a pale yellow liquid, R_f (SiO₂, hexane) 0.35; δ_H 3.24-3.38 (4H, m, 2xCH₂) and 7.15-7.37 (4H, m, ArH).

3.3.2 2-Bromophenalkyl Iodides

3.3.2.1 2-Bromophenylalkanoic Acids

2-Bromophenylpropanoic acid **61**³

A mixture of 2-bromobenzaldehyde **59** (3.2 cm³, 27 mmol) and Meldrum's Acid **60** (3.9 g, 2.7 mmol) in TEAF (15 cm³) (made by slow addition of triethylamine (10 cm³, 72 mmol) to formic acid (6.8 cm³, 180 mmol) with cooling) was heated to 95-100 °C and stirred at this temperature for 4 h. Ice and water (30 cm³) was added to the cool reaction mixture then its pH was adjusted to 1 with 6M hydrochloric acid and it was left to crystallise at 5-10 °C for a day. After having been filtered, the crystals were washed with water and recrystallised from petroleum ether 40-60 to afford the known acid **61** (5.12 g, 82 %); δ_H 2.71 (2H, t, $J=7.8$, CH₂), 3.08 (2H, t, $J=7.8$, CH₂), 7.06-7.12 (1H, m, ArH), 7.21-7.29 (2H, m, ArH) and 7.35-7.57 (1H, m, ArH) (COOH signal not observed).

2-Bromophenylbutanoic acid **68**

A mixture of 2-[3-(2-bromophenyl)propyl]-4,4-dimethyl-2-oxazoline **33b** (3.76 g, 12.7 mmol) and hydrochloric acid (12 cm³) was heated under reflux for 45 minutes and the cooled mixture extracted with dichloromethane (3x20 cm³). The combined organic layers were dried (MgSO₄) and the solvent removed to yield the known crude acid **68** (3 g, 92 %) which was used without further purification; (Lit., NMR⁴) δ_H 1.97 (2H, dt, $J=7.7$ & 7.5, CH₂), 2.42 (2H, t, $J=7.5$, CH₂), 2.80 (2H, t, $J=7.7$, CH₂), 7.03-7.09 (1H, m, ArH), 7.17-7.29 (2H, m, ArH) and 7.52-7.57 (1H, m, ArH) (COOH signal not observed).

2-Bromophenylpentanoic acid **65**

2-[4-(2-Bromophenyl)butyl]-4,4-dimethyl-2-oxazoline **64** was hydrolysed as above to yield the crude known acid (1.08 g, 83 %) which was used without further purification; (Lit., data⁵) $\nu_{\max}(\text{Film})/\text{cm}^{-1}$ 1707 (C=O) and 3029 (OH); δ_{H} 1.61-1.78 (4H, m, 2x CH₂), 2.41 (2H, t, $J=7.1$, CH₂), 2.75 (2H, t, $J=7.4$, CH₂), 7.02-7.07 (1H, m, ArH), 7.17-7.26 (2H, m, ArH), 7.48-7.53 (1H, m, ArH) and 11.15 (1H, br s, COOH); δ_{C} 24.3 (CH₂), 29.2 (CH₂), 33.8 (CH₂), 35.7 (CH₂), 124.4 (C_q), 127.4 (Ar), 127.6 (Ar), 130.3 (Ar), 132.8 (Ar) 141.2 (C_q) and 179.9 (C=O); m/z (TOF MS-ES-) 255 [100 %, (M-H⁺)], [Found: (M-H⁺), 255.0018. C₁₁H₁₂O₂⁷⁹Br requires 255.0021].

3.3.2.2 2-Bromophenylalkanols

General Alcohol Preparation

To a stirring solution the 2-bromophenylalkanoic acid (1eq) in freshly distilled dry ether (5.4 cm³/mmol) at 0 °C was added carefully LiAlH₄ (1.05 eq) in several portions. The resulting grey suspension was allowed to warm to room temperature over 20 min, at which time the suspension was immediately cooled to 0 °C and water (0.13 cm³/mmol) was added dropwise carefully! The mixture was then allowed to warm to room temperature with stirring. 15 % HCl solution (1.6 cm³/mmol) was added and stirred until all solids had dissolved. The aqueous layer was extracted and washed with ether (3x1 cm³/mmol). The combined organic layers were washed with saturated sodium hydrogen carbonate solution (1 cm³/mmol), brine (1 cm³/mmol) and water (1 cm³/mmol). The organic layers were dried (MgSO₄) and concentrated in vacuo to give the crude alcohol, which was used without further purification.

2-Bromophenylethanol **39b**

Clear viscous liquid; Yield (84 %);(Lit., NMR⁶) δ_{H} 3.01 (2H, t, $J=6.8$, CH₂), 3.81 (1H, s, OH), 3.86 (2H, t, $J=6.8$, CH₂O), 7.05-7.32 (3H, m, ArH) and 7.54-7.56 (1H, m, HCCBr).

2-Bromophenylpropanol 62

Clear Viscous Liquid; Yield (91 %); (Lit., NMR⁶) δ_{H} 1.35-2.08 (3H, m, OH & CH₂), 2.83 (2H, t, $J=7.8$, CH₂), 3.70 (2H, t, $J=6.4$, CH₂O), 7.01-7.09 (1H, m, ArH), 7.20-7.27 (2H, m, ArH) and 7.53 (1H, d, $J=7.9$, HCCBr).

2-Bromophenylbutanol 69

Clear Viscous Liquid; Yield (91 %); (Lit., NMR⁴) δ_{H} 1.56-1.92 (5H, m, OH & 2xCH₂), 2.76 (2H, t, $J=7.3$, CH₂), 3.67 (2H, dt, $J=6.1$ & 0.9, CH₂O), 7.00-7.08 (1H, m, ArH), 7.17-7.27 (2H, m, ArH) and 7.51 (1H, d, $J=7.9$, HCCBr).

2-Bromophenylpentanol 66

Clear Viscous Liquid; Yield (91 %); δ_{H} 1.40-1.50 (2H, m, CH₂), 1.58-1.70 (2H, m, CH₂), 2.51 (1H, br s, OH), 2.74 (2H, t, $J=7.8$, CH₂), 3.65 (2H, t, $J=6.5$, CH₂), 7.01-7.06 (1H, m, ArH), 7.19-7.22 (2H, m, ArH) and 7.50-7.53 (1H, m, HCCBr); δ_{C} 25.4 (CH₂), 29.7 (CH₂), 32.5 (CH₂), 36.1 (CH₂), 62.8 (CH₂OH), 124.4 (CBr), 127.3 (CH_{Ar}), 127.4 (CH_{Ar}), 130.2 (CH_{Ar}), 132.7 (CH_{Ar}) and 141.7 (C_q).

3.3.2.3 2-Bromophenylalkyl Iodides**General Iodide Preparation**

At 0 °C 2-bromophenylalkyl alcohol (1eq) in dichloromethane (2 cm³/mmol) was added dropwise to a stirring solution of triphenylphosphine (1.3eq) and imidazole (1.4eq) in dichloromethane (4 cm³/mmol). After 20 min iodine (1.5eq) was added and the resulting dark brown mixture was allowed to stir for 3 h at 0 °C. A saturated solution of sodium thiosulfate (4 cm³/mmol) was added and the mixture allowed to warm to room temperature over 10 min with stirring. The organic layer was then washed with further portions of saturated sodium thiosulphate solution until the organic layer was pale yellow in colour. The aqueous layers were extracted with dichloromethane (3x2 cm³/mmol) and the combined organic layers were then dried (MgSO₄) and concentrated until a white solid began to precipitate. Enough

dichloromethane was added to redissolve the precipitate and hexane (4 cm³/mmol) was added. The white precipitate was filtered off and the filtrate concentrated in vacuo to give the crude iodide which was purified by column chromatography (SiO₂, hexane).

2-Bromophenethyl Iodide **37b**

Pale Yellow Liquid; Yield (88 %); R_f (SiO₂, hexane) 0.3; (Lit., NMR⁷) δ_H 3.25-3.39 (4H, m, 2xCH₂), 7.07-7.34 (3H, m, ArH) and 7.52-7.55 (1H, m, HCCBr).

2-Bromophenylpropyl Iodide **63**

Pale Yellow Liquid; Yield (87 %); R_f (SiO₂, hexane) 0.3; (Lit., NMR⁷) δ_H 2.09-2.18 (2H, m, CH₂), 2.82-2.87 (2H, m, CH₂), 3.20 (2H, t, *J*=6.8, CH₂), 7.04-7.09 (1H, m, ArH) 7.20-7.26 (2H, m, ArH) and 7.51-7.54 (1H, m, HCCBr).

2-Bromophenylbutyl Iodide **70**

Pale Yellow Liquid; Yield (82 %); R_f (SiO₂, hexane) 0.3; ν_{max}(Film)/cm⁻¹ 658, 749, 1024, 1438, 1470, 2859, 2933; δ_H 1.67-1.79 (2H, m, CH₂), 1.85-1.95 (2H, m, CH₂), 2.75 (2H, t, *J*=7.7, CH₂), 3.2 (2H, t, *J*=6.9, CH₂), 7.02-7.07 (1H, m, ArH), 7.17-7.25 (2H, m, ArH) and 7.50-7.53 (1H, m, HCCBr); δ_C 6.5 (CH₂), 30.7 (CH₂), 33.0 (CH₂), 35.0 (CH₂), 124.3 (CBr), 127.4 (CH_{Ar}), 127.6 (CH_{Ar}), 130.2 (CH_{Ar}), 132.7 (CH_{Ar}) and 141.0 (C_q); *m/z* (CI) 338 [100 %, (M+H)⁺] [Found: (MH)⁺, 337.9174. C₁₀H₁₂⁷⁹BrI requires 337.9167].

2-Bromophenylpentyl Iodide **67**

Pale Yellow Liquid; Yield (91 %); R_f (SiO₂, hexane) 0.3; (Lit., NMR⁸) δ_H 1.43-1.53 (2H, m, CH₂), 1.59-1.68 (2H, m, CH₂), 1.88 (2H, q, *J*=7.2, CH₂), 2.73 (2H, t, *J*=7.7, ArCH₂), 3.20 (2H, t, *J*=7.1, CH₂I), 7.06-7.07 (1H, m, ArH), 7.18-7.25 (2H, m, ArH) and 7.50-7.53 (2H, m, ArH); δ_C 6.9 (CH₂), 28.8 (CH₂), 30.2 (CH₂), 33.2 (CH₂), 35.9 (CH₂), 124.4 (CBr), 127.3 (CH_{Ar}), 127.5 (CH_{Ar}), 130.2 (CH_{Ar}), 132.7 (CH_{Ar}) and 141.5 (C_q)

3.4 Chiral Aminoalcohols

3.4.1 (S)-Valinol

(S)-Valine methyl ester hydrochloride (**S**)-218⁹

To a suspension of (S)-Valine (50 g, 0.43 mol) in dry methanol (400 cm³) at -10 °C under nitrogen was added freshly distilled thionyl chloride (39 cm³, 0.54 mol) portionwise over 20 min, ensuring the temperature was maintained below -5 °C. The heterogeneous mixture was warmed to room temperature and heated at reflux for 2 h. The reaction mixture was allowed to cool and the solvent removed to afford a white crystalline solid. Recrystalliation from methanol/ether gave the pure hydrochloride salt (**S**)-218 (63 g, 88 % Lit.,⁹ 79 %) as white crystals; mp 162.5-163.5 (methanol-ether) [Lit.,¹⁰ 155-160 (methanol-ether)]; [α]_D²⁵ 24.6 (*c* 2.15 in MeOH) [lit.,¹¹ 24.5 (*c* 2.00 in MeOH)]; δ_{H} 1.14 (3H, d, *J*=5.3, CH₃), 1.16 (3H, d, *J*=4.8, CH₃), 2.42-2.53 (1H, m, (CH₃)₂CH), 3.83 (3H, s, OCH₃), 3.95 (1H, br s, CHN) and 8.88 (3H, br s, NH₃⁺).

(S)-Valine methyl ester (**S**)-91

Ammonia gas was bubbled through a stirring suspension of (S)-valine methyl ester hydrochloride (**S**)-218 (20 g, 119 mmol) in dichloromethane (200 cm³). After bubbling for 30 min water (75 cm³) was added. The aqueous layer was extracted with dichloromethane (2x50 cm³) and the combined organic layers were dried (Na₂SO₄). Removal of the solvent afforded the crude ester (**S**)-91 (14.7 g, 94 %) which was used without further purification; [α]_D²⁵ 49.1 (*c* 1.00 in EtOH) [lit.,¹² 42.2 (*c* 1.00 in EtOH)]; δ_{H} 0.91 (3H, d, *J*=6.8, CH₃), 0.97 (3H, d, *J*=6.8, CH₃), 1.43 (2H, br s, NH₂), 1.96-2.07 (1H, m, (CH₃)₂CH), 3.30 (1H, d, *J*=5.3, CHN) and 3.72 (3H, s, OCH₃).

(S)-Valinol (**S**)-73

To a refluxing stirring suspension of lithium aluminium hydride (3.5 g, 90 mmol) in dry ether (200 cm³) under nitrogen was added (S)-valine methyl ester (**S**)-91

(10 g, 76 mmol) in dry ether (100 cm³), dropwise over 50 min. The mixture was then heated under reflux for 1 h, at which time the mixture was cooled to 0 °C and water (3.3 cm³) was added dropwise cautiously. The mixture was allowed to warm to room temperature and stirred for a further 30 min. The solids were filtered, and washed with ether and dichloromethane. The filtrates were dried (Na₂SO₄) and concentrated in vacuo to give the crude product. Purification by distillation afforded the pure alcohol (**S**)-**73** (5.1 g, 64 %) as white waxy solid; $[\alpha]_D^{25}$ 17.3 (*c* 0.36 in EtOH) [Lit.,¹³ 17.4 (*c* 10.00 in EtOH)]; δ_H 0.92 (3H, d, *J*=6.8, CH₃), 0.93 (3H, d, *J*=6.8, CH₃), 1.60 (1H, dq, *J*=6.8 & 6.3, (CH₃)₂CH), 2.41 (3H, br s, OH & NH₂), 2.57 (1H, ddd, *J*=8.7, 6.3 & 3.9, CHN), 3.32 (1H, dd, *J*=10.6 & 8.7, CH_AH_BO) and 3.64 (1H, dd, *J*=10.6 & 3.9, CH_AH_BO).

3.4.2 (S)-Phenylglycinol

(S)-Phenylglycine methyl ester (**S**)-**93**

Ammonia gas was bubbled through a stirring suspension of (*S*)-phenylglycine methyl ester hydrochloride (**S**)-**92** (10 g, 50 mmol) in dichloromethane (100 cm³). After bubbling for 30 min water (50 cm³) was added. The aqueous layer was extracted with dichloromethane (2x50 cm³) and the combined organic layers were dried (Na₂SO₄). Removal of the solvent afforded the crude ester (**S**)-**93** (8 g, 97 %) which was used without further purification; $[\alpha]_D^{25}$ -118.3 (*c* 2.12 in CHCl₃) [Lit.,¹⁴ -121 (*c* 1.00 in H₂O)]; δ_H 1.93 (2H, s, NH₂), 3.68 (3H, s, CH₃), 4.60 (1H, s, CHN) and 7.27-7.38 (5H, m, Ph).

(S)-Phenylglycinol (**S**)-**75**

To a refluxing stirring suspension of lithium aluminium hydride (2.3 g, 60 mmol) in dry ether (160 cm³) under nitrogen was added (*S*)-phenylglycine methyl ester (**S**)-**93** (8 g, 48 mmol) in dry ether (40 cm³), dropwise over 50 min. The mixture was then heated under reflux for 1 hour, at which time the mixture was cooled to 0 °C and water (2.2 cm³) was added dropwise cautiously! The mixture was allowed to warm to room temperature and stirred for a further 30 min. The solids were filtered,

and washed with ether and dichloromethane. The filtrates were dried (NaSO_4) and concentrated in vacuo to give the crude product. Purification by distillation afforded the known pure alcohol (**S**)-**75** (2 g, 28 %) as off white crystals; mp 72.0-74.0 [Lit.,¹⁵ 76.0-79.0]; $[\alpha]_D^{25}$ -21.5 (c 1.77 in MeOH) [lit.,¹⁶ -26.1 (c 5.36 in MeOH)]; δ_H 2.30 (3H, br s, NH_2 & OH), 3.55 (1H, dd, $J=11.1$ and 8.2, $\text{CH}_A\text{H}_B\text{O}$), 3.73 (1H, dd, $J=11.1$ and 4.3, CH_AH_B), 4.04 (1H, dd, $J=8.2$ and 4.3, CHN) and 7.24-7.37 (5H, m, Ph).

3.4.3 (S)-Serine Methyl Ester Hydrogen Chloride (S)-78

Acetyl chloride (28 g, 25 cm³, 0.36 mol) was added dropwise to methanol (150 cm³) at 0 °C. The mixture was stirred for 15 min and L-serine (12.5 g, 119 mol) was then added portionwise to the solution. The resulting mixture was heated under reflux for 3 h. Concentration under reduced pressure provide the crude product, which was recrystallised from dichloromethane-ether to yield the pure chloride (**S**)-**78** (42.9 g, 77 % Lit.,¹⁷ 98 %); mp 162.0-162.8 dec. [Lit.,¹⁸ 161-162]; $[\alpha]_D^{25}$ 5.66 (c 1.14 in MeOH) [lit.,¹⁹ 5.5 (c 2.00 in MeOH)]; δ_H (D_2O) 3.90 (3H, s, CH_3), 4.04 (1H, dd, $J=12.5$ & 3.4, $\text{CH}_A\text{H}_B\text{O}$), 4.14 (1H, dd, $J=12.5$ & 4.3, $\text{CH}_A\text{CH}_B\text{O}$) and 4.32 (1H, t, $J=3.8$, CHN).

3.4.4 (S,S)-2-Amino-3-methoxy-1-phenylpropan-1-ol (S,S)-79

2-Methyl-4-hydroxymethyl-5-phenyl-2-oxazoline (**S,S**)-**219** (2 g, 10.5 mmol) in dry THF (20 cm³) was added dropwise at room temperature to a stirring heterogeneous solution of sodium hydride (60 % in mineral oil) (0.5 g, 12.6 mmol) in THF (10 cm³) at a rate to maintain a mild evolution of hydrogen. When addition was complete, the mixture was heated at 50-60 °C for 1.5 h and cooled to ambient temperature. A solution of methyl p-toluenesulfonate (2.55 g, 13.7 mmol) in dry THF (2 cm³) was added dropwise. The reaction was stirred for 3 h and slowly poured into ice-water (30 cm³), then extracted with ether (2x20 cm³). The combined extracts were dried (NaSO_4) and concentrated to give an oil, which was distilled in vacuo to give the 4-methoxymethyl-2-methyl-5-phenyl-2-oxazoline intermediate as a clear liquid. The 4-methoxymethyl-2-methyl-5-phenyl-2-oxazoline was then added to 3M hydrochloric acid (75 cm³) and the mixture was heated under reflux for 3h. After

cooling the aqueous mixture was washed with ether (10 cm³). The aqueous layer made alkaline to pH 10 with 3M sodium hydroxide solution and extracted with ether (3x 50 cm³). The ether portions were dried (MgSO₄) and concentrated to give an oil that crystallised on standing to give the known (*S,S*)-aminoalcohol (*S,S*)-79 (1 g, 54 %) which was used immediately; δ_{H} (Intermediate) 2.10 (3H, d, $J=1.3$, CH₃), 3.41 (3H, s, CH₃O), 3.52 (1H, dd, $J=9.7$ & 6.2, CH₃OCH_AH_B), 3.60 (1H, dd, $J=9.7$ & 4.4, CH₃OCH_AH_B), 4.07-4.13 (1H, m, CHN), 5.28 (1H, d, $J=7.0$, PhCH) and 7.27-7.39 (5H, m, Ph); δ_{H} (Final Product) 2.03 (3H, br s, OH & NH₂), 3.01-3.10 (1H, m, CHN), 3.34 (1H, dd, $J=9.4$ & 6.4, CH_AH_B), 3.35 (3H, s, CH₃), 3.42 (1H, dd, $J=9.4$ & 4.0, CH_AH_B), 4.60 (1H, d, PhCH) and 7.24-7.36 (5H, m, Ph).

3.5 Acetimidate Esters

Acetimidic acid ethyl ester hydrochloride **71**

Dry hydrogen chloride gas was bubbled through a solution of acetonitrile **42** (21 cm³, 393 mmol) in dry ethanol (30 cm³) at 0 °C. After the reaction flask had gained 14 g in weight, the cloudy mixture was left to stand at room temperature overnight. The mixture was then concentrated in vacuo to yield acetimidic acid ethyl ester hydrochloride **71** (37.3 g, 76 %) as a white crystalline solid; mp 112-114 [Lit.,²⁰ 112-114]; δ_{H} 1.49 (3H, t, $J=7.1$, CH₃CH₂), 2.48 (3H, s, CH₃), 4.64 (2H, q, $J=7.1$, CH₃CH₂), 11.48 (1H, br s, NH_AH_B) and 12.40 (1H, br s, NH_AH_B).

2-Phenylacetimidic acid ethyl ester hydrochloride **72**

Dry hydrogen chloride gas was bubbled through a solution of benzyl cyanide **43** (23 cm³, 193 mmol) in dry ethanol (15 cm³) at 0 °C. After the reaction flask had gained 7 g in weight the cloudy mixture was left to stand at room temperature overnight. The mixture was then concentrated in vacuo to yield 2-phenyl-acetimidic acid ethyl ester hydrochloride **72** (36.6 g, 95 %) as a white waxy solid; mp 78-79 [Lit.,²¹ 78-79]; δ_{H} 1.44 (3H, t, $J=6.9$, CH₃), 4.05 (2H, s, PhCH₂), 4.61 (2H, q, $J=6.9$, CH₂), 7.30-7.39 (3H, m, Ph), 7.43-7.46 (2H, m, Ph), 11.64 (1H, br s, NH_AH_B⁺) and 12.69 (1H, br s, NH_AH_B⁺).

3.6 2-Oxazolines

3.6.1 Non Chiral Oxazolines

2-Benzyl-4,4-dimethyl-2-oxazoline **27**

Phenylacetic acid **32** (20 g, 0.15 mol) and 2-amino-2-methylpropanol **31** (13.40 g, 0.15 mol) were dissolved in xylene (100 cm³). The reaction mixture was then heated under reflux using a Dean-Stark trap. After a calculated amount of water (5.4 cm³, 0.30 mol) was collected, the mixture was allowed to cool to room temperature. The mixture was washed with 10 % sodium bicarbonate solution (2x45 cm³), and the aqueous layers were extracted with xylene (2x25 cm³). The combined organic layers were dried (NaSO₄) and the product was vacuum distilled to give the known substituted oxazoline **27** (18.62 g, 66 %) as a clear oil. δ_{H} 1.26 (6H, s, 2x CH₃), 3.58 (2H, s, CH₂), 3.88 (2H, s, CH₂), 7.19-7.33 (5H, m, Ph).

3.6.2 Chiral Oxazolines

Method A

A solution of 1,2-aminoalcohol (1 eq) in dichloromethane (1.5 cm³/mmol) was added to a stirred solution of acetimidic acid ethyl ester hydrochloride (1.1 eq) in dichloromethane (3.6 cm³/mmol) at 0 °C. After stirring for 40 h the reaction mixture was washed with water (2x1.5 cm³/mmol). The aqueous layer was extracted with dichloromethane (3x1.5 cm³/mmol) and the combined organic layers dried (MgSO₄) and concentrated in vacuo. Purification was achieved by Kugelrohr distillation initially at room temperature to remove any EtOAc and then at a higher temperature to give the pure oxazoline.

Method B

Triethylamine (1.6 eq) was added dropwise to a stirred mixture of 1,2-aminoalcohol (1 eq), acetimidic acid ethyl ester hydrochloride (1.5 eq) and dichloromethane (5 cm³/mmol) at 0 °C. After stirring at room temperature overnight, the reaction mixture was poured into ice-water and the aqueous layer was extracted

with dichloromethane (3x5 cm³/mmol). The organic layer was dried (MgSO₄) and concentrated in vacuo to give an opaque viscous oil. Purification was achieved by column chromatography (SiO₂, hexanes:EtOAc) to give the pure oxazoline.

(S)-4-Isopropyl-2-methyl-2-oxazoline (S)-81

Method A: Clear oil; Yield (60 %); $[\alpha]_D^{25}$ -81.3 (*c* 3.44 in CHCl₃) [lit.,²² -86.2 (*c* 1.10 in CHCl₃)]; δ_H 0.88 (3H, d, *J*=6.6, (CH₃)₂CH), 0.97 (3H, d, *J*=6.6, (CH₃)₂CH), 1.72 (1H, oct, *J*=6.6, (CH₃)₂CH), 1.98 (3H, d, *J*=1.3, CH₃), 3.78-3.96 (2H, m, CHN & CH_AH_B) and 4.20-4.27 (1H, m, CH_AH_B).

(S)-2-Benzyl-4-iso-propyl-2-oxazoline (S)-82

Method B: Clear Oil; Yield (59 %); R_f (SiO₂, 9:1 hexane:EtOAc) 0.1; $[\alpha]_D^{25}$ -67.7 (*c* 2.16 in CHCl₃); δ_H 0.86 (3H, d, *J*=6.8, CH₃), 0.95 (3H, d, *J*=6.8, CH₃), 1.74 (1H, oct, *J*=6.8, (CH₃)₂CH), 3.62 (2H, s, PhCH₂), 3.83-3.94 (2H, m, CHN & CH_ACH_BO), 4.10-4.23 (1H, m, CH_ACH_BO) and 7.17-7.30 (5H, m, Ph).

(R)-2-Benzyl-4-iso-propyl-2-oxazoline (R)-82

Method B: Clear Oil; Yield (33 %); $[\alpha]_D^{25}$ 66.4 (*c* 1.56 in CHCl₃)

(S)-2-Benzyl-4-tert-butyl-2-oxazoline (S)-83

Method B: Clear Oil: Yield (33 %); R_f (SiO₂, 9:1 hexane:EtOAc) 0.25; $[\alpha]_D^{25}$ -69.2 (*c* 0.43 in CHCl₃); ν_{\max} (Film)/cm⁻¹ 1670 (C=N); δ_H 0.88 (9H, s, ^tBu), 3.63 (2H, d, *J*=2.6, PhCH₂), 3.85 (1H, dd, *J*=8.4 & 9.5, CHN), 4.01 (1H, t, *J*=8.2, CH_AH_BO), 4.08-4.17 (1H, m, CH_AH_BO) and 7.20-7.31 (5H, m, Ph); δ_C 25.7 (3x CH₃), 33.5 (C(CH₃)₃), 34.8 (PhCH₂), 68.7 (CH₂O), 75.6 (CHN), 126.8 (CH_{Ar}), 128.4 (CH_{Ar}), 128.8 (CH_{Ar}), 135.3 (C_q) and 165.5 (C=N); *m/z* (ES⁺) 218 [100 %, (M+H⁺)], [Found: (MH)⁺, 218.1540. C₁₄H₂₀NO requires 218.1545].

(R)-2-Benzyl-4-tert-butyl-2-oxazoline (R)-83

Method B: Clear Oil; Yield (34 %); $[\alpha]_D^{25}$ 68.5 (*c* 1.2 in CHCl₃).

(S)-2-Benzyl-4-phenyl-2-oxazoline (S)-84

Method B: Clear oil; Yield (75 %); R_f (SiO₂, 9:1 hexane:EtOAc) 0.25; $[\alpha]_D^{25}$ 70.4 (*c* 1.39 in CHCl₃) [lit.,²³ 95.4 (*c* 9.60 in CHCl₃)]; δ_H 3.64 (2H, s, PhCH₂), 4.08 (1H, m, CH_AH_B), 4.60 (1H, m, CH_AH_B), 5.19 (1H, t, *J*=9.2, CHN) and 7.20-7.39 (10H, m, 2xPh).

(S)-2,4-Dibenzyl-2-oxazoline (S)-85

Method B: Oil; Yield (55 %); R_f (SiO₂, 9:1 hexane:EtOAc) 0.20; $[\alpha]_D^{25}$ -41.9 (*c* 0.34 in EtOH) [Lit.,²⁴ -43.7 (*c* 1.08 in EtOH); δ_H 2.66 (1H, dd, *J*=13.8 & 8.4, PhCH_AH_BCHN), 3.09 (1H, dd, *J*=13.8 & 8.4, PhCH_AH_BCHN), 3.60 (2H, s, PhCH₂), 3.94 (1H, dd, *J*=8.4 & 7.3, CH_CH_DO), 4.16 (1H, dd, *J*=9.3 & 8.4, CH_CH_DO), 4.34-4.44 (1H, m, CHN), and 7.15-7.34 (5H, m, Ph).

(S)-2-Benzyl-4-cyclohexylmethyl-2-oxazoline (S)-86

Method B: Oil; Yield (56 %); R_f (SiO₂, 9:1 hexane:EtOAc) 0.23; $[\alpha]_D^{25}$ 67.1 (*c* 1.19 in MeOH); ν_{\max} (Film)/cm⁻¹ 1644 (C=N); δ_H 0.85-0.99 (2H, m, C₆H₁₁), 1.07-1.34 (4H, m, C₆H₁₁CH_AH_B & C₆H₁₁), 1.36-1.50 (1H, m, C₆H₁₁), 1.55-1.78 (6H, m, C₆H₁₁CH_AH_B & C₆H₁₁), 3.61 (2H, s, PhCH₂), 3.78 (1H, t, *J*=7.8, CH_CH_DO), 4.10-4.20 (1H, m, CHN), 3.78 (1H, dd, *J*=9.4 & 7.9, CH_CH_DO) and 7.21-7.35 (5H, m, Ph); δ_C 26.60 (CH₂), 26.62 (CH₂), 26.9 (CH₂), 33.9 (CH₂), 34.0 (CH₂), 35.2 (CH), 35.3 (CH₂), 44.7 (PhCH₂), 64.4 (CHN), 73.7 (CH₂O), 127.3 (CH_{Ar}), 129.0 (CH_{Ar}), 129.3 (CH_{Ar}), 135.7 (C_q) and 165.9 (C=N); *m/z* (TOF MS-CI+) 258 [100 %, (M+H⁺)], [Found: (MH)⁺, 258.1866. C₁₇H₂₄NO requires 258.1858].

(S)-2-Benzyl-2-oxazoline-4-carboxylic acid methyl ester (S)-87

Method B: Oil; Yield (30 %); R_f (SiO₂, 9:1 hexane:EtOAc) 0.2; $[\alpha]_D^{25}$ 65.9 (*c* 0.33 in CHCl₃) [lit.,²⁵ -14.75 (*c* 1.50 in CHCl₃)]; δ_H 3.62 (1H, d, $J=15.0$, PhCH_AH_B), 3.69 (1H, d, $J=15.0$, PhCH_AH_B), 3.76 (3H, s, OMe), 4.35 (1H, dd, $J=10.6$ & 8.7), 4.46 (1H, dd, $J=8.7$ & 7.8), 4.72 (1H, dd, $J=7.8$ & 10.6) and 7.20-7.30 (5H, m, Ph).

(S,S)-4-Hydroxymethyl-2-methyl-5-phenyl-2-oxazoline (S,S)-219

Method A: Recrystallisation from ether at -78 °C, instead of distillation; Pale yellow crystals; Yield (51 %); mp 62-63 [Lit.,²⁶ 63-64]; $[\alpha]_D^{25}$ -146.21 (*c* 2.27 in CHCl₃) [lit.,²⁶ -150.0 (*c* 1.00 in CHCl₃)]; δ_H 2.11 (3H, d, $J=1.5$, CH₃), 3.66 (1H, dd, $J=11.6$ & 4.1, CH_AH_B), 3.93 (1H, dd, $J=11.6$ & 3.6, CH_AH_B), 4.01-4.07 (1H, m, CHN), 5.34 (1H, d, $J=7.7$, PhCH) and 7.26-7.41 (5H, m, Ph).

(S,S)-2-Benzyl-4-methoxymethyl-5-phenyl-2-oxazoline (S,S)-88

Method B: Soft Yellow Wax; Yield (85 %); R_f (SiO₂, 9:1 hexane:EtOAc) 0.1; $[\alpha]_D^{25}$ -38.0 (*c* 0.16 in EtOH) [Lit.,²⁷ -38.2 (*c* 9.3 in EtOH)]; δ_H 3.40 (3H, s, CH₃), 3.50 (1H, dd, $J=9.7$ & 6.3, CH_AH_B), 3.63 (1H, dd, $J=9.7$ & 4.5, CH_AH_B), 3.93 (2H, d, $J=2.2$, PhCH₂), 4.08-4.14 (1H, m, CHN), 5.29 (1H, d, $J=6.8$, PhCH) 7.12-7.16 (2H, m, Ph) and 7.24-7.39 (8H, m, Ph).

(S)-1-(2-Benzyl-2-oxazolinyldiphenylmethanol (S)-89

Method B: Only unreacted starting materials observed, therefore alternative route from (S)-2-Benzyl-2-oxazoline-4-carboxylic acid methyl ester used.

A solution of (S)-2-benzyl-2-oxazoline-4-carboxylic acid methyl ester (S)-87 (2 g, 9.1 mmol) in THF (30 cm³) added to a freshly prepared solution of phenylmagnesium bromide (5 g, 27.4 mmol) in THF (10 cm³) (prepared by slow addition of neat bromobenzene (2.9 cm³) to Mg(0) (0.67 g, 27.4 mmol) in THF (10 cm³)). The resulting mixture was stirred at room temperature overnight, after which

the mixture was quenched by pouring into saturated ammonium chloride. Ether (50 cm³) was added and the aqueous layer extracted with ether (2x30 cm³) and the combined organic layers were washed with sat. NaHCO_{3(aq)}, NaCl_(aq) and water. Drying (MgSO₄) and concentration gave the crude product. Purification was achieved via column chromatography (SiO₂, 4:1, hexanes:EtOAc) to give waxy solid (**S**)-**89**; (1.55 g, 50 %); R_f (SiO₂, 4:1 hexane:EtOAc) 0.25; [α]_D²⁵ -33.8 (*c* 0.5 in CHCl₃); ν_{max}(Film)/cm⁻¹ 1660 (C=N) & 3400 (OH); δ_H 2.52 (1H, br s, OH), 3.64 (2H, s, PhCH₂), 4.01-4.11 (2H, m, CH₂O), 5.30-5.36 (1H, m, CHN), 7.14-7.36 (11H, m, Ph), 7.38-7.41 (2H, m, Ph) and 7.56-7.61 (2H, m, Ph); δ_C 35.0 (PhCH₂), 69.3 (CH₂O), 72.6 (CHN), 78.0 (Ph₂C), 125.6 (CH_{Ar}), 126.6 (CH_{Ar}), 126.8 (CH_{Ar}), 127.0 (CH_{Ar}), 127.1 (CH_{Ar}), 128.26 (CH_{Ar}), 128.3 (CH_{Ar}), 128.6 (CH_{Ar}) 135.0 (C_q), 144.0 (C_q), 145.7 (C_q) and 169.5 (C=N); *m/z* (TOF MS-ES+) 344 [100 %, (M+H⁺)], [Found: (MH)⁺, 344.1650. C₂₃H₂₂NO₂ requires 344.1651].

3.7 2-(Arylalkyl)-2-Oxazolines

Preparation of 2-(Arylalkyl) 2-oxazolines

2.5M n-BuLi in hexanes (1.05 eq) was added dropwise to a stirring solution of the 2-oxazoline (1 eq) in dry THF (0.75 cm³/mmol) and dry hexane (0.38 cm³/mmol) under nitrogen at -78 °C. After stirring for 5 min *o*-halophenethyl halide (1.05 eq) in dry THF (0.38 cm³/mmol) and dry hexane (0.2 cm³/mmol) was added over a 10 minute period. The solution was then allowed to warm to room temperature slowly over 3 h, then water (3x2 cm³/mmol) was added. The aqueous layer was extracted with ether (3x3.2 cm³/mmol), the combined organic layers were washed with water (3.2 cm³/mmol), dried (MgSO₄) and concentrated in vacuo to give the crude substituted 2-oxazoline. Purification was achieved by column chromatography using SiO₂ or Al₂O₃ and ethyl acetate/hexanes mixtures as elutant.

2-[3-(2-Chlorophenyl)propyl]-4,4-dimethyl-2-oxazoline **33a**

Clear oil; Yield (54 %); R_f (Al₂O₃, 9:1, hexane:EtAc) 0.3; ν_{max}(Film)/cm⁻¹ 1648 (C=N); δ_H 1.27 (6H, s, 2xCH₃), 1.91-2.01 (2H, m, CH₂(CH₂)₂), 2.31 (2H, t, *J*=7.5, CH₂), 2.79 (2H, t, *J*=7.7, ArCH₂), 3.91 (2H, s, CH₂O), 7.10-7.24 (3H, m, ArH) and 7.31-7.34 (1H, m, HCCCl); δ_C 26.1 (CH₂), 27.6 (CH₂), 28.4 (2xCH₃), 32.8 (CH₂), 66.9 ((CH₃)₂CH), 78.9 (CH₂O), 126.7 (CH_{Ar}), 127.4 (CH_{Ar}), 129.4 (CH_{Ar}), 130.5 (CH_{Ar}), 133.9 (CCl), 139.1 (C_q) and 165.6 (C=N); *m/z* (CI) 252 [100 %, (M+H)⁺] [Found: (MH)⁺, 252.1147. C₁₄H₁₉ON³⁵Cl requires 252.1155].

2-[3-(2-Bromophenyl)-propyl]-4,4-dimethyl-2-oxazoline **33b**

Clear oil; Yield (80 %); R_f (Al₂O₃, 9:1, hexanes:EtAc) 0.25; ν_{max}(Film)/cm⁻¹ 1668 (C=N); δ_H 1.27 (6H, s, 2xCH₃), 1.88-2.00 (2H, m, CH₂CH₂CH₂), 2.32 (2H, t, *J*=7.7, CH₂), 2.79 (2H, t, *J*=7.8, ArCH₂), 3.91 (2H, s, CH₂O), 7.01-7.07 (1H, m, ArH), 7.21-7.28 (2H, m, ArH) and 7.50-7.53 (1H, m, HCCBr); δ_C 26.2 (CH₂), 27.6 (CH₂), 28.4 (2xCH₃), 35.3 (CH₂), 66.9 ((CH₃)₂CH), 78.9 (CH₂O), 124.4 (CBr), 127.3 (CH_{Ar}),

127.6 (CH_{Ar}), 130.4 (CH_{Ar}), 132.7 (CH_{Ar}), 140.8 (C_q) and 165.5 (C=N); *m/z* (CI) 296 [100 %, (M+H)⁺].

2-[3-(2-Chlorophenyl)-1-phenylpropyl]-4,4-dimethyl-2-oxazoline **34a**

Clear Oil; Yield (48 %); R_f (Al₂O₃, 19:1, hexane:EtAc) 0.2; *v*_{max}(Film)/cm⁻¹ 1635 (C=N); *δ*_H 1.27 (3H, s, CH₃), 1.28 (3H, s, CH₃), 2.07-2.19 (1H, m, CHCH_AH_BCH₂), 2.32-2.44 (1H, m, CHCH_AH_BCH₂), 2.63-2.80 (2H, m, ArCH₂), 3.60 (1H, t, *J*=7.8, CH), 3.87 (2H, s, CH₂O), 7.07-7.20 (3H, m, ArH) and 7.22-7.37 (6H, m, ArH); *δ*_C 28.1 (CH₃), 28.3 (CH₃), 31.4 (CH₂), 33.5 (CH₂), 44.9 (CH), 66.8 ((CH₃)₂CH), 78.9 (CH₂O), 126.6 (CH_{Ar}), 127.0 (CH_{Ar}), 127.3 (CH_{Ar}), 127.7 (CH_{Ar}), 128.5 (CH_{Ar}), 129.3 (CH_{Ar}), 130.4 (CH_{Ar}), 133.8 (CCl), 139.0 (C_q), 139.6 (C_q) and 166.5 (C=N); *m/z* 328 (CI) [100 %, (M+H)⁺] [Found: (MH)⁺, 328.1478. C₂₀H₂₃ON³⁵Cl requires 328.1468].

2-[3-(2-Bromophenyl)-1-phenylpropyl]-4,4-dimethyl-2-oxazoline **34b**

White Solid; Yield (66 %); R_f (SiO₂, 9:1 hexanes:EtOAc) 0.25; mp 69.5-71.5 (EtOAc:hexanes); (Found C, 64.7; H, 5.75; N, 3.6. C₂₀H₂₂ONBr requires C, 64.5; H, 6.0; N, 3.8 %); *v*_{max}(Nujol)/cm⁻¹ 1668 (C=N); *δ*_H 1.28 (3H, s, CH₃), 1.30 (3H, s, CH₃), 2.05-2.19 (1H, m, CHCH_ACH_BCH₂), 2.31-2.43 (1H, m, CHCH_ACH_BCH₂), 2.60-2.81 (2H, m, ArCH₂), 3.61 (1H, t, *J*=7.8, CH), 3.90 (2H, s, CH₂O), 7.00-7.06 (1H, m, ArH), 7.16-7.38 (7H, m, ArH) and 7.48-7.51 (1H, m, HCCBr); *δ*_C 28.1 (CH₃), 28.3 (CH₃), 33.6 (CH₂), 34.0 (CH₂), 44.9 (CH), 67.0 ((CH₃)₂CH), 79.0 (CH₂O), 124.3 (CBr), 127.1 (CH_{Ar}), 127.3 (CH_{Ar}), 127.6 (CH_{Ar}), 127.8 (CH_{Ar}), 128.5 (CH_{Ar}H), 130.4 (CH_{Ar}), 132.7 (CH_{Ar}), 139.7 (C_q), 140.8 (C_q) and 166.6 (C=N); *m/z* (CI) 372 [95 %, (M+H)⁺] [Found: (MH)⁺ 372.0945. C₂₀H₂₃ON⁷⁹Br requires 372.0963].

(4*S*)-2-[3-(2-Bromophenyl)propyl]-4-isopropyl-2-oxazoline (*S*)-**102**

Yield (50 %); R_f (SiO₂, 4:1 hexanes:EtOAc) 0.25; *v*_{max}/cm⁻¹ (Film) 1670 (C=N); *δ*_H 0.88 (3H, d, *J*=6.9, CH₃), 0.96 (3H, d, *J*=6.7, CH₃), 1.74 (1H, dq, *J*=6.9, 6.9 & 6.7, (CH₃)₂CH), 1.75 (2H, qu, *J*=7.8, CH₂), 2.35 (2H, t, *J*=6.8, CH₂C=N), 2.80 (2H, t, *J*=6.8, ArCH₂), 3.84-3.95 (2H, m, CHN & CH_AH_BO), 4.14-4.23 (1H, m, CH_AH_BO),

7.00-7.10 (1H, m, ArH), 7.16-7.30 (2H, m, ArH) and 7.50-7.54 (1H, m, HCCBr); δ_C 18.1 (CH₃), 18.8 (CH₃), 26.3 (CH₂), 27.6 (CH₂C=N), 32.5 ((CH₃)₂CH), 35.4 (ArCH₂), 69.8 (CH₂O), 72.0 (CHN), 124.4 (CBr), 127.3 (CH_{Ar}), 127.6 (CH_{Ar}), 130.4 (CH_{Ar}), 132.7 (CH_{Ar}), 140.8 (C_q) and 166.6 (C=N); m/z (CI) 310 [100 %, (M+H)⁺] Found: (MH)⁺, 310.0807. C₁₅H₂₁NO⁷⁹Br requires 310.0807].

(4S)-2-[3-(2-Bromophenyl)-1-phenyl-propyl]-4-isopropyl-2-oxazoline (S)-103

2:1 Mixture of Diastereoisomers

White solid; Yield (71 %); R_f (SiO₂, 2:1 hexanes:EtOAc) 0.38; $\nu_{\max}/\text{cm}^{-1}$ 1664 (C=N); δ_H (500MHz, CDCl₃) 0.85 (3H, d, $J=6.8$, CH₃, major isomer), 0.87 (3H, d, $J=6.8$, CH₃, minor isomer), 0.93 (3H, d, $J=6.8$, CH₃, major isomer), 0.96 (3H, d, $J=6.8$, CH₃, minor isomer), 1.71-1.82 (1H, m, CH(CH₃)₂), 2.10-2.20 (1H, m, CH_AH_B), 2.33-2.43 (1H, m, CH_AH_B), 2.64-2.82 (2H, m, ArCH₂), 3.66 (1H, t, $J=7.8$, PhCH, major isomer), 3.69 (1H, t, $J=8.1$, PhCH, minor isomer), 3.88-3.95 (2H, m, CH_CH_DO, CHN), 4.01-4.21 (1H, m, CH_CH_D), 6.99-7.06 (1H, m, Ar), 7.15-7.27 (3H, m, Ar), 7.30-7.38 (4H, m, ArH) and 7.48-7.50 (1H, m, ArH); δ_C 17.9 (CH₃, major isomer), 18.0 (CH₃, minor isomer), 18.7 (CH₃, major isomer), 18.8 (CH₃, minor isomer), 32.4 ((CH₃)₂CH, minor isomer), 32.5 ((CH₃)₂CH, major isomer), 33.5 (CH₂, minor isomer), 33.7 (CH₂, major isomer), 34.1 (ArCH₂, minor isomer), 34.2 (ArCH₂, major isomer), 45.1 (PhCH, major isomer), 45.2 (PhCH, minor isomer), 69.8 (CH₂O), 71.7 (CHN), 124.3 (CBr), 127.0 (CH_{Ar}, major isomer), 127.1 (CH_{Ar}, minor isomer), 127.3 (CH_{Ar}), 127.6 (CH_{Ar}), 127.8 (CH_{Ar}, major isomer), 128.0 (CH_{Ar}, minor isomer), 128.5 (CH_{Ar}), 130.3 (CH_{Ar}), 132.7 (CH_{Ar}), 139.6 (C_q, minor isomer), 139.9 (C_q, major isomer), 140.8 (C_q, minor isomer), 140.9 (C_q, major isomer) and 167.8 (C=N), m/z (ES⁺) 386 [100 %, (M+H)⁺], [Found: (MH)⁺, 386.1122. C₂₁H₂₅NO⁷⁹Br requires 386.1120].

(4R)-2-[3-(2-Bromophenyl)-1-phenyl-propyl]-4-isopropyl-2-oxazoline (R)-103

Yield (68 %), See data for (S)-103

(4S)-2-[3-(2-Bromo-phenyl)-1-phenyl-propyl]-4-tert-butyl-2-oxazoline (S)-104

Mixture of diastereoisomers

White Solid; Yield (72 %); R_f (9:1 hexane:EtOAc) 0.2; (Found C, 65.8; H, 6.6; N, 3.3. $C_{22}H_{26}ONBr$ requires C, 66.0; H, 6.5; N, 3.5 %) ; ν_{max}/cm^{-1} 1669 (C=N); δ_H 0.86 (9H, s, $C(CH_3)_3$, minor isomer), 0.90 (9H, s, $C(CH_3)_3$, major isomer), 2.06-2.21 (1H, m, CH_AH_B), 2.29-2.46 (1H, m, CH_AH_B), 2.61-2.86 (2H, m, $ArCH_2$), 3.62-3.75 (1H, m, $PhCH$), 3.81-3.89 (1H, m, CHN), 3.99-4.10 (1H, m, $CH_C H_D O$), 4.10-4.18 (1H, m, $CH_C H_D O$), 7.00-7.08 (1H, m, ArH), 7.16-7.41 (7H, m, ArH) and 7.49-7.51 (1H, m, BrCCH); δ_C 25.8 (tBu , minor isomer), 26.0 (tBu , major isomer), 33.7 (CH_2 , major isomer), 33.7 (CH_2 , minor isomer), 34.2 (CH_2 , major isomer), 34.4 (CH_2 , minor isomer), 45.3 ($PhCH$, minor isomer), 45.4 ($PhCH$, major isomer), 68.6 (CH_2O , minor isomer), 68.6 (CH_2O , major isomer), 75.4 (CHN, minor isomer), 75.6 (CHN, major isomer), 124.4 (CBr), 127.0 (CH_{Ar}), 127.1 (CH_{Ar}), 127.4 (CH_{Ar}), 127.6 (CH_{Ar}), 127.9 (CH_{Ar}), 128.1 (CH_{Ar}), 128.5 (CH_{Ar}), 130.4 (CH_{Ar}), 132.8 (CH_{Ar}), 139.7 (C_q , major isomer), 140.0 (C_q , minor isomer), 141.0 (C_q , major isomer), 141.1 (C_q , minor isomer), 167.7 (C=N, minor isomer) and 167.8 (C=N, major isomer); m/z (ES+) 400 [100 %, (M+H⁺) [Found: (MH)⁺, 400.1279. $C_{22}H_{27}NO^{79}Br$ requires 400.1276].

(4R)-2-[3-(2-Bromo-phenyl)-1-phenyl-propyl]-4-tert-butyl-2-oxazoline (R)-104

Yield (80 %), See data for (S)-104

(4S)-2-[3-(2-Bromo-phenyl)-1-phenyl-propyl]-4-phenyl-2-oxazoline (S)-105

Mixture of Diastereoisomers

White Solid; Yield (40 %); R_f (9:1 hexanes:EtOAc) 0.1; ν_{max}/cm^{-1} 1656 (C=N); δ_H 2.16-2.30 (1H, m, CH_AH_B), 2.41-2.55 (1H, m, CH_AH_B), 2.68-2.89 (2H, m, $ArCH_2$), 3.73-3.79 (1H, m, $PhCH$), 4.03-4.11 (1H, m, $CH_C H_D O$), 4.53-4.63 (1H, m, $CH_C H_D O$), 4.53-4.63 (1H, m, CHN), 7.01-7.08 (1H, m, ArH), 7.18-7.45 (12H, m, ArH) and 7.49-7.52 (1H, m, BrCCH); m/z (CI) 420 [100 %, (M+H⁺)], [Found: (MH)⁺, 420.0957. $C_{24}H_{23}NO^{79}Br$ requires 420.0963].

(4S)-2-[3-(2-Bromophenyl)-1-phenylpropyl]-4-benzyl-2-oxazoline (S)-106

1:1 Mixture of diastereoisomers

White Solid; Yield (88 %); R_f (9:1 hexanes:EtOAc) 0.25; $\nu_{\max}/\text{cm}^{-1}$ 1645 (C=N); δ_H 2.04-2.20 (1H, m, PhCHCH_AH_B), 2.28-2.46 (1H, m, PhCHCH_AH_B), 2.58-2.78 (3H, m, ArCH₂ & PhCH_CH_D), 3.07-3.15 (1H, m, PhCH_CH_D), 3.56-3.66 (1H, m, PhCH), 3.88-3.96 (1H, m, CH_EH_FO), 4.06-4.16 (1H, m CH_EH_FO), 4.34-4.46 (1H, m, CHN), 7.00-7.05 (1H, m, Ar), 7.14-7.36 (12H, m, Ph & Ar) and 7.48-7.51 (1H, m, Ar); δ_C^{28} 33.5 (CH₂, isomer A), 33.7 (CH₂, isomer B), 34.0 (CH₂, isomer A), 34.1 (CH₂, isomer B), 41.5 (CH₂), 44.9 (PhCH, isomer A), 45.0 (PhCH, isomer B), 66.9 (CHN, isomer A), 67.0 (CHN, isomer B), 71.5 (CH₂O), 124.4 (CBr), 126.4 (CH_{Ar}), 127.1 (CH_{Ar}), 127.2 (CH_{Ar}), 127.3 (CH_{Ar}), 127.6 (CH_{Ar}), 127.88 (CH_{Ar}), 127.9 (CH_{Ar}), 128.38 (CH_{Ar}), 128.42 (CH_{Ar}), 128.5 (CH_{Ar}), 129.2 (CH_{Ar}), 129.3 (CH_{Ar}), 130.4 (CH_{Ar}), 132.7 (CH_{Ar}), 137.6 (C_q, isomer A), 137.7 (C_q, isomer B), 139.5 (C_q, isomer A), 139.6 (C_q, isomer B), 140.77 (C_q, isomer A), 140.8 (C_q, isomer B), 168.55 (C=N, isomer A) and 168.57 (C=N, isomer B); m/z (CI) 434 [100 %, (M+H⁺)], [Found: (MH)⁺, 434.1109. C₂₅H₂₅NO⁷⁹Br requires 434.1120].

(4S)-2-[3-(2-Bromo-phenyl)-1-phenylpropyl]-4-cyclohexylmethyl-2-oxazoline (S)-107

3:2 mixture of diastereoisomers

White Solid; Yield (49 %); R_f (9:1 hexanes:EtOAc) 0.25; $\nu_{\max}/\text{cm}^{-1}$ 1647 (C=N); δ_H 0.83-1.01 (2H, m, C₆H₁₁), 1.08-1.32 (4H, m, C₆H₁₁CH_AH_B & C₆H₁₁), 1.34-1.48 (1H, m, C₆H₁₁), 1.58-1.75 (6H, m, C₆H₁₁CH_AH_B & C₆H₁₁), 2.08-2.20 (1H, m, PhCHCH_AH_B), 2.30-2.44 (1H, m, PhCHCH_AH_B), 2.62-2.81 (2H, m, ArCH₂), 3.60-3.68 (1H, m, PhCH), 3.76-3.81 (1H, m, CH_CH_DO), 4.09-4.30 (1H, m, CHN & CH_CH_DO), 7.00-7.08 (1H, m, ArH), 7.16-7.38 (1H, m, ArH) and 7.48-7.51 (1H, m, HCCBr); δ_C 26.2 (CH₂), 26.5 (CH₂), 33.4 (CH₂), 33.57 (CH₂, minor isomer), 33.61 (CH₂, major isomer), 33.8 (CH₂), 34.1 (CH₂, minor isomer), 34.2 (CH₂, major isomer), 34.7 (CH, minor isomer), 34.8 (CH, major isomer), 44.2 (CH₂, major isomer), 44.3 (CH₂, minor isomer), 45.1 (PhCH), 63.8 (CHN, minor isomer), 63.9 (CHN, major isomer), 73.0 (CH₂O, major isomer), 73.1 (CH₂O, minor isomer), 124.4 (CBr), 127.1 (CH_{Ar}, major isomer), 127.2 (CH_{Ar}, minor isomer), 127.4 (CH_{Ar}), 127.9

(CH_{Ar}), 128.6 (CH_{Ar}), 130.4 (CH_{Ar}), 132.8 (CH_{Ar}), 139.7 (C_q, minor isomer), 139.8 (C_q, major isomer), 140.9 (C_q, minor isomer), 141.0 (C_q, major isomer) and 167.7 (C=N); *m/z* (CI) 440 [100 %, (M+H⁺)], [Found: (MH)⁺, 440.1570. C₂₅H₃₁NO⁷⁹Br requires 440.1589].

**(4*S*,5*S*)-2-[3-(2-Bromophenyl)-1-phenylpropyl]-4-methoxy-5-phenyl-2-oxazoline
(*S,S*)-108**

3:2 Mixture of diastereoisomers

White Solid; Yield (55 %); R_f (4:1 hexanes:EtOAc) 0.25; $\nu_{\max}/\text{cm}^{-1}$ 1640 (C=N); δ_{H} 2.15-2.39 (1H, m, PhCHCH_AH_B), 2.38-2.53 (1H, m, PhCHCH_AH_B), 2.70-2.88 (ArCH₂), 3.39 (3H, s, MeO, minor isomer), 3.41 (3H, s, MeO, major isomer), 3.46-3.54 (1H, m, CH_CH_DOMe), 3.65 (1H, dd, *J*=9.6, 4.3, CH_CH_DOMe, major isomer), 3.66 (1H, dd, *J*=9.7, 4.4, CH_CH_DOMe, minor isomer), 3.73 (1H, t, *J*=7.7, PhCHCH_AH_B, minor isomer), 3.80 (1H, t, *J*=7.8, PhCHCH_AH_B, major isomer), 4.08-4.17 (1H, m, CHN), 5.28 (1H, d, *J*=6.6, PhCHO), 7.00-7.12 (3H, m, ArH), 7.17-7.38 (8H, m, ArH), 7.40-7.44 (2H, m, ArH) and 7.49-7.52 (1H, m, ArH); δ_{C} 33.2 (CH₂, major isomer), 33.5 (CH₂, minor isomer), 34.1 (CH₂), 45.1 (PhCH, minor isomer), 45.3 (PhCH, major isomer), 59.2 (CHN), 74.26 (MeO, major isomer), 74.3 (CH₂O, major isomer), 74.39 (MeO, minor isomer), 74.42 (CH₂O, major isomer), 83.2 (PhCHO, minor isomer), 83.5 (PhCHO, major isomer), 124.4 (CBr), 125.2 (CH_{Ar}), 125.4 (CH_{Ar}), 127.3 (CH_{Ar}), 127.4 (CH_{Ar}), 127.7 (CH_{Ar}), 127.9 (CH_{Ar}), 127.96 (CH_{Ar}), 128.0 (CH_{Ar}), 128.1 (CH_{Ar}), 128.6 (CH_{Ar}), 130.5 (CH_{Ar}), 132.8 (CH_{Ar}), 139.4 (C_q, major isomer), 139.5 (C_q, minor isomer), 140.86 (C_q, major isomer), 140.88 ((C_q, minor isomer) & (C_q, major isomer)), 140.9 (C_q, minor isomer), 168.9 (C=N, major isomer) and 169.0 (C=N, minor isomer); *m/z* (CI) 464 [100 %, (M+H⁺)], [Found: (MH)⁺, 464.1219. C₂₆H₂₇NO₂⁷⁹Br requires 464.1225].

**(4*S*)-{2-[3-(2-Bromophenyl)-1-phenylpropyl]-2-oxazolin-4-yl}-diphenylmethanol
(*S*)-109**

2:1 Mixture of diastereoisomers

White Solid; Yield (41 %); R_f (9:1 hexanes:EtOAc) 0.2; $\nu_{\max}/\text{cm}^{-1}$ 1654 (C=N) and 3547 (OH); δ_{H} 2.05-2.17 (1H, m, PhCHCH_AH_B), 2.24-2.40 (2H, m, OH &

PhCHCH_AH_B), 2.61-2.78 (2H, m, ArCH₂), 3.73 (1H, t, *J*=7.7, PhCH), 4.02-4.13 (2H, m, CH₂O), 5.28 (1H, t, *J*=9.6, CHN, minor isomer), 5.32 (1H, t, *J*=9.4, CHN, major isomer), 6.99-7.06 (1H, m, ArH), 7.09-7.40 (16H, m, ArH), 7.46-7.51 (1H, m, ArH) and 7.55-7.60 (2H, m, ArH); δ_C 33.7 (CH₂, minor isomer), 33.8 (CH₂, major isomer), 34.2 (CH₂, minor isomer), 34.3 (CH₂, major isomer), 45.38 (PhCH, major isomer), 45.44 (PhCH, minor isomer), 69.1 (CH₂O, major isomer), 69.2 (CH₂O, minor isomer), 72.4 (CHN), 78.0 (Ph₂C, minor isomer), 78.2 (Ph₂C, major isomer), 124.3 (CBr, major isomer), 124.4 (CBr, minor isomer), 125.7 (CH_{Ar}), 126.7 (CH_{Ar}), 126.8 (CH_{Ar}), 127.0 (CH_{Ar}), 127.1 (CH_{Ar}), 127.3 (CH_{Ar}), 127.7 (CH_{Ar}), 128.0 (CH_{Ar}), 128.2 (CH_{Ar}), 128.6 (CH_{Ar}), 130.3 (CH_{Ar}), 130.4 (CH_{Ar}), 132.8 (CH_{Ar}), 139.4 (C_q, minor isomer), 139.7 (C_q, major isomer), 140.79 (C_q, major isomer), 140.84 (C_q, minor isomer), 144.0 (C_q, major isomer), 144.1 (C_q, minor isomer), 145.7 (C_q), 171.5 (C=N, minor isomer) and 171.6 (C_q, major isomer); *m/z* (CI) 526 [100 %, (M+H⁺)], [Found: (MH)⁺, 526.1372. C₃₁H₂₉NO₂⁷⁹Br requires 526.1354].

2-[3-(2-Bromophenyl)butyl]-4,4-dimethyl-2-oxazoline **64**

Acid-base work up employed and crude used without further purification; Clear oil; Yield (not determined see Section 3.3.2.1 for overall yield); ν_{max}(Film)/cm⁻¹ 1664 (C=N); δ_H 1.26 (6H, s, 2xCH₃), 1.61-1.78 (4H, m, ArCH₂CH₂CH₂), 2.30 (2H, t, *J*=7.1, CH₂), 2.74 (2H, t, *J*=7.4, ArCH₂), 3.89 (2H, s, CH₂O), 7.01-7.07 (1H, m, ArH), 7.19-7.24 (2H, m, ArH) and 7.51 (1H, d, *J*= HCCBr); δ_C 25.7 (CH₂), 27.9 (CH₂), 28.4 (2xCH₃), 29.3 (CH₂), 35.7 (CH₂), 66.8 ((CH₃)₂C), 78.8 (CH₂O), 124.3 (CBr), 127.3 (CH_{Ar}), 127.4 (CH_{Ar}), 130.2 (CH_{Ar}), 132.7 (CH_{Ar}), 141.4 (C_q) and 165.7 (C=N); *m/z* (-ES⁺) 310 [100 %, (M+H⁺)], [Found: (MH)⁺, 310.0807. C₁₅H₂₁NO⁷⁹Br requires 310.0807].

2-[3-(2-Bromophenyl)-1-phenylbutyl]-4,4-dimethyl-2-oxazoline **110**

Clear Oil; Yield (69 %); R_f (SiO₂, 9:1 hexanes:EtOAc) 0.2; (Found C, 65.3; H, 6.8; N, 3.8. C₂₁H₂₄ONBr requires C, 65.3; H, 6.3; N, 3.6 %); ν_{max}(Nujol)/cm⁻¹ 1660 (C=N); δ_H 1.26 (3H, s, CH₃), 1.27 (3H, s, CH₃), 1.46-1.74 (2H, m, ArCH₂CH₂), 1.84-1.96 (1H, m, PhCHCH_ACH_B), 2.11-2.23 (1H, m, PhCHCH_ACH_B), 2.66-2.82 (2H, m, ArCH₂), 3.58 (1H, t, *J*=7.8, PhCH), 3.86 (2H, s, CH₂O), 6.98-7.04 (1H, m, ArH),

7.12-7.36 (7H, m, ArH) and 7.48 (1H, d, $J=7.8$, HCCBr); δ_C 27.7 (CH₂), 28.2 (CH₃), 28.3 (CH₃), 33.5 (CH₂), 35.9 (CH₂), 45.2 (PhCH), 66.8 ((CH₃)₂C), 78.9 (CH₂O), 124.4 (CBr), 127.0 (CH_{Ar}), 127.3 (CH_{Ar}), 127.4 (CH_{Ar}), 127.7 (CH_{Ar}), 128.5 (CH_{Ar}), 130.2 (CH_{Ar}), 132.7 (CH_{Ar}), 140.0 (C_q), 141.4 (C_q) and 166.8 (C=N); m/z (ES⁺) 386 [100 %, (M+H⁺)], [Found: (MH)⁺, 386.1108. C₂₁H₂₅NO⁷⁹Br requires 386.1120].

2-[3-(2-Bromophenyl)-1-phenylpentyl]-4,4-dimethyl-2-oxazoline 111

Clear Oil; Yield (60 %); R_f (SiO₂, 9:1 hexanes:EtOAc) 0.2; ν_{\max} (Nujol)/cm⁻¹ 1661 (C=N); δ_H 1.25 (3H, s, CH₃), 1.26 (3H, s, CH₃), 1.15-1.47 (2H, m, CH₂), 1.54-1.74 (2H, m, ArCH₂CH₂), 1.77-1.91 (1H, m, PhCHCH_ACH_B), 2.03-2.17 (1H, m, PhCHCH_ACH_B), 2.68 (2H, t, $J=7.7$, ArCH₂), 3.53 (1H, t, $J=7.8$, PhCH), 3.85 (2H, s, CH₂O), 6.98-7.04 (1H, m, ArH), 7.11-7.33 (7H, m, ArH) and 7.49 (1H, dd, $J=8.0$ & 1.0, HCCBr); δ_C 27.1 (CH₂), 28.2 (CH₃), 28.3 (CH₃), 29.4 (CH₂), 33.6 (CH₂), 35.8 (CH₂), 45.3 (PhCH), 66.7 ((CH₃)₂C), 78.8 (CH₂O), 124.4 (CBr), 126.9 (CH_{Ar}), 127.2 (CH_{Ar}), 127.3 (CH_{Ar}), 127.7 (CH_{Ar}), 128.5 (CH_{Ar}), 130.2 (CH_{Ar}), 132.6 (CH_{Ar}), 140.2 (C_q), 141.7 (C_q) and 166.8 (C=N); m/z (ES⁺) 400 [100 %, (M+H⁺)], [Found: (MH)⁺, 400.1292. C₂₂H₂₇NO⁷⁹Br requires 400.1276].

2-[3-(2-Bromophenyl)-1-phenylhexyl]-4,4-dimethyl-2-oxazoline 112

Clear Oil; Yield (61 %); R_f (SiO₂, 9:1 hexanes:EtOAc) 0.2; ν_{\max} (Nujol)/cm⁻¹ 1661 (C=N); δ_H 1.27 (3H, s, CH₃), 1.28 (3H, s, CH₃), 1.20-1.45 (4H, m, 2x CH₂), 1.53-1.63 (2H, m, ArCH₂CH₂), 1.75-1.87 (1H, m, PhCHCH_ACH_B), 2.00-2.13 (1H, m, PhCHCH_ACH_B), 2.68 (2H, t, $J=7.7$, ArCH₂), 3.52 (1H, t, $J=7.8$, PhCH), 3.87 (2H, s, CH₂O), 6.99-7.05 (1H, m, ArH), 7.13-7.35 (7H, m, ArH) and 7.50 (1H, dd, $J=8.0$ & 0.9, HCCBr); δ_C 27.3 (CH₂), 28.2 (CH₃), 28.4 (CH₃), 29.0 (CH₂), 29.7 (CH₂), 33.7 (CH₂), 36.0 (CH₂), 45.4 (PhCH), 66.8 ((CH₃)₂C), 78.9 (CH₂O), 124.4 (CBr), 126.9 (CH_{Ar}), 127.2 (CH_{Ar}), 127.3 (CH_{Ar}), 127.7 (CH_{Ar}), 128.5 (CH_{Ar}), 130.2 (CH_{Ar}), 132.7 (CH_{Ar}), 140.3 (C_q), 141.9 (C_q) and 166.9 (C=N); m/z (ES⁺) 414 [100 %, (M+H⁺)], [Found: (MH)⁺, 414.1439. C₂₃H₂₉NO⁷⁹Br requires 414.1433].

4,4-Dimethyl-2-(3-phenylpropyl)-2-oxazoline **98** ²⁹

2.5M n-BuLi in hexanes (1.94 cm³, 4.8 mmol) was added dropwise to a stirring solution of 2,4,4-trimethyl-2-oxazoline **30** (0.5 g, 4.4 mmol) in dry THF (4 cm³) and dry hexane (2 cm³) under nitrogen at -78°C. After stirring for 5 min 2-bromoethylbenzene **101** (0.9 g, 4.84 mmol) in dry THF (2 cm³) was added over a 10 minute period. The solution was then allowed to warm to room temperature slowly over 3 h, after which water (10 cm³) was added. The aqueous layer was extracted with ether (3x10 cm³), the combined organic layers were washed with water (20 cm³), dried (MgSO₄) and concentrated in vacuo to give a crude product mixture which was analysed by ¹H-NMR. Analysis determined only starting materials present and the known product, substituted oxazoline **98** with no unwanted elimination products; δ_{H} 1.25 (6H, s, 2xCH₃), 1.90-2.00 (2H, m, CH₂(CH₂)₂), 2.27 (2H, t, *J*=7.6, CH₂), 2.66 (2H, t, *J*=7.6, ArCH₂), 3.88 (2H, s, CH₂O) and 7.14-7.30 (5H, m, ArH).

3.8 Substituted Propen-2-ols

2-Bromophenylacetyl chloride **38b**³⁰

Distilled thionyl chloride (11.7 cm³, 98 mmol) was added slowly via a syringe to 2-bromophenylacetic acid **40b** (7.00 g, 33 mmol). The solution was then heated under reflux at 75 °C for 1.5 h after which time heating was stopped and the reaction mixture was left to stand overnight at room temperature. The excess thionyl chloride was removed under vacuum to afford the known product **38b** in quantitative yield (7.81g) as a pale yellow liquid, δ_{H} 4.29 (2H, s, CH₂) 7.15-7.30 (3H, m, ArH) and 7.57 (1H, dd, $J=7.9$ & 1.3, HCCBr).

3-(2-Bromophenyl)-1-(4,4-dimethyl-2-oxazolin-2-yl)propen-2-ol **35b**

2-4,4-Trimethyloxazoline **30** (0.5 g, 4.3 mmol) was placed in a 3-necked round bottom flask fitted with a septum. The apparatus was flushed with N₂ for 10 min. The N₂ pressure was reduced and dry THF (12 cm³) was added via a syringe before the flask was cooled to -78 °C using acetone/dry ice. After 5 min 2.5M BuLi in hexane solution (3 cm³, 7.5 mmol) was added slowly with stirring and the reaction mixture became bright yellow in colour. After stirring for 5 min, a solution of 2-bromophenylacetyl chloride **38b** in dry THF (1.00 g, 4.3 mmol in 3 cm³) was added slowly via a syringe. The solution was then allowed to warm to room temperature over a period of 1.5 h with stirring. To the reaction mixture brine (100 cm³) was added, and the aqueous phase was extracted with ether (4x40 cm³). The combined organic portions were washed with water (100 cm³) and dried (MgSO₄) and the solvent removed. The crude product was then washed through alumina using hexane : ethyl acetate (200 cm³, 3:1) and the solvent removed. To the residue boiling hexane (30 cm³) was added and DCM was added dropwise until the residue fully dissolved. The solution was then covered and cooled (-20 °C) overnight. The solution was filtered and the filtrate washed with cold (-78 °C) ethyl acetate to afford the pure product **35b** (320 mg, 25 %) as a white crystals, δ_{H} (300 MHz, CDCl₃) 1.38 (6H, s, 2xCH₃), 3.75 (2H, s, CH₂), 4.07 (2H, s, CH₂O), 4.82 (1H, s, CH), 7.06-7.15 (1H, m, ArH), 7.23-7.33 (2H, m, ArH), 7.53-7.56 (1H, m, ArH) and 9.55 (1H, bs, OH); δ_{C}

27.1 (2xCH₃), 48.5 (ArCH₂), 58.3 (C(CH₃)₂), 76.2 (CH), 78.8 (CH₂O), 125.1, 127.3, 128.0, 131.6, 132.6, 137.1 (CBr), 168.7 and 192.8.

3-(2-Bromophenyl-1-(4,4-dimethyl-2-oxazolin-2-yl)-1-phenylpropen-2-ol **36b**

2-Benzyl-4,4-dimethyl-2-oxazoline **27** (0.80 g, 4.3 mmol) was placed in a 3-necked round bottom flask fitted with a septum. The apparatus was flushed with N₂ for 10 min. The N₂ pressure was reduced and dry THF (12 cm³) was added via a syringe before the flask was cooled to -78 °C using acetone/dry ice. After 5 min 2.5M BuLi in hexane solution (3 cm³, 7.5 mmol) was added slowly with stirring and the reaction mixture became bright yellow in colour. After stirring for 5 min, a solution of 2-bromophenylacetyl chloride **38b** in dry THF (1.00 g, 4.3 mmol in 3 cm³) was added slowly via a syringe. The solution was then allowed to warm to room temperature over a period of 1.5 h with stirring. To the reaction mixture brine (100 cm³) was added, the aqueous phase was extracted with ether (4x40 cm³). The combined organic portions were washed (water, 100 cm³) and dried (MgSO₄) and the solvent removed. The crude product was then washed through alumina using hexane : ethyl acetate (200 cm³, 3:1) and the solvent removed. Boiling hexane (30 cm³) was added to the residue and DCM was added dropwise until the residue fully dissolved. The solution was then covered and cooled (-20 °C) overnight. The solution was filtered and the filtrate washed with cold (-78 °C) ethyl acetate to afford the pure product **36b** (190 mg, 12 %) as white crystals, m.p 156-160, δ_H 1.38 (6H, s, 2xCH₃), 3.70 (2H, s, CH₂), 4.05 (2H, s, CH₂O), 7.02-7.51 (9H, m, ArH) and 10.22 (1H, bs, OH); δ_C 27.5 (CH₃), 46.4 (ArCH₂), 59.0 ((CH₃)₂C), 79.5 (CH₂O), 93.7, 125.5, 126.4, 127.2, 127.5, 128.3, 128.5, 128.6, 129.9, 132.2, 132.7, 132.8, 136.5, 138.1, 167.1 (OCN) and 192.0 (HOC); *m/z* (CI) 386 [33 %, (M+H)⁺], [Found: (MH)⁺, 386.0746. C₂₀H₂₁NO₂⁷⁹Br requires, 386.0756].

3.9 γ -Substituted Propionic acids

3-(2-Chlorophenoxy)propionic acid **123**³¹

A solution of 3-bromopropionic acid **122** (10 g, 66.0 mmol) and sodium hydrogencarbonate (5.54 g, 66.0 mmol) in water (30 cm³) was added gradually over one hour to 2-chlorophenol **48a** (6.74 cm³, 66.0 mmol) in aqueous potassium hydroxide (6 g in 20 cm³) at 100 °C. After heating for a further two hours, the solution was cooled to 0 °C and acidified with concentrated hydrochloric acid. The precipitate was collected and washed with water. The first aqueous filtrate was extracted with ether (3x30 cm³) and the combined organic layers extracted with saturated sodium hydrogencarbonate solution (3x30 cm³). Acidification of the aqueous layers with conc. HCl afforded a further quantity of the crude product. The crude product was suction dried to afford the known acid **123** (3.51 g, 26 %) as a white solid; mp 115.5-116.5 (MeOH) [Lit.,³¹ 112-113 (aq MeOH)]; δ_{H} 2.92 (2H, t, $J=6.4$, CH₂), 4.32 (2H, t, $J=6.4$, OCH₂), 6.89-6.98 (2H, m, ArH), 7.18-7.24 (1H, m, ArH) and 7.36 (1H, dd, $J=7.9$ & 1.5, ArH); δ_{C} 34.2 (CH₂), 64.4 (CH₂N), 114.0 (CH_{Ar}), 122.0 (CH_{Ar}), 123.2 (CCl), 127.7 (CH_{Ar}), 130.4 (CH_{Ar}), 154.0 (CO) and 175.7 (CO₂H). m/z (CI) 200 [100 %, (M)⁺] [Found: (M)⁺ 200.0247. C₉H₉O₃Cl requires 200.0240].

3-(2-Bromophenylamino)propionic acid **124**³²

A mixture of 2-bromoaniline **49b** (6.9 g, 40.0 mmol), 3-bromopropionic acid **122** (3.0g, 20.0mmol) and water (10 cm³) were heated to 85 °C for two hours with stirring. The hot mixture was then allowed to cool to 40 °C, at which point it was washed into a conical flask, firstly with ether (30 cm³), then water (20 cm³) and finally saturated sodium hydrogencarbonate solution (30 cm³). The ether was made up to approximately 60 cm³. Saturated sodium hydrogencarbonate solution was added until carbon dioxide was no longer evolved and all solids had been dissolved. The aqueous layer was washed with ether (3x30 cm³) and acidified to pH 4 with 5M hydrochloric acid. The precipitate was filtered and washed with aqueous HCl solution at pH 4 and allowed to dry by suction to give the known β -amino acid **124** (2.83 g, 58

%) as a white solid. The purity of the product, measured by $^1\text{H-NMR}$ was deemed sufficient; mp 149.8-151.0 °C [Lit.,³² 152.5-153.0 °C]; $\nu_{\text{max}}/\text{cm}^{-1}$ (nujol) 1711 (C=O) and 3330 (NH); δ_{H} (d^6 -acetone) 2.68 (2H, t, $J=6.6$, $\text{CH}_2\text{CO}_2\text{H}$), 3.51 (2H, t, $J=6.6$, CH_2N), 6.54-6.60 (1H, m, BrCCHCH), 6.80 (1H, dd, $J=8.3$ & 1.7), 7.18-7.24 (1H, m, NCCHCH) and 7.41 (1H, dd, $J=7.7$ & 1.4, HCCBr); δ_{C} (d^6 -acetone) 34.1 (CH_2), 40.2 (CH_2N), 110.4 (CBr), 112.7 (CH_{Ar}), 119.0 (CH_{Ar}), 129.9 (CH_{Ar}), 133.6 (CH_{Ar}), 146.1 (C=N) and 173.8 (CO_2H); m/z (CI) 242 [98 %, (M+H)⁺] [Found: (MH)⁺ 242.9911. $\text{C}_9\text{H}_{10}\text{O}_2\text{N}^{79}\text{Br}$ requires 242.9895].

3.10 Cyanoacetic acid Derivatives

2-Bromophenyl cyanoacetate **127**

Cyanoacetic acid **129** (8.5 g, 0.1 mol), 2-bromophenol **48b** (8.4 cm³, 0.08 mol) and phosphorus oxychloride (4.5 cm³) were heated under reflux until evolution of hydrogen chloride gas ceased (2-3 h). After cooling the solid product was broken up and washed with ice cold water. The solids were then dissolved in toluene (200 cm³) and filtered. The filtrate was then washed with 5 % sodium hydrogencarbonate solution. The organic layer was dried (Na₂SO₄) and concentrated in vacuo. Krugelrohr distillation afforded the pure ester **127** (70 %) as a clear oil; $\nu_{\max}/\text{cm}^{-1}$ 1778 (C=O) and 2268 (C≡N); δ_{H} 3.77 (2H, s, CH₂), 7.12-7.18 (2H, m, Ar), 7.30-7.35 (1H, m, Ar) and 7.58-7.61 (1H, m, HCCBr); δ_{C} 24.5 (CH₂), 112.5 (CBr), 115.4 (C≡N), 123.1 (CH_{Ar}), 128.1 (CH_{Ar}), 128.6 (CH_{Ar}), 133.3 (CH_{Ar}), 147.2 (C-O) and 160.9 (C=O); m/z (CI) 240 [95 %, (M+H⁺) [Found: (MH)⁺, 239.9666. C₉H₇NO₂⁷⁹Br requires 239.9660].

N-(2-Bromophenyl)-2-cyanoacetamide **128**

Cyanoacetic acid **129** (4.3 g, 50.0 mmol), and 2-bromoaniline **49b** (9.5 g, 55.0 mmol), were dissolved in dichloromethane (50 cm³) and stirred at reflux. Dicyclohexylcarbodiimide (10.8 g, 52.5 mmol) was added with care over 15 min. The reaction was then stirred overnight at room temperature. The mixture was then filtered and solvent removed. The residue was washed with a little cold dichloromethane. Recrystallisation from dichloromethane/pentane to gave the pure product **127** (6.29 g, 52 %); mp 139.1-140.6; (Found: C, 46.3; H, 3.1; N, 11.6 C₉H₇N₂OBr requires C, 45.2; H, 3.0; N, 11.7 %); $\nu_{\max}/\text{cm}^{-1}$ 1670 (C=O), 2268 (C≡N) and 3250 (NH); δ_{H} 3.62 (2H, s, CH₂), 7.07 (1H, ddd, $J=7.9, 7.7$ & 1.5, BrCCHCH), 7.36 (1H, ddd, $J=8.2, 7.7$ & 1.5, HNCCHCH), 7.59 (1H, dd, $J=7.9$ & 1.5, BrCCH) and 8.26 (2H, br dd, $J=8.2$ & 1.5, HNCCH & NH); δ_{C} 28.1 (CH₂), 116.6 (C_q), 117.4 (C_q), 126.7 (CH_{Ar}), 128.6 (CH_{Ar}), 130.0 (CH_{Ar}), 134.6 (CH_{Ar}), 137.6 (C_q) and 163.0 (C=O); m/z (CI) 238 [100 %, (M+H⁺) and 159 (16) [Found: (MH)⁺, 238.9812. C₉H₈N₂O⁷⁹Br requires 238.9820].

3.11 S_{RN}1 Reactions

3.11.1 ^tBuOK/DMSO

3.11.1.1 General Procedure

Freshly sublimed potassium *tert*-butoxide (1.1 eq) was dissolved up in dry distilled dimethyl sulfoxide (6 cm³/mmol). The substrate oxazoline (1 eq) in dimethyl sulfoxide (6 cm³/mmol) was then added and stirred for 5 min. Triethylamine (1 eq) was added and the resulting mixture was irradiated for 3-4 h. Water (6 cm³/mmol) was added and the aqueous phase was extracted with dichloromethane (3x12 cm³/mmol). The combined organic extracts were washed (water (24 cm³/mmol)), dried (MgSO₄) and concentrated in vacuo to give the crude product.

3.11.1.2 2-[3-(2-Chlorophenyl)propyl]-4,4-dimethyl-2-oxazoline **33a**

2-[3-(2-Chlorophenyl)propyl]-4,4-dimethyl-2-oxazoline **33a** was reacted as outline above with 3 h irradiation. After work up the crude ¹H-NMR spectrum showed only the presence of starting material.

3.11.1.3 2-[3-(2-Bromophenyl)-1-phenylpropyl]-4,4-dimethyl-2-oxazoline **34b**

2-[3-(2-Bromophenyl)-1-phenylpropyl]-4,4-dimethyl-2-oxazoline **34b** was reacted as shown above with 4 h irradiation. Analysis of the crude ¹H-NMR and GCMS revealed the presents of a 1 : 2 mixture of the starting material **34b** and the dehalogenated product 2-[1,3-diphenylpropyl]-4,4-dimethyl-2-oxazoline **141** R_f (Al₂O₃, 19:1, hexane:EtAc) 0.3, δ_H 1.25 (3H, s, CH₃), 1.26 (3H, s, CH₃) 2.09-2.18 (1H, m, CH_ACH_B), 2.37-2.44 (1H, m, CH_ACH_B), 2.59 (2H, t, J=7.7, ArCH₂), 3.54 (1H, t, J=7.7, PhCH), 3.81 (1H, s, CH_CH_DO), 3.82 (1H, s, CH_CH_DO) and 7.11-7.34 (10H, m, ArH); δ_C 28.6 (CH₃), 28.8 (CH₃), 34.0, 35.9, 45.1, 67.3, 79.3, 126.3, 127.5, 128.3, 128.6, 128.8, 129.0, 129.1, 140.5, 141.9 and 167.1; m/z (EI) 293 (1 %, M⁺), 189 (100, M-C₈H₈), 91 (16).

3.11.2 MNH₂/NH₃

3.11.2.1 General Procedure

To a solution of ferric nitrate (0.03 eq) in liquid ammonia (15 cm³/mmol) at -78 °C, was added with caution, either lithium or potassium metal (3 eq). The resulting mixture was warmed to -33 °C and stirred until the blue colour faded to a grey suspension (c.a 30 min). The substrate oxazoline (1 eq) in dry THF (1 cm³/mmol) was added dropwise over 5 min and stirred for a further 10 min. After allowing the mixture to warm to reflux (-33 °C), it was irradiated with UV for either 1 or 2 h, after which solid NH₄Cl was added with extreme caution! The liquid ammonia was allowed to evaporate while being slowly replaced by ether (20 cm³/mmol). The ethereal solution was decanted and the solids washed with ether (2x50 cm³/mmol). The combined portions were dried (MgSO₄) and concentrated in vacuo to give the crude product.

3.11.2.2 2-[3-(2-Chlorophenyl)propyl]-4,4-dimethyl-2-oxazoline **33a**

Following the procedure above 2-[3-(2-chlorophenyl)propyl]-4,4-dimethyl-2-oxazoline **33a** was reacted with LiNH₂ in liquid ammonia with irradiation for 2 h to yield after work up a 5 : 1 mixture of starting material **33a** and the reduced product 2-[3-phenylpropyl]-4,4-dimethyl-2-oxazoline **98** (for data see Section 3.7) as determined by ¹H-NMR analysis.

3.11.2.3 2-[3-(2-Bromophenyl)-1-phenylpropyl]-4,4-dimethyl-2-oxazoline **34b**

2-[3-(2-Bromophenyl)-1-phenylpropyl]-4,4-dimethyl-2-oxazoline **34b** was added to a stirring solution of potassium amide in liquid ammonia as detailed above. After 1 h irradiation and work up, the crude mixture was weighed and a portion placed in an NMR tube and CDCl₃ was added followed by 5 μl of dibromomethane as an internal standard. The ¹H-NMR revealed three separate species, these were starting material **34b**, yield (51 %), diphenylpropyl-2-oxazoline **141**, yield (31 %); (for data see Section 3.11.1.3) and the desired 4,4-dimethyl-2-(1'-phenyl-indan-1'-yl)-2-oxazoline **140** yield (16 %); R_f (SiO₂, 9:1 hexanes:EtOAc) 0.35; ν_{max}(film)/cm⁻¹

1649 (C=N); δ_{H} 1.24 (3H, s, CH₃), 1.40 (3H, s, CH₃), 2.30 (1H, ddd, $J=12.6, 7.7, 5.1$, CH_AH_B), 2.82 (1H, ddd, $J=15.6, 7.7$ & 7.4 , ArCH_CH_D), 3.00 (1H, ddd, $J=15.6, 7.9, 5.1$, ArCH_CH_D), 3.18 (1H, ddd, $J=12.6, 7.9$ & 7.4 , CH_AH_B), 3.90 (1H, AB doublet $J\sim 7.9$, CH_EH_FO), 3.97 (1H, AB doublet $J\sim 7.9$, CH_EH_FO), 7.06-7.11 (2H, m, ArH), 7.18-7.31 (6H, m, ArH) and 7.48-7.51 (1H, m, ArH); δ_{C} 28.0 (CH₃), 28.3 (CH₃), 30.3 (CH₂), 41.3 (ArCH₂), 58.2 ((CH₃)₂C), 66.8 (PhC), 79.4 (CH₂O), 124.7 (CH_{Ar}), 126.4 (CH_{Ar}), 126.5 (CH_{Ar}), 126.6 (CH_{Ar}), 126.7 (CH_{Ar}), 127.7 (CH_{Ar}), 128.3 (CH_{Ar}), 143.6 (C_q), 144.3 (C_q), 144.8 (C_q) and 167.6 (C=N); m/z (CI) 292 [100 %, (M+H)⁺] [Found: (MH)⁺ 292.1708. C₂₀H₂₂ON requires 292.1701].

The reaction was repeated under identical conditions but at a dilution of one tenth, the yields of which are shown in Table 6, Section 2.4.2.

3.11.3 LDA/THF & LDA THF/Hexane Without Iron(II) Salts

3.11.3.1 General Procedure

To a solution of LDA (3 equiv.) in either THF or 2:1 hexane:THF mixture (6 cm³/mmol) at -78 °C under nitrogen was added a solution of the substrate (1 eq) in the reaction solvent (3 cm³/mmol). After stirring for 10 min the solution was allowed to warm to room temperature over 30 min, at which time more solvent was added (18 cm³/mmol). The mixture was then stirred for between 0 and 48 h at between -30 °C and reflux, either with or without irradiation. After this time a saturated solution of ammonium chloride (10 cm³/mmol) was added and the aqueous layer was extracted with three portions of ether (5 cm³/mmol). The combined organic layers were washed with water (10 cm³/mmol) and dried (MgSO₄) to give the crude product.

3.11.3.2 2-[3-(2-Bromophenyl)-propyl]-4,4-dimethyl-2-oxazoline **33b**

Using the general procedure detailed above 2-[3-(2-bromophenyl)-propyl]-4,4-dimethyl-2-oxazoline **33b** was reacted under UV radiation in quartz glassware for 4 h to yield after column chromatography starting material **33b**, yield (29 %), desired 4,4-dimethyl-2-indan-1'-yl-2-oxazoline **139**, yield (58 %); R_f (SiO₂, 9:1 hexanes:EtOAc) 0.2; $\nu_{\text{max}}/\text{cm}^{-1}$ 1653 (C=N); δ_{H} 1.28 (3H, s, CH₃), 1.30 (3H, s, CH₃), 2.29-2.47 (2H, m, CH₂), 2.87-2.98 (1H, m, ArCH_AH_B), 3.03-3.13 (1H, m, ArCH_AH_B), 3.93 (2H, s,

CH₂O), 4.09, (1H, t, *J*=7.9, CH), 7.08-7.27 (3H, m, ArH) and 7.30-7.34 (1H, m, ArH); δ_C 28.2 (CH₃), 25.5 (CH₃), 29.2 (CH₂), 31.8 (ArCH₂), 44.4 (CH), 66.8 (C(CH₃)₂), 79.2 (CH₂O), 124.3 (CH_{Ar}), 124.6 (CH_{Ar}), 126.4 (CH_{Ar}), 127.3 (CH_{Ar}), 141.3 (C_q), 144.0 (C_q) and 167 (C=N); *m/z* (CI) 216 [100 %, (M+H)⁺] [Found: (MH)⁺ 216.1396. C₂₀H₂₂ON requires 216.1388]; and a mixture of styrenes **142** & **143**, yield (10 %); 2-bromostyrene **142** δ_H 5.40 (1H, dd, *J*=8.1 & 1.1, CH), 5.75 (1H, dd, *J*=16.0 & 1.1), 7.20 (1H, dd, *J*=16.0 & 8.1, CH) and 7.30-7.52 (4H, m, CH_{Ar}); styrene **143** δ_H 5.22 (1H, dd, *J*=10.9 & 0.9, CH), 5.70 (1H, dd, *J*=17.6 & 0.9, CH), 6.68 (1H, dd, *J*=10.9 & 17.6) & 7.15-7.45 (1H, m, Ph).

Yields for the identical reaction carried out in Pyrex glassware are shown in Table 8, Section 2.4.3.2.

3.11.3.3 2-[3-(2-Bromophenyl)-1-phenylpropyl]-4,4-dimethyl-2-oxazoline **34b**

2-[3-(2-Bromophenyl)-1-phenylpropyl]-4,4-dimethyl-2-oxazoline **34b** was reacted as detailed in the general procedure above for 48 hours without irradiation using THF as solvent. Column chromatography, using 9:1 hexanes:EtOAc as elutant, afforded indane **140**, yield (75 %) (for data see Section 3.11.2.3), starting material **34b**, yield (<1 %) and a mixture of styrenes **142** & **143**, yield (2 %) (for data see Section 3.11.3.2).

Yields for the same reaction in the dark and under irradiation for between 0-20 h, with 1-3 eq of LDA are detailed in Table 7, Section 2.4.3.1 for reaction in THF and Table 9, Section 2.4.4 for reaction in 2:1 THF:hexanes. Yields for these reactions were either determined via isolation or by ¹H-NMR analysis using 5 μ l of dibromomethane as an internal standard.

3.11.3.4 2-[3-(2-Bromophenyl)-1-phenylbutyl]-4,4-dimethyl-2-oxazoline **110**

2-[3-(2-Bromophenyl)-1-phenylbutyl]-4,4-dimethyl-2-oxazoline **110** reacted in THF for 48 h in the dark using the general procedure detailed in Section 3.11.3.1 to afford, after column chromatography, a 55 % yield of the desired 4,4-dimethyl-2-(1-phenyl-1,2,3,4-tetrahydronaphthalen-1-yl)-2-oxazoline **144**; *R_f* (SiO₂, 9:1 hexanes:EtOAc) 0.25; Found: C, 81.8; H, 8.0; N, 4.7. C₂₁H₂₃NO requires C, 82.6; H, 7.6; N, 4.6 %; ν_{\max} (film)/cm⁻¹ 1638 (C=N); δ_H 1.28 (3H, s, CH₃), 1.38 (3H, s, CH₃),

1.54-1.69 (1H, m, CH_AH_B), 1.80-1.93 (1H, m, CH_AH_B), 2.03-2.12 (1H, m, CH_CH_D), 2.70-2.79 (1H, m, CH_CH_D), 2.83-2.89 (2H, m, $ArCH_2$), 3.93 (1H, AB doublet $J \sim 8.2$, CH_EH_FO), 3.96 (1H, AB doublet $J \sim 8.2$, CH_EH_FO), 7.00-7.04 (2H, m, ArH), 7.07-7.27 (6H, m, ArH) and 7.31-7.34 (1H, m, ArH); δ_C 19.2 (CH_2), 28.1 (CH_3), 28.3 (CH_3), 29.8 (CH_2), 37.8 ($ArCH_2$), 50.5 (PhC), 66.8 ($(CH_3)_2C$), 79.1 (CH_2O), 125.4 (CH_{Ar}), 126.3 (CH_{Ar}), 126.8 (CH_{Ar}), 127.8 (CH_{Ar}), 127.9 (CH_{Ar}), 129.2 (CH_{Ar}), 130.9 (CH_{Ar}), 137.3 (C_q), 137.9 (C_q), 146.6 (C_q) and 168.7 ($C=N$); m/z (CI) 306 [100 %, $(M+H)^+$] [Found: $(MH)^+$ 306.1853. $C_{21}H_{24}ON$ requires 306.1858]; Crystal data $C_{21}H_{23}NO$ $M = 305.40$, colourless cubes, crystal dimensions 0.2 x 0.2 x 0.2 mm, triclinic, space group P-1, $a = 8.588$ (2), $b = 10.0389$ (19), $c = 10.8881$ (13) Å, $\alpha = 115.888$ (16), $\beta = 98.06$ (5), $\gamma = 92.69$ (2)°, $V = 830.0$ (3) Å³, $D_c = 1.222$ Mg/m³, $T = 93$ (2) K, $Z = 2$, $R = 0.0462$, $R_w = 0.1257$ for 2811 reflections with $I > 2\sigma(I)$ and 210 variables.

The reaction of oxazoline **110** under similar conditions in THF after 6 h UV irradiation gave the tetralin **144** in a 50 % yield.

3.11.3.5 2-[3-(2-Bromophenyl)-1-phenylpentyl]-4,4-dimethyl-2-oxazoline **111**

To a solution of LDA in THF was added 2-[3-(2-bromophenyl)-1-phenylpentyl]-4,4-dimethyl-2-oxazoline **111** and after warming to room temperature the mixture was stirred for 48 hours as described in the general procedure (Section 3.11.3.1). Column chromatography was performed, which gave several products as follows:

2-(1-Butyl-1,5-diphenylpentyl)-4,4-dimethyl-2-oxazoline **145**

Yield (13 %); R_f (SiO_2 , 4:1 hexanes:EtOAc) 0.4; ν_{max} (Film)/cm⁻¹ 1655 ($C=N$); δ_H 0.81-0.88 (3H, m, CH_3), 0.93-1.34 (6H, m, 3x CH_2), 1.27 (3H, s, $(CH_3)_2C$), 1.30 (3H, s, $(CH_3)_2C$), 1.62 (2H, q, $J = 7.6$, CH_2), 1.89-2.15 (4H, m, 2x CH_2), 2.49-2.65 (2H, m, CH_2), 3.73 (1H, d, $J = 8.1$, CH_AH_BO), 1H, d, $J = 8.1$, CH_AH_BO) and 7.10-7.34 (10H, m, 2x Ph); δ_C 14.0 (CH_3), 23.0 (CH_2), 23.1 (CH_2), 25.9 (CH_2), 28.2 ($(CH_3)_2C$), 31.5 (CH_2), 33.8 (CH_2), 34.0 (CH_2), 35.5 (CH_2), 47.2 (PhC), 66.8 ($(CH_3)_2C$), 78.7 (CH_2O), 125.5 (CH_{Ar}), 126.2 (CH_{Ar}), 126.4 (CH_{Ar}), 128.1 (CH_{Ar}), 128.3 (CH_{Ar}), 142.4 (C_q), 143.8 (C_q), 169.5 ($C=O$); m/z (ES⁺) 378 [100 %, $(M+H)^+$], [Found: $(MH)^+$, 378.2811. $C_{26}H_{36}NO$ requires 378.2797].

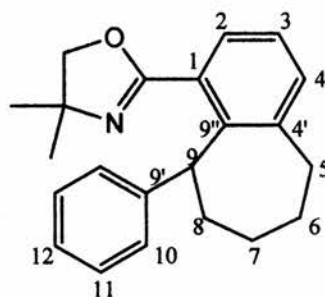
4,4-Dimethyl-2-(9-phenyl-6,7-dihydro-5H-benzocyclohepten-1-yl)-2-oxazoline 148

Yield (25 %); δ_{H} 0.72 (3H, s, CH₃), 1.07 (3H, m, CH₃), 1.22-1.32 (2H, m, CH₂), 2.01-2.20 (2H, m, CH₂), 2.56-2.69 (2H, m, CH₂), 3.23 (1H, d, $J=7.8$, CH_AH_BO), 3.71 (1H, d, $J=7.8$, CH_AH_BO), 6.54 (1H, t, $J=7.4$, vinyl), 7.13-7.35 (6H, m, CH_{Ar}), 7.39 (1H, dd, $J=7.6$ & 1.5) & 7.65 (1H, dd, $J=7.6$ & 1.5); δ_{C} 25.0 (CH₂), 27.7 (CH₃), 28.1 (CH₃), 32.4 (CH₂), 34.1 (CH₂), 66.6 (C_q), 79.0 (CH₂O), 126.5 (CH_{Ar}), 126.7 (CH_{Ar}), 127.2 (CH_{Ar}), 128.1 (CH_{Ar}), 128.4 (vinyl), 128.7 (CH_{Ar}), 131.1 (CH_{Ar}), 138.3 (C_q), 141.5 (C_q), 141.7 (C_q), 142.1 (C_q) & 163.4 (C=N); m/z 318 [100 %, (M+H)⁺] [Found: (MH)⁺ 318.1865. C₂₂H₂₄ON requires 318.1858]; Crystal data C₂₂H₂₃NO $M = 317.41$, colourless needles, crystal dimensions 0.3 x 0.05 x 0.01 mm, monoclinic, space group P2(1)/c, $a = 12.9895$ (12), $b = 11.5790$ (10), $c = 11.5517$ (11) Å, $\alpha = 90$, $\beta = 93.777$ (3) (5), $\gamma = 90$ °, $V = 1733.7$ (3) Å³, $D_c = 1.216$ Mg/m³, $T = 173$ (2) K, $Z=4$, $R = 0.0406$, R_w 0.0982 for 2948 reflections with $I > 2\sigma(I)$ and 217 variables.

4,4-Dimethyl-2-(4,5,6,7-tetrahydro-cyclohepta[jk]fluoren-7a-yl)-2-oxazoline 149

Yield (6 %); δ_{H} 1.24-1.30 (2H, m, CH₂), 1.26-(3H, m, CH₃), 1.27 (3H, m, CH₃), 1.95-2.18 (2H, m, CH₂), 2.25-2.42 (1H, m, CH_AH_B), 2.72-2.85 (2H, m, CH₂), 2.94-3.01 (1H, m, CH_AH_B), 3.76 (1H, d, $J \sim 8.1$, CH_CH_DO), 3.81 (1H, d, $J \sim 8.1$, CH_CH_DO), 7.06 (1H, d, $J=7.4$, CH_{Ar}), 7.30 (1H, d, $J=7.4$, CH_{Ar}), 7.31 (1H, dd, $J=7.4$ & 1.3, CH_{Ar}), 7.37 (1H, dt, $J=7.4$ & 1.3, CH_{Ar}), 7.57-7.62 (2H, m (~t), CH_{Ar}) & 7.69-7.71 (1H, m (~d), CH_{Ar}); δ_{C} Unfortunately insufficient material to obtain a clear spectrum; m/z (EI) 317 [100 %, (M⁺)], 274 (65), 203 (70), 100 (84); Crystal data C₂₂H₂₃NO $M = 317.41$, colourless needles, crystal dimensions 0.27 x 0.1 x 0.05 mm, orthorhombic, space group Pbca, $a = 7.2553$ (3), $b = 18.2486$ (6), $c = 25.7308$ (9) Å, $\alpha = \beta = \gamma = 90$ °, $V = 3406.7$ (2) Å³, $D_c = 1.238$ Mg/m³, $T = 173$ (2) K, $Z=8$, $R = 0.0446$, R_w 0.1174 for 2960 reflections with $I > 2\sigma(I)$ and 219 variables.

4,4-Dimethyl-2-(9-phenyl-6,7,8,9-tetrahydro-5H-benzocyclohepten-1-yl)-2-oxazoline
150



Yield (19 %); δ_{H} 1.24 (3H, s, CH₃), 1.28 (3H, s, CH₃), 1.30-1.40 (1H, m, C⁶H_AH_B), 1.68-1.89 (3H, m, C⁶H_AH_B & C⁷H₂), 1.95-2.06 (1H, m, C⁸H_CH_D), 2.47-2.66 (3H, m, C⁸H_CH_D & C⁵H₂), 3.89 (1H, d, AB doublet $J \sim 8.1$, CH_EH_FO), 3.94 (1H, d, AB doublet $J \sim 8.1$, CH_EH_FO), 5.01 (1H, dd, $J = 5.9$ & 2.7 , C⁹H), 7.02 (2H, d, $J = 8.1$, C¹⁰H), 7.10-7.31 (5H, m, C³H, C⁴H, C¹¹H & C¹²H), 7.44 (1H, dd, $J = 5.8$ & 3.4 , C²H); δ_{C} 25.1 (C⁷), 27.4 (C⁶), 28.0 (CH₃), 28.1 (CH₃), 30.7 (C⁸), 35.9 (C⁵), 44.4 (C⁹), 67.5 ((CH₃)₂C), 78.9 (CH₂O), 125.1 (C¹²), 126.3 (C³), 127.4 (C¹⁰), 127.8 (C²), 128.0 (C¹¹), 130.2 (C¹), 132.5 (C⁴), 142.2 (C^{9'} or C^{9''}), 142.3 (C^{9'} or C^{9''}), 144.2 (C^{4'}) and 163.9 (C=N); m/z (EI) 319 [100 %, (M⁺)], 291 (27), 290 (20), 247 (20), 228 (16), 219 (24), 202 (25), 189 (24) [Found: (M)⁺, 319.1933 C₂₂H₂₅NO requires 319.1936].

2-[1,5-Diphenylpentyl]-4,4-dimethyl-2-oxazoline **147**

Yield (7 %); m/z (EI) 321 [20 %, (M⁺)], 202 (100, M-PhCH₂CH₂CH₂), 188 (82, M-PhCH₂CH₂CH₂CH₂), 91 (38).

Yields indicated were determined by a combination of ¹H-NMR and GCMS analysis. Alkene **148** and fluorene **149** were obtained pure by crystallisation from the impure fractions obtained from column chromatography. Fluorene **149** was contained in the same fraction as alkane **150**. Only butylated product **145** was obtained pure from column chromatography.

Reactions under similar conditions in THF, either in the dark or under irradiation for 6-48 h were carried out and the yields are shown in Table 13, Section 2.5.2.2

3.11.3.6 2-[3-(2-Bromophenyl)-1-phenylhexyl]-4,4-dimethyl-2-oxazoline 112

Reactions of 2-[3-(2-bromophenyl)-1-phenylhexyl]-4,4-dimethyl-2-oxazoline **112** were carried out in THF, using the standard conditions (Section 3.11.3.1), for 6 h with UV irradiation and for 48 h in the dark. $^1\text{H-NMR}$ spectroscopy revealed both reactions produced a multitude of products. Due to the small scale of these reactions (ca. 0.24 mmol), it was decided to combine the crude mixtures from both reactions to enable column chromatography to be carried out with hope of identifying reaction products. The many fractions (ca. 8) obtained from the column were analysed via $^1\text{H-NMR}$ spectroscopy and GCMS. The analysis and discussion of these results are shown in Table 14, Section 2.5.3.

3.11.3.7 (4S)-2-[3-(2-Bromophenyl)-1-phenyl-propyl]-4-isopropyl-2-oxazoline (S)-103

(4S)-2-[3-(2-Bromophenyl)-1-phenyl-propyl]-4-isopropyl-2-oxazoline (**S**)-**103** was placed in a solution of LDA in THF and the resulting mixture stirred for 48 h in the dark as described in Section 3.11.3.1. After work up, column chromatography was performed, using 9:1 hexanes:EtOAc as elutant, to yield diastereomeric indanes (**S**, **R**)-**174** and (**S,S**)-**175** in a combined yield of 72 %. The d. e. was 42 % with (**S,S**)-**174** found to be the major isomer after hydrolysis to amide (**S**)-**175** and subsequent X-ray analysis.

(4S,1'R)-4-Isopropyl-2-(1'-phenyl-indan-1'-yl)-2-oxazoline (S,R)-174

R_f (SiO₂, 9:1 hexanes:EtOAc) 0.2; $[\alpha]_D^{25}$ 96.8 (*c* 1.02 in MeOH); $\nu_{\max}/\text{cm}^{-1}$ 1655(C=N); δ_{H} 0.94 (3H, d, $J=6.7$, CH₃), 1.02 (3H, d, $J=6.7$, CH₃), 1.90 (1H, sept, $J=6.7$, CH), 2.26-2.34 (1H, m, CH_AH_BCH_CH_D), 2.79-2.89 (1H, m, CH_AH_BCH_CH_D), 2.97-3.07 (1H, m, CH_AH_BCH_CH_D), 3.19-3.28 (1H, m, CH_AH_BCH_CH_D), 3.87-4.04 (2H, m, CH_EH_F & CHN), 4.19-4.25 (1H, m, CH_EH_F), 7.09-7.38 (8H, m, ArH) and 7.46-7.49 (1H, m, ArH); δ_{C} 17.9 (CH₃), 19.2 (CH₃), 30.5 (CH₂), 32.4 ((CH₃)₂CH), 41.2 (ArCH₂), 58.6 (PhC), 70.1 (CH₂O), 71.8 (CHN), 124.6 (CH), 126.3 (CH), 126.6 (CH), 126.7 (CH), 126.8 (CH), 127.7 (CH), 128.2 (CH), 143.9 (C), 144.4 (C), 144.7 (C) and 168.8

(C=N); m/z (CI) 306 [100 %, (M+H)⁺] [Found: (MH)⁺, 306.1862. C₂₁H₂₄NO requires, 306.1858].

(4*S*,1'*S*)-4-Isopropyl-2-(1'-phenyl-indan-1'-yl)-2-oxazoline (*S,S*)-174

R_f (SiO₂, 9:1 hexanes:EtOAc) 0.15; $[\alpha]_D^{25}$ 106.9 (*c* 0.32 in CHCl₃); $\nu_{\max}/\text{cm}^{-1}$ 1654 (C=N); δ_H 0.74 (3H, d, *J*=6.8, CH₃), 0.85 (3H, d, *J*=6.8, CH₃), 1.70 (1H, sept, *J*=6.8, CH), 2.26-2.35 (1H, m, CH_AH_BCH_CH_D), 2.80-2.90 (1H, m, CH_AH_BCH_CH_D), 2.98-3.08 (1H, m, CH_AH_BCH_CH_D), 3.15-3.24 (1H, m, CH_AH_BCH_CH_D), 3.95-4.06 (2H, m, CH_EH_F & CHN), 4.19-4.26 (1H, m, CH_EH_F), 7.09-7.13 (1H, m, ArH), 7.17-7.30 (7H, m, ArH) and 7.41-7.48 (1H, m, ArH); δ_C 17.6 (CH₃), 18.5 (CH₃), 30.5 (CH₂), 32.6 (CH(CH₃)₂), 41.3 (CH₂), 70.3 (CH₂O), 71.4 (CHN), 124.6 (CH_{Ar}), 126.3 (CH_{Ar}), 126.5 (CH_{Ar}), 126.6 (CH_{Ar}), 126.7 (CH_{Ar}), 127.7 (CH_{Ar}), 128.2 (CH_{Ar}), 144.0 (C_q), 144.2 (C_q), 144.6 (C_q) and 168.9 (C=N); m/z (CI) 306 [100 %, (M+H)⁺] [Found: (MH)⁺, 306.1865. C₂₁H₂₄NO requires 306.1858].

(1*S*, 1'*S*)-1'-Phenyl-indan-1'-carboxylic acid (2-hydroxy-1-isopropylethyl)-amide (*S,S*)-175

(4*S*, 1'*R*)-4-Isopropyl-2-(1'-phenyl-indan-1'-yl)-2-oxazoline (0.5 g, 1.6 mmol) in 2 % hydrochloric acid solution (50 cm³) was stirred at room temperature overnight. The reaction mixture was extracted with ether (50 cm³) and the aqueous layer was treated with 10 % sodium hydrogencarbonate solution. The resulting mixture was extracted with dichloromethane (3x50 cm³). The combined organic layers were washed with brine, dried (MgSO₄) and evaporated in vacuo to give a yellowish oil. The oil was left to stand for 2 days or until the oil had all crystallised. The crude product was then recrystallised from EtOAc/hexanes to give amide **87** (0.5 g, 95 %) as white needles; mp 115.5-117.0; $[\alpha]_D^{25}$ 8.9 (*c* 0.96 in MeOH); (Found: C, 78.2; H, 8.0; N, 4.4. C₂₁H₂₅NO₂ requires C, 78.0; H, 7.7; N, 4.3 %); $\nu_{\max}/\text{cm}^{-1}$ 1638 (C=O), 3290 and 3357; δ_H 0.65 (3H, d, *J*=6.9, CH₃), 0.77 (3H, d, *J*=6.9, CH₃), 1.66-1.82 (1H, m, CH(CH₃)₂), 2.17 (1H, br s, OH), 2.36-2.45 (1H, m, CH_AH_BCH_CH_D), 2.84-2.93 (1H, m, CH_AH_BCH_CH_D), 2.96-3.07 (1H, m, CH_AH_BCH_CH_D), 3.18-3.27 (1H, m, CH_AH_BCH_CH_D), 3.57-3.63 (1H, m, OCH_EH_F), 3.68-3.78 (2H, m, CHN and OCH_EH_F),

5.68 (1H, d, $J=7.4$, NH) and 7.18-7.37 (9H, m, ArH); δ_C 18.0, 19.5, 28.8, 30.8, 41.0, 57.9, 64.8, 66.0, 124.9 (CH_{Ar}), 125.4 (CH_{Ar}), 126.8 (CH_{Ar}), 127.1 (CH_{Ar}), 127.7 (CH_{Ar}), 128.1 (CH_{Ar}), 128.6 (CH_{Ar}), 143.2, 145.0, 145.1 and 175.4 (C=O); m/z (CI) 324 [100 %, (M+H⁺) [Found: (MH)⁺, 324.1964. C₂₁H₂₆NO₂ requires 324.1964]; Crystal data C₂₁H₂₅NO₂ $M = 323.42$, colourless needles, crystal dimensions 0.13 x 0.05 x 0.03 mm, monoclinic, space group P2₁, $a = 11.408$ (4), $b = 6.736$ (2), $c = 12.400$ (4) Å, $\beta = 107.562$ (5)°, $V = 908.5$ (5) Å³, $D_c = 1.182$ Mg/m³, $T = 125$ (2) K, $Z=2$, $R = 0.0625$, $R_w = 0.1293$ for 2993 reflections with $I > 2\sigma(I)$ and 228 variables.

Results of reactions under UV irradiation for 6 hours and at lower temperatures in THF using the same procedure are shown in Table 19, Section 2.7.1.

3.11.3.8 2-[3-(2-Bromo-phenyl)-1-phenyl-propyl]-4-*tert*-butyl-2-oxazoline

(4*S*)-2-[3-(2-Bromo-phenyl)-1-phenyl-propyl]-4-*tert*-butyl-2-oxazoline (*S*)-**104** was reacted in THF for either 6 h under irradiation or 48 h in the dark at r. t. as prescribed in the general procedure Section 3.11.3.1. After work up the ¹H-NMR spectrum of the crude material showed only diastereomeric indanes (*S,R*)-**174** and (*S,S*)-**174** the results of which are detailed in Table 20, Section 2.7.2., as are the selectivities which were determined by either ¹H-NMR (integration of ^tBu signals) or GCMS (peak areas). The yields were determined by analysis of crude ¹H-NMR spectra. An attempt was made to separate the two isomers from each other by the use of column chromatography which gave only the hydrolysis products (*S,R*)-**220** and (*S,S*)-**220** as an isomeric mixture in a yield of 80 %.

(4*S*)-4-*tert*-Butyl-2-(1'-phenyl-indan-1'-yl)-2-oxazoline (*S*)-**176**

Mixture of isomers

δ_H 0.63 (9H, s, (CH₃)₃, major isomer), 0.82 (9H, s, (CH₃)₃, minor isomer), 2.10-2.20 (1H, m, CH_AH_BCH_CH_D), 2.63-2.78 (1H, m, CH_AH_BCH_CH_D), 2.82-2.97 (1H, m, CH_AH_BCH_CH_D), 3.00-3.18 (1H, m, CH_AH_BCH_CH_D), 3.69 (1H, dd, $J=10.4$ & 8.2 , CHN, minor isomer), 3.79 (1H, dd, $J=10.0$ & 6.7 , CHN, major isomer), 3.90-3.95 (1H, m, CH_AH_BO), 4.01-4.07 (1H, m, CH_AH_BO), 6.95-7.02 (2H, m, ArH), 7.02-7.16

(6H, m, ArH) and 7.28-7.37 (1H, m, ArH); Isolated after purification as the β -hydroxyamide (**S**)-220.

(1'*S*)-1-Phenyl-indan-1-carboxylic acid (1'-hydroxymethyl-2',2'-dimethyl-propyl)-amide (**S**)-220

Mixture of isomers (3:2)

Yield (80 %), R_f (9:1 hexane:EtOAc) 0.1; ν_{\max} (Film)/ cm^{-1} 1629 (C=N) & 3344 (NH & OH); δ_H 0.68 (9H, s, (CH₃)₃, major isomer), 0.81 (9H, s, (CH₃)₃, minor isomer), 2.38-2.48 (1H, m, CH_AH_BCH_CH_D), 2.79-3.07 (2H, m, CH_AH_BCH_CH_D & CH_AH_BCH_CH_D), 3.18-3.30 (1H, m, CH_AH_BCH_CH_D), 3.35-3.49 (1H, m, CHN), 3.74-3.88 (2H, m, CH₂O), 5.67 (1H, d, $J=8.0$, NH, minor isomer), 5.73 (1H, d, $J=8.0$, NH, major isomer) and 7.16-7.37 (9H, m, ArH); δ_C 26.6 ((CH₃)₃C, major isomer), 26.8 ((CH₃)₃C, minor isomer), 30.7 (CH₂, minor isomer), 30.8 (CH₂, major isomer), 33.0 ((CH₃)₃C, major isomer), 33.3 ((CH₃)₃C, minor isomer), 40.4 (CH₂, minor isomer), 41.2 (CH₂, major isomer), 60.5 (CHN, minor isomer), 60.6 (CHN, major isomer), 63.8 (CH₂O, minor isomer), 63.9 (CH₂O, major isomer), 65.9 (PhC, minor isomer), 66.1 (PhC, major isomer), 124.9 (CH_{Ar}), 125.38 (CH_{Ar}, minor isomer), 125.44 (CH_{Ar}, major isomer), 126.7 (CH_{Ar}, minor isomer), 126.8 (CH_{Ar}, major isomer), 127.1 (CH_{Ar}, major isomer), 127.2 (CH_{Ar}, minor isomer), 127.6 (CH_{Ar}), 127.9 (CH_{Ar}, minor isomer), 128.1 (CH_{Ar}, major isomer), 128.5 (CH_{Ar}, minor isomer), 128.6 (CH_{Ar}, major isomer), 142.9 (C_q, minor isomer), 143.0 (C_q, major isomer), 144.8 (C_q, major isomer), 144.9 (C_q, minor isomer), 145.0 (C_q, major isomer), 145.3 (C_q, minor isomer), 175.5 (C=O, major isomer) and 175.8 (C=O, minor isomer); m/z (ES+) 360 [100 %, (M+Na⁺)], [Found: (MNa)⁺, 360.1935. C₂₂H₂₇NO₂Na requires 360.1939].

3.11.3.8.1 With (-)-Spartiene

(*S*) and (*R*)-2-[3-(2-Bromophenyl)-1-phenyl-propyl]-4 isopropyl-2-oxazoline (**S**)-104 & (**R**)-104 were reacted for 48 hours at r.t in a THF solution of LDA using the general procedure (Section 3.11.3.1) with the exception that 3.5-10 eq of (-)-Spartiene (-)-183 was added prior to addition of the oxazoline. The amount of THF added on reaching r. t. was adjusted such that the oxazoline concentration was equal

to either 0.036 or 0.1 M. After a standard workup a small amount of crude material was analysed via GCMS to obtain the diastereoeccess of the formed indane **104**.

3.11.3.9 (4*S*)-2-[3-(2-Bromo-phenyl)-1-phenyl-propyl]-4-phenyl-2-oxazoline (S)-**105**

(4*S*)-2-[3-(2-Bromo-phenyl)-1-phenyl-propyl]-4-phenyl-2-oxazoline (S)-**105** was reacted using the standard conditions (Section 3.11.3.1) with 3 eq. LDA and stirred for 48 h at r.t.. After work up the crude product was identified as 4-phenyl-2-(1'-phenyl-indan-1'-yl)-oxazole **177** (NMR yield 60 %); δ_{H} 2.30-2.40 (1H, m, CH_AH_B), 2.78-2.88 (1H, m, CH_AH_B), 2.96-3.06 (1H, m, CH_AH_B), 3.15-3.24 (1H, m, CH_AH_B) and 6.98-7.70 (15H, m, vinyl & CH_{Ar}).

3.11.3.10 (4*S*)-2-[3-(2-Bromo-phenyl)-1-phenylpropyl]-4-cyclohexylmethyl-2-oxazoline (S)-**107**

Using the standard conditions (Section 3.11.3.1) (4*S*)-2-[3-(2-bromo-phenyl)-1-phenylpropyl]-4-cyclohexylmethyl-2-oxazoline (S)-**107** was reacted in THF. The reaction mixture was worked up to afford the crude 4-cyclohexylmethyl-2-(1'-phenylindan-1'-yl)-2-oxazoline **181** *m/z* (EI) 359 [100 %, (M⁺)], 193 (90, M - 4-cyclohexylmethyloxazolin-2yl), 115 (28). Analysis of the crude product mixture by GCMS gave the diasteric excesses, 16 % 48 h, r.t and 16 % 6 h, UV.

3.11.4 LDA/THF & LDA THF/Hexane With Iron(II) Salts

General Procedure

To a solution of LDA (3 eq) in either THF or 2:1 hexane:THF mixture (6 cm³/mmol) at -78 °C under nitrogen was added a solution of the substrate in the reaction solvent (3 cm³/mmol). After stirring for 10 min the solution was allowed to warm to room temperature over 30 min. After which time more solvent was added (18 cm³/mmol) followed by the addition of either 10 mol % or 1 eq of anhydrous Iron(II) chloride. The mixture was then stirred for 1 hour, after which a saturated solution of ammonium chloride (10 cm³/mmol) was added. The aqueous layer was extracted with

three portions of ether (5 cm³/mmol), and the combined organic layers were washed with water (10 cm³/mmol) and dried (MgSO₄) to give the crude product.

Following the general procedure above 2-[3-(2-Bromophenyl)-1-phenylpropyl]-4,4-dimethyl-2-oxazoline **34b** reacted in either THF or 2:1 THF:hexanes with addition of 0.1 or 1 eq. of iron(II)chloride anhydrous. The reaction was worked up to give the crude products. ¹H-NMR analysis revealed the formation of several products, these were 4,4-dimethyl-2-(1'-phenyl-indan-1'-yl)-2-oxazoline **140** (for data see Section 3.11.2.3), 2-[1,3-diphenylpropyl]-4,4-dimethyl-2-oxazoline **141** (for data see Section 3.11.1.3) and styrenes **142** & **143** (for data see Section 3.11.3.2) plus starting material. The product distributions for reactions in THF are shown in Table 7, Section 2.4.3.1 and 2:1 THF:hexanes in Table 9, Section 2.4.4.1.

3.11.5 NaH/DMSO

NaH (60 % dispersion in mineral oil) (32.4 mg, 0.81 mmols), was weighed out into a 25 cm³ three necked flask and placed under a stream of nitrogen. Dry THF (1 cm³) was added and stirred. The NaH was allowed to settle to the bottom of the flask and the THF withdrawn using a syringe. This was repeated. Dry distilled dimethyl sulfoxide (4 cm³) was then added slowly with stirring. After ten min 2-propyl-2-oxazoline **34b** (1 cm³, 0.27M solution in dry DMSO) was added dropwise with stirring. Then with either heating and/or UV irradiation and/or Fe(II)Cl₂ (1eq) the mixture was stirred for between 10 min and 4h. Finely ground ammonium chloride (0.5 g), was added and stirred for ten min. Water (5 cm³) and ether (10 cm³) were added and the aqueous layer extracted with ether (2x5 cm³). The combined organic extracts were washed (water (5 cm³)), dried (MgSO₄) and concentrated in vacuo to give the crude reaction mixture. The crude reaction mixture was then washed into an NMR tube with CDCl₃ and 5µl of dibromomethane was added, and the product distribution analysed by comparison of the integration of the product signals.

2-[3-(2-Bromophenyl)-1-phenylpropyl]-4,4-dimethyl-2-oxazoline **34b** was reacted as detailed above and the following products were identified by ¹H-NMR spectroscopy: 4,4-dimethyl-2-(1'-phenyl-indan-1'-yl)-2-oxazoline **140** (for data see Section 3.11.2.3) and 2-[1,3-diphenylpropyl]-4,4-dimethyl-2-oxazoline **141** (for data

see Section 3.11.1.3). Conditions and yields of these products are shown in Table 10, Section 2.4.5.

3.11.6 With Phenanthrene Radical Anion

General Procedure

To a stirring solution of diisopropylamine HCl (18 mg, 0.13 mmol) in THF (5 cm³) was added at 0 °C under N₂, *n*-BuLi (2.5 M solution in hexanes) (0.1 cm³, 0.26 mmol). After stirring for 10 min the mixture was cooled to -78 °C and oxazoline **34b** (50 mg, 0.13 mmol) in THF (2 cm³) was added. The mixture was then stirred at -78 °C for 15 min, after which 0.02M phenanthrene radical anion solution in THF (prepared by the addition of stoichiometric amounts of phenanthrene and sodium metal in THF and stirred overnight under nitrogen) (0.65 – 6.5 cm³) was added. The resultant mixture was then stirred for 3 h at -78 °C and saturated ammonium chloride solution (5 cm³) was added and a standard aqueous workup with ether was performed.

In the case where no diisopropylamine HCl was added the reaction was carried out as above keeping reactant concentrations the same with only one equivalent of *n*-BuLi.

2-[3-(2-Bromophenyl)-1-phenylpropyl]-4,4-dimethyl-2-oxazoline **34b** was reacted using the standard conditions above. After work up 2-[1,3-diphenylpropyl]-4,4-dimethyl-2-oxazoline **141** (for data see Section 3.11.1.3). and styrenes **142** & **143** (for data see Section 3.11.3.2) were identified by ¹H-NMR analysis and the distribution determined (Table 7, Section 2.4.3.1).

3.11.7 Preparation of EPR Samples

The EPR tube was prepared by the drawing out a 1 mm ID capillary from the bottom of a standard 4 mm OD quartz EPR tube. The open end of the tube was then capped with a rubber septum and a fine needle connected to a nitrogen line was inserted through the septum, as was an exit needle. The tube was heated hard with an industrial airgun for at least 10 min under nitrogen to expel any moisture. The solutions of the substrates were prepared as detailed in Section 3.11.3 and a sample

was taken after warming to r.t. via a nitrogen flushed syringe and injected carefully into the prepared EPR tube. The nitrogen inlet needle in the tube was then pushed below the surface of the liquid to degas the sample. After 10 min all needles were removed and the septum protectively covered with Parafilm[®] and the EPR measurements carried out immediately.

3.12 Oxazolidinones

4-(2-Bromophenyl)-2-phenylbutyric acid **189**

To a solution of phenyl acetic acid **23** (1 g, 7.3 mmol) in THF (30cm³), under N₂ at -78 °C was added carefully dropwise 2 eq n-BuLi (5.9 cm³, 14.7 mmol). After stirring for 20 min 2-bromophenethyl iodide **37b** (2.3 g, 7.3 mmol) in THF (5 cm³) was added dropwise over 5 min. The mixture was allowed to warm to room temperature over 2 h and stirred overnight. The mixture was quenched by addition of solid ammonium chloride and the solvent removed. The residue was dissolved in 2M hydrochloric acid (100 cm³), and the cloudy mixture extracted with dichloromethane (3x 50cm³). The combined organic layers were dried (MgSO₄) and concentrated in vacuo to give the crude acid **189** (1.8 g, 77 %) which was used without further purification; $\nu_{\max}(\text{Nujol})/\text{cm}^{-1}$ 1705 (C=O) & 3060 (OH); δ_{H} 2.05-2.18 (1H, m, CHCH_ACH_B), 2.33-2.46 (1H, m, CHCH_ACH_B), 2.62-2.78 (2H, m, ArCH₂), 3.61 (1H, t, $J=7.6$, PhCH), 7.00-7.05 (1H, m, ArH), 7.13-7.35 (7H, m, ArH) and 7.48-7.51 (1H, m, HCCBr), CO₂H not observed; δ_{C} 32.8 (CH₂), 34.0 (CH₂), 51.0 (PhCH), 124.4 (CBr), 127.5 (CH_{Ar}), 127.7 (CH_{Ar}), 127.8 (CH_{Ar}), 128.2 (CH_{Ar}), 128.8 (CH_{Ar}), 130.5 (CH_{Ar}), 132.9 (CH_{Ar}), 137.9 (C_q), 140.5 (C_q) and 179.5 (C=O); m/z (CI) 319 [100 %, (M+H⁺)], [Found: (MH)⁺, 319.0326. C₁₆H₁₅O₂⁷⁹Br requires 319.0334].

4-(2-Bromophenyl)-2-phenylbutyryl chloride **187**

Distilled thionyl chloride (1.2 cm³, 17 mmol) was added slowly via syringe to 4-(2-Bromophenyl)-2-phenylbutyric acid **189** (1.8 g, 5.6 mmol). The solution was then heated under reflux at 75 °C for 1.5 h and left to stand over night at room temperature. The excess thionyl chloride was removed under vacuum to afford the crude product **187** (1.89 g, 99 %) which was used immediately without further purification; δ_{H} 2.10-2.22 (1H, m, CHCH_ACH_B), 2.42-2.54 (1H, m, CHCH_ACH_B), 2.62-2.79 (2H, m, ArCH₂), 4.01 (1H, t, $J=7.5$, PhCH), 7.03-7.41 (8H, m, ArH) and 7.51 (1H, d, $J=7.9$, HCCBr); δ_{C} 33.0 (CH₂), 33.6 (CH₂), 62.8 (PhCH), 124.3 (CBr), 127.6 (CH_{Ar}), 128.0 (CH_{Ar}), 128.4 (CH_{Ar}), 128.43 (CH_{Ar}), 129.1 (CH_{Ar}), 130.4 (CH_{Ar}), 133.0 (CH_{Ar}), 135.4 (C_q), 139.8 (C_q) and 174.6 (C=O).

4,4-Dimethyloxazolidin-2-one 185

A stirred mixture of 2-amino-2-methylpropan-1-ol **31** (15.5 g, 174 mmol), diethylcarbonate (21 cm³, 174 mmol) and potassium carbonate (2.4 g, 18 mmol) were heated at 120-126 °C with removal of ethanol (20 cm³, 348 mmol). After cooling, ethanol (500 cm³) was added and the solution was filtered through a pad of celite to remove potassium carbonate. After the solution was concentrated to ca. 180 cm³, it was slowly cooled to 0 °C and allowed to crystallise, filtrating afforded the known oxazolidinone as a white solid **185** (13.4 g, 67 %); mp 54.8-56.8 (EtOH-Et₂O) [Lit.,³³ 56.5-58.0 (EtOH-Et₂O)]; δ_{H} 1.37 (6H, s, 2x CH₃), 4.09 (2H, s, CH₂O) and 6.11 (1H, br s, NH).

4,4-Dimethyl-3-phenylacetyloxazolidin-2-one 186

To a solution of 4,4-dimethyloxazolidinone **185** (5 g, 43 mmol) in dry distilled THF (130 cm³) under nitrogen at -78 °C was added 2.5 M n-BuLi solution in hexanes (20 cm³, 50 mmol). After stirring for 10 min, freshly distilled phenylacetyl chloride (6.6 cm³, 50 mmol) was added via a syringe. The resulting nearly colourless solution was stirred for 30 min at -78 °C and then allowed to warm to room temperature over 30 min. Excess acid chloride was quenched by addition of saturated ammonium chloride solution (25 cm³). The THF and hexane were removed in vacuo and the resultant slurry extracted with dichloromethane (2x 35 cm³). The combined organic layers were washed with sodium hydroxide solution (30 cm³) and brine (30 cm³). After drying (Na₂SO₄) and removal of the solvent, the crude product was purified via column chromatography (SiO₂, 9:1 hexanes:EtOAc) to give the pure oxazolidinone **186** as a clear oil (7.7 g, 77 %); R_f (SiO₂, 9:1 hexanes:EtOAc) 0.1; ν_{max} (Nujol)/cm⁻¹ 1702 (C=O) & 1777 (C=O); δ_{H} 1.55 (6H, s, 2x CH₃), 3.98 (2H, s, PhCH₂), 4.24 (2H, s, CH₂O) and 7.19-7.38 (5H, m, Ph); δ_{C} 24.7 (2x CH₃), 43.1 (PhCH₂), 60.5 ((CH₃)₂C), 75.1 (CH₂O), 127.0 (CH_{Ar}), 128.4 (CH_{Ar}), 129.6 (CH_{Ar}), 133.8 (C_q), 153.9 (CON) and 172.1 (CO₂); m/z (CI) 234 [100 %, (M+H⁺)], [Found: (MH)⁺, 234.1134. C₁₃H₁₆NO₃ requires 234.1130].

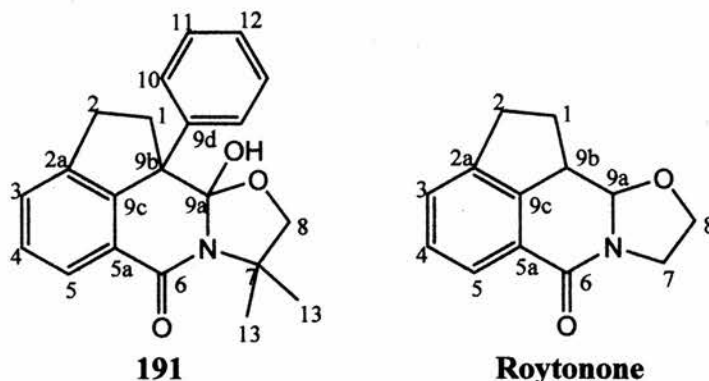
3-[4-(2-Bromophenyl)-2-phenylbutyryl]-4,4-dimethyloxazolidin-2-one **188**

To a solution of 4,4-dimethyloxazolidinone **185** (0.65 g, 5.6 mmol) in dry distilled THF (17 cm³) under nitrogen at -78 °C was added 2.5 M n-BuLi solution in hexanes (2.24 cm³, 5.6 mmol). After stirring for 10 min, 4-(2-bromophenyl)-2-phenylbutyryl chloride **187** (1.9 cm³, 5.6 mmol) in THF (5 cm³) was added via a syringe. The resulting nearly colourless solution was stirred for 30 min at -78 °C and then allowed to warm to room temperature over 30 min. Excess acid chloride was quenched by addition of saturated ammonium chloride solution (10 cm³). The THF and hexane were removed in vacuo and the resultant slurry extracted with dichloromethane (2x 15 cm³). The combined organic layers were washed with sodium hydroxide solution (10 cm³) and brine (10 cm³). After drying (Na₂SO₄) and removal of the solvent, the crude product was purified via column chromatography (SiO₂, 9:1 hexanes:EtOAc) to give the pure oxazolidinone **188** as a clear oil (1.5 g, 64 %); R_f (SiO₂, 9:1 hexanes:EtOAc) 0.1; ν_{\max} (Nujol)/cm⁻¹ 1698 (C=O) & 1778 (C=O); δ_{H} 1.39 (3H, s, CH₃), 1.58 (3H, s, CH₃), 1.98-2.14 (1H, m, PhCHCH_AH_B), 2.33-2.45 (1H, m, PhCHCH_AH_B), 2.51-2.76 (2H, m, ArCH₂), 3.76 (1H, d, *J*=8.4, CH_CH_DO), 3.91 (1H, d, *J*=8.4, CH_CH_DO), 5.03 (1H, t, *J*=7.4, PhCH), 6.98-7.03 (1H, m, ArH), 7.14-7.37 (1H, m, ArH) and 7.46-7.49 (1H, m, HCCBr); δ_{C} 24.2 (CH₃), 25.2 (CH₃), 34.0 (CH₂), 34.2 (CH₂), 49.9 (PhCH), 60.6 ((CH₃)₂C), 74.9 (CH₂O), 124.4 (CBr), 127.3 (CH_{Ar}), 127.5 (CH_{Ar}), 127.7 (CH_{Ar}), 128.6 (CH_{Ar}), 128.7 (CH_{Ar}), 130.4 (CH_{Ar}), 132.8 (CH_{Ar}), 138.8 (C_q), 141.0 (C_q), 153.6 (CON) and 174.5 (CO₂); *m/z* (CI) 416 [100 %, (M+H⁺)], [Found: (MH)⁺, 416.0855. C₂₁H₂₃NO₃⁷⁹Br requires 416.0861].

7,7-Dimethyl-9a-hydroxy-9b-phenylroytonone **191**³⁴

To a solution of 0.48 M LDA in THF (7.5 cm³) -78 °C under nitrogen was added a solution of oxazolidinone **188** (0.5 g, 1.2 mmol) in THF (3.5 cm³). After stirring for 10 min the solution was allowed to warm to room temperature over 30 min, at which time more THF (21 cm³) was added. The mixture was then stirred 48 h at r. t. in the dark. After this time a saturated solution of ammonium chloride (4 cm³) was added and the aqueous layer was extracted with three portions of ether (2 x 6 cm³). The combined organic layers were washed with water (10 cm³) and dried

(MgSO₄) to give the crude product. Column chromatography (SiO₂, 9:1 hexanes:THF) yielded the pure Roytonone **191** as a white wax (301 mg, 75 %);



R_f (SiO₂, 9:1 hexanes:EtOAc) 0.2; δ_H 0.70 (3H, s, CH₃), 1.60 (3H, s, CH₃), 2.64-2.69 (1H, m, C²H_AH_B), 2.76-2.85 (1H, m, C¹H_CH_D), 2.91-2.99 (2H, m, C²H_AH_B & C¹H_CH_D), 3.13 (1H, br. s, OH), 3.42 (1H, d, *J*=8.2, CH_EH_FO), 3.94 (1H, d, *J*=8.2, CH_EH_FO), 7.07-7.10 (2H, m, C¹⁰H_{Ar}), 7.17-7.21 (3H, m, C¹¹H_{Ar} & C¹²H_{Ar}), 7.40-7.45 (2H, m, C³H_{Ar} & C⁴H_{Ar}), & 7.80-7.82, (1H, m (~d), C²H_{Ar}) δ_C 22.4 (C13), 25.0 (C13), 31.3 (C1), 36.3 (C2), 58.9 (C7), 59.5 (C9b), 78.1 (C8), 112.4 (C9a), 123.8 (C5), 127.1 (C12), 127.4 (C11), 128.0 (C5a), 128.5(C3), 128.8 (C4), 129.6 (C10), 139.1 (C9d), 142.5 (C2a), 145.8 (C9c) & 162.6 (C6); *m/z* (CI) 336 [100 %, (M+H⁺)], [Found: (MH)⁺, 336.1604. C₂₁H₂₂NO₃ requires 336.1600].

4.13 Cycloalkylcarbaldehydes

4.13.1 Synthesis

Commercial cyclohexane carbaldehyde **205** was redistilled before use. 4-Methylcyclohexane carboxylic acid **209** (*cis/trans* mixture), 4-*tert*-butylcyclohexane carboxylic acid **207** (*cis/trans* mixture) and tetrahydropyran-2-methanol **212** were obtained commercially.

4.13.1.1 Carboxylic Acids

cis-4-Methylcyclohexane carboxylic acid **cis-209** was isolated, after hydrolysis, from the calcium salt **210** of the commercial isomeric mixture.³⁵ *cis* & *trans* 4-*tert*-Butylcyclohexane carboxylic acids **207** were separated from the commercial mixture of acids (*cis/trans* 55/45) via column chromatography using a column of silica (20 x 3.5 cm) eluting with dichloromethane. The R_f s of the *cis* and *trans* acids were 0.12 and 0.05 respectively.

cis-4-Methylcyclohexane carboxylic acid calcium salt **cis-210**³⁶

A portion of the commercial *cis/trans* 4-methylcyclohexane carboxylic acid **209** was dissolved in water and excess CaCO_3 added. The mixture was then heated to reflux and stirred for one hour. After cooling, the heterogeneous mixture was filtered to remove excess CaCO_3 . The water was evaporated until solid began to precipitate. The resulting mixture was heated to redissolve the solid and the solution covered and left to cool slowly. The first crop of crystals was collected and via $^1\text{H-NMR}$ was found to contain a 1:1 mixture of the *cis/trans*, the second crop contained 5:4 with the *cis* isomer predominating. The fourth crop yielded a 9:2 ratio and was deemed a suitable ratio; δ_{H} 0.84-0.90 (4H, m, *c*- C_6H_{11}), 1.15-1.26 (2H, m, *c*- C_6H_{11}), 1.41-1.53 (4H, m, *c*- C_6H_{11}), 1.53-1.18 (2H, m, *c*- C_6H_{11}), 2.14-2.23 (1H, m, *c*- C_6H_{11}).

cis-4-*t*-Butylcyclohexane carboxylic acid *cis*-207³⁷

δ_{H} 0.83 (9H, s, ^tBu), 0.93-1.03 (1H, m, *c*-C₆H₁₁), 1.08-1.25 (2H, m, *c*-C₆H₁₁), 1.41-1.52 (2H, m, *c*-C₆H₁₁), 1.63-1.68 (2H, m, *c*-C₆H₁₁), 2.21-2.27 (2H, m, *c*-C₆H₁₁), 2.67-2.71 (1H, m, *c*-C₆H₁₁), 11.58 (1H, br s, CO₂H).

4.13.1.2 Cycloalkylmethanols

To a suspension of lithium aluminium hydride (1.05 eq) in dry ether (30 cm³) at 0 °C under nitrogen was added dropwise a solution of the carboxylic acid (11 mmol) (in the case of the *cis*-4-methylcyclohexane carboxylic acid, the calcium salt was acidified with 1M hydrochloric acid and extracted in dichloromethane and the solvent dried and removed prior to use) in dry ether (20 cm³). After stirring for 10 min the mixture was heated under reflux for 2 h, cooled to 0 °C and water (5 cm³) was added dropwise with caution. The mixture was then stirred for 10 min and allowed to warm to room temperature over 20 min. Aqueous HCl (5M, 50 cm³) was added and the salts were allowed to dissolve. The aqueous layer was extracted with ether (3x 20 cm³). The combined organic layers were washed with saturated sodium bicarbonate (50 cm³), brine (50 cm³) and water (50 cm³). The organic layers were then dried (MgSO₄) and the solvent evaporated.

trans-4-*tert*-Butylcyclohexane methanol *trans*-208³⁸

Pale yellow liquid; δ_{H} 0.84 (9H, s, ^tBu), 0.86-1.07 (5H, m, *c*-C₆H₁₁), 1.35-1.46 (1H, m, *c*-C₆H₁₁), 1.76-1.88 (4H, m, *c*-C₆H₁₁), 1.93 (1H, br s, OH), 3.44 (2H, d, *J*=6.4, CH₂O).

cis-4-*tert*-Butylcyclohexane methanol *cis*-208³⁹

Pale yellow liquid; δ_{H} 0.83 (9H, s, ^tBu), 0.96-1.12 (3H, m, *c*-C₆H₁₁), 1.40-1.58 (4H, m, *c*-C₆H₁₁), 1.71-1.87 (4H, m, *c*-C₆H₁₁), 3.63 (2H, d, *J*=7.4, CH₂O) (OH not observed).

3.13.1.3 Cycloalkylmethanals

To a stirred solution of sodium acetate (1 eq) and sodium bicarbonate (1 eq) in dichloromethane (125 cm³), was added pyridinium chlorochromate (3 eq) followed by the alicyclic alcohol (6 mmol). The resultant suspension was stirred at room temperature for 1 h. After this time ether (200 cm³) was added and the mixture stirred for an additional 15 min. The suspension was poured through a pad of silica and the solvent evaporated. Distillation under reduced pressure afforded the pure aldehyde.

Cyclohexane carbaldehyde (*axial/equatorial* mixture) **205**.

δ_{H} (CD₂Cl₂) 1.2-1.45 (4H, m, *c*-C₆H₁₁), 1.6-1.8 (3H, m, *c*-C₆H₁₁), 1.8-1.95 (2H, m, *c*-C₆H₁₁), 2.2-2.35 (1H, m, *c*-C₆H₁₁), 5.31 (1H, m, *c*-C₆H₁₁), 9.61 (1H, d, *J*=1.3, CHO). At lower temperatures the spectrum broadened, coalescence was at ca. 213 K and below this temperature separate spectra for the axial and equatorial aldehydes were observed. Their concentration ratio [**205ax**]/[**205eq**] was determined from the formyl signals at 9.65 (**205ax**) and 9.52 (**205eq**).

T/K	204	203	198	193	188	183
[205ax]/[205eq]	0.119	0.118	0.118	0.106	0.118	0.105

trans-4-*tert*-Butylcyclohexane carbaldehyde *trans*-**203**⁴⁰

δ_{H} 0.86 (9H, s, ^tBu), 0.94-1.11 (3H, m, *c*-C₆H₁₁), 1.14-1.32 (2H, m, *c*-C₆H₁₁), 1.85-2.08 (2H, m, *c*-C₆H₁₁), 1.99-2.08 (2H, m, *c*-C₆H₁₁), 2.08-2.20 (1H, m, *c*-C₆H₁₁), 9.61 (1H, d, *J*=1.8, CHO).

cis-4-*tert*-Butylcyclohexane carbaldehyde *cis*-**203**⁸

δ_{H} 0.80 (9H, s, ^tBu), 0.82-0.88 (1H, m, *c*-C₆H₁₁), 0.88-1.00, (2H, m, *c*-C₆H₁₁), 1.40-1.60 (2H, m, *c*-C₆H₁₁), 1.60-1.72 (2H, m, *c*-C₆H₁₁), 2.24-2.34 (2H, m, *c*-C₆H₁₁), 2.38-2.44 (1H, m, *c*-C₆H₁₁), 9.72 (1H, d, *J*=0.8, CHO). δ_{C} 23.8, 24.1, 25.4, 27.3, 46.5, 47.8, 206.0.

cis-4-Methylcyclohexane carbaldehyde *cis*-204⁴¹

δ_{H} 0.91 (3H, d, $J=6.3$, CH₃), 1.18-1.32 (3H, m, *c*-C₆H₁₁), 1.50-1.62 (4H, m, *c*-C₆H₁₁), 1.98-2.09 (2H, m, *c*-C₆H₁₁), 2.53-2.60 (1H, m, *c*-C₆H₁₁) 9.60 (1H, s, CHO).

Tetrahydropyran-2-carbaldehyde (*axial/equatorial* mixture) 206⁴²

δ_{H} 1.38-1.65 (4H, m, *c*-C₅H₉O), 1.83-1.93 (2H, m, *c*-C₅H₉O), 3.41-3.60 (2H, m, *c*-C₅H₉O), 3.99-4.10 (1H, m, *c*-C₅H₉O), 9.62 (1H, s, CHO). The ¹H NMR was studied at lower temperatures in CD₂Cl₂ solution. The formyl signal broadened and showed a shoulder at 185 K, the lowest accessible temperature (~coalescence), but separate signals for the axial and equatorial conformers were not resolved.

3.13.2 EPR Sample Preparation

Solutions of freshly distilled aldehyde (ca. 0.1-0.2 M) and DTBP (20 μ l) were made up in 0.4 mm od quartz tubes and the solvent was distilled in. For reactions performed in cyclopropane or *n*-propane (up to 0.5 cm³), the solution was degassed on a vacuum line using the freeze-pump-thaw technique, and the quartz tube was flame sealed.

3.13.3 Computations.

Most of the computations for the cycloalkylacyl radicals were carried by Dr G. DiLabio at the National Institute of Nanotechnology, NRCC, Edmonton, Canada.

The following method of averaging hfs over rotational potentials was adopted because of the irregularity of the PES shape. For each minimum on the PES, rotational states up to RT ($T = 140$ K) should be occupied. The dihedral boundaries on the PES that corresponded to RT were obtained and assigned to the hfs vs. dihedral plot. An unweighted average of the area bounded by the dihedral boundaries and the hfs curve was obtained. This approach should be good to within a few tenths of a Gauss despite not taking into account explicit rotational energy levels.

3.14 Bibliography

- 1 R. A. Glennon, J. J. Salley, O. S. Steinstand and S. Nelson, *J. Med. Chem.*, 1981, **24**, 678-683.
- 2 P. L. Ornstein, T. J. Bleisch, M. B. Arnold, J. H. Kennedy, R. A. Wright, B. G. Johnson, J. P. Tizzano, D. R. Helton, M. J. Kallman, and D. D. Schoepp, *J. Med. Chem.*, 1998, **41**, 358-378.
- 3 G. Toth and K. E. Koeber, *Synth. Commun.*, 1995, **25**, 3067-3074.
- 4 J. P. Wolfe, R. A. Rennels, S. L. Bulchwald, *Tetrahedron*; 1996, **52**, 7525-7546.
- 5 R. G. Woolford and W. S. Lin, *Can. J. Chem.*, 1996, **44**, 2783-2791.
- 6 H. J. Reich, W. S. Goldenberg, A. W. Sanders, K. L. Jantzi and C. C. Tzschucke, *J. Am. Chem. Soc.*, 2003, **125**, 3509-3521.
- 7 P. A. Wender and A. W. White, *J. Am. Chem. Soc.*, 1988, **110**, 2218-2223.
- 8 P. A. Beak and D. J. Allen, *J. Am. Chem. Soc.*, 1992, **114**, 3420-3425.
- 9 K. Alexander (née Gillon), S. Cook, C. L. Gibson and A. R. Kennedy, *J. Chem. Soc., Perkin Trans. 1*, 2001, 1538-1549.
- 10 E. P. Kyba, J. M. Timko, L. J. Kaplan, F. De Jong, G. W. Gokel and D. J. Cram, *J. Am. Chem. Soc.*, 1978, **100**, 4555-4568.
- 11 B. D. White, J. Mallen, K. A. Arnold, F. R. Fronczek, R. D. Gandour, L. M. B. Gehrig and G. W. Gokel, *J. Org. Chem.*, 1989, **54**, 937-947.
- 12 H. Eckert and I. Ugi, *Liebigs Ann. Chem.*, 1979, 278-295.
- 13 D. L. J. Clive and J. Wang, *J. Org. Chem.*, 2004, **69**, 2773-2784.
- 14 Y. N. Belokon, L. K. Pritula, V. I. Tararov, V. I. Bakhmutov and Y. T. Struchkov, *J. Chem. Soc., Dalton Trans.*, 1990, 1867-1872.
- 15 J. M. Janey, T. Iwama, S. A. Kozmin and V. H. Rawal, *J. Org. Chem.*, 2000, **65**, 9059-9068.
- 16 K. Kamata, I. Agata and A. I. Meyers, *J. Org. Chem.*, 1998, **63**, 3113-3116.
- 17 A. N. Hulme, C. H. Montgomery and D. K. Henderson, *J. Chem. Soc., Perkin Trans. 1*, 2000, 1837-1841.
- 18 Y-A. Kim, H-M. Chung, J-S. Park, W. Choi, J. Min, N-H. Park, K-H. Kim, G-J. Jhon and S-Y. Han, *J. Org. Chem.*, 2003, **68**, 10162-10165.

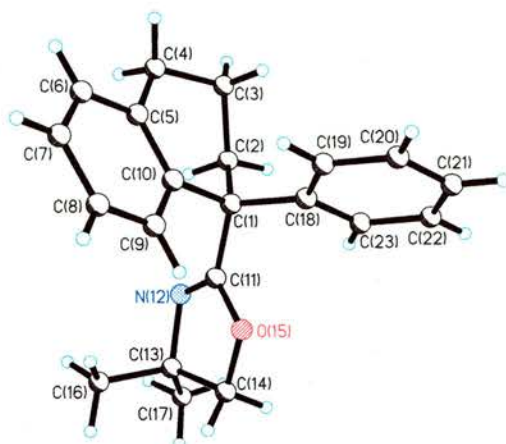
- 19 B Guttmann, *Helv. Chim. Acta*, 1958, 1852-1864.
- 20 G. Mackenzie, H. A. Wilson, G. Shaw and D. Ewing, *J. Chem. Soc., Perkin Trans. 1*, 1988, 2541-2546.
- 21 M. T. H. Liu, N. H. Chishti, M. Tencer, H. Tomioka and Y. Izawa, *Tetrahedron*, 1984, **40**, 887-892.
- 22 J. F. Bower, C. J. Martin, D. J. Rawson, A. M. Z. Slawin and J. M. J. Williams, *J. Chem. Soc., Perkin Trans. 1*, 1996; 333-342.
- 23 A. I. Meyers and J. Slade, *J. Org. Chem.*, 1980, **45**, 2785-2791.
- 24 S. Shibata, H. Matsushita, H. Kaneko, M. Noguchi, M. Saburi and S. Yoshikawa, *Bull. Chem. Soc. Jpn.*, 1982, **55**, 3546-3551.
- 25 S. Cossu, G. Giacomelli, S. Conti and M. Falorni, *Tetrahedron*, 1994, **50**, 5083-5090.
- 26 A. I. Meyers and P. M. Kendall, *Tetrahedron Lett.*, 1974, **14**, 1337-1340.
- 27 A. I. Meyers, G. Knaus, K. Kamata, and M. E. Ford, *J. Am. Chem. Soc.*, 1976, **98**, 567-576.
- 28 Assignment of isomer A or B is arbitrary.
- 29 D. S. Clarke, and R. Wood, *Synth. Commun.*, 1996, **26**, 1335-1340.
- 30 E. Martinez, J. C. Estevez, J. Ramon and L. Castedo, *Tetrahedron*, 2001, **57**, 1973-1980.
- 31 D. Chakravarti, *J. Indian Chem. Soc.*, 1939, **16**, 639-644.
- 32 G. Bradley, J. Clark and W. Kernick, *J. Chem. Soc., Perkin Trans. 1*, 1972, 2019-2023.
- 33 W. J. Close, *J. Am. Chem. Soc.*, 1951, **73**, 95-96.
- 34 Roytonone - 1,2,7,8,9a,9b hexahydro-9-oxa-6a-aza-cyclopenta[d]acenaphthyl-en-6-one.
- 35 T. Q. Chou and W. H. Perkin Jr., *J. Chem. Soc., Trans.*, 1911, 526-538.
- 36 J. Furukawa, T. Tsuyuki, N. Morisaki, N. Uemura and Y. Koiso, *Chem. Pharm. Bull.*, 1986, **34**, 5176-5179.
- 37 H. Van Bekkum, *Recl. Trav. Chim. Pays-Bas.*, 1970, **89**, 521-534.
- 38 P. Wessig and O. Muehling, *Helv. Chim. Acta.*, 2003, **86**, 865-893.
- 39 K. Hiroya, J. Hasegawa, T. Watanabe and K. Ogasawara, *Synthesis*, 1995, 379-381.

- 40 G. Accrombessi, P. Geneste, J-L Olive and A. A. Pavia, *Bull. Soc. Chim. Fr.*, 1981, 19-23.
- 41 X. Hou, Q. Xie and L. Dai, *J. Chem. Res. (M)*, 1997, **12**, 2665-2678.
- 42 P. Bianchi, G. Roda, S. Riva, B. Danieli, A. Zabelinskaja-Mackova and H. Griengl, *Tetrahedron*, 2001, **57**, 2213-2220.

Appendix A

X-Ray Crystal Data

Tetrahydronaphthalene 144

Table 1. Crystal data and structure refinement for **144**.

Identification code	144	
Empirical formula	C ₂₁ H ₂₃ N O	
Formula weight	305.40	
Temperature	93(2) K	
Wavelength	0.71073 Å	
Crystal system	Triclinic	
Space group	P-1	
Unit cell dimensions	a = 8.588(2) Å	$\alpha = 115.888(16)^\circ$.
	b = 10.0389(19) Å	$\beta = 98.06(2)^\circ$.
	c = 10.8881(13) Å	$\gamma = 92.69(2)^\circ$.
Volume	830.0(3) Å ³	
Z	2	
Density (calculated)	1.222 Mg/m ³	
Absorption coefficient	0.074 mm ⁻¹	
F(000)	328	
Crystal size	0.2000 x 0.2000 x 0.2000 mm ³	
Theta range for data collection	2.41 to 25.32°.	
Index ranges	-8 ≤ h ≤ 10, -12 ≤ k ≤ 10, -13 ≤ l ≤ 12	
Reflections collected	5017	
Independent reflections	2811 [R(int) = 0.0221]	
Completeness to theta = 25.32°	92.4 %	
Absorption correction	MULTISCAN	
Max. and min. transmission	1.0000 and 0.3816	
Refinement method	Full-matrix least-squares on F ²	
Data / restraints / parameters	2811 / 0 / 210	
Goodness-of-fit on F ²	1.074	
Final R indices [I > 2σ(I)]	R1 = 0.0462, wR2 = 0.1198	
R indices (all data)	R1 = 0.0519, wR2 = 0.1257	
Extinction coefficient	0.027(12)	
Largest diff. peak and hole	0.317 and -0.426 e.Å ⁻³	

Table 2. Atomic coordinates ($\times 10^4$) and equivalent isotropic displacement parameters ($\text{\AA}^2 \times 10^3$) for 144. $U(\text{eq})$ is defined as one third of the trace of the orthogonalized U^{ij} tensor.

	x	y	z	$U(\text{eq})$
C(1)	3498(2)	3861(1)	1570(1)	16(1)
C(2)	5325(2)	3987(1)	1734(1)	18(1)
C(3)	5972(2)	2735(1)	2009(1)	21(1)
C(4)	5660(2)	2915(1)	3407(1)	21(1)
C(5)	3959(2)	3140(1)	3578(1)	18(1)
C(6)	3372(2)	2886(1)	4603(1)	22(1)
C(7)	1817(2)	3051(1)	4795(1)	23(1)
C(8)	813(2)	3482(1)	3954(1)	22(1)
C(9)	1373(2)	3755(1)	2947(1)	19(1)
C(10)	2947(2)	3595(1)	2742(1)	16(1)
C(11)	2984(2)	5348(1)	1689(1)	16(1)
N(12)	3797(1)	6617(1)	2363(1)	18(1)
C(13)	2704(2)	7737(1)	2368(1)	19(1)
C(14)	1321(2)	6773(1)	1210(1)	22(1)
O(15)	1467(1)	5271(1)	1056(1)	22(1)
C(16)	2205(2)	8409(2)	3785(1)	28(1)
C(17)	3486(2)	8946(1)	2093(2)	28(1)
C(18)	2773(2)	2583(1)	128(1)	16(1)
C(19)	1947(2)	1273(1)	-38(1)	18(1)
C(20)	1356(2)	130(1)	-1357(1)	21(1)
C(21)	1604(2)	270(1)	-2522(1)	21(1)
C(22)	2445(2)	1565(2)	-2369(1)	22(1)
C(23)	3013(2)	2711(1)	-1053(1)	20(1)

Table 3. Bond lengths [\AA] for 144.

$\bar{C}(1)$ -C(11)	1.5321(17)	C(11)-O(15)	1.3679(15)
C(1)-C(10)	1.5422(18)	N(12)-C(13)	1.4958(16)
C(1)-C(18)	1.5465(17)	C(13)-C(17)	1.521(2)
C(1)-C(2)	1.5472(18)	C(13)-C(16)	1.523(2)
C(2)-C(3)	1.5244(17)	C(13)-C(14)	1.5309(19)
C(2)-H(2A)	0.9900	C(14)-O(15)	1.4561(15)
C(2)-H(2B)	0.9900	C(14)-H(14A)	0.9900
C(3)-C(4)	1.5165(19)	C(14)-H(14B)	0.9900
C(3)-H(3A)	0.9900	C(16)-H(16A)	0.9800
C(3)-H(3B)	0.9900	C(16)-H(16B)	0.9800
C(3)-H(3C)	0.9900	C(16)-H(16C)	0.9800
C(4)-C(5)	1.5132(19)	C(17)-H(17A)	0.9800
C(4)-H(4A)	0.9900	C(17)-H(17B)	0.9800
C(4)-H(4B)	0.9900	C(17)-H(17C)	0.9800
C(5)-C(6)	1.3992(19)	C(18)-C(23)	1.3880(19)
C(5)-C(10)	1.4046(18)	C(18)-C(19)	1.3910(19)
C(6)-C(7)	1.386(2)	C(19)-C(20)	1.3922(18)
C(6)-H(6A)	0.9500	C(19)-H(19A)	0.9500
C(7)-C(8)	1.388(2)	C(20)-C(21)	1.3799(19)
C(7)-H(7A)	0.9500	C(20)-H(20A)	0.9500
C(8)-C(9)	1.3818(19)	C(21)-C(22)	1.388(2)
C(8)-H(8A)	0.9500	C(21)-H(21A)	0.9500
C(9)-C(10)	1.4049(19)	C(22)-C(23)	1.3883(19)
C(9)-H(9A)	0.9500	C(22)-H(22A)	0.9500
C(11)-N(12)	1.2673(16)	C(23)-H(23A)	0.95

Table 4. Bond angles [°] for 144.

C(11)-C(1)-C(10)	107.93(10)	C(11)-N(12)-C(13)	106.35(10)
C(11)-C(1)-C(18)	110.16(10)	N(12)-C(13)-C(17)	112.05(11)
C(10)-C(1)-C(18)	111.24(10)	N(12)-C(13)-C(16)	107.02(10)
C(11)-C(1)-C(2)	107.90(10)	C(17)-C(13)-C(16)	110.73(11)
C(10)-C(1)-C(2)	110.72(10)	N(12)-C(13)-C(14)	102.52(9)
C(18)-C(1)-C(2)	108.83(10)	C(17)-C(13)-C(14)	112.34(11)
C(3)-C(2)-C(1)	111.35(11)	C(16)-C(13)-C(14)	111.81(12)
C(3)-C(2)-H(2A)	109.4	O(15)-C(14)-C(13)	103.92(10)
C(1)-C(2)-H(2A)	109.4	O(15)-C(14)-H(14A)	111.0
C(3)-C(2)-H(2B)	109.4	C(13)-C(14)-H(14A)	111.0
C(1)-C(2)-H(2B)	109.4	O(15)-C(14)-H(14B)	111.0
H(2A)-C(2)-H(2B)	108.0	C(13)-C(14)-H(14B)	111.0
C(4)-C(3)-C(2)	109.25(10)	H(14A)-C(14)-H(14B)	109.0
C(4)-C(3)-H(3A)	109.8	C(11)-O(15)-C(14)	104.55(9)
C(2)-C(3)-H(3A)	109.8	C(13)-C(16)-H(16A)	109.5
C(4)-C(3)-H(3B)	109.8	C(13)-C(16)-H(16B)	109.5
C(2)-C(3)-H(3B)	109.8	H(16A)-C(16)-H(16B)	109.5
H(3A)-C(3)-H(3B)	108.3	C(13)-C(16)-H(16C)	109.5
C(5)-C(4)-C(3)	112.73(11)	H(16A)-C(16)-H(16C)	109.5
C(5)-C(4)-H(4A)	109.0	H(16B)-C(16)-H(16C)	109.5
C(3)-C(4)-H(4A)	109.0	C(13)-C(17)-H(17A)	109.5
C(5)-C(4)-H(4B)	109.0	C(13)-C(17)-H(17B)	109.5
C(3)-C(4)-H(4B)	109.0	H(17A)-C(17)-H(17B)	109.5
H(4A)-C(4)-H(4B)	107.8	C(13)-C(17)-H(17C)	109.5
C(6)-C(5)-C(10)	118.76(13)	H(17A)-C(17)-H(17C)	109.5
C(6)-C(5)-C(4)	119.07(11)	H(17B)-C(17)-H(17C)	109.5
C(10)-C(5)-C(4)	122.17(12)	C(23)-C(18)-C(19)	118.32(11)
C(7)-C(6)-C(5)	121.64(13)	C(23)-C(18)-C(1)	119.07(11)
C(7)-C(6)-H(6A)	119.2	C(19)-C(18)-C(1)	122.55(12)
C(5)-C(6)-H(6A)	119.2	C(18)-C(19)-C(20)	120.70(13)
C(6)-C(7)-C(8)	119.51(14)	C(18)-C(19)-H(19A)	119.7
C(6)-C(7)-H(7A)	120.2	C(20)-C(19)-H(19A)	119.7
C(8)-C(7)-H(7A)	120.2	C(21)-C(20)-C(19)	120.41(12)
C(9)-C(8)-C(7)	119.81(13)	C(21)-C(20)-H(20A)	119.8
C(9)-C(8)-H(8A)	120.1	C(19)-C(20)-H(20A)	119.8
C(7)-C(8)-H(8A)	120.1	C(20)-C(21)-C(22)	119.40(12)
C(8)-C(9)-C(10)	121.34(12)	C(20)-C(21)-H(21A)	120.3
C(8)-C(9)-H(9A)	119.3	C(22)-C(21)-H(21A)	120.3
C(10)-C(9)-H(9A)	119.3	C(23)-C(22)-C(21)	120.01(13)
C(5)-C(10)-C(9)	118.93(13)	C(23)-C(22)-H(22A)	120.0
C(5)-C(10)-C(1)	121.73(12)	C(21)-C(22)-H(22A)	120.0
C(9)-C(10)-C(1)	119.29(11)	C(22)-C(23)-C(18)	121.15(12)
N(12)-C(11)-O(15)	118.35(11)	C(22)-C(23)-H(23A)	119.4
N(12)-C(11)-C(1)	126.30(11)	C(18)-C(23)-H(23A)	119.4
O(15)-C(11)-C(1)	115.25(10)		

Symmetry transformations used to generate equivalent atoms:

Table 5. Anisotropic displacement parameters ($\text{\AA}^2 \times 10^3$) for **144**. The anisotropic displacement factor exponent takes the form: $-2\pi^2 [h^2 a^{*2} U^{11} + \dots + 2 h k a^* b^* U^{12}]$

	U^{11}	U^{22}	U^{33}	U^{23}	U^{13}	U^{12}
C(1)	14(1)	13(1)	20(1)	5(1)	2(1)	4(1)
C(2)	14(1)	15(1)	22(1)	7(1)	1(1)	4(1)
C(3)	15(1)	17(1)	27(1)	7(1)	1(1)	6(1)
C(4)	19(1)	17(1)	25(1)	9(1)	-2(1)	5(1)
C(5)	19(1)	10(1)	18(1)	2(1)	-1(1)	2(1)
C(6)	28(1)	16(1)	20(1)	7(1)	-1(1)	4(1)
C(7)	29(1)	18(1)	19(1)	6(1)	5(1)	2(1)
C(8)	21(1)	16(1)	22(1)	3(1)	5(1)	2(1)
C(9)	19(1)	14(1)	21(1)	5(1)	0(1)	3(1)
C(10)	17(1)	9(1)	16(1)	2(1)	0(1)	2(1)
C(11)	12(1)	17(1)	17(1)	7(1)	1(1)	5(1)
N(12)	17(1)	13(1)	21(1)	6(1)	1(1)	5(1)
C(13)	17(1)	14(1)	22(1)	6(1)	1(1)	7(1)
C(14)	24(1)	13(1)	27(1)	7(1)	-1(1)	7(1)
O(15)	17(1)	14(1)	30(1)	7(1)	-4(1)	5(1)
C(16)	31(1)	25(1)	24(1)	7(1)	5(1)	15(1)
C(17)	27(1)	18(1)	37(1)	12(1)	5(1)	7(1)
C(18)	12(1)	14(1)	20(1)	7(1)	2(1)	8(1)
C(19)	17(1)	17(1)	21(1)	8(1)	5(1)	6(1)
C(20)	18(1)	15(1)	26(1)	7(1)	5(1)	4(1)
C(21)	18(1)	19(1)	19(1)	2(1)	1(1)	7(1)
C(22)	21(1)	26(1)	19(1)	10(1)	5(1)	9(1)
C(23)	17(1)	18(1)	25(1)	11(1)	5(1)	4(1)

Table 6. Hydrogen coordinates ($\times 10^4$) and isotropic displacement parameters ($\text{\AA}^2 \times 10^3$) for **144**.

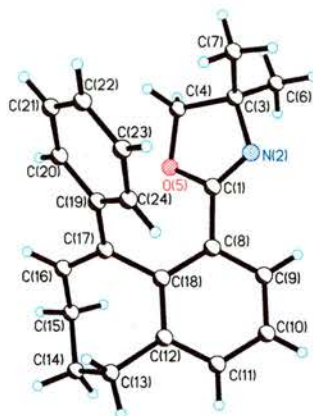
	x	y	z	$U(\text{eq})$
H(2A)	5640	3943	878	21
H(2B)	5790	4961	2513	21
H(3A)	5451	1757	1270	25
H(3B)	7126	2772	2005	25
H(4A)	5918	2017	3514	25
H(4B)	6368	3783	4150	25
H(6A)	4055	2594	5182	27
H(7A)	1443	2871	5495	27
H(8A)	-258	3588	4072	26
H(9A)	681	4058	2381	23
H(14A)	294	7090	1475	27
H(14B)	1411	6831	338	27
H(16A)	1703	7614	3942	41
H(16B)	1451	9121	3815	41
H(16C)	3140	8925	4508	41
H(17A)	4359	9534	2859	41
H(17B)	2704	9599	2016	41
H(17C)	3898	8484	1224	41
H(19A)	1783	1157	756	22
H(20A)	780	-753	-1455	25
H(21A)	1203	-512	-3422	25
H(22A)	2631	1667	-3165	26
H(23A)	3575	3598	-958	24

Table 7. Torsion angles [°] for 144.

C(11)-C(1)-C(2)-C(3)	165.12(10)	C(10)-C(1)-C(11)-O(15)	-84.69(12)
C(10)-C(1)-C(2)-C(3)	47.21(13)	C(18)-C(1)-C(11)-O(15)	36.95(15)
C(18)-C(1)-C(2)-C(3)	-75.35(13)	C(2)-C(1)-C(11)-O(15)	155.63(11)
C(1)-C(2)-C(3)-C(4)	-65.79(13)	O(15)-C(11)-N(12)-C(13)	5.64(16)
C(2)-C(3)-C(4)-C(5)	49.48(14)	C(1)-C(11)-N(12)-C(13)	-170.50(12)
C(3)-C(4)-C(5)-C(6)	161.35(11)	C(11)-N(12)-C(13)-C(17)	-136.80(12)
C(3)-C(4)-C(5)-C(10)	-18.65(16)	C(11)-N(12)-C(13)-C(16)	101.64(12)
C(10)-C(5)-C(6)-C(7)	1.01(18)	C(11)-N(12)-C(13)-C(14)	-16.13(14)
C(4)-C(5)-C(6)-C(7)	-178.99(11)	N(12)-C(13)-C(14)-O(15)	20.34(13)
C(5)-C(6)-C(7)-C(8)	-0.13(19)	C(17)-C(13)-C(14)-O(15)	140.81(12)
C(6)-C(7)-C(8)-C(9)	-0.65(18)	C(16)-C(13)-C(14)-O(15)	-93.98(12)
C(7)-C(8)-C(9)-C(10)	0.55(18)	N(12)-C(11)-O(15)-C(14)	8.21(15)
C(6)-C(5)-C(10)-C(9)	-1.09(17)	C(1)-C(11)-O(15)-C(14)	-175.23(11)
C(4)-C(5)-C(10)-C(9)	178.91(10)	C(13)-C(14)-O(15)-C(11)	-17.57(13)
C(6)-C(5)-C(10)-C(1)	-178.59(10)	C(11)-C(1)-C(18)-C(23)	53.92(15)
C(4)-C(5)-C(10)-C(1)	1.41(17)	C(10)-C(1)-C(18)-C(23)	173.56(10)
C(8)-C(9)-C(10)-C(5)	0.34(18)	C(2)-C(1)-C(18)-C(23)	-64.19(14)
C(8)-C(9)-C(10)-C(1)	177.89(10)	C(11)-C(1)-C(18)-C(19)	-129.03(13)
C(11)-C(1)-C(10)-C(5)	-133.42(12)	C(10)-C(1)-C(18)-C(19)	-9.38(16)
C(18)-C(1)-C(10)-C(5)	105.62(13)	C(2)-C(1)-C(18)-C(19)	112.86(13)
C(2)-C(1)-C(10)-C(5)	-15.53(15)	C(23)-C(18)-C(19)-C(20)	-0.90(18)
C(11)-C(1)-C(10)-C(9)	49.09(14)	C(1)-C(18)-C(19)-C(20)	-177.97(11)
C(18)-C(1)-C(10)-C(9)	-71.87(13)	C(18)-C(19)-C(20)-C(21)	0.99(19)
C(2)-C(1)-C(10)-C(9)	166.98(10)	C(19)-C(20)-C(21)-C(22)	-0.17(19)
C(10)-C(1)-C(11)-N(12)	91.56(15)	C(20)-C(21)-C(22)-C(23)	-0.72(19)
C(18)-C(1)-C(11)-N(12)	-146.81(13)	C(21)-C(22)-C(23)-C(18)	0.8(2)
C(2)-C(1)-C(11)-N(12)	-28.13(17)	C(19)-C(18)-C(23)-C(22)	0.00(18)
		C(1)-C(18)-C(23)-C(22)	177.17(12)

Symmetry transformations used to generate equivalent atoms:

Benzosuberene 148

Table 1. Crystal data and structure refinement for **148**.

Identification code	mrjw4	
Empirical formula	C ₂₂ H ₂₃ N O	
Formula weight	317.41	
Temperature	173(2) K	
Wavelength	1.54178 Å	
Crystal system	Monoclinic	
Space group	P2(1)/c	
Unit cell dimensions	a = 12.9895(12) Å	$\alpha = 90^\circ$.
	b = 11.5790(10) Å	$\beta = 93.777(3)^\circ$.
	c = 11.5517(11) Å	$\gamma = 90^\circ$.
Volume	1733.7(3) Å ³	
Z	4	
Density (calculated)	1.216 Mg/m ³	
Absorption coefficient	0.570 mm ⁻¹	
F(000)	680	
Crystal size	0.300 x 0.050 x 0.010 mm ³	
Theta range for data collection	3.41 to 67.62°.	
Index ranges	-15 ≤ h ≤ 15, -13 ≤ k ≤ 13, -12 ≤ l ≤ 12	
Reflections collected	21400	
Independent reflections	2948 [R(int) = 0.0628]	
Completeness to theta = 67.62°	94.1 %	
Absorption correction	Multiscan	
Max. and min. transmission	1.0000 and 0.9505	
Refinement method	Full-matrix least-squares on F ²	
Data / restraints / parameters	2948 / 0 / 217	
Goodness-of-fit on F ²	1.078	
Final R indices [I > 2σ(I)]	R1 = 0.0406, wR2 = 0.0939	
R indices (all data)	R1 = 0.0481, wR2 = 0.0982	
Largest diff. peak and hole	0.158 and -0.175 e.Å ⁻³	

Table 2. Atomic coordinates ($\times 10^4$) and equivalent isotropic displacement parameters ($\text{\AA}^2 \times 10^3$) for 148. $U(\text{eq})$ is defined as one third of the trace of the orthogonalized U^{ij} tensor.

	x	y	z	$U(\text{eq})$
C(1)	6715(1)	6867(1)	4140(1)	25(1)
N(2)	5775(1)	6893(1)	3768(1)	33(1)
C(3)	5218(1)	7575(1)	4622(1)	31(1)
C(4)	6089(1)	8031(1)	5470(1)	37(1)
O(5)	7001(1)	7421(1)	5149(1)	29(1)
C(6)	4488(1)	6776(1)	5222(2)	41(1)
C(7)	4640(1)	8552(2)	3991(2)	43(1)
C(8)	7550(1)	6242(1)	3587(1)	25(1)
C(9)	7299(1)	5181(1)	3074(1)	30(1)
C(10)	8045(1)	4534(1)	2575(1)	32(1)
C(11)	9046(1)	4942(1)	2586(1)	29(1)
C(12)	9320(1)	6002(1)	3085(1)	25(1)
C(13)	10416(1)	6436(1)	3063(1)	30(1)
C(14)	11003(1)	6457(1)	4258(1)	34(1)
C(15)	10352(1)	6967(1)	5198(1)	32(1)
C(16)	9700(1)	7970(1)	4775(1)	28(1)
C(17)	8855(1)	7849(1)	4055(1)	24(1)
C(18)	8564(1)	6677(1)	3590(1)	23(1)
C(19)	8218(1)	8853(1)	3650(1)	25(1)
C(20)	8083(1)	9808(1)	4366(1)	29(1)
C(21)	7486(1)	10737(1)	3981(1)	34(1)
C(22)	6992(1)	10731(1)	2879(2)	37(1)
C(23)	7125(1)	9795(1)	2159(1)	35(1)
C(24)	7733(1)	8867(1)	2536(1)	29(1)

Table 3. Bond lengths [\AA] for 148.

C(1)-N(2)	1.2672(18)	C(12)-C(13)	1.5108(19)
C(1)-O(5)	1.3616(16)	C(13)-C(14)	1.533(2)
C(1)-C(8)	1.4825(19)	C(13)-H(13A)	0.9900
N(2)-C(3)	1.4881(18)	C(13)-H(13B)	0.9900
C(3)-C(7)	1.518(2)	C(14)-C(15)	1.537(2)
C(3)-C(6)	1.523(2)	C(14)-H(14A)	0.9900
C(3)-C(4)	1.540(2)	C(14)-H(14B)	0.9900
C(4)-O(5)	1.4472(17)	C(15)-C(16)	1.5002(19)
C(4)-H(4A)	0.9900	C(15)-H(15A)	0.9900
C(4)-H(4B)	0.9900	C(15)-H(15B)	0.9900
C(6)-H(6A)	0.9800	C(16)-C(17)	1.3401(19)
C(6)-H(6B)	0.9800	C(16)-H(16A)	0.9500
C(6)-H(6C)	0.9800	C(17)-C(19)	1.4852(19)
C(7)-H(7A)	0.9800	C(17)-C(18)	1.4986(18)
C(7)-H(7B)	0.9800	C(19)-C(24)	1.396(2)
C(7)-H(7C)	0.9800	C(19)-C(20)	1.3982(19)
C(8)-C(9)	1.3943(19)	C(20)-C(21)	1.382(2)
C(8)-C(18)	1.4101(19)	C(20)-H(20A)	0.9500
C(9)-C(10)	1.381(2)	C(21)-C(22)	1.388(2)
C(9)-H(9A)	0.9500	C(21)-H(21A)	0.9500
C(10)-C(11)	1.383(2)	C(22)-C(23)	1.384(2)
C(10)-H(10A)	0.9500	C(22)-H(22A)	0.9500
C(11)-C(12)	1.392(2)	C(23)-C(24)	1.386(2)
C(11)-H(11A)	0.9500	C(23)-H(23A)	0.9500
C(12)-C(18)	1.4114(19)	C(24)-H(24A)	0.9500

Table 4 Bond angles [°] for 148

N(2)-C(1)-O(5)	118.75(12)	C(12)-C(13)-H(13A)	108.8
N(2)-C(1)-C(8)	125.58(13)	C(14)-C(13)-H(13A)	108.8
O(5)-C(1)-C(8)	115.63(11)	C(12)-C(13)-H(13B)	108.8
C(1)-N(2)-C(3)	106.73(12)	C(14)-C(13)-H(13B)	108.8
N(2)-C(3)-C(7)	108.86(12)	H(13A)-C(13)-H(13B)	107.7
N(2)-C(3)-C(6)	108.89(12)	C(13)-C(14)-C(15)	112.19(12)
C(7)-C(3)-C(6)	111.63(13)	C(13)-C(14)-H(14A)	109.2
N(2)-C(3)-C(4)	103.55(11)	C(15)-C(14)-H(14A)	109.2
C(7)-C(3)-C(4)	111.65(13)	C(13)-C(14)-H(14B)	109.2
C(6)-C(3)-C(4)	111.88(13)	C(15)-C(14)-H(14B)	109.2
O(5)-C(4)-C(3)	104.45(11)	H(14A)-C(14)-H(14B)	107.9
O(5)-C(4)-H(4A)	110.9	C(16)-C(15)-C(14)	113.10(12)
C(3)-C(4)-H(4A)	110.9	C(16)-C(15)-H(15A)	109.0
O(5)-C(4)-H(4B)	110.9	C(14)-C(15)-H(15A)	109.0
C(3)-C(4)-H(4B)	110.9	C(16)-C(15)-H(15B)	109.0
H(4A)-C(4)-H(4B)	108.9	C(14)-C(15)-H(15B)	109.0
C(1)-O(5)-C(4)	105.51(10)	H(15A)-C(15)-H(15B)	107.8
C(3)-C(6)-H(6A)	109.5	C(17)-C(16)-C(15)	122.91(13)
C(3)-C(6)-H(6B)	109.5	C(17)-C(16)-H(16A)	118.5
H(6A)-C(6)-H(6B)	109.5	C(15)-C(16)-H(16A)	118.5
C(3)-C(6)-H(6C)	109.5	C(16)-C(17)-C(19)	122.04(12)
H(6A)-C(6)-H(6C)	109.5	C(16)-C(17)-C(18)	119.62(12)
H(6B)-C(6)-H(6C)	109.5	C(19)-C(17)-C(18)	118.27(11)
C(3)-C(7)-H(7A)	109.5	C(8)-C(18)-C(12)	118.49(12)
C(3)-C(7)-H(7B)	109.5	C(8)-C(18)-C(17)	122.53(12)
H(7A)-C(7)-H(7B)	109.5	C(12)-C(18)-C(17)	118.91(12)
C(3)-C(7)-H(7C)	109.5	C(24)-C(19)-C(20)	118.01(13)
H(7A)-C(7)-H(7C)	109.5	C(24)-C(19)-C(17)	120.51(12)
H(7B)-C(7)-H(7C)	109.5	C(20)-C(19)-C(17)	121.48(12)
C(9)-C(8)-C(18)	120.55(13)	C(21)-C(20)-C(19)	121.00(13)
C(9)-C(8)-C(1)	117.09(12)	C(21)-C(20)-H(20A)	119.5
C(18)-C(8)-C(1)	122.35(12)	C(19)-C(20)-H(20A)	119.5
C(10)-C(9)-C(8)	120.29(14)	C(20)-C(21)-C(22)	120.46(14)
C(10)-C(9)-H(9A)	119.9	C(20)-C(21)-H(21A)	119.8
C(8)-C(9)-H(9A)	119.9	C(22)-C(21)-H(21A)	119.8
C(9)-C(10)-C(11)	119.76(13)	C(23)-C(22)-C(21)	119.13(14)
C(9)-C(10)-H(10A)	120.1	C(23)-C(22)-H(22A)	120.4
C(11)-C(10)-H(10A)	120.1	C(21)-C(22)-H(22A)	120.4
C(10)-C(11)-C(12)	121.35(13)	C(22)-C(23)-C(24)	120.63(14)
C(10)-C(11)-H(11A)	119.3	C(22)-C(23)-H(23A)	119.7
C(12)-C(11)-H(11A)	119.3	C(24)-C(23)-H(23A)	119.7
C(11)-C(12)-C(18)	119.55(13)	C(23)-C(24)-C(19)	120.76(13)
C(11)-C(12)-C(13)	120.14(12)	C(23)-C(24)-H(24A)	119.6
C(18)-C(12)-C(13)	120.30(12)	C(19)-C(24)-H(24A)	119.6
C(12)-C(13)-C(14)	113.81(12)		

Symmetry transformations used to generate equivalent atoms:

Table 5. Anisotropic displacement parameters ($\text{\AA}^2 \times 10^3$) for **148**. The anisotropic displacement factor exponent takes the form: $-2\pi^2 [h^2 a^{*2} U^{11} + \dots + 2 h k a^* b^* U^{12}]$

	U ¹¹	U ²²	U ³³	U ²³	U ¹³	U ¹²
C(1)	31(1)	22(1)	22(1)	1(1)	1(1)	-2(1)
N(2)	29(1)	35(1)	34(1)	-7(1)	1(1)	3(1)
C(3)	28(1)	31(1)	34(1)	-5(1)	4(1)	1(1)
C(4)	32(1)	40(1)	38(1)	-11(1)	5(1)	3(1)
O(5)	29(1)	34(1)	23(1)	-4(1)	2(1)	1(1)
C(6)	41(1)	34(1)	50(1)	-3(1)	11(1)	-3(1)
C(7)	42(1)	39(1)	47(1)	1(1)	5(1)	7(1)
C(8)	30(1)	22(1)	23(1)	3(1)	0(1)	2(1)
C(9)	33(1)	26(1)	31(1)	0(1)	0(1)	-2(1)
C(10)	43(1)	22(1)	31(1)	-4(1)	-2(1)	2(1)
C(11)	35(1)	26(1)	26(1)	-1(1)	2(1)	8(1)
C(12)	31(1)	26(1)	20(1)	4(1)	1(1)	4(1)
C(13)	30(1)	32(1)	30(1)	0(1)	7(1)	3(1)
C(14)	29(1)	36(1)	36(1)	-1(1)	-1(1)	4(1)
C(15)	34(1)	35(1)	27(1)	1(1)	-4(1)	1(1)
C(16)	31(1)	27(1)	26(1)	-1(1)	2(1)	-1(1)
C(17)	28(1)	24(1)	21(1)	1(1)	5(1)	0(1)
C(18)	29(1)	23(1)	19(1)	3(1)	0(1)	3(1)
C(19)	26(1)	23(1)	26(1)	0(1)	4(1)	-3(1)
C(20)	32(1)	27(1)	28(1)	-2(1)	5(1)	-3(1)
C(21)	36(1)	25(1)	41(1)	-4(1)	10(1)	1(1)
C(22)	37(1)	27(1)	47(1)	8(1)	4(1)	6(1)
C(23)	37(1)	31(1)	36(1)	7(1)	-4(1)	0(1)
C(24)	34(1)	23(1)	29(1)	0(1)	0(1)	-1(1)

Table 6. Hydrogen coordinates ($\times 10^4$) and isotropic displacement parameters ($\text{\AA}^2 \times 10^3$) for **148**.

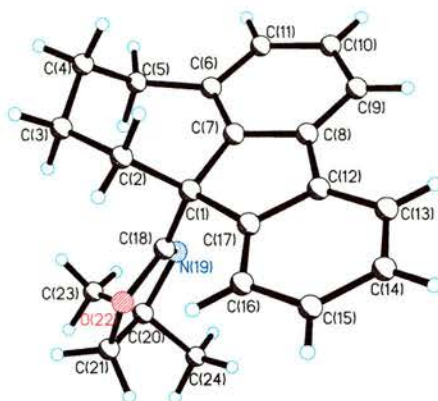
	x	y	z	U(eq)
H(4A)	6174	8875	5381	44
H(4B)	5943	7861	6283	44
H(6A)	3948	6501	4656	62
H(6B)	4172	7198	5842	62
H(6C)	4876	6114	5554	62
H(7A)	5132	9050	3619	64
H(7B)	4270	9006	4547	64
H(7C)	4146	8231	3399	64
H(9A)	6611	4901	3067	36
H(10A)	7872	3811	2226	38
H(11A)	9557	4491	2246	35
H(13A)	10403	7228	2738	36
H(13B)	10794	5938	2539	36
H(14A)	11639	6921	4213	41
H(14B)	11210	5659	4479	41
H(15A)	9899	6356	5480	39
H(15B)	10819	7222	5862	39
H(16A)	9895	8724	5028	33
H(20A)	8406	9819	5127	35
H(21A)	7413	11383	4475	40
H(22A)	6568	11361	2622	44
H(23A)	6796	9788	1400	42
H(24A)	7820	8233	2030	35

Table 7. Torsion angles [°] for 148.

O(5)-C(1)-N(2)-C(3)	-0.32(17)	C(15)-C(16)-C(17)-C(19)	179.74(13)
C(8)-C(1)-N(2)-C(3)	177.51(13)	C(15)-C(16)-C(17)-C(18)	-3.4(2)
C(1)-N(2)-C(3)-C(7)	125.19(13)	C(9)-C(8)-C(18)-C(12)	-1.44(19)
C(1)-N(2)-C(3)-C(6)	-112.90(14)	C(1)-C(8)-C(18)-C(12)	177.40(12)
C(1)-N(2)-C(3)-C(4)	6.29(15)	C(9)-C(8)-C(18)-C(17)	175.60(12)
N(2)-C(3)-C(4)-O(5)	-9.56(15)	C(1)-C(8)-C(18)-C(17)	-5.6(2)
C(7)-C(3)-C(4)-O(5)	-126.52(13)	C(11)-C(12)-C(18)-C(8)	1.02(19)
C(6)-C(3)-C(4)-O(5)	107.56(14)	C(13)-C(12)-C(18)-C(8)	179.74(12)
N(2)-C(1)-O(5)-C(4)	-6.25(17)	C(11)-C(12)-C(18)-C(17)	-176.13(12)
C(8)-C(1)-O(5)-C(4)	175.71(12)	C(13)-C(12)-C(18)-C(17)	2.59(18)
C(3)-C(4)-O(5)-C(1)	9.43(15)	C(16)-C(17)-C(18)-C(8)	132.97(14)
N(2)-C(1)-C(8)-C(9)	-36.6(2)	C(19)-C(17)-C(18)-C(8)	-50.04(18)
O(5)-C(1)-C(8)-C(9)	141.28(13)	C(16)-C(17)-C(18)-C(12)	-50.00(18)
N(2)-C(1)-C(8)-C(18)	144.52(15)	C(19)-C(17)-C(18)-C(12)	126.99(13)
O(5)-C(1)-C(8)-C(18)	-37.59(18)	C(16)-C(17)-C(19)-C(24)	145.73(14)
C(18)-C(8)-C(9)-C(10)	0.9(2)	C(18)-C(17)-C(19)-C(24)	-31.19(18)
C(1)-C(8)-C(9)-C(10)	-177.97(13)	C(16)-C(17)-C(19)-C(20)	-34.4(2)
C(8)-C(9)-C(10)-C(11)	0.0(2)	C(18)-C(17)-C(19)-C(20)	148.74(13)
C(9)-C(10)-C(11)-C(12)	-0.4(2)	C(24)-C(19)-C(20)-C(21)	0.1(2)
C(10)-C(11)-C(12)-C(18)	-0.1(2)	C(17)-C(19)-C(20)-C(21)	-179.82(13)
C(10)-C(11)-C(12)-C(13)	-178.82(13)	C(19)-C(20)-C(21)-C(22)	1.1(2)
C(11)-C(12)-C(13)-C(14)	-110.90(15)	C(20)-C(21)-C(22)-C(23)	-1.5(2)
C(18)-C(12)-C(13)-C(14)	70.39(17)	C(21)-C(22)-C(23)-C(24)	0.7(2)
C(12)-C(13)-C(14)-C(15)	-45.06(17)	C(22)-C(23)-C(24)-C(19)	0.4(2)
C(13)-C(14)-C(15)-C(16)	-38.48(17)	C(20)-C(19)-C(24)-C(23)	-0.9(2)
C(14)-C(15)-C(16)-C(17)	73.02(18)	C(17)-C(19)-C(24)-C(23)	179.07(13)

Symmetry transformations used to generate equivalent atoms:

Flourene 149

Table 1. Crystal data and structure refinement for **149**.

Identification code	149	
Empirical formula	C ₂₂ H ₂₃ N O	
Formula weight	317.41	
Temperature	173(2) K	
Wavelength	1.54178 Å	
Crystal system	Orthorhombic	
Space group	Pbca	
Unit cell dimensions	a = 7.2553(3) Å	α = 90°.
	b = 18.2486(6) Å	β = 90°.
	c = 25.7308(9) Å	γ = 90°.
Volume	3406.7(2) Å ³	
Z	8	
Density (calculated)	1.238 Mg/m ³	
Absorption coefficient	0.580 mm ⁻¹	
F(000)	1360	
Crystal size	0.270 x 0.100 x 0.050 mm ³	
Theta range for data collection	3.44 to 67.74°.	
Index ranges	-7 ≤ h ≤ 8, -21 ≤ k ≤ 21, -30 ≤ l ≤ 30	
Reflections collected	40869	
Independent reflections	2960 [R(int) = 0.0762]	
Completeness to theta = 67.74°	95.9 %	
Absorption correction	Multiscan	
Max. and min. transmission	1.0000 and 0.2522	
Refinement method	Full-matrix least-squares on F ²	
Data / restraints / parameters	2960 / 0 / 219	
Goodness-of-fit on F ²	0.974	
Final R indices [I > 2σ(I)]	R1 = 0.0446, wR2 = 0.1162	
R indices (all data)	R1 = 0.0455, wR2 = 0.1174	
Extinction coefficient	0.0016(2)	
Largest diff. peak and hole	0.239 and -0.231 e.Å ⁻³	

Table 2. Atomic coordinates ($\times 10^4$) and equivalent isotropic displacement parameters ($\text{\AA}^2 \times 10^3$) for 149. $U(\text{eq})$ is defined as one third of the trace of the orthogonalized U^{ij} tensor.

	x	y	z	$U(\text{eq})$
C(1)	6779(2)	1564(1)	6247(1)	26(1)
C(2)	8744(2)	1879(1)	6331(1)	29(1)
C(3)	10284(2)	1463(1)	6051(1)	33(1)
C(4)	10654(2)	684(1)	6241(1)	36(1)
C(5)	9145(2)	125(1)	6107(1)	34(1)
C(6)	7468(2)	175(1)	6450(1)	30(1)
C(7)	6482(2)	827(1)	6513(1)	26(1)
C(8)	5028(2)	873(1)	6870(1)	28(1)
C(9)	4483(2)	269(1)	7164(1)	34(1)
C(10)	5414(2)	-386(1)	7090(1)	38(1)
C(11)	6880(2)	-427(1)	6743(1)	35(1)
C(12)	4332(2)	1626(1)	6876(1)	28(1)
C(13)	2958(2)	1948(1)	7177(1)	34(1)
C(14)	2591(2)	2690(1)	7113(1)	39(1)
C(15)	3567(2)	3101(1)	6753(1)	38(1)
C(16)	4942(2)	2780(1)	6449(1)	33(1)
C(17)	5327(2)	2043(1)	6516(1)	27(1)
C(18)	6345(2)	1528(1)	5672(1)	26(1)
N(19)	5786(2)	983(1)	5415(1)	31(1)
C(20)	5557(2)	1227(1)	4866(1)	34(1)
C(21)	6065(2)	2045(1)	4886(1)	37(1)
O(22)	6611(2)	2179(1)	5418(1)	36(1)
C(23)	6851(4)	787(1)	4525(1)	70(1)
C(24)	3563(3)	1108(1)	4706(1)	55(1)

Table 3. Bond lengths [\AA] for 149.

C(1)-C(18)	1.5157(17)	C(11)-H(11A)	0.9500
C(1)-C(7)	1.5252(17)	C(12)-C(17)	1.3990(18)
C(1)-C(17)	1.5342(18)	C(12)-C(13)	1.3921(19)
C(1)-C(2)	1.5515(18)	C(13)-C(14)	1.389(2)
C(2)-C(3)	1.5295(19)	C(13)-H(13A)	0.9500
C(2)-H(2A)	0.9900	C(14)-C(15)	1.389(2)
C(2)-H(2B)	0.9900	C(14)-H(14A)	0.9500
C(3)-C(4)	1.526(2)	C(15)-C(16)	1.395(2)
C(3)-H(3A)	0.9900	C(15)-H(15A)	0.9500
C(3)-H(3B)	0.9900	C(16)-C(17)	1.3848(19)
C(4)-C(5)	1.536(2)	C(16)-H(16A)	0.9500
C(4)-H(4A)	0.9900	C(18)-N(19)	1.2595(17)
C(4)-H(4B)	0.9900	C(18)-O(22)	1.3706(15)
C(5)-C(6)	1.508(2)	N(19)-C(20)	1.4896(16)
C(5)-H(5A)	0.9900	C(20)-C(24)	1.520(2)
C(5)-H(5B)	0.9900	C(20)-C(23)	1.516(2)
C(6)-C(7)	1.3965(19)	C(20)-C(21)	1.540(2)
C(6)-C(11)	1.3990(19)	C(21)-O(22)	1.4450(16)
C(7)-C(8)	1.4021(18)	C(21)-H(21A)	0.9900
C(8)-C(9)	1.3925(18)	C(21)-H(21B)	0.9900
C(8)-C(12)	1.4645(19)	C(23)-H(23A)	0.9800
C(9)-C(10)	1.387(2)	C(23)-H(23B)	0.9800
C(9)-H(9A)	0.9500	C(23)-H(23C)	0.9800
C(10)-C(11)	1.390(2)	C(24)-H(24A)	0.9800
C(10)-H(10A)	0.9500	C(24)-H(24B)	0.9800
		C(24)-H(24C)	0.9800

Table 4. Bond Angles [°] for 149

C(18)-C(1)-C(7)	111.68(10)	C(17)-C(12)-C(13)	120.53(13)
C(18)-C(1)-C(17)	108.89(10)	C(17)-C(12)-C(8)	108.98(11)
C(7)-C(1)-C(17)	101.71(10)	C(13)-C(12)-C(8)	130.47(12)
C(18)-C(1)-C(2)	110.03(10)	C(14)-C(13)-C(12)	118.88(13)
C(7)-C(1)-C(2)	113.22(10)	C(14)-C(13)-H(13A)	120.6
C(17)-C(1)-C(2)	110.99(10)	C(12)-C(13)-H(13A)	120.6
C(3)-C(2)-C(1)	115.02(11)	C(15)-C(14)-C(13)	120.52(14)
C(3)-C(2)-H(2A)	108.5	C(15)-C(14)-H(14A)	119.7
C(1)-C(2)-H(2A)	108.5	C(13)-C(14)-H(14A)	119.7
C(3)-C(2)-H(2B)	108.5	C(14)-C(15)-C(16)	120.77(14)
C(1)-C(2)-H(2B)	108.5	C(14)-C(15)-H(15A)	119.6
H(2A)-C(2)-H(2B)	107.5	C(16)-C(15)-H(15A)	119.6
C(4)-C(3)-C(2)	116.09(11)	C(17)-C(16)-C(15)	118.85(13)
C(4)-C(3)-H(3A)	108.3	C(17)-C(16)-H(16A)	120.6
C(2)-C(3)-H(3A)	108.3	C(15)-C(16)-H(16A)	120.6
C(4)-C(3)-H(3B)	108.3	C(16)-C(17)-C(12)	120.43(12)
C(2)-C(3)-H(3B)	108.3	C(16)-C(17)-C(1)	129.45(12)
H(3A)-C(3)-H(3B)	107.4	C(12)-C(17)-C(1)	110.12(11)
C(3)-C(4)-C(5)	114.95(12)	N(19)-C(18)-O(22)	118.67(11)
C(3)-C(4)-H(4A)	108.5	N(19)-C(18)-C(1)	127.84(11)
C(5)-C(4)-H(4A)	108.5	O(22)-C(18)-C(1)	113.48(10)
C(3)-C(4)-H(4B)	108.5	C(18)-N(19)-C(20)	107.27(11)
C(5)-C(4)-H(4B)	108.5	N(19)-C(20)-C(24)	108.69(12)
H(4A)-C(4)-H(4B)	107.5	N(19)-C(20)-C(23)	108.85(12)
C(6)-C(5)-C(4)	113.75(11)	C(24)-C(20)-C(23)	110.90(15)
C(6)-C(5)-H(5A)	108.8	N(19)-C(20)-C(21)	103.43(10)
C(4)-C(5)-H(5A)	108.8	C(24)-C(20)-C(21)	112.02(13)
C(6)-C(5)-H(5B)	108.8	C(23)-C(20)-C(21)	112.58(15)
C(4)-C(5)-H(5B)	108.8	O(22)-C(21)-C(20)	105.08(10)
H(5A)-C(5)-H(5B)	107.7	O(22)-C(21)-H(21A)	110.7
C(7)-C(6)-C(11)	116.80(13)	C(20)-C(21)-H(21A)	110.7
C(7)-C(6)-C(5)	122.19(12)	O(22)-C(21)-H(21B)	110.7
C(11)-C(6)-C(5)	120.95(12)	C(20)-C(21)-H(21B)	110.7
C(6)-C(7)-C(8)	120.80(12)	H(21A)-C(21)-H(21B)	108.8
C(6)-C(7)-C(1)	128.85(12)	C(18)-O(22)-C(21)	105.45(10)
C(8)-C(7)-C(1)	110.31(11)	C(20)-C(23)-H(23A)	109.5
C(9)-C(8)-C(7)	121.43(13)	C(20)-C(23)-H(23B)	109.5
C(9)-C(8)-C(12)	129.69(13)	H(23A)-C(23)-H(23B)	109.5
C(7)-C(8)-C(12)	108.85(11)	C(20)-C(23)-H(23C)	109.5
C(10)-C(9)-C(8)	117.99(13)	H(23A)-C(23)-H(23C)	109.5
C(10)-C(9)-H(9A)	121.0	H(23B)-C(23)-H(23C)	109.5
C(8)-C(9)-H(9A)	121.0	C(20)-C(24)-H(24A)	109.5
C(9)-C(10)-C(11)	120.50(13)	C(20)-C(24)-H(24B)	109.5
C(9)-C(10)-H(10A)	119.8	H(24A)-C(24)-H(24B)	109.5
C(11)-C(10)-H(10A)	119.7	C(20)-C(24)-H(24C)	109.5
C(10)-C(11)-C(6)	122.41(13)	H(24A)-C(24)-H(24C)	109.5
C(10)-C(11)-H(11A)	118.8	H(24B)-C(24)-H(24C)	109.5
C(6)-C(11)-H(11A)	118.8		

Symmetry transformations used to generate equivalent atoms:

Table 5. Anisotropic displacement parameters ($\text{\AA}^2 \times 10^3$) for 149. The anisotropic displacement factor exponent takes the form: $-2\pi^2 [h^2 a^{*2} U^{11} + \dots + 2 h k a^* b^* U^{12}]$

	U ¹¹	U ²²	U ³³	U ²³	U ¹³	U ¹²
C(1)	26(1)	28(1)	24(1)	-1(1)	0(1)	-2(1)
C(2)	27(1)	31(1)	28(1)	0(1)	0(1)	-4(1)
C(3)	27(1)	41(1)	31(1)	0(1)	0(1)	-4(1)
C(4)	29(1)	42(1)	36(1)	-2(1)	-1(1)	4(1)
C(5)	37(1)	32(1)	34(1)	-4(1)	-3(1)	5(1)
C(6)	32(1)	31(1)	27(1)	-2(1)	-7(1)	-1(1)
C(7)	27(1)	30(1)	22(1)	-1(1)	-4(1)	-4(1)
C(8)	26(1)	35(1)	24(1)	2(1)	-4(1)	-5(1)
C(9)	32(1)	41(1)	30(1)	5(1)	-2(1)	-8(1)
C(10)	43(1)	34(1)	36(1)	8(1)	-8(1)	-11(1)
C(11)	43(1)	28(1)	35(1)	0(1)	-11(1)	-2(1)
C(12)	25(1)	35(1)	23(1)	-1(1)	-4(1)	-4(1)
C(13)	28(1)	48(1)	26(1)	-1(1)	1(1)	-3(1)
C(14)	34(1)	48(1)	34(1)	-8(1)	2(1)	7(1)
C(15)	41(1)	37(1)	37(1)	-5(1)	-2(1)	7(1)
C(16)	35(1)	32(1)	32(1)	0(1)	-1(1)	-2(1)
C(17)	25(1)	33(1)	23(1)	-2(1)	-2(1)	-2(1)
C(18)	24(1)	27(1)	26(1)	2(1)	2(1)	0(1)
N(19)	38(1)	31(1)	25(1)	1(1)	-4(1)	-1(1)
C(20)	47(1)	32(1)	23(1)	1(1)	-2(1)	4(1)
C(21)	45(1)	38(1)	27(1)	6(1)	-4(1)	-3(1)
O(22)	54(1)	30(1)	26(1)	4(1)	-1(1)	-7(1)
C(23)	111(2)	57(1)	43(1)	6(1)	29(1)	30(1)
C(24)	68(1)	44(1)	53(1)	8(1)	-30(1)	-11(1)

Table 6. Hydrogen coordinates ($\times 10^4$) and isotropic displacement parameters ($\text{\AA}^2 \times 10^3$) for 149.

	x	y	z	U(eq)
H(2A)	8758	2394	6211	35
H(2B)	9013	1880	6708	35
H(3A)	9978	1442	5677	39
H(3B)	11437	1749	6086	39
H(4A)	10808	695	6623	43
H(4B)	11832	514	6089	43
H(5A)	8762	199	5741	41
H(5B)	9668	-375	6135	41
H(9A)	3502	305	7407	41
H(10A)	5047	-810	7277	45
H(11A)	7506	-881	6704	42
H(13A)	2283	1665	7422	41
H(14A)	1664	2917	7318	47
H(15A)	3296	3607	6711	46
H(16A)	5603	3062	6202	39
H(21A)	7092	2154	4644	44
H(21B)	4993	2353	4790	44
H(23A)	6474	271	4526	105
H(23B)	8111	829	4658	105
H(23C)	6803	977	4169	105
H(24A)	3294	582	4701	83
H(24B)	3362	1314	4359	83
H(24C)	2746	1351	4956	83

Table 7. Torsion angles [°] for 149.

C(18)-C(1)-C(2)-C(3)	-56.16(14)	C(12)-C(13)-C(14)-C(15)	0.6(2)
C(7)-C(1)-C(2)-C(3)	69.60(14)	C(13)-C(14)-C(15)-C(16)	-0.4(2)
C(17)-C(1)-C(2)-C(3)	-176.75(10)	C(14)-C(15)-C(16)-C(17)	-0.4(2)
C(1)-C(2)-C(3)-C(4)	-66.50(15)	C(15)-C(16)-C(17)-C(12)	0.9(2)
C(2)-C(3)-C(4)-C(5)	70.57(15)	C(15)-C(16)-C(17)-C(1)	-178.43(13)
C(3)-C(4)-C(5)-C(6)	-77.41(15)	C(13)-C(12)-C(17)-C(16)	-0.80(19)
C(4)-C(5)-C(6)-C(7)	55.28(17)	C(8)-C(12)-C(17)-C(16)	-179.56(12)
C(4)-C(5)-C(6)-C(11)	-121.57(14)	C(13)-C(12)-C(17)-C(1)	178.69(11)
C(11)-C(6)-C(7)-C(8)	2.68(18)	C(8)-C(12)-C(17)-C(1)	-0.07(14)
C(5)-C(6)-C(7)-C(8)	-174.29(11)	C(18)-C(1)-C(17)-C(16)	-63.49(17)
C(11)-C(6)-C(7)-C(1)	-179.47(12)	C(7)-C(1)-C(17)-C(16)	178.49(13)
C(5)-C(6)-C(7)-C(1)	3.6(2)	C(2)-C(1)-C(17)-C(16)	57.78(17)
C(18)-C(1)-C(7)-C(6)	67.63(17)	C(18)-C(1)-C(17)-C(12)	117.09(11)
C(17)-C(1)-C(7)-C(6)	-176.37(12)	C(7)-C(1)-C(17)-C(12)	-0.93(13)
C(2)-C(1)-C(7)-C(6)	-57.24(16)	C(2)-C(1)-C(17)-C(12)	-121.64(11)
C(18)-C(1)-C(7)-C(8)	-114.33(11)	C(7)-C(1)-C(18)-N(19)	0.72(19)
C(17)-C(1)-C(7)-C(8)	1.66(13)	C(17)-C(1)-C(18)-N(19)	-110.81(15)
C(2)-C(1)-C(7)-C(8)	120.80(11)	C(2)-C(1)-C(18)-N(19)	127.34(14)
C(6)-C(7)-C(8)-C(9)	-1.84(18)	C(7)-C(1)-C(18)-O(22)	-179.49(10)
C(1)-C(7)-C(8)-C(9)	179.94(11)	C(17)-C(1)-C(18)-O(22)	68.98(13)
C(6)-C(7)-C(8)-C(12)	176.42(11)	C(2)-C(1)-C(18)-O(22)	-52.87(14)
C(1)-C(7)-C(8)-C(12)	-1.80(13)	O(22)-C(18)-N(19)-C(20)	-0.01(16)
C(7)-C(8)-C(9)-C(10)	-0.48(19)	C(1)-C(18)-N(19)-C(20)	179.77(12)
C(12)-C(8)-C(9)-C(10)	-178.33(13)	C(18)-N(19)-C(20)-C(24)	-121.01(13)
C(8)-C(9)-C(10)-C(11)	1.8(2)	C(18)-N(19)-C(20)-C(23)	118.10(16)
C(9)-C(10)-C(11)-C(6)	-0.9(2)	C(18)-N(19)-C(20)-C(21)	-1.81(15)
C(7)-C(6)-C(11)-C(10)	-1.35(19)	N(19)-C(20)-C(21)-O(22)	2.85(15)
C(5)-C(6)-C(11)-C(10)	175.66(12)	C(24)-C(20)-C(21)-O(22)	119.72(13)
C(9)-C(8)-C(12)-C(17)	179.24(13)	C(23)-C(20)-C(21)-O(22)	-114.48(15)
C(7)-C(8)-C(12)-C(17)	1.17(14)	N(19)-C(18)-O(22)-C(21)	1.96(16)
C(9)-C(8)-C(12)-C(13)	0.6(2)	C(1)-C(18)-O(22)-C(21)	-177.84(11)
C(7)-C(8)-C(12)-C(13)	-177.43(13)	C(20)-C(21)-O(22)-C(18)	-2.87(15)
C(17)-C(12)-C(13)-C(14)	0.03(19)		
C(8)-C(12)-C(13)-C(14)	178.49(13)		

Symmetry transformations used to generate equivalent atoms:

Table 2. Atomic coordinates ($\times 10^4$) and equivalent isotropic displacement parameters ($\text{\AA}^2 \times 10^3$) for (S,S)-175. U(eq) is defined as one third of the trace of the orthogonalized U_{ij} tensor.

	x	y	z	U(eq)
C(1)	12593(3)	2880(7)	12981(3)	20(1)
C(2)	13113(4)	4397(7)	13951(3)	24(1)
C(3)	14463(4)	4749(7)	14014(3)	28(1)
C(4)	14802(4)	2875(7)	13497(3)	22(1)
C(5)	15947(4)	2252(7)	13482(3)	32(1)
C(6)	16055(4)	444(7)	12976(3)	31(1)
C(7)	15028(4)	-680(7)	12492(3)	26(1)
C(8)	13876(4)	-54(7)	12486(3)	21(1)
C(9)	13768(4)	1768(7)	12976(3)	20(1)
C(10)	12180(3)	3950(7)	11833(4)	21(1)
O(10)	12394(3)	5749(5)	11785(2)	27(1)
N(11)	11663(3)	2845(3)	10920(3)	19(1)
C(12)	11425(3)	3579(7)	9759(3)	21(1)
C(13)	10222(3)	2771(7)	9008(3)	25(1)
O(13)	9226(3)	3592(4)	9340(2)	25(1)
C(14)	12505(4)	3087(8)	9295(3)	33(1)
C(15)	12711(4)	867(8)	9185(4)	42(1)
C(16)	13702(4)	4075(9)	10000(4)	48(2)
C(17)	11561(4)	1690(7)	13221(3)	20(1)
C(18)	11795(4)	-77(7)	13841(3)	25(1)
C(19)	10885(4)	-1013(7)	14174(3)	30(1)
C(20)	9706(4)	-209(8)	13886(3)	29(1)
C(21)	9443(4)	1530(8)	13249(4)	30(1)
C(22)	10386(4)	2440(7)	12932(3)	28(1)

Table 3. Bond lengths [\AA] for (S,S)-175.

C(1)-C(17)	1.525(6)	C(12)-C(14)	1.545(5)
C(1)-C(9)	1.538(6)	C(12)-H(12A)	1.0000
C(1)-C(10)	1.538(5)	C(13)-O(13)	1.431(4)
C(1)-C(2)	1.553(5)	C(13)-H(13A)	0.9900
C(2)-C(3)	1.537(5)	C(13)-H(13B)	0.9900
C(2)-H(2A)	0.9900	O(13)-H(13O)	0.9799(11)
C(2)-H(2B)	0.9900	C(14)-C(15)	1.526(7)
C(3)-C(4)	1.518(6)	C(14)-C(16)	1.534(6)
C(3)-H(3A)	0.9900	C(14)-H(14A)	1.0000
C(3)-H(3B)	0.9900	C(15)-H(15A)	0.9800
C(4)-C(5)	1.378(6)	C(15)-H(15B)	0.9800
C(4)-C(9)	1.380(5)	C(15)-H(15C)	0.9800
C(5)-C(6)	1.393(6)	C(16)-H(16A)	0.9800
C(5)-H(5A)	0.9500	C(16)-H(16B)	0.9800
C(6)-C(7)	1.372(6)	C(16)-H(16C)	0.9800
C(6)-H(6A)	0.9500	C(17)-C(22)	1.375(5)
C(7)-C(8)	1.379(5)	C(17)-C(18)	1.398(5)
C(7)-H(7A)	0.9500	C(18)-C(19)	1.380(6)
C(8)-C(9)	1.391(6)	C(18)-H(18A)	0.9500
C(8)-H(8A)	0.9500	C(19)-C(20)	1.393(6)
C(10)-O(10)	1.242(5)	C(19)-H(19A)	0.9500
C(10)-N(11)	1.335(5)	C(20)-C(21)	1.394(6)
N(11)-C(12)	1.468(5)	C(20)-H(20A)	0.9500
N(11)-H(11N)	0.9800(11)	C(21)-C(22)	1.394(6)
C(12)-C(13)	1.508(5)	C(21)-H(21A)	0.9500
		C(22)-H(22A)	0.9500

Table 4. Bond angles [°] for (S,S)-175.

C(17)-C(1)-C(9)	118.0(4)	C(13)-C(12)-H(12A)	107.8
C(17)-C(1)-C(10)	112.8(3)	C(14)-C(12)-H(12A)	107.8
C(9)-C(1)-C(10)	104.4(3)	O(13)-C(13)-C(12)	109.7(3)
C(17)-C(1)-C(2)	109.4(3)	O(13)-C(13)-H(13A)	109.7
C(9)-C(1)-C(2)	101.2(3)	C(12)-C(13)-H(13A)	109.7
C(10)-C(1)-C(2)	110.3(4)	O(13)-C(13)-H(13B)	109.7
C(3)-C(2)-C(1)	106.5(3)	C(12)-C(13)-H(13B)	109.7
C(3)-C(2)-H(2A)	110.4	H(13A)-C(13)-H(13B)	108.2
C(1)-C(2)-H(2A)	110.4	C(13)-O(13)-H(13O)	108(3)
C(3)-C(2)-H(2B)	110.4	C(15)-C(14)-C(16)	110.0(4)
C(1)-C(2)-H(2B)	110.4	C(15)-C(14)-C(12)	113.9(4)
H(2A)-C(2)-H(2B)	108.6	C(16)-C(14)-C(12)	111.5(4)
C(4)-C(3)-C(2)	103.2(3)	C(15)-C(14)-H(14A)	107.0
C(4)-C(3)-H(3A)	111.1	C(16)-C(14)-H(14A)	107.0
C(2)-C(3)-H(3A)	111.1	C(12)-C(14)-H(14A)	107.0
C(4)-C(3)-H(3B)	111.1	C(14)-C(15)-H(15A)	109.5
C(2)-C(3)-H(3B)	111.1	C(14)-C(15)-H(15B)	109.5
H(3A)-C(3)-H(3B)	109.1	H(15A)-C(15)-H(15B)	109.5
C(5)-C(4)-C(9)	120.6(4)	C(14)-C(15)-H(15C)	109.5
C(5)-C(4)-C(3)	128.5(4)	H(15A)-C(15)-H(15C)	109.5
C(9)-C(4)-C(3)	110.9(4)	H(15B)-C(15)-H(15C)	109.5
C(4)-C(5)-C(6)	119.0(4)	C(14)-C(16)-H(16A)	109.5
C(4)-C(5)-H(5A)	120.5	C(14)-C(16)-H(16B)	109.5
C(6)-C(5)-H(5A)	120.5	H(16A)-C(16)-H(16B)	109.5
C(7)-C(6)-C(5)	120.0(4)	C(14)-C(16)-H(16C)	109.5
C(7)-C(6)-H(6A)	120.0	H(16A)-C(16)-H(16C)	109.5
C(5)-C(6)-H(6A)	120.0	H(16B)-C(16)-H(16C)	109.5
C(6)-C(7)-C(8)	121.4(4)	C(22)-C(17)-C(18)	117.7(4)
C(6)-C(7)-H(7A)	119.3	C(22)-C(17)-C(1)	120.3(4)
C(8)-C(7)-H(7A)	119.3	C(18)-C(17)-C(1)	121.6(4)
C(7)-C(8)-C(9)	118.5(4)	C(19)-C(18)-C(17)	121.2(4)
C(7)-C(8)-H(8A)	120.7	C(19)-C(18)-H(18A)	119.4
C(9)-C(8)-H(8A)	120.7	C(17)-C(18)-H(18A)	119.4
C(4)-C(9)-C(8)	120.4(4)	C(18)-C(19)-C(20)	120.1(4)
C(4)-C(9)-C(1)	111.0(4)	C(18)-C(19)-H(19A)	120.0
C(8)-C(9)-C(1)	128.6(4)	C(20)-C(19)-H(19A)	120.0
O(10)-C(10)-N(11)	123.1(4)	C(19)-C(20)-C(21)	119.9(4)
O(10)-C(10)-C(1)	119.5(4)	C(19)-C(20)-H(20A)	120.1
N(11)-C(10)-C(1)	117.3(4)	C(21)-C(20)-H(20A)	120.1
C(10)-N(11)-C(12)	123.2(4)	C(20)-C(21)-C(22)	118.5(4)
C(10)-N(11)-H(11N)	118(4)	C(20)-C(21)-H(21A)	120.8
C(12)-N(11)-H(11N)	118(4)	C(22)-C(21)-H(21A)	120.8
N(11)-C(12)-C(13)	110.4(3)	C(17)-C(22)-C(21)	122.7(4)
N(11)-C(12)-C(14)	111.1(3)	C(17)-C(22)-H(22A)	118.7
C(13)-C(12)-C(14)	111.8(3)	C(21)-C(22)-H(22A)	118.7
N(11)-C(12)-H(12A)	107.8		

Symmetry transformations used to generate equivalent atoms:

Table 5. Anisotropic displacement parameters ($\text{\AA}^2 \times 10^3$) for (S,S)-175. The anisotropic displacement factor exponent takes the form: $-2\pi^2 [h^2 a^{*2} U^{11} + \dots + 2 h k a^* b^* U^{12}]$

	U ¹¹	U ²²	U ³³	U ²³	U ¹³	U ¹²
C(1)	27(2)	12(2)	17(2)	-3(2)	2(2)	0(2)
C(2)	36(3)	14(3)	19(2)	-1(2)	5(2)	4(2)
C(3)	38(3)	19(3)	25(2)	-2(2)	7(2)	-3(2)
C(4)	27(3)	22(3)	14(2)	0(2)	2(2)	-1(2)
C(5)	27(3)	37(3)	29(3)	-3(2)	6(2)	-9(2)
C(6)	27(3)	42(4)	26(3)	3(2)	10(2)	6(2)
C(7)	31(3)	27(3)	23(2)	-1(2)	10(2)	4(2)
C(8)	33(3)	7(2)	19(2)	2(2)	2(2)	-8(2)
C(9)	21(3)	18(3)	19(2)	3(2)	6(2)	2(2)
C(10)	19(2)	15(3)	28(3)	2(2)	5(2)	3(2)
O(10)	36(2)	10(2)	27(2)	2(1)	-2(2)	-3(1)
N(11)	25(2)	14(2)	16(2)	3(2)	3(2)	-1(2)
C(12)	31(3)	15(3)	15(2)	3(2)	4(2)	-3(2)
C(13)	29(3)	24(3)	20(2)	-1(2)	6(2)	1(2)
O(13)	30(2)	14(2)	29(2)	0(1)	6(1)	1(2)
C(14)	37(3)	44(4)	21(2)	5(2)	13(2)	-1(3)
C(15)	42(3)	46(4)	39(3)	-9(3)	12(3)	6(3)
C(16)	39(3)	67(4)	37(3)	0(3)	11(2)	-13(3)
C(17)	21(2)	22(3)	15(2)	-6(2)	1(2)	0(2)
C(18)	32(3)	20(3)	26(2)	9(2)	10(2)	3(2)
C(19)	34(3)	32(3)	21(2)	7(2)	6(2)	0(2)
C(20)	30(3)	38(3)	21(2)	-2(2)	11(2)	-5(2)
C(21)	22(3)	33(3)	34(3)	-1(2)	9(2)	5(2)
C(22)	32(3)	28(3)	24(2)	2(2)	8(2)	1(2)

Table 6. Hydrogen coordinates ($\times 10^4$) and isotropic displacement parameters ($\text{\AA}^2 \times 10^3$) for (S,S)-175.

	x	y	z	U(eq)
H(2A)	12645	5656	13787	28
H(2B)	13057	3861	14677	28
H(3A)	14548	5938	13573	34
H(3B)	14984	4916	14806	34
H(5A)	16653	3045	13813	38
H(6A)	16840	-11	12966	37
H(7A)	15112	-1916	12154	32
H(8A)	13171	-849	12155	25
H(11N)	11320(50)	1560(40)	11030(50)	130(30)
H(12A)	11350	5057	9777	25
H(13A)	10126	3118	8210	30
H(13B)	10217	1306	9071	30
H(13O)	8530(30)	2660(50)	9110(40)	46(14)
H(14A)	12298	3664	8517	40
H(15A)	13377	666	8849	63
H(15B)	11955	260	8699	63
H(15C)	12932	250	9935	63
H(16A)	13926	3571	10777	72
H(16B)	13585	5516	10004	72
H(16C)	14361	3769	9670	72
H(18A)	12595	-642	14038	31
H(19A)	11063	-2207	14600	36
H(20A)	9082	-846	14122	35

H(21A)	8639	2084	13037	36
H(22A)	10210	3625	12498	34

Table 7. Torsion angles [°] for (S,S)-175.

C(17)-C(1)-C(2)-C(3)	151.8(3)	C(17)-C(1)-C(10)-N(11)	-54.6(5)
C(9)-C(1)-C(2)-C(3)	26.5(4)	C(9)-C(1)-C(10)-N(11)	74.8(4)
C(10)-C(1)-C(2)-C(3)	-83.5(4)	(2)-C(1)-C(10)-N(11)	-177.3(3)
C(1)-C(2)-C(3)-C(4)	-24.0(4)	O(10)-C(10)-N(11)-C(12)	7.3(6)
C(2)-C(3)-C(4)-C(5)	-169.7(4)	C(1)-C(10)-N(11)-C(12)	-168.8(3)
C(2)-C(3)-C(4)-C(9)	11.7(4)	C(10)-N(11)-C(12)-C(13)	-142.4(4)
C(9)-C(4)-C(5)-C(6)	-2.8(6)	C(10)-N(11)-C(12)-C(14)	93.0(5)
C(3)-C(4)-C(5)-C(6)	178.7(4)	N(11)-C(12)-C(13)-O(13)	67.3(5)
C(4)-C(5)-C(6)-C(7)	0.6(6)	C(14)-C(12)-C(13)-O(13)	-168.4(3)
C(5)-C(6)-C(7)-C(8)	0.5(6)	N(11)-C(12)-C(14)-C(15)	63.8(5)
C(6)-C(7)-C(8)-C(9)	0.6(6)	C(13)-C(12)-C(14)-C(15)	-60.0(5)
C(5)-C(4)-C(9)-C(8)	3.9(6)	N(11)-C(12)-C(14)-C(16)	-61.4(5)
C(3)-C(4)-C(9)-C(8)	-177.4(4)	C(13)-C(12)-C(14)-C(16)	174.7(4)
C(5)-C(4)-C(9)-C(1)	-173.2(4)	C(9)-C(1)-C(17)-C(22)	-161.7(4)
C(3)-C(4)-C(9)-C(1)	5.6(4)	C(10)-C(1)-C(17)-C(22)	-39.8(5)
C(7)-C(8)-C(9)-C(4)	-2.7(6)	C(2)-C(1)-C(17)-C(22)	83.4(4)
C(7)-C(8)-C(9)-C(1)	173.7(4)	C(9)-C(1)-C(17)-C(18)	25.2(5)
C(17)-C(1)-C(9)-C(4)	-139.3(3)	C(10)-C(1)-C(17)-C(18)	147.2(4)
C(10)-C(1)-C(9)-C(4)	94.5(4)	C(2)-C(1)-C(17)-C(18)	-89.6(5)
C(2)-C(1)-C(9)-C(4)	-20.0(4)	C(22)-C(17)-C(18)-C(19)	-1.4(6)
C(17)-C(1)-C(9)-C(8)	44.0(6)	C(1)-C(17)-C(18)-C(19)	171.9(4)
C(10)-C(1)-C(9)-C(8)	-82.2(5)	C(17)-C(18)-C(19)-C(20)	0.5(6)
C(2)-C(1)-C(9)-C(8)	163.2(4)	C(18)-C(19)-C(20)-C(21)	0.7(6)
C(17)-C(1)-C(10)-O(10)	129.1(4)	C(19)-C(20)-C(21)-C(22)	-0.9(6)
C(9)-C(1)-C(10)-O(10)	-101.5(4)	C(18)-C(17)-C(22)-C(21)	1.2(6)
C(2)-C(1)-C(10)-O(10)	6.4(5)	C(1)-C(17)-C(22)-C(21)	-172.2(4)
		C(20)-C(21)-C(22)-C(17)	0.0(6)

Symmetry transformations used to generate equivalent atoms

Table 8. Hydrogen bonds for (S,S)-175 [Å and °].

D-H...A	d(D-H)	d(H...A)	d(D...A)	<(DHA)
N(11)-H(11N)...O(13)#1	0.9800(11)	2.10(3)	3.024(4)	156(5)
O(13)-H(13O)...O(10)#1	0.9799(11)	1.817(19)	2.733(4)	154(4)

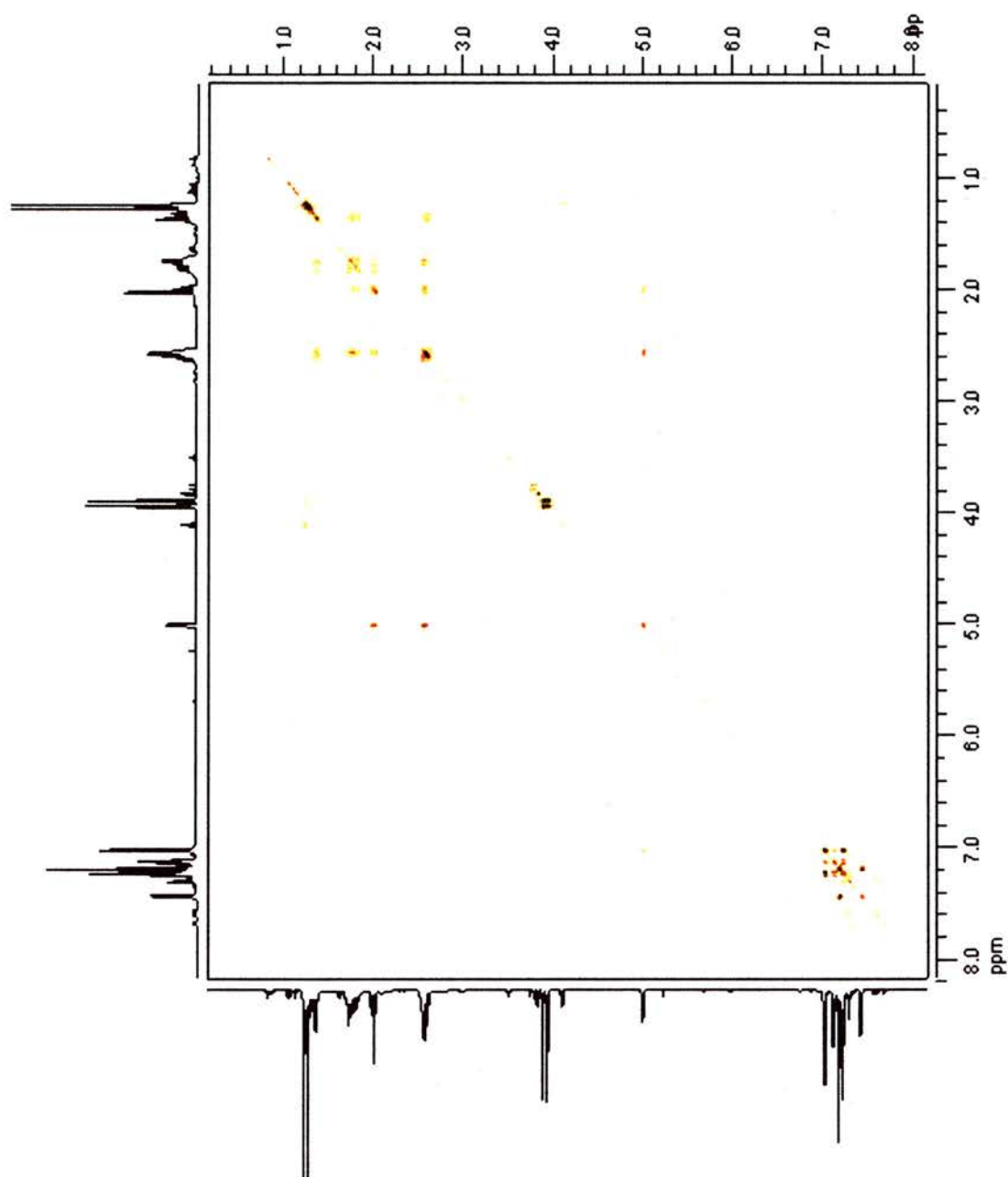
Symmetry transformations used to generate equivalent atoms:

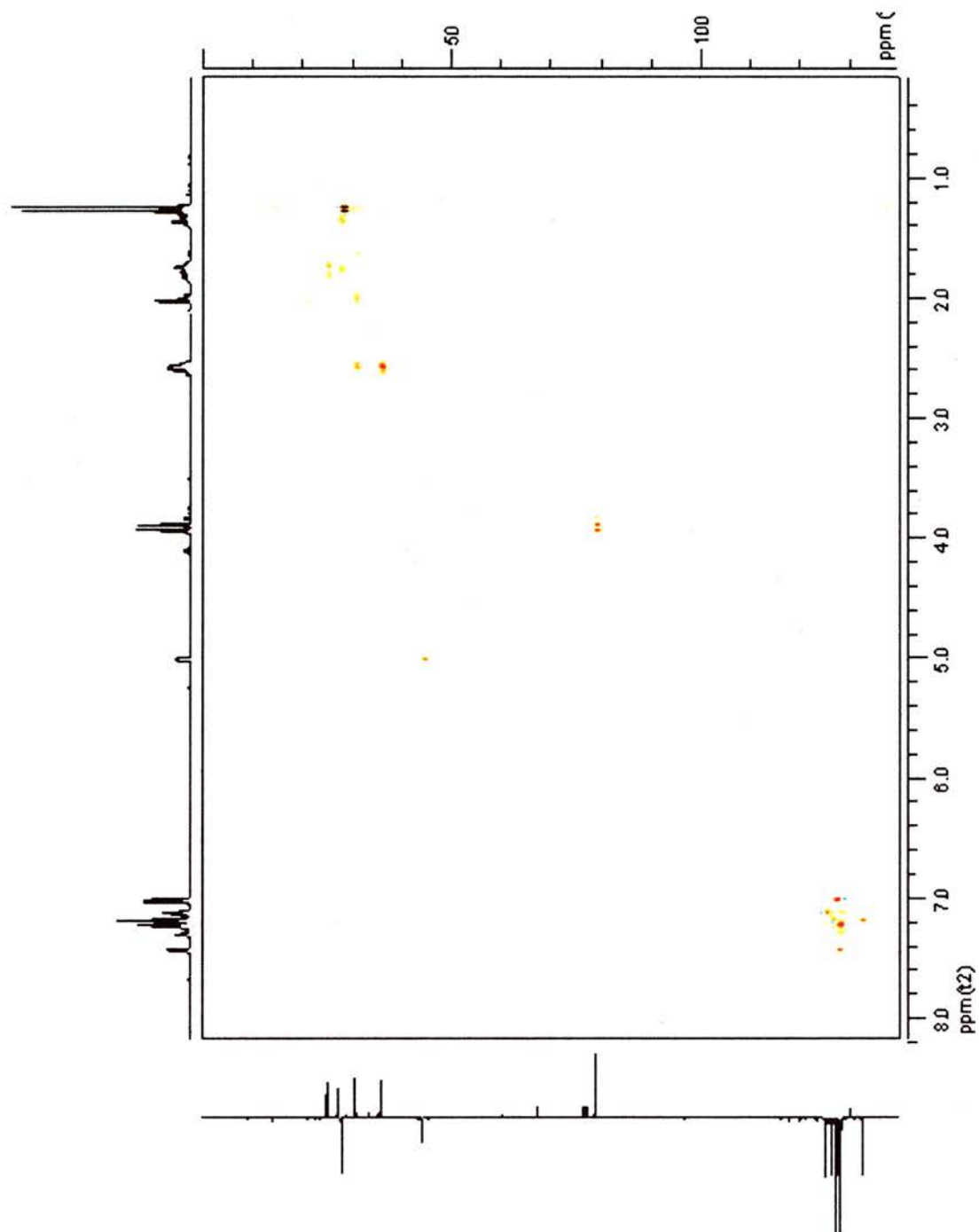
#1 -x+2,y-1/2,-z+2

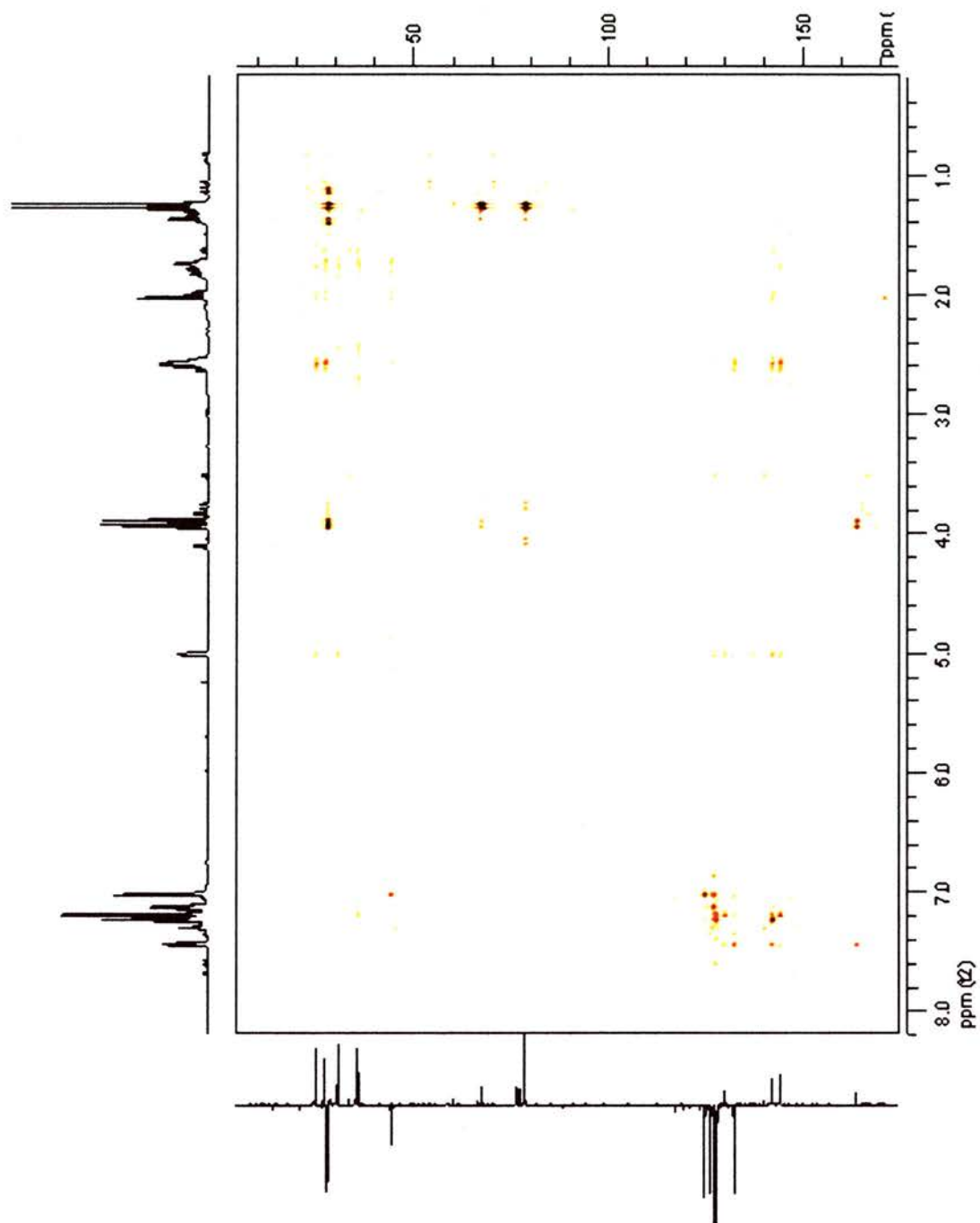
Appendix B

NMR Data

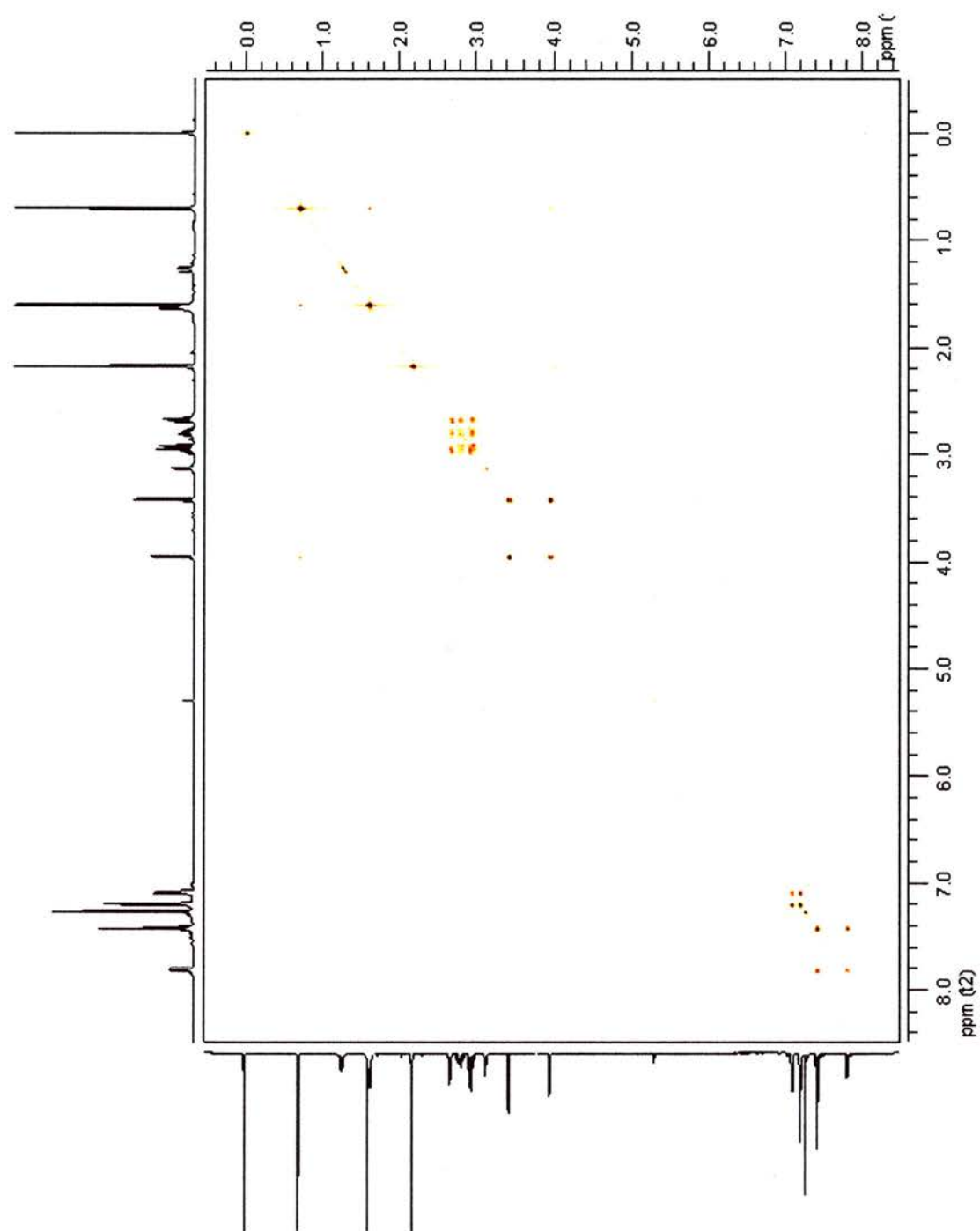
Benzosuberene 150

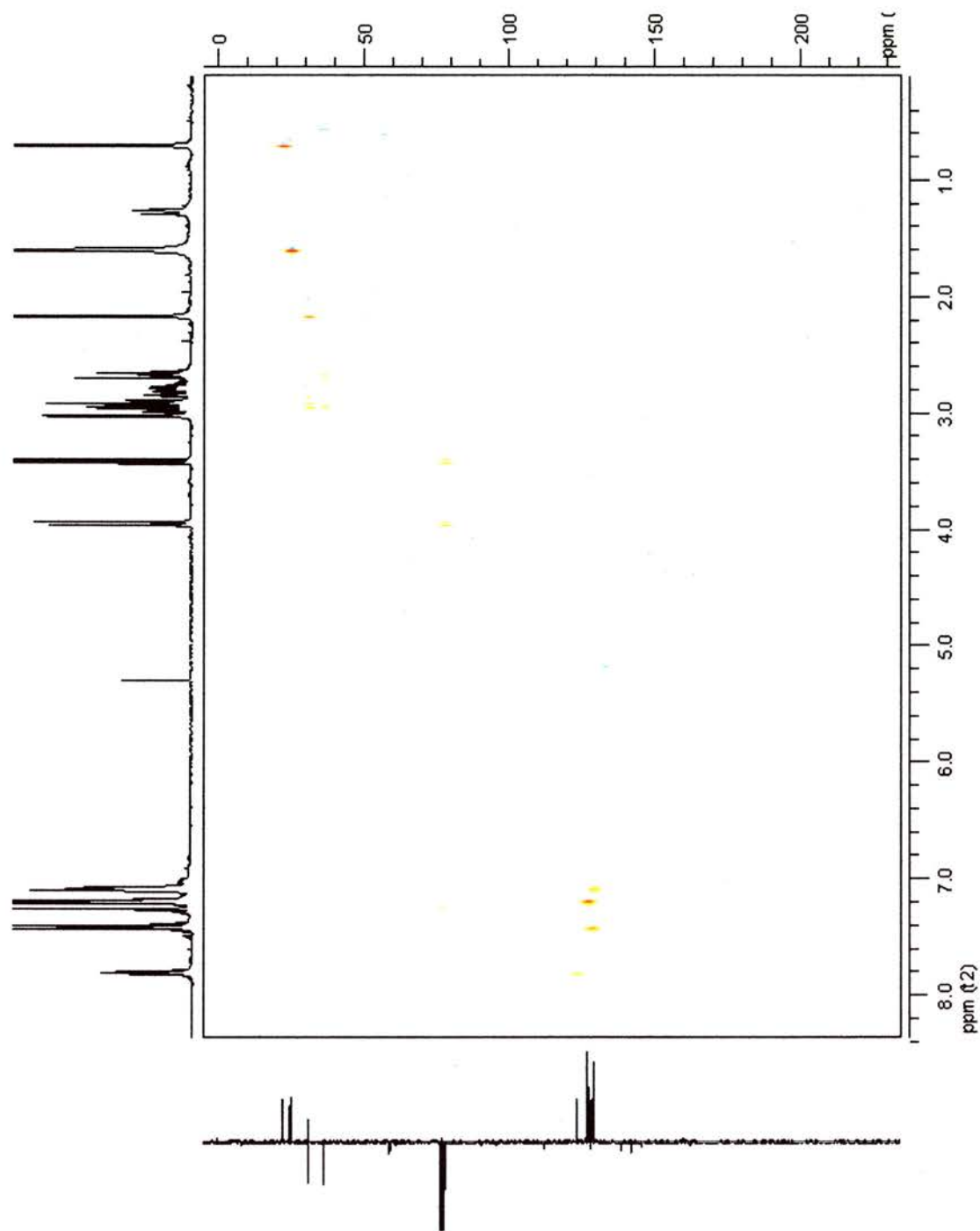
500 MHz (CDCl₃) ¹H-¹H-COSY Spectrum of 150

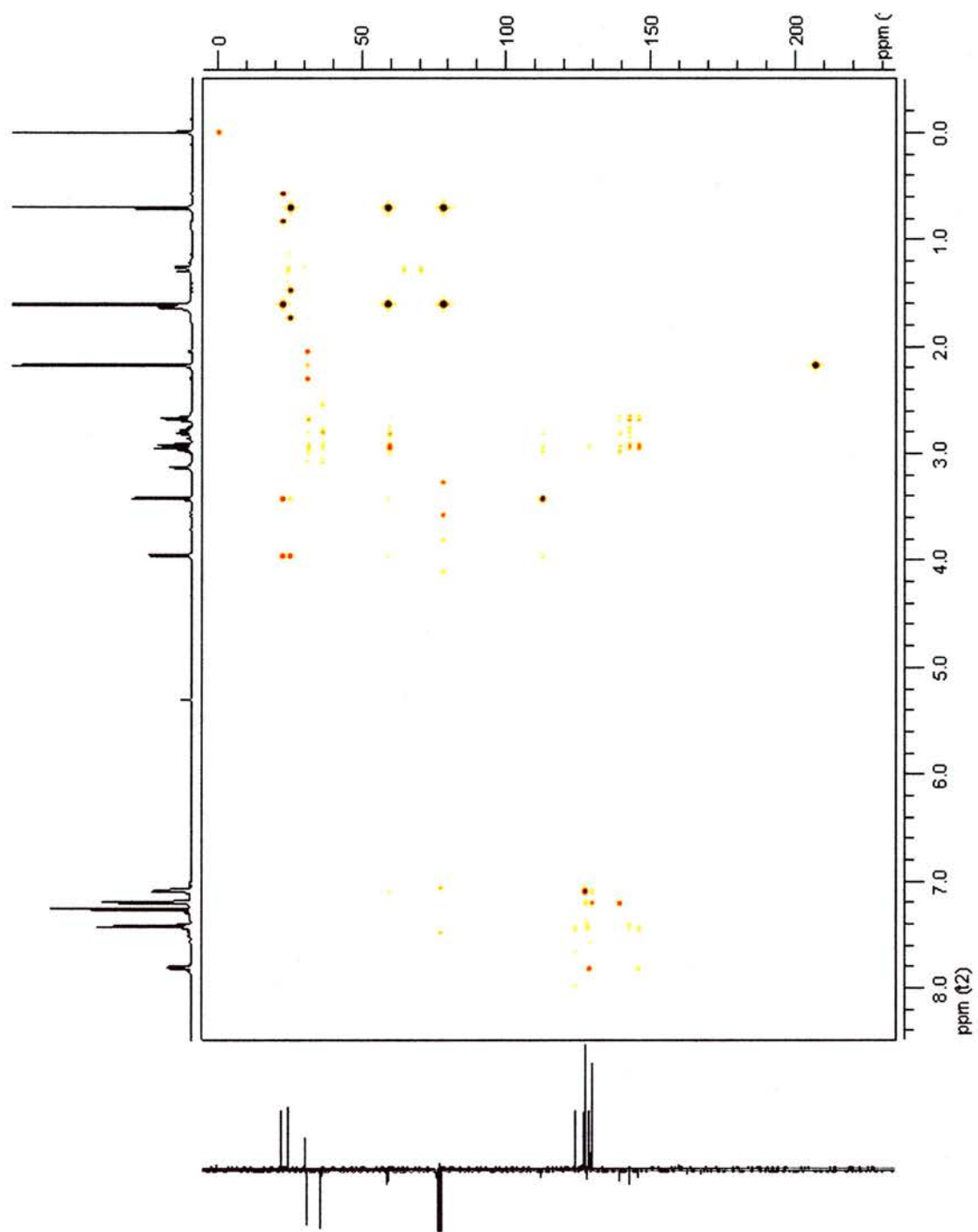
500MHz (CDCl₃) HSQC Spectrum of **150**

500MHz (CDCl₃) HMBC Spectrum of **150**

Roytonone 191



500MHz (CDCl₃) HSQC Spectrum of 191

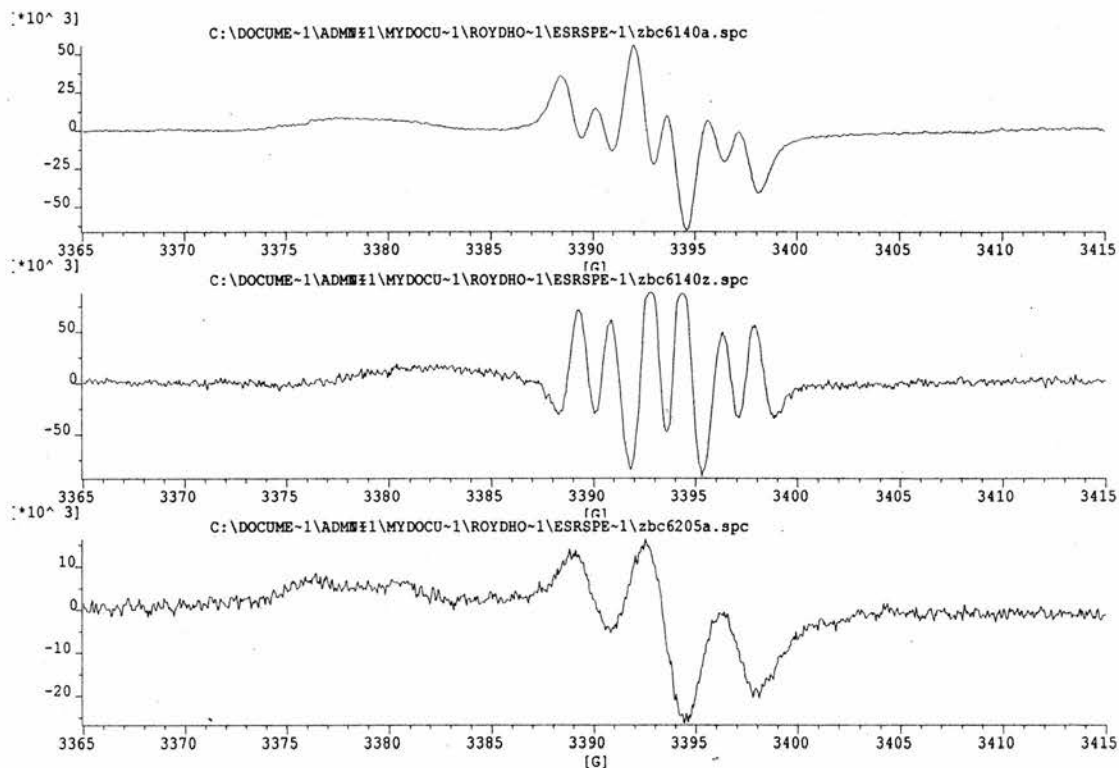
500MHz (CDCl₃) HMBC Spectrum of 191

Appendix C

EPR Spectra

Carbaldehyde cis-203

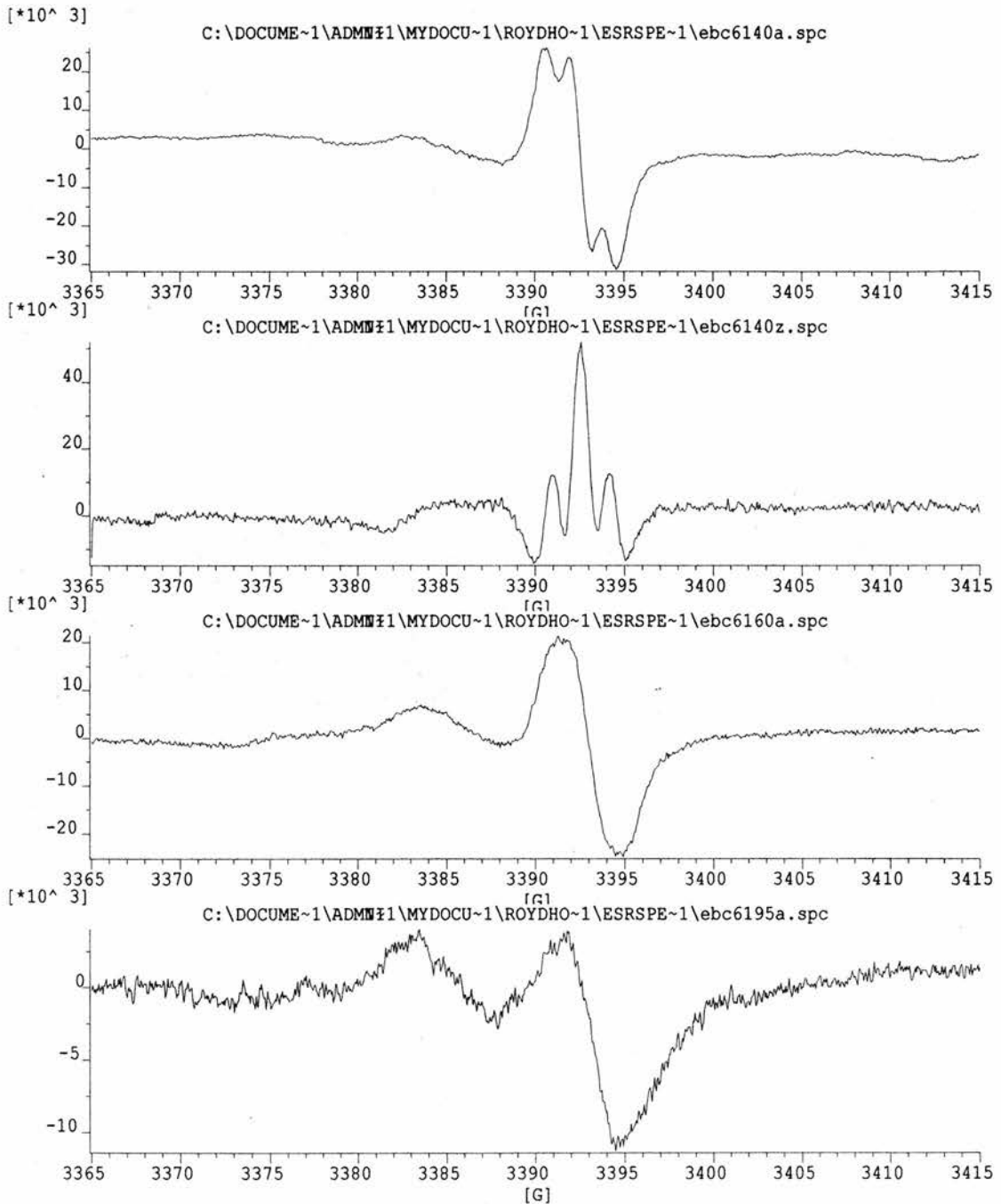
EPR Spectra from DTBP and *cis*-4-t-butylcyclohexane carbaldehyde (**cis-203**) in cyclopropane



Top at 140 K, 1st derivative. Middle at 140 K, 2nd derivative. Bottom at 205 K, 1st derivative.

Carbaldehyde *trans*-203

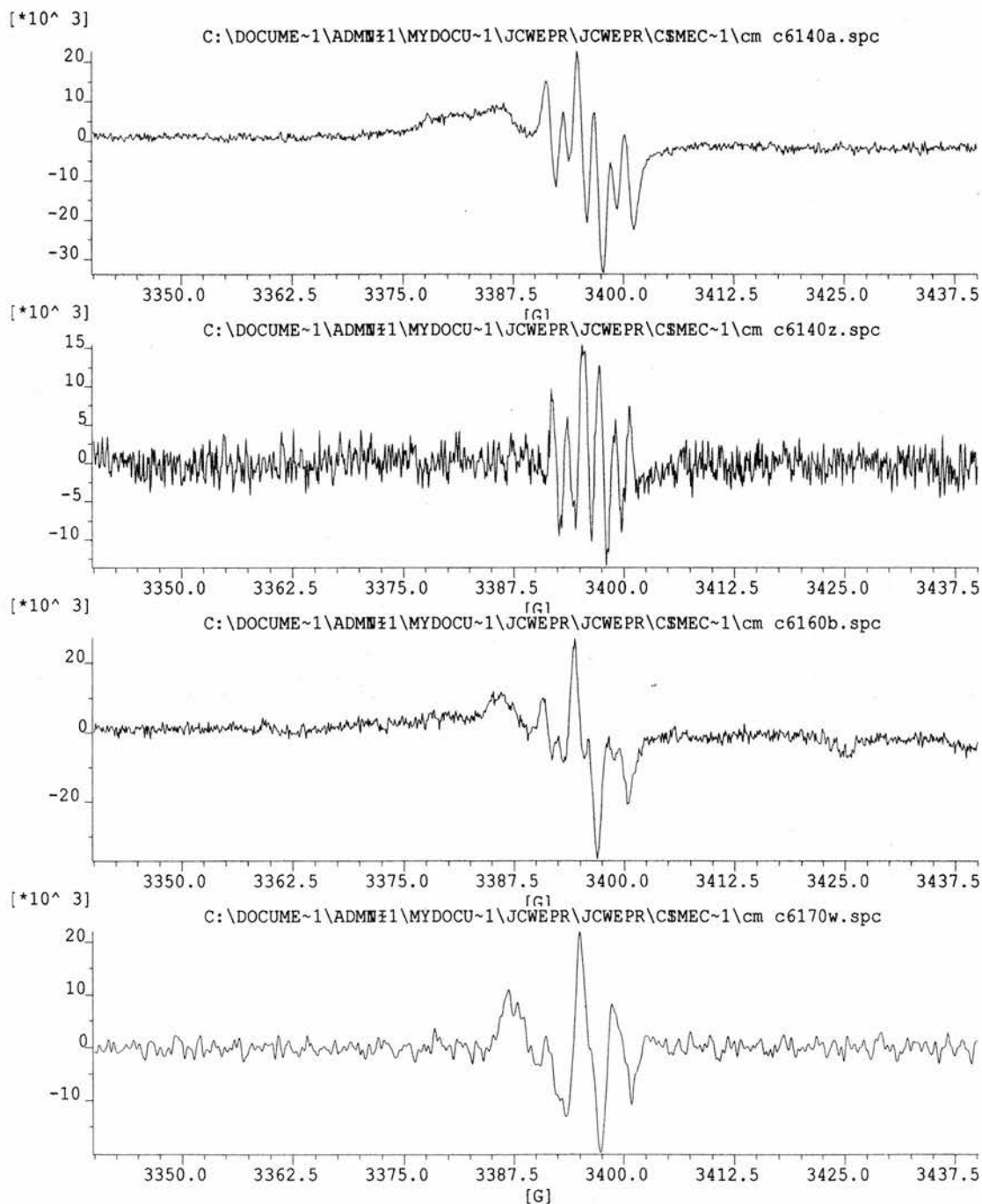
EPR Spectra from DTBP and *trans*-4-t-butylcyclohexane carbaldehyde (*trans*-203) in cyclopropane



Top at 140 K, 1st derivative. Next: at 140 K 2nd derivative. Next at 160 K, 1st derivative.
Bottom at 195 K 1st derivative.

Carbaldehyde cis-204

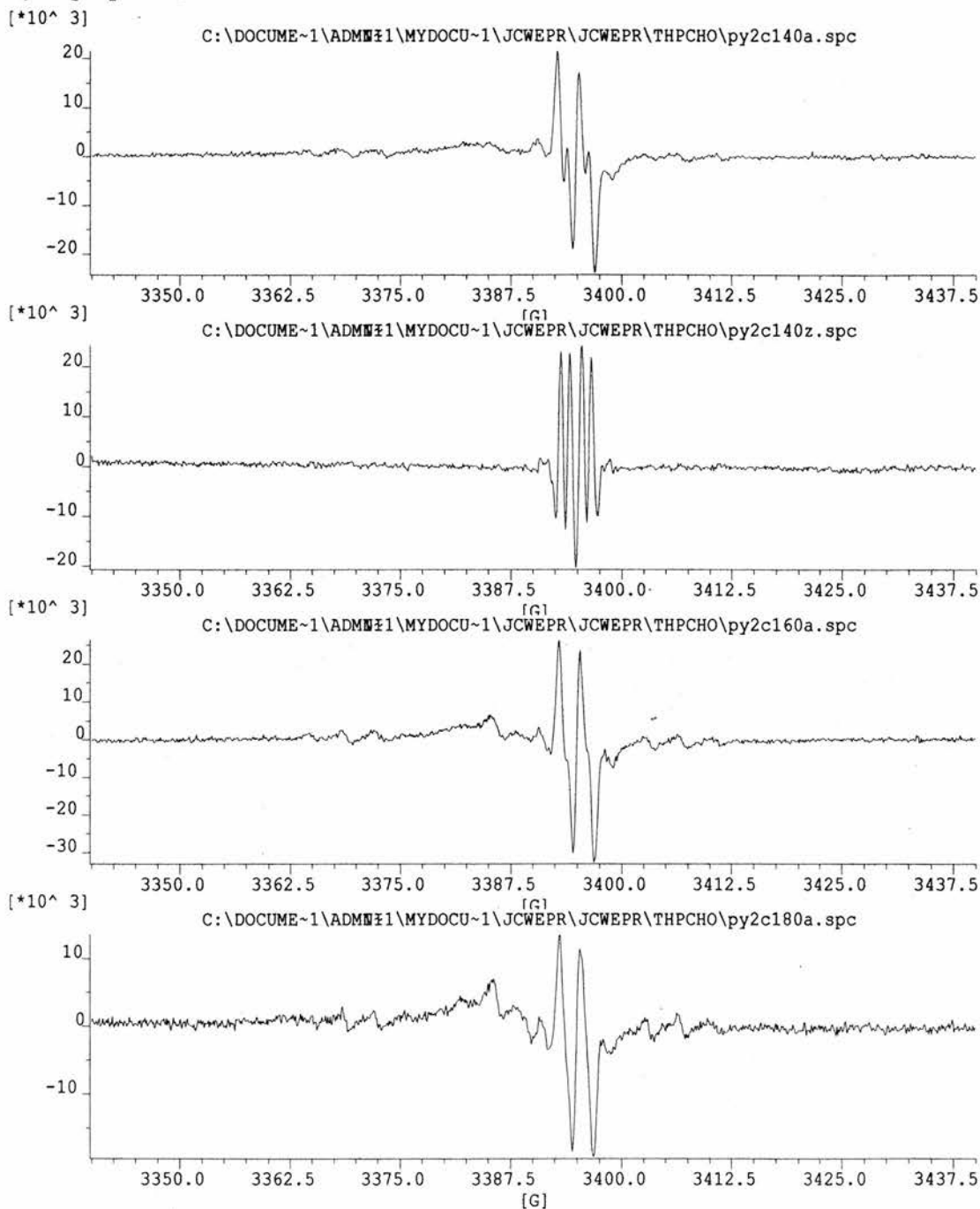
EPR Spectra from DTBP and *cis*-4-methylcyclohexancarbaldehyde (*cis*-204) in cyclopropane



Top at 140 K, 1st derivative. Next: at 140 K 2nd derivative. Next at 160 K, 1st derivative.
Bottom at 170 K 1st derivative.

Carbaldehyde 206

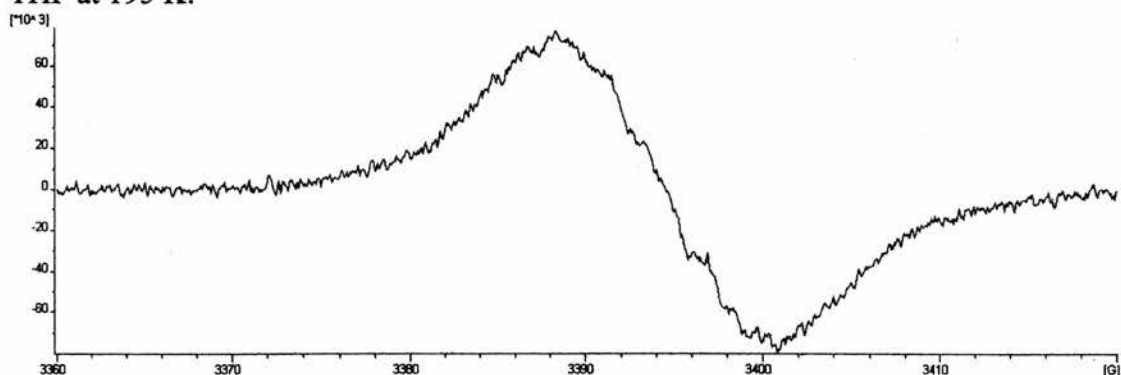
9.5 GHz EPR Spectra from DTBP and tetrahydropyranyl-2-carbaldehyde (3) in cyclopropane



Top: spectrum at 140K, 1st derivative. Next down, spectrum at 140 K, 2nd derivative. Next down, spectrum at 160 K, 1st derivative. Bottom, spectrum at 180K, 1st derivative.

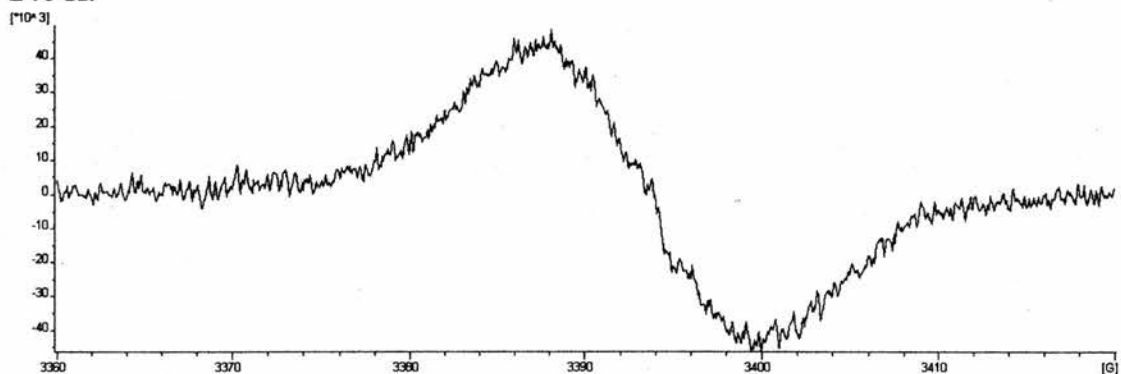
Tetrahydronaphthalene Radical Anion 171

9.5 GHz EPR 1st derivative spectrum from tetrahydronaphthalene radical anion 171 in THF at 195 K.



Benzosuberene Radical Anion 172

9.5 GHz EPR 1st derivative spectrum from benzosuberene radical anion 172 in THF at 240 K.



Appendix D

Kinetic Data

Cyclohexylacetyl Radical 214

Measurement of the concentrations of **214ax** and **214eq** by EPR spectroscopy.

T/K	Gain	D.I. (Ax)	D. I. (Eq)	[Ax]/M	[Eq]/M	[Ax]/[Eq]	log [Ax/Eq]
139.22	5.0E+05	10	572	5.48E-08	3.92E-07	0.140	-0.85
139.22	5.0E+05	9	380	4.93E-08	2.60E-07	0.189	-0.72
144.31	5.0E+05	14	499	7.95E-08	3.54E-07	0.224	-0.65
144.31	5.0E+05	15	577	8.52E-08	4.10E-07	0.208	-0.68
149.41	5.0E+05	11	393	6.47E-08	2.89E-07	0.224	-0.65

EPR measurements from solutions of *c*-C₆H₁₁CHO (*axial/equatorial* mixture) in cyclopropane (0.14 M) with DTBP photolysed at various temperatures.¹

T/K	Gain	D.I. (Ax)	D. I. (Eq)	[Ax]/M	[Eq]/M	[Ax]/[Eq]	log [Ax/Eq]
118.84	5.0E+05	25	905	1.17E-07	5.29E-07	0.221	-0.66
129.03	5.0E+05	20	705	1.02E-07	4.48E-07	0.227	-0.64
134.12	5.0E+05	16	700	8.45E-08	4.62E-07	0.183	-0.74
139.22	5.0E+05	15	639	8.22E-08	4.38E-07	0.188	-0.73
144.31	5.0E+05	15	542	8.52E-08	3.85E-07	0.221	-0.65
149.41	5.0E+05	15	514	8.82E-08	3.78E-07	0.233	-0.63

EPR measurements from solutions of *c*-C₆H₁₁CHO (*axial/equatorial* mixture) in *n*-propane (0.13 M) with DTBP photolysed at various temperatures.

¹ D.I. = double integral of EPR signal (the Ax D.I. has been multiplied by 8 (F=8) because it refers to the outer line only). DPPH = diphenylpicrylhydrazyl standard. Signals were too broad at higher temperatures for accurate measurements of individual lines to be made. DPPH dailT = 270, [DPPH]/M = 0.001, Gain DPPH = 1000, D.I. DPPH = 374, TrueT DPPH = 271.7, F[Ax] = 8 and F[Eq] = 1.